WOFEX 2007

proceedings of the 5th annual workshop

Faculty of Electrical Engineering and Computer Science,
VŠB – Technical University of Ostrava

ISBN 978-80-248-1571-8

WOFEX 2007

www.fei.vsb.cz/wofex

5th annual workshop,
Ostrava, 24th – 25th September 2007
Proceedings of papers

Organized by

VŠB – Technical University of Ostrava
Faculty of Electrical Engineering and Computer Science

WOFEX 2007
© Václav Snášel, editor

ISBN 978-80-248-1571-8

This work is subject to copyright. All rights reserved. Reproduction or publication of this material, even partial, is allowed only with the editors' permission.

Technical editors:
Pavel Moravec `pavel.moravec@vsb.cz`
Jiří Dvorský `jiri.dvorsky@vsb.cz`

Faculty of Electrical Engineering and Computer Science,
VŠB – Technical University of Ostrava

Page count: 456
Impression: 200
Edition: 1st
First published: 2007

This proceedings was typeset by PDFLaTeX.
Printed and bound in Ostrava, Czech Republic by TiskServis Jiří Pustina.

Published by Faculty of Electrical Engineering and Computer Science, VŠB – Technical University of Ostrava

Preface

The workshop WOFEX 2007 (PhD workshop of Faculty of Electrical Engineering and Computer Science) was held on September 24th – 25th, 2007 at the VŠB – Technical University of Ostrava. The workshop offers an opportunity for students to meet and share their research experiences, to discover commonalities in research and studentship, and to foster a collaborative environment for joint problem solving. PhD students are encouraged to attend in order to ensure a broad, unconfined discussion. In that view, the Workshop is intended for students, young researchers, and engineers offering opportunities to meet new colleagues.

The proceedings of WOFEX 2007 are also available at WOFEX Web site http://www.fei.vsb.cz/wofex/2007/. I would like to thank the authors and the Organising Committee from Department of Computer Science for their arduous editing work.

September 2007

Václav Snášel
Evaluation Committee Chair
WOFEX 2007

Organization

Evaluation Committee

Chair:
Václav Snášel (VŠB – Technical University of Ostrava)

Members:
Zdeněk Dostál (VŠB – Technical University of Ostrava)
Zdeněk Diviš (VŠB – Technical University of Ostrava)
Pavel Brandštetter (VŠB – Technical University of Ostrava)

Organizing Committee

Jiří Dvorský (VŠB – Technical University of Ostrava)
Jana Mlatečková (VŠB – Technical University of Ostrava)
Pavel Moravec (VŠB – Technical University of Ostrava)

Workshop Location:

Campus of VŠB – Technical University of Ostrava
17. listopadu 15, 708 33 Ostrava–Poruba, Czech Republic
24th – 25th September 2007

`www.fei.vsb.cz/wofex`

Sponsor

Workshop WOFEX 2007 and its proceeding is supported by:

Visteon

AUTOPAL

AUTOPAL

Visteon

VISTEON-AUTOPAL, s.r.o.

- VISTEON-AUTOPAL, s.r.o.
se sídlem v Novém Jičíně je centrem vývoje a předním světovým výrobcem světelné, chladící a klimatizační techniky, forem a nástrojů pro automobilový průmysl. Visteon-Autopal dodává své výrobky hlavním výrobcům automobilů včetně firem Aston Martin, Audi, Fiat, Ford, Daimler-Chrysler, General Motors, Jaguar, Kia, Mercedes-Benz, Porsche, PSA Peugeot-Citroen, Renault, Seat, Škoda Auto, Volvo a VW

OPEL ASTRA
Rear Lamp

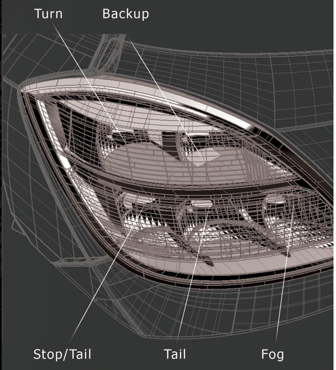

- Kontakty
Visteon-Autopal, s.r.o.
Lužická 14 7410 01 Nový Jičín

Tel.: +420 556 780 388
Fax: +420 556 780 477

www.visteon.com

Pokud máte zájem o práci v naší společnosti kontaktuje: Tamara Bernatíková
email: tbernatikova@dmc-cz.com
tel.: +420 602 102 501

- Našim zaměatnancům nabízíme široké spektrum benefitů :

Motivující plat a zajímavý bonusový systém
Zázemí silné mezinárodní společnosti
(Za)školení
Příležitost i pro absolventy
Pracoviště vybavená špičkovou technikou
Věrnostní odměny
Flexibilní pracovní doba
Zajištění přechodného ubytování s možností přidělení bytu
Příplatky na stravování
5 týdnů dovolené
Životní a penzijní připojištění
Příspěvek na dopravné
Sportovní aktivity v areálu závodu v Novém Jičíně

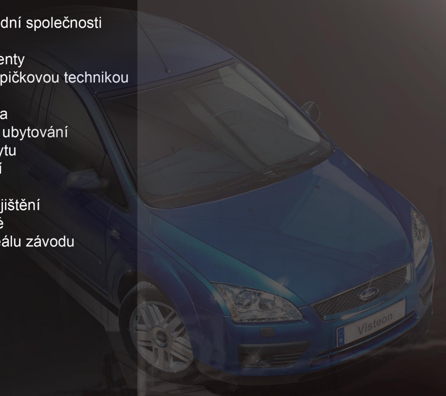

- Mezi základní požadavky spolupráce považujeme :

Schopnost komunikovat v anglickém jazyce
Technické vzdělání
Flexibilitu
Samostatnost
Zájem o osobní a profesní rozvoj
Prezentační dovednosti
Povědomí a zájem o automobilový sektor
Ochota cestovat

- S více než 4500 zaměstnanci provozuje Visteon-Autopal dvě specializovaná technická centra zaměřená na klimatizaci a světelnou techniku, pět výrobních závodů a nástrojárnu nacházejících se v Novém Jičíně, Hluku a Rychvaldě, dále pak prodejní kancelář pro náhradní díly v Praze, sklad náhradních dílů pro střední a východní Evropu v Novém Jičíně a v neposlední řadě zákaznické středisko pro firmu Škoda Auto v Mladé Boleslavi. Visteon-Autopal je součástí americké nadnárodní společnosti Visteon Corporation, která je přední světový dodavatel pro automobilový průmysl, má více než 170 závodů ve 26 zemích a zaměstnává přibližně 49, 000 lidí.

Visteon-Autopal nabízí pracovní příležitosti mladým, dynamickým a samostatným individualitám s technickým vzděláním. Za důležitý předpoklad spolupráce považujeme slušnost, spolehlivost, loajalitu, práci v týmu a zájem o osobní a profesní rozvoj.

VISTEON-AUTOPAL, s.r.o.

Visteon-Autopal C. 2007

Sponsor

Workshop WOFEX 2007 and its proceeding is supported by:

Schneider Electric
www.schneider-electric.cz

The new electric world

Devising solutions for all needs

Aligning growth and responsibility

Commitment to all our stakeholders

The world leader in electricity and automation management, Schneider Electric harnesses electricity to support customer performance and enhance quality of life. Thanks to a unique portfolio of products and services, we offer integrated, intelligent and networked solutions that allow customers to use electricity in complete safety, develop automation everywhere, improve energy efficiency, ensure a high quality power supply and manage building utilities and communication networks. By leveraging the deep commitment of our 105,000 team members in 106 countries, Schneider Electric gives the best of the New Electric World to everyone, everywhere, at any time.

Schneider Electric

Ve Schneider Electric víme, ...

... že spokojenosti našich zákazníků dosáhneme pouze díky našim zaměstnancům. Proto klademe velký důraz na jejich výběr a profesní i kariérový rozvoj.

Ve Schneider Electric věříme, ...

... že vzdělávání je jedním z klíčových nástrojů personální práce, podporujeme rozvoj zaměstnanců, jejich motivaci a efektivitu pracovního výkonu.

Volné pozice pro absolventy:

- Aplikační specialisté
  pro automatizaci PLC, HW, SW
- Servisní technici pro automatizaci budov
  (EZS, měření a regulace, bezpečnostní kamerové systémy)
- Specialisté v oboru slaboproud a silnoproud

Pro bližší informace prosím kontaktujte:
Lenka Blahetová, personální oddělení,
Schneider Electric CZ, s. r. o., Thámova 13, 186 00 Praha 8
tel.: 281 088 618, 603 884 254, e-mail: lenka.blahetova@cz.schneider-electric.com

Schneider Electric

Sponsor

Workshop WOFEX 2007 and its proceeding is supported by:

SIEMENS

Siemens s.r.o.

Automation and Drives

Siemens s.r.o., Automation and Drives, offers products, systems and end-to-end solutions for industrial automation: systems for process control and regulation, automation systems and drives, production control, measuring and testing technology, automation in the machine tool industry, drives and drive technology, low-voltage switching and installation technology.

Products, services and solutions

1.) Industrial automation systems
2.) Low-voltage switching and installation technology
3.) Automotive Industry Control Systems
4.) Control systems and drives for machine tools and robots
5.) Process instrumentation and analytics
6.) Electric drives for dynamically demanding applications
7.) Large drives
8.) Standard drives
9.) Transmissions & clutches

SIEMENS

Automatizace a pohony

Určujeme standardy a vývojové trendy v oblasti automatizace průmyslových procesů. Všem zákazníkům prostřednictvím svých produktů a řešení umožňujeme zvyšovat produktivitu při současné úspoře nákladů. Již delší dobu jsme vedoucím světovým dodavatelem technologií v oblasti automatizace a pohonů a tuto pozici stále posilujeme díky neustálým inovacím svých produktů, systémů i komplexních řešení v oblasti systémů pro řízení a regulaci procesů, automatizačních systémů a pohonů, řízení výroby, měřicí a zkušební techniky, automatizace v obrábění, pohonů a techniky pohonů i nízkonapěťové a spínací techniky. Nedílnou součástí naší nabídky je také špičkový servis po celém světě a průběžná inovace a modernizace již dodaných produktů, systémů a řešení podle přání našich zákazníků.

Koncepce plně integrované automatizace

Koncepce plně integrované automatizace (TIA – Totally Integrated Automation) je ve světě ojedinělá. Nabízí zákazníkům koncepci řízení, která má jednotnou hardwarovou i softwarovou platformu pro libovolnou automatizační úlohu ve všech průmyslových odvětvích, a to jak při výrobě sériových produktů, tak i ve zpracovatelském průmyslu.

Automatizace se týká všech fází výrobního procesu – od logistiky, přes vlastní výrobu, až po řízení podniku. TIA umožňuje průchodnou a přehlednou horizontální a vertikální integraci všech výrobních procesů. Zahrnuje řídicí a automatizační systémy, techniku pohonů, spínací techniku, procesní instrumentaci a v neposlední řadě integrované IT technologie, které v dnešní době hrají stále důležitější úlohu.

TIA je zárukou flexibility celého řešení, absolutní spolehlivosti a vysoké produktivity. Systém podstatně zkracuje také dobu projektování všech zařízení a jejich uvádění do provozu, zvyšuje efektivitu výrobních procesů a výrazně snižuje celkové náklady na údržbu zařízení po dobu jeho životnosti. TIA řídí a vyhodnocuje výrobní procesy, které jsou pak přehledné a snadno řiditelné pro provozní i podnikové úrovně řízení.

Koncepce plně integrované automatizace (TIA) umožňuje zvýšit konkurenceschopnost ve všech průmyslových odvětvích

Pro všechna průmyslová odvětví

Plně integrovaná automatizace poskytuje propracovanou, přesto však přehlednou architekturu pro automatizaci všech výrobních a dalších průmyslových procesů - od kontinuálních a sériových výrobních procesů až po nespojitou (diskrétní) výrobu.

Komplexní přístup k výrobnímu procesu

Plně integrovaná automatizace je integrovaná platforma pro celý výrobní podnik - od vstupní logistiky, přes výrobní proces a řízení, až po výstupní logistiku.

Životní cyklus výroby

Díky plně integrované automatizaci, která nabízí řídicí systémové prostředí monitorující výrobní proces, standardizovanou otevřenou komunikaci a sofistikovanou diagnostiku, lze výrazně zefektivnit životní cyklus výroby.

Kontakt:

Siemens, s.r.o., divize Automatizace a pohony,
Evropská 33a, 160 00 Praha 6
www.siemens.cz/ad

Prodej:
tel.: 233 032 411, fax: 233 032 449, e-mail: adprodej.cz@siemens.com

Marketing:
tel.: 233 032 474, fax: 233 032 482, e-mail: admarketing.cz@siemens.com

Jedině bezchybná synchronizace
přináší ten správný efekt
plně integrovaná
automatizace
optimalizace
bezpečnost

modularita

Dokonalé procesy vyžadují dokonalou souhru všech součástí. Plně integrovaná automatizace (Totally Integrated Automation - TIA) nabízí spolehlivé a modulární řešení pro veškeré výrobní procesy a splňuje nejnáročnější požadavky na jednotné řízení, bezpečnost, efektivitu i úsporu nákladů pro všechna průmyslová odvětví.

SIEMENS

Siemens, s.r.o., Automatizace a pohony, Evropská 33a, 160 00 Praha 6,
tel.: 233 032 474, e-mail: admarketing.cz@siemens.com, www.siemens.cz/ad

produktivita

Sponsor

Workshop WOFEX 2007 and its proceeding is supported by:

TietoEnator

TietoEnator

greater together.

Zvolte si to správné místo
v Ostravě!

Jsme evropská IT společnost s působností v 30 zemích celého světa.
S více než 16 tisíci zaměstnanci patříme
k největším hráčům na poli informačních technologií v Evropě.
Za svého spolehlivého partnera nás volí přední světové společnosti
z vybraných odvětví, jako jsou bankovnictví, telekomunikace
a média, zdravotnictví, lesní průmysl a energetika.
Nabízíme jim nová řešení a stojíme za jejich úspěchem.
Dosáhli jsme už mnoha cílů, ale abychom se stali ještě lepšími,
potřebujeme vaši pomoc, vaše nápady a zkušenosti.

www.tietoenator.cz
www.greatertogether.cz

Váš životopis v českém
a anglickém jazyce zašlete na
csc.recruitment@tietoenator.com.

TietoEnator TE

greater together.

Přidejte se k našemu
IT týmu!

Hledáte zajímavé perspektivní zaměstnání v oblasti informačních technologií v silné mezinárodní společnosti?

Přijmeme absolventy nebo studenty (i na kratší pracovní úvazek) se znalostí angličtiny na tyto pozice:
Programátor - znalost některého z uvedených jazyků
- Java (J2ME, J2EE), .NET, C#, C++, Symbian
Administrátor - základní znalost administrace některé z oblastí
- Windows, UNIX/Linux, Security, SAP, databáze

Nabízíme:
- mezinárodní prostředí, denní využití angličtiny
- odborná školení, technické kurzy, výuku anglického jazyka
- osobní i profesní růst
- odpovídající finanční ohodnocení
- program zaměstnaneckých výhod (týden dovolené navíc, stravenky, teambuildingové aktivity, příspěvek na kapitálové životní a důchodové pojištění)
- pracovní smlouvu na dobu neurčitou

Kontakt:
TietoEnator Czech s.r.o.
Recruitment Team
Technologická 373/4, 708 00 Ostrava
Tel.: +420 597 459 982, +420 597 459 979
www.tietoenator.cz

www.tietoenator.cz
www.greatertogether.cz

Table of Contents

Study Programme P 2645 Electrical Engineering, Communication and Computer Systems

Electrical machines, apparatus and drives (2642V004)

Execution of IGBT Drivers for Electric Vehicle Inverter 1
Petr Adamovský

Realization of the Vector Control of the Electric Vehicle Drive with DSP TMS 320F2812 7
Zbyněk Adamovský

Sensorless Methods Based on Estimation of Rotor Magnet Flux-Linkage Components in Drive with PMSM 13
Michal Božek

A Comparison of Characteristics of Less Common Methods of Direct Torque Control with the Classic Takahashi Method 19
Libor Hrdina

Single-phase direct AC/AC converter 26
Michal Kabašta

Sensorless Control of Induction Machine with Signal Injection 31
Petr Korbel

Sensorless Vector Control of a Permanent Magnet Synchronous Motor Using High Frequency Injection 36
Tomáš Křeček

Direct Torque Control for Three-level Voltage Inverter 42
Petr Moravčík

Matrix Converters by DSP Controlled 48
Lukáš Osmančík

Adhesion Regulator with Doppler Radar 54
Pavel Pivoňka

Control of the Switched Reluctance Motor with Current and Voltage Controller 59
Martin Polák

Loss-Minimization Algorithm for Induction Motors with Vector Control . . 65
Petr Skotnica

Aplication of Radial Basis Function Network in Rotor Time Constant Adaptation 71
Ondřej Škuta

Electric power engineering (3907V001)

Propagation of Voltage Dips in Transmission System 77
Josef Cigánek

Accuracy of DACF Models in Year 2006 83
Martin Galetka

Confrontation of Reliability Indices of Chosen Equipment and Elements . 87
Martin Golasowski, Radomír Goňo

Resonance in power supply system of AC traction 93
Pavel Hořínek

Power and Reliability Test of Wind Power Plant 99
Jan Lindovský

Laboratory of Fuel Cells VŠB-TUO in period 2006/2007 104
Daniel Minařík, Karel Sokanský

Methods of Multi-criterial Analysis for Optimum Utilization New Materials in Industrial Establishments 110
Leopold Paszek, Petr Moldřík

Determination of Optimal Order of 110 kV/MV Transformers to Maintenance 116
Břetislav Stacho, Stanislav Rusek, Radomír Goňo

Fuel Cells for Accumulation Electrical Energy from Renewable Energy Sources 123
Robert Šebesta

Regulation of Quality of Electric Power Supply in Czech Republic and Assessment Costs of Electric Power Suppliers Caused by Interruption of Supply 129
Marek Tinka

Optimal Economic Dispatch in Electrical Power System Using Genetic Algorithm 135
Khanh Hung Tran

A Study of New Supply Way the Non-traction Take off at Czech Railways 142
Viktor Vik

Methodology of Tunnel Luminance Measurement Using LMK Mobile Advanced Luminance Camera 148
Zdislav Žwak

Electronics (2612V015)

The Current Sensor for Power Electronic Applications 155
Martin Dostalík

Measurement of the Energy Consumption of Railcars 161
Martin Škopek

Technical cybernetics (2612V045)

Filtering Signal by Using ICA 167
Branko Babušiak, Michal Gála

HomeCare Project Evolution 173
Martin Černý

ZigBee Networks 178
Jan Floder

Application of Neural Network by Signal Classification 184
Michal Gála, Branko Babušiak

Verification of Temperature Fields in the Bimetallic Thermometer 190
David Grobelný, Pavel Nevřiva

Measuring of Vibrations in Medicine 196
Lukáš Martinák

Strain Gages and Position on Circular Diaphragm 200
Aleš Oujezdský

Using Knowledge System Module in Genetic Algorithm 206
Pavel Petránek, Miroslav Pokorný

The V4DB Real-time Database System: Admission Control and Priority Assignment 212
Jan Pokorný

Flow Sensor for Biomedical Applications 215
Jan Spišak

A Benchmark on Dynamic Reliability: Analysis of the Modeled System . . 219
Petra Škňouřilová

Adaptive Filter for Speech Signal Processing 225
Jan Vaňuš

Using FPGA Technology in Medical Diagnostic Ultrasonography 231
Petr Žůrek

Study Programme P2646 Information Technology

Information science and applied mathematics (1801V002)

An Indexing Approaches to Efficient Processing XPath Queries 237
Radim Bača, Michal Krátký, Václav Snášel

Parallelization of Process Functional Language 243
Marek Běhálek

Adaptive Mechanisms and Adaptation of Navigation in Virtual Education Environment 249
Marek Bober, Jana Šarmanová

DSP in Image Processing - Face Detection 255
Petr Delong, Michal Krumnikl, Boris Polikarpov

Projector Preconditioning for the Solution of Quadratic Programming Problems 261
Marta Domorádová

Task Generators, and Environment Simulator, Evaluation of Special Tasks 267
Radoslav Fasuga

An Image Analysis Based Method for Measuring the Surface Tension of Liquids 273
Jan Gaura, Michal Krumnikl, Eduard Sojka, Rostislav Dudek

The Analogy between Polymorfic Gates and Linear Threshold Units 279
Vladimír Havel

Spectral Graph Partitioning 285
Pavla Kabelíková

Brain for Agents in Multi-agent Systems 291
Ondřej Kohut

Control System for Robot Soccer Game Category MiroSot and SimutoSot 297
Jan Kožaný, Petr Tučník

Embedded Vehicle Systems and Networks 303
Michal Krumnikl, Jan Martinovič

The Usage of Polarization During Logic Synthesis Using Ashenhurst Disjunctive Decomposition 309
Pavel Moravčík

Compression of Small Text Files 315
Jan Platoš, Václav Snášel, and Eyas El-Qawasmeh

A Detection of Structural Damage of Brain Tissue in Parkinson's Disease Patients 321
Josef Schreiber

Using of BIBD Designs with Parallel Class for B-trees 327
Jan Šútora

Ontology Based Course Structure for Adaptive Web-based Systems...... 333
Zdeněk Velart

Study Programme P2612 Electrical Engineering and Computer Science

Telecommunication technology (2601V013)

DRM Reception - the Practical Experience 339
Marek Dvorský

Fiber Optical Sensors in Biomedical 345
František Hanáček

The Influence of the Network Load on a Quality of IP Telephony 350
František Hromek

Mathematical Modeling of EDCF Media Access Mechanism 356
Petr Machník

Mode Field Visualization Near of Normalized Frequency 362
Leoš Maršálek, Václav Hamerský, and Vladimír Vašinek

Bitrate Determination for GPRS/EDGE Service Using Markov Chains... 367
Libor Michalek

Reflectivity of the Wall Surfaces and Its Influence on Fibreless Optical Diffused Networks within Interiors 373
Jaromír Nečesaný

Interleaver Improvement for the New Scheme of Combined Turbo Code with Public Key Cryptosystem 379
Nabil Ouddane

Analysis of Optical-Power Redistribution for Hybrid Optical Fiber Sensors 386
Jan Skapa, Jan Vanda

The Hybrid Optical Fibers Based on Redistribution of Power 392
Petr Šiška

Using Fourier Transform for Solving Problems with Photonic Crystals by PWM 398
Jan Vanda, Jan Skapa

External Authors

Languages of the Environment in PM-Colonies 405
Adam Kožaný

Using Artifical Intelligence in e-Commerce 411
Radek Šilhavý, Petr Šilhavý

Codeviation Project - Analyzing Software Project From Its History 416
Petr Zajac

Author Index 421

Execution of IGBT Drivers for Electric Vehicle Inverter

Petr Adamovský

Department of Electronics, FEECS,
VŠB – Technical University of Ostrava, 17. listopadu 15, 708 33 Ostrava – Poruba
`petr.adamovsky.fei@vsb.cz`

Abstract. This paper is dealing with the driving circuits for IGBT modules which are used in voltage inverter. This inverter is used in Beta electric vehicle and feeds induction machine from traction accumulator. There are summarized requirements on the drivers at the first. Description and results of driver circuit design are following.

1 Required Parameters

The Beta electric vehicle is powered by induction machine fed by voltage inverter. There will be used 400 A Fuji 1MBI400F-060 IGBT modules for voltage 600 V or Semikron SKM400GA123 for 1200 V in the inverter. The charge which is necessary for switching the Fuji transistor at voltage $V_{CE} = 200$ V and $V_{GE} = 15$ V is $Q_G = 4500$ nC. The required average driver power 0.54 W and peak current 1.3 A with the gate resistance $R_G = 15\ \Omega$ were determined computationally (see [1]). Decreasing this resistance to 3.3 Ω results in increase of peak current up to 6 A.

2 Design and Execution

The above-mentioned requirements accommodate the compact driver SEMIKRON SKHI 22A H4. In one case of the circuit SKHI 22A H4 are integrated two drivers for two transistors connected in half-bridge. Peak current supplied into the gate can be up to 8 A, allowed average value of the current is up to 40 mA. At the extend of the gate voltage from –7 V to +15 V is the average power of the driver

$$P_{Gavg} = \left(V_{GE+} + \left|V_{GE-}\right|\right)\cdot I_{Gavg} = \left(15 + \left|-7\right|\right)\cdot 0{,}04 = 0.88\ \text{W}\,. \tag{1}$$

© Václav Snášel (Ed.): WOFEX 2007, pp. 1–6, ISBN 978-80-248-1571-8.
VŠB – Technical University of Ostrava, FEECS, 2007.

The driver has built-in various types of protection:

- short circuit protection by V_{CE} monitoring and switch off
- drive interlock which avoids switching top and bottom together
- dead time generator
- supply under voltage protection at 13 V
- error latch

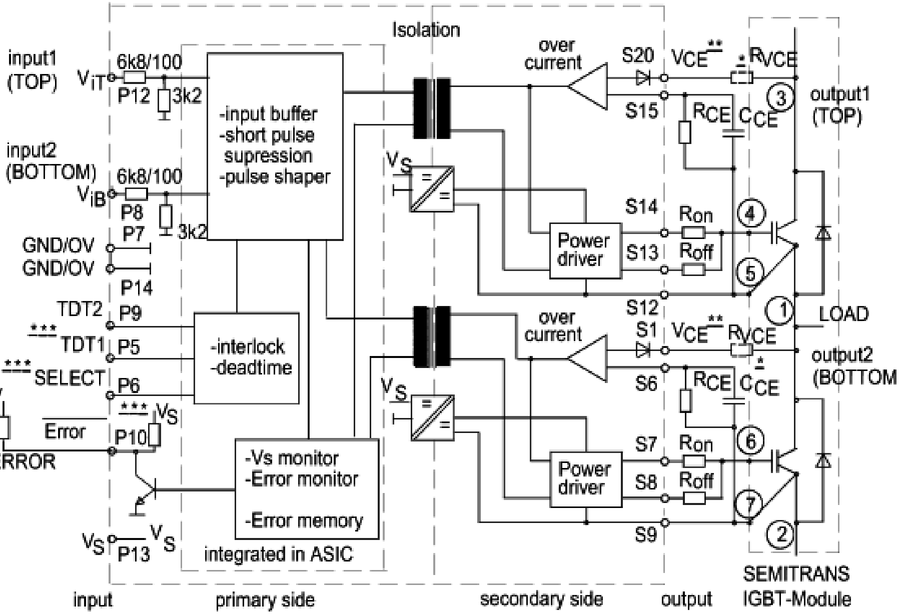
Isolation
input1
(TOP)
V_iT
6k8/100
P12
3k2
-input buffer
-short pulse
supression
-pulse shaper
input2
(BOTTOM)
6k8/100
V_iB
P8
P7
3k2
GND/OV
GND/OV
P14
TDT2
P9
***TDT1
P5
***SELECT
P6
-interlock
-deadtime
V
Error
***
V_S
P10
R_ERROR
-Vs monitor
-Error monitor
-Error memory
V_S
P13
V_S
integrated in ASIC
V_S
V_S
over
current
S20
V_CE**
*R_VCE
S15
R_CE
C_CE
③
output1
(TOP)
S14
R_on
④
Power
driver
S13
R_off
⑤
S12
①
LOAD
over
current
S1
V_CE**
R_VCE
*
output2
(BOTTOM)
S6
R_CE
C_CE
S7
R_on
⑥
Power
driver
S8
R_off
⑦
S9
②
SEMITRANS
IGBT-Module
input
primary side
secondary side
output

Fig. 1. Internal connection of integrated circuit and connection to IGBT half-bridge

The primary and secondary sides are isolated by transformers. The signal inputs are treated by pulse shaper, which patterns the edge slope of driving pulse and eliminates too short pulses generated by interference, for example.

Generally are the new driver circuits divided into four double-sided printed circuit boards. The core is the SKHI 22A H4 circuit mounted on board, which is used three times. The fourth board carries the logical circuits for the unification of error reports from the particular arms and the circuits for the division of inputs. The board with the logical circuits can be fixed to any main–board with the driver by four distance columns. Individual parts are connected by twisted cables. Although individual main–boards distance differently from the logical board, all the cables have the same length, so that their impedance could be approximately similar.

The main-board is fixed directly to the power modules by screws. Apart from the integrated circuit itself the board includes the network of discrete parts for the user settings. It includes the dead time setting junction. The dead time is the delay between the turn-off of the first transistor in the arm and turn-on of the second. This prevents short circuit in the arm. The dead time can be set to 3.3 μs or 4.3 μs according to position of junction connected to either low or high logical level. Further the board includes delay element for setting the delay between the rise of switching pulse and saturation voltage measurement. The delay is given by expression

$$t_{\min} = \tau_{CE} \cdot \ln\left[\frac{15 - V_{CEstat}}{10 - V_{CEstat}}\right], \tag{2}$$

where

$$\tau_{CE} = C_{CE} \cdot \frac{10 \cdot R_{CE}}{10 + R_{CE}} \tag{3}$$

and

$$V_{CEstat} = \frac{10 \cdot R_{CE}}{10 + R_{CE}} - 1{,}4\,. \tag{4}$$

The resistance is substituted in kΩ, capacitance in nF. Then voltage result in V and time in μs. Resistor of this delaying element is a part of voltage divider, which determines reference value for voltage measurement. The size of gate resistance can influence the IGBT turn-on and turn-off speed. The driver has separated output for turn-on and turn-of pulse and therefore it is possible to set the turn-on and turn-off time independently. The integrated driver inputs work with positive logic but the control system outputs are enhanced by open collector transistors and they work with the negative logic. Therefore there is invertor created by PNP transistor inserted on the driver input. The whole integrated circuit input is protected against voltage peaks by fast diodes. There is also light signalling of error in particular arm. The integrated driver has error output with transistor. In case of fault, the transistor connects the output to zero potential. This is used by red LED connected against supply voltage. The error indication is written into latch and this is deleted only if both control signals are zero.

On the logic board the error signals from all three arms are joined by AND gate which further controls the open collector transistor. The supply voltage level is also evaluated on this board. If the voltage is lower than 12 V, an error is indicated. The joined error output is equipped with green LED, which indicates, that everything is correct.

In sight of control system, all together the driver circuits have six control signal inputs, that is one for each inverter IGBT, and one output with error indication for interrupt call. The supplying requires voltage of 15 V.

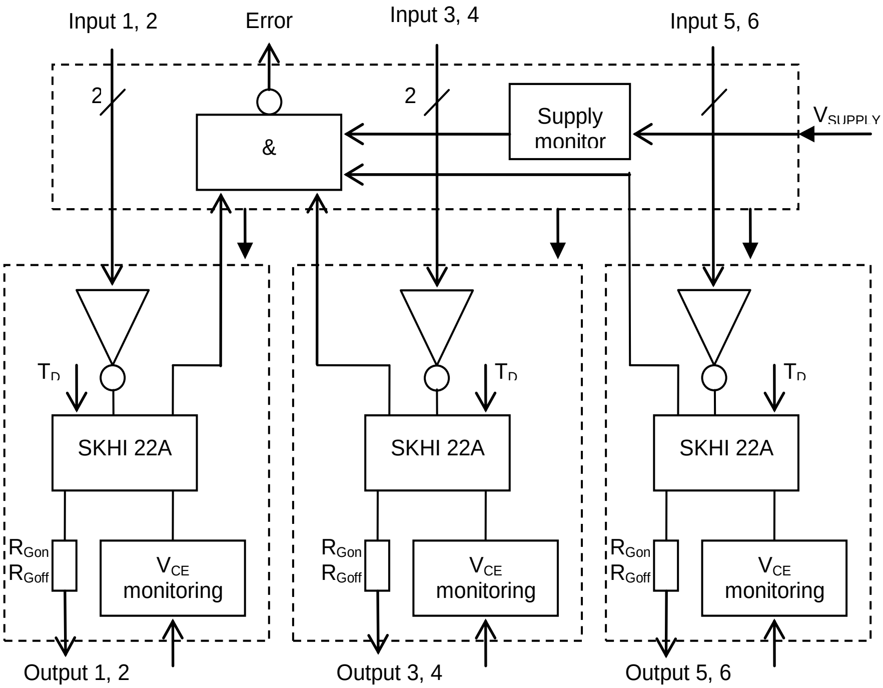
Input 1, 2
Error
Input 3, 4
Input 5, 6
2
2
&
Supply monitor
V_{SUPPLY}
T_D
T_D
T_D
SKHI 22A
SKHI 22A
SKHI 22A
R_{Gon}
R_{Goff}
R_{Gon}
R_{Goff}
R_{Gon}
R_{Goff}
V_{CE} monitoring
V_{CE} monitoring
V_{CE} monitoring
Output 1, 2
Output 3, 4
Output 5, 6

Fig. 2. Overall block diagram

3 Results

During the main-board printed circuit design the importance of channel insulation distances was not considered. This has not appeared to be wrong up till now. Recently a new board version solving this mistake has been designed. The possibilities are limited by integrated driver size and its pins placement, by each power module distance and by generally limited area meant driver circuits placement.

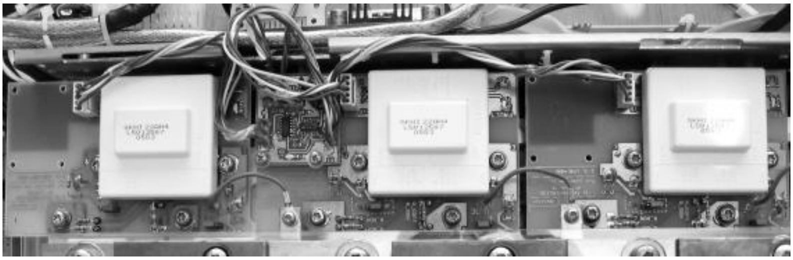

Fig. 3. General view

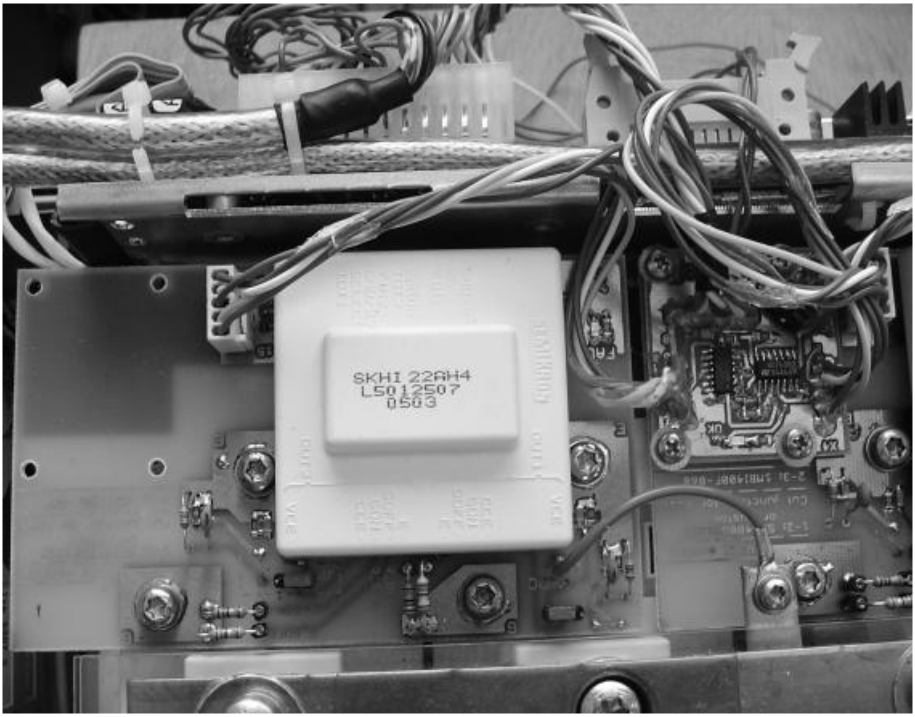
SKHI 22AH4
L5012507
0503

Fig. 4. The main-board and the logic board (on the right side)

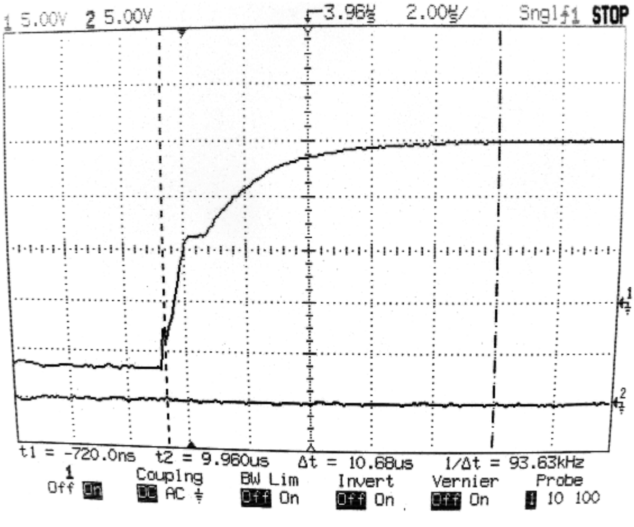

Fig. 5. Turn-on gate voltage (channel 1); $V_{GE} = -7..+15$ V, $R_{Gon} = 15\ \Omega$. Voltage range is 5 V/div., time-base 2 μs/div.

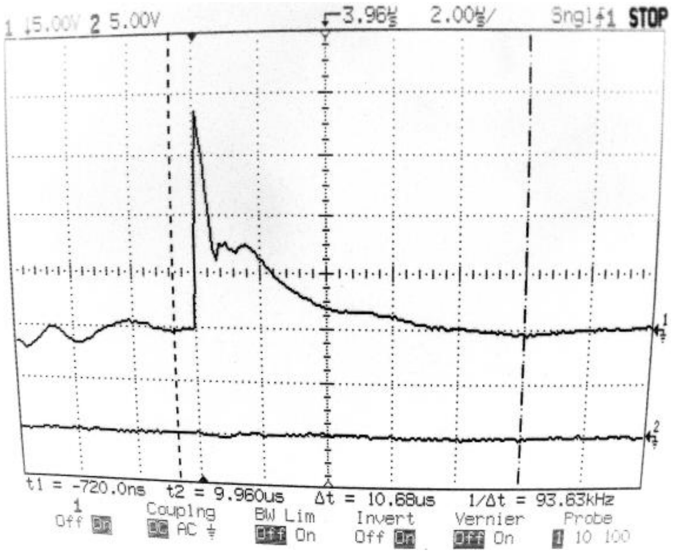

Fig. 6. Gate resistor $R_{Gon} = 15\ \Omega$ current during turn-on (channel 1). Voltage range is 5 V/div., time-base 2 μs/div.

References

1. Adamovský, P.: Improvement of electric vehicle drive in sight of power electronics. In *WOFEX 2006*, Ostrava, Czech republic: VŠB-Technical university of Ostrava, 2006, p. 1-6, ISBN 80-248-1152-9
2. SEMIKRON: SKHI 21/22 A/B H4 datasheet, http://www.semikron.com/internet/webcms/online/pdf/SKHI21_22_A_B_H4.pdf

Realization of the Vector Control of the Electric Vehicle Drive with DSP TMS 320F2812

Zbyněk Adamovský

Department of Electronics, FEECS,
VŠB – Technical University of Ostrava, 17. listopadu 15, 708 33 Ostrava – Poruba
`zbynek.adamovsky.fei@vsb.cz`

Abstract. In this paper the realization of the vector control of the electric vehicle drive using the digital signal processor TMS 320F2812 is described. The drive comprises of squirrel-cage induction motor driven by voltage inverter with IGBTs. The drive supply in the vehicle is realized by traction accumulators and in the laboratory was provided by Ward-Leonard motor control system. The inverter is driven by high-performance control system allowing the use of the modern ways of electric drive control. For the verification of the behavior of the whole drive with the mentioned control system, was firstly created a simulation model of the vehicle drive in the Matlab Simulink program and based on the established information a controlling algorithm was realized in the development system for DSP. For the drive control and for setting of the parameters of the controllers a control panel was created in the Labview program.

1 Introduction

The paper deals with implementation of the vector control method used at the Department of electronics on the electric vehicle drive. The electric vehicle drive is comprised by 3-phase squirrel-cage induction motor supplied from voltage inverter with IGBTs. The inverter is controlled by high performance digital signal processor TMS 320F2812. The electric drive in the vehicle is supplied by traction accumulators. In the laboratory during the development and verification of the control algorithms was the electric drive supplied by Ward-Leonard motor control system. The first step to the realization of the vector control was the creation of the simulation model of the electric vehicle drive with the mentioned control method in the Matlab Simulink program. Here was simulatively verified the behavior of the whole drive by the change of the particular parameters of the control structure and the parameters of the electric drive. In the light of the knowledge obtained from these simulations, in the development system designed for programming of the signal processors by Texas Instruments Co., an algorithm of the vector oriented control of the asynchronous motor was created. For the setting of the main parameters of the regulation structure, demanded values and the measurement of the demanded quantities a control panel with multimeters was created in the visualization program Labview. Subsequently, in the laboratory, experimental results were measured on the electric drive.

© Václav Snášel (Ed.): WOFEX 2007, pp. 7–12, ISBN 978-80-248-1571-8.
VŠB – Technical University of Ostrava, FEECS, 2007.

2 Simulation of vector controlled electric vehicle drive

Based on the method of the vector control used on the Department of electronics on VSB- TU Ostrava for the control of the AC motors, a model of the controlled electric vehicle drive was created in the Matlab Simulink program.

2.1 Structure of vector control electric vehicle drive

The core of the regulation structure based on the vector oriented control lies in the decomposition of the stator current space vector into two mutually perpendicular components in the rotating coordinate system oriented to the space vector of the stator flux linkage possibly rotor or magnetizing flux. The component of the stator vector current lying in the direction of the magnetizing flux vector i1x (so-called direct-axis component) represents magnetization of the machine (reactive power). The second quadrature-axis component i1y represents with the respective magnetic flux vector the torque of the machine (active power). The algorithm of the vector control has the ability to provide the control of both components of the stator current without mutual influence. The block scheme of the control structure is shown in the Fig. 1. The detailed description of the this structure is described in the [1] [2].

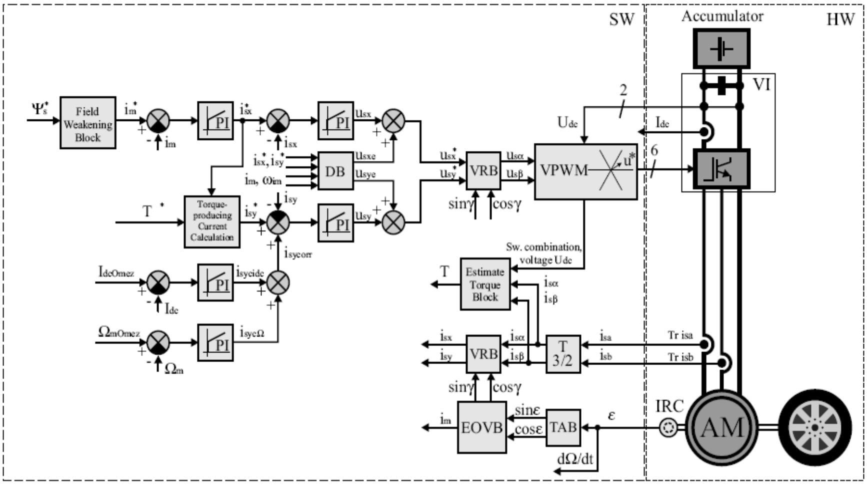
SW
Accumulator
HW
VI
Ψ_s^*
Field Weakening Block
i_m^*
i_m
PI
i_{sx}^*
i_{sx}
u_{sx}
i_{sx}^*, i_{sy}^*
i_m, ω_{im}
DB
u_{sxe}
u_{sye}
i_{sy}
T^*
Torque-producing Current Calculation
i_{sy}^*
u_{sy}
i_{sycorr}
I_{dcOmez}
I_{dc}
i_{sycidc}
Ω_{mOmez}
Ω_m
$i_{syc\Omega}$
u_{sx}^*
u_{sy}^*
VRB
$u_{s\alpha}$
$u_{s\beta}$
sinγ
cosγ
U_{dc}
2
VPWM
u^*
6
I_{dc}
Sw. combination, voltage Udc
T
Estimate Torque Block
$i_{s\alpha}$
$i_{s\beta}$
i_{sx}
i_{sy}
T 3/2
i_{sa}
i_{sb}
Tr isa
Tr isb
i_m
EOVB
sinε
cosε
TAB
ε
dΩ/dt
IRC
AM

Fig. 1. Block diagram of the vector control electric vehicle drive

2.2 Simulation model of the whole electric vehicle drive

In this subchapter the model of the whole drive is briefly described. During the simulations was the drive divided into two parts - electrical and kinematic. Electrical part includes the model of the control system with algorithms, the model of the voltage inverter with the inclusion of the voltage drop of IGBT, the model of the asynchronous motor, the model of the speed evaluation from IRC and the model of the power losses of the induction motor and voltage inverter. Kinematical part is represented by the model of the train resistances of the vehicle and by the equation of motion of the drive. In the model it is possible to change gears, camber of the road, speed of the headwind and other parameters. It is also possible to exclude these resistances and enter the constant drive load, i.e. the case corresponding to the laboratory conditions, where the load by DC motor is provided. Block scheme of the model can be seen in the Fig. 2. [2] [5].

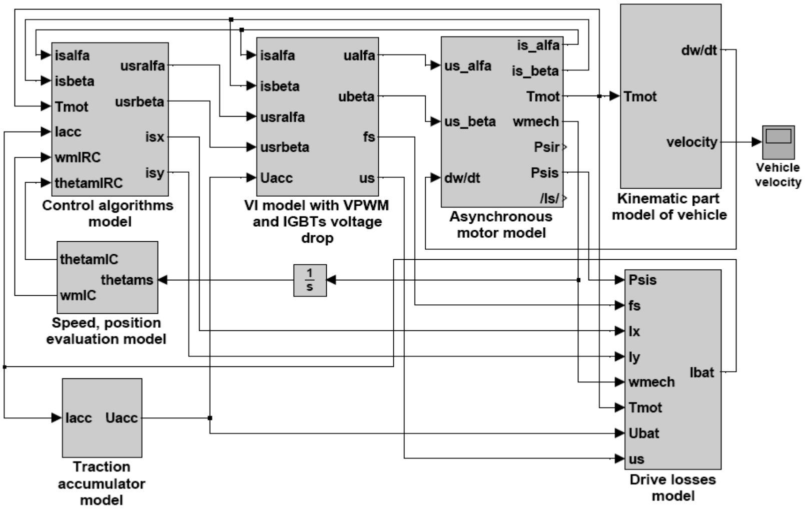
isalfa
isbeta
Tmot
Iacc
wmIRC
thetamIRC
usralfa
usrbeta
isx
isy
Control algorithms model
isalfa
isbeta
usralfa
usrbeta
Uacc
ualfa
ubeta
fs
us
VI model with VPWM and IGBTs voltage drop
us_alfa
us_beta
dw/dt
is_alfa
is_beta
Tmot
wmech
Psir
Psis
/Is/
Asynchronous motor model
Tmot
dw/dt
velocity
Kinematic part model of vehicle
Vehicle velocity
thetamIC
wmIC
thetams
Speed, position evaluation model
1/s
Psis
fs
Ix
Iy
wmech
Tmot
Ubat
us
Ibat
Drive losses model
Iacc
Uacc
Traction accumulator model

Fig. 2. Main parts of the electric vehicle drive model in Matlab Simulink

3 The realization of the vector control algorithms

3.1 The creation of the control algorithms in the development system CCS for DSP Texas Instruments Co.

Based on the knowledge obtained by the simulation of regulation algorithms of the drive and on the tutorial for the development system Code Composer Studio a program for the vector control of the electric vehicle drive was created in the programming language C. For driving of the inverter was chosen a control system with high-performance 32-bit digital signal processor TMS 320F2812 including peripheries usable in applications of electric drives (12-bit, 16-channels A/D converter; D/A converter; capture unit; pulse-width modulator; SCI, SPI units; Event managers; universal input/output unit etc.). For this processor system I have made supportive board, which was designed at the Department of electronics (Fig. 3).

Development system on PC communicated with the control system via parallel port. To the supportive board were further connected outputs from the sensors of the current and the voltage. The output of the speed sensor was connected to the input of the Capture unit providing processing of the sensor signal [3] [4].

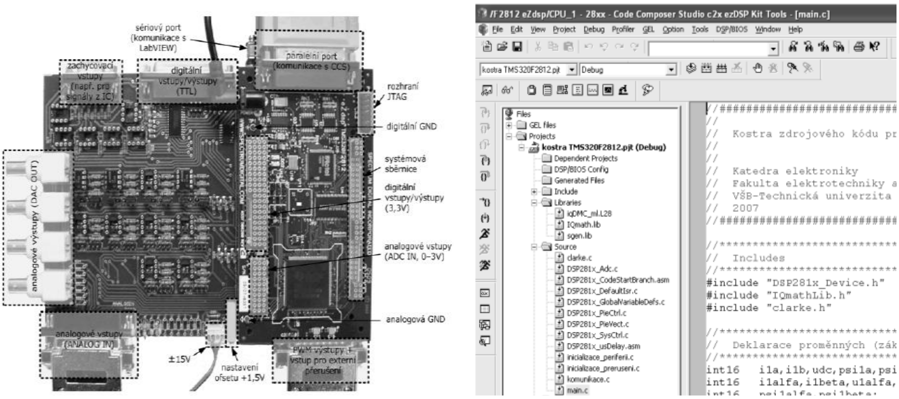
sériový port (komunikace s LabVIEW)
paralelní port (komunikace s CCS)
zachycovací vstupy (např. pro signály z IC)
digitální vstupy/výstupy (TTL)
rozhraní JTAG
digitální GND
systémová sběrnice
digitální vstupy/výstupy (3,3V)
analogové výstupy (DAC OUT)
analogové vstupy (ADC IN, 0–3V)
analogová GND
analogové vstupy (ANALOG IN)
±15V
nastavení ofsetu +1,5V
PWM výstupy + vstup pro externí přerušení
/F2812 eZdsp/CPU_1 - 28xx - Code Composer Studio c2x ezDSP Kit Tools - [main.c]
File Edit View Project Debug Profiler GEL Option Tools DSP/BIOS Window Help
kostra TMS320F2812.pjt
Debug
Files
GEL files
Projects
kostra TMS320F2812.pjt (Debug)
Dependent Projects
DSP/BIOS Config
Generated Files
Include
Libraries
iqDMC_ml.L28
IQmath.lib
sgen.lib
Source
clarke.c
DSP281x_Adc.c
DSP281x_CodeStartBranch.asm
DSP281x_DefaultIsr.c
DSP281x_GlobalVariableDefs.c
DSP281x_PieCtrl.c
DSP281x_PieVect.c
DSP281x_SysCtrl.c
DSP281x_usDelay.asm
inicializace_periferii.c
inicializace_preruseni.c
komunikace.c
main.c

```
//############################
//
//  Kostra zdrojového kódu pr
//
//
//  Katedra elektroniky
//  Fakulta elektrotechniky a
//  VŠB-Technická univerzita
//  2007
//############################

//****************************
//  Includes
//****************************
#include "DSP281x_Device.h"
#include "IQmathLib.h"
#include "clarke.h"

//****************************
//  Deklarace proměnných (zák
//****************************
int16   i1a,i1b,udc,psi1a,psi
int16   i1alfa,i1beta,u1alfa,
int16   psi1alfa,psi1beta;
```

Fig. 3. Supportive board with eZdsp TMS 320F2812 and window with development system Code composer studio

The structure of the main file of the vector control program of the electric vehicle drive *VOC_elmobil.c* can be briefly summarized into several basic parts:

• input of the head files (connection of the data prototypes defined in other files eg. connection of the macros defined in the file *regmacro.c* including functions for the regulation) → declarations of the used variables (eg. i_{lafa}) → definitions of the tables (SIN,COS) → definitions of the constants (eg. sampling period of the current control loop) → main functions of the program including →→ initialization of the control system →→ initialization of the unit for the control of the interruption →→ initialization of peripheries (EVx, A/D, GPIO, SCI, SPI, VPWM, QEP) →→ initialization and redirecting of the interrupts →→ starting initialization of the variables →→ infinite loop for communication with PC →→ definition of the functions of the interrupt service = vector control algorithms (reading of the values from A/D converter, calling of the macros of transformations, PI and I controllers etc.) →→ definition of the self-functions •

3.2 The creation of the control panel for the vector control electric vehicle drive

A control panel was made in the visualizing program LABVIEW for the vector control program operation. On this panel it is possible to change gain (proportional) constants, time constants and restrictions of PI and I controllers. Further it is possible to set the required torque of the motor, restriction of the motor speed and frequency of the vector pulse-width modulation. On the panel are displayed extends of the measured quantities (current and voltage of the DC link, stator currents). The panel further enables setting of important quantities of the control structure sent to the 4 channel D/A converter. These can be further on the outputs of D/A converter monitored by oscilloscope. The program with the control system communicates via serial port. The Control panel is shown in Fig. 4. [6].

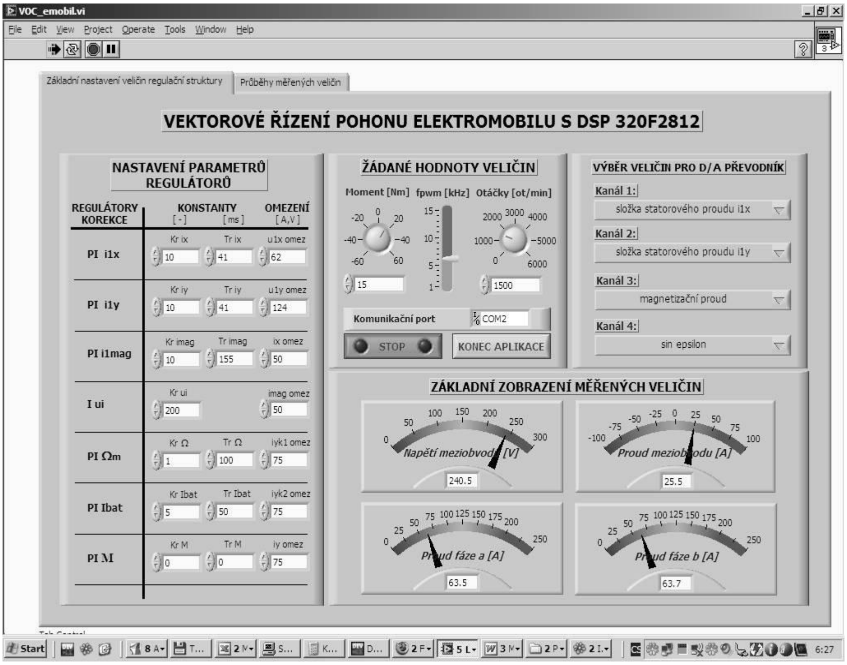
VOC_emobil.vi
File Edit View Project Operate Tools Window Help
Základní nastavení veličin regulační struktury
Průběhy měřených veličin
STOP
KONEC APLIKACE
Start
6:27

VEKTOROVÉ ŘÍZENÍ POHONU ELEKTROMOBILU S DSP 320F2812

NASTAVENÍ PARAMETRŮ REGULÁTORŮ

REGULÁTORY KOREKCE	KONSTANTY [-]	[ms]	OMEZENÍ [A,V]
PI i1x	Kr ix 10	Tr ix 41	u1x omez 62
PI i1y	Kr iy 10	Tr iy 41	u1y omez 124
PI i1mag	Kr imag 10	Tr imag 155	ix omez 50
I ui	Kr ui 200		imag omez 50
PI Ωm	Kr Ω 1	Tr Ω 100	iyk1 omez 75
PI Ibat	Kr Ibat 5	Tr Ibat 50	iyk2 omez 75
PI M	Kr M 0	Tr M 0	iy omez 75

ŽÁDANÉ HODNOTY VELIČIN

Moment [Nm]: 15

fpwm [kHz]

Otáčky [ot/min]: 1500

Komunikační port: COM2

VÝBĚR VELIČIN PRO D/A PŘEVODNÍK

Kanál 1: složka statorového proudu i1x

Kanál 2: složka statorového proudu i1y

Kanál 3: magnetizační proud

Kanál 4: sin epsilon

ZÁKLADNÍ ZOBRAZENÍ MĚŘENÝCH VELIČIN

Napětí meziobvodu [V]: 240.5

Proud meziobvodu [A]: 25.5

Proud fáze a [A]: 63.5

Proud fáze b [A]: 63.7

Fig. 4. Control panel of the vector control electric drive

4 Simulated and measured results

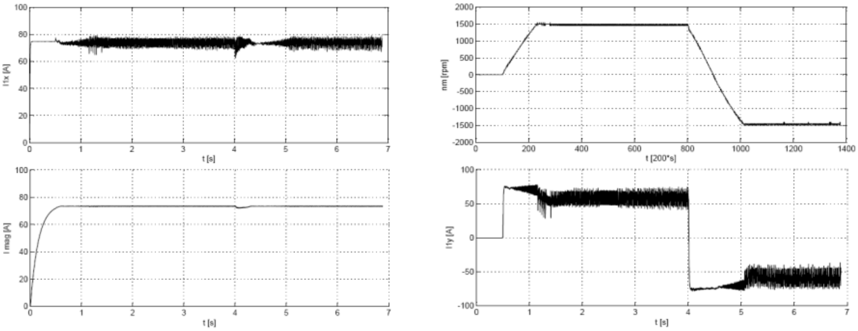

Fig. 5. The waveforms of simulated flux-producing current 75 A (left-up), magnetizing current 75 A (left-down), rpm 1500 min^{-1} (right-up) and torque-producing current 75 A (right-down); t: 1 s/div, Ix,y,m: 20 A/div, Ω: 500 rpm/div, T_L = 20 Nm, with speed closed-loop

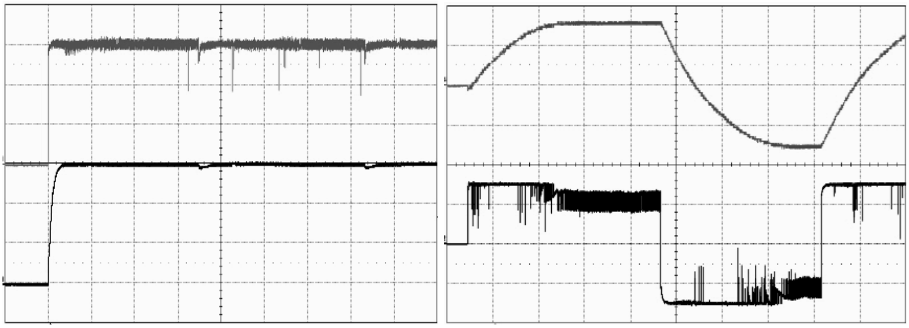

Fig. 6. The waveforms of measured flux-producing current 75 A (left-up), magnetizing current 75 A (left-down), rpm 1500 min^{-1} (right-up) and torque-producing current 75 A (right-down); t: 2 s/div, Ix,m: 25 A/div, Iy: 50 A/div, Ω: 1000 rpm/div, T_L = 20 Nm, with speed closed-loop

On the simulated and measured waveforms can be seen enlarged ripple of the motor speed and stator currents. This is caused by smaller number of IRC impulses, which is designed for the higher speeds. This sensor is the part of the used asynchronous motor. The ripple could by lowered by the change of the sampling frequency of the IRC impulses or by the change of the used speed sensor.

3 Conclusion

In this paper was briefly described the procedure of realization of the vector control of electric vehicle drive. In the future this control algorithm will be supplemented by other optimizing blocks. The improvement of the control panel is also presumed. For the practical use of this control directly in the electric vehicle will be useful the use of the control panel of the physical form without the need of the notebook. Further a more complex vizual representation of the quantities of the regulatory structure.

References

1. Brandštetter, P.: A.C. Control Drives, Modern Control Method, VSB - Technical University of the Ostrava, 1999. ISBN 80-7078-668
2. Neborák, I.; Modelling and simulation of the electric control drives, VSB - Technical University of the Ostrava, 2002.
3. Šaloun, P.: Programming in language C, Ostrava 1996, http://docs.linux.cz /programming/c/
4. Texas Instruments: TMS 320C28xx Manuals and User's Guide, http://focus.ti.com
5. The Mathworks Inc.: Getting started with Matlab 7,March 2007, http://www.mathworks.com
6. National Instruments: Labview 8.2 Help, August 2006, http://digital.ni.com/ manuals.nsf

Sensorless Methods Based on Estimation of Rotor Magnet Flux-Linkage Components in Drive with PMSM

Michal Božek

Department of Electronics, FEECS,
VŠB – Technical University of Ostrava, 17. listopadu 15, 708 33 Ostrava – Poruba
`michal.bozek.fei@vsb.cz`

Abstract. In the paper was described a method for speed and position estimation using estimation of rotor magnet flux-linkage component. By using measured stator voltage, currents and algorithm, it is possible to implement high dynamic performance permanent magnet synchronous motor (PMSM). It this case were using pseudo sliding mode observer (SMO) and model reference adaptive system (MRAS) for estimation speed and position based on estimation rotor magnet flux-linkage components. The instruction for design of the both ways is presented with simulation results in Matlab-simulink software.

1 Introduction

The PMSM modern control method is direct torque moment, vector control and especially variation of sensorless vector control for their advantages. The vector control of PMSM requires knowledge of the rotor position to perform an effective stator current control. For speed control, the speed signal is also required. However, for evaluation of rotor position and rotor speed, it is possible to eliminate these sensors in vector-controlled drives. We speak about so-called “Sensorless control”. Advantages of sensorless control is e.g. reduction of hardware complexity and cost, increased mechanical robustness and overall ruggedness, operation in hostile environments, increased noise immunity, unaffected machine inertia, higher reliability and decreased maintenance requirements. For sensorless vector control is suitable using many methods. This paper shown SMO and MRAS methods based on the rotor magnet flux-linkage components.

2 PMSM sensorless vector control with SMO

In the fig. 1 is the regulation structure of PMSM sensorless vector control. Block CB1 is computation block for reconstruction of the phasor of the induced back e.m.f.. Block CB2 is computation block for maximal value specification of torque-producing stator current component, BD is decoupling block, SMO is block of sliding mode observer. SMO block output $\Omega_{est\ vf}$ is filtrated by the first order delay or can be filtrated by low-pass filter which is complicated.

© Václav Snášel (Ed.): WOFEX 2007, pp. 13–18, ISBN 978-80-248-1571-8.
VŠB – Technical University of Ostrava, FEECS, 2007.

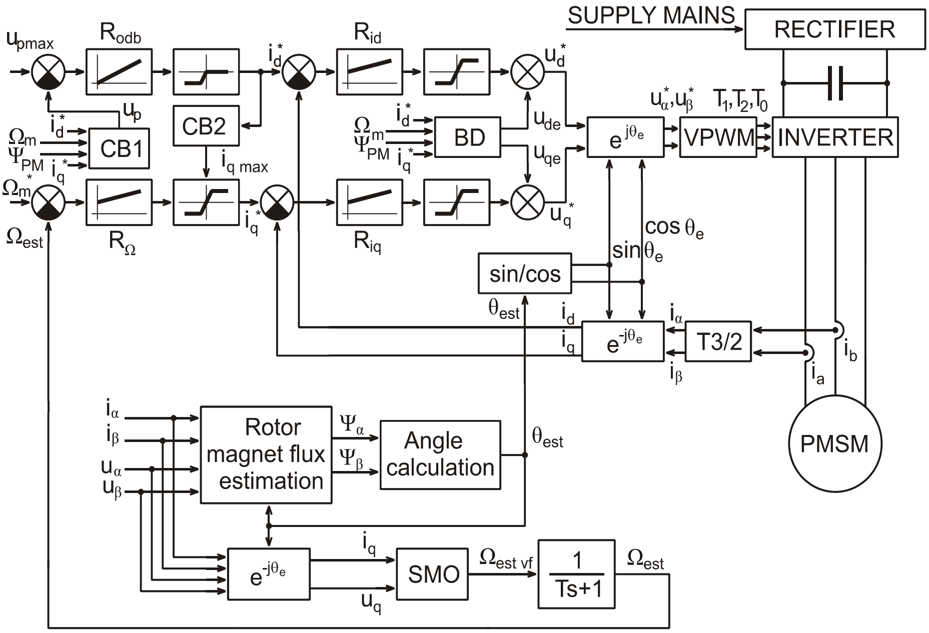
SUPPLY MAINS
RECTIFIER
u_{pmax}
R_{odb}
i_d^*
R_{id}
u_d^*
u_p
CB2
u_α^*, u_β^*
T_1, T_2, T_0
Ω_m
i_d^*
Ψ_{PM}
i_q^*
CB1
$i_{q\,max}$
BD
u_{de}
$e^{j\theta_e}$
VPWM
INVERTER
u_{qe}
Ω_m^*
i_q^*
u_q^*
Ω_{est}
R_Ω
R_{iq}
$\cos\theta_e$
$\sin\theta_e$
sin/cos
θ_{est}
i_d
i_q
$e^{-j\theta_e}$
i_α
i_β
T3/2
i_b
i_a
PMSM
i_α
i_β
u_α
u_β
Rotor magnet flux estimation
Ψ_α
Ψ_β
Angle calculation
θ_{est}
$e^{-j\theta_e}$
i_q
u_q
SMO
$\Omega_{est\,vf}$
$\frac{1}{Ts+1}$
Ω_{est}

Fig. 1. Sensorless vector control block diagram using SMO

The important block is rotor magnet flux estimation. However, inputs of this block, only the stator currents are monitored together with d.c. link voltage. This block is described in [2]. Outputs are rotor magnet flux-linkage components in α, β orthogonal coordinates which can be expressed as follows:

$$\begin{bmatrix}\Psi_\alpha\\ \Psi_\beta\end{bmatrix} = \int\left(\begin{bmatrix}u_\alpha\\ u_\beta\end{bmatrix} - R_S\begin{bmatrix}i_\alpha\\ i_\beta\end{bmatrix} + K\begin{bmatrix}\Psi_{PM}\cos\theta_{e\_est} - \Psi_\alpha\\ \Psi_{PM}\sin\theta_{e\_est} - \Psi_\beta\end{bmatrix}\right)dt - L_S\begin{bmatrix}i_\alpha\\ i_\beta\end{bmatrix} \tag{1}$$

The rotor angle is calculated by the equation (2):

$$\theta_{e\_est} = \tan 2^{-1}\left(\frac{\Psi_\beta}{\Psi_\alpha}\right) \tag{2}$$

The stator current component i_q together with voltage component u_q are obtained by using the transformation exp ($-j\theta_{e\_est}$). These components are inputs in sliding mode observer (SMO) block in Fig. 2. SMO principle is obviously from equations (3)-(6).

$$\frac{di_q}{dt} = \left(u_q - R_S i_q - \Omega_m p\left(L_d i_d + \Psi_{PM}\right)\right)\frac{1}{L_q} \tag{3}$$

Right aspect of equation (3) we can substitute v_{ekv}. Equation (4) is obtained. Equation (4) compare with equation (5), mechanical speed is obtained by the equation (6).

$$\frac{di_{q\_est}}{dt} = \left(u_q - R_S i_{q\_est} - v_{ekv}\right)\frac{1}{L_q} \tag{4}$$

$$v_{ekv} = \Omega_m p\left(L_d i_d + \Psi_{PM}\right) = K_{SM}\left(i_q - i_{q\_est}\right) \tag{5}$$

$$\Omega_m = \frac{v_{ekv}}{p\left(L_d i_d + \Psi_{PM}\right)} \tag{6}$$

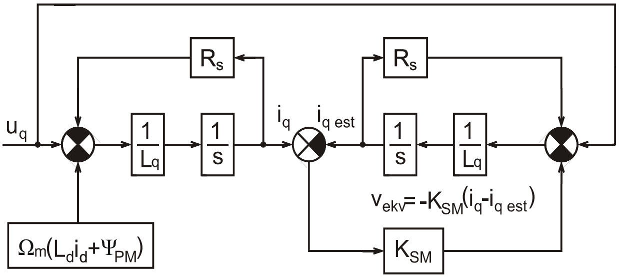

Fig. 2. SMO principle

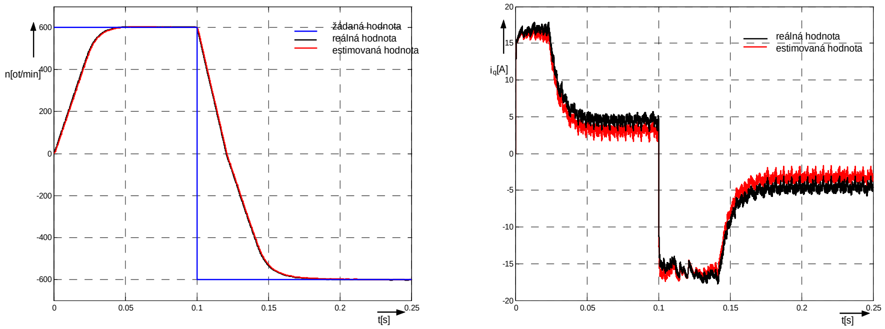

Fig. 3. The waveforms of the required, actual and estimated rpm and actual and estimated i_q

There is SMO principle in fig. 2. SMO principle is based on compare current component i_q with current estimated component i_{q_est}. Difference of this compare is gained by the K_{SM}. This term substitute left part of equation (5). Estimated mechanical speed is computed by the equation (6). We can see the waveforms of the rpm on the left part of fig. 3. On the right part of fig. 3 we can see waveforms of the actual current component i_q with estimated i_{q_est}. If we compare both waveforms of current, it is equivalent between i_q and i_{q_est}.

3 PMSM sensorless vector control with MRAS

In the fig. 4 is the regulation structure of PMSM sensorless vector control with MRAS. Structure is very similar with structure in fig. 1. MRAS principle is based on comparision of two estimators. One of them does not include speed and is called the reference system. The other, which contains speed, is the adjustable model. The error between the two models is used to derive an adaptive that produces the estimated speed for the adjustable model [3].

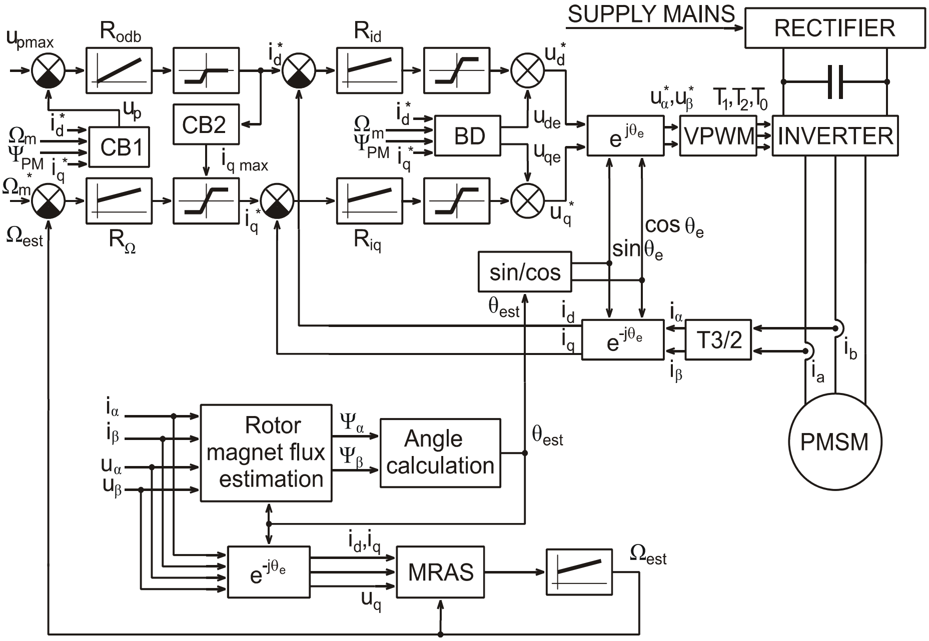
SUPPLY MAINS
RECTIFIER
u_{pmax}
R_{odb}
i_d^*
R_{id}
u_d^*
u_p
i_d^*
Ω_m
Ψ_{PM}
i_q^*
CB1
CB2
$i_{q\,max}$
Ω_m
Ψ_{PM}
i_d^*
i_q^*
BD
u_{de}
u_{qe}
$e^{j\theta_e}$
u_α^*, u_β^*
T_1, T_2, T_0
VPWM
INVERTER
Ω_m^*
Ω_{est}
R_Ω
i_q^*
R_{iq}
u_q^*
$\cos\theta_e$
$\sin\theta_e$
sin/cos
θ_{est}
i_d
i_q
$e^{-j\theta_e}$
i_α
i_β
T3/2
i_b
i_a
PMSM
i_α
i_β
u_α
u_β
Rotor magnet flux estimation
Ψ_α
Ψ_β
Angle calculation
θ_{est}
$e^{-j\theta_e}$
i_d, i_q
u_q
MRAS
Ω_{est}

Fig. 4. Sensorless vector control block diagram using MRAS

Equation (7) is presents reference model. Equation (8) is PMSM formula expressed in rotor oriented system. Estimated value Ψ_{est} is derived from (8), it is presents adjustable model. This procedure is shown in fig. 5. Difference between reference model output and adjustable model output is input of PI-regulator.

$$\Psi_q = L_q i_q \tag{7}$$

$$\frac{d\Psi_q}{dt} = u_q - R_S i_q - p\Omega_m L_d i_d - p\Omega_m \Psi_{PM} \tag{8}$$

$$\Psi_{est} = \Psi_q = \int \left(u_q - R_S i_q - p\Omega_m L_d i_d - p\Omega_m \Psi_{PM} \right) dt \tag{9}$$

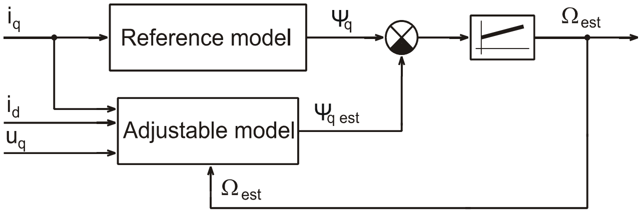

Fig. 5. Principle of the MRAS

PI-regulator output is Ω_{est} which can be determined by the equation (10), where K_p is proportional component and K_i is integral component of PI-regulator.

$$\Omega_{est} = \left(K_p + \frac{K_i}{s} \right) \left(\Psi_q - \Psi_{q\_est} \right) \tag{10}$$

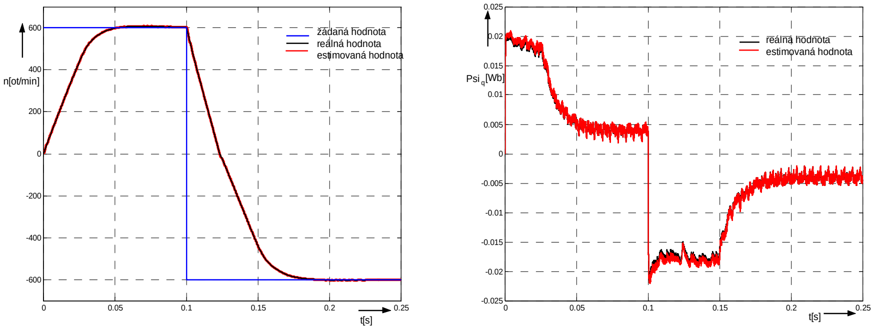

Fig. 6. The waveforms of the required, actual and estimated rpm and actual and estimated Ψ_q

The both sensorless vector control of PMSM has been simulated in program MATLAB-Simulink. Parameters of the PMSM: P_n=890W, M_n=17Nm, n_n=500rpm, p_p=3, Φ_b=0.378Wb, J_m=0.0104kgm^2, U_{sn}=78/45V, I_{sn}=16A, R_s=0.14Ω, L_d=L_q=1.29mH. On the simulation start the required rpm was set n=600rpm, reversation starts at time t=0.1s, and required n=-600rpm.

Conclusion

Two ways of the sensorless PMSM vector control are described in this paper. The both methods are adequate and is not possible said which is better. If we compare both methods with EKF implementation, both methods are more quickly and simplicity.

References

1. Brandštetter, P.: A.C. Control Drives, Modern Control Method. VSB - Technical University of the Ostrava, 1999. ISBN 80-7078-668
2. Štulrajter, M.: Bezsnímačový polohový servomechanizmus so synchrónnym motorom s permanentnými magnetmi, Doktorandská dizertačná práca, Žilinská univerzita v Žiline, 2006
3. Boldea, I., Nasar, S.A.: Electric drives, 1999. ISBN 0-8493-2521-8

List of author's publications

1. Božek, M., Fišer, O., Brandštetter, P., Palacký, P.: AC Drive without Speed Sensor, EPE 2005, Dresden, 2005
2. Božek, M.: Vector Control Simulation of Permanent-Magnet Synchronous Motor, WOFEX 2005, Ostrava, 2005
3. Božek, M., Fišer, O., Brandštetter, P., Palacký, P.: Střídavý regulační pohon se synchronním motorem s permanentními magnety, ELOSYS 2005, Trenčín, 2005
4. Božek, M., Brandštetter, P.: Simulace vektorového řízení synchronního mototru s permanentními magnety, EPVE 2005, Brno, 2005
5. Božek, M., Brandštetter, P., Palacký, P., Fišer, O., Hrdina, L., Vaverka, T.: Přímé řízení momentu pohonů se střídavými motory, SYMEP 2006, Plzeň, 2006
6. Božek, M., Brandštetter, P., Palacký, P.: Moderní způsoby řízení pohonu elektromobilu, ELEN 2006, Praha, 2006
7. Božek, M., Brandštetter, P., Palacký, P., Vaverka, T.: Přímé řízení momentu synchronního motoru s permanentními magnety, ELOSYS 2006, Trenčín, 2006
8. Božek, M.: Using observers for estimation state vector and parameters in drive with PMSM, WOFEX 2006, Ostrava, 2006
9. Božek, M., Brandštetter, P., Korbel, P., Křeček, T.: Bezsenzorové vektorové řízení synchronního motoru s permanentími magnety, ELOSYS 2007, Trenčín, 2007. In print.

A Comparison of Characteristics of Less Common Methods of Direct Torque Control with the Classic Takahashi Method

Libor Hrdina

Department of Electronics, FEECS,
VŠB – Technical University of Ostrava, 17. listopadu 15, 708 33 Ostrava – Poruba
`libor.hrdina.fei@vsb.cz`

Abstract Direct torque control is one of the most modern methods of torque regulation. Several methods of direct torque control have been proposed. One of the oldest and practically useful is the Depenbrock and Takahashi method. Many other methods intended as improvements or simplifications have been devised. Among these is the so-called Modified Method (M_DTC) and the Twelve-Sector Method (12_DTC). In the article, I discuss important quantities that were measured on a real model drive with induction motor. The basic characteristics of these methods will be compared with the classic Takahashi Method.

1 Introduction

Currently the induction motor is the most widely used active unit for regulated drives in general usage with a range up to hundreds of kW. The technical means for the realization of converters and their regulators are now at such a high level that the practical implementation of complicated control algorithms does not cause any significant problems. The calculation speed of contemporary processors provides plenty of room for seeking new algorithms of direct torque control.

2 Direct Torque Control (DTC)

Methods of direct torque control AC machines are characterized by their simplicity with regard to vector control; this simplicity allows for easy implementation on a control microcomputer. The high robustness and the ability of quick changes of motor torque, thanks to which it is possible to attain very good dynamic qualities, are among the advantages of these methods. Such methods do not regulate the vector of stator current, but rather directly regulate torque within certain selected tolerances and the course of the space vector of magnetic flux along the desired curve. Both quantities are calculated from measured values with the help of a mathematical model of an induction motor. A clear advantage of the method of direct torque is the virtual elimination of overshoot.

© Václav Snášel (Ed.): WOFEX 2007, pp. 19–25, ISBN 978-80-248-1571-8.
VŠB – Technical University of Ostrava, FEECS, 2007.

3 Methods of Direct Torque Control

All methods of direct torque control use a similar basic principle: a rotating magnetic field in the stator is created on the basis of a calculating algorithm with the help of switching vectors $\underline{\mathbf{u}}_1$ to $\underline{\mathbf{u}}_6$ (Fig. 1b), where the rotation speed of the magnetic field, and subsequently the amount of motor torque, can be controlled by the switching of zero vectors or the switching of active vectors working in the opposite direction of the magnetic field [1]. Stator flux and internal motor torque are calculated on the basis of the measured voltage of the DC bus and phase currents in this relationship:

$$\begin{aligned}\Psi_{1\alpha} &= \int \left(u_{1\alpha} - R_S \cdot i_{1\alpha}\right)dt \\ \Psi_{1\beta} &= \int \left(u_{1\alpha} - R_S \cdot i_{1\beta}\right)dt \\ \left|\Psi_1\right| &= \sqrt{\Psi_{1\alpha}^2 + \Psi_{1\beta}^2}\end{aligned} \qquad \textbf{(1)}$$

$$m = \frac{3}{2} \cdot p_p \cdot \left(\Psi_{1\alpha} \cdot i_{1\beta} - \Psi_{1\beta} \cdot i_{1\alpha}\right) \qquad \textbf{(2)}$$

3.1 Takahashi's Method

In Takahashi's method of direct torque control, the magnetic flux of the stator is controlled so that the final point of the vector of stator magnetic flux moves within a annulus, whereby its trajectory in a simplified case approaches a circle. A diagram of regulation can be seen at Fig. 1a.

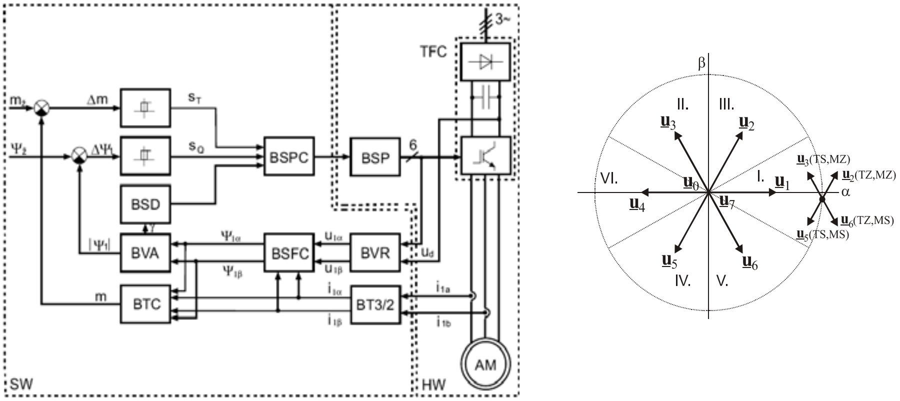
3~
TFC
m₂
Δm
s_T
Ψ₂
ΔΨ₁
s_Q
BSPC
BSP
6
BSD
γ
|Ψ₁|
BVA
Ψ_1α
Ψ_1β
BSFC
u_1α
u_1β
BVR
u_d
m
BTC
i_1α
i_1β
BT3/2
i_1a
i_1b
AM
SW
HW
β
II.
III.
u₃
u₂
u₃(TS,MZ)
u₂(TZ,MZ)
VI.
u₀
I.
u₁
α
u₄
u₇
u₆(TZ,MS)
u₅(TS,MS)
u₅
u₆
IV.
V.

a) b)

Fig. 1. a) The diagram of AC drive with Takahashi's method of direct torque control
b) The principle of selection of voltage vector in the first sector of the plane α , β according to Takahashi's method

For control of motor excitation, the module of the space vector of magnetic flux is determined according to the relationships (1) and consequently is compared with the desired value. The regulator is two-level with hysteresis. Then it must be determined in which sector the vector of magnetic flux is located. Regulation of torque is based upon a comparison of the calculated value of internal motor torque according to the relationship (2) and the desired torque value. The regulator is three-level with hysteresis.[2].

3.2 Modified method of direct torque control (M_DTC)

The regulation structure of this method is the same as that of the Takahashi method. The difference of this method is in the shifting of the sectors and in the content of the switching table, on the basis of which the selection of the voltage vector is made. The first sector is shifted from the original -30° to 30° to the new 0° to 60°. In determining the switching table, we attempt to avoid vectors with which it is unclear whether they will cause in a particular sector an increase or decrease of torque (flux). The following table shows the influence of the switching of individual vectors in the first sector for Takahashi's and the Modified Method.

	Takahashi's Method -30°→ 30°	**Modified Method** 0° → 60°
$\underline{u}_1$	Torque ambiguity	MS , TZ
$\underline{u}_2$	MZ , TZ	MZ , TZ
$\underline{u}_3$	MZ , TS	Flux ambiguity
$\underline{u}_4$	Torque ambiguity	MZ , TS
$\underline{u}_5$	MS , TS	MS , TS
$\underline{u}_6$	MS , TZ	Flux ambiguity

Table 1. The influence of switching of individual vectors in the first sector of plane α , β first sector

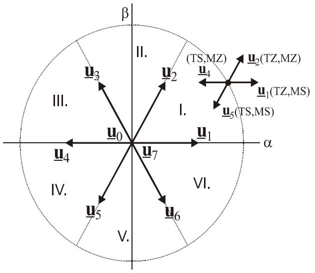

Fig. 2. The principle of selection of voltage vector in the of plane α , β according to the Modified Method

The abbreviations MZ and MS denote respectively the increase and decrease of torque and TZ and TS denote the increase and decrease of flux.

From Table 1 we can see that with Takahashi's Method, vectors $\underline{\mathbf{u}}_1$ and $\underline{\mathbf{u}}_4$ are not used, because it is not clear whether they will cause an increase or decrease of torque in a given sector. Their influence is dependent on the position of the vector of magnetic flux. In selecting the vector according to the Modified Method, vectors $\underline{\mathbf{u}}_3$ and $\underline{\mathbf{u}}_6$ are not used. In switching these vectors it is not clear whether there will be an increase or decrease of flux. This is considered to be the main advantage of the Modified Method compared to the Takahashi Method [3]. The switching table of the Takahashi and Modified Methods can be determined on the basis of Fig. 1b, Fig. 2 and Table 1. Each of these tables contains 36 elements.

3.3 Twelve-Sector Method of Direct Torque Control (12_DTC)

For methods with the α , β plane divided into 6 sectors, it is possible to find in each sector 2 situations that are not used because of the amibiguity of the torque or flux. For this reason it is good to divide the plane α , β into twelve sectors. With this division, all 6 active vectors in each sector may be used, as long as it is clear what kind of change of flux or torque they will cause. The following table shows what change of flux and torque is caused by the switching of individual active vectors in sectors S_1 and S_{12}.

S_1	INCREASE	DECREASE
Stator Flux	$\underline{u}_1$, $\underline{u}_2$, $\underline{u}_6$	$\underline{u}_3$, $\underline{u}_4$, $\underline{u}_5$
Torque	$\underline{u}_2$, $\underline{u}_3$, $\underline{u}_4$	$\underline{u}_5$, $\underline{u}_6$, $\underline{u}_1$
S_{12}	INCREASE	DECREASE
Stator Flux	$\underline{u}_1$, $\underline{u}_2$, $\underline{u}_6$	$\underline{u}_3$, $\underline{u}_4$, $\underline{u}_5$
Torque	$\underline{u}_1$, $\underline{u}_2$, $\underline{u}_3$	$\underline{u}_4$, $\underline{u}_5$, $\underline{u}_6$

Table 2. The influence of switching of active vectors on flux and torque in sectors S1 and S12

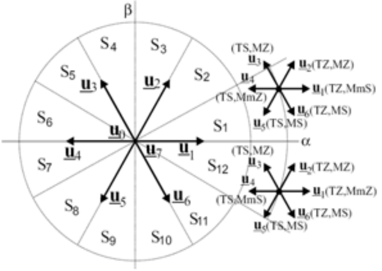
β
α
S_1
S_2
S_3
S_4
S_5
S_6
S_7
S_8
S_9
S_{10}
S_{11}
S_{12}
$\underline{u}_0$
$\underline{u}_1$
$\underline{u}_2$
$\underline{u}_3$
$\underline{u}_4$
$\underline{u}_5$
$\underline{u}_6$
$\underline{u}_7$
(TS,MZ) $\underline{u}_3$
$\underline{u}_2$(TZ,MZ)
$\underline{u}_4$ (TS,MmZ)
$\underline{u}_1$(TZ,MmS)
$\underline{u}_6$(TZ,MS)
$\underline{u}_5$(TS,MS)
(TS,MZ) $\underline{u}_3$
$\underline{u}_2$(TZ,MZ)
$\underline{u}_4$ (TS,MmS)
$\underline{u}_1$(TZ,MmZ)
$\underline{u}_6$(TZ,MS)
$\underline{u}_5$(TS,MS)

Fig. 3. The principle of selection of voltage vector in the first and twelfth sectors of plane α , β according to the Twelve-Sector Method

For more precise regulation ot torque it is necessary to further define small and large changes of torque; therefore, the abbreviations MmZ for small torque increase and MmS for small torque decrease were used in Fig. 3. It is obvious that in the case of a positive desired torque, vector $\underline{\mathbf{u}}_1$ insector S_{12} will create a large increase of flux and a small increase of torque. On the other hand, $\underline{\mathbf{u}}_2$ will considerably increase torque and flux will be increased only minimally [3]. For a finer distinction between changes of torque, it is necessary to use a hysteresis regulator of torque with four levels, where the output values 0, 1 represent small changes of torque and -1, 2 represent large changes of torque.

For selection suitable voltage vector the next logical variables are used:

Sector	Sector = 1, 2, 3, 4, 5, 6, 7, 8, 9, 10, 11, 12
Flux	SQ = 0, 1
Torque	ST = -1, 0, 1, 2

The regulation structure of this method differs from Takahashi's Method (Fig. 1a) only by the four-level comparator of torque. The resultant switching table, which applies for all twelve sectors, can be determined on the basis of Fig. 3 and Table 2. This table contains 96 elements.

4 Experimental Results

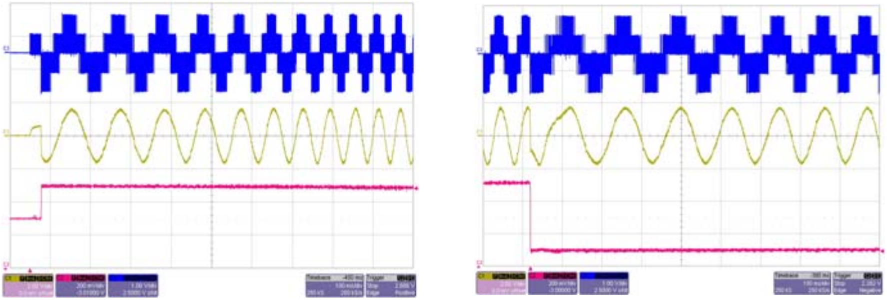

Fig. 4. Takahashi's Method

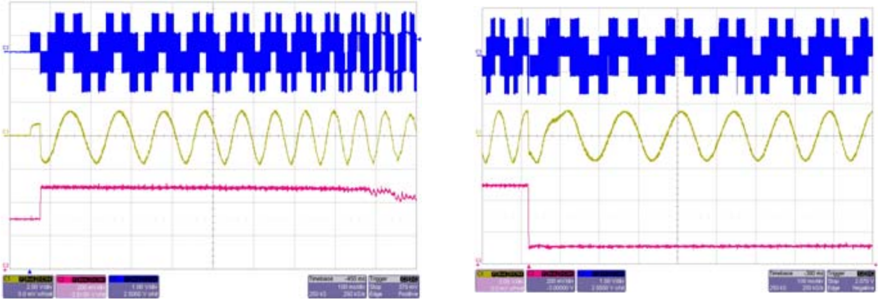

Fig. 5. Modified Method

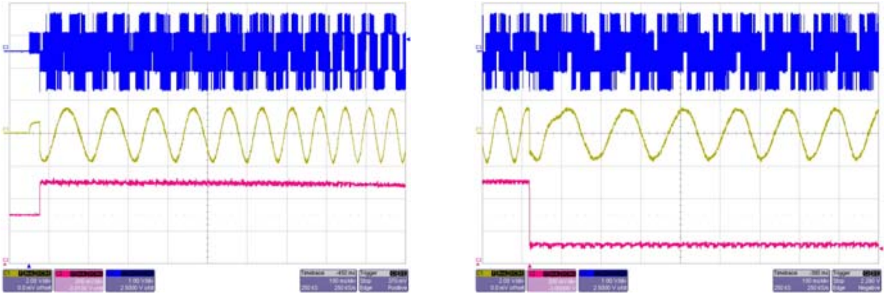

Fig. 6. Twelve-Sector Method

In Figures 4-6, in the lefthand side of each, the course of the start of the method is shown, where at first the excitation of the motor is caused by the pulsing switching of vector $\underline{\mathbf{u}}_2$ to the desired flux and subsequently the regulatory algorithm of the method is started. In the righthand side of the figures is shown the course of the reverse from the desired torque of 4Nm to -4Nm. In all cases, the voltage of the DC bus was 200V and the desired flux was 0.7 Wb and the starting revolutions before the reverse were 500r/min. The measures were made on a induction motor of 2.7 kW.

5 Comparison of the Methods

A comparison of the basic characteristics of each method can be made from teh above measured courses :

- *peak-to-peak value of torque rozkmit momentu* – The Modified Method is most advantageous from the point of view of peak-to-peak value of torque. The measured results corrspond to theoretical models, which arise from the principle of selection of the proper active vector. From Fig. 2 it is clear that the selection of vectors of the Modified Method prefers active vectors, which affect mainly flux. In the course of individual cycles of the calculation of the method's regulation structure there are minute changes of torque. On the other hand an apparent advantage of the Twelve-Sector Method, where larges and small changes of torque are distinguished, turned out to be a disadvantage. For the regulation of torque, mainly active vectors are used. In comparison with zero vectors, active vectors cause a much larger change of torque, and therefore the overall peak-to-peak value of torque isa larger compared to other methods.
- *voltage use of the DC bus* – this criterion can be assessed according to how many revolutions the motor attains given a constant voltage of the DC bus without a drop in torque below the desired value. The maximum revolutions of the Modified Method are considerably lower, which is apparent from Fig. 5, where we can see a drop in torque below the desired value in the course of starting the motor. This drop in torque occurs during lower revolutions than is the case in Takahashi's Method and the Twelve-Sector Method. The maximum possible revolutions of these two methods are similar.
- *content of higher harmonics in output voltage* – due to the most frequent switching of active vectors, the Twelve-Vector Method seems to be the least advantageous

From the above comparison, Takahashi's Method appears to be the best, which, even though it is one of the oldest methods, shows the best characteristics copmared to the other methods. For instance, the company ABB uses this method for all of its products. The use of a DC bus is a basic disadvantage of the Modifed Method. A disadvantage of the Twelve-Sector Method is the large amount of switching of active vectors during torque regulation. This is seen mainly in the content of higher harmonics in output voltage and also in increased switching losses.

References

1. Brandštetter, P.: A.C. Control Drives – Modern Control Method. VSB Technical University of the Ostrava, 1999. ISBN 80-7078-668
2. Javůrek, J.: Regulace moderních elektrických pohonů. VŠB-TU, Grada Publiching, a.s., ISBN 80-247-0507-9.

3. Meziane, S., Toufouti, R., Benalla, H.: Direct torque control strategy of induction motor. Acta Electrotechnica et Informatica, 2001.

Single-phase direct AC/AC converter

Michal Kabašta

Department of Electronics, FEECS,
VŠB – Technical University of Ostrava, 17. listopadu 15, 708 33 Ostrava – Poruba
`michal.kabasta.fei@vsb.cz`

Abstract. This paper is concerned in implementations of the Three-Phase Matrix Converter (TPMC) as Single-Phase Matrix Converter (SPMC) as a direct AC-AC converter with passive load conditions. It was the output voltage was synthesized using the well-known Sinusoidal Pulse Width Modulation (SPWM) technique. Simulations was performed. A laboratory model test-rig of the SPMC is under developed from TPMC to experimentally verify the result.

1 Introduction

Many parts of industrial application request ac/ac power conversion and ac/ac converters take power from one ac system and deliver it to another with waveforms of different amplitude, frequency, or phase. The ac/ac converters are commonly classified into indirect converter which utilizes a dc link between the two ac systems and direct converter that provides direct conversion. Indirect converter consists of two converter stages and energy storage element, which convert input ac to dc and then reconverting dc back to output ac with variable amplitude and frequency as shown in Fig. 1.1 (a).

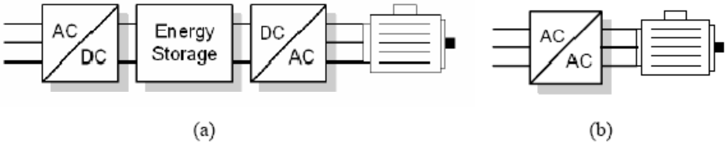

(a)

(b)

Fig. 1. Indirect ac/ac converter (a) direct ac/ac converter(b)

The operation of these converter stages is decoupled on an instantaneous basis by means of energy storage element and controlled independently, so long as the average energy flow is equal. Therefore, the instantaneous power flow does not have to equal the instantaneous power output. The difference between the instantaneous input and output power must be absorbed or delivered by an energy storage element within the converter. The energy storage element can be either a capacitor or an inductor. However, the energy storage element is not needed in direct converter as shown in Fig. 1 (b) [1].

© Václav Snášel (Ed.): WOFEX 2007, pp. 26–30, ISBN 978-80-248-1571-8.
VŠB – Technical University of Ostrava, FEECS, 2007.

Matrix converter replaces the multiply conversion stages and the intermediate energy storage element by a single power conversion stage, and uses a matrix of semiconductor bidirectional switches, with a switch connected between each input terminal to each output terminal as shown in Fig. 2.

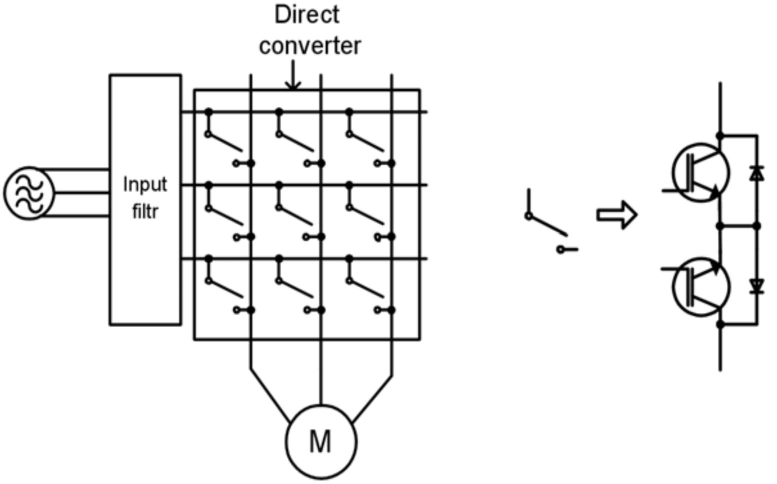

(a) (b)

Fig. 2. Three phase matrix converter(a) bi-directional switches (b)

With this general arrangement of switches, the power flow through the converter can reverse. Because of the absence of any energy storage element, the instantaneous power input must be equal to the power output, assuming idealized zero-loss switches. Therefore, the matrix converter topology is promising for universal power conversion such as: ac to dc, dc to ac, dc to dc or ac to ac.

2 Single-Phase Matrix Converter (SPMC)

The SPMC it is created from TPMC [3] using only four switches bi-directional switches Figure 2 (b). Each switch is capable of conducting current in both directions, blocking forward and reverse voltages. The power grid of SPMC is shown on Figure 3.

The input and output voltage of the SPMC [1] is given by (1) and (2) respectively with loads represented in (3).

$$v_i(t) = \sqrt{2}V_i sin(\omega_i t) \tag{1}$$

$$v_O(t) = \sqrt{2}V_O sin(\omega_O t) \tag{2}$$

$$v_O(t) = Ri_Ot + L\frac{i_O(t)}{dt} \tag{3}$$

Where v_i is input voltage, v_O is output voltage and R,L are parameters of load.

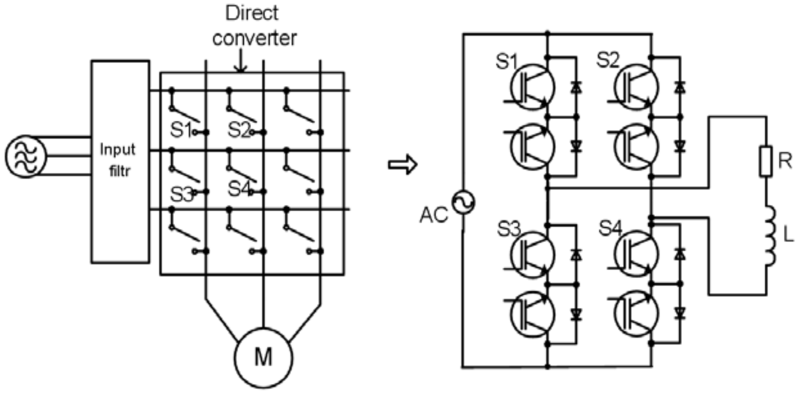

Fig.3. Power grid of single-phase matrix converter

3 Sinusoidal Pulse Width Modulation (SPWM)

The SPWM as illustrated in Fig. 4 has been used in this work and has been known to synthesize a variable voltage output from a fixed input. The use of this technique will result with existence of switching transients relating to the inductive load available during switch turn-off. Theoretically the switching sequence in the SPMC must be instantaneous and simultaneous, but unfortunately this is impossible for practical realization due to the turn-off IGBT characteristic, where the tailing-off of the collector current will create a short circuit with the next switch turn-on. This problem occurs when inductive loads are used. So it is necessary to choose the right commutation strategy [2].

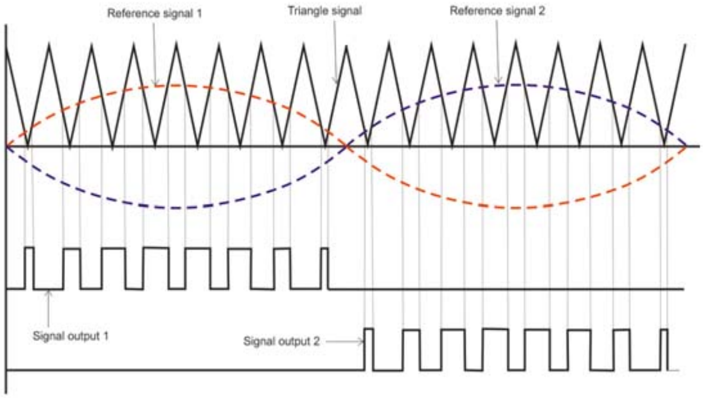

Fig.4. Explanation of SPWM

4 Simulation Results

To predict the behaviour, a simulation model was developed in MATLAB/Simulink. The following parameters are used for this simulation:

- Input voltage V=200V
- Input frequency 50Hz
- RL Load with $R = 50\Omega$ and $L = 50mH$
- Time of simulation 0.04s

Sample results from simulation are shown in subsequent Fig. 5 and 6.

Simulation result for 100Hz

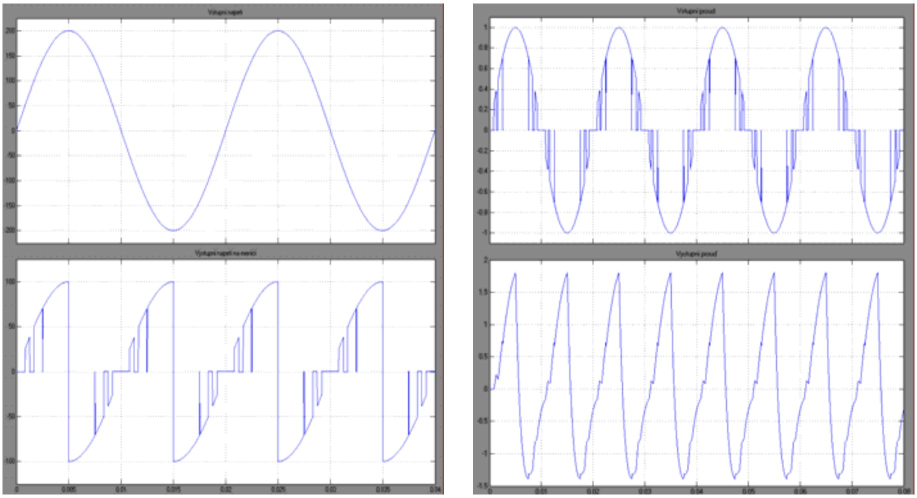

(a) (b)

Fig. 5. Input (top line) and output voltage (bottom line) for 100Hz (a) and input (top line) and output (bottom line) current (b)

Simulations result for 25Hz

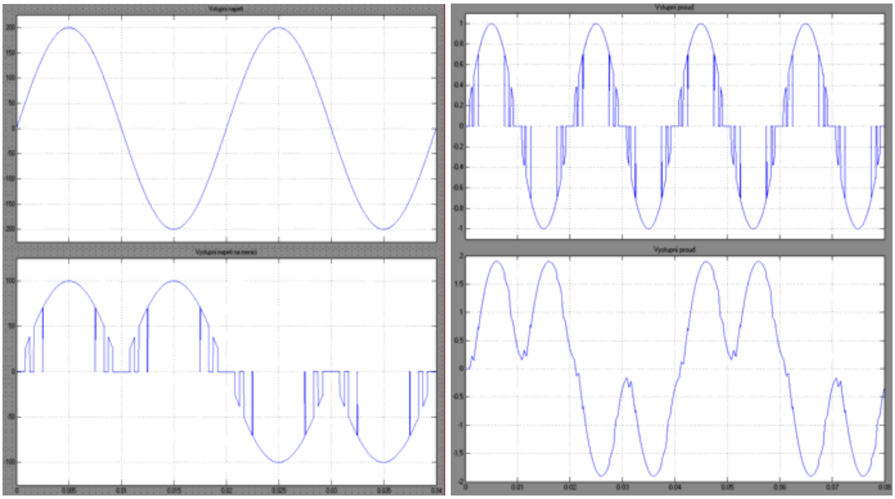

(a) (b)

Fig. 6. Input (top line) and output voltage (bottom line) for 25Hz (a) and input (top line) and output (bottom line) current (b)

5 Conclusion

In this paper, a direct AC-AC converter using single phase matrix converter with passive load condition was presented without the need of DC link. Results of the SPMC for simulation illustrates that it is feasible to realize the converter in the various basic AC-AC conversion that includes step-up frequency changer and step-down frequency changer. For control of SPMC was developed the communications interface for digital signal processor Freescale 56F8013 with inputs of the A/D converter and outputs for PWM outputs. The inputs were boosted in such a way that the input voltage level was changed to 0 - 3V. PWM outputs were boosted for directly connected to the desk for IGBT drivers (from 3.3V to 5V). This interface is under construction now. This is necessary for practical realization SPMC and check simulation results.

References

1. Zuckerberger, A., Weinstock, D., Alexandrovitz A., Single-phase Matrix Converter, IEE Proc. Electric Power App, Vol.144 (4), Jul 1997 pp. 235-240
2. Zahirrudin I., Mohamad F. S., Mustafar K. H., Implementation of Single-Phase Matrix Converter as a Direct AC-AC Converter with Commutation Strategies
3. Kabasta M., Matrix Converter for control AC drive, Diploma thesis, VSB-TU Ostrava 2006

Sensorless Control of Induction Machine with Signal Injection

Petr Korbel

Department of Electronics, FEECS,
VŠB – Technical University of Ostrava, 17. listopadu 15, 708 33 Ostrava – Poruba
`petr.korbel.fei@vsb.cz`

Abstract. Controlled induction motor drives without mechanical speed sensors at the motor shaft have the attractions of low cost and high reliability. To replace the sensor, the information on the rotor speed is extracted from measured stator voltages and currents at the motor terminals**.** Vector controlled drives require estimating the magnitude and spatial orientation of the fundamental magnetic flux waves in the stator or in the rotor. Open loop estimators or closed loop observers are used for this purpose. They differ with respect to accuracy, robustness, and sensitivity against model parameter variations. Dynamic performance and steady-state speed accuracy in the low speed range can be achieved by signal injection, exploiting the anisotropic properties of the machine.

1 Introduction

AC drives based on full digital control have reached the status of a mature technology. The world market volume is about 12,000 millions US$ with an annual growth rate of 15%.

Ongoing research has concentrated on the elimination of the speed sensor at the machine shaft without deteriorating the dynamic performance of the drive control systém. Speed estimation is an issue of particular interest with induction motor drives where the mechanical speed of the rotor is generally different from the speed of the revolving magnetic field. The advantages of speed sensorless induction motor drives are reduced hardware complexity and lower cost, reduced size of the drive machine, elimination of the sensor cable, better noise immunity, increased reliability and less maintenance requirements. The operation in hostile environments mostly requires a motor without speed sensor. A variety of different solutions for sensorless ac drives have been proposed in the past few years. Their merits and limits are reviewed based on a survey of the related literature [1].

© Václav Snášel (Ed.): WOFEX 2007, pp. 31–35, ISBN 978-80-248-1571-8.
VŠB – Technical University of Ostrava, FEECS, 2007.

2 Sensorless Control of Induction Motor

Controlled induction motor drives without speed sensor have emerged as a matur technology in the past decade. The advantages of sensorless control are reduced hardware complexity and lower cost, reduced size of the drive machine, elimination of the sensor cable, better noise immunity, increased reliability and less maintenance requirements. A motor without speed sensor is indicated for operation in hostile environments. Notwithstanding the rapid progress at which the new technologies have emerged, the requirement of operating a sensorless drive at very low speed constitutes a persisting challenge.

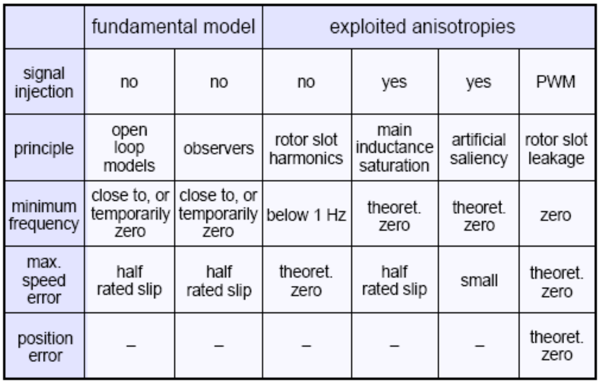

	fundamental model		exploited anisotropies			
signal injection	no	no	no	yes	yes	PWM
principle	open loop models	observers	rotor slot harmonics	main inductance saturation	artificial saliency	rotor slot leakage
minimum frequency	close to, or temporarily zero	close to, or temporarily zero	below 1 Hz	theoret. zero	theoret. zero	zero
max. speed error	half rated slip	half rated slip	theoret. zero	half rated slip	small	theoret. zero
position error	–	–	–	–	–	theoret. zero

Fig. 1. Methods of sensorless speed control

Fig. 1 gives a schematic overview of the methodologies applied to sensorless speed control. A first category comprises the methods that model the induction motor by its state equations. A sinusoidal flux density distribution in the airgap is then assumed, neglecting space harmonics and other secondary effects. The approach defines the class of fundamental models. They are either implemented as open loop structures, like the stator model, or as closed loop observers. The latter make use of error signals between measured and estimated quantities that are fed back to the observers in order to increase their robustness and improve their dynamics. Fundamental models have their limits at zero stator frequency. The rotor induced voltage is then zero, which renders the induction motor an unobservable system.

It is particularly the low speed range where anisotropic properties of the machine can provide additional information on the field angle or the position of the rotor. Voltages induced in the stator windings by spatial rotor slot harmonics can be utilized to determine accurate speed signals. Transient excitation by injected signals having other frequencies than the fundamental serves to detect the spatial orientations of existing anisotropies. The response of the motor is used to identify the field angle or the rotor position angle.

Both the fundamental model methods and the signal injection techniques are competing to improve the low speed performance of sensorless drives [2].

3 Sensorless Control Through Signal Injection

Signal injection methods exploit machine properties that are not reproduced by the fundamental machine model. The injected signal excites the machine at a much higher frequency than that of the fundamental field. The resulting high-frequency currents generate flux linkages that close through the leakage paths in the stator and the rotor, leaving the mutual flux linkage with the fundamental wave almost unaffected. High-frequency signal injection is used to detect anisotropic properties of the machine.

3.1 Anisotropies of an induction machine

Magnetic anisotropy can be caused by saturation of the leakage paths through the fundamental field. Other anisotropic structures are the discrete rotor bars in a cage rotor. A rotor may be also custom designed so as to exhibit periodic variations within a fundamental pole pitch of local magnetic or electrical characteristics, for example the dimensions of the rotor slots. Detecting such anisotropy serves to identify the rotor position angle, the changes of which define the shaft speed. Detecting such anisotropy serves to identify the rotor position angle, the changes of which define the shaft speed.

The case of a saturation-induced anisotropy is considered first. The fundamental field saturates the stator and rotor iron in the region of higher flux density, there producing higher magnetic resistivity of the local leakage paths. A transient excitation by an injected voltage $\mathbf{u}_{tr}$ changes the leakage fluxes in the direction of the forcing voltage vector, $u_{tr}=d\psi_{\sigma tr}/d\tau$. The transient currents change accordingly.

There is generally more than one anisotropy present in an induction motor. The existing anisotropies have different spatial orientations, such as the actual angular position of the fundamental field, the position of the rotor bars within a rotor bar pitch, and, if applicable, the angular position within a fundamental pole pair of a custom designed rotor.

The response to an injected high-frequency signal necessarily reflects all anisotropies, field dependent and rotor position dependent. While intending to extract information on one particular anisotropy, the other anisotropies act as disturbances.

3.2 Signal injection

The injected signals may be periodic, creating either a highfrequency revolving field, or an alternating field in a specific, predetermined spatial direction. Such signals can be referred to as carriers, being periodic at the carrier frequency with respect to space, or time. The carrier signals, mostly created by additional components of the stator voltages, get modulated by the actual orientations in space of the machine anisotropies. The carrier frequency components are subsequently extracted from the machine currents. They are demodulated and processed to retrieve the desired information.

Instead of injecting a periodic carrier, the high-frequency content of the switched waveforms in a PWM controlled drive system can be exploited for the same purpose. The switching of the inverter produces a perpetual excitation of the transient leakage fields [3]. Their distribution in space is governed by the anisotropies of the machine. Measuring and processing of adequate voltage or current signals permits identifying their spatial orientations.

3.3 Estimators which unused motor model

Observer, which unused motor model, are based on usage nonlinear characteristics and by this way try estimate position of magnetic flow or position of rotor.
Piece of knowledge about it, that the in motor exist phenomena, which directly bears with position of magnetic flow or with position of rotor, is base of all strategy centred on estimation reminiscent magnitude, how leave out using model motor. Main diffrences used methods is only way, how these effects „ extract" from motor, to applicable for estimation. All method use definite way „ injection" voltage or current signal.
By kind injection we can devide injection method subsequently:

- ➢ injection periodic signal
    - injection synchronic pulsating signal - Blaschke
    - injection high-frequency signal – Lorenz, Sul
    - zero- sequence technique - Consoli
    - injection synchronic pulsating high-frequency signal - Lipo

- ➢ injection discreet voltage impulses
    - INFORM - Schroedl
    - injection testing impulses „ zero- sequence voltage" - Holtz
    - injection testing impulses „ zero- sequence current"

Among discreet injection voltage impulses belongs to exploitation switching converters, which disuses no additional injected signal.

Injection periodic signal – structures are easy implement, whereas is more exacting operation signal processing in order to get desired information of position magnetic flow or position of rotor

Injection discreet signal – these method are more exacting on implementation, demand exact terms synchronized injection signal with measurent responses magnitude, whereas but offer signal higher qualities (less harmonic, lower share murmur) thereby is desired information on position easily accessible.

Acknowledgement

In the paper there are the results of the project 102/05/2080 which was supported by The Czech Science Foundation(GA CR)

References

1. Holtz, J.: *Sensorless Speed and Position Control of Induction Motor Drives*. IECON Roanoke VA, Germany, 2003.
2. Holtz, J.: *Sensorless Control of Induction Machines – with or without Signal Injection?* Proceedings of the IEEE, Germany, 2003.
3. Holtz, J.: *On the Spatial Propagation of Transient Magnetic Fields in AC Machines.* Proceedings of the IEEE, august 1996, pp. 927-937.
4. Makyš, P.: *Polohový servopohon s asynchronním motorem bez snímača na hriadeli.* Disertačná práca. Žilinská univerzita. Žilina 2006

Sensorless Vector Control of a Permanent Magnet Synchronous Motor Using High Frequency Injection

Tomáš Křeček

Department of Electronics, FEECS,
VŠB – Technical University of Ostrava, 17. listopadu 15, 708 33 Ostrava – Poruba
tomas.krecek.fei@vsb.cz

Abstract. Sensorless control of permanent magnet synchronous machine (PMSM) is popular for several reasons: cost saving and system reliability. In this paper, rotor position and speed estimation, i.e., sensorless control, of PMSM is discussed. The injection methods describe in the paper is a new sensorless strategy for control A.C drives with low and zero speed. A brief overview different methods found in the literature is presented. The basis for the injection method is that there exist a difference in the direct and quadrature inductance of the machines. This difference is reefer to as saliency. The saliency of PMSM is discussed too.

1 Introduction

As is well known, there are (in principle), two difference methods of obtaining estimates of speed and rotor position in a vector control PMSM.

In the first category, information is obtaining from the back electromotive force (EMF). These estimation techniques show good performance in the medium and high speed regions. Since the back EMF is vanishes at low speed, low and zero speed operation is challenging [5].

In the second category, a high frequency (HF) carried signal is added, and information about the rotor position or speed is obtained from the current response. The basis for the injection methods is certain amount saliency present in the machine [1, 2, 3, 4, 5].

There are several sources of saliencies in PM machines. In this paper a single saliency is consideration: rotor construction saliency, saturation based saliency.

2 Description of Saliency

A necessary requirement of the injection method is a known magnetic saliency ($L_q \neq L_d$) in the machine. The saliency in PMSM is manifested as change in the stator inductance. This change is better analyzed in the synchronous d-q reference frame. Saliency of the PMSM is mainly caused by two dominant effects: geometrical saliency such as the IPMSM, and magnetic saturation of the stator, which appears in all type of PMSMs. Most PMSM inherently some magnetic saliency with interior PM synchronous machine (IPMSM) exhibiting the most saliency (L_q=2 to 3 times L_d) and

© Václav Snášel (Ed.): WOFEX 2007, pp. 36–41, ISBN 978-80-248-1571-8.
VŠB – Technical University of Ostrava, FEECS, 2007.

surface mount permanent magnet synchronous machine (SMPMSM) exhibiting a very small saliency.

2.1 Geometrical saliency

Though the SMPMSM of cylindrical rotor is non-salient machine small amount of geometrical asymmetry is normal present due to inset or partially inset magnets into the rotor iron [3, 4]. In a surface mounted PM with inset and partially inset magnets, as show in fig. 1, the extra iron in the quadrature magnetic path q and the stator's teeth saturation in the flux direction d result in small saliency in the effective air gap length. As a result, the inductance in the flux axis L_d is smaller than the inductance in the quadrature axis L_q producing the stator inductance to be function of the position.

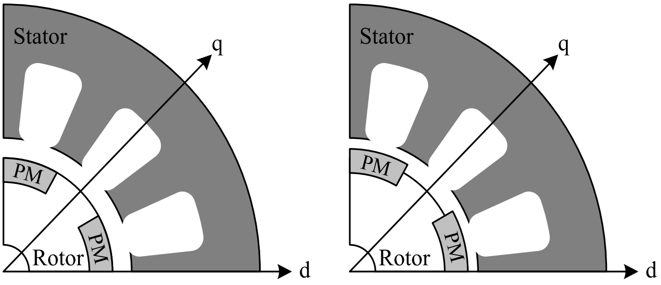

Fig. 1. Inset and partially inset magnet motor

The IPMSM unlike an SMPMSM, the magnets are mounted inside the rotor. A typical configuration is shown in the fig. 2. The difference in the geometry gives the effective air gap in the d axis is larger than that in the q axis, which makes the machine a salient pole with $L_d<L_q$.

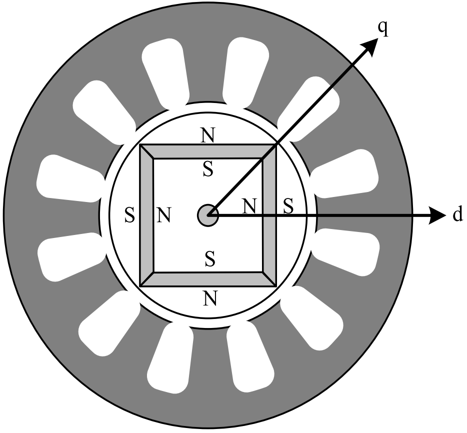

Fig. 2. Typical cross-section of IPMSM

2.2 Saturation saliency

SMPMSM without structural saliency will present a spatial difference in the synchronous inductance caused by the magnetic saturation of some section of the machine iron core due to the high air gap flux-density produced by the PM [1, 3]. As it is well known, the saturated iron presents a sharp reduction in the permeability decreasing the inductance value of any coil whose flux path crosses through saturated section. The saturation of the machine's iron may affect the main flux path or the leakage flux path producing a spatial modulation in the magnetizing and leakage inductances.

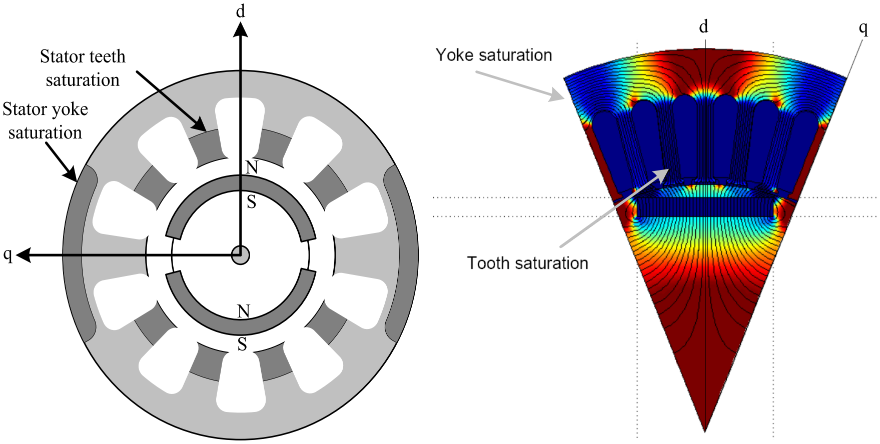

Fig. 3. Source of saliency by magnetic saturation of the stator regions

2.2.1 Saturation saliency in the magnetizing inductance – L_{mdq}

Under no load the rotor magnets establishes a flux-density with its maximum in the d-axis direction. The stator iron directs and concentrates the flux producing saturation (fig. 3) stator teeth, tooth tips (in the proximity d-axis) and yoke (in the proximity q-axis). These stator saturations produce an increase in the effective air gap length for the main d-axis flux resulting in a reduction of L_{md}. On the other hand, L_{mq} remains unchanged (the yoke saturation is assumed to have minimal impact) and $L_{md}<L_{mq}$ [2].

2.2.2 Saturation saliency in the leakage inductance – $L_{\sigma dq}$

Due to the orthogonal position of the stator windings and their magnetic axis, under no load the main flux saturation produced by the PM in the d-axis affects the stator teeth and tooth tips around the q-axis winding as illustrated in fig. 3.The reduction in the permeance of the leakage flux path of the q-axis causes a reduction of $L_{\sigma q}$. Because there is almost no main flux in the q-axis direction, the d-axis leakage inductance remains largely unchanged resulting in $L_{\sigma q}< L_{\sigma d}$ [2, 3, 4].

3 High Frequency (HF) Injection Techniques

Knowledge of the rotor position is needed for the vector control of the PMSM. In sensorless control, an estimation algorithm is used instead of a mechanical position sensor, resulting in reduced overall cost and increase reliability. The methods used for the estimation of the rotor speed and position can be classified into model-based methods and non-model based methods. Model-based methods rely on a dynamics model of the motor. These methods have good dynamic properties but are not suitable for low and zero speed operation. In signal injection method (non-model based), a HF voltage signal is superimposed on the stator voltage, and the resulting current response is used for detecting the anisotropy caused by the saliency [1].

There is several HF injection methods found in the literature and they can be classified into three types: α-β frame rotating injection, d-q frame rotating injection and d-q frame pulsating injection. This paper will be concentrated with the α-β frame persistent HF rotating carrier injection [3, 4, 5].

3.1 Rotating α-β Injection

The most common approach is to superimpose a HF voltage carrier on the fundamental excitation. The rotor position is than extracted from resulting HF currents. The HF, ω_{vf}, should be high enough to ensure sufficient spectral separation between itself and the fundamental excitation to reduce the requirements of the band-pass filters.

One form of the HF voltage carrier injection, with constant amplitude U_{vf} and frequency ω_{vf}, is as follows [1, 3]:

$$\begin{bmatrix} u_{\alpha\_vf} \\ u_{\beta\_vf} \end{bmatrix} = U_{vf} \cdot \begin{bmatrix} -\sin(\omega_{vf} \cdot t) \\ \cos(\omega_{vf} \cdot t) \end{bmatrix} \tag{1}$$

The voltage model for the PMSM in the stationery reference frame can be written:

$$\begin{bmatrix} u_{\alpha} \\ u_{\beta} \end{bmatrix} = R_s \cdot \begin{bmatrix} i_{\alpha} \\ i_{\beta} \end{bmatrix} + \frac{d}{dt}\left\{ \begin{bmatrix} L - \Delta L \cdot \cos(2 \cdot \theta_r) & -\Delta L \cdot \cos(2 \cdot \theta_r) \\ -\Delta L \cdot \cos(2 \cdot \theta_r) & L + \Delta L \cdot \cos(2 \cdot \theta_r) \end{bmatrix} \cdot \begin{bmatrix} i_{\alpha} \\ i_{\beta} \end{bmatrix} + \psi_{PM} \cdot \begin{bmatrix} \cos(\theta_r) \\ \sin(\theta_r) \end{bmatrix} \right\} \tag{2}$$

Using a carrier between 600 Hz to 1 kHz, the stator impedance of (2) is dominated by the stator inductance, as $\omega_{vf} \cdot L_s >> R_s$, thus (2) can be approximated to [1, 3]:

$$\begin{bmatrix} u_{\alpha\_vf} \\ u_{\beta\_vf} \end{bmatrix} = \frac{d}{dt}\left\{ \begin{bmatrix} L - \Delta L \cdot \cos(2 \cdot \theta_r) & -\Delta L \cdot \cos(2 \cdot \theta_r) \\ -\Delta L \cdot \cos(2 \cdot \theta_r) & L + \Delta L \cdot \cos(2 \cdot \theta_r) \end{bmatrix} \cdot \begin{bmatrix} i_{\alpha\_vf} \\ i_{\beta\_vf} \end{bmatrix} \right\} \tag{3}$$

Substituting (1) in (3), the resulting HF current is given by:

$$\begin{bmatrix} i_{\alpha\_vf} \\ i_{\beta\_vf} \end{bmatrix} = \frac{U_{vf}}{\omega_{vf} \cdot L_d \cdot L_q} \begin{bmatrix} L_s \cdot \cos(\omega_{vf} \cdot t) + \Delta L_s \cdot \cos(2 \cdot \theta_r - \omega_{vf} \cdot t) \\ L_s \cdot \sin(\omega_{vf} \cdot t) + \Delta L_s \cdot \sin(2 \cdot \theta_r - \omega_{vf} \cdot t) \end{bmatrix} \tag{4}$$

An equation shows that the resulting current contains both positive and negative sequences components. The position information is contained in the negative sequence [1, 3, 4].

3.2 Demodulation

The demodulator must be used in order to extract the position angle information. There are several methods for extract the position information. This paper will be concentrated with homodyne signal processing which use as a synchronous filter [4].

3.2.1 Homodyne Signal Processing (HSP)

The HSP (shown in fig. 4) can be derived from equation (4). The band-pass filter removes the fundamental component and leaves HF component. The first rotation of coordinates transforms the HF currents to a rotating frame synchronous with the voltage injection, converting the positive sequence current into DC. Therefore, by means of a high-pass filter it can be completely removed. Finally, a rotation back attached to the frame synchronous with the negative sequence produced the position signal at base band, as given in equation (5). The angle θ_r can be that extracted by an directly arc tangent [1, 3, 4]:

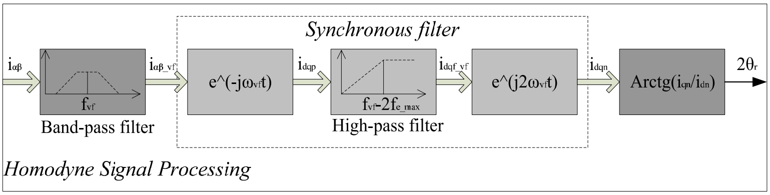

Fig. 4. Synchronous filter for homodyne demodulation of HF current vector

$$\begin{bmatrix} i_{dn} \\ i_{qn} \end{bmatrix} = \frac{U_{vf}}{\omega_{vf} \cdot L_d \cdot L_q} \begin{bmatrix} \Delta L_s \cdot \cos(2 \cdot \theta_r) \\ \Delta L_s \cdot \sin(2 \cdot \theta_r) \end{bmatrix} \tag{5}$$

3 α-β Injection in a Vector Controlled drive

The developed instantaneous torque by the PMSM can be found in the form:

$$T_e = \frac{3 \cdot p_p}{2} \cdot \left(\underbrace{\psi_{PM} \cdot i_q}_{\text{magnet toeque}} + \underbrace{i_d \cdot i_q \cdot \{L_d - L_q\}}_{\text{reluctance torque}} \right) \tag{6}$$

In the SMPMSM, the reluctance torque is zero and therefore the torque is controlled only by changes in i_q. This makes the control structure very simple (fig. 5) [3].

The reluctance torque is significant on IPMSM. In these motors more torque per each ampere of stator current can be achieving by advancing the stator current vector angle and forcing some negative i_d current. The particular mapping (function gen. 1, 2) of torque reference T_e^* into i_d^* and i_q^* is not unique but is given optimization criteria such as maximum torque per ampere (criterion for maximum torque/ampere).

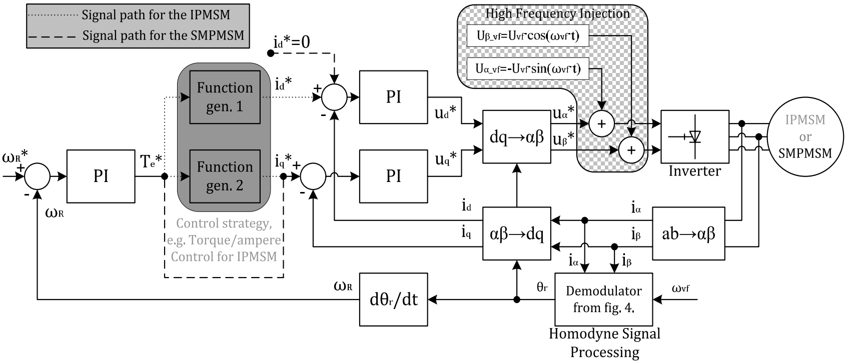
Signal path for the IPMSM
Signal path for the SMPMSM
i_d*=0
High Frequency Injection
$U_{\beta\_vf}=U_{vf}\cdot\cos(\omega_{vf}\cdot t)$
$U_{\alpha\_vf}=-U_{vf}\cdot\sin(\omega_{vf}\cdot t)$
Function gen. 1
Function gen. 2
i_d*
i_q*
PI
PI
PI
u_d*
u_q*
dq→αβ
u_α*
u_β*
Inverter
IPMSM or SMPMSM
ω_R*
T_e*
ω_R
Control strategy, e.g. Torque/ampere Control for IPMSM
i_d
i_q
αβ→dq
i_α
i_β
ab→αβ
ω_R
$d\theta_r/dt$
θ_r
Demodulator from fig. 4.
ω_{vf}
Homodyne Signal Processing

Fig. 5. Sensorless vector control of the IPMSM and SMPMSM using α-β injection

The implementation of α-β HF voltage carrier injection is relative straightforward in the vector controlled drive, as shown in fig. 5. The vector control identifies the reference voltage vector $\underline{\mathbf{u}}_{\alpha\beta}^*$ and the carrier can be superimposed with no hardware modification [1].

The main disadvantages implementation of the α-β HF voltage carrier injection is the largely rippled current and thus the torque is rippled too. This does the electric drive somewhat noisy.

Acknowledgements: In the paper there are the results of the project 102/05/2080 which was supported by The Czech Science Foundation (GA CR).

References

1. Ortega, C., Arias, A., Caruana, C., Staines, C., Balcells, J., Cilia, J.: Sensorless Direct Torque Control of a Surface Mounted PMSM using High Frequency Injection. In: Industrial electronics, IEEE International symposium on, vol. 3, pp. 2332-2337, July 2006.
2. Overbo, R., Nilssen, R., Nilssen, R.: Saliency Modelling in Radial Flux Permanent Magnet Synchronous Mechines. In: NORPIE 2004, Trondheim, Norway.
3. Silva, C. A.: Sensorless Vector Control of Surface Mounted Permanent Magnet Machines Without Restriction of Zero Frequency. In: Ph.D Dissertation, Dep. Power Electronics, Machines and Control, University of Nottingham, May 2003.
4. Štulrajter, M.: Bezsnímačový polohový servomechanizmus so synchronným motorom s permanentnými magnetmi. In: Doktorandská disertačná práca, Kat. Výkonových elektrotechnických systémov, Žilinská Univerzita v Žilině, Slovensko 2006.
5. Wallmark, O.: On Control of Permanent-Magnet Synchronous Motors in Hybrid-Electric vehicle Applications. In: Thesis for the degree of licentiate of engineering, Dep. Of Electric Power Engineering, Chalmers University of technology, Sweden 2004.

Direct Torque Control for Three-level Voltage Inverter

Petr Moravčík

Department of Electronics, FEECS,
VŠB – Technical University of Ostrava, 17. listopadu 15, 708 33 Ostrava – Poruba
petr.moravcik.fei@vsb.cz

Abstract. This paper presents a new Method of control based on Direct Torque Control (DTC) strategy. This method is designed to be applied in the control of Induction Motors (IM) fed with a three-level Voltage Source Inverter (VSI). This type of inverter has several advantages comparison with standard two-level VSI, such as a greater number of levels in the output voltage waveforms, lower dV/dt, less harmonic distortion in voltage and current waveforms and lower switching frequencies. In the new method, torque and stator flux errors are used together with the stator flux angular frequency to generate a reference voltage vector. Further operation of designated converters are documented on experimental results.

1 Introduction

Direct Torque Control (DTC) is a method that has emerged to become one possible alternative to the well-known Vector Control of Induction Motors. This method provides a good performance with a simpler structure and control diagram. In DTC it is possible to control directly the stator flux and the torque by selecting the appropriate Voltage Source Inverter state. The main advantages offered by DTC are:

- Decoupled control of torque and stator flux.
- Excellent torque dynamics with minimal response time.

Inherent motion-sensorless control method since the motor speed is not required to achieve the torque control.

- Absence of coordinate transformation (required in Field Oriented Control (FOC)).
- Absence of voltage modulator, as well as other controllers such as PID and current controllers (used in FOC).
- Robustness for rotor parameters variation. Only the stator resistance is needed for the torque and stator flux estimator.

These merits are counterbalanced by some drawbacks:

- Possible problems during starting and low speed operation and during changes in torque command.
- Requirement of torque and flux estimators, implying the consequent parameters identification (the same as for other vector controls).

© Václav Snášel (Ed.): WOFEX 2007, pp. 42–47, ISBN 978-80-248-1571-8.
VŠB – Technical University of Ostrava, FEECS, 2007.

- Variable switching frequency caused by the hysteresis controllers employed.
- Inherent torque and stator flux ripples.
- Flux and current distortion caused by sector changes of the flux position.
- Higher harmonic distortion of the stator voltage and current waveforms compared to other methods such as FOC.
- Acoustical noise produced due to the variable switching frequency. This noise can be particularly high at low speed operation.

2 The principle of the New Method of Direct Torque Control

The basic principle of all methods of direct torque control is the same: The three-level voltage inverter is able to provide maximally twenty-seven correct switching combinations, which, on the basis of a theory of complex vectors, corresponds to twenty-seven voltage vectors from $\underline{\mathbf{u}}_1$ to $\underline{\mathbf{u}}_{27}$. Rotating magnetic field in the stator is created on the basis of an algorithm using switching of active vectors, in which the speed of rotation of the magnetic field, as well as the amount of motor torque, can be driven by switching of zero vectors, or switching active vectors working in the opposite direction of the magnetic field rotation.

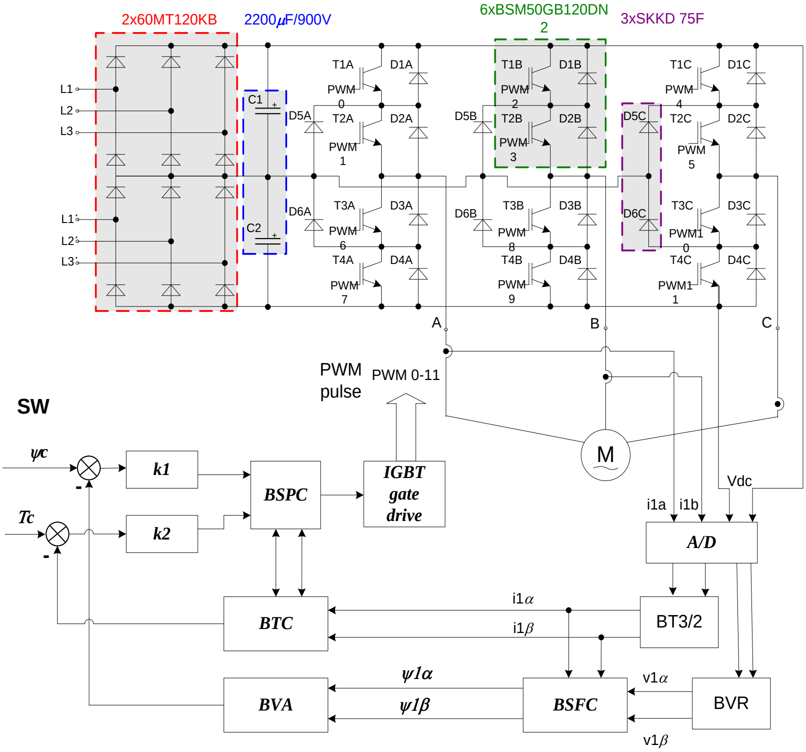
2x60MT120KB
2200μF/900V
6xBSM50GB120DN2
3xSKKD 75F
L1
L2
L3
L1
L2
L3
C1
C2
D5A
D6A
T1A
D1A
T2A
D2A
T3A
D3A
T4A
D4A
PWM 0
PWM 1
PWM 6
PWM 7
D5B
D6B
T1B
D1B
T2B
D2B
T3B
D3B
T4B
D4B
PWM 2
PWM 3
PWM 8
PWM 9
D5C
D6C
T1C
D1C
T2C
D2C
T3C
D3C
T4C
D4C
PWM 4
PWM 5
PWM 10
PWM 11
A
B
C
PWM pulse
PWM 0-11
SW
ψc
Tc
k1
k2
BSPC
IGBT gate drive
M
Vdc
i1a
i1b
A/D
BTC
i1α
i1β
BT3/2
BVA
ψ1α
ψ1β
BSFC
v1α
v1β
BVR

Fig. 1. Block diagram with the New Method of Direct Torque Control

Note:

M - induction motor
BSP - block of pulse creation
BT3/2 - block of transformation 3/2
BVA - block of vector analyzer
BTC - block of calculation of torque
BVR - block of reconstruction of voltage
BSFC - block of calculation of stator flux
BSPC – block of calculation of switching combination

The stator flux and inner motor torque are calculated on the basis of measured voltage of the DC-link and phase currents. In the Fig.1 is illustrated block diagram with the New method of direct torque control.

2.1 The Calculation of Switching Combination

The advantage of the New Method compared to earlier ones is the fact that the algorithm provides a direct vector of voltage, which is to be switched for every position of stator flux. In Fig. 2 it is possible to see vectors **g1** and **g2**, in which **g1** is always coaxial with the flux, whereas **g2** is always perpendicular to the flux.

$$\begin{aligned} \Delta\Psi_1 &= \Psi_{\check{z}} - \left|\Psi_1^S\right| \\ \Delta m &= m_{\check{z}} - m \\ \left|\mathbf{g1}\right| &= k_1\,\Delta\Psi_1 \\ \left|\mathbf{g2}\right| &= k_2\,\Delta m \end{aligned} \qquad \mathbf{(1)}$$

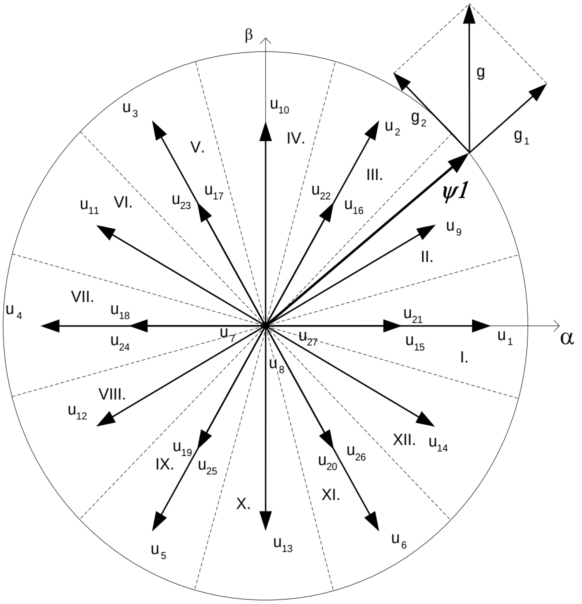
β
α
g
g_2
g_1
$\psi 1$
u_1
u_2
u_3
u_4
u_5
u_6
u_7
u_8
u_9
u_{10}
u_{11}
u_{12}
u_{13}
u_{14}
u_{15}
u_{16}
u_{17}
u_{18}
u_{19}
u_{20}
u_{21}
u_{22}
u_{23}
u_{24}
u_{25}
u_{26}
u_{27}
I.
II.
III.
IV.
V.
VI.
VII.
VIII.
IX.
X.
XI.
XII.

Fig. 2. Trajectory of the vector of stator magnetic flux according to the New Method

By adding vectors **g1** and **g2**, we arrive at the resultant vector **g**. If the vector of voltage is switched on , whose direction is the same as the direction of vector **g**, then it is apparent that the value of vector **g1** determines the amount of activation, and the amount of vector **g2** determines the speed of rotation of the vector of stator flux, as well as the amount of torque.

Considering that the three-level voltage inverter uses twenty-seven voltage vectors, of which three are zero vectors, it is necessary to select the vector whose direction most closely resembles that of vector **g** coaxial with the flux, whereas **g2** is always perpendicular to the flux.

2.2 Implementation of five-level hysteresis torque comparator

The SV diagram is divided into twelve sectors and one sector have 30° (See you in the Fig.2). Input values for five-level hysteresis torque comparator are: number of sector, torque errors, voltages on capacity divider vc1, vc2, value of comparator hysteresis. Five-level hysteresis comparator is included in block of calculation of switching combination. Comparator has five level of torque namely: zero change of torque, positive small change of torque, negative small change of torque, positive large change of torque, negative large change of torque. On the based input values of variables is executed selection of switching combination.

Example of a Program Code in the C Language from Code Composer Studio C2x eyDSP Kit Tools.

```
dM=vstupni_promenna[0]-m;

g1=((int32)(vstupni_promenna[3])*(int32)(vstupni_promen
na[1]-psimodul))>>13;

g2=((int32)(vstupni_promenna[4])*(int32)(dM))>>13;

temp=((int32)(modul)*2120)>>13; //0,258*modul

temp1=((int32)(modul)*5792)>>13;//0,707*modul

temp2=((int32)(modul)*7912)>>13;//0,965*modul
```

3 Experimental results

Some experimental results have been obtained for the Classical DTC (Takahashi's methods) with a three-level VSI and New Method of Direct Torque Control with a three-level VSI to establish a comparison between both systems. In the first method of

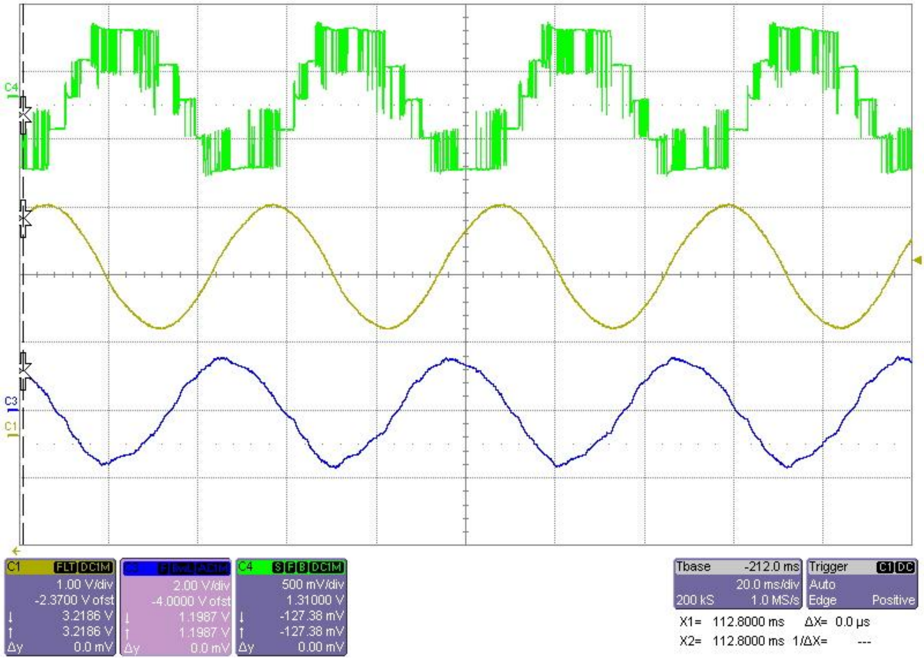

Fig. 3. Values of asynchronous motor, (fs = 10kHz) C1: $\psi 1\alpha = f(t)$ C3: $i_{1\alpha} = f(t)$, C4: V_{L-L}
The second method: New Method of Direct Torque Control

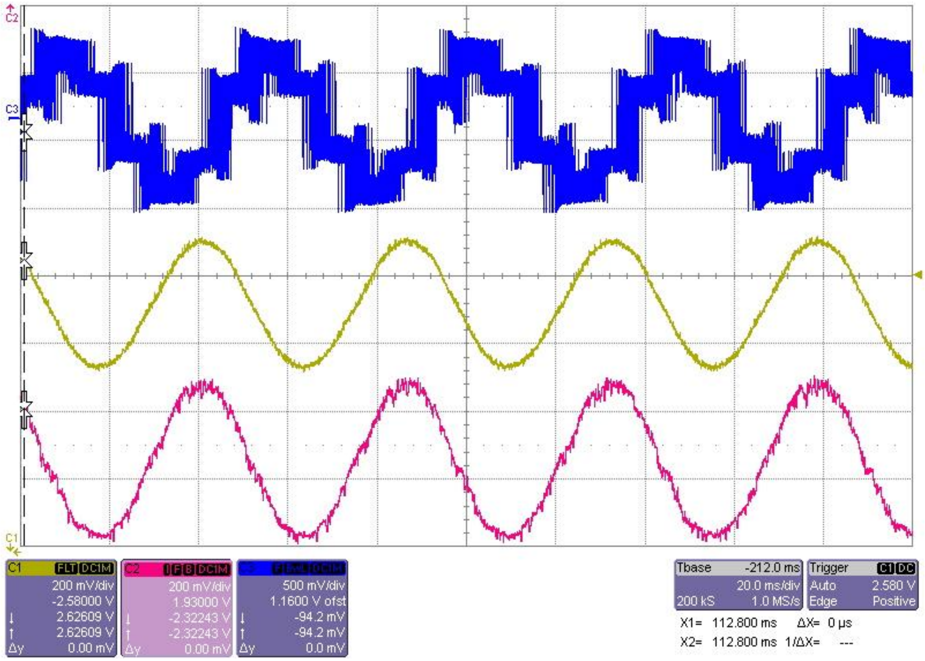

Fig. 4. Values of asynchronous motor, (fs = 10kHz) C1: $\psi 1\alpha = f(t)$ C3: $i_{1\alpha} = f(t)$, C4: V_{L-L}
The first method: Modified Takahashi's methods for three-level VSI.

control – Classical DTC was switched only twelve active vectors and two zero vectors. In the Fig.3 are illustrated measure waveforms for first method: First waveform is output line to line voltage V_{L-L} on asynchronous motor , second waveform is stator flux component $\psi_{1\alpha}$ and last waveform is phase stator current $i_{1\alpha}$.

In the second method: New Method of Direct Torque Control, was switched all active vectors (24) and three zero vectors. Reconstruction voltage is realized with all vectors (27). In the Fig.4 are illustrated measure waveforms for second method: First waveform is output line to line voltage V_{L-L} on asynchronous motor, second waveform is stator flux component $\psi_{1\alpha}$ and last waveform is phase stator current $i_{1\alpha}$. The measurement was implement for following parameters: Vdc = 120[V], fs = 10kHz,

4 Conclusion

There was proved some methods of control for Three-level inverter results acknowledge the right way in development of those modulation strategies and was confirmed some advantages of conception of Three-level voltage inverter. The Three-level voltage inverter have better reduction in torque ripple, flux ripple, harmonic distortion in stator currents and switching frequency when compared with classical DTC system utilising two-level VSI.

5 Acknowledgements

The support for this research work has been provided by the GAČR project 102/05/H525: The Postgraduate Study Rationalization at Faculty of Electrical Engineering and Computer Science VSB-TU Ostrava. Next acknowledgments are intended to my supervisor prof. Petr Chlebiš, CSc and the Department of Electronics. My studies has been also supported by the scholarship of Ostrava.

References

[1] Brandštetter, P.: A.C. Control Drives – Modern Control Method. VSB Technical University of the Ostrava, 1999. ISBN 80-7078-668

[2] Javůrek, J.: Regulace moderních elektrických pohonů. VŠB-TU, Grada Publiching, a.s., ISBN 80-247-0507-9.

Matrix Converters by DSP Controlled

Lukáš Osmančík

Department of Electronics, FEECS,
VŠB – Technical University of Ostrava, 17. listopadu 15, 708 33 Ostrava – Poruba
`lukas.osmancik.fei@vsb.cz`

Abstract. This paper deals with a special types of converters. Those converters are classified as direct type of converters. First is three-phase Four Quadrant Current Source Rectifier in operation like Matrix Converter 3/2. The power part, control circuits and control method are described there. Second is Indirect Matrix Converter 3/3. A power part and basic type of modulation method are described there. Further, practical application and operation of designated converters are documented on experimental results.

1 Introduction

Currently, the majority of the electrical drives are the three phase variable speed AC drives, but DC drives are still used and many parts of industrial application request power conversion from ac power supply to the dc electrical power. Currently, standard approach of modern AC drive is the asynchronous motor fed from Voltage Source Inverter (VSI) with input diode rectifier. This converters have a lot of shortcomings. The currents drawn by the rectifier content harmonics and they are far from being sinusoidal. The capacitance of DC link limit a dimensions of converter and there is no way to recovered the brake energy to the mains, so it must be abduced to bulky, heat produce brake resistor. There exist a modern configuration with active input pulse width controlled rectifier with sine modulated input currents and recuperation, but the problem with big capacitor in the DC link is persisting. Further, the DC link capacitor limits the use of this converter in aggressive environment. This shortcomings and more are addressed the direct power converters – the Matrix Converters.

2 Matrix Converter 3/2

The three-phase Four Quadrant Current Source Rectifier (Fig. 1) is built with semiconductors with gate-turn-off capability. This feature confers the following advantages. The current can be modulated (Space Vector PWM or other type of suitable control method), generating less harmonic contamination. The power factor can be con-

© Václav Snášel (Ed.): WOFEX 2007, pp. 48–53, ISBN 978-80-248-1571-8.
VŠB – Technical University of Ostrava, FEECS, 2007.

trolled and with this arrangement of the power part, the four quadrant operation is possible to achieve. The switching ripples are filtered by the input capacitors and phase inductances. The power part was arranged using IGBTs. The reverse blocking capability is achieved with anti serial combination of transistors – bidirectional switch. This rectifier could be used like direct power conversion stage from three phase constant frequency system to one phase variable amplitude and frequency system. The label 3/2 is rather complicated, because two phases, half turn, are in appearance to ground – center point of mains. From the output point of view it could be in some literature labeled as Matrix Converter 3/1.

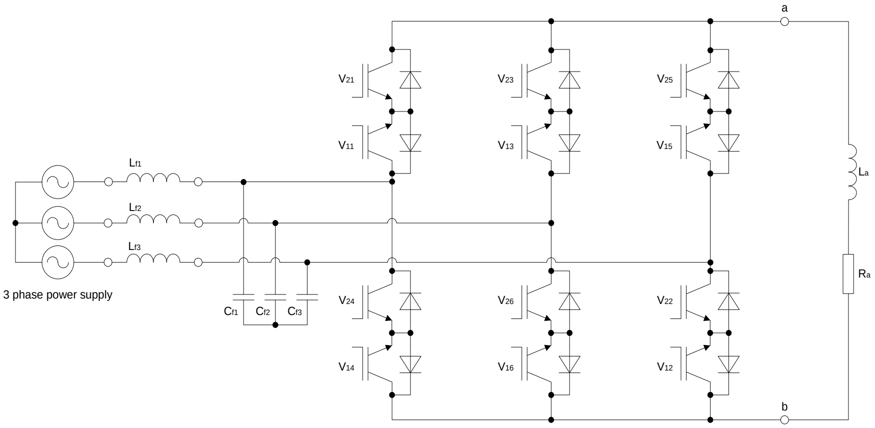

Fig. 1. Power part of the Matrix Converter 3/2

2.1 Method of Control

There was used the Space Vector Pulse Width Modulation (SVPWM). The pulses of the SVPWM are send on switches according to vector diagram (Fig. 2.). Vector diagram is divided by active vectors into the six sectors. Every active vector is represented by the switching combination, which effect conducting of current from the power supply to the load (or conversely). In the centre, there are located three zero vectors. This zero vectors effect disconnecting the load from the supply and the current is closed (fade) trough switches and the load. The vector diagram is synchronized by space vector of three input phase voltages. This space vector is observed and all of his transitions are respected by the algorithm. The position of the vector in sector is constituted by the duty ratio of switching active vectors inherent to this sector. The magnitude of this vector is confered by duration of switching zero vector. The control algorithm principle is downward represented on Fig. 3. The control algorithm was implemented for modern DSP TMS 320F2812. Input phase voltages are transformed from three phase to the two axis system (alpha, beta). Then is calculated the angle of space vector. Sector and duty ratios are calculated in the modulator and with use of compare registers the pulse timing is to be operated. There were also realised an external control circuits for overlap of the PWM pulses, because of current character of the converter.

AV_{1-6}	Active Vector
ZV_{1-3}	Zero Vector
V_{fa}, V_{fb}, V_{fc}	phase voltages
I. – VI.	sector

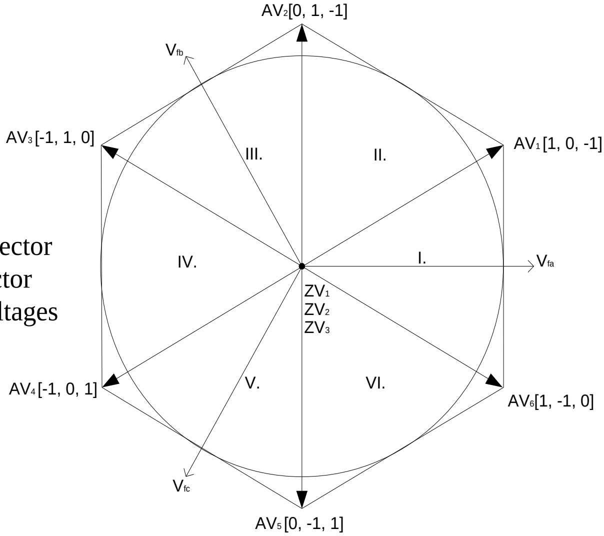
AV₂[0, 1, -1]
Vfb
AV₃[-1, 1, 0]
III.
II.
AV₁[1, 0, -1]
IV.
I.
Vfa
ZV₁
ZV₂
ZV₃
AV₄[-1, 0, 1]
V.
VI.
AV₆[1, -1, 0]
Vfc
AV₅[0, -1, 1]

Fig. 2. The diagram of the SVPWM

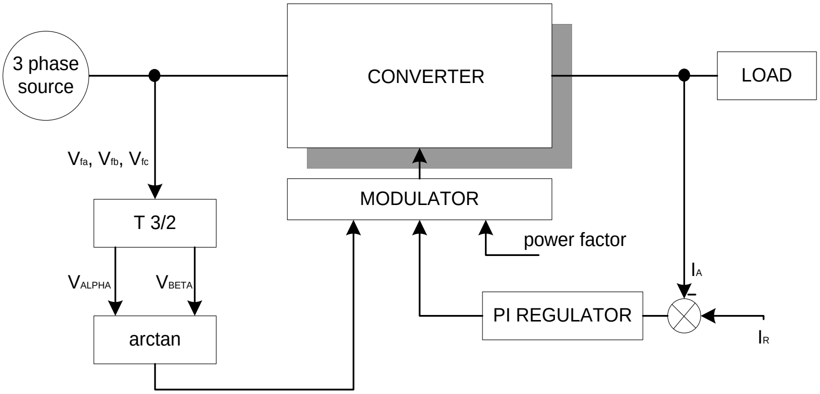
3 phase source
CONVERTER
LOAD
Vfa, Vfb, Vfc
MODULATOR
T 3/2
power factor
IA
VALPHA
VBETA
PI REGULATOR
arctan
IR

Fig. 3. Control algorithm principle

2.2 Experimental Results

Realised converter was used for fed RL load. Software sine generator was add instead of constant request value. In this way, the algorithm was modified for operation such as Matrix Converter 3/2.

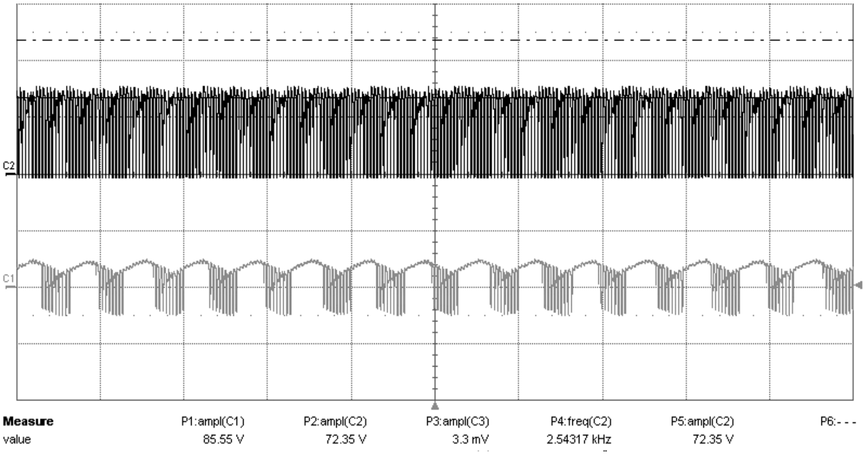

Measure	P1:ampl(C1)	P2:ampl(C2)	P3:ampl(C3)	P4:freq(C2)	P5:ampl(C2)	P6:- - -
value	85.55 V	72.35 V	3.3 mV	2.54317 kHz	72.35 V	

Fig. 4. Maximum output voltage (up- at output 50V/div, down-output to ground 100V/div)

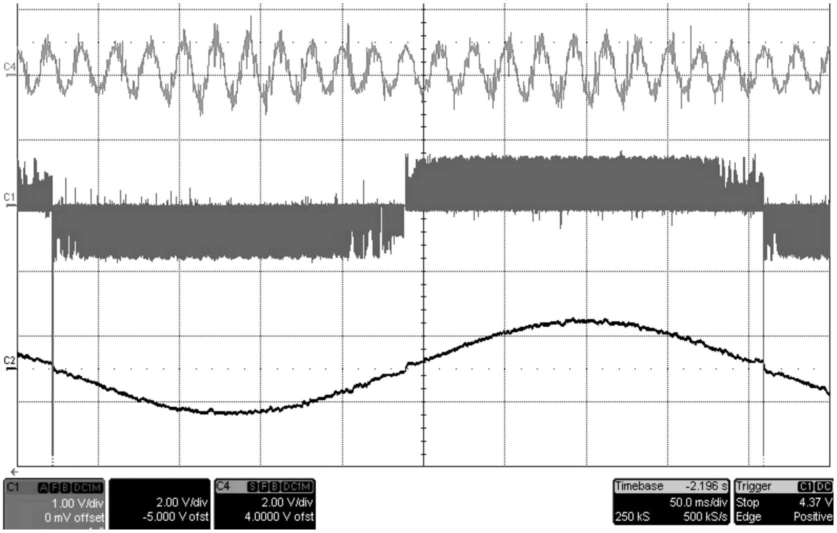

C1 1.00 V/div 0 mV offset
2.00 V/div -5.000 V ofst
C4 2.00 V/div 4.0000 V ofst
Timebase -2.196 s 50.0 ms/div 250 kS 500 kS/s
Trigger Stop 4.37 V Edge Positive

Fig. 5. Matrix Converter 3/2 (up – input phase current 2V/div 1V≈1A , center – output voltage 1V/div 1V≈50V , down – output current 2V/div 1V≈1A)

3 Indirect Matrix Converter 3/3

Two-stage or generally called Indirect Matrix Converter is a special type of direct frequency converter. In comparison with conventional Matrix Converter 3/3 makes possible to practice detach input and output stage connected through DC link, without big energy storage elements. The power part of the converter is illustrated on Fig. 7. The power part is composed from input Four Quadrant Current Source Rectifier, which was described previously and output part formed on VSI. This configuration bears some important benefits: simplest commutation of output and whole converter (compared to conventional Matrix Converter) and possibilities of multi-output stage converter.

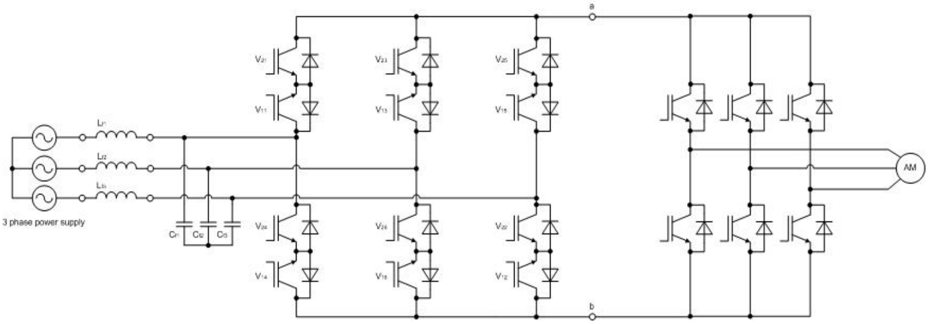

Fig. 6. Indirect Matrix Converter 3/3

3.1 Experimental Results

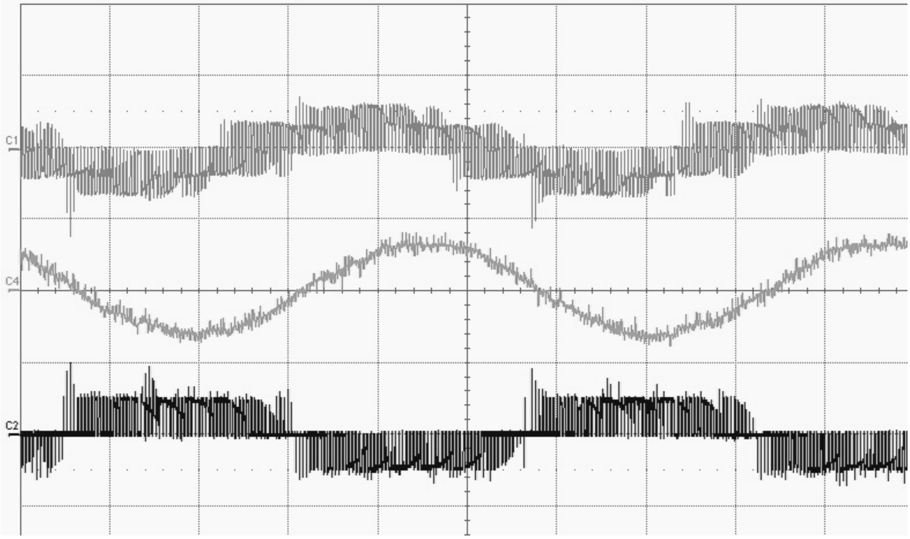

Fig. 7. Indirect Matrix Converter 3/3 (up – output phase voltage 50V/div, center – output phase current 200mV/div 1V≈1A, down – output line to line voltage 100V/div), output frequency 18Hz

4 Conclusion

There was proved some methods of control for Matrix Converters. Experimental results acknowledge the right way in development of those modulation strategies and was confirmed some advantages of conception of Indirect Matrix Converter. Matrix converters have better operation in cases where is needed four quadrant operation, lower harmonic emission and low compact dimensions then conventional voltage source inverter. Complicated commutation, rather complex method of control, behavior during distortion of input voltage and lower voltage at output are disadvantages of those converters. Future work will be focused on tune of those methods for implementation of modern regulation algorithms (vector control or direct torque control).

5 Acknowledgements

The support for this research work has been provided by the GAČR project 102/05/H525: The Postgraduate Study Rationalization at Faculty of Electrical Engineering and Computer Science VSB-TU Ostrava. Next acknowledgments are intended to my supervisor prof. Petr Chlebiš, CSc and the Department of Electronics. My studies has been also supported by the scholarship of Ostrava.

References

1. Jussila, M., Salo, M., Kähkönen, L. Tuusa, H..: A Vector Modulated Three Phase Four Quadrant Rectifier, Institute of Power Electronics, Finland (2004)
2. Osmancik, L.: The Four Quadrant Current Source Pulse Rectifier by DSP Controlled, Diploma thesis, VSB-TU Ostrava (2005)
3. Kolar, J.W., Baumann, M., Schafmeister, F., Ertl, H.: Novel Three Phase AC-DC-AC Sparse Converter, Interactive Power Electronics Seminar
4. Empringham, L., Wheeler, P., W., Clare, J., C..: Intelligent Commutation of Matrix Converter Bi-directional Switch Cells using Novel Gate Drive Techniques, PESC (1998)

Adhesion Regulator with Doppler Radar

Pavel Pivoňka

Department of Electronics, FEECS,
VŠB – Technical University of Ostrava, 17. listopadu 15, 708 33 Ostrava – Poruba
`pavel.pivonka.fei@vsb.cz`

Abstract. In this paper there is described the principle of adhesion regulator with Doppler radar as a sensor of real velocity of locomotive. Advantages and disadvantages of different velocity sensors are also explained. Finally, there are presented simulation results of such regulator. Results are simply showing how this regulator works. Also they show, that regulator works fast and precise. This kind of regulator should be used on tramway, metro, suburb railways and any other transport, where accelerating and stopping is very often.

1 Introduction

Adhesion limit sets maximal power, what is possible to transform into traction force. If adhesion limit is exceed, wheels start spinning and overall traction force decreases dramatically. Adhesion limit is affected by many elements: shape of rails, mechanical construction of bogie, humidity, leaves, ice and other contaminants, what gets between wheel and rail. It is proved, that there is enough adhesion in little spin. With raising spin adhesion reach its top and then fall quickly, this leads into uncontrolled spin. Spin control is needed from beginning, because it is only way to prevent uncontrolled spin. To determine amount of spin, reference speed sensor is used. Reference sensor could be real (non tractive axle, Doppler radar, GPS), or mathematical model. By comparing spin, we are trying to keep tractive axle on top of μ-λ curve, where μ is friction coefficient between wheel and rail, λ is wheel slip and F_x is tractive force. Operating point is not exactly on top, it could even be in non stable part of curve. Behavior of F_x is hardly non linear and unpredictable, because we don't know value of μ at each time. The easiest way to get real speed is use of GPS, but it has one big disadvantage. It can't be used in tunnels, where due to air humidity μ is lower. It is necessary to use sensor, what works in tunnels. That's why Doppler radar is used. Doppler radar measures real speed of locomotive. System compares this speed with wheel speed and control traction engine to adhesion top. Slip is best between 5 – 15% and adhesion top is at about 10%.

© Václav Snášel (Ed.): WOFEX 2007, pp. 54–58, ISBN 978-80-248-1571-8.
VŠB – Technical University of Ostrava, FEECS, 2007.

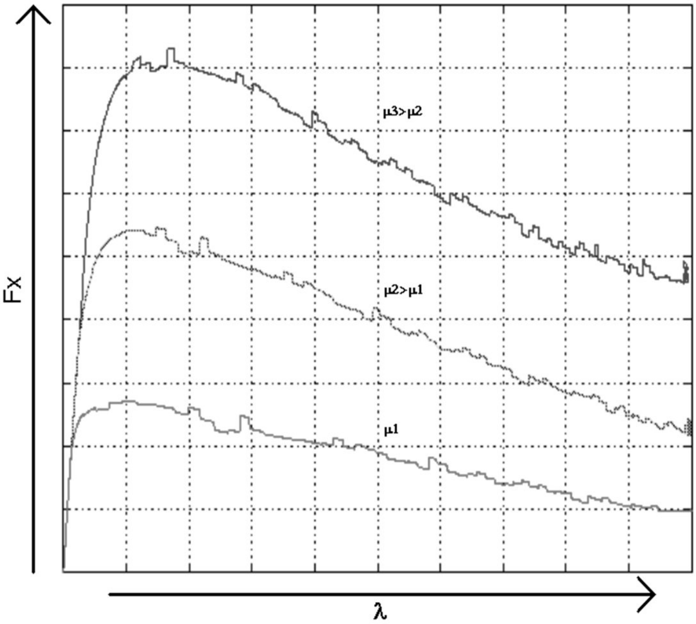

Fig. 1. Behavior of tractive force depending on friction and spin

2 Doppler radar

Doppler effect applies to electromagnetic waves same as to sound waves. Doppler effect is change of frequency originating from relative movement of receiver and transmitter. Amount of effect depends on frequency and velocity of wave (velocity of light for electromagnetic waves). Practically it is the same radar as police use to speed controls. Radar uses ground echo to determine its own speed.

3 Locomotive with 400t train – accelerate in areas with reduced adhesion

Simulation of train acceleration with tractive force limited to 250kN. Two areas with reduced adhesion.

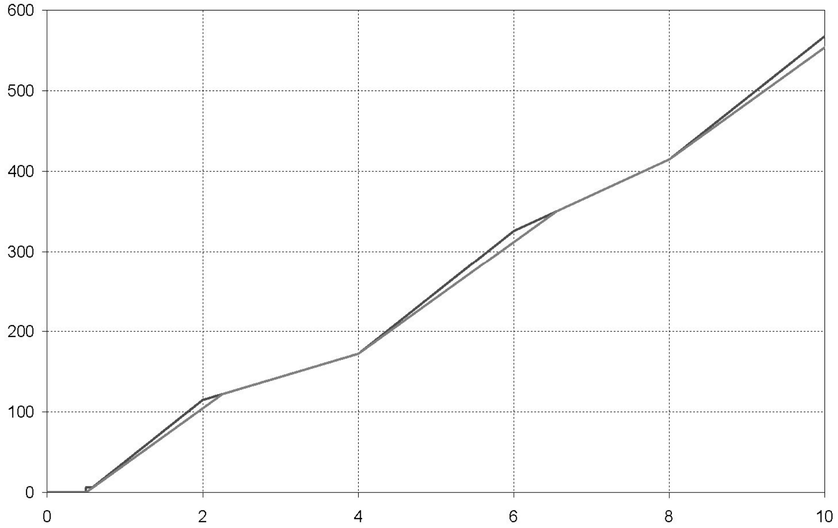

Fig. 2. RPM of traction engine

Axes: x – Time [s]; y – RPM [RPM]
Traces: Real speed + 10%; Wheel speed

In figure 2 we can see that in areas, where adhesion is enough, wheels are spinning in stable area of adhesion curve. Stable is spinning less than 10%. Blue trace is exactly 10% spin. In areas with lower adhesion wheel speed is about 10% spin. 10% spin is adhesion top, it is evident, that locomotive is accelerating as fast as possible.

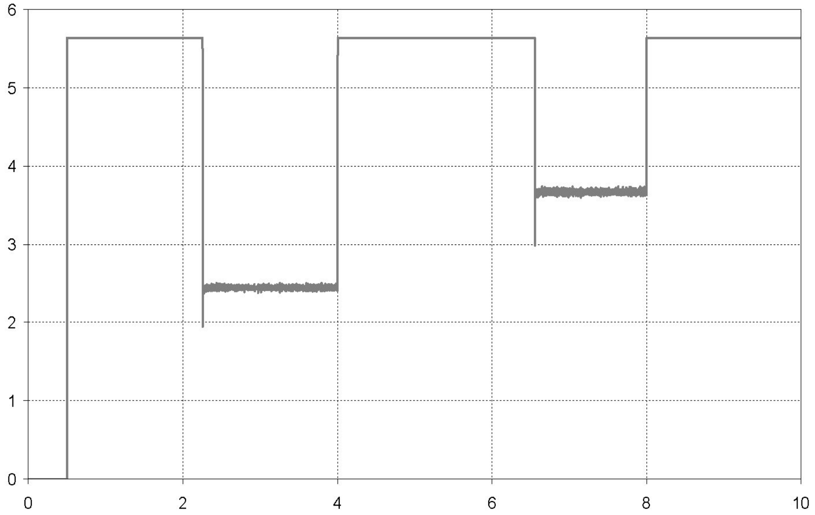

Fig. 3. Torque requested

Axes: x – Time [s]; y – Torque request [V]

Comparing Torque request with adhesion limit (Fig.5), we can see, that regulation is very fast. Amplitude of torque request is small and frequency is high. Torque request can't be constant, because we don't know adhesion level, but we are trying to maintain it.

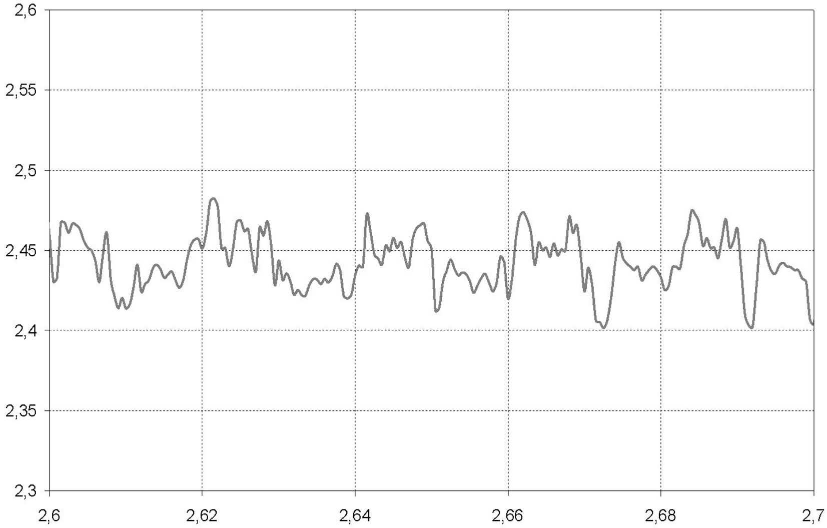

Fig. 4. Detail of torque request

Axes: x – Time [s]; y – Torque request [V]

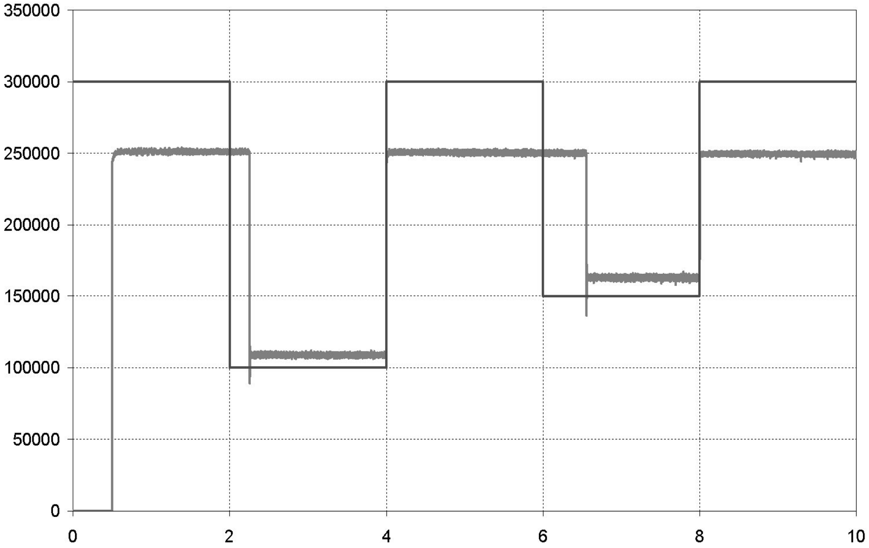

Fig. 5. Tractive force at wheels

Axes: x – Time [s]; y – Tractive force at wheels [N]
Traces: Adhesion limit; Real tractive force

In figure 5 we can see, that real tractive force is following adhesion limit. Differences are caused by simplification in Doppler radar model. If Doppler radar model is exact, tractive force is exactly following adhesion limit. Delay in fall of tractive force is caused by presumption of constant moment of inertia until wheel slip. At wheel slip, moment of inertia is step reduced. Really, if adhesion limit is lower than tractive force, moment of inertia is reduced fluently. Axle reach faster 10% slip and then is no more accelerated. In this simulation motor has to accelerate mass of all the train. That is why fall in tractive force is delayed. Difference in value of tractive force is caused by asynchronous motor model. Motor model presume all frictional forces at motor shaft. That is why tractive force is taller by all friction forces than adhesion limit. Really, friction forces are uniformly distributed all over the train and their points of action are behind point of limited adhesion, touch of wheel and rail.

4 Acknowledgment

The research was supervised by Prof. Ing. Petr Chlebiš, CSc. I would like also to express thanks to Department of Electronics, VŠB – TU Ostrava.

References

1. Kenneth R. Buckholtz: Reference Input Wheel Slip Tracking Using Sliding Mode Control, SAE 2002 World Congress Detroit, 2002
2. Christopher W. Jenks: Improved Methods for Increasing Wheel/Rail Adhesion in the Presence of Natural Contaminants, Transit Cooperative Research Program, 1997
3. Police Traffic Radar Handbook, http://copradar.com/

Control of the Switched Reluctance Motor with Current and Voltage Controller

Martin Polák

Department of Electronics, FEECS,
VŠB – Technical University of Ostrava, 17. listopadu 15, 708 33 Ostrava – Poruba
martin.polak.fei@vsb.cz

Abstract. Much of the classical theory in electric drives is based on the d.c. machine, in which torque is proportional to flux and current. The flux and current are controlled independently; both in space and in time. In switched reluctance machines unfortunately, there is no equivalent of field-oriented control. Torque is produced in impulses and the flux in each phase must usually by built up from zero and returned to zero each stroke [1]. This paper introduces main advantages of the switched reluctance machines. Then the paper takes controlling quantities and block diagram of current and voltage control this machine. There are simulation results at the conclusion.

1 Introduction

A reluctance motor is an electric motor in which torque is produced by the tendency of its moveable part to move to a position where the inductance of the excited winding is maximized. The motion may be rotary or linear, and the rotor may be interior or exterior. Generally the moveable part is a simple component made of soft magnetic iron, shaped in such a way as to maximize the variation of inductance with position. The geometrical simplicity is one of the main attractive features: since no windings or permanent magnets are use, the manufacture cost appears to be lower than other types of motor, while the reliability and robustness appear to be improved.

Electrical drives with switched reluctance motors (SRM), which are characterised especially by their simple construction, low price and high efficiency, also belong to the group of A.C. electrical drives. In spite of the mentioned advantages of switched reluctance motors, and the rapidly developing semiconductor and micro-processor technique, the number of commercially produced products is still very low, and to this day there is no universal way of design of electrical drive with switched reluctance motor and its control for a wider area of applications. At present many scientist workplaces try to develop mentioned universal design way of SRM drives.

Their main advantages are:

- simplicity and robustness
- high torque overload capacity
- high efficiency over wide speed-range
- low machine inertia

© Václav Snášel (Ed.): WOFEX 2007, pp. 59–64, ISBN 978-80-248-1571-8.
VŠB – Technical University of Ostrava, FEECS, 2007.

- decreased maintenance requirements

High efficiency of SRM results to use this motor in application of the runabout with battery source. Brushless construction allowed using in explosive environments. One of troubles of the control is strongly nonlinear motor model [1]. For example, in fig. 1 is complete set of magnetization curves of motor SR90.

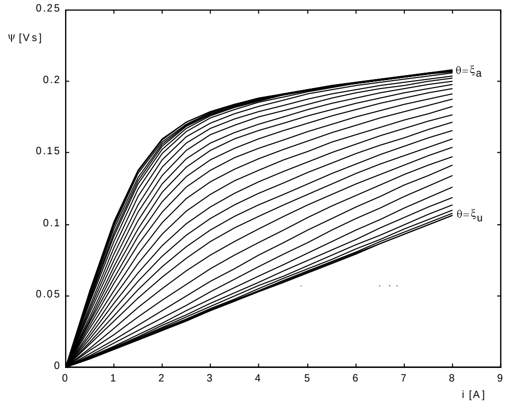

Fig. 1. Complete set of magnetization curves, showing flux-linkage vs. current for one phase, with the rotor at several positions between the unaligned and aligned positions. The aligned curve is the highest, and the unaligned curve is the lowest.

2 Control of SRM

The basic principle control of SRM is different from the routine method control of electrical drives with asynchronous motor or synchronous motors with permanent magnet. For SRM cannot be used specification space vector, show oneself very profitable be used numerical method in touch modern software resources at own description machinery and investigation his quality.

2.1 Controlling Quantities

The controlling quantities are amplitude of the phase current I_c with range 0 - I_{cmax}, turn-on angle θ_{on} and turn-off angle θ_{off} . The angle θ_{on} is determined by demand for braking or motoring regime. The control of the SRM can be described like the control in the range of low and high speed (fig. 2.). At lower speeds the torque is limited only by the current, which is regulated either by voltage-PWM, or instantaneous current regulation. As the speed increases the back-EMF increases to a level at which there is insufficient voltage available to regulate the current; the torque can then be controlled only by the timing of the current pulses. This control mode is called ‚single-pulse mode’ or ‚firing angle control‘, since the firing angles alone are controlled to produce the desired torque. Many applications require a combination of the high-speed and low-speed control modes. Even at lower speeds with voltage-PWM or current regulation, the firing angles are typically scheduled with speed to optimise performance [1].

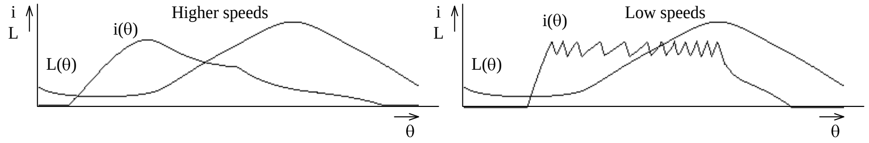
i
L
Higher speeds
i(θ)
L(θ)
θ
i
L
i(θ)
Low speeds
L(θ)
θ

Fig. 2. The waveform of stator inductance in one phase of SRM

2.2 Control of SRM with Current Controller

Figure 3 shows a speed control structure. Speed controller output is reference current i_{ref}, which is restricted to maximal value and to the current controller enter his absolute value at the beginning of each working motor cycle. To the block BRS enter in the desired speed of rotation Ω_{mref}, the speed of rotor rotation Ω_{mfb} from the block of speed calculation BVR and the speed controller output i_{ref}. Desired and actual speed is compared in the first step. If signs of both speeds are various then there are determined switching angle for braking motor operation and the motor is braking with commutation phase sequence destined for direction of rotation according by real speed Ω_{mfb}. After crossing the zero, the motor works with switching phases in sequence destined for rotation direction according to desired speed, and switching angles are determined according to sign of speed controller output i_{ref} for braking or motoring regime.

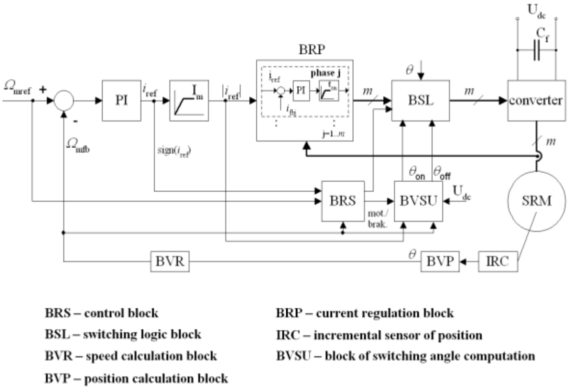
Ωmref
+
-
Ωmfb
PI
iref
Im
|iref|
BRP
iref
phase j
PI
ton
ifbj
j=1..m
m
θ
BSL
m
converter
Udc
Cf
m
sign(iref)
θon
θoff
BRS
BVSU
Udc
mot./brak.
SRM
BVR
θ
BVP
IRC
BRS – control block
BSL – switching logic block
BVR – speed calculation block
BVP – position calculation block
BRP – current regulation block
IRC – incremental sensor of position
BVSU – block of switching angle computation

Fig. 3. Block diagram of SRM speed control with current controller

The pulse signals from output position sensor IRC are evaluated in block of evaluation position BVP. Block of switch logic BSL interlock in dependence on motor operation, operating angles and rotor position, conduction times of individual phases with closure time of appropriate switching devices, which is determined by current controller in individual phases [2].

2.3 Control of SRM with Voltage Controller

Figure 4 shows a voltage control structure. Difference at that there is leaved out the current regulation block in the figure 3. The reference current i_{ref} is replaced proportional of time z. Meaning of the blocks is same as in the figure 3. Current waveform is given phase voltage. At least one of switches turns on and turns off with f_{PWM} and proportional of time z which is speed controller output at the beginning working cycle of motor [2].

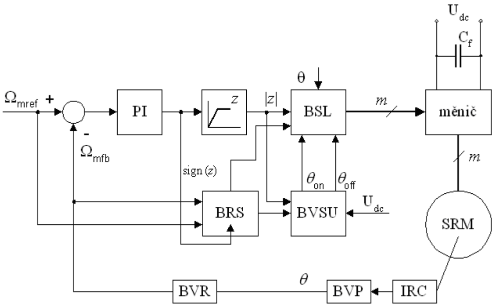

Fig. 4. Block diagram of SRM speed control with voltage controller. Meaning of the blocks is same as in the figure 3.

3 Simulation results

There are simulation results in figures 5 and 6. Figure 5 shows control of SRM with current controller where there is hysteresis regulation in the current regulation block. The hysteresis regulation is very simple. The main disadvantage is variable switch frequency. The frequency is depending on width hysteresis band. There is control of SRM with voltage controller in figure 6. There is demand on high switch frequency, so fast switching component and fast micro-processor technique.

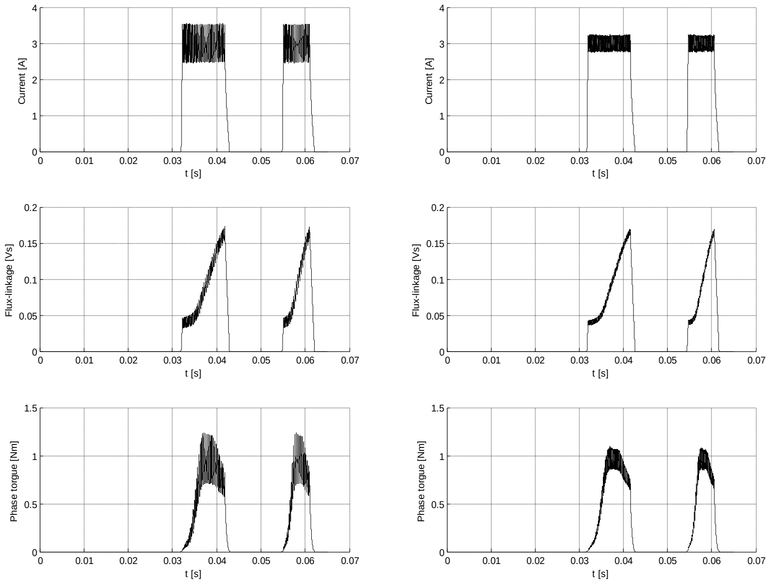

Fig. 5. Control of SRM with current controller. There is hysteresis regulation in the current regulation block. There is hysteresis band 2.5A – 3.5A on the left and 2.8A – 3.2A on the right.

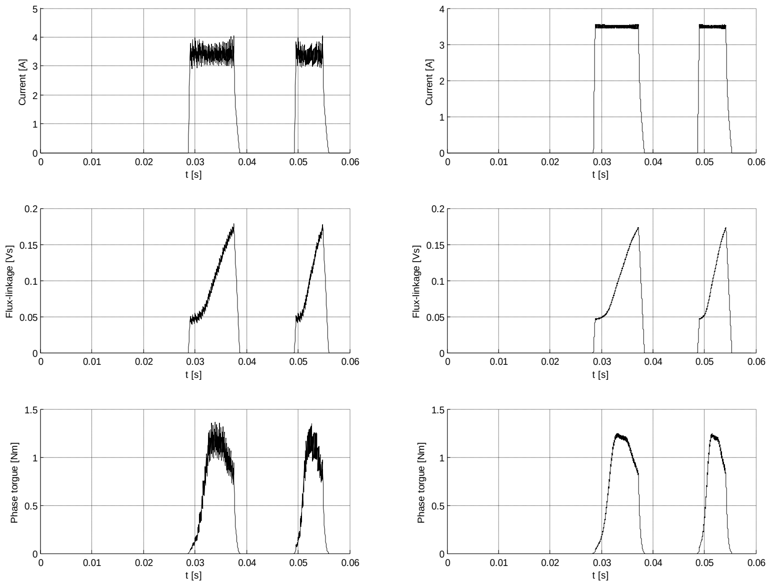

Fig. 6. Control of SRM with voltage controller. There is switch frequency 1kHz on the left and 10kHz on the right.

Acknowledgement

The support for this research work has been provided by the GAČR project 102/05/H525: The Postgraduate Study Rationalization at Faculty of Electrical Engineering and Computer Science VSB-TU Ostrava.

References

1. Miller, T. J. M.: Electronic of Control Switched Reluctance Machines. ISBN 0 7506 50737
2. Brandstetter P.: A.C. Control Drives – Modern Control Methods. VŠB-Technical University of Ostrava, 1999. ISBN 80-7078-668-X.

Loss-Minimization Algorithm for Induction Motors with Vector Control

Petr Skotnica

Department of Electronics, FEECS,
VŠB – Technical University of Ostrava, 17. listopadu 15, 708 33 Ostrava – Poruba
`petr.skotnica.fei@vsb.cz`

Abstract. This paper deals with the problem of loss minimization in the induction motor. Loss-minimization algorithm creates an optimal flux level. Loss minimization is dependent on the choice of the flux level. The higher of the flux level brings on the larger the loss in iron. Across higher minimization causes a high copper loss. In the paper are presented the simulations results of loss-minimization algorithm (LMA) with vector control of voltage-powered induction drive. These simulations were created in software Matlab-Simulink.

1 Introduction

There is many researchers, who are engaged with optimization of vector control drive. We can use optimization of IM drive with minimal stator current criterion, efficiency optimization and loss minimizing control. This paper introduces with loss-minimization algorithm, which guarantees optimal rotor magnetic flux level. Derivation of loss-minimization algorithm is mentioned in [1].

1.1 Region derivation

The torque speed plane is separated by different constraints into three regions (Fig. 1).
Region I: the constant torque limit region (below the rated speed)
Region II: the constant power limit region (field weakening region)
Region III: the constant power-speed limit region (above boundary speed)
Rated speed ω_n is expressed

$$\omega_n = \frac{U_{\max}}{\sqrt{L_s^2 I_{sxn}^2 + \sigma^2 L_s^2 \left(I_{\max}^2 - I_{sxn}^2\right)}} \tag{1}$$

and the boundary speed

$$\omega_c = \sqrt{\frac{L_s^2 + \sigma^2 L_s^2}{2\sigma^2 L_s^4}} \frac{U_{\max}}{I_{\max}} \tag{2}$$

The voltage constraint is given by

© Václav Snášel (Ed.): WOFEX 2007, pp. 65–70, ISBN 978-80-248-1571-8.
VŠB – Technical University of Ostrava, FEECS, 2007.

$$U_{\max}^2 \geq \left(\omega_e L_s I_{sx}\right)^2 + \left(\omega_e \sigma L_s I_{sy}\right)^2 \tag{3}$$

And current constraint

$$I_{\max}^2 \geq I_{sx}^2 + I_{sy}^2 \tag{4}$$

In each region we can derive the maximum available torque. For Region I is the maximum available torque expressed as

$$M_{m1} = \frac{3}{2} p \frac{L_h^2}{L_r} \sqrt{I_{\max}^2 - I_{sxn}^2} \tag{5}$$

Maximum torque M_{m1} is determined by the rated flux producing component and torque producing component of stator current at the rated speed.
For region II is expressed as

$$M_{m2} = \frac{3p}{2} \frac{L_h^2}{L_r} \sqrt{\frac{\left(U_{\max}/\omega_e\right)^2 - \left(\sigma L_s I_{\max}\right)^2}{L_s^2 - \sigma^2 L_s^2}} \sqrt{\frac{\left(L_s I_{\max}\right)^2 - \left(U_{\max}/\omega_e\right)^2}{L_s^2 - \sigma^2 L_s^2}} \tag{6}$$

The maximum torque is a function of ω_e and is determined by the intersecting point between the voltage limit curve and current limit curve. As the frequency increases, the stator voltage limit ellipse shrinks down gradually. Therefore, the level of intersecting point M_{m2} decreases with ω_e (shown in Fig. 2b).
And for Region III we obtain

$$M_{m3} = \frac{3}{2} p \frac{L_h^2}{L_r} \frac{U_{\max}}{\sqrt{2}\omega_e L_s} \frac{U_{\max}}{\sqrt{2}\omega_e \sigma L_s} \tag{7}$$

On the Figure 1 we can see characteristics of output torque at a fixed speed in each region.

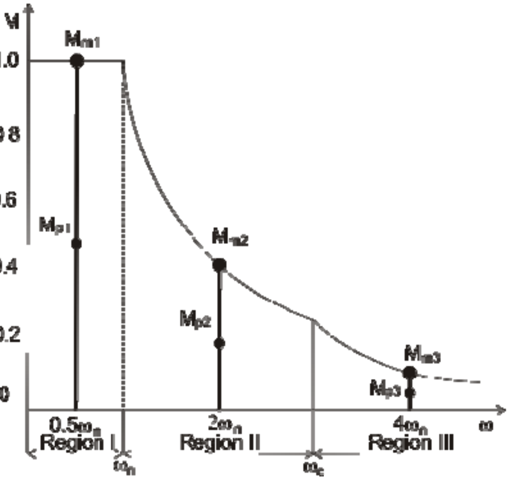

Fig. 1. Torque plot against speed

Fig. 2a, b and c represent the corresponding contours. In Region III, the total voltage limit curve can be contained inside current limit circle. Maximum torque boundary M_{m3} has nothing to do with the current limit.

The crossing points M_p are determined for each region. For Region I we obtain equation

$$M_{p1} = k_t I_{sxn} I_{sxn} \sqrt{\frac{R_x}{R_y}} = k_t \sqrt{\frac{R_x}{R_y}} I_{sxn}^2 \tag{8}$$

In Region II is M_{p2} the point where the linear curve intersect the voltage limit ellipse

$$M_{p2} = k_t \frac{\sqrt{R_x R_y}\, U_{\max}^2}{\left(R_x + R_y \sigma^2\right) \omega_e^2 L_s^2} \tag{9}$$

From M_{p2} to M_{m2} lies the optimal trajectory of the torque at a fixed speed on the voltage limit ellipse.

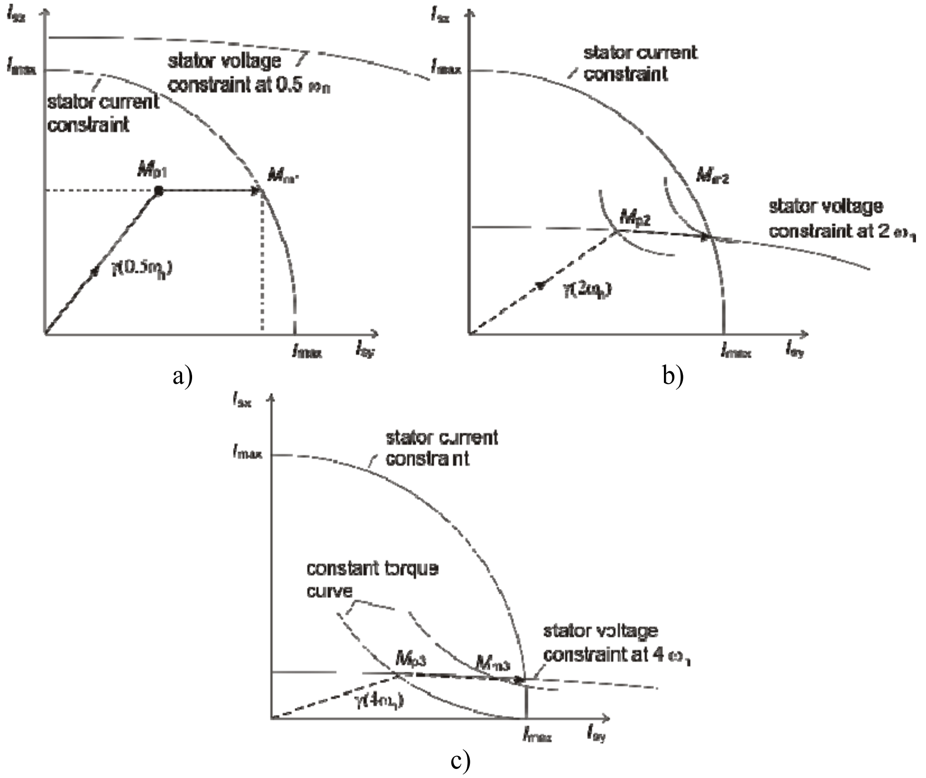
I_{sx}
I_{max}
stator voltage constraint at 0.5 ωn
stator current constraint
M_{p1}
$M_{m'}$
γ(0.5ωn)
I_{max}
I_{sy}
I_{sx}
I_{max}
stator current constraint
M_{m2}
M_{p2}
stator voltage constraint at 2 ω1
γ(2ωn)
I_{max}
I_{sy}
I_{sx}
I_{max}
stator current constraint
constant torque curve
stator voltage constraint at 4 ω1
M_{p3}
M_{m3}
γ(4ωn)
I_{max}
I_{sy}

a)

b)

c)

Fig. 2. Optimal constant speed contour **a)** Optimal constant speed ($0.5\omega_n$) contour in Region I; **b)** Optimal constant speed ($2\omega_n$) contour in Region II; **c)** Optimal constant speed ($4\omega_n$) contour in Region III

1.2 Control scheme

At the Fig. 3 we can see flux level generation scheme. At first we evaluate region, which is depended on given ω_e. Region I is given, if $\omega_e \leq \omega_n$. If $\omega_n \leq \omega_e \leq \omega_c$, it belongs to Region II. Region III is given, if $\omega_e \geq \omega_c$. Further happens to comparing actual torque M with precomputed values M_{p1}, M_{p2}, and M_{p3}. We can determine, that the point is in the interior or on the boundaries. If $M<M_{p1}$, $M<M_{p2}$ or $M<M_{p3}$ the operating point is located in the interior. If $M>M_{p1}$, $M>M_{p2}$ or $M>M_{p3}$ the operating point is located on the boundaries.

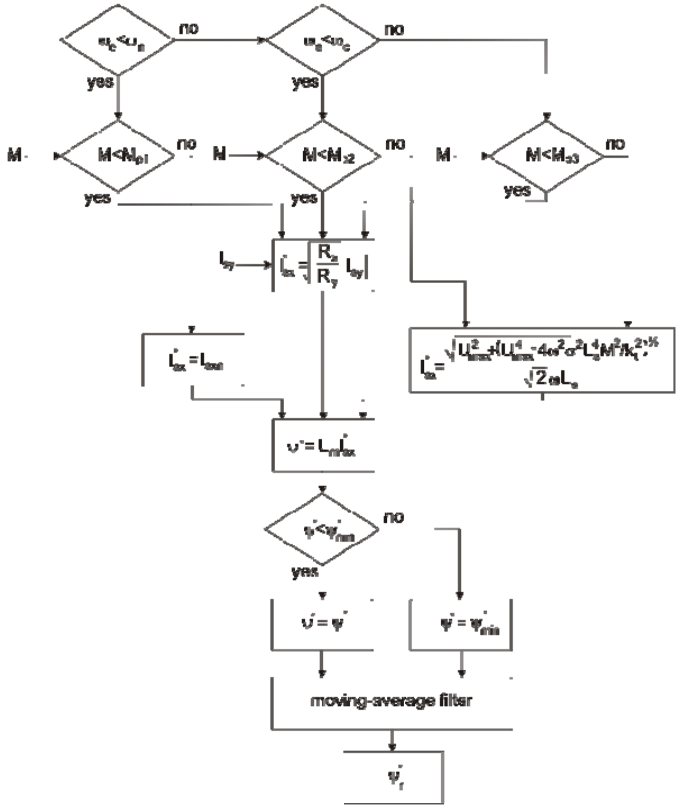

ω_e<ω_n
no
yes
ω_e<ω_c
no
yes
M
M<M_p1
no
yes
M
M<M_p2
no
yes
M
M<M_p3
no
yes
I_sy
I*_sx = √(R_x/R_y) |I_sy|
I*_sx = I_sxn
I*_sx = √(U²_smax + (U⁴_smax − 4ω²σ²L⁴_sM²/k_t²)^½) / (√2 ωL_s)
ψ* = L_m I*_sx
ψ*<ψ*_min
no
yes
ψ* = ψ*
ψ* = ψ*_min
moving-average filter
ψ*_f

Fig. 3. Optimal flux command generating strategy

If is $M<M_p(\omega_e)$, then we operate in interior. At the interior points, the optimal flux producing current level is proportional to torque producing current level. Then the optimal flux is given by

$$\psi^* = L_m \sqrt{\frac{R_x}{R_y}} \left| I_{sy} \right| \tag{10}$$

If $M>M_{p1}(\omega_e)$ in Region I, then the optimal flux is given by

$$\psi^* = L_m I_{sxn} \tag{11}$$

and it is constant.

If $M > M_{p2}(\omega_e)$ in Region II or $M > M_{p3}(\omega_e)$ in Region III, the optimal flux is given by

$$\psi^* = L_m \frac{\sqrt{U_{\max}^2 + (U_{\max}^4 - 4\omega_e^4 \sigma^2 L_s^4 M^2 / k_t^2)^{1/2}}}{\sqrt{2}\omega_e L_s} \tag{12}$$

If is calculated magnetic flux less than minimal, then is magnetic flux restricted to minimal value $\psi_{\min}$, which is constant.

2 Simulation results

In this section are presented simulation results of LMA. Simulation was performed with parameters of induction motor Siemens 1PV 5105-4WS15. Fig. 4 represents simulation results when speed command is set to 4000 rev/min and Fig. 5 when speed command is set to 2000 rev/min. Load torque 45 Nm is applied from 0.5 to 1.5 s and from 1.5 s is 10 Nm.

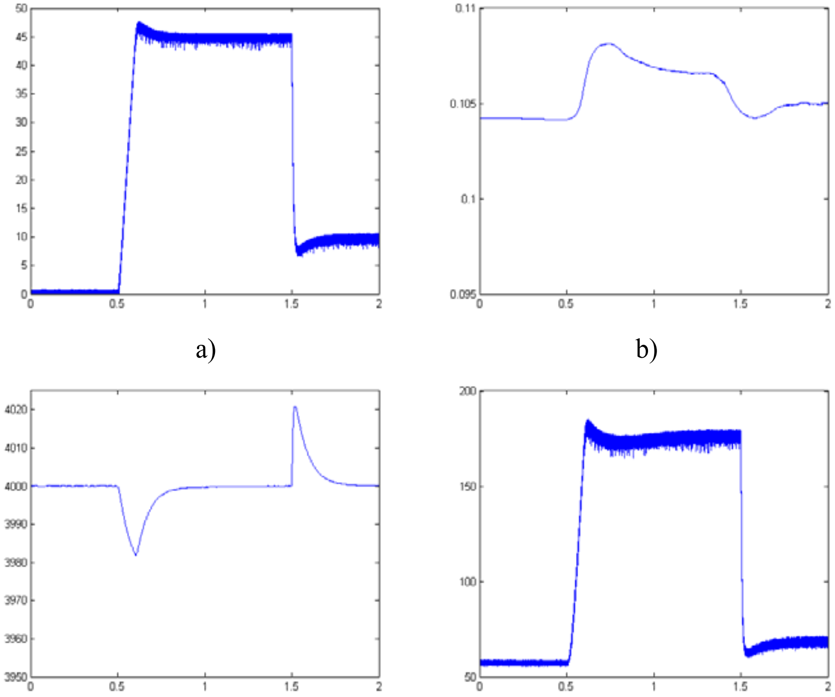

a) b)

c) d)

Fig. 4. Simulation results – speed command is set to 4000 rev/min a) Actual torque M [Nm,s]; b) Rotor magnetic flux ψ_r [Wb,s]; c) Actual speed n [rev/min,s]; d) Actual stator current I_s [A,s]

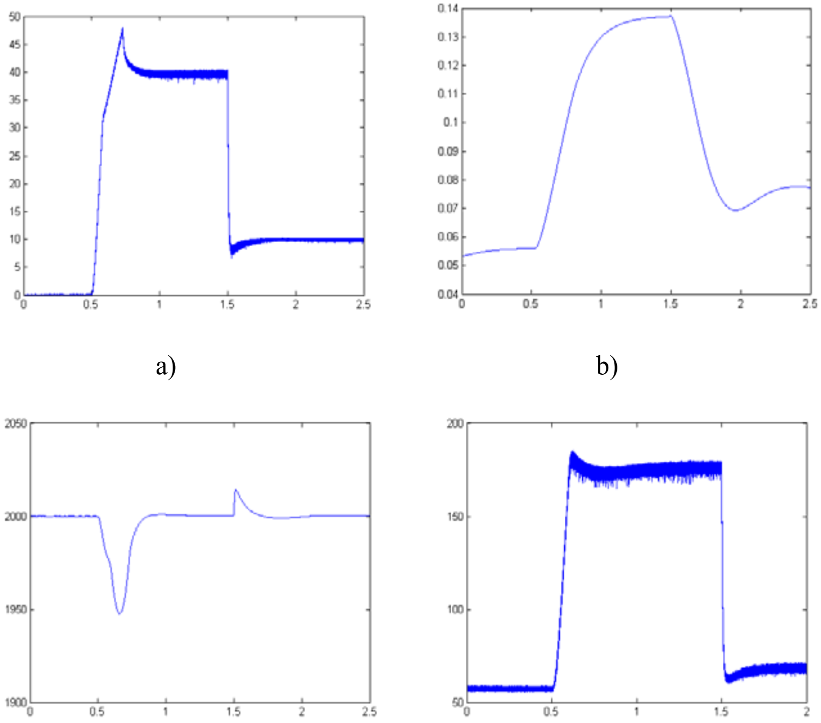

a) b)

c) d)

Fig. 5. Simulation results – speed command is set to 2000 rev/min a) Actual torque M [Nm,s]; b) Rotor magnetic flux ψ_r [Wb,s]; c) Actual speed n [rev/min,s]; d) Actual stator current I_s [A,s]

3 Conclusions

In this paper are presented simulations results of loss minimization algorithm. This algorithm was investigated in three regions by considering the voltage and current constraints. Algorithm ensures optimal rotor magnetic flux all over speed range for any load.

References

1. Lim, S., Nam, K.: Loss-minimising control scheme for induction motors. In IEE, p. 385-397. (2004)
2. Neborák, I.: Modelování a simulace elektrických regulovaných pohonů. VŠB – TU Ostrava, Ostrava. ISBN 80-248-0083-7 (2002)

Aplication of Radial Basis Function Network in Rotor Time Constant Adaptation

Ondřej Škuta

Department of Electronics, FEECS,
VŠB – Technical University of Ostrava, 17. listopadu 15, 708 33 Ostrava – Poruba
ondrej.skuta.fei@vsb.cz

Abstract. The paper presents simulation results of the method of rotor time constant adaptation with radial basis function network implemented. The estimated rotor time constant is used in vector control of A.C. drive with induction motor. The radial basis function neural network offers a viable alternative to the multi-layer feed-forward neural networks in many aspects. There were used various types of radial basis function at this work and they were compared with feed-forward ANN. In many cases, it presents higher training speed in comparison with ANN based on back-propagation training methods, they don't suffer from local minima in the same way as multilayer perceptrons, etc…

1 Introduction

Artificial neural networks (ANN) are mainly used in these types of application where the realization of another methods would be very difficult, expensive or even unrealizable. In these applications there is possible to take the advantage of the main features of neural networks, namely: approximation ability of different nonlinear functions, possibility to set their parameters in virtue of the experimental or learning data set, the quickness of information processing and their robustness. There is no necessary mathematical or structure description, there is possible to solve the problem just like the black box task with their inputs and outputs. In the field of praxis there is possible use of ANN in many tasks e.g.: classification, prediction, autoassociation, noise suppression, function approximation, etc…

The Radial Basis Functions (RBF) emerged like a variant of ANN in late 80`s by Broomhead and Love and their work opened another frontier. The radial basis function networks are powerful techniques which are built into a distance criterion with a respect to the centre. Such networks have 3 layers, the input layer, the hidden layer with the RBF non-linearity and the linear output layer. RBF networks have the advantage of non-suffering from local minima in the same way as multilayer perceptrons. The most popular choice for the non-linearity is the Gaussian. The output layer is in

© Václav Snášel (Ed.): WOFEX 2007, pp. 71–76, ISBN 978-80-248-1571-8.
VŠB – Technical University of Ostrava, FEECS, 2007.

regression problems a linear combination of hidden layer values representing mean predicted output.

Rotor time constant adaptation methods are used in the modern control of induction drive. The value of rotor resistor changes in dependence on drive load. To improve the motor power it’s necessary the identification of these parameters and adjusts them.

2 Method of Rotor Time Constant Adaptation

There where derivate the proper adaptive method of rotor time constant in the work [1]. There is displayed the block structure of vector control of induction motor with

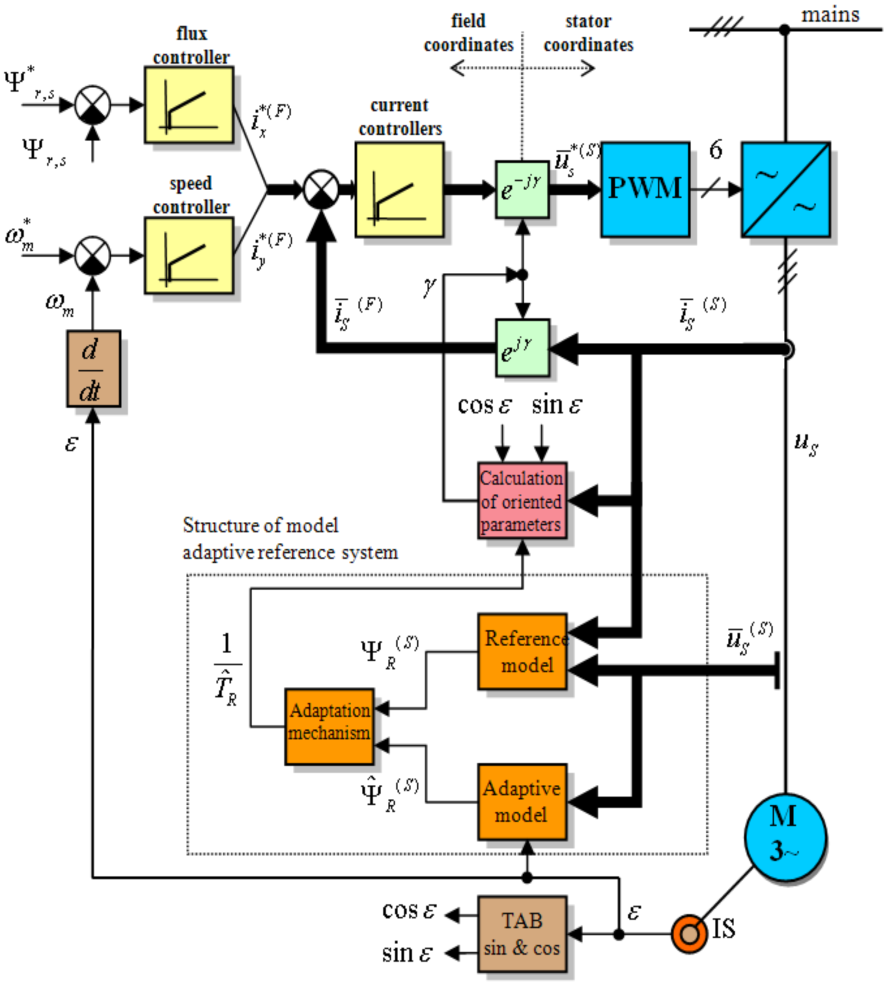
flux controller
field coordinates
stator coordinates
mains
$\Psi^*_{r,s}$
$\Psi_{r,s}$
$i_x^{*(F)}$
current controllers
$\bar{u}_s^{*(S)}$
$e^{-j\gamma}$
PWM
6
speed controller
ω^*_m
$i_y^{*(F)}$
ω_m
γ
$\bar{i}_S^{(F)}$
$\bar{i}_S^{(S)}$
$e^{j\gamma}$
$\frac{d}{dt}$
ε
$\cos\varepsilon$
$\sin\varepsilon$
u_S
Calculation of oriented parameters
Structure of model adaptive reference system
$\frac{1}{\hat{T}_R}$
$\Psi_R^{(S)}$
Reference model
$\bar{u}_S^{(S)}$
Adaptation mechanism
$\hat{\Psi}_R^{(S)}$
Adaptive model
M 3~
$\cos\varepsilon$
TAB sin & cos
$\sin\varepsilon$
ε
IS

Fig. 1. Control structure with adaptive system

the adaptation method of rotor time constant in the figure 1. The method is based on the comparison of two estimators, where one of them includes rotor time constant and we call it adaptive model. The other one does not include rotor time constant and is the so-called reference model. The error between them is used to derive an adaptation algorithm which produces the estimated value of rotor time constant for adaptive model. This value can be used for adaptation of rotor time constant in current model, which is used in the control structure of induction motor drive with vector control.
The adaptive model is based on application of current model of rotor flux. We often use it for the determination of the value and position of the magnetizing current vector or rotor flux vector. Current model contains the rotor time constant which is a changing parameter. The adaptive model it's described by following equation:

$$\hat{\Psi}_R^S = \int \left[\left(j\omega_R - \frac{1}{\hat{T}_R} \right) \hat{\Psi}_R^S + \frac{1}{\hat{T}_R} L_m \bar{i}_S^S \right] dt \tag{1}$$

The reference model is based on application of voltage model of rotor flux and is described by the following equation:

$$\bar{\Psi}_R^S = \frac{L_R}{L_m} \left[\int \left(\bar{u}_S^S - R_S \bar{i}_S^S \right) dt - \frac{L_S L_R - L_m^2}{L_R} \bar{i}_S^S \right] \tag{2}$$

The adaptation algorithm was derived in the work [1] and it's described by the following equations:

$$\Phi(e) = e_\alpha \left(L_m i_{S\alpha} - \hat{\Psi}_{R\alpha} \right) + e_\beta \left(L_m i_{S\beta} - \hat{\Psi}_{R\beta} \right) \tag{3}$$

$$e_\alpha = \left(\Psi_{R\alpha} - \hat{\Psi}_{R\alpha} \right), \quad e_\beta = \left(\Psi_{R\beta} - \hat{\Psi}_{R\beta} \right) \tag{4}$$

$$\frac{1}{\hat{T}_R} = K_1 \Phi(e) + K_2 \int \Phi(e) dt \tag{5}$$

$$\text{kde} \quad K_1 > 0, \quad K_2 > 0 \tag{6}$$

3 Types and training methods of RBF networks

The aim of this work was the application and comparison of artificial neural feed-forward network and the radial basis function network in the control of induction motor. These networks were used like an adaptation mechanism in the rotor time constant adaptation (fig.2). The proper radial basis neural networks were described in paper [2]. The aim it's also to describe the features of particular radial basis neural network types. There were used three training algorithms to test the main features of RBS neural networks [3]:

1. Forward subset selection
2. Ridge regression
3. Regression trees 1 & 2

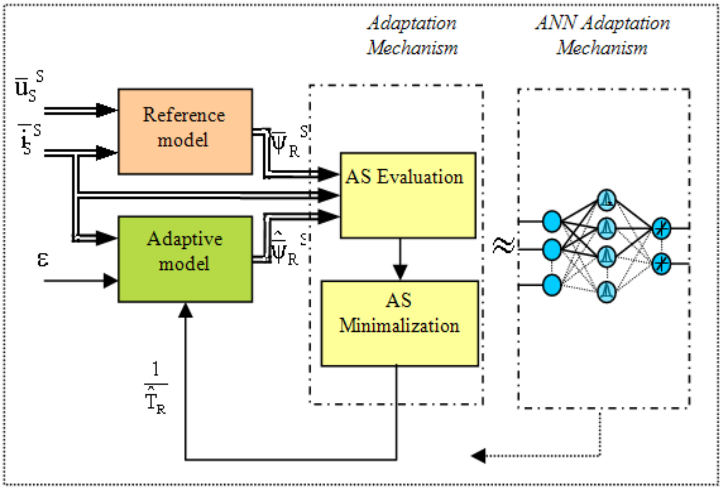

Fig. 2. Adaptation mechanism

From these training algorithms there were chosen like a useful for ours purpose just the Forward subset selection algorithm. The other methods should be useful for some other problems.

Figures 3 and 4 depicts RBF networks curve, which where trained by virtue of Forward subset selection algorithm. This algorithm was variously modified together with changes of the RBF network (e.g. activation function, radius…). Then there were presented different amount and types of training data sets. In the followed figures there are always two curves. The first curve, lighter one, shows the differences between the adaptation model output and the feed-forward ANN network. The feed-forward ANN were used in the work [1]. The second one shows the differences between the adaptation model output and the RBF network.

Figure 3 depict output of the most accurate estimation of rotor time constant, but the "price" of this accuracy is the higher number of radial basis units (136) in the hidden layer.

There weren't used the typical activation Gaussian function in the second type of RBF network, but Cauchy function. There were made other differences like changed parameters of the shape of radial activation function (bigger radius of coverage), etc… In the result there are less radial units (75).

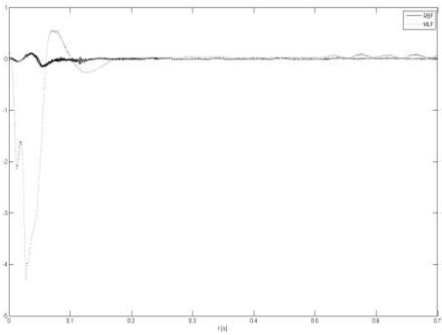

Fig. 3. RBF(136) and ANN network

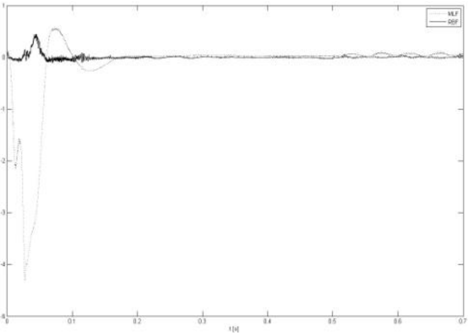

Fig. 4. RBF(75) and ANN network

4 Types and training methods of RBF networks

The structure of vector control of electric motor drive, depicted above, was simulated in Matlab-Simulink software and used for neural network verification. Also neural networks were trained in Matlab-Workspace. There were used modified m-files from the literature [3]. There were implemented many variations of RBF network. Figures shown below depict important curves of electrical drives with implemented RBF neural network. The controllers in this control structure of induction electric drive were adjusted in accordance with the parameters of this motor [1].

In these curves there is obvious smaller amplitude of estimated value instead of reference value (lighter curve). Electrical drive was set to start without load and after 0.5 seconds with load.

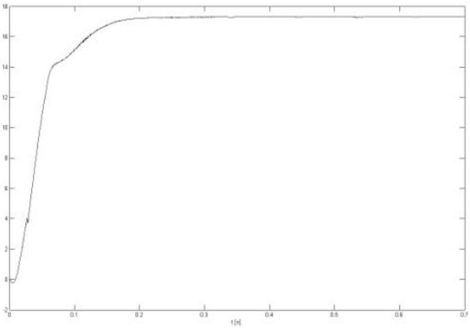

Fig. 5. 1/Tr = f(t) [s-1,s]

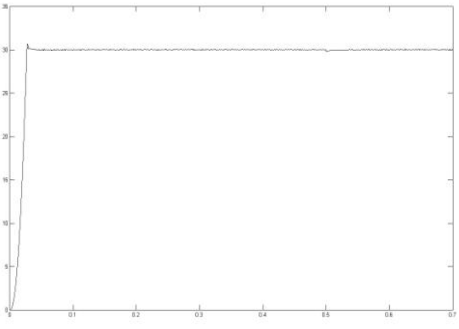

Fig. 6. n = f(t) [rpm., s]

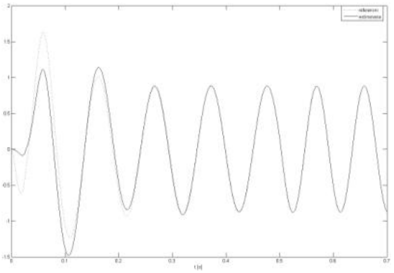

Fig. 7. $\psi_{s\alpha}$= f(t) [Wb, s]

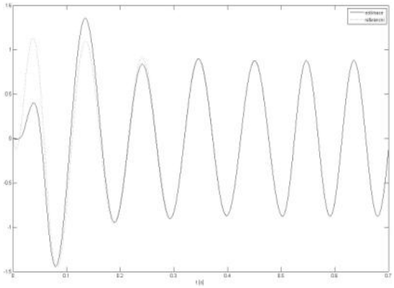

Fig. 8. $\psi_{s\beta}$= f(t) [Wb, s]

5 Conclusion

Presented implementation possibilities of radial basis function networks instead of feed-forward neural networks have a lot of advantages, but also some disadvantages. One of the most important features is the linear output combination of the values from the hidden nonlinear layer and their appropriate weights. This network architecture gives us the opportunity of online network weights adjusting, depending on the output of the whole network. Apparently disadvantage seems to be higher number of neural units. Not just only this but also the implementation on the signal processors is the field of the future research.

Acknowledgement

This research was supervised by Prof. Ing. Pavel Brandštetter, CSc. We would like also to express thanks to Department of Power Electronics and Electrical Drives, VSB-TU Ostrava. The research was supported by the Grant Agency of the Czech Republic with project No. 102/05/2080.

References

1. Čajka, R.: Application of artificial intelligence in electrical drives, dissertation work, Department of Electronic, VŠB-TUO, November 2006
2. Škuta,O.: Estimation of time-varying parameter of induction motor using radial basis function network, Workshop of Faculty of Electrical Engineering and Computer Science WOFEX, Ostrava, September, 2006
3. Orr, M. J. L.: Introduction to radial basis function networks, Centre of Cognitive Science, University of Edinburgh, 1996

Propagation of Voltage Dips in Transmission System

Josef Cigánek

Department of Electrical Measurements, FEECS,
VŠB – Technical University of Ostrava, 17. listopadu 15, 708 33 Ostrava – Poruba
`ciganekjosef@seznam.cz`

Abstract. A voltage dip is short duration, usually caused by a fault on the power system. In this paper I introduce a category of three-phase balanced and unbalanced voltage dips and a method for their characterization.

1 Introduction

Voltage dip is a sudden reduction of the supply voltage to a value between 90 % and 1 % of the declared voltage Uc, followed by a voltage recovery after a short period of time. Conventionally the duration of a voltage dip is between 10 ms and 1 minute. The depth of a voltage dip is defined as the difference between the minimum rms voltage during the voltage dip and the declared voltage. Voltage changes which do not reduce the supply voltage to less than 90 % of the declared voltage Uc are not considered to be dips.

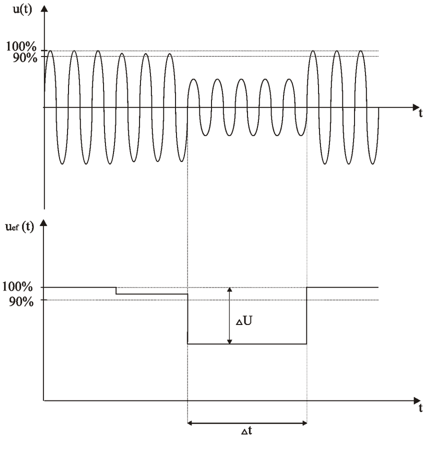

Fig. 1. Example of voltage dip

© Václav Snášel (Ed.): WOFEX 2007, pp. 77–82, ISBN 978-80-248-1571-8.
VŠB – Technical University of Ostrava, FEECS, 2007.

2 Causes of voltage dips

1. Motor starts:
    - sharp drop, slow recovery of voltage;
    - balanced voltage dip.
2. Transformer energizing:
    - sharp drop, slow recovery;
    - unbalanced voltage dip.
3. Short-circuit faults:
    - sharp drop, sharp recovery;
    - balanced voltage dip;
    - unbalanced voltage dip.

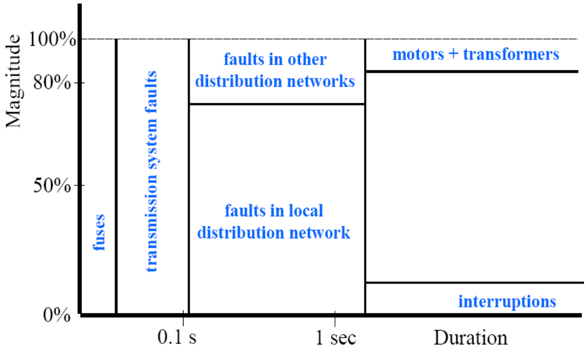
Magnitude
100%
80%
50%
0%
fuses
transmission system faults
faults in other distribution networks
faults in local distribution network
motors + transformers
interruptions
0.1 s
1 sec
Duration

Fig. 2. Causes of voltage dips

3 Voltage dip classification

The voltage dips can be classified into seven groups (figure 3). Type A is due to three-phase faults, types B, C and D are due to single-phase and phase-to-phase faults. Type B contains a zero-sequence component which is rarely transferred down to the equipment terminals. The voltage dips of type E, F and G are due to a two-phase-to-ground fault. An overview of the different types of voltage dips due faults is shown in Table 1.

Three-phase equipment is normally connected in delta or in star without neutral connection. Single-phase low-voltage equipment is connected between phase and neutral, but the number of dips originating in the low-voltage system is small. Therefore the vast majority of three-phase unbalanced dips at the equipment terminals are of type C or type D.

We considered for interpretation of voltage dips only dip type A for balanced faults and dip types C and D for unbalanced faults. For types C and D a further subdivision is needed to include the symmetrical phase (the phase with the large voltage drop for type D, the phase without voltage drop for type C). As a result is six types of three-phase unbalanced dips (C_A, C_B, C_C, D_A, D_B, D_C).

For description of voltage dips we use characteristics: characteristic voltage V and PN-factor F (positive-negative factor). Characteristic voltage is remaining complex voltage. Characteristic voltage is defined as:

$$V = \min(U_{A0}, U_{B0}, U_{C0}, \frac{U_{AB}}{\sqrt{3}}, \frac{U_{BC}}{\sqrt{3}}, \frac{U_{CA}}{\sqrt{3}}) \quad (1)$$

PN-factor is defined as:

$$F = \max(U_{A0}, U_{B0}, U_{C0}, \frac{U_{AB}}{\sqrt{3}}, \frac{U_{BC}}{\sqrt{3}}, \frac{U_{CA}}{\sqrt{3}}) \quad (2)$$

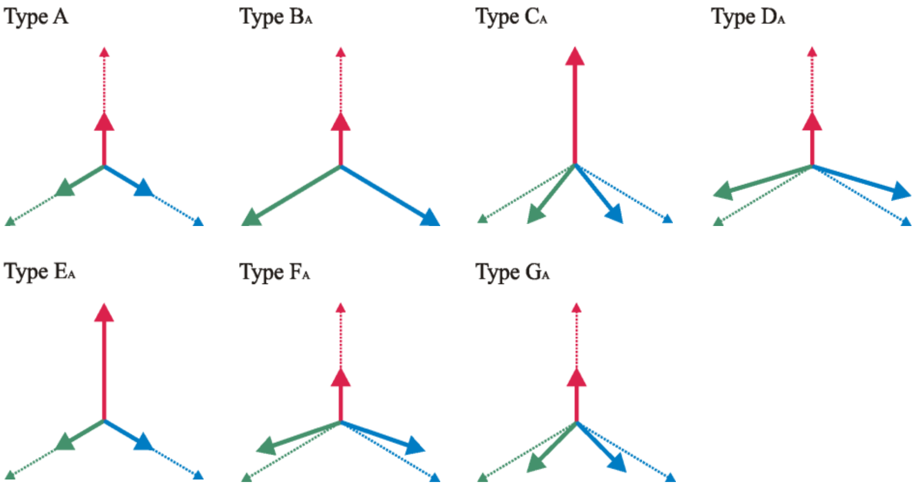

Fig. 3. Seven type of voltage dips

Table 1. Overview of different types of voltage dips

Dip type	Fault type
Type A	Three-phase
Type B	Single-phase-to-ground
Type C	Phase-to-phase (wye connected load)
Type D	Phase-to-phase (delta connected load) Single-phase-to-ground (zero-sequence-component removed)
Type E	Two-phase-to-phase (wye connected load)
Type F	Two-phase-to-phase (delta connected load)
Type G	Two-phase-to-phase (zero-sequence-component removed)

By introducing a second characteristic F, three additional effects are included:

- Positive and negative-sequence impedance are not exactly equal.

- The slowing down of induction motors due to the dip, leads to an apparent drop in source voltage. This will cause all three voltages to drop, but the effect is most obvious in the phases with a small initial drop.
- Two-phase-to-ground faults lead to a relatively large drop in voltage magnitude in the non-faulted phase.

4 Voltage dip propagation in transmission systems

Voltage dips in transmission systems are mainly due to system faults on transmission lines. Dips originating in transmission systems influence all the connected distribution systems since they can propagate downward without attenuation.

Transmission systems are normally loop-connected or mesh-connected. To predict the propagation of voltage dips, computer simulations are often performed.

Figure 4 shows a loop-connected system with five sites supplied by the generator at site A, which I created by using software ATP/EMTP. Table 2 gives the parameters of the system. The transmission lines between the stations are assumed all of length 50 km.

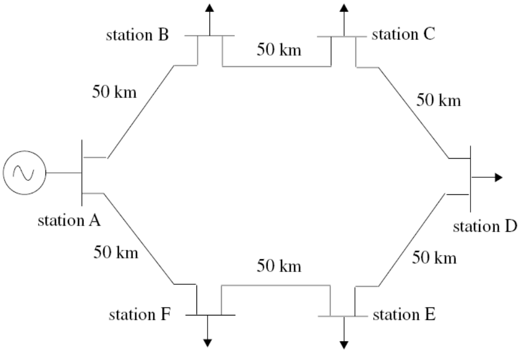

Fig. 4. A hypothetical loop-connected transmission network.

Table 2. Transmission line's parameters

Voltage	R_1 [Ω/km]	X_1 [Ω/km]	R_0 [Ω/km]	X_0 [Ω/km]	l [km]
400 kV	0,016	0,288	0,112	0,8	50

Simulations are performed for different types of faults at stations A, B, C, and D. Figure 5 through 7 show the characteristic magnitude and PN-factor at each site for four different types of fault.

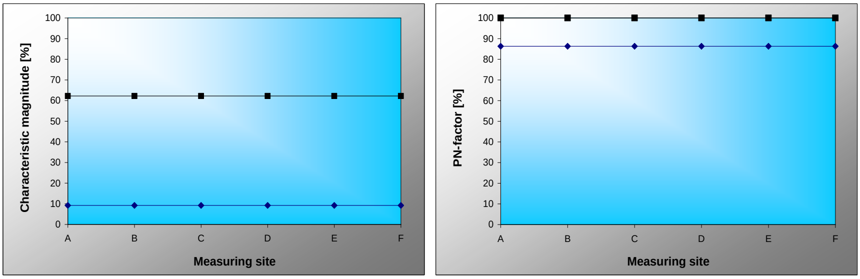

Fig. 5. Voltage dips resulting from faults at site A. (a) Characteristic magnitude vs. measuring site. ■ SLGF, ◆ LLF, 2LGF, 3ØF. (b) PN-factor vs. measuring site. ■ LLF, SLGF, ◆ 2LGF.

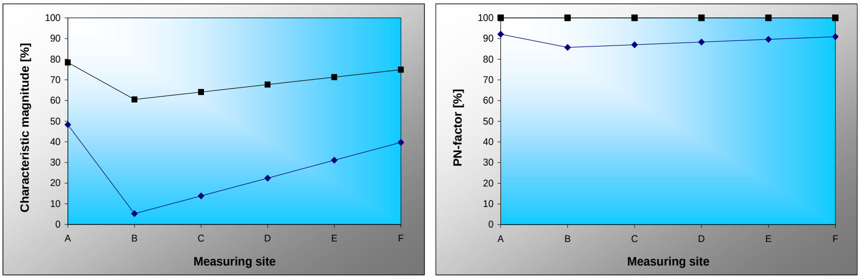

Fig. 6. Voltage dips resulting from faults at site B. (a) Characteristic magnitude vs. measuring site. ■ SLGF, ◆ LLF, 2LGF, 3ØF. (b) PN-factor vs. measuring site. ■ LLF, SLGF, ◆ 2LGF.

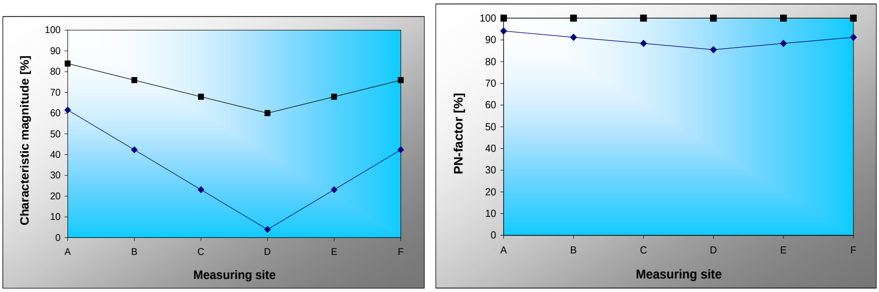

Fig. 7. Voltage dips resulting from faults at site D. (a) Characteristic magnitude vs. measuring site. ■ SLGF, ◆ LLF, 2LGF, 3ØF. (b) PN-factor vs. measuring site. ■ LLF, SLGF, ◆ 2LGF.

4 Conclusion

The characteristics of voltage dips in transmission systems show a similar behavior as dips in distribution systems:

- Dips due to SLGF and LLF have a PN-factor equal to 1, and the PN-factor doesn't change when the dips propagate through the power system. 2LGF has a non-unity PN-factor.
- Dips due to LLF, 2LGF, 3ØF at the same fault place have the same characteristic voltage, while dips due to SLGF have a higher characteristic magnitude.

However, in a mesh-connected network, it is hard to predict the characteristic magnitude when a dip propagates to different stations. Generally we can observe: The dip characteristic magnitude decreases when the fault moves nearer to the station bus-bar.

Acknowledgement

The support for this research work has been provided by the GAČR project 102/05/H525: The Postgraduate Study Rationalization at Faculty of Electrical Engineering and Computer Science VSB-TU Ostrava.

References

1. Cigánek, J., Turča, R., Barbořík, P.: Transmission of voltage dips in power system. Electric Power Engineering. Hotel Dlouhé Stráně, Kouty nad Desnou (2005). ISBN 80-248-0842-0.
2. Cigánek, J.: Charakter poklesů napětí v distribučních sítích. Kvalita elektrické energie, 3th Scientific Workshop. Penzion Beskydy, Visalaje (2006). ISBN 80-248-1033-6.
3. Cigánek, J.: Šíření poklesů napětí v distribučních sítích. Electric Power Engineering, 7th International Scientific Conference. Brno (2006), ISBN 80-214-3180-6.
4. Cigánek, J.: Propagation of voltage dips in three-phase system. VŠB-TU Ostrava FEI. Sborník konference Wofex (2006). ISBN 80-248-1152-9.
5. Cigánek, J.: Šíření poklesů napětí v distribučních sítích II. 6th Scientific Workshop. Duszniki Zdrój, Polsko (2006). ISBN 83-923118-3-3.
6. Cigánek, J.: Šíření poklesů napětí v přenosových sítích. Electric Power Engineering. Hotel Dlouhé Stráně, Kouty nad Desnou (2007).

Accuracy of DACF Models in Year 2006

Martin Galetka

Department of Electrical Power Engineering, FEECS,
VŠB – Technical University of Ostrava, 17. listopadu 15, 708 33 Ostrava – Poruba
`martin.galetka@vsb.cz`

Abstract. In this article is described the evaluation of accuracy DACF models in year 2006. DACF means Day ahead congestion forecast process which is running among European transmission systems operators and this process deals with prediction of congestion on next day in European power grid. Every transmission system operator (TSO) must prepare four mathematic models of his power grid on next day and must provide these models others TSOs. After acquisition and merging all models every TSO can calculate flows in his power grid and can prepare a measure for the secure system operation.

1 Introduction

In continental Europe power transmission grids all users are connected synchronously from Portugal to Greece in one European grid. Purpose of connecting power grids served originally only for increasing of the grid operation reliability.

Grid behaviour and power flows were forecasted simply and grid operation was very stable. With extension of UCTE on whole continental Europe and because of changes in power engineering sector during last year's there are high transits of power across the Europe and unexpected changes of power flow in interconnected network. Main reasons of this situation are:

- Opening of the electricity market - This is connected with increasing quantum of cross border transmission exchange and their high variability, which are given the trend of prices in the whole region.
- Increasing of wind power plants capacity - Wind power plants have a very changeable production and they are used preferentially instead of classical power plants.
- Power engineering sector restructuring - separating of electricity production, transmission and distribution. Transmission system operators (TSO) have limited measures for the power flow control.

Due to the lack of timely information about neighbourhood's power grids and for necessity of the power flows prediction it has been established a process DACF – Day - ahead congestion forecast. This process deals with changing of the power grid data

© Václav Snášel (Ed.): WOFEX 2007, pp. 83–86, ISBN 978-80-248-1571-8.
VŠB – Technical University of Ostrava, FEECS, 2007.

by the mathematic models form. These models contain information about the topology, the generation, the consumption, the voltage in nodes, the balance and electrical parameters of grid elements. After downloading and merging of models each TSO can calculate load flow and on the base of the results analyse behaviour and congestions in the network. Then each TSO can prepare effective measures for congestion solution.

The expression congestion means a situation, when an arbitrary element in power grid is overloaded in base case or in the case of disconnection of arbitrary else element. In this case we are speaking about so-called N-1 criterion, which says, that loss of any power system element (transmission circuit, transformer, generating set, compensating installation) must not jeopardise the security of operation of interconnected network as a result of limits being reached or exceeded for current, voltage magnitude, stability etc. (UCTE operation handbook – policy 3).

There can be many reasons of grid congestions: disturbances in the grid, insufficient interconnection transmission grid, insufficient coordination, etc.

2 Statistical evaluation of the accuracy DACF models

The accuracy of DACF models is given of the difference between calculated forecasted power flows from DACF models and real flows which then flowed in power grid. Differences between DACF values and real values were evaluated on border connection of Czech power grid (Figure 1).

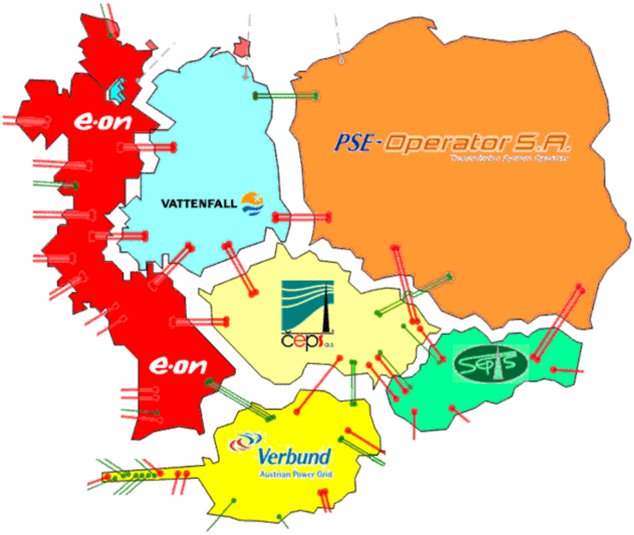

Fig. 1. Border connection of Czech power grid

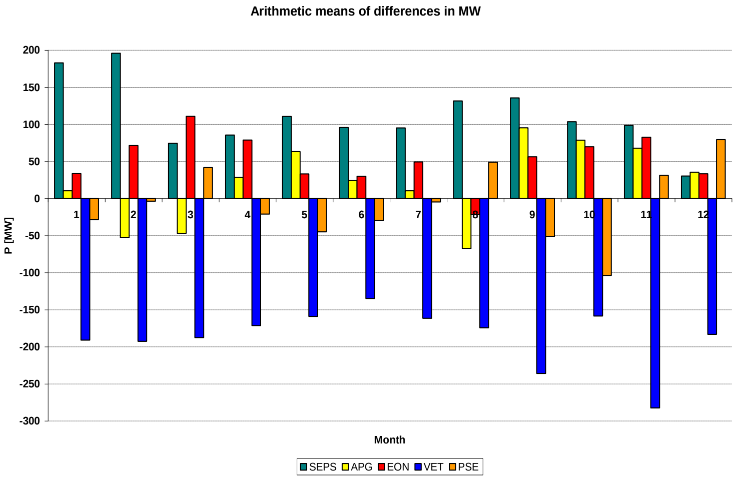

Fig. 2. Monthly arithmetic means of differences on border connection in year 2006

Figure 2 shows monthly arithmetic means of differences on Czech border connection in year 2006. The highest differences are on the border connection with Vattenfall (VET). After VET the border connection with SEPS has high differences too but these differences have the downward tendency. The border connection with EON has the similar trend like the border connection with VET. Border connections with PSE and APG have the most accuracy of Czech border connections.

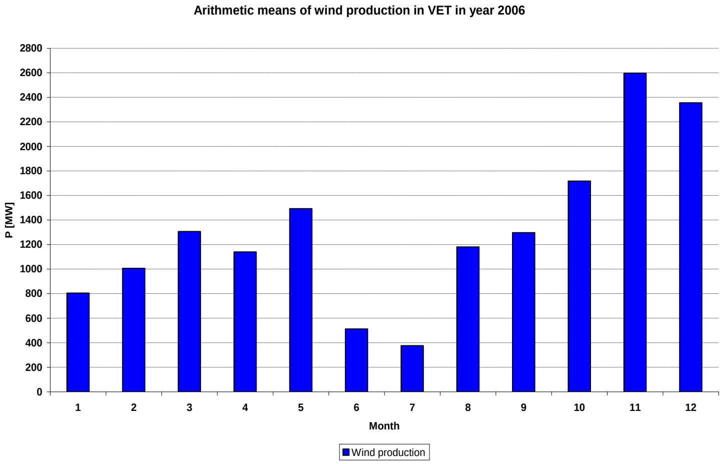

Fig. 3. Monthly arithmetic means of wind power production in Vattenfall

Figure 3 shows monthly arithmetic means of wind power production in area of German TSO Vattenfall in year 2006. It is evident from the graph that wind power capacity in Vattenfall is increasing. In comparison figure 2 with figure 3 we can see that monthly differences on the Vattenfall border connection have the similar trend like monthly arithmetic means of wind power production in Vattenfall because the highest differences are in spring and autumn when the wind production was highest in year 2006. We can say that differences on the border connection with Vattenfall depend probably on the accuracy of wind power prediction. The inaccurate wind power prediction causes probably the high difference on the border connection with Vattenfall and so this border connection has the highest differences of Czech border connection. The inaccuracy of wind power prediction has the influence on differences on the border connection with EON because the power generated in wind power plants in North Germany flows to place of consumption in South Germany in one part through the Czech power grid.

3 Conclusion

In year 2006 the highest differences between forecasted values from DACF and real values were on the border connection with German TSO Vattenfall. This border connection had the highest inaccuracy from all Czech border connection. This Situation was probably caused with the inaccuracy prediction of wind power production in German DACF models. We can say that with increasing wind power capacity the accuracy of DACF model depends more and more on prediction of wind power production.

References

1. Galetka, Chrapek: DACF in CEPS, Electric Power Engineering 2007
2. Chrapek, Švejnar, Máslo: Řešení úzkých míst v přenosové soustavě, Konference ČK CIRED 2006

Confrontation of Reliability Indices of Chosen Equipment and Elements

Martin Golasowski, Radomír Goňo

Department of Electrical Power Engineering, FEECS,
VŠB – Technical University of Ostrava, 17. listopadu 15, 708 33 Ostrava – Poruba
{martin.golasowski.fei,radomir.gono}@vsb.cz

Abstract. This paper deals with confrontation of reliability indices for conductor 22 kV and transformer MV/LV. We will use two distribution regions, database, which is created at the Department of Electrical Power Engineering VŠB-TU Ostrava and ČEZ 22/80 directive as input database. Results show that ČEZ 22/80 directive is out of date. This directive needs update. We can find causes of different values of particular databases.

1 Introduction

Principal aim of monitoring of events in distribution network is ensured reliability supply of electrical energy to customers conformable with network codex of distribution networks. Measure of reliability is possible to find from database of events by the help of global indices of reliability supply or else reliability indices of particular elements.

Reliability was begun to observe in the past Czechoslovakia in the year 1974. Operation technical rules ČEZ and SEP 2/74 was published in this year. Exclusive database of failures and outages rose in the year 1975 and was stopped in the year 1990. Department of Electrical Power Engineering VŠB-TU Ostrava helped to restore observation of reliability of distribution networks of the Czech Republic in the year 2000.

To determine the reliability of network elements and the supply of electrical energy to consumers, it is necessary to observe failures and outages in the transmission and distribution of electrical energy. The calculation of probably unsupplied energy is only possible just on the basis of results of reliability calculations. What is of great importance is the connection of databases of distribution regions to the overall database that will be continuously supplemented and broadened. In this way the statistically significant set of data will be created that will better and more quickly describe the real condition of network equipment.

© Václav Snášel (Ed.): WOFEX 2007, pp. 87–92, ISBN 978-80-248-1571-8.
VŠB – Technical University of Ostrava, FEECS, 2007.

2 Description of input database

For correct reliability analysis of systems is necessary the knowledge of input parameters. Best system behaviour apposite database record his condition. The result of analyses is the determination of the failure rate and mean failure duration for particular items of equipment or for group of equipments. With more detailed databases, other pieces of information may be found that are important for operators, such as the most frequent cause of failures, areas of the greatest amounts of undelivered energy, etc.
Data about reliability of equipment and elements of distribution system is as follows:

- failure rates of particular pieces of equipment and elements,
- outages of the piece of equipment due to maintenance and inspections,
- outages of the piece of equipment due to operating works on the piece itself and labour safety securing in the vicinity of live parts of the distribution system.

This data serves to evaluate properties of pieces of equipment already operated (or a piece of equipment of the certain type of the selected supplier), to select new pieces of equipment, to assess the time suitable for restoring pieces of equipment at the end of their lives, to choose the operating mode of the MV network node, and others.

2.1 Distribution regions

There was used only data for two distribution regions.

Database distribution region 10 is formed for year:
2000: 756 records and 83 arrays
2001: 850 records and 83 arrays
2002: 1273 records and 83 arrays
2003: 1109 records and 64 arrays
2004: 1077 records and 86 arrays
2005: 1161 records and 84 arrays

Database distribution region 11 is formed for year:
2000: 3125 records and 35 arrays
2001: 3243 records and 35 arrays
2002: 2965 records and 35 arrays
2003: 2684 records and 35 arrays
2004: 2829 records and 35 arrays
2005: 1895 records and 47 arrays

2.2 ČEZ 22/80 directive

ČEZ 22/80 directive is only one accessible file of input reliability parameters. ČEZ 22/80 directive determine identical reliability data for circuit breaker and outgoing circuit. Circuit breaker is more important element substation from the point of view of reliability, so it determines reliability of outgoing circuit.

These parameters are valid for whole ČEZ without consideration to specific conditions of each of distribution power utility. We can specify and divide these reliability parameters according to different rules. We have to know system of database of failures to do that.

2.3 Database of VŠB – TUO (Kat451)

This database consists of 7 distribution regions. We can determine failure rate of more equipment and elements than ČEZ 22/80 regulation. Database of distribution regions are different. So we can evaluate failure rate (in single distribution regions) for different number of equipment and elements.

3 Method of calculation of reliability indicators of equipment and elements

For the failure rate the following equation may be written:

$$\lambda = \frac{N}{Z \cdot P} \qquad (\text{year}^{-1}) \qquad (1)$$

where N = the number of failures (-),
Z = the number of elements of the given type in the network (-),
P = the considered period (year).

For the failure rate of the line (provided the uniform distribution of failure rate per unit of line length) the following is valid:

$$\lambda = \frac{N}{L \cdot 0{,}01 \cdot P} \qquad (\text{year}^{-1} \,.\, (100\ \text{km})^{-1}) \qquad (2)$$

where N = the number of failures (-),
L = the length of line of the certain (km),
P = the considered period (year).

For the mean duration of the failure the following is valid:

$$\tau = \frac{\sum_{i=1}^{N} t_i}{N} \qquad (\text{h}) \qquad (3)$$

where N = the number of failures of the element of the certain type (-),
t_i = the duration of the failure of the element of the certain type (h).

4 Evaluation of reliability indices of equipment and elements

These graphs represent reliability indices above cited database for conductor 22 kV.

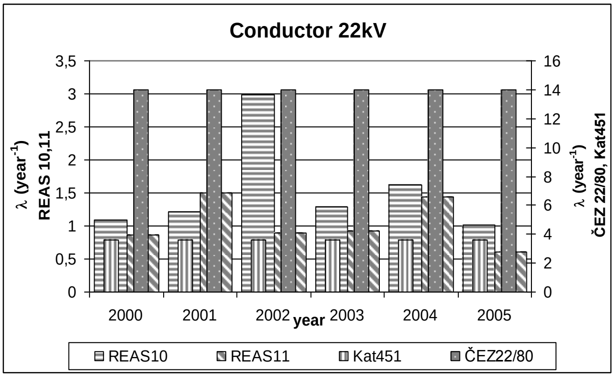

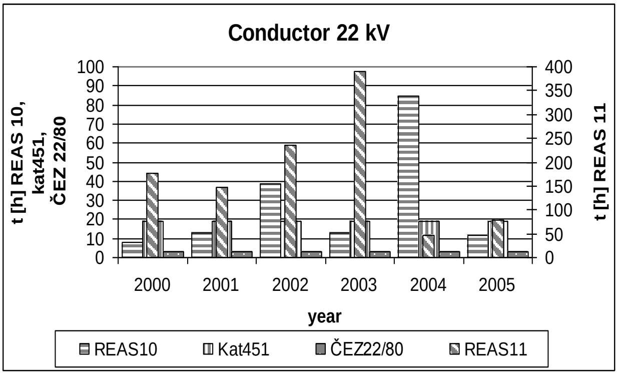

Graph 1 Tendency of reliability indices of conductor 22kV.

These graphs represent reliability indices above cited database for transformer MV/LV.

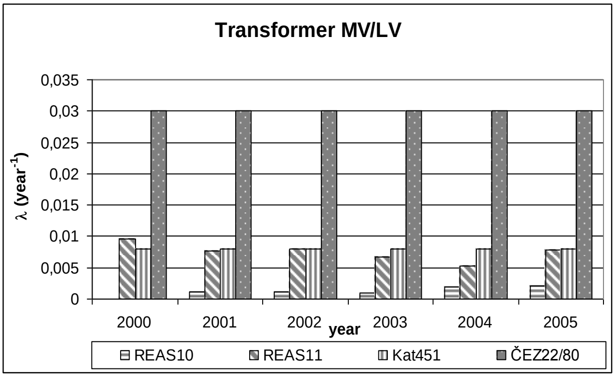

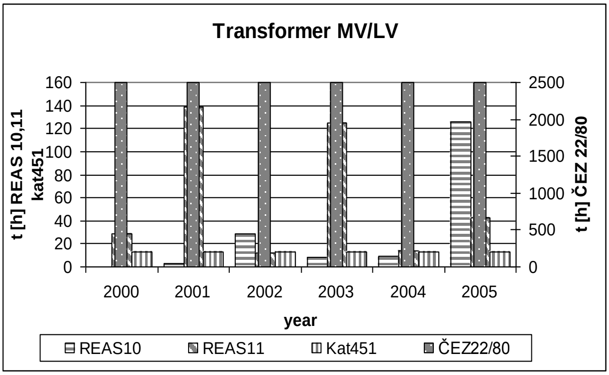

Graph 2 Tendency of reliability indices of transformer MV/LV.

5 Evaluation results of reliability indices of equipment and elements

Resultant graphs show that the failure rate of particular distribution regions is not such different. If we compare failure rate of distribution regions with VŠB-TUO database and consequently with ČEZ 22/80 directive, than we can see big differences.

Database of VŠB-TUO has not such different values for conductor 22 kV and transformer MV/LV than ČEZ 22/80. Database VŠB-TUO contains all distribution regions as well as two chosen for this article. Failure rate of ČEZ 22/80 directive has such different values because it is out of date.

Resultant graphs for mean time to failure show that values of particular distribution regions and kat451 have overvalues then ČEZ 22/80 directive for conductor 22 kV. Whereas values of ČEZ 22/80 for transformer MV/LV have overvalues then other database again. We can see values are out of data again.

6 Conclusion

This article deals with confrontation of failure rate in 2 distribution regions with ČEZ 22/80 directive and database, which is created at the Department of Electrical Power Engineering VŠB-TU Ostrava.

The biggest differences reliability of indices are between ČEZ 22/80 and other databases. Database VŠB-TUO contain all distribution regions (and two chosen for this article) has not such different values than ČEZ 22/80 directive. Different results of particular distribution regions are caused by territorial locality of particular distribution regions and appropriate climatic conditions. It primarily shows on conductors. Distribution regions, which have most of area location in mountain areas more effortful in time of disaster events (threatened points - fall of tree, branches etc.) and then longer mean time to failure occurs at failure. This mean time to failure can be lengthened by accessibility of the failure site.

Many years elapsed since the time directive was introduced and equipment and elements began to be made more advanced manufactured, better materials are used, isolated overhead lines are installed, cables with paper insulation were replaced by polyethylene insulated etc. Power network is much greater and much more appliances are connected into this network. This everything shows that ČEZ 22/80 directive is out of date. This directive needs update.

Department of Electrical Power Engineering VŠB-TU Ostrava wants determine new values of reliability indices by the help of creating database.

Acknowledgment:

This work is supported by the Czech Science Foundation - project No: GA ČR 102/05/H525.
This work is supported by The Ministry of Education, Youth and Sports of the Czech Republic - project No: CEZ MSM6198910007.

7 References

1. Rusek S.: Spolehlivost elektrických sítí, VŠB - TU Ostrava, ISBN 80-7078-847-X, 2001
2. Provozovatelé distribučních soustav: Pravidla provozování distribučních soustav, příloha č. 2. - Metodika určování spolehlivosti dodávky elektřiny a prvků distribučních sítí., 2004
3. Richtr a kol.: Provozně technická pravidla ČEZ 22/80
4. Golasowski M.,Rusek S., Goňo R.: Usage of database in electricity sector, Žilina, ELEKTRO 2006

Resonance in Power Supply System of AC Traction

Pavel Hořínek

Department of Electrical Power Engineering, FEECS,
VŠB – Technical University of Ostrava, 17. listopadu 15, 708 33 Ostrava – Poruba
`pavel.horinek@vsb.cz`

Abstract. This article be concerned with influence classification of alternating current system on overhead lines 110 kV and distribution point 400/110 kV. Spektrum of current harmonic components in distribution point 400/110kV needn´t be identical with a spektrum of current harmonic components on collector of driving vehicle, thanks rezonance in electric supply system.

1 Introduction

The electrical locomotives use at single-phase traction current system 25kV, 50 Hz behave like current power supply of harmonics. The size of current harmonic components at the distribution point 400/110 kV depends on the size of locomotive current harmonic components and on the traction supply circuit configuration. This circuit presents RLC circuit, in which resonances are generated. Some of the current harmonics are amplified during these resonances in the circuit traction. This one is characterized by current increment coefficient K.

$$K_{(\mathrm{n})} = \frac{I_{2(\mathrm{n})}}{I_{1(\mathrm{n})}} \qquad \mathbf{(1)}$$

where
$I_{2(\mathrm{n})}$ - (A) is the size of current n harmonic
component which is generated by locomotive
$I_{1(\mathrm{n})}$ - (A) is the n harmonic current increment coefficient

2. Mathematical model of AC traction

This chapter shows the model and the way of modeling of an unilaterally supply AC traction section for the resonant frequence calculation and the increment current coefficient K. There is a case, modeling a locomotive at the end of the fed section and case, when the locomotive is at the beginning of the supply section. In the models are influenced calculations of lengths of the outside leading 110kV (for 30, 40, 50 km).

© Václav Snášel (Ed.): WOFEX 2007, pp. 93–98, ISBN 978-80-248-1571-8.
VŠB – Technical University of Ostrava, FEECS, 2007.

The AC traction supply system is divided at these components:
equivalent system scheme 400kV
equivalent scheme of distribution point 400/110kV
equivalent lead schema 110kV
equivalent scheme of traction substation
equivalent scheme of contact line

Every mentioned schemes are replaced by two-port network, which is described by array. At the fig. 1 there is mentioned scheme of two-part network for the case, when the locomotive is at the end of the supply section and at the beginning of the supply section.

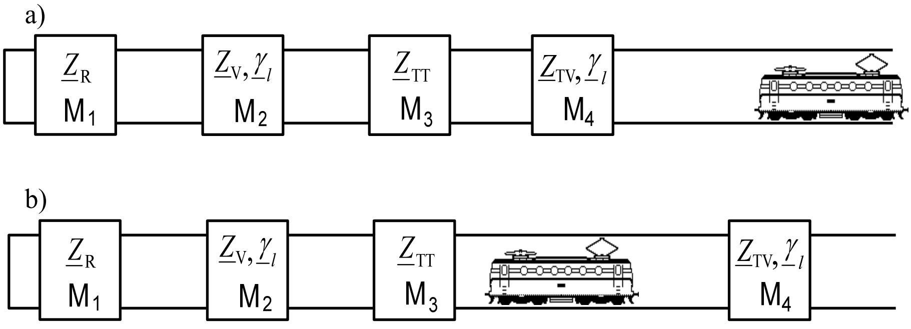
a)
$\underline{Z}_R$
M1
$\underline{Z}_V, \underline{\gamma}_l$
M2
$\underline{Z}_{TT}$
M3
$\underline{Z}_{TV}, \underline{\gamma}_l$
M4
b)
$\underline{Z}_R$
M1
$\underline{Z}_V, \underline{\gamma}_l$
M2
$\underline{Z}_{TT}$
M3
$\underline{Z}_{TV}, \underline{\gamma}_l$
M4

Figure 1. The supply AC traction model in bloc ordering
a) tractive unit (locomotive) at the end of the supply section
b) tractive unit (locomotive) at the beginning of the supply section

2.1 Equivalent scheme of system 400kV and substation 400/110kV

Substation 400/110kV contains transformer and his primary part is fed from lead 400kV. This equivalent scheme describes array M1:

$$\mathrm{M}_1 = \begin{pmatrix} 1 & \underline{Z}_R \\ 0 & 1 \end{pmatrix} = \begin{pmatrix} 1 & \underline{Z}_{TR} + \underline{Z}_{400kV} \\ 0 & 1 \end{pmatrix} \qquad \textbf{(2)}$$

where
$\underline{Z}_{TR}$ - (Ω) is an equivalent impedance of traction transformer, which is calculated from the short-circuit paramater
$\underline{Z}_{400kV}$ - (Ω) is an equivalent impedance of the supergrid, which is calculated from the short-circuit power in substation 400/110kV
In the calculation it is included dependence transformer active resistance.

2.2 Equivalent scheme of electric line 110kV

In the electric line 110kV it is necessary to account with wave characteristics of this electric line and for modeling to use a model with the spread parameters. The electric line 110kV is considered like homogenous and we model this one via equations which describes a long homogenous electric line.

$$\mathrm{M}_2 = \begin{pmatrix} \underline{A}_1 & \underline{B}_1 \\ \underline{C}_1 & \underline{D}_1 \end{pmatrix} = \begin{pmatrix} \cosh(\underline{\gamma} \cdot l_1) & \underline{Z}_\mathrm{V} \sinh(\underline{\gamma} \cdot l_1) \\ \dfrac{\sinh(\underline{\gamma} \cdot l_1)}{\underline{Z}_\mathrm{V}} & \cosh(\gamma \cdot l_1) \end{pmatrix} \tag{3}$$

where

$\underline{Z}_\mathrm{V}$ is a wave impedance of airline 110kV (Ω)
γ is specific a transfer coefficient
l_1 is a total electric line length (km)

In the calculation it is considered skin effect.

2.3 Equivalent scheme of traction substation

Equivalent scheme of traction substation, which includes single phase traction transformer 110/27kV is the same like the equivalent distribution point 400/110kV scheme. That means, that it is replaced by the resistance and transformer inductance.

$$\mathrm{M}_3 = \begin{pmatrix} 1 & \underline{Z}_\mathrm{TT} \\ 0 & 1 \end{pmatrix} \tag{4}$$

2.4 Equivalent traction line scheme

The contact line is considered as homogenous line (same like the electric line 110kV) and in the calculation it is modeled by equations which describes a long homogenous electric line.

2.5 The total supply circuit model of AC traction.

For the resonant rate determination it is necessary to calculate a total array M, which describes the total supply circuit from electric referent tractive unit header. It is showed in fig. 2.

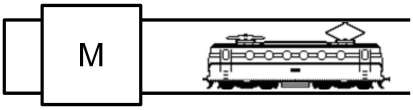

Figure 2. The total model of AC traction supply in the bloc ordering

The equivalent scheme array **M** (according to fig.1a), for case when traction unit is at the end of the supply section, it ensues from this equation:

$$M = M_4 \cdot M_3 \cdot M_2 \cdot M_1 \tag{5}$$

The case, when referential traction unite is at the beginning of the section (supply place), it is showed in fig. 1b. An array M is calculated according to equation 5.:

$$M = M_4' \cdot M_3 \cdot M_2 \cdot M_1 \tag{6}$$

For the increment current coefficient value it is possible to derive, that it is even like reciprocal coefficient D value of the total array M. According to this calculate methodics were calculated the increment current coefficients depending on the multiple of basic frequency 50Hz for two section case of traction unite at supply section.

3. Calculation results

There are dependences examples calculated for free different length of airline 110 kV (30, 40, 50 km) see fig. 3 and fig. 4. At fig. 3 there is a dependence of absolute value of rise current coefficient at basic frequency 50Hz multiple for traction unite at the supply section end. For confrontation, at fig. 4 there is traction unite at the supply section beginning. An increment current coefficient max value corresponds to parallel resonance in the traction circuit. Round about the resonant frequency there is the coefficient K values greater then one. It means, that the current harmonics, which corresponds to these frequencies, are more expressive in substation 400/110 kV than in current at referent traction unite header.

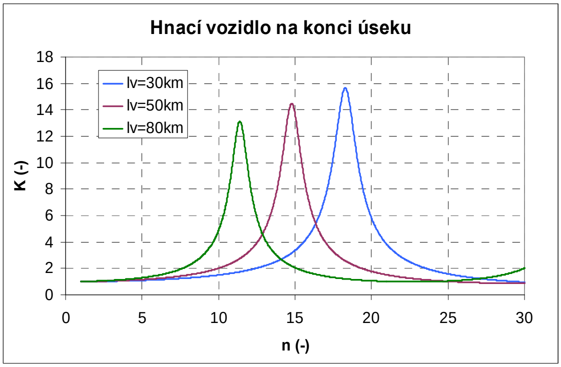

Figure 3. An increment current coefficient absolute value depends on frequence for traction unite at the section end.

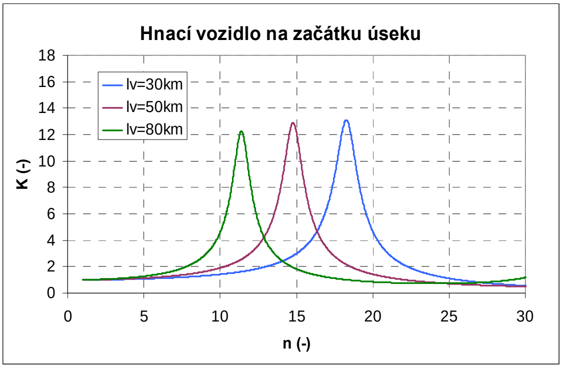

Figure 4. An increment current coefficient of the absolute value depends on the frequence for traction unite at the section beginning.

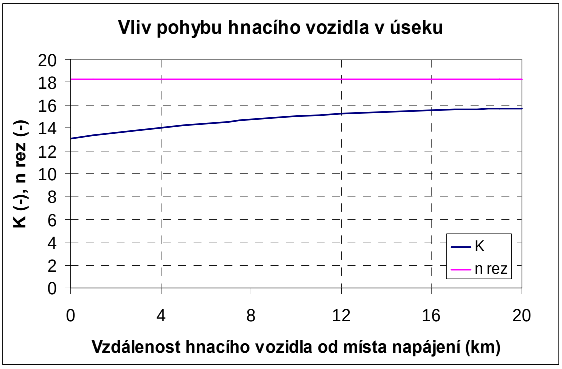

Figure 5. A coefficient K max value and a resonant frequnce value (for the traction unite in feed section) depends on electric line length 110kV – 30km.

4. Conclusion

The parallel resonant frequency value, of the AC traction supply circuit, declines with increasing length of the electric line 110 kV and it is not depend on the traction unite movement at supply section of the contact line. The series resonant value depends on traction unite movement at supply section.

5. Acknowledgement

The support for this research work has been provided by the GAČR project 102/05/H525: The Postgraduate Study Rationalization at Faculty of Electrical Engineering and Computer science VSB-TU Ostrava.

7. Published articles

1. HOŘÍNEK, P.: Fyzikální modely. In XXVII. Sešitu katedry teoretické elektrotechniky, Ostrava:VŠB - TU Ostrava, 2005, 92-102, 80-248-0770-X
2. HOŘÍNEK, P., PALEČEK, J.: Load balancing converters for 50 Hz railways. In sborník WOFEX 2005, 2005, 98-102, ISBN 80-248-0866-8
3. HORÁK, Z.; HOŘÍNEK, P.: Diagnostika napěťové nesymetrie trakční transformovny, XXVIII. Seminář Katedry teoretické elektrotechniky, Ostrava, r. 2005, VŠB – Technická univerzita Ostrava, ISBN 80-248-0853-6
4. HOŘÍNEK, P.: Výpočet elektrických parametrů venkovních vedení s podporou LabView. In Sešitu katedry teoretické elektrotechniky, Ostrava:VŠB – TU Ostrava, 2006,
5. HOŘÍNEK, P.: The analysis of the electric factor line with regard to transverse deflection in the overhead power transmission with LabView. In sborník WOFEX 2006, Ostrava:VŠB – TU Ostrava, 2006, ISBN 80-248-1152-9
6. HOŘÍNEK, P.: The computation of the electric characteristics in the overhead power transmission line with LabView. In sborník IWCIT´06, Gliwice, Polsko, 2006, EAN-9788390840994
7. HOŘÍNEK, P.: Rezonance v napájecím systému zabezpečovacích zažízení. In XXXV. Sešitu katedry teoretické elektrotechniky, VŠB – TUO, 2007, ISBN 978-80-248-1323-3
8. HOŘÍNEK, P., VIK, V., KIJONKA, J.: Prezentace studií z Teorie obvodů v PowerPointu. XXV. International Colloquium on the Management of Educational Process, Brno, Univerzita obrany, 2007, ISBN 978-80-7231-228-3
9. HOŘÍNEK, P., VIK, V., KHANH HUNG T.: Hodnocení zpětných vlivů trakčních odběrů na síť 110 kV. In Sborník ELECTRIC POWER ENGINEERING 2007, Dlouhé Stráně, VŠB – TU Ostrava, 2007, ISBN 978-80-248-1391-2
10. HOŘÍNEK, P.; HORÁK, Z.: Rezonanční poměry v trakčním obvodu jednofázové soustavy 25 kV, 50 Hz; XXXVI. Seminář Katedry teoretické elektrotechniky – Elektrizace železnic, Ostrava, r. 2007, VŠB – Technická univerzita Ostrava, ISBN 978-80-248-1444-5
11. HOŘÍNEK, P.: Use of virtual instrumentation to computation of electrical parameters of overhead lines. In sborník Transcom 2007, Žilina, Slovensko, 2007, ISBN-978-80-8070-694-4

Power and Reliability Test of Wind Power Plant

Jan Lindovský

Department of Electrical Power Engineering, FEECS,
VŠB – Technical University of Ostrava, 17. listopadu 15, 708 33 Ostrava – Poruba
`jan.lindovsky.fei@vsb.cz`

Abstract. Basic for evaluation is measuring, which run on wind power plant Mravenecnik 220kW in phase from 11.10.2005 to the 23.5.2006. Analysis has been carried out in light of average rate wind, instantaneous power and produced energy. Further there are analyzed types and failure frequency that occurred during running. Measured data was viewed, how long the power station was able to supply electric energy, how long was in failure and what was time of single failures.

1 Introduction

The purpose of this study was estimation of the trial running of wind power plant Mravenecnik with rate power 220 kW in term of power and reliability test. The measurement on the wind power plant of duration of 5 months was the basis for the evaluation of the study. Followed measured data was source for setting of time percentage from general time when the wind power station was able supply electric energy, types of failures, the lifetime of single failures.

2 Characteristics of wind power plants as energy resources

Wind power plants are ecologic resources of electric energy. When wind power plants work - greenhouse gas are not emitted into the atmosphere so that no produce global clime changes. Energy from the wind power plants is more expensive than energy from the fossil firings, but fossil firings is exhaustible resource with the negative environmental impact (e.g. fouling and heat water contamination). Wind power plants are safe (there is no danger of contaminate radiation as it is at the breakdown of the nuclear plant). Build – up of wind power plants presents concentrate of big electricity sources to more small ones. That reduces hazard of big power outages in the event of breakdowns of power grid and terrorist attacks. The cost of distribution of electricity and losses are lower too.

But wind power plants have some disadvantages [1]. Wind most time blows too slowly or too speedily, so that wind power plants supply at average only low part of nominal power. Practical result is essentially more highly price energy compared to classical power station. Energy output of wind power plants is very variable, no con-

© Václav Snášel (Ed.): WOFEX 2007, pp. 99–103, ISBN 978-80-248-1571-8.
VŠB – Technical University of Ostrava, FEECS, 2007.

trollable and unrelated with variability power consumption. Electrical energy has very bad storability so energy of wind sources must advance next source able instantaneous production. In reference to legislative regulation in ČR these costs pay common consumer instead of operator wind power station. Build-up wind power plants faces to cost increase on distribution of electricity. Happens to increasing power losses in consequence bigger load in a system and at the same time springs necessity their strengthening. It everything results in an additional cost that the again will pay final consumer. At major enlargement wind power plants faces every speed conversion fluxion to vehement changes supplied by power that the deteriorate stability power system. As an example it is possible bring in power system of Germany that isn´t controllable and for her stabilization is use Czech energy resources. There is a higher risk of blackout in power system [3].

3 Negative effect of wind power plants to electricity grid

The powers of wind power plant that is supplied to the power grid are very variable and they influence that way the power regulation (secondary, tertiary) inclusive dispatcher power reserve. At running electricity sector system is important that the production must stow consumption and it is always necessary to ensure reserve power for elimination of variation of power that the wind power station implicate.

Voltage variations of amplitude and frequency mainly result from the wind speed, but other factors play an important part, too. Voltage variations are directly related to real and reactive power variations. Wind power plant with asynchronous generator are consumers of reactive power, which can cause additional negative problem for the grid. Flicker effect results directly from this voltage variations, which occurs on the consumer load (lamp bulbs).

Next problem are harmonics, which result mainly from the operation of power electronic systems (converters). The effects of harmonics (voltage or currents) in the power system can lead to degradation of power quality at the consumer terminals, increase of the power losses, communication system malfunction, etc.

4 Results of measurement wind power plant Mravenecnik 220 kW

This wind power plant is operated by the CEZ company within a wind farm about general site rated power 1,165 MW in locality called Mravenecnik above Kouty nad Desnou. The farm is situated in the gap of the Medvedi mountain not far from Dlouhe Strane pumped storage hydro plant in Jeseniky mountains at the level of 1160 m above sea. It consists of three wind power plants of type designation Wind World W-2500, EWT 315 kW and EWT 630 kW.

In Fig.1 there is time behavior of instantaneous power of this power plant from 20.5.2006. We can see big power variability in dependence on the wind speed. At normal operation, the power output of a wind power plant can vary up to 15 % of installed capability within 15 minutes. Considerably larger variations of power production may occur during and after extreme wind conditions. This variability makes lot of trouble at integration of bigger number of wind power plants in the regulation system [3]. In the case of an imbalance between production and consumption, primary and secondary control is used to return to a balanced system.

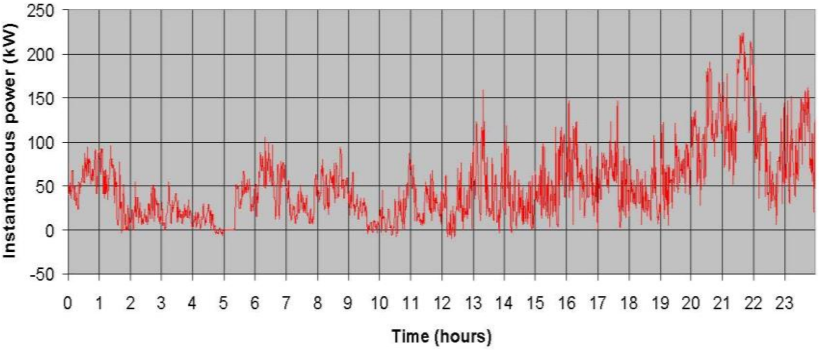

Fig. 1. Instantaneous power of Mravenecnik 220 kW from day 20.5.2006

For examination of a wind power plant in term of good location is wind speed priority in the area, which is represented in the Fig.2.

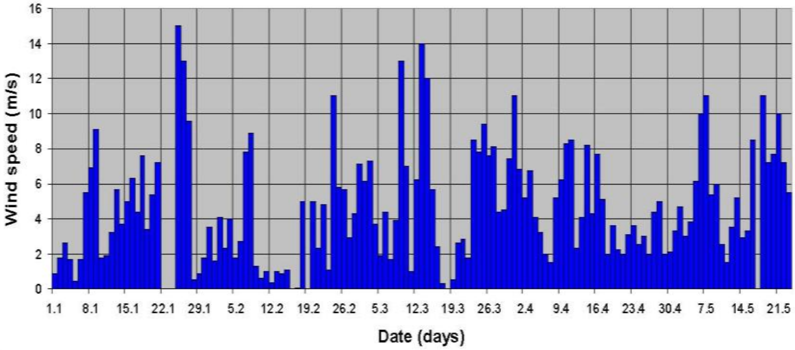

Fig. 2. Average wind speed in Mravenecnik locality

In the Fig. 3, there is produced energy of the period from 1.1.2006 until 23.5.2006. Wind power plant owing to failures (see Fig. 4) don′t use fully potential of wind and has very low availability ratio power. The energy costs (kWh) are higher then.

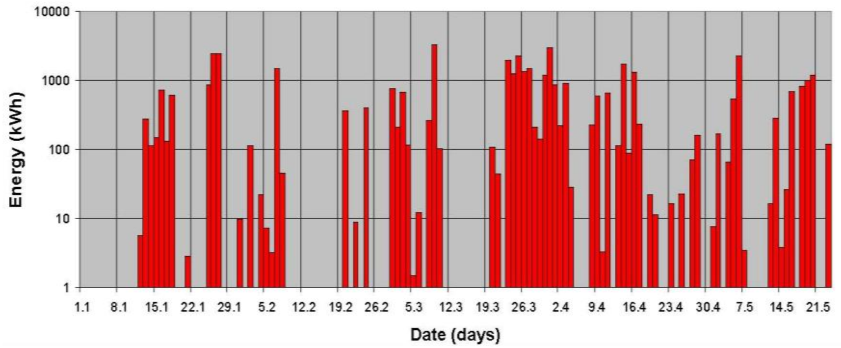

Fig. 3. Average power production of Mravenecnik 220 kW wind power plant

In term of failure frequency the low oil level hydraulics, overtemperature generator or missing signal from sensors signaling distortion cables was most often offer (see Fig. 4).

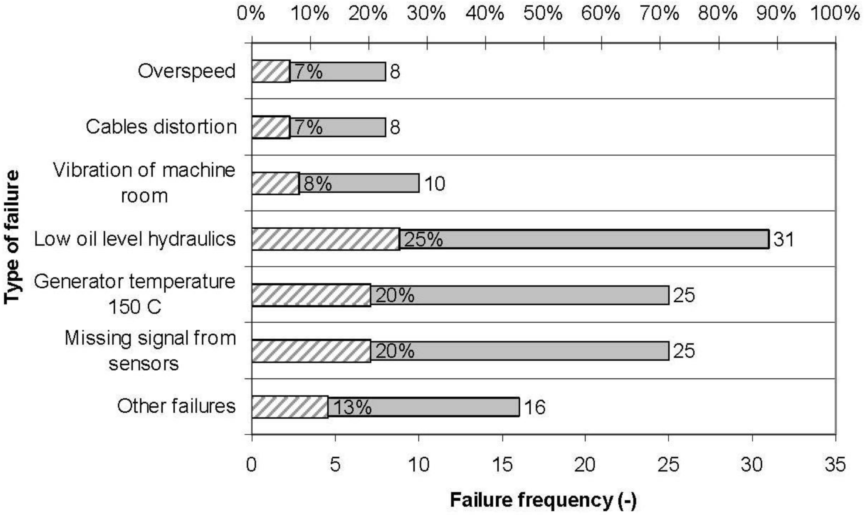

Fig. 4. Failure frequency of wind power plant

In term of total fault time was the longest failure due to overspeed. This failure takes 12 days out of servise from period under consideration. Long failure was cables distortion too when it takes 9 days out of servise from period under consideration. In the Fig. 5 there is mean time of single failures.

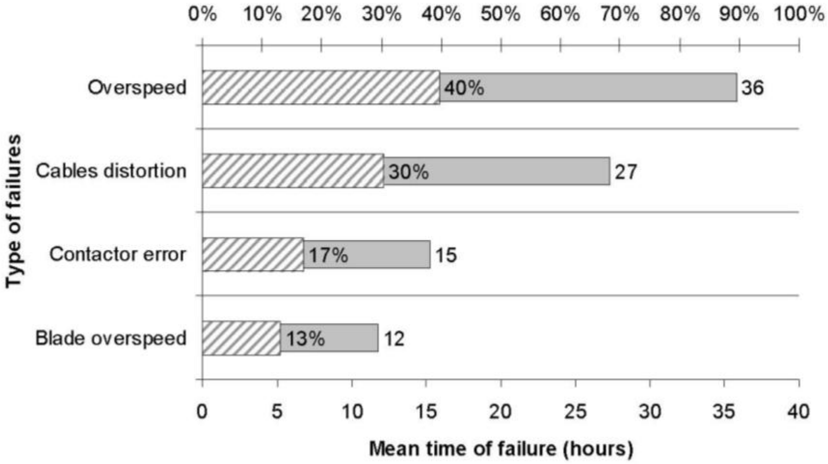

Fig. 5. Mean time of the longest failures

5 Conclusion

This paper was made for Danish Wind World W-2500 with rated power 220 kW. It results from measured that the wind power plant was in period from 1.1.2006 until 21.5.2006 (141 days) 25 days out of service in all. This statistic data show big fault liability of wind power plant given by amount of failures which are pointing to the system shutdown for few days. In therm of availability this locality and changing meteorological conditions that this wind power plant becomes problematic.

Because the energy contained in the wind is a function of the cube of its speed, small differences in average wind speeds can results in large differences in production output, and therefore cost.

This article was presented on the 8th international scientific conference electric power engineering 2007.

References

1. The free encyclopedia.: <http://cs.wikipedia.org/ >, (2006)
2. Ackermann, T.: Wind power in power systems, Royal Institute of Technology, Stockholm (2005)
3. Lubosny, Z.: Wind Turbine operation in electric power system, Poland (2003)

Acknowledgements:
This article was prepared in research within project VZMSM 6198910007.

Laboratory of Fuel Cells VŠB-TUO in period 2006/2007

Daniel Minařík, Karel Sokanský

Department of Electrical Power Engineering, FEECS,
VŠB – Technical University of Ostrava, 17. listopadu 15, 708 33 Ostrava – Poruba
{daniel.minarik.fei,karel.sokansky}@vsb.cz

Abstract. Hydrogen is the topic of the day. Mankind is challenged by depletion of fossil energy reserves to research and development new “alternative” source of electric energy. Very perspective for use in the electrical power engineering are fuel cells especially combination with renewable energy source. Subject and main intention of this papers is acquaint with fresh knowledge from research activities form new laboratory of fuel cells at VŠB-TUO. Concretely area of interest fuel cells technology, their characteristics, electric and operational characteristic and personal experience gained at experiments on low - temperature fuel cell. Experiments, tests and metering was done on the low-temperature NEXA Power Module with PEM technologies - Proton Exchange Membrane. Basic characteristic like load and operational characteristic are very important for better understand some process, which are following operation of fuel cell and his connecting to the electrical power network. Basic characteristic and some aspects of connecting to the network are explain in this article.

Keywords. Fuel Cell, PEM Fuel Cells, Hydrogen, Electricity Generation, Connecting of Fuel Cell, Inverter.

1 Opening new laboratory of fuel cells.

In June 11th 2007 was festively begun operation new laboratory of fuel cell at VŠB-TU Ostrava. In this new laboratory scope of research is oriented by two basic direction namely mobile application using hydrogen as energy carrier (project HYDROGENIX where is develop vehicle prototype for competition Shell Eco-marathon or new project Hydrogenix CITY where is developed prototype real vehicles for city traffic) and further, research of stationary application fuel cells for generation electrical energy. In December 2006 was activity of research, develop and realization team of laboratory appreciated by SIEMENS award for research.

© Václav Snášel (Ed.): WOFEX 2007, pp. 104–109, ISBN 978-80-248-1571-8.
VŠB – Technical University of Ostrava, FEECS, 2007.

2 Description and basic characteristic of NEXA Power Module.

Laboratory is equipped low temperature fuel cell type PEM - Proton Exchange Membrane, concretely fuel cell series NEXA Power Module with DC rated power 1200 W and rated voltage 43 – 26 V depend on operational load. The Nexa power module is a fully integrated system that produces unregulated DC power from a supply of hydrogen and air. Water and heat are the only by-products of their reaction. It contains a fuel cell stack, as well as all the ancillary equipment necessary for fuel cell operation. Ancillary subsystems include hydrogen delivery, oxidant air supply and cooling air supply. Onboard sensors monitor system performance and the control board and microprocessor fully automate operation.

1.1 Static characteristic of fuel cell.

Most important characteristic of fuel cell for interconnection with inverter and subsequent connecting to the electrical power network is his load characteristic (Fig.2). Load characteristic of FC module is very soft and output voltage is changed up to approx. 40% within output power range. This feature putting big demands to inverter and his parameters by reason of stabilization of output AC voltage.

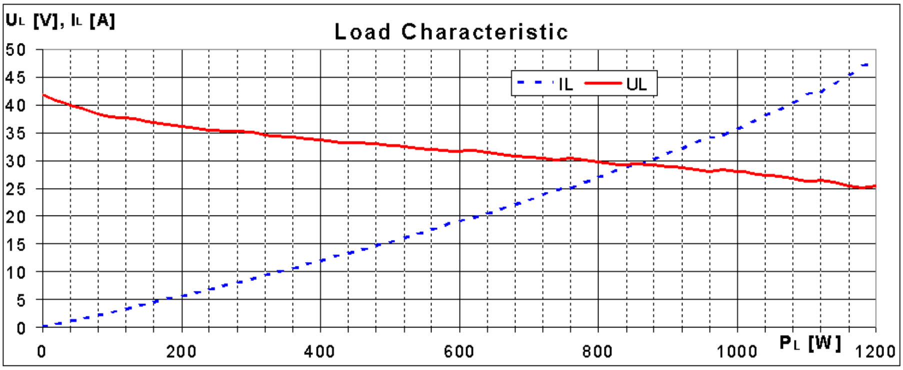

Fig. 1. Load characteristic of PEM fuel cell - NEXA Power Module

Module Nexa has two specific output power. Firs of them is power, which is available at output terminal connector of Nexa module for connecting load (P_L) and second output power is power, which is measurable at output terminal connector of stack of fuel cells (P_S). Power on load P_L compared to power on stack P_S is reduced by self-consumption power (P_{SC}). Self-consumption power in load range is between 2,3% and 18,5% of stack power. For rated load and rated power P_Z=1200W is stack power P_S=1470W. These parameters are shown in graph at Fig. 2.

Fuel cell needs for his function sufficient supply gaseous hydrogen and necessary reaction oxygen, which is extracting from air. The consumption these gases and their course are shown in Fig. 3. For example: for application of fuel cell as little independent source of electric energy with output power P_L=1,2 kW is consumption of hydrogen about 1,2 m^3 per one hour or else for average load P_L=0,5 kW is

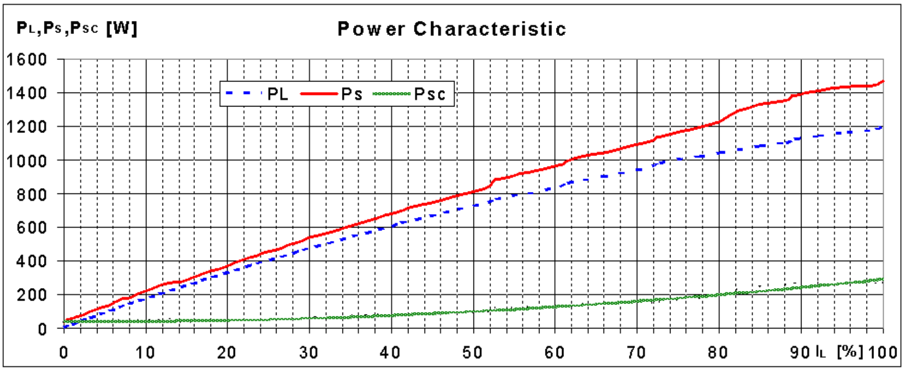

Fig. 2. Power characteristic of NEXA Power Module.

consumption of hydrogen about 8,8 m^3 per day. For better imagine this quantity is stored in one standard pressure gas bottle with pressure 200 bar.

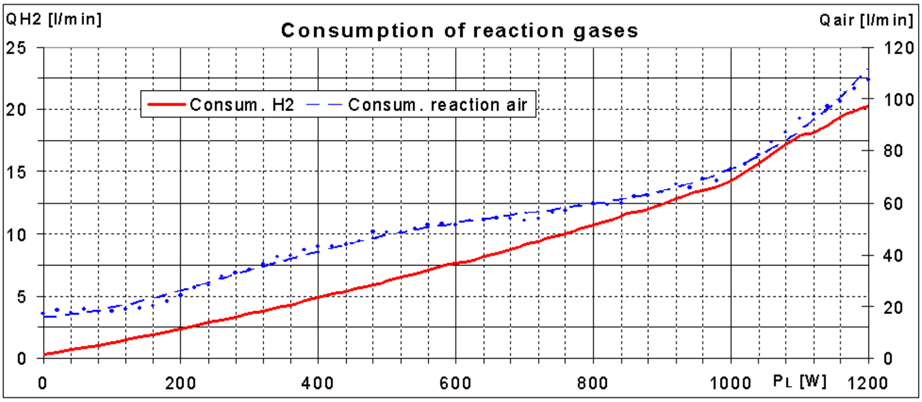

Fig. 3. Consumption of reaction gases depend on load power.

1.2 Dynamic characteristic of fuel cell.

Very interesting phenomenon influencing stack output voltage is “purge blow” effect. Because nitrogen and product water vapour in the air stream slowly migrates across the fuel cell membranes and gradually accumulates in the hydrogen stream in colder or more exposed place. The accumulation of nitrogen and water vapour in the anode results in the steady decrease in performance of certain key fuel cells, which are termed “purge cells”. In response to the purge cell voltage, a hydrogen purge valve at the stack outlet is periodically opened to flush out inert constituents in the anode and restore performance and output voltage. At the same time sheer grows output voltage as shown in Fig. 4. Frequency of opening purge valve is depends on load or otherwise, depends on consumption of hydrogen. For possibility of connecting fuel cell with voltage converter have to be set working voltage characteristic. This work characteristic take into account purge blow effect.

Closely before purge blow is output voltage lowest. Output voltage must not to decrease outside of voltage converter work area, which evoke unwanted voltage failure and interrupt power supply.

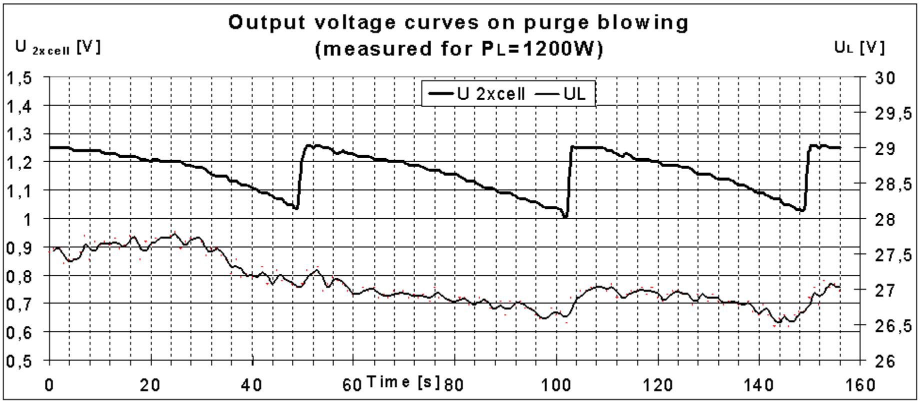

Fig. 4. Output voltage curves on purge blowing. Measured on two purge cell (U $_{2xcell}$)

2 Connection fuel cell to the electrical power network.

Electricity is produced by one or two Nexa modules, which are connecting to the network according to measurement demands. Nexa modules are placed in safety digester with ventilation and hydrogen leak detector. Hydrogen leak are continuously monitored to ensure they stay within desired limits. Hydrogen is stored in two packs at 12 pressure bottle in hydrogen storage.

For power supply to the electrical power network are fuel cells modules linked to voltage inverter and they creates one production block. There are used voltage inverter type SUNNYBOY 1100LV with output power 1,1 kW. From converter power line continues to switchboard and out of him to the network. Switchboard is equipped by short-circuit protection, over-voltage protection, switches, electrometer and signalization of operational status. All of necessary parameters are measured by measured card. Data are saved to PC and backed up at server.

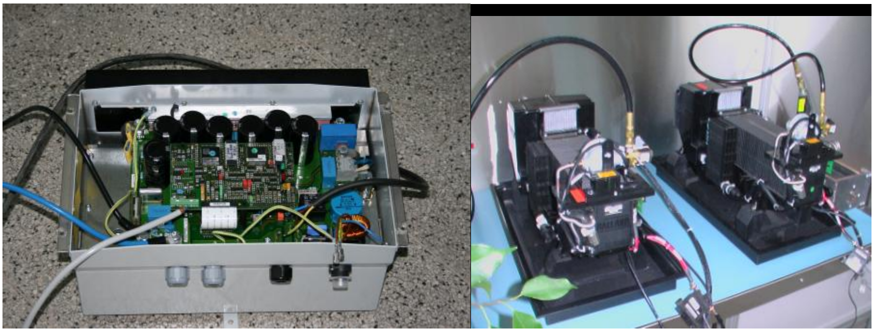

Fig. 5. On the left: Inverter Sunnyboy, On the right: Two connected Nexa modules in digester.

Total efficiency of one production block is about 37% now. At present, whole arrangement running trial operation, when are monitoring and valuating working states so that arrangement worked reliably with optimal parameters and highest possible efficiency in future. The electrical circuit diagram is shown on the Fig. 6.

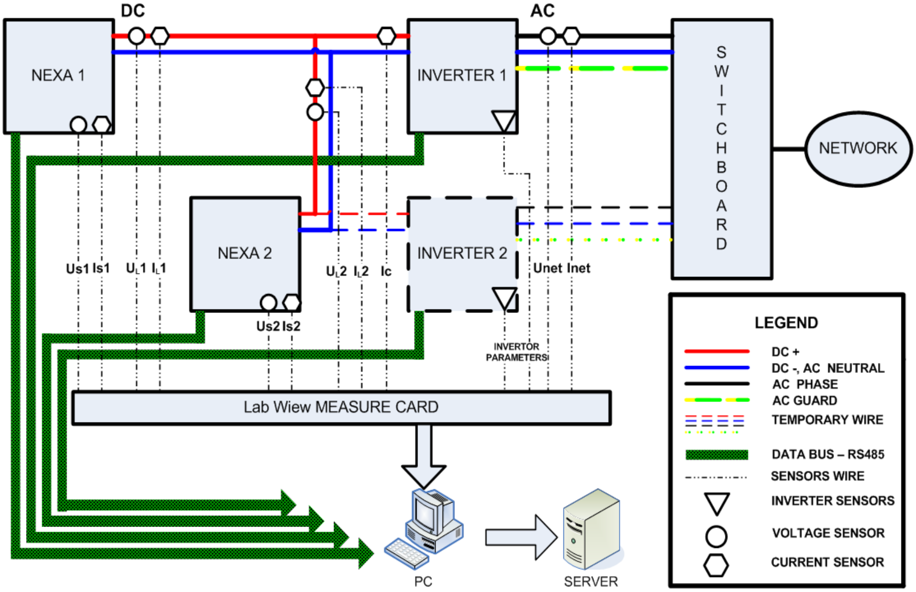
DC
AC
NEXA 1
INVERTER 1
SWITCHBOARD
NETWORK
NEXA 2
INVERTER 2
Us1 Is1
U_L1 I_L1
U_L2 I_L2 Ic
Unet Inet
Us2 Is2
INVERTOR PARAMETERS
Lab Wiew MEASURE CARD
PC
SERVER
LEGEND
DC +
DC -, AC NEUTRAL
AC PHASE
AC GUARD
TEMPORARY WIRE
DATA BUS – RS485
SENSORS WIRE
INVERTER SENSORS
VOLTAGE SENSOR
CURRENT SENSOR

Fig. 6. Electrical circuit diagram.

3 Activities

The team of LFC VSB-TU of Ostrava is concentrating on other activities to represent VSB-TUO and spread the knowledge about fuel cell technologies into public too.

3.1 Exhibitions and publishing activities

In the academic year 2006/2007 were published with members team of LFC VSB-TUO these articles:

1. “Diagnostika a provozní zkoušky na palivových článcích typu PEM.” (Diagnostics and operational tests of PEM fuel cells), Diagnostika 2007 – National Scientific Conference ZČU Plzeň, CZ
2. “Operational characteristic and operational tests of PEM fuel cell” Electric Power Engineering 2007 - International Scientific Conference, Kouty nad Desnou, CZ.

Team of LFC VSB-TUO took part in several exhibitions. The main of them are “Věda v ulicích” (Science in the streets) in Prague and “Chemie na hradě” (Chemistry at castle) in Ostrava both in June 2007.

To hear more about technology of fuel cells and hydrogen technologies, visit Workshop “Hydrogen Technologies, Fuel Cells and Applications, HT-FCA 2007” organized by FCL VSB-TUO in September 2007 at VSB-TUO, more on webpage http://ht-fca.vsb.cz .

Acknowledgements

The support for this research work has been provided by the GAČR project 102/05/H525: The Postgraduate Study Rationalization at Faculty of Electrical Engineering and Computer Science VSB-TU Ostrava.
The support for this research work has been provided by the IGS2007 project: The unconventional source of electrical energy.

References

1. EG&G Technical Services, Inc: Fuel Cell Handbook – Seventh Edition; US DOE, OFE, NETL; West Virginia, USA, 2004.
2. Education materials from Ballard company delivery with Nexa Power Module
3. Fuel Cells and Their Applications, Kordesh K. Simader G., Weinheim, 1996

Methods of Multi-criterial Analysis for Optimum Utilization New Materials in Industrial Establishments

Leopold Paszek, Petr Moldřík

Department of Electrical Power Engineering, FEECS,
VŠB – Technical University of Ostrava, 17. listopadu 15, 708 33 Ostrava – Poruba
{`leopold.paszek.fei`,`petr.moldrik`}`@vsb.cz`

Abstract. This paper takes down the knowledge of multicriterial analysis and their methods (IPA, WSA, TOPSIS, CDA). These analyses we can use at installing superconductive reactors in industrial plants. In future some interesting material instead copper could be superconductor. Generally is well-known that the superconductor is a nature of material when at so-called critical temperature T_c from material of certain resistance became superconductor. It means that the resistance of material sags at critical temperature on zero. Nowadays we know these superconductors (superconductor of the I. type, superconductors of II. type and high temperature superconductors). Reactors used in the electric networks are air core inductors which are applying for limitation of short - circuit currents. Reactors are connected in to mains from single sources, among single partitions of bus bars, to bays of appliances.

Keywords: multi-criteria analysis, reactor, superconductors

1 Introduction

Methods of multi-criteria analysis (MCA) are used for selecting the most suitable from offered variants. In power engineering practice, we can use the multi-criteria analysis for example for selecting the most suitable device, which we need to replace by a new device (remote-controlled switch-disconnector in this paper). These devices are very expensive, and thus we are not able to replace all hand operated disconnectors with these remote-controlled switch-disconnectors. MCA8 software application is used to selecting the most suitable variants. This application enables to perform applicated computation of the hereby used methods and it was developed by us for such purposes.

Following methods appear as advisable methods for solution of existing problems:

- Weighted Sum Approach (WSA)
- Ideal Points Analysis (IPA)

© Václav Snášel (Ed.): WOFEX 2007, pp. 110–115, ISBN 978-80-248-1571-8.
VŠB – Technical University of Ostrava, FEECS, 2007.

- Technique for Order Preference by Similarity to Ideal Solution (TOPSIS)
- Concordance-Discordance Analysis (CDA)

2 Multi-criteria analysis (MCA)

The initial step of each MCA analysis is to form an evaluating matrix, the elements of which reflect the evaluation of particular criteria for each alternative. The matrix *S* consists then of elements S_{ij} where $i = 1,...,I$ alternatives and $j = 1,..., J$ criteria.

The evaluating matrix:

$$S = \begin{matrix} s_{11} & \cdots & s_{1J} \\ \cdots & & \\ s_{I1} & \cdots & s_{IJ} \end{matrix} \tag{1}$$

Because particular evaluations are not measured against the same units, it is necessary to carry out the standardization of the matrix to the standard condition. For the case when the higher evaluation of the criterion means also the better evaluation (i.e. 1 = max, 0 = min), we can write the standardization as follows:

$$e_{ij} = \frac{S_{ij} - \min_i S_{ij}}{\max_i S_{ij} - \min_i S_{ij}} \tag{2}$$

In the contrary case, when the higher evaluation means the worse evaluation (i.e. 1 = min, 0 = max), the standardization will be as follows:

$$e_{ij} = \frac{\max_i S_{ij} - S_{ij}}{\max_i S_{ij} - \min_i S_{ij}} \tag{3}$$

2.1. Ideal Point Analysis (IPA)

The Ideal Point Analysis rests upon the deviation between the set of ideal solutions and the set of effective solutions. Although the ideal solution surely almost does not exist, it serves as an important reference model. The best compromise solution is determined as that solution that is the nearest to the ideal one. The increasing distance from the ideal solution for factors located upper on the scale of importance induces greater consequences than the increasing distance from the ideal solution for factors located lower on the scale of importance.

2.2. Weighted Sum Approach (WSA)

The Weighted Sum Approach method comes from principle of maximization of benefit, simplification of this method is that it is assumed only linear function of benefit. Process of this method is comfortable to IPA method; resulting sequence of alternatives is opposite.

2.3. TOPSIS

In case of TOPSIS method this is again the question of principle of maximization of distance from ideal variant. The ideal variant means that all criteria have the best assessments. Ideal variant is mostly suppositional; the best of variants is that one which is the nearest to ideal variant. Vector $(H_1, H_2, \ldots, H_J)$ represents ideal variant, vector $(D_1, D_2, \ldots, D_J)$ represents basal variant.

2.4. Concordance-Discordance Analysis (CDA)

The Concordance-Discordance Analysis is a method widely used in MCA. It consists of comparison of alternatives of pair selection. It measures the degree by which the alternatives of selection and the weights of factors prove or disprove the ratio between the alternatives. The differences in the weights of factors and in the evaluations of criteria are analysed by means of the procedures of concordance and discordance separately.

The index of concordance between the alternative A and the alternative B is defined as a proportion of the sum of weights of those criteria, for which the evaluation A is greater than or equal to the evaluation B, and the sum of weights of all criteria.

2.5 Usage of multicriterial analyses

This helps to solve multicriterial analysis (MCA). MCA engages in plotting of single alternatives according to more criterials and it was described many times for example in new methods of multi–criteria analysis for increasing of reliability of electrical networks. It is necessary to remind that no methods MCA substitute in the human determination process when this person is decider, but it rather transports its action for qualitatively higher level. In these methods there always gets off some subjective factor (e.g. at determination of relative importance single criterials - stress criteria). Effectiveness of these methods MCA consists of making decider to orientate in a case of big set off variants and criteria very well.

3. Reactors

Reactors used in the electric networks are air core inductors which are applying for limitation of short - circuit currents. Reactors have even to reduce an amplitude of transitional short - circuit current for such valuable which can't threaten instruments transformers of current, bus-bars or disconnectors. Reactors reduce an interrupting capacity of switches and so they are cheaper.

Connecting of reactors:

- to mains from single sources
- among single partitions of bus-bars
- to bays of appliances

Dividing of reactors according to type of cooling:

- air cooled
- oil cooled

Dividing of reactors according to type of their placing:

- indoor
- outdoor

For higher voltage there are generally used reactors with higher voltage in outdoor substation and they are engineered as oily ones. Reactors are similar to oily transformers however they miss iron core. The oily reactors are blocked similarly as transformers. The reactor is specified by its rated current, rated voltage and impedance voltage in percent (%) of rated voltage network, which means size of reactor impedance.

3.1 Reactors with superconductive material

The reactors are formed by air core inductors. In future some interesting material instead copper could be superconductor.

Superconductor is an element, inter-metallic alloy, or compound will conduct electricity without resistance below a certain temperature. Resistance is undesirable because it produces losses in the energy flowing through the material. To superconductive state 24 absolute materials and hundreds of casting alloy can gradate (at present time more than 600).

Generally is well-known that the superconduction is a nature of material when at so-called critical temperature T_c from material of certain resistance became superconductor. It means that the resistance of material sags at critical temperature on zero. This status is maintainable all the time when this temperature of material will be minimally on limits of critical temperature.

3.2 Superconductors of the I. type

The Type 1 category of superconductors is mainly comprised of metals and metalloids that show some conductivity at room temperature. They require incredible cold to slow down molecular vibrations. These superconductors are characterized as the "soft" superconductors - were discovered first and require the coldest temperatures to become superconductive. They exhibit a very sharp transition to a superconducting state (see above graph) and "perfect" diamagnetism.

3.3 Superconductors of the II. type

The type 2 category of superconductors is comprised of metallic compounds and alloys. The recently-discovered superconducting "perovskites" (metal-oxide ceramics that normally have a ratio of 2 metal atoms to every 3 oxygen atoms) belong to this Type 2 group. They achieve higher Tc's than Type 1 superconductors by a mechanism that is still not completely understood. These superconductors are also known as the "hard" superconductors - differ from Type 1 in that their transition from a normal to a superconducting state is gradual across a region of "mixed state" behavior.

3.4 High temperature superconductors

High temperature superconductors were real technological break-through. These materials are possible to cool down only by very cheap liquid nitrogen (it supplied earlier used helium). Gradually there was found a number of superconductive materials. Values of reach temperatures are from 30 to 130 K.

Since acquisition costs for superconductors are quite high, it is suitable to choose multicriterial analysis for their optimal situation. There isn't thinkable to exchange all reactors in the industrial plant at a time, because financial taxes would be very high.

4. Conclusion

This paper is engaged in usage of new materials for reactor construction by reason of short-circuits currents decrease in an industrial plant. Short-circuit in industrial plant is very dangerous and there can be great breakdowns. The usage of superconductive materials in industrial plant leads to reduction of losses. It is advisable to use some of methods multicriterial analyses for substitution because their investments are enormous. Therefore it is necessary to carry out this substitution where it is mostly needed.

This helps to solve multicriterial analysis (MCA). MCA engages in plotting of single alternatives according to more criterials and it was described many times for example in new methods of multi–criteria analysis for increasing of reliability of electrical networks. It is necessary to remind that no methods MCA substitute in the human determination process when this person is decider, but it rather transports its action for qualitatively higher level. In these methods there always gets off some subjective factor (e.g. at determination of relative importance single criterials - stress criteria). Effectiveness of these methods MCA consists of making decider to orientate in a case of big set off variants and criteria very well.

Nowadays superconductive materials of I. type, II. type and high temperature are exploited, however they are expensive, because they are cooled of necessity by nitrogen or helium.

Acknowledgements

This work is supported by The Ministry of Education, Youth and Sports of the Czech Republic – project No: CEZ MSM6198910007.

References

1. Kulhánek P.,Vysokoteplotní supravodivost, Týdeník věnovaný aktualitám a novinkám z fyziky a astronomie 36/2004
2. www.superconductors.org
3. Korviny P.: Aplikace multikriteriální analýzy při nasazování dálkově řízených prvků v distribučních sítích vysokého napětí, disertační práce, Ostrava 200397
4. Fiala P., Jablonský J., Maňas M.: Vícekriteriální rozhodování, Vysoká škola ekonomická v Praze
5. Gurecký J.: Optimalizace řízení sítí vn dálkově ovládanými úsečníky, disertační práce, Ostrava 1998

Determination of Optimal Order of 110 kV/MV Transformers to Maintenance

Břetislav Stacho, Stanislav Rusek, Radomír Goňo

Department of Electrical Power Engineering, FEECS,
VŠB – Technical University of Ostrava, 17. listopadu 15, 708 33 Ostrava – Poruba
{bretislav.stacho.fei, stanislav.rusek, radomir.gono}@vsb.cz

Abstract. This Paper deals with putting on the reliability centred maintenance (RCM) to the 110 kV/MV transformers. The paper deals with determination of technical condition and operational importance of transformers. Also it presents methodology of evaluation of possibility of a connected point of supply backup, which is one of the operational importance criterion of 110 kV/MV transformers. An example of possible evaluation of RCM program output data is presented in the last chapter. This program was developed at the Department of Electrical Power Engineering VŠB-TU Ostrava in order to apply RCM to the selected elements of distribution network.

1 Introduction

Optimal order to maintenance is one of the two approaches by the help of them we can apply reliability centred maintenance to distribution network elements. Optimization of maintenance cycle length is the second approach, but it is not appropriate to use it to the110 kV/MV transformers, because it is applied to elements, which are thousands in distribution network.

So we chose the optimal order to maintenance as an approach for the 110 kV/MV transformers. It means that inspections and diagnostic measurements, incorporated in the Preventive Maintenance Code, are performed in regular intervals on the equipment. The maintenance activity depends on the results of these inspections, diagnostic measurements and operational importance of appropriate equipment.

2 General determination of optimal order of elements to maintenance

If we want to use this approach for application of RCM, elements of distribution network have to fulfil these conditions:

- the number of certain elements is not such high,
- element of certain type has a high importance,
- there have to be determined limits, from when the maintenance has worth,

© Václav Snášel (Ed.): WOFEX 2007, pp. 116–122, ISBN 978-80-248-1571-8.
VŠB – Technical University of Ostrava, FEECS, 2007.

- It's possible to find out concrete element at analysis of event (failure, outage),
- equipment monitoring is possible (eventually on-line monitoring,
- we have to be able to determine condition and importance of equipment.

Relation between operational importance and technical condition is essential to determine maintenance order. So it is needed to specify importance and condition of element by appropriate parameters. There is needed besides technical condition and importance to punctually identify each element too. Identification is the third group of information about element.

Input data for each equipment can be divided into three groups:

- identification data about equipment,
- data determining technical condition of equipment,
- data determining equipment importance.

If we want to apply this RCM approach, it is needed to create different structure of input data for each element type, mainly for evaluation of technical condition.

3 Technical condition

Four criteria were chosen to evaluate technical condition of a 110 kV/MV transformer:

- climatic conditions,
- diagnostic tests evaluation,
- date of the last regular maintenance or repair,
- transformer age,
- tank condition (corrosion, paint),
- tank, pipeline and armature seal,
- condition of a control box and its equipment,
- cabling,
- type of a tap changer,
- tap changer age,
- sort of drive,
- number of switch-overs,
- bushing seal,
- bushing age,
- date of internal inspection,
- number of hours in operation,
- average load per hour.

Weights and ranges of evaluating of these criteria were determined by qualified estimations of operating and maintenance employees at the beginning. After having performed evaluation of all machines, the appropriate weight values were specified so that the resulting evaluation of technical condition was as real as possible. Thus the set weights of criteria and ranges of their evaluations were not changed at all. Weights of the particular criteria are in Tab. 1.

Climatic conditions	5	Tap changer age	10
Date of the last common maintenance or repair	30	Sort of drive	20
Type of transformer	50	Number of switch-over	30
transformer age	50	Bushing seal	40
tank condition	10	Bushing age	20
Tank seal	40	Date of internal revision	50
Condition of control box	20	Number of hours in operation	80
Cabling	10	average load per hour	80
Type of a tap changer	50	Diagnostic tests evaluation	100

Tab. 1 Weights of technical conditions criteria

4 Operational importance

Technical condition is actually determined by the transformer itself. Considering operational importance of a transformer, we are interested in its position in the network. Three criteria were chosen to evaluate operational importance of a 110 kV/MV transformer:

- possibility of a connected point of supply backup,
- importance of supplied distribution transformers (number and type of connected customers),
- transferred energy in a year.

These three criteria were considered coessential, so the value of weight of each criterion equals one third. The range of importance evaluation of MV lines was determined by the help of so-called credit evaluation according to the number and type of customers, which are connected to the transformer. The following methodology was designed to evaluate a criterion - possibility of a connected point of supply backup

5 Evaluation of a criterion – possibility of a connected point of supply backup

The following criteria were chosen for evaluation of this operational importance criterion:

- reserve by the transformer (%),
- manipulating time of reserve by the transformer (min),
- reserve by the MV line (%),
- manipulating time of reserve by the MV line (min).

The most important criterion for evaluation is the reserve by the transformer. Namely, if the reserve is 100%, there is no reserve, or the reserve is between these two extreme values.

Design of methodology for evaluation of the criterion - possibility of a connected point of supply backup - is in Tab. 2.

No back up	100
T0/- MV(0-100)/120	90
T0/- MV100/120	85
T0/- MV(0-100)/60	80
T0/- MV100/60	75
T0/- MV(0-100)/20	70
T0/- MV100/20	65
T(0-100)/15 MV(0-100)/120	60
T(0-100)/15 MV100/120	55
T(0-100)/15 MV(0-100)/60	50
T(0-100)/15 MV100/60	45
T(0-100)/15 MV(0-100)/20	40
T(0-100)/15 MV100/20	35
T100/15 MV0	30
T100/15 MV(0-100)/120	25
T100/15 MV100/120	20
T100/15 MV(0-100)/60	15
T100/15 MV100/60	10
T100/15 MV(0-100)/20	5
T100/15 MV100/20	0

T0 - záloha transformátorem není možná
T(0-100) - záloha transformátorem existuje, ale není 100%
T100 - záloha transformátorem je 100%
vn0 - záloha po vedení vn není možná
vn(0-100) - záloha po vedení vn existuje, ale není 100%
vn100 - záloha po vedeních vn je 100%
15,20,60,120 - zprovoznění do (min)

Tab. 2 Design of methodology for evaluation of the criterion - possibility of a connected point of supply backup

In the coming time new methodology for determination of the criterion value range -possibility of a connected point of supply backup - shall be completed. It will contain determination of weights for the particular criteria mentioned above. Consequently the possibility of a connected point of supply backup will be determined more accurately by the multicriteria analysis (MCA), probably by concordance and discordance analysis.

6 Resulting evaluation of RCM application to 110 kV/MV transformers

As it was mentioned in chapter 2, the relation between operational importance and technical condition is essential to determine optimal order of technical evidence elements for maintenance. In our case, the 110 kV/MV transformers are the above mentioned elements. Ratio of the resulting values of operational importance and technical condition is respected and may be changed deliberately in RCM computer application, which was developed at the Department of Electrical Power Engineering VŠB-TU Ostrava. For the primary theoretical consideration this ratio is 1:1.

Fig. 2 describes one of the possible approaches of evaluation of application of RCM for the ratio mentioned above. On this picture the three-level decision model is presented. These three levels determine the contingent maintenance activity for individual transformers. It is possible to determine a multilevel model, however, this approach seems to be quite adequate. At present it is necessary to determine more accurately limits between individual levels so that they correspond to reality as best as they can.

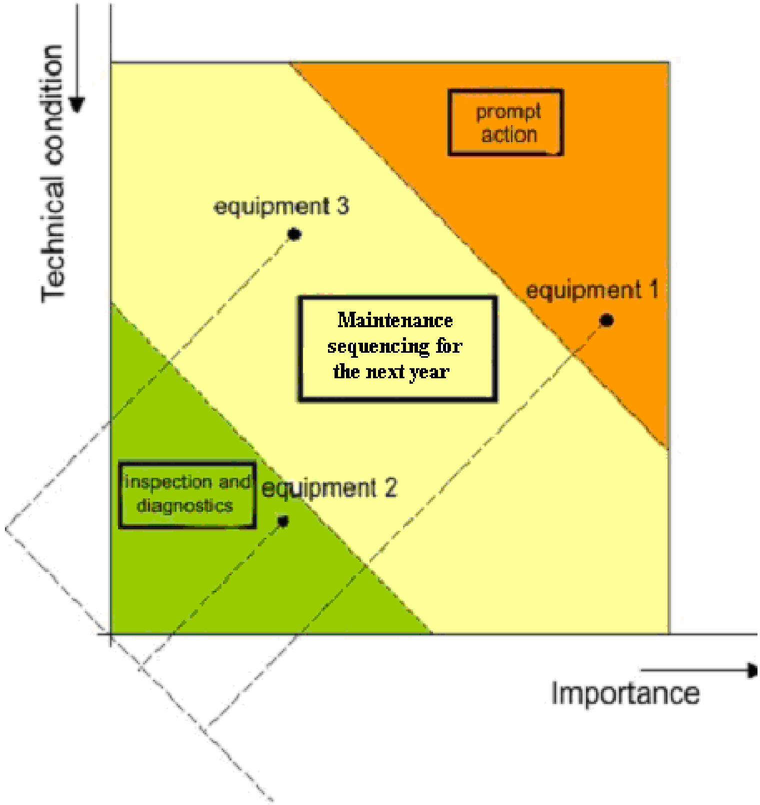
Technical condition
prompt action
equipment 3
equipment 1
Maintenance sequencing for the next year
inspection and diagnostics
equipment 2
Importance

Fig. 2 Three-level decision model

7 Conclusion

This paper deals with determination of optimal order for maintenance of 110 kV/MV transformers in network of the distribution company. The paper presents determination a classification method of technical conditions and operational importance.

Further there is presented methodology of evaluation of possibility of connected point of supply backup. Resultant evaluation range of this criterion will be more specified at stepwise evaluation of collected data in terms of periodic revisions of transformers.

Technical condition and operational importance ratio (we use 1:1 ratio in this paper) will also be specified more accurately. We may expect the resulting ratio between the operational importance and technical condition about 2:3.

Acknowledgment:

This work is supported by The Ministry of Education, Youth and Sports of the Czech Republic - project No: CEZ MSM6198910007.

8 References

1. Rusek S. : Spolehlivost elektrických sítí, VŠB - TU Ostrava, ISBN 80-7078-847-X, 2001
2. Goňo, R., Rusek, S., Král, V.: Application of Reliability Centered Maintenance in Electricity Distribution Company. In Proceedings of the IASTED International Conference PEA 2006. Ed. G. O. Anderson, Calgary:ACTA Press, 2006, p. 96 - 101, ISBN 0-88986-616-3
3. Stacho B., Rusek S., Goňo, R., Král V., Raška T.: Maintenance optimization of 110 kV/MV transformers in distribution networks, Conference Electric Power Engineering, 2007

Fuel Cells for Accumulation Electrical Energy from Renewable Energy Sources

Robert Šebesta

Department of Electrical Power Engineering, FEECS,
VŠB – Technical University of Ostrava, 17. listopadu 15, 708 33 Ostrava – Poruba
robert.sebesta.fei@vsb.cz

Abstract. Goal of this article is to present possibilities of accumulation of redundant electric energy which has been produced by unconventional sources of electric energy and their use at the time of increased load of electric supply system. This work deals with different ways of design systems of accumulation of electric energy in parks of wind power plants. There are described five options of accumulation of electricity in parks of wind power plants. These options are also analyzed. There are also mentioned fuel cells and their advantages and disadvantages. Fuel cells are compared with other sources of electric energy - batteries and internal combustion engines - in terms of efficiency and number of energy conversions.

1 Introduction

It is typical for generation of electricity from renewable sources that amount of power supplied to the grid fluctuates in time. In addition electric energy is generated also in time of low load of electricity supply system. It is connected with changeability of weather which is also difficulty to accurately forecast. It forces transmission system operator to maintain large regulating power reserves in conventional power plants. Reduction or elimination of these unfavourable impacts may be achieved using accumulation of electrical energy.

2 Storage systems

As for storage systems for electricity we can divide them into accumulators of power and accumulators of energy. Both of them consist of two converters (rectifier – inverter) double conversion and accumulation unit.

© Václav Snášel (Ed.): WOFEX 2007, pp. 123–128, ISBN 978-80-248-1571-8.
VŠB – Technical University of Ostrava, FEECS, 2007.

2.1 Accumulators of power

Accumulators of power allow provide great charging and discharging powers for a brief period. Capacitors, superconductive magnetic accumulators and fly-wheel accumulators belong to this category. Accumulation size of these accumulators is low.

2.2 Accumulators of energy

Accumulators of energy have a huge accumulation size (MWh) and they are able to accumulate electricity and get it out for many hours. Pumped storage hydro plants, accumulators of compressed air, chemical accumulators (batteries) and hydrogen systems belong to this category. Pumped storage hydro plants and systems of compressed air are technically and commercially mature. Special case is heat accumulation (hot water).

Available capacities are limited when geographical conditions absent. Electrochemical storage system is option for short-time accumulation of large amount of energy. Lead acid batteries may be assembled to large units whereas power variation can be balanced during several seconds. Redox-Flow batteries are just launched into the market and they are suitable for large size units but there is short of experiences.

2.3 Options of setting accumulation

There were investigated these options of setting accumulation in farms of wind power plants:

1. Supply of Peak Energy
2. Minimal Supply
3. Prediction of Supply of Power
4. Cover of Own Consumption
5. Overdesign of Accumulation

Options 1, 2 and 3 allow better planning.

2.3.1 Supply of Peak Energy

This option allows to operator of wind power plants to supply electricity during peak load of electricity supply system. In addition there is possible to conclude supplied power as well as daily amount of electricity and supply period (MWh/day) individually. Part of power of wind power plants is thus certificated as peak source of electricity and also thus financially evaluated.

2.3.2 Minimal Supply

There can be agreed minimal performance supplied for a period of 24 hours, this also matches to design of accumulation and evaluation of electricity at the level of power plant working in base load. Size of accumulation is determined by the longest predicted time of windlessness. There also can be agreed certain number of drop-outs (days) whereby usage of accumulation rises.

2.3.3 Prediction of Supply of Power

This option allows prediction at least part of power of wind power plants by the help of accumulation of electricity. Electricity is supplied directly by wind power plant or it is supplied across accumulation system. If there is redundant wind energy then supply of energy is higher than predicted minimal power with all consequences.

2.3.4 Cover of Own Consumption

Farm of wind power plants has own consumption, which must be covered even through windlessness (i.e. electricity must be bought from public grid). This consumption can be covered with the aid of accumulation. Saved (prevented) costs can be used to refund of accumulation system.

2.3.5 Overdesign of Accumulation

Power of farm of wind power plants exceeds transmission capacity of power lines (grid) connector that's why power peak must be accumulated and then supplied to grid during lower power of wind power plants

2.3.6 Analysis of results

Analysis of these five variants related to specific farm of wind power plants pointed to that there are necessary large accumulation capacities to supply reliable wind energy (variants Supply of Peak Energy and Minimal Supply). There are necessary accumulation capacities 14 or 70 kWh per a MW installed power of wind power plants [2] for both of these variants to overcome windlessness, which lasts several days in each year. So the utilization of accumulation is very low. In case of options Prediction of Supply of Power and Cover of Own Consumption can be used any size of accumulation. Option Prediction of Supply of Power looks like the most economical one of these five variants.

3. Description of principle and properties of fuel cell and comparison with other sources

Fuel cells use clean hydrogen (or hydrogen containing fuel) and oxygen to produce electricity during electrochemical process. Fuel cell consists of two electrodes – negative anode and positive cathode which surround electrolyte. Anode is supplied by hydrogen and cathode is supplied by oxygen. Hydrogen atoms are then activated by catalyst and divide into protons and electrons. Electrons go through external electric circuit producing electricity while protons go throw the electrolyte to the cathode where they join up with oxygen and electrons producing water and heat. Fuel cell is equipment which allows direct conversion of chemical energy bound in fuel to electric energy without heat or mechanic transition stage. Energy is released every time that fuel chemically reacts with oxygen from air. Energy is released in the form of DC low voltage electric energy and heat.

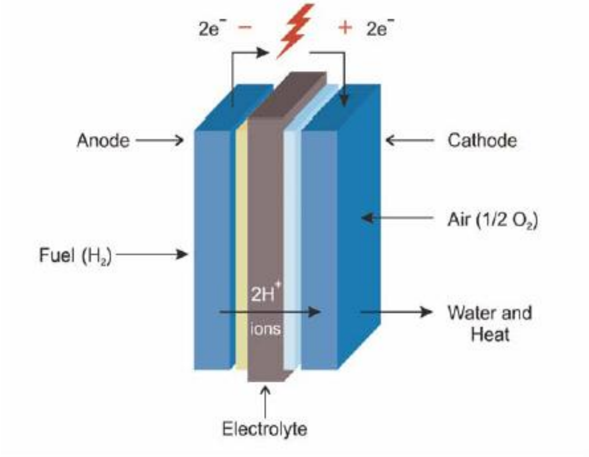

Fig. 1. Demonstration of function of fuel cell PEM type [1]

Fuel gas and oxidizing gas feed anode and cathode in fuel cell respectively. Gases flow through channels which are placed at both sides of electrolyte. We can distinguish between various types of fuel cells according to the type of electrolyte. Various types of electrolyte conduct variety of ions. Electrolyte may be in liquid state or in solid state. Some fuel cells operate at high operating temperatures and some fuel cells operate at low operating temperature. Low-temperature fuel cells require catalysts which are made of noble metals especially platinum. The task of catalyst is to dispatch reactions which take place on electrodes.

3.1 Advantages of fuel cells

Fuel cells are usually compared with internal combustion engines and with batteries. However fuel cells offer certain advantages in comparison with these power sources. These advantages should be considered when new suitable resource is chosen.

Fuel cells (PEM type) which work only with pure hydrogen operate without polluting matters. Products of reaction are next to the electricity also water and heat. That’s why fuel cells may be used for combined heat and power applications. If it is so done then general efficiency of system increases.

Fuel cells work with higher thermodynamic efficiency than internal combustion engines. Internal combustion engines convert chemical energy to heat through combustion and making use of fact that heat does useful work.

Efficiency of fuel cells is not connected with their maximal operating temperature because they don’t use combustion process. Result is that efficiency of energy conversion (real electrochemical reaction) can be significantly higher than real combustion reaction. Efficiency of electrochemical reaction isn’t same as general efficiency. Comparison of efficiency characteristics of power sources is displayed in figure 2. As well as higher relative thermodynamic efficiency fuel cells show also higher efficiency than internal combustion engines at their part load. Fuel cells don't show sharp underflows in efficiency as it is in case of great power plants. Internal combustion engines achieve the highest efficiency operating at designed rated state and they show rapid drops at part load. Fuel cells as well as batteries show higher efficiency at part load than at full load.

If fuel cell is used as electric generator then it requires less energy conversions than internal combustion engine (figure 3). Each energy conversion is connected with energy losses so that the less number of conversions are done the efficiency is better.

Fuel cells don't require charging-up however fuel feed must be recovered which is faster than charging-up of batteries. They can offer longer supply of electricity. It depends on size of tanks with fuel and oxidant. Fuel cells have low level of noise.

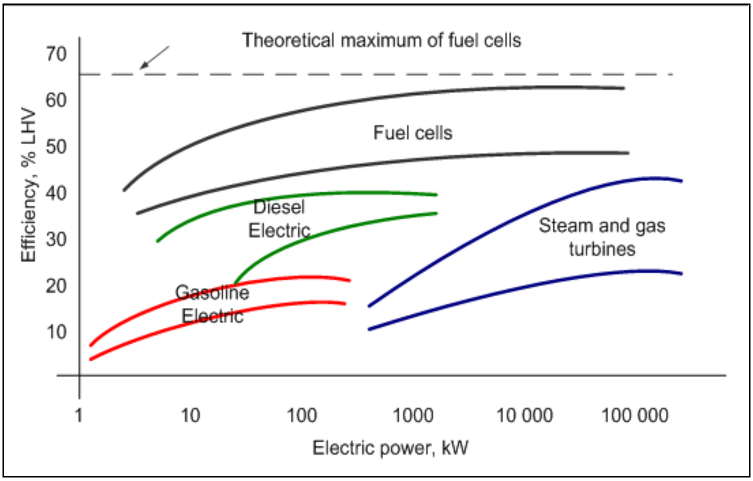

Fig. 2. Comparison of efficiencies of different ways of electric power generation [1]

3.2 Disadvantages of fuel cells

Fuel cells have following disadvantages in comparison with internal combustion engines and batteries:

Hydrogen is very difficult to produce and to storage. Current production processes are expensive and they require large number of energy.

Hydrogen gaseous storage system are huge and difficulty adaptable to low power volume density of hydrogen. Hydrogen liquid storage systems are much smaller and lighter but they must be operated at cryogenic temperatures. Possibility also presents storage of hydrogen in the form of hydrocarbons and alcohols. It is true that storage and manipulation with hydrogen is then simplified but some ecological advantages will be irretrievably lost.

Even slight residual water in fuel cell can evoke irreversible destructional expansion when fuel cell is exposed to frost. Operating fuel cells produce enough heat to prevent freeze at outdoor temperatures below freezing point. If fuel cells are switched off at cold weather then they must be permanent warming or residual water must be completely removed from them.

PEM fuel cells use proton exchanging membranes and they can’t dry up and they must be wet even when they are stored. Effort to start of these cells with dry membranes can lead to destruction of membranes.

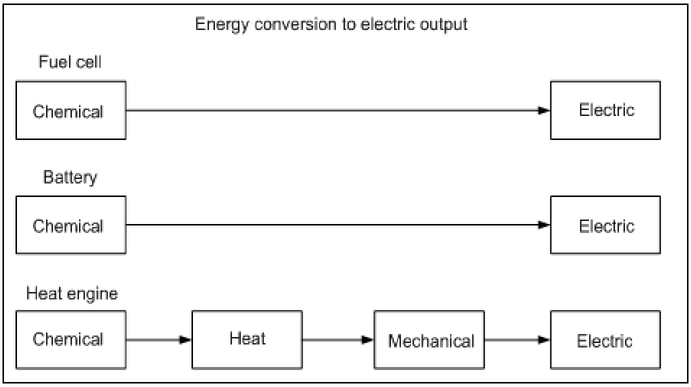

Fig. 3. Comparison of energy conversions [1]

4. Conclusion

Goal of this work was to explore particular options of accumulation of electric energy gained from renewable energy sources at their stochastic production. There were described these five options of accumulation of electricity in parks of wind power plants: Supply of Peak Energy, Minimal Supply, Prediction of Supply of Power, Cover of Own Consumption and Overdesign of Accumulation. There were mentioned principle and function of fuel cells, their advantages and disadvantages in comparison with other energy sources. There is presumption that this work will be developed with purpose of choose an optimal storage system with the help of multicriterial analysis method.

Acknowledgements:
This article was prepared in research within project VZMSM 6198910007.

References

1. Kopřiva, M., Horák, B., Koziorek, J., Papoušek, M., Slanina, Z.: Studie pohonu mobilního prostředku s palivovým článkem VŠB, ČEA 2005
2. Distribuce a obchod s elektrickou energií – Odborný bulletin č. 54 Listopad, 2004
3. IEA, OECD: Prospects for Hydrogen and Fuel Cells, 2005
4. Kordesch, K., Simander, G.: Fuel Cells and Their Applications, VCH 1995
5. Sammers, N.: Fuel Cell Technology Reaching Towards Commercialization, Springer 2006
6. EG&G Technical Services, Inc.: Fuel Cells (Seventh Edition), US Department of Energy 2004
7. Hradílek, Z., Šebesta, R.: Fuel cells for storage of electric energy gained from wind power plants, ELECTRIC POWER ENGINEERING 2007, Kouty nad Desnou

Regulation of Quality of Electric Power Supply in Czech Republic and Assessment Costs of Electric Power Suppliers Caused by Interruption of Supply

Marek Tinka

Department of Electrical Power Engineering, FEECS,
VŠB – Technical University of Ostrava, 17. listopadu 15, 708 33 Ostrava – Poruba
`marek.tinka@cz.abb.com`

Abstract. This contribution deal with the problems of regulation of electric power quality in Czech Republic, especially in connection with interruption of electric power supply to customers. There is described now valid regulation about quality of electric power supply and related services in electrical power engineering n. 540/2005 Sb. in this paper. In next part of contribution I deal with assessment costs of electric power suppliers caused by interruption supply. Total costs I divide into five groups. These are costs independent on system reliability parameters, costs dependent on system reliability parameters, cost of investments for increase of system reliability, other costs for increase of system reliability, costs for compensation of customers by interruption of electric power supply.

1 Introduction

The electric power supply in required capacity and with acceptable level of quality and supply reliability for acceptable price is a basic task of electric power system. On liberalized electricity market two opposed interests meet. On the one hand there are operators of distribution systems, who have natural effort to reduce costs, inclusive of costs for development and operation of distribution system and they would like to make good results of their business by this way. On the other side there are customers, who demand quality and reliable electric power supply for acceptable price. In respect of monopoly environment in the area of electric power distribution customers don't have chance for choice of supplier, therefore it's necessary determine specific level of quality electric power supply, that every supplier has to carry out.

2 Electric power quality

The electric power quality it's possible judge from these points of view:

- voltage quality expressed by deviations from nominal values
- voltage quality in light of deviations from sinusoidal voltage

© Václav Snášel (Ed.): WOFEX 2007, pp. 129–134, ISBN 978-80-248-1571-8.
VŠB – Technical University of Ostrava, FEECS, 2007.

- short-term interruptions or voltage drops in power take-off point
- long-term interruptions of supply caused by planned works on distribution system and failures of distribution system devices
- disintegrations of electric power supply system
- other services of distribution system operators resulting from needs of contact with customers

3 Regulation of quality of electric power supply in Czech Republic

In Czech Republic electric power quality is regulated by regulation about quality of electric power supply and related services in electrical power engineering n. 540/2005 Sb. on the present.

Standards of quality of electric power supply and related services are divided in accordance with this regulation into:

a) guaranteed standards of electric transmission or electric power distribution and guaranteed standards of supplies, that set out quality of electric transmission or electric power distribution and electric power supplies, that must be reach for every individual case.

b) general standard of electric transmission or electric power distribution, that is used for comparison performance and its time process of distribution systems operators and for judgment of performance and its time process of transmission system operator.

Guaranteed standards of electric transmission or electric power distribution:

- standard renewal of electric transmission or electric power distribution after failure
- standard compliance of planned restriction or interruption of electric power distribution
- standard replacement of damaged fuse
- standard electric power quality
- standard term for settlement of a claim of electric power quality
- standard term for elimination causes of reduced electric power quality
- standard consignment of attitude to request for connection customer's device to transmission system or distribution system
- standard permission of electric transmission or electric power distribution
- standard renewal of electric power distribution after interruption of distribution caused by delay customer or supplier of compound service with payment for provided electric power distribution
- standard renewal of electric power distribution after interruption distribution by request of supplier or supplier of compound service
- standard term for settlement of a claim of electric power supply measure
- standard transfer of measure data

- standard term for settlement of claim of account for electric power distribution
- standard compliance deadline of meeting with customer

General standards of electric transmission or electric power distribution and its declaration:

- standard continuity of electric transmission or electric power distribution
- declaration compliance of standard continuity of electric transmission or electric power distribution

Standard continuity of electric transmission or electric power distribution is judged by values of indicators of electric transmission or electric power distribution. These indicators for distribution system operators are:

- interruptions frequency of electric power distribution given number of interruptions of electric power distribution in a year
- total time period of all interruptions of electric power distribution in minutes in a year
- average time period of one interruption of electric power distribution in minutes in a year

Distribution system operator is obliged to show compliance of standard continuity of electric transmission or electric power distribution and release achieved level of electric power distribution.

For an example I present compliance statement of standard continuity of electric transmission or electric power distribution for company ČEZ Distribuce, a.s. in a year 2006.

Table 1.

Month	**Distributor**	**Interruption frequency**		
		number of interruptions in a month		
		nn	vn	vvn
January	ČEZ Distribuce, a.s.	0,025	0,208	0,008
February	ČEZ Distribuce, a.s.	0,027	0,141	0,008
March	ČEZ Distribuce, a.s.	0,034	0,204	0,017
April	ČEZ Distribuce, a.s.	0,027	0,174	0,004
May	ČEZ Distribuce, a.s.	0,025	0,221	0,004
June	ČEZ Distribuce, a.s.	0,031	0,285	0,029
July	ČEZ Distribuce, a.s.	0,026	0,314	0,04
August	ČEZ Distribuce, a.s.	0,027	0,216	0,028
September	ČEZ Distribuce, a.s.	0,022	0,206	0,025
October	ČEZ Distribuce, a.s.	0,022	0,127	0,052
November	ČEZ Distribuce, a.s.	0,026	0,251	0,03
December	ČEZ Distribuce, a.s.	0,02	0,103	0,025

Table 2.

Month	Distributor	Total time period of all interruptions		
		minutes in a month		
		nn	vn	vvn
January	ČEZ Distribuce, a.s.	3,23	14,105	0,197
February	ČEZ Distribuce, a.s.	3,474	11,642	0,069
March	ČEZ Distribuce, a.s.	3,81	14,725	0,997
April	ČEZ Distribuce, a.s.	4,011	18,099	0,251
May	ČEZ Distribuce, a.s.	3,826	21,868	0,028
June	ČEZ Distribuce, a.s.	4,929	25,178	0,44
July	ČEZ Distribuce, a.s.	3,818	20,409	0,491
August	ČEZ Distribuce, a.s.	3,884	16,074	0,226
September	ČEZ Distribuce, a.s.	2,926	20,021	0,747
October	ČEZ Distribuce, a.s.	3,604	17,709	3,69
November	ČEZ Distribuce, a.s.	4,187	22,647	0,302
December	ČEZ Distribuce, a.s.	2,661	11,217	0,256

Table 3.

Month	Distributor	Average time period of one interruption		
		minutes for one interruption		
		nn	vn	vvn
January	ČEZ Distribuce, a.s.	129,2	67,813	24,625
February	ČEZ Distribuce, a.s.	128,667	82,567	8,625
March	ČEZ Distribuce, a.s.	112,059	72,181	58,647
April	ČEZ Distribuce, a.s.	148,556	104,017	62,75
May	ČEZ Distribuce, a.s.	153,04	98,95	7
June	ČEZ Distribuce, a.s.	159	88,344	15,172
July	ČEZ Distribuce, a.s.	146,846	64,997	12,275
August	ČEZ Distribuce, a.s.	143,852	74,417	8,071
September	ČEZ Distribuce, a.s.	133	97,189	29,88
October	ČEZ Distribuce, a.s.	163,818	139,441	70,962
November	ČEZ Distribuce, a.s.	161,038	90,227	10,067
December	ČEZ Distribuce, a.s.	133,05	108,903	10,24

4 Costs of electric power supplier

In connection with interruption of electric power supply to customers financial expenses rise to suppliers. These expenses it's possible express by equation:

$$N_C = N_{NEZ} + N_{ZAV} + N_{INV} + N_{DAL} + N_{OZ} \tag{1}$$

N_{NEZ} – costs independent on system reliability parameters
N_{ZAV} – costs dependent on system reliability parameters
N_{INV} – cost of investments for increase of system reliability

N_{DAL} – other costs for increase of system reliability
N_{OZ} – costs for compensation of customers by interruption of electric power supply

4.1 Costs independent on system reliability parameters

These costs are forced by interruption of electric power supply, but they don't directly depend on system reliability parameters. Costs independent on system reliability parameters it's possible express by equation:

$$N_{NEZ} = N_{PPC} + N_{SPZ} \tag{2}$$

N_{PPC} – costs for arrangement of operation of breakdown service
N_{SPZ} – costs for other services for customers associated with interruption supply

4.2 Costs dependent on system reliability parameters

These costs are directly dependent on interruptions frequency and interruptions duration. That's evident these costs is possible decrease by increase of system reliability. Costs dependent on system reliability parameters it's possible express by equation:

$$N_{ZAV} = N_{MAN} + N_{VOPZ} + N_{NEE} \tag{3}$$

N_{MAN} – costs for manipulation in system
N_{VOPZ} – costs for replacement or reparation of damaged devices
N_{NEE} – costs for not sell electric power

Costs for not sell electric power refer to only suppliers, who deal not only distribution but so sell electric power.

4.3 Costs of investments for increase of system reliability

Most of costs that rise to electric power supplier in connection with interruption supply are dependent on reliability system. By increase system reliability is possible decrease other costs of supplier and in light of future process total costs too. Cost of investments for increase of system reliability it's possible express by equation:

$$N_{INV} = N_{ZA} + N_{VNC} + N_{INP} \tag{4}$$

N_{ZA} – costs for processing analysis about state and development of system
N_{VNC} – costs for building new parts of system
N_{INP} – costs for installation new modern components (for example reclosers, new switching or isolating components)

4.4 Other costs for increase of system reliability

These costs isn't possible judge as costs of investments, however they can contribute to increase system reliability. These costs it's possible express by equation:

$$N_{DAL} = N_{RPO} + N_{ZDPO} + N_{OOV} \quad \textbf{(5)}$$

N_{RPO} – costs for revision and planned reparation
N_{ZDPO} – costs for arrangement of supply during planned interruption (costs for operation of mobile distribution substation)
N_{OOV} – costs for disposal and lopping of vegetation

4.5 Costs for compensation of customers by interruption of electric power supply

Supplier is obligated to pay these costs to customers in the event that he isn't able to meet guaranteed standards of electric transmission or electric power distribution defined by regulation n. 540/2005 Sb. From mentioned above guaranteed standards three these standards direct relate to interruption of electric power supply to customers. Costs for compensation of customers by interruption of electric power supply it's possible express by equation:

$$N_{OZ} = N_{OPD} + N_{DPOP} + N_{VPP} \quad \textbf{(6)}$$

N_{OPD} – costs for non-performance standard renewal of electric transmission or electric power distribution after failure
N_{DPOP} – costs for non-performance standard compliance of planned restriction or interruption of electric power distribution
N_{VPP} – costs for non-performance standard replacement of damaged fuse

References

1. Tinka M.: Estimation of energy not supply, Wofex 2006, Ostrava
2. Willmann B. Gohler M.: Pohled na ekonomickou stránku kvality dodávky elektřiny a poskytovaných služeb distribuce, CIRED 2006, Tábor
3. Peleška S.: Zpráva CEER o kvalitě dodávek elektřiny v roce 2005, CIRED 2006, Tábor
4. ERÚ: Vyhláška o kvalitě dodávek elektřiny a souvisejících služeb v elektroenergetice č. 540/2005 Sb.

Optimal Economic Dispatch in Electrical Power System Using Genetic Algorithm

Khanh Hung Tran

Department of Theoretical Electrical Engineering, FEECS,
VŠB – Technical University of Ostrava, 17. listopadu 15, 708 33 Ostrava – Poruba
`khanh.hung.tran.st@vsb.cz`

Abstract. The optimal operations of power system are the major task in the power system generation. The objective of economic dispatch problem is to calculate the output power of every generation unit so that all demands are satisfied at minimum cost, while satisfying different technical constraints of network and generators. Until now several classical optimization techniques has been applied to solve this problem. Hence, dispatch result is inaccurate due to get trap in the local optimal. In order to overcome the above-mentioned drawbacks, genetic algorithms (GAs) has demonstrated to be an efficient tool for solving the economic dispatch problem. GAs search optimization in three ways: it search from population of candidates, it uses direct fitness information of function and it uses probabilistic. As a result, GAs can identify near global region. The IEEE 26 bus has been used to simulate in this paper, and the results are compared between LaGrange method and GAs.

1 Introduction

Genetic algorithms (GAs) was introduced by John Holland in the early 1970's. GAs has been applied to a lot of optimization problem. The characters of GAs are different from other search techniques in several aspects. First, the algorithm is not limited restrictive assumption about search space, and hence reducing the possibility of local minimum trapping. Second, GAs works with a coding of parameters instead of the parameters themselves. Thirdly, GAs evaluates the fitness of each individual instead of the optimization function. Therefore, there is no need for computation of derivatives. Finally, GAs explores the search space where the probability of finding improved performance is high.

In recent decays, soft computing techniques such as artificial neural networks (ANNs) and genetic algorithms (GAs) are increasing applied in a various applications. As an optimization tool ANNs and GAs are successfully applied in constrained optimization problems. The economic dispatch of electric power system is also a constrained optimization problem. Recently, GAs which is a probabilistic heuristic algorithm has been studied to solve the power optimization problems. Hence, GAs is an

© Václav Snášel (Ed.): WOFEX 2007, pp. 135–141, ISBN 978-80-248-1571-8.
VŠB – Technical University of Ostrava, FEECS, 2007.

attractive tool for economic dispatch problems. In this problem, the aim is to calculate the most economical schedule generation of very generator units, while satisfying load demand and operational constraints.

2 Overview of genetic algorithms

The GAs may find the several suboptimum solutions within a realistic computation time, even though there is no guaranty that the GAs may find the globally optimal solution in a finite time. GAs is based on the process of biological evolution, natural selection and population genetics. The mechanism of natural selection has been applied to the optimization problem of searching for a global optimization solutions.

The algorithm starts from a population which is a randomly selected initial solution set. The process searching for a global optimum is executed by moving individuals from the initial population to new population using genetic operators such as selection, crossover and mutation. Each individual represents a candidate to the optimization solution and is modeled by a value called chromosome. In the evolutionary process, in order to produce a new generation so that solution at the optimum may be obtained. The operation is based on a selective nature, the best individuals are chosen as parents so that the new generation holds best genetic heritage. For this purpose, a fitness function is used to calculate a fitness value of each individual within the population. This fitness value is measure for the quality of an individual. A typical GAs cycle included four majors' processes of fitness evaluation, selection, recombination and creation of a new generation. Based on fitness criterion, poorer individuals are progressively taken out, and best individuals are chosen to the next generation. The process of GAs includes three different phases: initial population generation, fitness evaluation and genetic operations (selection and reproduction, crossover and mutation).

3 Mathematical formulation of economic dispatch problem

The main purpose of economic dispatch problem is determine the amount of power that each generator in a system should produce so that the total cost of generation is minimized and meet fully the customers demands while satisfying system constraints.

Consider a system consisting of N_G thermal units connected to electric network, in case of steady-state operation of the power system, the economic dispatch problem is mathematically expressed by minimum the object function:

$$F_T = \sum_{i=1}^{n_G} (a_i + b_i P_{Gi} + c_i P_{Gi}^2), \$/h \tag{1}$$

And the operation system constraints:

$$\begin{cases} \sum_{i=1}^{n_G} P_{Gi} - P_T - \sum_{k=1}^{n_L} P_{Dk} - \sum_{i=1}^{n_G} P_{Di} = \varphi \\ P_{Gi}^{\min} \le P_{Gi} \le P_{Gi}^{\max}; i = 1, \dots, n_G \end{cases} \tag{2}$$

Where

P_{Gi}	power output of unit i
n_G	total number of online thermal units
P_{Dk}	load demand at node k
P_{Di}	load equipment of unit i
P_T	power transmission losses
n_L	number of loads
a_i, b_i and c_i	cost coefficients of generating unit i
φ	power balance tolerance
$P_{Gi}^{\min}, P_{Gi}^{\max}$	lower and upper real power limits of unit i

The economic dispatch problem (1) is a constrained optimization and often solved using the LaGrange multiplier. The solution states that the minimum fuel cost is obtained when the incremental fuel cost λ ($/MWh) is the same for all operating units of the system. The solution of this problem is found in the following iterative procedure. The process repeat until satisfy convergent conditions.

4 Genetic algorithm for economic power dispatch

There is several GAs, which has been applied to economic power dispatch; the lambda–based encoding method is presented in this paper.

In this method, the system incremental cost λ is used as coding parameter. The binary code is used in the encoding schemes, and the length of coding strings is entirely independent of the number of generating units. At the initialization stage, the initial population include n_p individuals using b_l number of bits are randomly generated C_k^m, $m = 1, 2, \dots, n_p$; $k = 1, 2, \dots, b_l$ with n_p, b_l are the population size and the number bits of a chromosome, respectively.

Each individual represents the system incremental costs. The individuals are decoded to the real value equivalent of the normalized system incremental cost. To calculate the system incremental cost, the normalized system incremental cost of the m^{th} individual is calculated as,

$$\lambda_{sys}^{m} = \lambda_{sys}^{min} + \frac{\sum_{k=1}^{b_l} S_k^m .2^{b_l - k}}{2^{b_l} - 1} \lambda_{sys}^{max} - \lambda_{sys}^{min} \tag{3}$$

Where λ_{sys}^{min} and λ_{sys}^{max} are respectively the minimum and maximum of the system incremental cost and defined as $\lambda_{sys}^{min} = \min\left(\frac{dF_i}{dP_{Gi}}\right)$ and $\lambda_{sys}^{max} = \max\left(\frac{dF_i}{dP_{Gi}}\right)$ for i = 1, 2, …, n_G.

The power outputs of n_G synchronized generating units are determined by applying the LaGrange method and the Kuhn-Tucker conditions [10].

$$\begin{cases} \lambda_{sys}^{m} = b_i + 2c_i P_{Gi} & \text{if } P_{Gi}^{min} \le P_{Gi} \le P_{Gi}^{max} \\ \lambda_{sys}^{m} \ge b_i + 2c_i P_{Gi} & \text{if } P_{Gi} = P_{Gi}^{max} \\ \lambda_{sys}^{m} \le b_i + 2c_i P_{Gi} & \text{if } P_{Gi} = P_{Gi}^{min} \end{cases} \tag{4}$$

If the generation power output is out of the operation limits, then the unit's power output is adjusted to operate at the lower or upper limit depending on the situation.

The object of the economic power dispatch is to minimize the total generation cost (1), while satisfying the constraints (2). To minimize the objective function F_T is equivalent to getting a maximum fitness value in searching process. A individual that has lower cost function should be assigned a larger fitness value, and the function is computed as follow:

$$\text{fitness}_i = \frac{1}{1 + \frac{1}{\sum_{i=1}^{n_G} F_i}} \tag{5}$$

After computing the fitness of each individual, the GA operators reproduction, crossover and mutation are applied to generate a new population, and this process continues until the convergence criterion is satisfied. The GA is converged when conditional convergences are satisfied as, the operation system constraints (2) are met, and there is no improvement in the solution after a number of generations (50 – 100 generations).

After the algorithm has converged, the final power flow is then executed to calculate the power output of each generating units, the total generating cost and the total system transmission losses.

5 Case studies

The IEEE 26-bus system was used to test the proposed algorithm for economic dispatch. The numeral results are compared between the LaGrange multiplier method and the lambda–based encoding method.

The generator's operating costs in \$/h, with P_i in MW are as follow

Gen	Min, MW	Max, MW	a (\$/h)	b (\$/MWh)	c (\$/MW^2/h)
1	100	500	240	7.0	0.0070
2	50	200	200	10.0	0.0095
3	80	300	220	8.5	0.0090
4	50	150	200	11.0	0.0090
5	50	200	220	10.5	0.0080
26	50	120	190	12.0	0.0075

Table 1. Generator's operating costs

The numeral results are given by in table 2. and respectively table 3.

Gen	LaGrange, MW	Lambda-based, MW
1	420.276	458.41
2	176.50	171.48
3	300	264.34
4	129.39	125.45
5	200	172.38
26	50	83.88

Table 2. Optimal dispatch of generation

	LaGrange	Lambda-based
Initial system loss, MW	15.53	15.53
Final system loss, MW	13.17	12.96
Total generation power output, MW	1276.17	1275.96
Incremental system cost λ, \$/MWh	13.79	13.26
Total generation cost, \$/h	15482.09	15296.70
Calculation time, Second	0.51	19.36
Number of iterations	6	66

Table 3. Parametric values

The total generation cost with LaGrange multiplier method is 15,408.09 $/h and the total generation cost with Lambda-based coding GA is 15,296.70 $/h. This results in a saving 112.2 $/h, with this loading, the total annual saving is nearly $1,0 million. From table 3the Lambda-based coding GA is given the least final system loss than the LaGrange method.

However, There are some disadvantages which are recognized in GA search. First, there are a large number of function evaluations. Therefore, the resulting of search process needs long execution time. Second, there is no way to definitely know whether the optimal solution has been found. In order overcome the processing time drawback, the modern computer hardware could considerably improve the computational time issue.

6 Conclusion

With the above-highlighted advances, the GAs has been extensively applied in the field of power system operation, economic dispatch, reactive power control, load flow analysis, distribution network planning, unit commitment, voltage optimization, optimal capacitor placement, and so on. And this is a very attractive method for the solution of the economic dispatch in electric power system.

References

1. Khanh Hung Tran, "Genetic Algorithm applied to optimal economic dispatch in electric power system", Master thesis, Ho Chi Minh City University of Technology – Viet Nam, July 2005.
2. Mr. S. O. Orero and Dr. M. R. Irving, "A genetic algorithm for generator scheduling in power system", Brunel Institute of power system, Dept. of electrical Eng. & electronics, Brunel University, Uxbridge, UB8 3PH, U.K.
3. Vladimiro Miranda and Luís Miguel Procenca, "Chapter 5 genetic/ evolutionary algorithm and application to power system", INESC Port Instituto Enga Sist. Computadores, Portugal and FEUP – Fac. Engenharia Universidade do Porto.
4. Tarek Bouktir, Slimani L. Bouktir, M. Belkacemi, "A genetic algorithm for solving the optimal power flow problem", Department of Electrical Engineering – University of Oum El Bouaghi – Algeria, Department of Electrical Engineering – University of Batna – Algeria, Leonardo Journal of Sciences, Issue 4, January – June 2004.
5. Ouiddir, M. Rahli and L. Abdelhakem - Koridak ,"Economic dispatch using a genetic algorithm: Application to Western Algeria's electric power network", Power system optimization laboratory, Faculty of electrical engineering – University of Science and technology of Oran – Algeria, Journal of Information Science and Engineering 21, 659 – 668, 2005.
6. Anastasios G. Bakirtzis, Christoforos E. Zoumas ,"Optimal power flow by enhanced genetic algorithm", IEEE Transactions on power systems, Vol 17, No. 2, May 2002.
7. Ashish Saini, Devendra K. Chaturvedi, A. K. Saxena, "Optimal power flow solution: GA – Fuzzy system approach, International Journal of Emerging Electric Power Systems, Volume 5, Issue 2, 2006.

8. John J. Grainger, William D. Stevenson, Jr., Power System Analysis, McGraw-Hill, Inc., 1994.
9. Allen J. Wood, Bruce F. Wollenberg, Power generation operation and control, Second edition, John Wiley & Sons, Inc., 1996.
10. O. I. Elgerd, Electric energy systems theory: An introduction, McGraw-Hill, 1971.

A Study of New Supply Way the Non-traction Take off at Czech Railways

Viktor Vik

Department of Theoretical Electrical Engineering, FEECS,
VŠB – Technical University of Ostrava, 17. listopadu 15, 708 33 Ostrava – Poruba
viktor.vik@seznam.cz

Abstract. The benefit deals with proposal outside self-contained aerial cable with voltage 22kV in environment of Czech course. In the benefit are determination mechanical and electrical qualities. This cable should serve for power supply not traction equipments on the railway (lighting, building, block system etc.). Project is creates under the support computer technique with concretely created software for this problems. This studie is subject of my dissertation thesis.

1 Introduction

A modernization of Czech railways is running now. Shorter track sections are electrified and main investments are directed to construction of railway corridors.

During construction of transit corridor in Czech Republic is running reconstruction of existing railways and adjustment or reconstruction of contiguous electrical apparatus and technologies. These arrangements are necessary part for running the railway transport. We talk about installation of reliable interlocking plants. Further there are necessary reconstructions of electrical apparatus of railway stations and intermediate stops, subway constructions, lighting adjustment and changing and laying cables.

I want to make proposal and evaluation of new supply way of non-train power take-off on electrified traction. It is the theme of my thesis.

Goal is proposing self-supporting suspension cable which will supply non-train appliances (lighting, traction buildings, block system etc.). The cable has 22kV and this voltage level will be reduced to the voltage level of single appliances. It was selected HV cable 12,7/22kV with wire supporting stainless-steel blank rope 22 – AXEKV-CEz.

2 Calculation of mechanical parameters of cable 22-AXEKVCEz

I am using programme *Průhyb vodiče* to determinate mechanical quality of cable, which be formed directly for these purposes. Programme should easy calculate the airline mechanical parameters. At determination of lead parameters it calculates me-

© Václav Snášel (Ed.): WOFEX 2007, pp. 142–147, ISBN 978-80-248-1571-8.
VŠB – Technical University of Ostrava, FEECS, 2007.

chanical tension in conductor and his deflection for different temperatures of outside environment.

2.1 Calculation

Leading role in the mechanical calculation of electric line has making-up an assembly tablet (portrayal assembly waveform), what is dependence of a stress and a conductor sag on outside temperature.

State equation of catenary:

$$\upsilon-\upsilon_o=\frac{\gamma^2\cdot a^2}{24\cdot\alpha}\cdot\left[\left(\frac{z}{\sigma_H}\right)^2-\left(\frac{z_0}{\sigma_{H0}}\right)^2\right]-\frac{\sigma_H-\sigma_{H0}}{E\cdot\alpha} \qquad \textbf{(1)}$$

where: α - thermal extensibility factor of material conductor (°C^{-1})
E - modulus of elasticity material of conductor (MPa)
υ - temperature of conductor (°C)
σ_H - horizontal component mechanical tension in conductor (MPa)
γ - specific weight of conductor ($N.m^{-1}.mm^{-2}$)
z - overfreight of conductor (-)
a - span of pole (m)

Calculation of conductor sag:

$$f=\frac{a^2\cdot\gamma\cdot z_0}{8\cdot\sigma_H}\ \text{(m)} \qquad \textbf{(2)}$$

2.2 Programme *Průhyb vodiče*

Programme was created in programmatic environment C-sharp (shortcut C#). At setting parameters of lead it calculates mechanical tension in conductor and his deflection for different temperatures of outside environment. This programme reflects temperature and weather conditions.
Programme goes out from fundamental equation of catenarian curve and it respects conditions on Czech railways (like magnitude of tension, height of posts etc.). In calculation isn't respected a deflection of poles or a strong wind. Programme respects standard specification ČSN EN 50341-3-19.

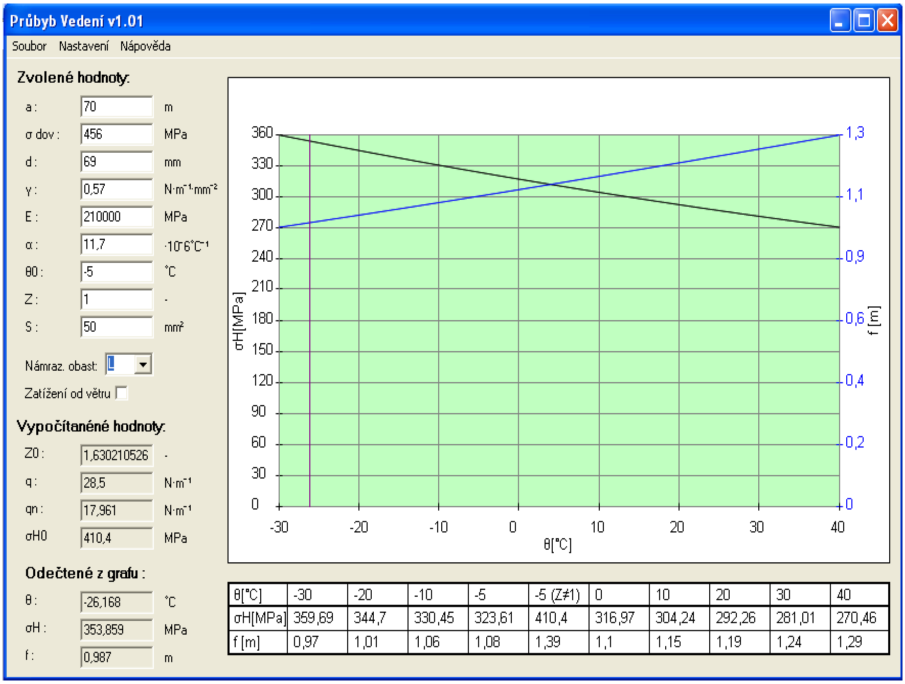

Zvolené hodnoty:

a : 70 m

σ dov : 456 MPa

d : 69 mm

γ : 0,57 $N \cdot m^{-1} \cdot mm^{-2}$

E : 210000 MPa

α : 11,7 $\cdot 10^{-6}$°C^{-1}

θ0 : -5 °C

Z : 1 -

S : 50 mm^2

Námraz. obast: L

Zatížení od větru ☐

Vypočítanéné hodnoty:

Z0 : 1,630210526 -

q : 28,5 $N \cdot m^{-1}$

qn : 17,961 $N \cdot m^{-1}$

σH0 410,4 MPa

Odečtené z grafu :

θ : -26,168 °C

σH : 353,859 MPa

f : 0,987 m

θ[°C]	-30	-20	-10	-5	-5 (Z≠1)	0	10	20	30	40
σH[MPa]	359,69	344,7	330,45	323,61	410,4	316,97	304,24	292,26	281,01	270,46
f [m]	0,97	1,01	1,06	1,08	1,39	1,1	1,15	1,19	1,24	1,29

Fig. 1. Status box of programme *Průhyb vedení* – assembly tablet 22- AXEKVCEz 50mm^2

Table 1. Assembly tablet 22-AXEKVCEz 50 mm^2, a = 70m

υ (C°)	-30	-20	-10	-5	-5(z≠1)
σ_H (MPa)	359,7	344,7	330,4	323,6	410,4
f (m)	0,97	1,01	1,06	1,08	1,39
υ (C°)	0	10	20	30	40
σ_H (MPa)	316,9	304,2	292,2	281	270,4
f (m)	1,1	1,15	1,19	1,24	1,29

Calculation of mechanical quality cable was effected for its bearer wire rope, which bears head cable weight. In reckonings isn't inclusion mechanics self conductor and single isolation, which escalate cable mechanical tension.

3 Electric line transmission capacity

At projection electric line is fundamental requirements add into consumption places requisite achievement at voltage rating. It means, that tension must overmatch the voltage drop, which is restricted crest of tension and crest of tension mustn't be overfull filled in normal operation. Electric line is dimensioned to not overfull fill permissible voltage drop.

3.1 Theory

Three-phase active power at the end of electric line:

$$P = \sqrt{3} \cdot U_2 \cdot I \cdot \cos\varphi_2 \quad \text{(W; V, A, -)} \tag{3}$$

Longitudinal voltage drop is:

$$\Delta U = \sqrt{3} \cdot R \cdot I \cdot \cos\varphi_2 + \sqrt{3} \cdot X \cdot I \cdot \sin\varphi_2 \tag{4}$$

Percentual voltage drop:

$$p_n = \frac{P \cdot l}{U_2^2 \cdot \cos\varphi_2} \cdot \left(R_K \cdot \cos\varphi_2 + X_K \cdot \sin\varphi_2\right) \cdot 100 \tag{5}$$

For existent electric line type (R_K, X_K), voltage system (U_2), $\cos\varphi_2$ and p_n we can write:

$$P \cdot l = konst. \tag{6}$$

$$P \cdot l = \frac{U_2^2 \cdot p_n}{R_K \cdot K \cdot 100} \quad \text{(MW, km; kV, \%, } \Omega\text{/km, -)} \tag{7}$$

Where:

$$K = 1 + tg\psi_2 \cdot tg\varphi_2 \tag{8}$$

Quadratic locution electric line transmission capacity depends on mileages transmission in the area, where's volt drop restrictive factor for transmission.

Distance l is:

$$l = \frac{U_2^2 \cdot p_n}{P_{\max} \cdot K \cdot R_K \cdot 100} \quad \text{(km; kV, \%, MW, -, } \Omega\text{/km)} \tag{9}$$

$$P_{\max} = \sqrt{3} \cdot U_2 \cdot I_{\max} \cdot \cos\varphi_2 \quad \text{(MW; kV, A, -)} \tag{10}$$

$P_{\max}$ is restrictive factor permissible load of conductor by current $I_{\max}$. Practically is criterion warming authority thereby, that every conductor has in a given environment determination maximum current load, so his temperature at normal operation could not exceed permission limits.

3.1 Cable analysis

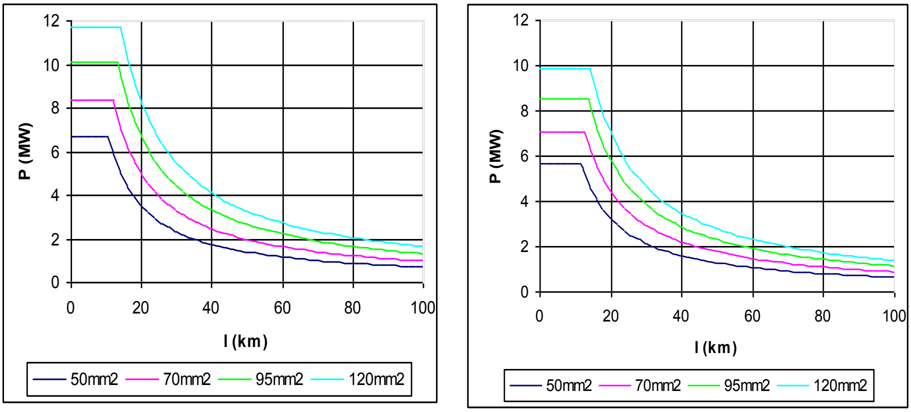

Fig. 2. Graphic illustration of electric line transmission capacity 50mm^2,70 mm^2, 95 mm^2, 120mm^2 22-AXEKVCEz, U_2 = 22kV, p_n =10%.
a) cosφ_2 = 0,95 b) cosφ_2 = 0,8

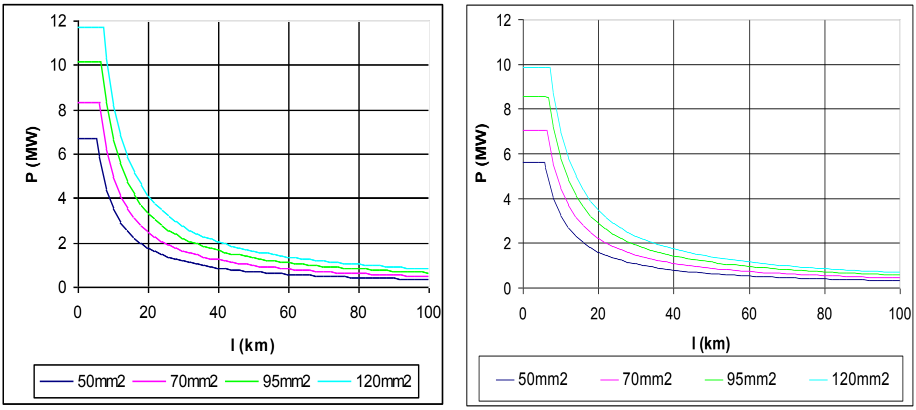

Fig. 3. Graphic illustration of electric line transmission capacity 50mm^2,70 mm^2, 95 mm^2, 120mm^2 22-AXEKVCEz, U_2 = 22kV, p_n =5%.
a) cosφ_2 = 0,95 b) cosφ_2 = 0,8

When cosφ_2 declines, then maximal transmitted electric power is proportionately declined. That is the reason for compensation of power factor cosφ_2. The maximal distance of l' does not depend on this loss of power but it depends on the percentual voltage drop. For this transmitted electric power decrease this distance to the half when this voltage drop declines from 10% to 5%. When the distance is longer than l', the transmitted electric power is limited by the voltage drop. The maximal transmission capacity is usually not use for the reason of big losts.

3 Structure of cable AXEKVCEz

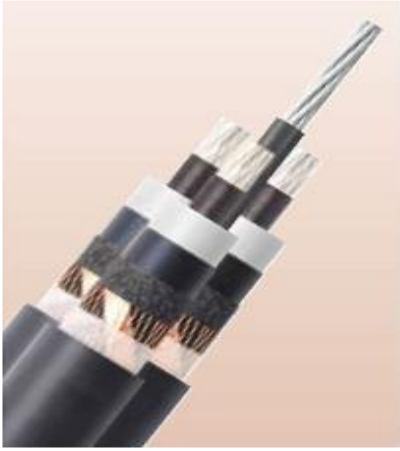

Fig. 4. Cable 22-AXEKVCEz

Aerial cable is made from three single-core cable which is right regular laid by the PN05/96. Aerial line is made from stainless-steel and it is hot-dip galvanized without cable sheathing. It is produced in many different versions.

Price:
22-AXEKVCEz 50mm^2… . 500 000 Kč/km
22-AXEKVCEz 70mm^2 …..530 000 Kč/km
22-AXEKVCEz 95 mm^2…..570 000 Kč/km
22-AXEKVCEz 120mm^2….610 000 Kč/km

4 Conclusion

By the requirements on electric power from Czech railways and calculations of electric parameters (transmission capacity of electric line, voltage drop) and mechanical parameters will be chosen the adequate type of cable 22-AXEKVCEz. The requirements will be probably various, so many versions of the cable are processed.

References

1. PALEČEK, J a kol.:Elektorenergetika 1., Skripta VŠDS Žilina, 1990
2. VARGA, L a kol.: Výpočet mechanických pomerov vonkajších silových vedeí, Edícia vedeckých spisov FEI TU Košice, 2002
3. Lánková, G.: Vybrané state z pevných trakčných zariadení, Skripta VSDS Žilina, 1987
4. Kiesling, F., Puschmann, R., Schmieder, A.: Contact lines for electric railways, Siemens, Mnichov 2001

Acknowledgement

The support for this research work has been provided by the GAČR project 102/05/H525: The Postgraduate Study Rationalization at Faculty of Electrical Engineering and Computer Science VSB-TU Ostrava.

Methodology of Tunnel Luminance Measurement Using LMK Mobile Advanced Luminance Camera

Zdislav Žwak

Department of Electrical Power Engineering, FEECS,
VŠB – Technical University of Ostrava, 17. listopadu 15, 708 33 Ostrava – Poruba
`zdislav.zwak.fei@vsb.cz`

Abstract. This work deals with luminance measuring of tunnel Sitina in Bratislava. Measured values are compared with designed values, which are in separate reports. Calculations and measuring are outgoing from CR 14380:2003 document.

1 Introduction

Measured tunnel is situated in Bratislava. It has two tubes, which are titled as a West tube and an East tube. Length of West tube is 1440 meters and length of East tube is 1415 meters. Both tubes are designed as a one way in normal mode.

Lighting system contains three switchable groups, every third luminaire has power reduction down to 50% of light flux. Adaptation, interior and exit zones were evaluated. Last measured mode was opposite direction, which is used in emergency state or when one tube is maintained. This paper contains two chosen modes.

1.1 LMK mobile advanced

Special luminance analyzer LMK mobile advanced is used to measure luminance. This device uses digital reflex camera for measuring and special software for evaluation of measured situation.

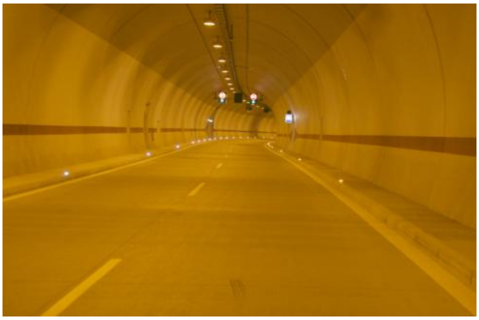

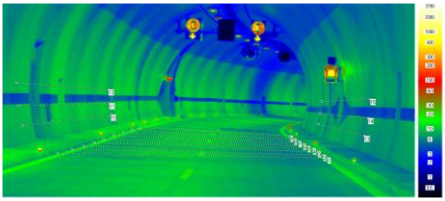

Fig. 1. Measured situation (left). Evaluated situation presented by luminance field (upper).

Measured zones (threshold, transition, interior, exit) were divided to areas of length of 35 m, where initial point of measuring was 60 m before beginning of measured field in

© Václav Snášel (Ed.): WOFEX 2007, pp. 148–154, ISBN 978-80-248-1571-8.
VŠB – Technical University of Ostrava, FEECS, 2007.

an axis of driving lane, 1,5 m over road surface. Measured road field contains net of measured points with longitudinal pitch equal 5 m y=(0, 5, 10, 15, 20, 25, 30, 35) m and with cross pitch x=(1,63; 2,88; 4,13; 5,38; 6,63; 7,88) m. Measured wall field contains cross net of measured points with pitch z=(0,5; 1,1; 1,7) m with the same longitudinal pitch as a road field. This applies for both left and right walls.

1.2 Physical description of tunnel Sitina [2]

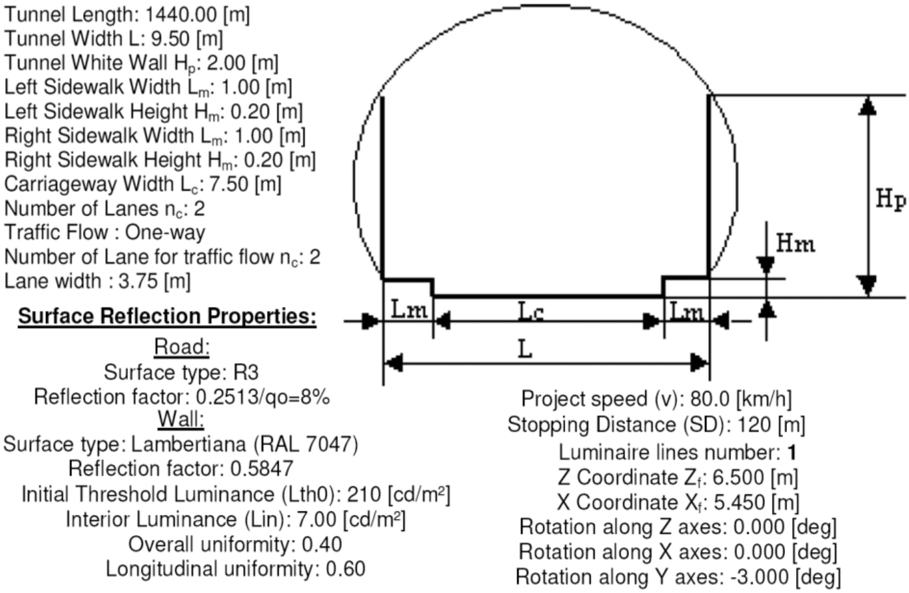
Tunnel Length: 1440.00 [m]
Tunnel Width L: 9.50 [m]
Tunnel White Wall H_p: 2.00 [m]
Left Sidewalk Width L_m: 1.00 [m]
Left Sidewalk Height H_m: 0.20 [m]
Right Sidewalk Width L_m: 1.00 [m]
Right Sidewalk Height H_m: 0.20 [m]
Carriageway Width L_c: 7.50 [m]
Number of Lanes n_c: 2
Traffic Flow : One-way
Number of Lane for traffic flow n_c: 2
Lane width : 3.75 [m]

Surface Reflection Properties:
Road:
Surface type: R3
Reflection factor: 0.2513/qo=8%
Wall:
Surface type: Lambertiana (RAL 7047)
Reflection factor: 0.5847
Initial Threshold Luminance (Lth0): 210 [cd/m²]
Interior Luminance (Lin): 7.00 [cd/m²]
Overall uniformity: 0.40
Longitudinal uniformity: 0.60

Project speed (v): 80.0 [km/h]
Stopping Distance (SD): 120 [m]
Luminaire lines number: **1**
Z Coordinate Z_f: 6.500 [m]
X Coordinate X_f: 5.450 [m]
Rotation along Z axes: 0.000 [deg]
Rotation along X axes: 0.000 [deg]
Rotation along Y axes: -3.000 [deg]

Fig. 2. Physical dimensions of tunnel and luminaire location

1.3 CR 14380:2003 – Tunnel lighting

The aim of tunnel lighting is to ensure that users, both during the day and by night, can approach, pass through, and exit the tunnel without changing direction or speed with the degree of safety commensurate to that on the approach on the road. [1]

Principal characteristics required to describe the quality of tunnel lighting are [1]:

- the luminance and illuminance levels of the road surface;
- the luminance level of the walls up to 2 m in height above the road surface;
- the uniformity of the luminance distribution on the road and walls;
- the control of induced glare;
- the avoidance of critical flicker frequencies.

Adaptation zone contains threshold and transition zones. The luminance level of the threshold zone L_{th} must be provided during daytime from the beginning of the threshold zone and for a length of 0,5 stopping distance SD. From half the SD onwards, the light level may linearly decrease to a value equal 0,4 L_{th} at the end of threshold zone. In the transition zone, luminance level is described by equation:

$$L_{tr}=L_{th}(1,9+t)^{-1,4}\ (cd/m^2),\text{ where } t = \text{time in sec.} \qquad (1)$$

At the end of transition zone, luminance level reaches luminance value of interior zone.

Overall uniformity is computed from all luminance values included in evaluated area and is computed from following equation:

$$Uo=L_{minUo}/L_{meanUo}\ (-) \qquad (2)$$

Longitudinal uniformity is computed from all luminance values lying in axis of driving line in evaluated area and is computed from following equation:

$$U_l=L_{min}/L_{max}\ (-) \qquad (3)$$

1.4 Measured situations

To evaluate tunnel light parameters were measured following modes:

a) day mode (West + East tube)
- adaptation zone 16,67; 50 and 100 %
- interior zone 100%
- exit zone
- opposite direction

b) night mode (West + East tube)
- interior zone 50%

1.5 Evaluation of chosen situation (Adaptation zone 100%)

Adaptation zone contains threshold and transition zone. Length of threshold zone is 0,5 of stopping distance.

Fig. 3 contains graphs of designed and measured luminance. Luminance values presented by curves respects maintenance factor equal to 0,7. Maintained L (left) and R (right) values represent average measured luminance values of each driving lane. Values in left driving lane are measured from left driving lane axis. Identical condition applies for right driving lane. Luminance values computed by SiTunnel software are presented by the curve “designed value”. Minimal luminance values requested in document CR 14380 are presented by the curve “14380”, which definition is described in 1.3. Measured values should not fall below this curve.

Wall luminance values are drawn as mean maintained luminance value.

LL (left driving lane DR, left wall W), LR (left DR, right W), RL (right DR, left W) and RR (right DR, right W)

Table 1 shows overall and longitudinal uniformity of adaptation zone. Requested minimal values are for overall uniformity equal or higher to 0,4 and for longitudinal uniformity equal or higher 0,6.

Table 1. Overall and longitudinal uniformity computed from measured values.

Overall and longitudinal uniformity of left driving lane						
Distance [m]	LminUo [cd/m2]	Lmin [cd/m2]	Lmax [cd/m2]	LmeanUo [cd/m2]	Overall uniformity Uo [-]	Longitudinal uniformity Ul [-]
1-20	301,4	460,9	587,3	519,2	0,58	0,78
21-40	356,9	478,5	511,1	490,2	0,73	0,94
41-60	329,3	428,9	522,5	459,6	0,72	0,82
61-80	193,4	374,6	419,6	374,4	0,52	0,89
81-100	244,9	339,9	395,0	351,9	0,70	0,86
101-120	183,4	244,0	309,3	263,6	0,70	0,79
121-140	94,5	140,5	214,0	161,9	0,58	0,66
141-160	66,4	94,4	109,3	95,7	0,69	0,86
161-180	53,4	78,9	90,0	81,5	0,66	0,88

Overall and longitudinal uniformity of right driving lane						
Distance [m]	LminUo [cd/m2]	Lmin [cd/m2]	Lmax [cd/m2]	LmeanUo [cd/m2]	Overall uniformity Uo [-]	Longitudinal uniformity Ul [-]
1-20	250,4	281,2	378,5	383,5	0,65	0,74
21-40	288,9	348,6	369,4	386,0	0,75	0,94
41-60	274,4	329,3	355,9	371,2	0,74	0,93
61-80	235,7	294,5	332,5	338,2	0,70	0,89
81-100	199,6	237,7	290,6	286,6	0,70	0,82
101-120	132,8	181,5	225,3	221,0	0,60	0,81
121-140	74,9	99,0	168,3	142,8	0,52	0,59
141-160	53,8	63,6	93,4	87,2	0,62	0,68
161-180	44,4	55,5	64,6	63,6	0,70	0,86

West tube, average road luminance measured from the axes of driving lanes

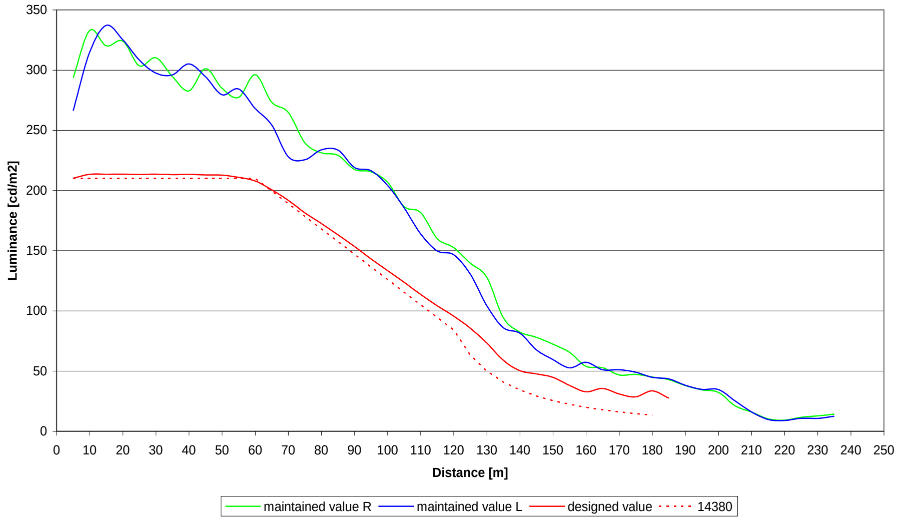

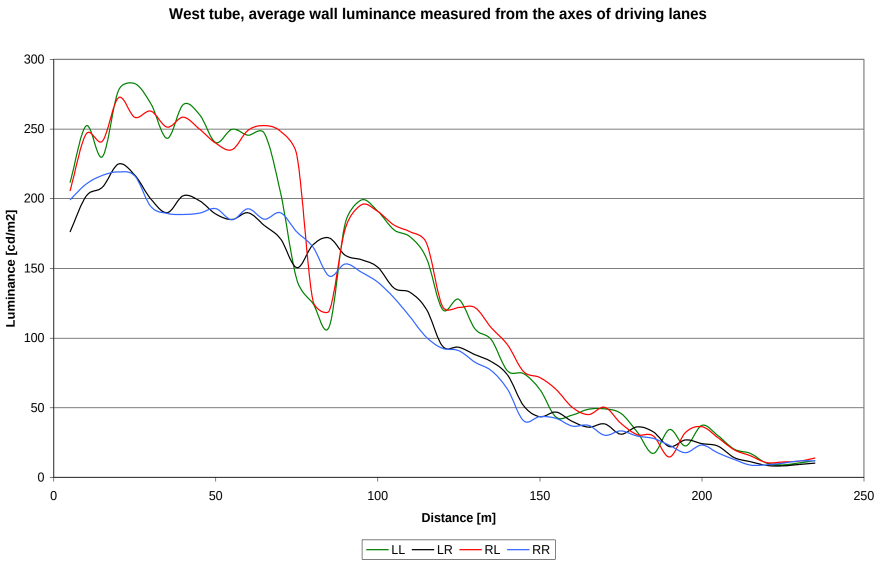

Fig. 3. luminance diagrams of adaptation zone

Deep fall of luminance on the left wall (Fig. 3) is caused by exhauster, which is mounted at the top of the tube. You may recognize it in Fig. 1.

1.6 Evaluation of chosen situation (Interior zone 50%)

Interior zone has nearly uniform luminance distribution and therefore measuring and evaluation is not such complicated as in adaptation zone.

	Computed from measured values	Values from SiTunnel
Overall uniformity L_{minUo}/L_{meanUo}:		
- left driving lane	0,79	0,59
- right driving lane	0,78	0,59
Longitudinal uniformity L_{min}/L_{max}:		
- left driving lane	0,73	0,87
- right driving lane	0,83	0,83

Luminance values SiTunnel:

Mean luminance in axis of right driving lane: 3,66 cd/m^2
Mean luminance of left wall: 5,9 cd/m^2
Mean luminance of right wall: 6,12 cd/m^2

Luminance values computed from measured values:

Mean luminance in axis of right driving lane: 8,1 cd/m^2
Mean luminance of left wall: 9 cd/m^2
Mean luminance of right wall: 7,3 cd/m^2

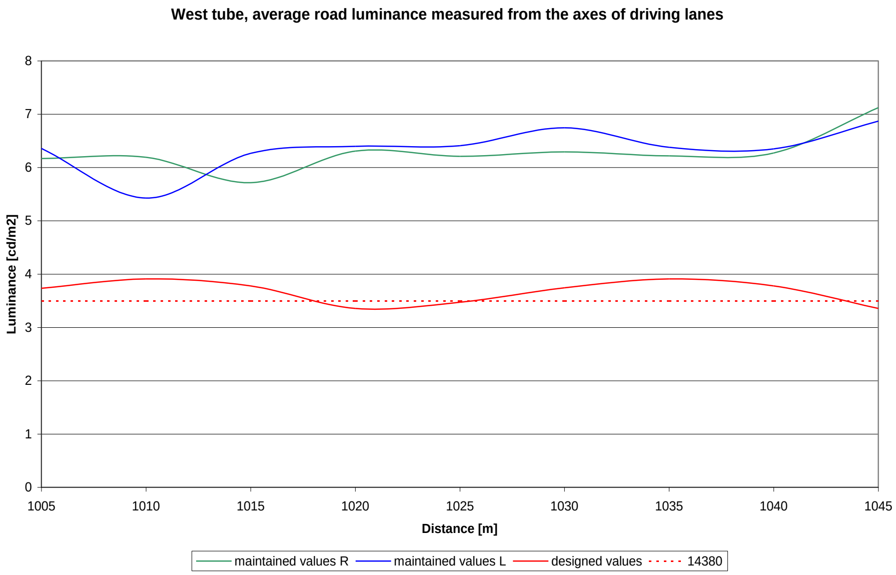

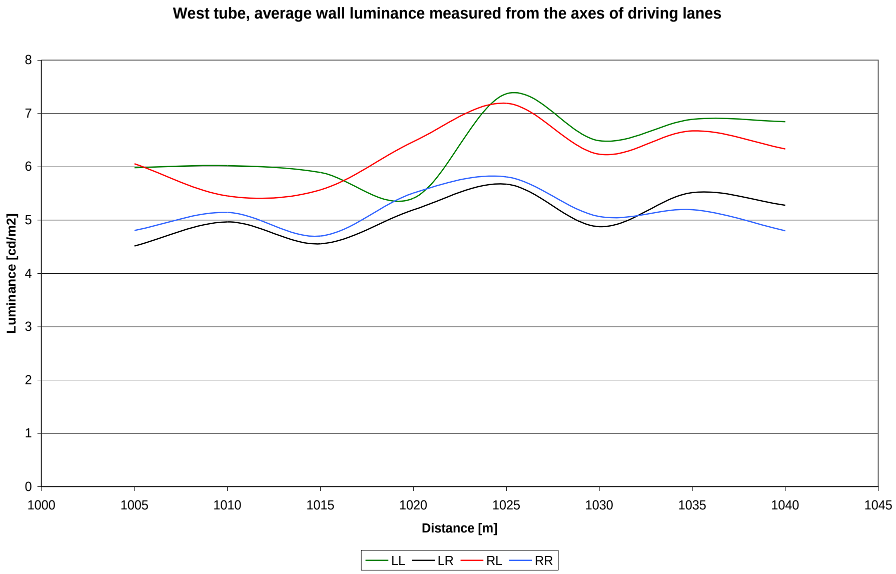

Fig. 4. luminance diagrams of interior zone

2 Conclusion

Measured road luminance values are over luminance values computed in SiTunnel. Mean wall luminance values should reach at least 50% of road luminance value. This requirement is also fulfilled.

Uniformity values do not fall below requested values, therefore tunnel lighting fulfill requests of CR 14380:2003 document.

References

1. European Committee for Standardization: CEN Report, Brussels (2003) 14380:2003E
2. Background papers, protocols with computed values.

The Current Sensor for Power Electronic Applications

Martin Dostalík

Department of Electronics, FEECS,
VŠB – Technical University of Ostrava, 17. listopadu 15, 708 33 Ostrava – Poruba
martin.dostalik.fei@vsb.cz

Abstract. This paper presents a method of current measurement with the use of the magnetic Hall sensors. That is an indirect current measurement method, based on sensing of magnetic field around the conductor wire. There isn't used a ferrite magnetic field concentrators and the sensor unit it's possible to connect it with a microprocessor system. There was selected a modern magnetic sensor by LEM manufacturer with the bandwidth up to 100 kHz. To follow the correct magnetization of Hall sensor there were performed the simulation of magnetic field around the Hall sensor in depending on the geometric construction of current measurement unit.

1 Introduction

The aim of my work is the design of current sensor in the power electronics usage. Whereas is the current sensor used in the power converters and in the power switching applications, they is necessary respect a high requirements of this area. The sensors and DSP unit for signal processing are situated in hard conditions with high differences of temperature and high disturbances of magnetic field. There has been selected a modern integrated Hall sensor by LEM.

2 Requirements to the measurement system

To the relevant requirements on power electronics it's necessary to do the galvanic isolation between the measured side and signal side. Also is necessary to ensure the alternately and direct currents measurement with the minimal bandwidth about 30 kHz. The current sensor must be resistant to overloading and high differences of temperature. In the area with high disturbances where are data communications between the sensor, DSP board and master control system of the power unit.

© Václav Snášel (Ed.): WOFEX 2007, pp. 155–160, ISBN 978-80-248-1571-8.
VŠB – Technical University of Ostrava, FEECS, 2007.

3 Designed system

The designed system uses the indirect current measurement. Hall sensors sensing a magnetic field around the conductor wire. The situation is illustrated on the figure 3.1. Principe of current sensing is based on Biot-Savart law, which is represented by the equations 3.1 and 3.2. The equation 3.2 we can use with a few simplifying conditions (infinitely long and thin wire).

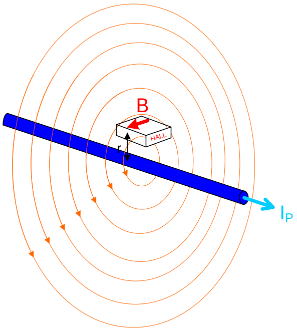

Fig. 3.1. The sensor orientation in the magnetic field.

$$i = \oint_{l} \overline{H} \cdot \overline{dl} \tag{3.1}$$

$$B = \frac{\mu_0 \cdot I}{2 \cdot \pi \cdot r} \tag{3.2}$$

3.1 New conception with four field sensing elements

New conception of current measurement unit is consisting of four chips with integrated Hall sensors and magnetic field concentrators (Fig. 3.1.1).

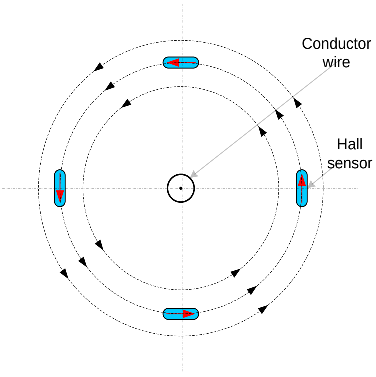

Fig. 3.1.1. The geometric structure with four Hall sensors around the conductor wire.

The Hall sensors are situated in two upright axes in the equivalent proximity of the axes center. Value of measured current will equal the total sum of the all signals from Hall sensors. More information about Hall sensor is referenced in chapter 4.

3.2 The magnetic field simulation

For find a correct shape of magnetic field around the sensors and conductor were processed the simulations. Simulation data were achieved by the simulation software names Quick Field. Results of the simulations are used to find a maximum current flow there is acceptable for the range of flux density of Hall sensor. On the picture 3.2.1 and 3.2.2 are solved a magnetic field with the current flow J = 620A/cm2. When the wire conductor and current sensor are in the tight proximity, the flux density is in the upper limit of sensor range 3,3mT. With the increasing proximity between conductor wire and Hall sensor is the flux density decreased.

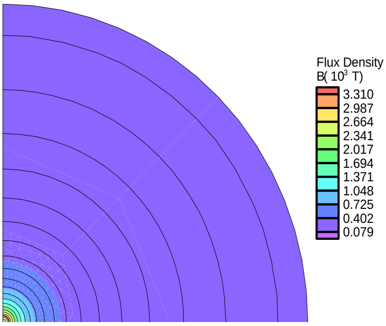

Fig. 3.2.1. The results of simulation by Qfield (magnetic field view in color scale).

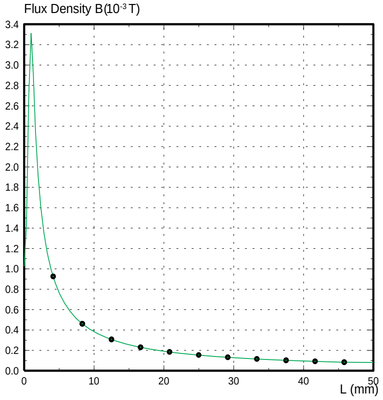

Fig. 3.2.2. The results of simulation by Qfield (The flux density in depending on the sensor-wire proximity).

3.3 Basic characteristic

With the usage of the aforesaid technology, we can keep all the requirements on the current sensor presented in the chapter 2. The bandwidth of Hall sensors (100 kHz) is very high thanks to LEM technology and is possible design a higher bandwidth with the usage of the software DSP algorithms. The construction with the four Hall sensors bring there automatic cancellation of the external disturbances (Fig. 3.3.1 and 3.3.2). In the case, that the conductor wire won't be in the axis center of sensors, there must be recalculated the output data of all sensors by the figure 3.3.3. All outputs of the sensors are therefore connected to the DSP board, which makes recalculation with parametric linearization.

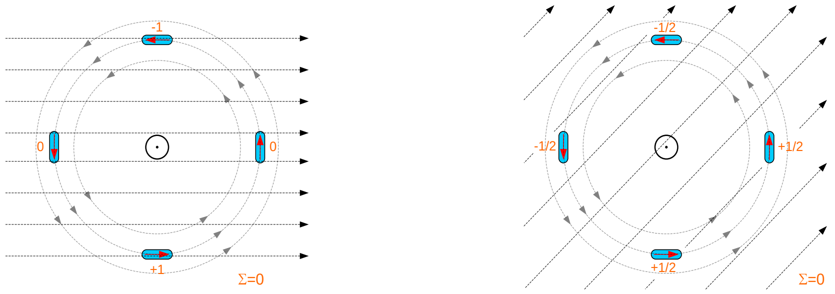

Fig. 3.3.1, 3.3.2. The sensors immunity in the disturbing fields.

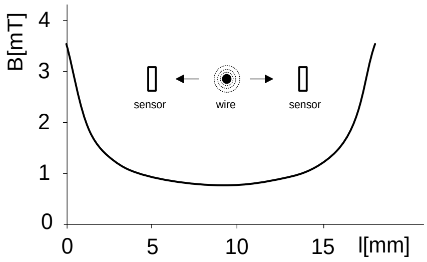

Fig. 3.3.3. The flux density summation by the opposed sensors.

4 Hall sensor

The modern Hall sensor (current transducer) is by the family LEM minisens type FHS40-P/SP600. It is an ultra flat SMD-SO8 open loop integrated circuit current transducer based on the Hall effect principle.

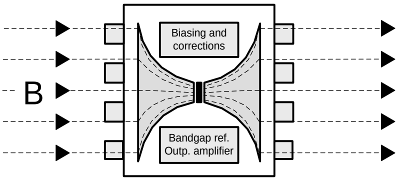

Fig. 4.1. Block diagram with internal magnetic field concentrators.

In the chip are integrated also the magnetic field concentrator, the circuits for Hall sensor compensation, the reference voltage source with outside adjustment, the temperature compensation circuit and the output operational amplifiers with the selectable low-pass filter. The lower power consumption can be obtained with the stand-by mode usage.

Parameter	value	unit	tolerance
Voltage supply	5	V	± 10%
Power consumption	15	mA	
Measurement range	± 3,3	mT	
Output voltage range	± 2.0	V	
Bandwidth	100	kHz	
Reaction time	3	μs	

Table 4.1. The basic parameters of the LEM minisens.

5 Measured characteristic

For the sensor accuracy verification were processed the measurement in static and dynamic conditions. In the static mode were increased the basic sensitivity trough the five coils around the current transducer. The dynamic characteristics were measured on the half bridge MOSFET switch controlled by the external arbitrary square generator. The transistors ware switched a resistance load with minimized inductions. The current transducer was placed in the near proximity by the wire conductor.

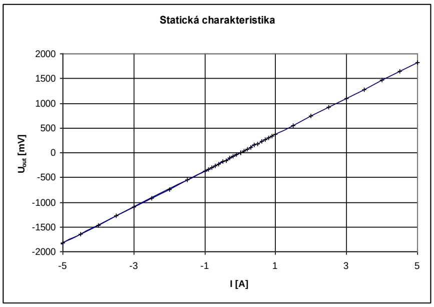

Fig. 5.1. The static diagram of the LEM sensor.

On the static characteristic (Fig. 5.1) can we see the basic offset of the sensor, which we can eliminate this, by the DSP software algorithms in the init conditions. These characteristic were measured with internal low-pass filter. The excellent linearity by the LEM datasheet was confirmed.

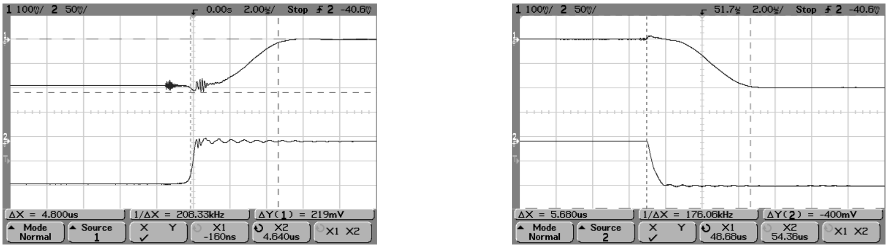
1 100mV/ 2 50mV/
0.00s 2.00us/ Stop 2 -40.6mV
ΔX = 4.800us
1/ΔX = 208.33kHz
ΔY(1) = 219mV
Mode Normal
Source 1
X Y ✓
X1 -160ns
X2 4.640us
X1 X2
1 100mV/ 2 50mV/
51.7us 2.00us/ Stop 2 -40.6mV
ΔX = 5.680us
1/ΔX = 176.06kHz
ΔY(2) = -400mV
Mode Normal
Source 2
X Y ✓
X1 48.68us
X2 54.36us
X1 X2

Fig. 5.2, 5.3. The fall time and rise time edges at the switching. The upper line pertains to the output of LEM sensor and the lower line pertains to the reference probe LEM PR55.

In the figures 5.2 and 5.3 are shown the output sensor responses of the dynamic switching. The upper characteristic belongs to the minisens sensor output with the low-pass filter and the lower characteristic belongs to the oscilloscopic probe LEM PR55 with the bandwidth 1MHz.

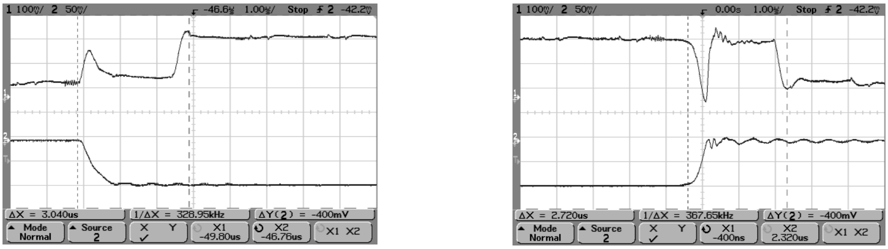
1 100mV/ 2 50mV/
-46.6us 1.00us/ Stop 2 -42.2mV
1
2
T
ΔX = 3.040us
1/ΔX = 328.95kHz
ΔY(2) = -400mV
Mode Normal
Source 2
X Y ✓
X1 -49.80us
X2 -46.76us
X1 X2
1 100mV/ 2 50mV/
0.00s 1.00us/ Stop 2 -42.2mV
1
2
T
ΔX = 2.720us
1/ΔX = 367.65kHz
ΔY(2) = -400mV
Mode Normal
Source 2
X Y ✓
X1 -400ns
X2 2.320us
X1 X2

Fig. 5.4, 5.5. The fall time and rise time edges at the switching. The upper line is the fast output of the LEM sensor and the lower line pertains to the reference probe LEM PR55.

The output of the minisens sensor without the low-pass filter can we see on the figures 5.4 and 5.5. The fast sensor output generate a quicker signal differences, but with bigger signal disturbances. The signal of fast output pin is inverted. It follows from internal circuits of the sensor chip.

6 Conclusion

The paper presents one of possibilities for next developing in the measurement electronics for power electronic systems. From a known magnetic sensors were selected the modern Hall sensor by LEM. According to results of measurement, the Hall sensor is suitable for usage in power electronic applications. I will find now new software solutions for increasing the sensor's output quality. I think the better offset correction process with minimizing the temperature depending, better linearity accuracy and mainly the summation method for all signals of sensors output.

7 Acknowledgment

The paper was supported by grant Agency of Czech Republic by project No. 102/05/H525. This research was supervised by Prof. Ing. Petr Chlebiš, CSc.

References

1. Popović, Z., Popović, B.: Introductory electromagnetics, Prentice Hall, New Jersey (2000), ISBN 0-201-32678-7, 183-301
2. Datasheet LEM minisens FHS40-P/SP600, www.lem.com, 2007 Feb 13.
3. LEM - Minisens/FHS design guide – CA070201, ver. 0, www.lem.com.

Measurement of the Energy Consumption of Railcars

Martin Škopek

Department of Electronics, FEECS,
VŠB – Technical University of Ostrava, 17. listopadu 15, 708 33 Ostrava – Poruba
martin.skopek.fei@vsb.cz

Abstract. In this paper, there are described the arguments why energy measurement is needed on board of electric railcars. Used multi-system energy meter for required measuring is presented here. In this document is shown connection of current and voltage sensors to the energy meter. There is also explained measurement principle and following calculation required value based on presented formulas. In the next part of the text, there is introduced process storage of values, parameters and relevant events. In the end, there is described transmission data from energy meter into central server.

1 Introduction

At the present time, it is very topical problem of electromagnetic compatibility driver (EMC) and saving of energy. Associated with this problem is requirement of measurement of actual consumption energy of the traction vehicles, including record of relevant values for the harmonic analysis and identification of the backward effects influencing supply traction network. Record of actual consumption of electrical energy result above all from arguments of energy efficiency and exact value the consumed and regenerated energy by the train (control drive).

2 Why energy measurement is needed?

- Increasing privatization of rail networks
- More and more private electricity utilities
- Demand for competitiveness between railway companies by the European Union
- More leasing of trains – freight and passenger
- Dual system suburban trains, metros & trams (AC outside, DC inside cities)
- Energy efficiency (control of power consumption / driver control)

Energy Meters EM4T use on trains of these arguments

- To know exactly the consumed and regenerated energy by the train
- To pay only the consumed energy

© Václav Snášel (Ed.): WOFEX 2007, pp. 161–166, ISBN 978-80-248-1571-8.
VŠB – Technical University of Ostrava, FEECS, 2007.

- For accounting independent, certified measuring system needed (PTB Approval)
- New multi voltage locomotives for cross border traffic

3 Measurement of the energy consumption

For measurement of the energy consumption in traction applications has been developed energy meter EM4T by the company LEM. The EM4T is a single-phase version of the multi-system energy meter, which can be connected to any existing traction network (600 V to 3 000 V DC, 15kV / 16,7Hz and 25kV / 50 Hz AC). It has 4 input channels to connect AC and DC measurement equipment at the same time (is needed for multi-network train) (Fig.1.)

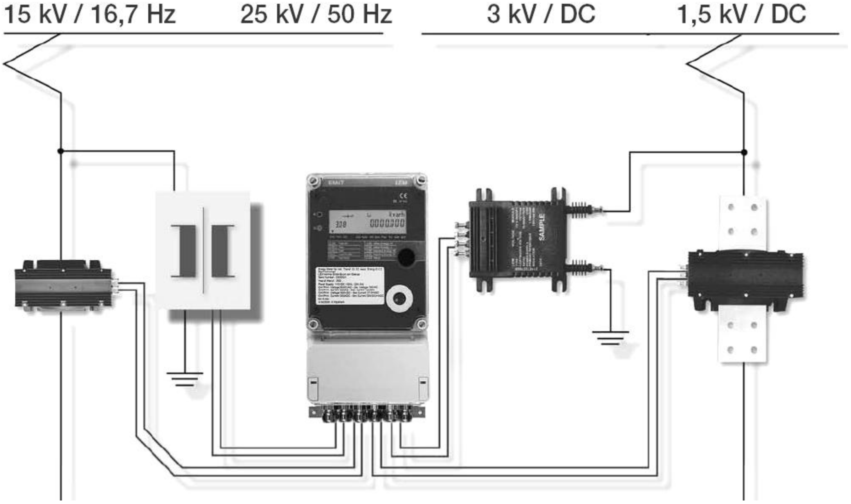

Fig. 1. Circuit diagram of current and voltage sensors connected to the energy meter EM4T

3.1 Main technical parameters of Energy Meters EM4T

Measuring ranges:	Nominal voltage:	AC: 90V to 300V AC/DC: 25mA to 300mA
	Nominal current:	AC: 25mA to 1A, 5A AC/DC: 25mA to 1,5A
Frequency range:	First harmonic:	DC, 16 2/3 and 50 Hz
	Harmonics:	up to 1000 Hz
Accuracy:	0,2; 0,5 and 1	
AD Conversion:	1 Sigma Delta converter ADC per channel	
ADCs Resolution:	16 Bits	
Sampling rate:	4000 Hz	

Interface: RS232, RS422, optical

4 Energy Meter EM4T

4.1 Measurement principle

The inputs of current and voltage are directly connected to the measuring circuit via differential inputs (insulation in the converters). The measuring circuit consists of one sigma-delta ADC per measuring channel, providing for simultaneous detection of measuring values at a sampling rate of 4 kHz. The sigma-delta method effectively suppresses high-frequency disturbances in both channels with identical frequency responses.

A 16-bit microprocessor reads the sampling values and calculates both the active power and the active energy via intervals that can be set (standard value = 15 minutes). The data records include the date, time, events, train identification number and the absolute energy for consumption and feedback. They are saved in flash memories (a special type of EEPROM) eliminating the need to replace internal batteries or accumulators.

The data can be transferred by one of the two insulated interfaces (RS232 or RS422). There is also an additional optical interface.

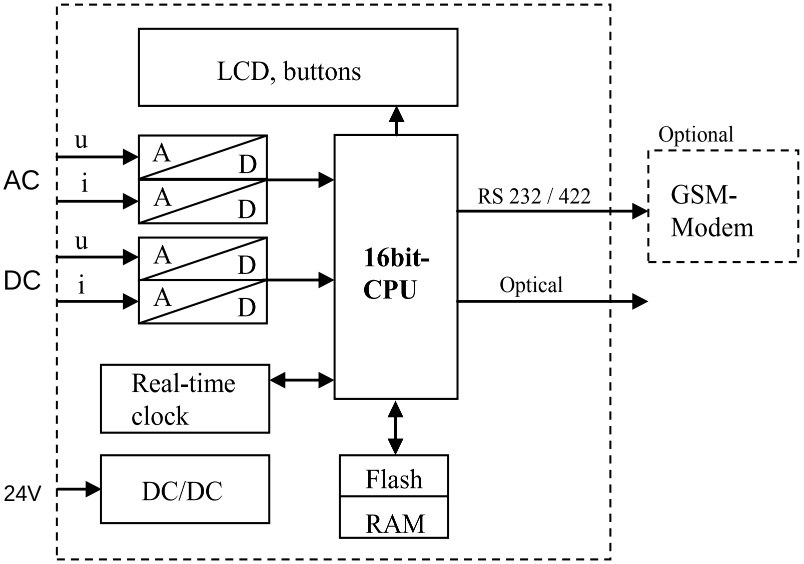

Fig. 2. Block diagram energy meter EM4T

4.2 Calculating powers

The apparent, active and reactive powers are calculated using the following data:

Voltage time value:	u(t)
Current time value:	i(t)
Shifted current time value:	i90(t) for calculating the reactive power

Calculating AC powers

Calculations per sampling time (1 ms)

Individual summations:

$$\sum p = \sum p + u(t) \times i(t) \qquad \textit{Sum of active powers} \tag{1}$$

$$\sum q = \sum q + u(t) \times i90(t) \qquad \textit{Sum of reactive powers} \tag{2}$$

$$\sum u^2 = \sum u^2 + u(t) \times u(t) \qquad \textit{Sum of voltage (squared)} \tag{3}$$

$$\sum i^2 = \sum i^2 + i(t) \times i(t) \qquad \textit{Sum of current (squared)} \tag{4}$$

Calculations per half-wave (10 ms or 30 ms)

Calculating powers:

$$P_{T/2} = \frac{\sum p}{Number\_of\_samples} \qquad \textit{Active power} \tag{5}$$

$$\mathrm{S}_{\mathrm{T/2}} = \frac{\sum u^2 \times \sum i^2}{Number\_of\_samples} \qquad \textit{Apparent power} \tag{6}$$

$$\mathrm{Q}_{\mathrm{T/2}} = \sqrt{\mathrm{S}_{\mathrm{T/2}} - \mathrm{P}_{\mathrm{T/2}}} \qquad \textit{Reactive power} \tag{7}$$

Calculating DC power

Calculations per sampling time (1 ms)

Individual summations:

$$\sum p = \sum p + u(t) \times i(t) \qquad \textit{Sum of active powers} \tag{8}$$

Calculations per half-wave (10 m)

Calculating powers:

$$P_{T/2} = \frac{\sum p}{Number\_of\_samples} \qquad Active\,power \qquad (9)$$

5 Data processing

The EM4T energy meter performs a cyclic storage of energy data in an integrated load profile memory. Changing operating conditions are also saved in a logbook. Once the load profile memory has reached its capacity, the oldest data is overwritten. All events and disturbances detected by the energy meter are logged in the logbook. The logbook is part of the load profile memory. A message is entered into the logbook when at least one status bit is changing. Setting a train number is entered into the logbook as well as setting the date and the time or the occurrence of a voltage failure. According to the default configuration, the energy meter will save the recorded power and the fed-back power of the locomotive in its load profile memory in 15 minute intervals (i.e. every full quarter of an hour 8:15, 8:30, etc.). The read-out time of the entire load profile memory including the logbook at a 9600Bd transmission rate is approx. 30minutes. A partial read-out of the load profile memory takes correspondingly less time.

6 Data transmission

This description explains how the communication (see Fig. 3.) between the energy meter and a computer installed on an electric railcar (train computer).

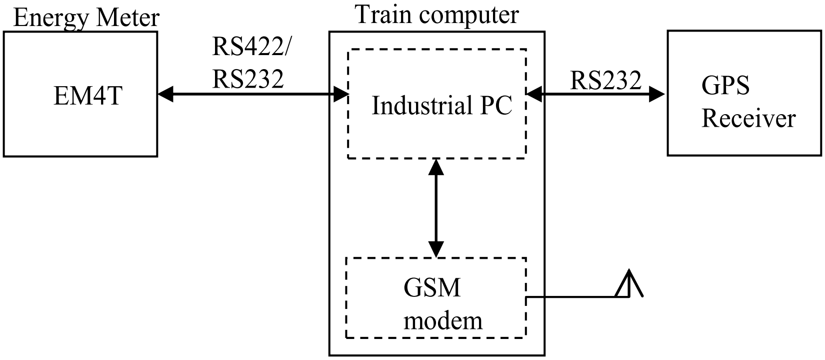

Fig. 3. Data transmission

The train computer reads the data collected by the energy meter and saved it for future analysis.

Example of output file from energy meter:

Load Profiles from 2007/03/25 08:48 to 2007/03/25 10:05

Date	Time	1.08 [kWh]	2.08 [kWh]	3.08 [kvarh]	4.08 [kvarh]	34.04 [Hz]	54.04 [Hz]
25.03.07	08:59:59	0,016	0	0,024	0	50	
25.03.07	09:14:59	0,018	0	0,026	0	50	
25.03.07	09:29:59	0,019	0	0,029	0	50	
25.03.07	09:44:59	0,021	0	0,032	0	50	
25.03.07	09:59:59	0,023	0	0,034	0	50	

Position of the traction vehicle is recorded by GPS receiver. Data are also transmitted into train computer via serial interface (RS232).

GPS output message includes:

- Time
- Position (latitude, longitude)
- Velocity

The data from the energy meter's load profile memory, which is saved in train computer's memory, and data from GPS receiver will be linked in single time and then will be protected to next transmission. After that the data can be read by a stationary workstation via the train computer's GSM modem at any time. All data will be accumulated in central server. There is possible next process and analyse of these accepted data.

7 Acknowledgment

The research was supervised by Prof. Ing. Petr Chlebiš, CSc. I would like also to express thanks to Department of Electronics, VŠB – TU Ostrava. The research is supported by the Grant Agency of the Czech Republic with project No. 102/05/H525.

References

1. Danzer J.: Elektrická trakce I, Západočeská univerzita Plzeň, 2000
2. LEM, www.lem.com

Filtering Signal by Using ICA

Branko Babušiak, Michal Gála

Department of Measurement and Control, FEECS,
VŠB – Technical University of Ostrava, 17. listopadu 15, 708 33 Ostrava – Poruba
{`branko.babusiak,michal.gala`}`@vsb.cz`

Abstract. Independent component analysis (ICA) is a computational method for separating a multivariate signal into additive subcomponents supposing the mutual statistical independence of the non-Gaussian source signals. It is a special case of blind source separation. ICA is useful in signal description, optimal feature extraction, and data compression. This paper deals with non-typical using of ICA – filtering signal. Filtering signal by using ICA is another possibility how to remove undesirable frequencies from signal without using classic digital filter.

1 Introduction

Blind Source/Signal Separation (BSS) is a group of methods of digital signal processing. Target of this methods is to restore initial source signals from mixture of signals by the help of separation process (Fig. 1.). One way how to solve this problem is using Independent Component Analysis (ICA).

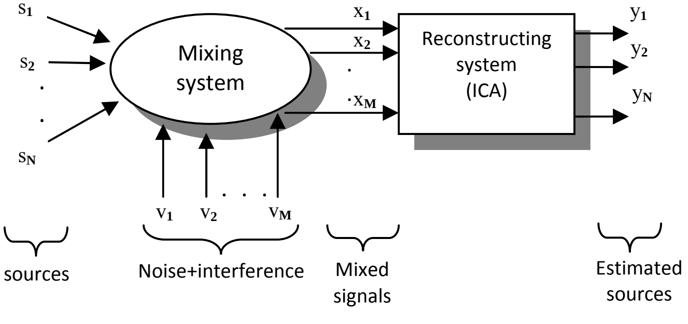

Fig. 1. Blind source separation process

© Václav Snášel (Ed.): WOFEX 2007, pp. 167–172, ISBN 978-80-248-1571-8.
VŠB – Technical University of Ostrava, FEECS, 2007.

2 Independent Component analysis (ICA)

The method of the ICA is technique which can separate linear mixed signals. In the simplest case are mixed signals $x(k)=[x_1(k),x_1(k),...,x_M(k)]^T$ linear combination of N (usually $M \geq N$) unknown source signals $s(k)=[s_1(k),s_2(k),...,s_N(k)]^T$ which are statistically independent to each other. In addition mixed signals are wasted with noise and interference. Symbol $[\;]^T$ means operation of transposition and *k* is index of discrete time sequence. The mixed signals

$$x_i(k)=\sum_{j=1}^{M} a_{ij}s_j(k)+v_i(k) \text{ or}$$

$$\mathbf{x}(k)=\mathbf{A}.\mathbf{s}(k)+\mathbf{v}(k),$$

where **x**(*k*) is column vector of mixed signals in each discrete time *k*, **s**(*k*) is column vector of source signals, **v**(*k*) is column vector of additive noise. The presence of additive noise will not be included in the further text. **A** is unknown mixture matrix with dimension MxN and with a_{ij} elements.

In general case source signals and number of source signals are unknown. Only mixed vectors **x**(*k*) are known. To estimate sources making of forward or recurrent neural network with suitable adaptive algorithm is needed.

The goal of ICA is to find inverse matrix of **A** matrix. Inverse matrix $\mathbf{A}^{-1}$ is called separative matrix **S** with NxM dimension. We try to solve transformation

$$y_j(k)=\sum_{i=1}^{M} s_{ji}x_j(k) \text{ or } \mathbf{y}(k)=\mathbf{S}.\mathbf{x}(k)$$

so that all output signals

$$y(k)=[y_1(k),y_2(k),...,y_N(k)]^T$$

will be maximal independent.

Process of the computation is shown on Fig. 2.

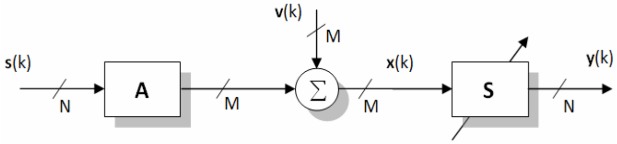

Fig. 2. Block diagram of blind source separation represented by vectors and matrices. ***A*** is mixture matrix, ***S*** is separative matrix, ***N*** is number of sources ***s(k)*** and output signals ***y(k)***, ***M*** is number of mixed signals ***x(k)*** and additive noises ***v(k)***

3 Basic properties of ICA

- ICA can only separate linearly mixed sources.
- Permutation of index of separated sources. Separated sources are not in the same order like initial sources.
- Separated signals aren’t restored with amplitude of source signals.
- If mean value of input signals equals to zero and dispersion equals to one, ICA will not have to identify value sign correctly.

4 Assumption of ICA

- Number of sensors is greater or equal to number of sources $M \geq N$
- Source signals ***s(k)*** are independent in every moment.
- Only signals without additive noise of sensors or with small level of additive degradation noise of sensors are acceptable.
- Maximum one source signal can be stochastic vector with Gaussian distribution

5 Filtering signal by using ICA

Method is simulated on signal ***s*** which is described with following mathematical equation:

$$s(t) = 2 \cdot \sin(7t) + 3 \cdot \sin(11t) + \sin(20t)$$

The shape of signal ***s*** and its frequency spectrum is in the figure 3.

Let us assume that last part of signal ***s*** is undesirable. We want to remove sin(20*t*) element from signal.

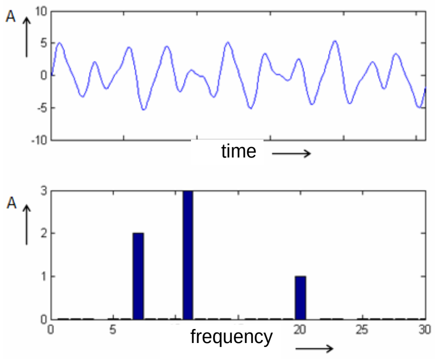

Fig. 3. Signal *s(t)* and its frequency spectrum

At first we must divide signal ***s*** to two source signals $\boldsymbol{s_1}$ and $\boldsymbol{s_2}$. Signal $\boldsymbol{s_1}$ has needed elements (frequencies) from primary signal **s** and $\boldsymbol{s_2}$ includes element which we want to remove:

$$s_1(t) = 2 \cdot \sin(7t) + 3 \cdot \sin(11t)$$

$$s_2(t) = \sin(20t)$$

The signals $\boldsymbol{s_1}$ and $\boldsymbol{s_2}$ are combined linearly and they are making $\boldsymbol{x_1}$ signal:

$$x_1(t) = a_{11} \cdot s_1(t) + a_{12} \cdot s_2(t)$$

The coefficients $\boldsymbol{a_{11}}$ and $\boldsymbol{a_{12}}$ in previous expression equal to one. We can retype the signal $\boldsymbol{x_1}$:

$$x_1(t) = 2 \cdot \sin(7t) + 3 \cdot \sin(11t) + \sin(20t)$$

To the reconstruction system of ICA enter also a signal $\boldsymbol{x_2}$ which corresponds with signal to remove:

$$x_2(t) = s_2(t) = \sin(20t)$$

Only signals $\boldsymbol{x_1}$ and $\boldsymbol{x_2}$ are known. To estimate source signals from known signals is used best-known and most sophisticated algorithm FastICA. A result of this algorithm will be signals $\boldsymbol{y_1}$ and $\boldsymbol{y_2}$ which are called estimations of sources. Both of estimated signals are in the figure 4.

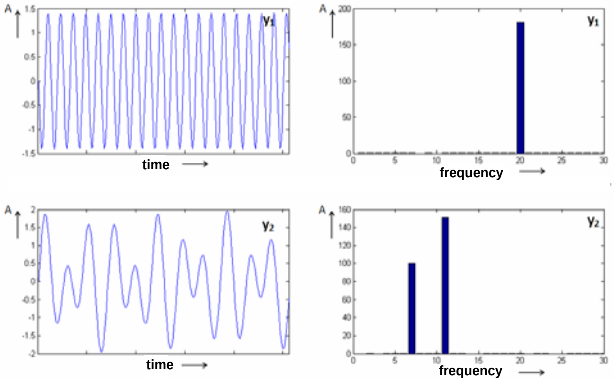

Fig. 4. Estimation of source signals by FastICA algorithm.

The signal $\boldsymbol{y_1}$ corresponds to signal which we wanted to remove. On the contrary signal $\boldsymbol{y_2}$ corresponds to signal without undesirable element (frequency 20 Hz). This fact is visible on the right side in the figure 4. In the two previous figures we can see that magnitude isn't reconstructed correctly but shape of reconstructed signals is saved and that is significant.

5 Filtering EEG record by using ICA

Let’s apply method described above to filtering EEG record which consist of 19 channels. The record includes noise (50 Hz) from electrical power network (fig. 5).

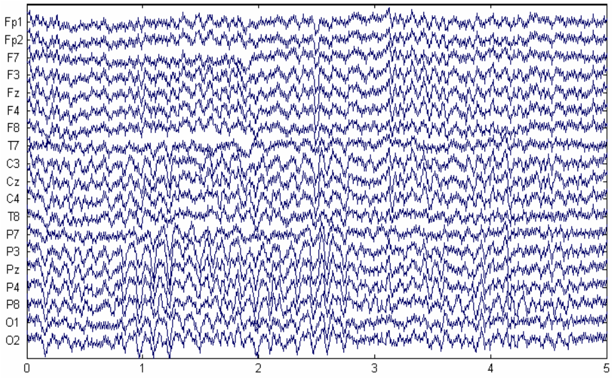

Fig. 5. The original EEG record with noise from electrical network

At first let’s use classical digital filter to remove undesirable frequency 50 Hz. The digital filter is bandstop type with boundaries at 48 and 52 Hz. The result after using this digital filter is in the figure 6.

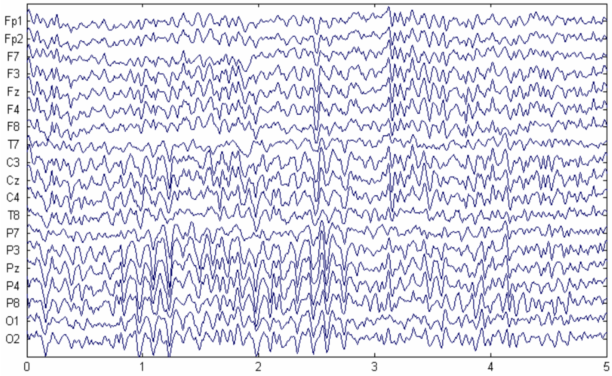

Fig. 6. The EEG record after removing frequency 50 Hz by using bandstop digital filter

In the second case we try to remove noise by help of independent component analysis. To the ICA algorithm always enter two signals. The one of them is one noised EEG channel and the second signal is simulated signal with frequency of electrical power network (50 Hz) and suitable magnitude. After application of this progress on all of the EEG channels we get signals displayed in the figure 7. In the figure 7. we can see that some channels have incorrect interpretation of sign. This fact does't create problem because the shape of the signal is preserve and signal is only inverted. This insufficiency can be removed by multiplying inverted channels with coefficient -1.

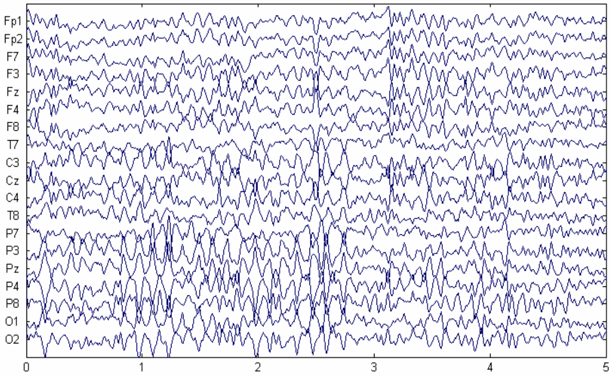

Fig. 7. The EEG record after removing frequency 50 Hz by using ICA method

6. Conclusion

In this paper was represented unusual case of using independent component analysis (ICA) method – filtering signal. If we compare fig. 6 and fig. 7, we can say that filtering signal by using classical digital filter and filtering signal by using ICA method have the same result. This shows that in some special applications filtering by using ICA can be another alternative to using digital filters.

7. References

1. Eksler,V.: Analýza hlavních komponent v problematice separace naslepo. Časopis Elektrorevue, číslo 2005/29.
2. Hyvärinen, A., Karhunen, J., Oja, E.: Independent component analysis. John Wiley & Sons, Toronto, 481 pp. 2001. ISBN 0-471-40540-X.
3. Mohylová, J.: Analýza EEG signálů nezávislými komponentami. Sešit katedry teoretické elektrotechniky, říjen 2004, ISBN 80-248-0644-4
4. Černošek, A., Krajča, V., Petránek, S., Mohylová, J.: Praktické zkušenosti s aplikací metody analýzy nezávislých komponent a analýzy hlavních komponent pro eliminaci EEG artefaktů. Časopis Lékař a technika, roč. 32, leden 2001.

HomeCare Project Evolution

Martin Černý

Department of Measurement and Control, FEECS,
VŠB – Technical University of Ostrava, 17. listopadu 15, 708 33 Ostrava – Poruba
`martin.cerny@vsb.cz`

Abstract. HomeCare is part of assistive technologies. It is a special monitoring system of the basic life functions which is primary designed for elderly people. But many of designed devices could be used in other branches of biotelemetry. This year progress, in so huge project like HomeCare is, is design and test of some in last phase project designed devices in critical conditions. Next important evolution is design and test of system for monitoring of position of people in his flat. Monitoring of the movement of people is very important in HomeCare. It was used different kind of modern technologies to permit useful detection, communication and visualization of the data. That is why, PIR sensor, ZigBee communication and Labview was the tools of this project. This system function with known technologies like PIR sensor, Labview but with a powerful system of wireless communication thanks to provide our system very flexible. Thanks too cooperation with Ostrava university it is prepared test flat, which is designed for in vivo tests of our HomeCare system.

1 Introduction

HomeCare is main project of laboratory of biomedical engineering, which is placed in our faculty in department of measurtement and control. This project employs most of Ph.D. students in biomedical engineering laboratory. There are in the project the best students of study branch measurement and control in human medicine. Project is the best way how to take advantage of our knowledges, which could be used to help to other people. We can say, HomeCare is one branch of assistive technologies.

One of evolutions of this project is design and test of the monitoring movement of people system. This system is designed it to detect the people position in an intelligent flat, to collect data by wireless communication and to display it. You can see below the designed measuring chain.

© Václav Snášel (Ed.): WOFEX 2007, pp. 173–177, ISBN 978-80-248-1571-8.
VŠB – Technical University of Ostrava, FEECS, 2007.

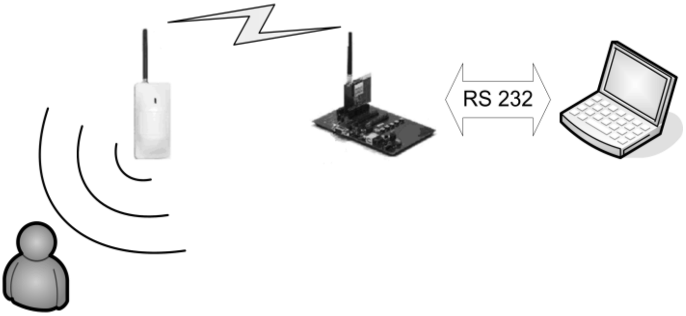

Fig. 1: Designed telemetry chain

The movement is detected by standard PIR sensor, measure data are transmit by ZigBee and finally, displayed in Personal Computer via software developed in Labview.

2 Hardware solution

The hardware realization is divided into two parts. First off all the detection, and finally the wireless communication.

In this part, I will not explain in details the power supply. This one of realized electronics board is an important thing. It is used two different kings of power supply, a lithium ion battery and a solar panel. Thanks to this both power supply, the system will be the most autonomous as long as possible.

3 Detection

For the detection was used standard PIR sensor. This one detects changes in infra-red radiation, in the form of heat emitted by a number of bodies including people, dogs or small animals. It is easy to understand that it is impossible to use directly the signal of the PIR sensor because this one gives an output signal of about 15mV with a frequency around 5 Hz.

To treat the signal from the sensor, there were two possible solutions. One of them is to treat the signal by electronics and the second solution is to treat this signal with a microcontroller. The electronic solution was chosen because in this system the microcontroller is not power supply all the time, it is in sleep mod when nobody are detect. The electronics' treatment of the data is composed of two steps. First of all the amplifier part. And finally the comparator's step. This one is realised by a standard hysteresis comparator. This solution was chosen in order to decrease the oscillation of the output. For this application it is used an amplifier OP481, due to the ultra low power supply.

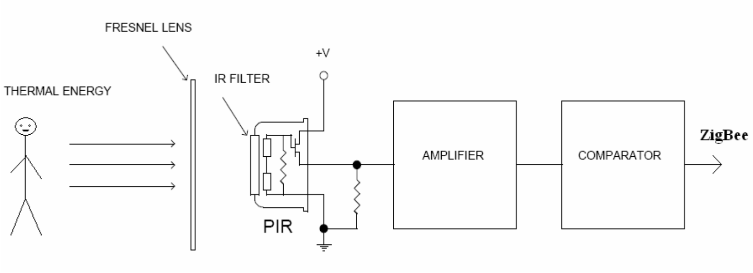

Fig. 2: PIR sensor.

4 Wireless communication

ZigBee is new standard for wireless data transmission. First generation of ZigBee compatible products came on market in 2005. ZigBee is designed for low distance data transmission at lower speeds with low energy consumption. ZigBee is good for data transmission from sensors and to some control peripherals, which could be powered by accumulators or for example solar panels.

PAN4551 (from Panasonic) ZigBee modules was used in this project. SIP PAN4551 consists of transceiver MC13193 and MCU HC9S08GT60 both from Freescale. Data transmission frequencies are placed in band 2.4GHz (divided into 16 channels). Data transmission is done in packet or stream mode (both with CRC checking in HW). Maximal distance between two nodes is tenths of meters (when using suitable mini-antennas). Power consumption of chosen PAN4551 is at around 30 / 35 mA during transmission (receive or send), 4 µA in idle state.

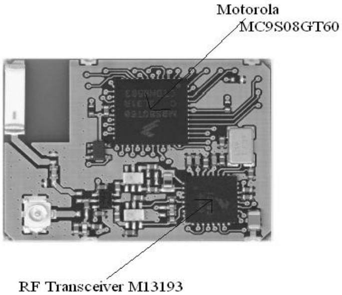

Fig. 3: ZigBee module.

5 Visualization

For data processing and visualization of measured values was created software in development system Labview 7.1.

User interface of this software is divided into two parts. In the first part you can see layout of flat. There is in each room minimally one LED which indicate the movement in area. Each LED represents one sensor.

The second part of user interface serves for statistics. There you can see bar graphs with show movement statistics of each room, more exactly of each sensor. X-coordinate represents the hours and Y-coordinate represents the numbers of passage. These values are updated each hour.

6 Devices test in critical conditions

Thank too cooperation with spa in Teplice nad Bečvou were tested most of designed devices prepared for HomeCare project in critical onditions. It took place in vivo test of devices for HomeCare in very low temperature. We we invited with ou colleagues form other part of our department to the Polarium. It is special place where are very lov temperatures around -160°C used for therapeutic purposes. There were realized test of ECG devices and electrodes. All tested devices pass these tests.

7 Results

The system of monitoring movement was fully integrated in a HomeCare.

Now, with this kind of system it is possible to follow the movement of people clearly. This data collected by the system permits to display with different kinds of technical graphics. Doctors will have helped to deduce the health of the patient in order to make the most powerful treatment at the better period of the life's patient.

Most of designed devices were tested in critical conditions in spa Teplice nad Becvou.

HomeCare project is still evaluated, we prepare new version of hardware, which use the most modern technologies of technical cybernetics. Thanks too cooperatiuon with Ostrava University we can test all devices and system in vivo in test flat, which is placed in Ostrava University building in Ostrava Zábřeh.

Acknowledgement

This project was supported in part by the Grant Agency of Czech Academy of Science under Grant 102/05/0467, Architectures of embedded system networks

This project was supported by the faculty internal project," Biomedical engineering systems".

The software was created in development system Labview and with cooperation of Department of electrical measurement on Technical University of Ostrava.

References

1. Černý, M., Penhaker, M., Martinák, L., Spišak, J., Válková, A.: Vzdálené monitorování pacientů v domácí péči, Ostravské traumatologické dny, 12-13.October.2006, Rožnov pod Radhošťem
2. Černý, M., Penhaker, M., Martinák, L., Spišak, J., Válková, A.: HomeCare – Smart embedded biotelemetry system, Worlg congress in biomedical engineering 2006, Soul, Korea.
3. Černý, M., Poujaud, J., Martinak, M..: Monitoring of Movement with ZigBee in a HomeCare In International Carpathian Conference of Control, ICCC 2007, March2007, Štrbské pleso, Slovakia
4. Černý, M.: HomeCare, Technické a medicínské aspekty biomedicínského inženýrství, setkání univerzit a lékařů, 18.6.2007, Nová aula VŠB-TUO, Ostrava Poruba
5. Černý, M., Poujaud, J., Martinak, M..: ZigBee based movement monitoring in HomeCare, In IWCIT 2007, 5.-7. September 2007, Ostrava. Ostrava: VŠB- TU Ostrava, Department of measurement and control, 2007,

ZigBee Networks

Jan Floder

Department of Measurement and Control, FEECS,
VŠB – Technical University of Ostrava, 17. listopadu 15, 708 33 Ostrava – Poruba
`jan.floder@vsb.cz`

Abstract. This paper is summary of work on ZigBee networks created for different applications. Applications are biomedical data acquisition (version based on SMAC was presented eg. in previous IWCIT) and vehicle tire pressure and temperature monitoring system. Networks based on 802.15.4 standard full MAC vs. S-MAC are compared.

1 Introduction

The tire temperature and pressure monitoring system is used for demonstration car model (for educational purposes). It is created to demonstrate car tire sensors and its data transmission to the embedded car system (and back to set sensors tresholds etc.). It uses the Freescale MPXY80xx sensor family together with the Freescale ZigBee transciever. The aim of this is to teach students to create sensor SW and communication with the car embedded system.

The Biomedical transmission part is continuation (and finishing) of the last year TeleCare project: The low distance wireless biomedical data transmission and data analysis system. It was created using proprietary network (using only PHY layer of the IEEE 802.15.4 standard) and newly the 802.15.4 standard network (due to cooperation of different ZigBee solutions). As basic the PAN4551/4555 was used (for proprietary network) and combination of PAN4551/4555 with Maxstream's Xbe/XBee-Pro modem for 802.15.4. Collected biomedical signals are SpO2, body temperature and pulse (ChipOx) and ECG (modules were different – one for proprietary and another for IEEE).

2 Wireless Tire Monitoring System

This wireless sensor is designed for educational purposes of the car model. It is designed to be fully programmable (together with receive station) and to be easy to debug (via standard BDM and UART). Unlike market solutions it has also replaceable batteries, it is not covered into a shelter (shelter is used to survive huge g shocks and centripetal forces) and operates at 2.4GHz (with about three times bigger power consumption while transmitting – compared to a market). Range is at tenths of me-

© Václav Snášel (Ed.): WOFEX 2007, pp. 178–183, ISBN 978-80-248-1571-8.
VŠB – Technical University of Ostrava, FEECS, 2007.

ters. Advantage of using ZigBee transciever is bilateral communication where receiver device can set sensor's treshold level etc.

The tire sensor is based on Freescale's MPXY80xx family of tire pressure and temperature sensors. The sensor ranges are from 50-900/637.5 kPa and 2000g for centripetal forces. These sensors are made to operate in embedded systems (generate interrupt signal every 3 seconds and reset signal every 57 minutes). The sensors communicate via SPI as SPI slaves. Resolution is 8-bit and temperature and pressure error fill requirements for these applications.

Figure 1 shows wireless tire sensor. MCU + transmitter is PAN4555 which also drives the sensor, BDM and UART are carried out on the right.

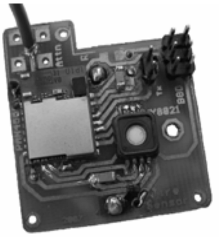

Fig. 1. Tire Sensor board (sensor + MCU-transmitter, BDM, serial line), battery from the bottom, antenna on the top

2.1 Network

In this case situation is little complicated. For a tire pressure and temperature monitoring system power consumption is crucial (is powered from own battery and have to work for years). On the other hand data sent from a sensor do not have to be sent real-time and can even be lost from a time to time. Vehicle tire pressure and temperature monitoring systems are used to catch slow degradation changes (like pressure loss due to time) which take at least tenths of minutes/hours or even days. They are not used to detect devastating sudden events like huge tire puncture/rupture. So it means data is send only few times a minute or even an hour and it drastically prolongs their lifetime.

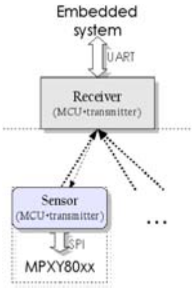

Fig. 2. Network Topology – wireless tire sensor

The only way to save power is to put the sensor to standby and MCU+transmitter to the deep sleep mode. MCU is then periodically waken by the sensor, measures data, turns on the transmitter and sends data to the receiver and goes back to the deep sleep mode.

802.15.4MAC is designed to be small and fast – to fit to 8bit MCUs but despite of this fact it requires relatively much computing (consists of MLME, MCPS and ASP layer – ASP is Freescale's proprietary) and user does not have full control of the MCU all the time. It results in increased power consumption due to longer times to handle messages and process all the operations. The only advantage is possibility of using enhanced security (up to 128bit AES encryption).

In case of 802.15.4 better network is peer-to-peer than star and it all without acknowledge response. 802.15.4 start network requires a PAN coordinator which associates disassociates devices which adds more problems to end devices.

To obtain full control over the MCU and to fill minimum computing requirements SimpleMAC has to be used. In fact SimpleMAC library contains only functions to control a ZigBee transciever (with 802.15.4 PHY layer implemented in HW) and send data over it. In case of using the SimpleMAC MCU can be used “freely”.

2.2 Chosen Solution

SimpleMAC was also chosen in the demonstration software of the tire sensor and the receiver. Access to the network is nondeterministic with channel energy detection and collision avoidance. MCUs default state is the deep sleep from which it is woken every 3 seconds by the tire sensor. Temperature and pressure data is send approximately every 30 seconds and then waits 10ms for the receiver to send ack/settings. Besides temperature and pressure also a low voltage warning is sent when battery power goes low.

The receiver sends received data immediately to the UART. In fact it is not decided yet whether communication with the car embedded system will be via UART or CAN (which is used in automotive industry). In case of CAN, UART-CAN gateway will have to be created (MCU contains only UART).

3 Biomedical Data Transmission system

Working prototype of low distance wireless biomedical (and any other) data transmission and data analysis system was created for TeleCare project. System was used in prototype of hydrogen vehicle (in year 2006). System transfers data about vehicle driver’s condition and some additional data about ride. These drivers’ signals are collected: pulse, ECG, SpO2 and body temperature. Besides these signals data about acceleration of vehicle in X and Y axis (front-back, left-right) and air temperature is measured. System network was based on proprietary solution (only IEEE 802.15.4 PHY used).

Second version (year 2007) omit X and Y axis acceleration and changed ECG collection device ECG100 to direct grabbing of analog signal (one recording ECG). This year system network was based directly on IEEE 802.15.4 due to collaboration with XBee (sending data from ChipOx).

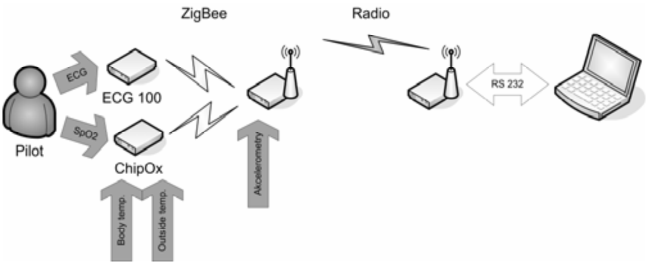
ZigBee
Radio
ECG
ECG 100
SpO2
Pilot
ChipOx
Akcelerometry
RS 232
Body temp.
Outside temp.

Fig. 3. System Scheme

3.1 Network

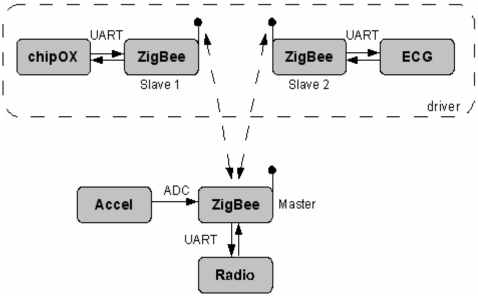
chipOX
UART
ZigBee
Slave 1
ZigBee
Slave 2
UART
ECG
driver
Accel
ADC
ZigBee
Master
UART
Radio

Fig. 4. Network Scheme – first version

In both cases (proprietary, 802.15.4) network consists of two end nodes and one main. In case of proprietary network the two end nodes are configured as slaves, main as master. In second case end nodes are end devices (configured as RFD devices without beacon and security) and main node is a PAN coordinator.

Proprietary network: ZigBee net consists of two slave units (Slave 1 and Slave 2) and one master unit (Master). Master polls each slave for data from peripheries. Except this, master collects data from AD converter (outputs of accelerometer). Collected data from two slaves and ADC are than sent to PC via Radiomodem (radio). This wireless net (star-like) is most suitable for our and similar tasks when all senosrs or other peripherals are in range of central node, low delay and fast data transmission (no node needs to re-transmit other node's data) is needed and slaves do not need to transfer too much data between (can be sent over master). Anything here is controlled by master and “way” of signal is known and never changes.

Communication is done in master-slave mode where master polls slaves and requires (numbered) data packet and slave sends data (or replies that no new data is available and sends error code). Except data request, master sends also commands to start/stop slaves and init peripherals. Data are buffered for 0.4 second to avoid possible data loss.

First slave (with chipOX) sends at about 200 Bps and second slave (with ECG meter) sends at about 100 Bps. So data sent size is about 300 Bps what is far below border of 10 kBps and it is possible to make delays in communication (transmitter turned to idle mode) to save batteries. Master collects data from these two slaves and adds data from accelerometer from X and Y axis with sampling rate of 100Hz or 50Hz. Amount of data send from master to PC is at about 500Bps maximum.

802.15.4: IEEE 802.15.4 standard network was chosen because of cooperation with XBee. XBee can participate in 802.15.4 star networks as an end device or a coordinator or in peer-to-peer networks. Because the structure of communication is mostly from data-gathering nodes to the storage and analysis device (computer in this case), star network was chosen (one PAN coordinator and two end devices). But in fact the peer-to-peer network can be used too.

Parameters of the network are: nonbeacon, no security, acknowledge, logical channel is one of 13-23 selected by PAN on its startup (the one with the least energy / the preset one). Addressing is 16-bit in default but the coordinator handles also 64-bit (device serial number). Coordinator's PAN ID is preset.

The coordinator allows end device association by comparing with its table of granted devices (table of serial numbers) non-granted devices are refused automatically. End devices have the same table of granted coordinators so it cannot happen that device will associate to different coordinator.

Main data flow is from the ECG node (it has to transmit huge amount of sampled and filtered analog data) it transmits approximately 100ms and total amount is about 600B per second. Second node (ChipOx) with XBee sends significantly lower amount of data - at about 200 Bytes per second.

The PAN coordinator translates all the data and retransmits them to the PC (Data is translated to the same format as in last year version).

Data flow from the coordinator to the end devices is minimal and it is only an initialization and de-initialization sequence.

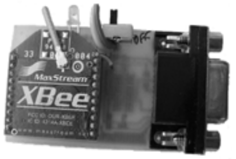

Fig. 5. ChipOx node (bottom side) with XBee

4 Conclusion

4.1 Proprietary versus 802.15.4 compatible network

Proprietary network is more advantageous especially in cases where users need to use more of MCU resources (like in case of FIR filter), to have full control over communication or sources (like master-multislave network described in [1]) or to have full control over MCU and peripherals (eg. when power consumption is essential). Disadvantage is that devices cannot participate in 802.15.4 networks and with devices handling only 802.15.4 protocol (eg. Xbee). It is also hard and slow to program networks with complicated structure.

On the other hand IEEE802.15.4 std. networks are useful when nodes have to participate biggger networks like big trees or mesh networks and when different types of devices (or from different producers). But it is much more complicated to program devices control resources etc. In fact Frescale IEEE802.15.4 MAC implementation we used probably contained some buffer bugs which cause random temporary MAC unavailability.

According to our experience it is always better to use SimpleMAC whenever possible.

5 Acknowledgement

This work is being solved on the VSB Technical University of Ostrava, Czech Republic. Most of this work was created under the GAČR grant no. 102/05/0467 (Network Architectures of Embedded Systems).

References

1. Bronzino, J. D.: The Biomedical Engineering Handbook, CRC Press 1995
2. Vitovec, J.: Telemetrie a přenos dat, první vydání, Praha: ČVUT, 1979
3. Panasonic:PAN4551 datasheets, www.pedeu.panasonic.de
4. J. Floder, M. Černý, “ZigBee in Biotelemetry”, IWCIT 2006, EAN-9788390840994, 2006, pp. 212-216

Application of Neural Network by Signal Classification

Michal Gála, Branko Babušiak

Department of Measurement and Control, FEECS,
VŠB – Technical University of Ostrava, 17. listopadu 15, 708 33 Ostrava – Poruba
{michal.gala, branko.babusiak}@vsb.cz

Abstract. Analysis of long-term EEG requires that it is segmented into piecewise stationary sections and classified. A neural network architecture is introduced for the problem of classification of EEG signals. This paper deals with basic signal classification into two classes. This work is a ground towards creating an algorithm to sleep status analysis. The signal is processed first by signal segmentation and then is used the neural network to classification into two classes.

1 Introduction

A Computer processing and a biological signal classification have great value for better diagnosis resulting. Therefore is it a strong tool in a doctor's hands. The effectivity rest on: software read the signal and marks only significant element of signal, which is important for result diagnosis. The doctor will save a time in this way. One of possibilities for a signal classification is using that neural network. These neural networks are possible for using signal segmentation too. For example will be an 8 seconds long real record of brain activity used as a test signal. This signal is segmented. For this signal segmentation is used by software. It name is EEGsegmentation. With this program we can display all EEG channels, ECG channel if exist too and many more.

2 Neural networks (NN)

A biological neural network is composed of a group or groups of physically connected or functionally associated neurons. A single neuron can be connected to many other neurons and the total number of neurons and connections in a network can be extremely large. Connections, called synapses, are usually formed from axons to dendrites, though dendrodentritic microcircuits and other connections are possible. Neural networks are extremely complex. Artificial intelligence and cognitive modeling try to simulate some properties of neural networks. An artificial neural network is an interconnected group of artificial neurons that uses a mathematical or computational model

© Václav Snášel (Ed.): WOFEX 2007, pp. 184–189, ISBN 978-80-248-1571-8.
VŠB – Technical University of Ostrava, FEECS, 2007.

for information processing based on a connectionist approach to computation. In most cases an artificial neural network is an adaptive system that changes its structure based on external or internal information that flows through the network.

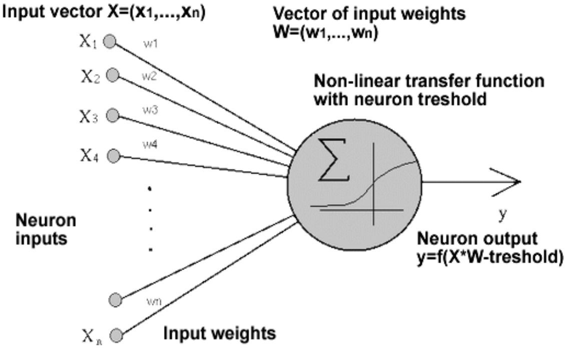
Input vector X=(x1,...,xn)
Vector of input weights
W=(w1,...,wn)
X1
X2
X3
X4
w1
w2
w3
w4
Non-linear transfer function
with neuron treshold
Neuron
inputs
y
Neuron output
y=f(X*W-treshold)
wn
Xn
Input weights

Fig. 1. Neuron model

The neural networks have got more good attributes. For example learn ability: network changes its structure following information for better artificial neural network performance. According to propagation of the signal, two main groups of neural networks are possible:

- Feed-forward – Data enters at the inputs and passes through the network, layer by layer, until it arrives at the outputs. During normal operation, that is when it acts as a classifier, there is no feedback between layers.
- Recurrent - a network of neurons with feedback connections between layers.

Learning is classified into: learning with teacher and learning without teacher. Learning is a systematic process, where knowledge is saved into synaptic weights of the neural network. In learning state:

$$\frac{\partial W}{\partial t} \neq 0 \qquad (2.1.)$$

W is a matrix of all synaptic weights of the neural network. After learning is the network learnt and then:

$$\frac{\partial W}{\partial t} = 0 \qquad (2.2.)$$

2.1. Backpropagation

In real 90% applications from neural networks are based on backpropagation algorithm. It is a basic algorithm for controlled learning. Backpropagation is recursive gradient method for the neural network weights adjusting with heed on learning error *J* minimalization.

$$J = \frac{1}{2}\sum_{i=1}^{N_0}(ev_i - x_i)^2 \tag{2.3.}$$

N_0 is a number of input neurons, ev_i is required activation value of i-neuron, x_i is activation of i-neuron and p index means that it belongs to p-pattern. For each neuron hold:

$$x_i = f_i(i_i) \qquad i_i = \sum_{j=1}^{M} w_{ij}x_j + \theta_i \tag{2.4.}$$

i_i is input of i-neuron, f_i is activation function of i-neuron, M is number of i-neuron inputs, w_{ij} is weight from z-neuron to i-neuron and θ_i is threshold value of i-neuron. Backpropagation is gradient method and therefore for weight change Δw_{ij} holds:

$$\Delta w_{ij} = -\gamma\frac{\partial J}{\partial w_{ij}} = -\gamma\frac{\partial J}{\partial i_i}\frac{\partial i_i}{\partial w_{ij}} = \gamma\delta_i x_j \tag{2.5.}$$

Calculated synaptic weight change between neuron from hidden layer and output neuron is then increment with current weight value:

$$w_{ij} = w_{ij} + \Delta w_{ij} \tag{2.6.}$$

For learning rate γ (2.5.) hold:

$$\delta_i = -\frac{\partial J}{\partial i_i} = -\frac{\partial J}{\partial x_i}\frac{\partial x_i}{i_i} = -\frac{\partial J}{\partial x_i}f'(i_i) \tag{2.7.}$$

If is i-neuron output neuron, then hold:

$$\delta_i = -\frac{\partial J}{\partial x_i}f'(i_i) = (ev_i - x_i)f'(i_i) \tag{2.8.}$$

If is it not output neuron:

$$\begin{aligned}\delta_i &= -f'(i_i)\sum_{h=1}^{N_h}\frac{\partial J}{\partial i_h}\frac{\partial i_h}{\partial x_i} = -f'(i_i)\sum_{h=1}^{N_h}\frac{\partial J}{\partial i_h}\frac{\partial}{\partial x_i}\sum_{l=1}^{N_l}w_{hl}x_l = \\ &= -f'(i_i)\sum_{h=1}^{N_h}\frac{\partial J}{\partial i_h}w_{hi} = f'(i_i)\sum_{h=1}^{N_h}\delta_h w_{hi}\end{aligned} \tag{2.9.}$$

Formula 2.9. is main backpropagation relationship and shows recursive propagation of an error signal δ from output neurons to network input.

3 EEG classification by neural network

As a test signal is used 20 channels (19 + marker), 8 seconds long real record of brain activity. From this record are 15 segments of various channel extracted (Fig. 2.). All segments are defined by using an adaptive segmentation algorithm with easy test method to segments boundaries indication. These 15 segments are separated into two classes (A and B). Each class has got training signals and testing signals. In class A are 5 signals, 3 training signals (FP1, F7, F3) and 2 testing signals (FP2, FZ). In class

B are 10 signals, 8 training signals (PZ, P3, C4, CZ, C3, F4, F8, *F3*) and 2 testing signals (*FZ*, *F7*).

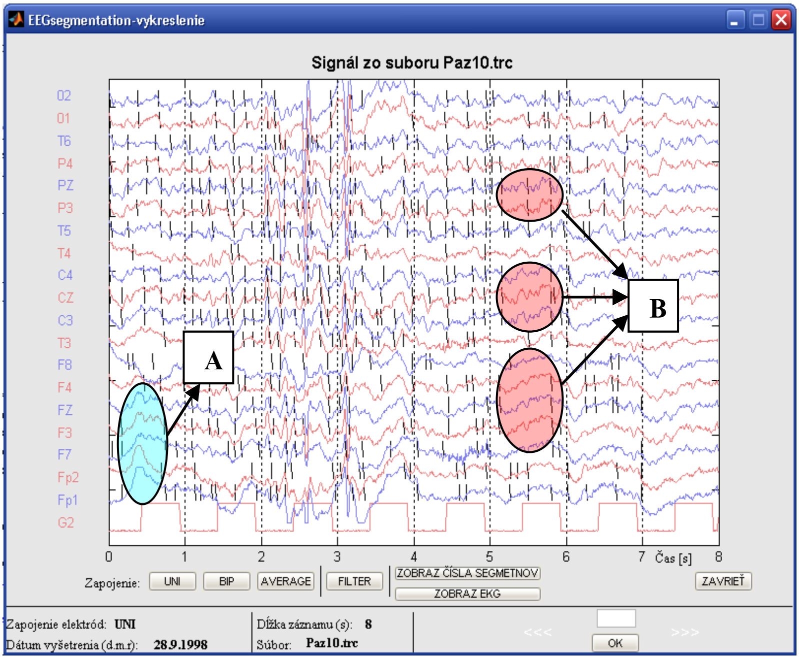
EEGsegmentation-vykreslenie
Signál zo suboru Paz10.trc
02
01
T6
P4
PZ
P3
T5
T4
C4
CZ
C3
T3
F8
F4
FZ
F3
F7
Fp2
Fp1
G2
A
B
0
1
2
3
4
5
6
7
Čas [s]
8
Zapojenie:
UNI
BIP
AVERAGE
FILTER
ZOBRAZ ČÍSLA SEGMETNOV
ZOBRAZ EKG
ZAVRIEŤ
<<<
>>>
OK

Zapojenie elektród: UNI
Dátum vyšetrenia (d.m.r): 28.9.1998
Dĺžka záznamu (s): 8
Súbor: Paz10.trc

Fig. 2. Real record of brain activity with two class of used segments

3.1. Neural network realization

The neural network is based on backpropagation algorithm. The network has one hidden layer with 20 neurons, 40 input neurons and one output. This is network with teacher. For creating and training the network is used a MATLAB algorithm. As activation function is used log-sigmoid function. The signal must be edited before neural network is trained. At first the signal must be transferred from time domain to frequency domain by using fast Fourier transform, so a problem with displacement between signals is solved.

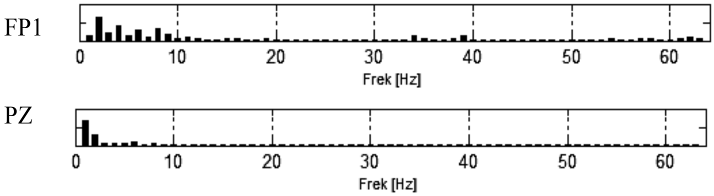

Fig. 3. Frequency domain of FP1 and PZ signal

This frequency range is then narrowing down to 0 – 40 Hz and it is dissociated to 40 elements. For EEG computer processing are these frequencies important:

- Delta (0,5 – 4Hz) – total unconsciousness, deep, dreamless sleep
- Theta (4 – 8Hz) – daydreaming, fantasy, imagination, ideas
- Alfa (8 – 13Hz) – occur an adult who is awake but relaxed with eyes closed
- Beta (13 – 22Hz) – occur during deep sleep, REM sleep when the eyes switch back and forth.

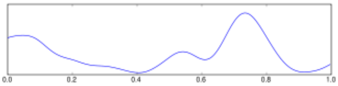

Fig. 4. Delta activity

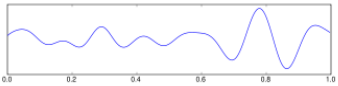

Fig. 5. Theta activity

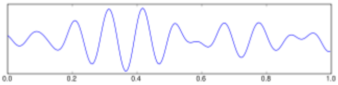

Fig. 6. Alfa activity

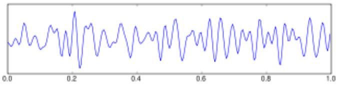

Fig. 7. Beta activity

Then the signals are normalized, number 1 has a max value of the signal and number 0 has a min value of the signal, a log-sigmoid function is used. I tried to learn the neural network following way:

- Output equals 1 in the case of signal from group A (FP2, FZ) as input signal.
- Output equals 0 in the case of signal from group B (*FZ*, *F7*) as input signal.

Table 1. Outputs values of neural network by testing signals using

	FZ	**FP2**	***FZ***	***F7***
1	0,9107	0,9982	$3,21.10^{-3}$	$5,91.10^{-5}$
2	0,2860	0,8100	$1,01.10^{-4}$	$6,52.10^{-3}$
3	0,0962	0,9560	$7,36.10^{-4}$	$1,70.10^{-3}$
4	0,0246	0,9706	$1,91.10^{-4}$	$4,84.10^{-2}$
5	0,1786	0,9672	$2,60.10^{-3}$	$1,25.10^{-4}$
6	0,8552	0,9431	$1,84.10^{-5}$	$4,66.10^{-2}$

Table shows if work the network correct or not. By using test signals from class B (*FZ, F7*) as input signal, output equals 0. Network is learnt and works correct. Problem is if I used test signals from class A (FZ, FP2). Network is learnt but works not correct (signal FZ, line 1 and 6). The output value by class A must be near value 0 but when is used signal FZ, output values are incorrect in two cases (0,9107 (line 1) or 0,8552 (line 6)). It is due to small training group. Training group A is not too large to correct network learning and to correct signal classification.

4 Conclusion

In this paper is presented an application method of the neural network by signal classification in two classes. The network has one hidden layer with 20 neurons, 40 input neurons and one output. The network is classifying signal into two classes. It is only basic network and it has low applying ability in praxis. At the present there are existing around 120 classes of segments. It requires a bigger and more accurately network with bigger training group of signals. The network is getting faster when the neurons and weights counts are reduced, but the knowledge is became generalized. It is very big optimizing problem. If is small number of neurons, network may be not able to correct signal classification. Other way, if there is large number of network neurons, network may be unnecessarily loaded. The largeness of training group is important, too. By the small training group, the network is not possible to right learning and to correct signal classification. In the future work the neural network will be used to sleep status analysis.

References

1. Vondrák, I.: Umělá inteligence a neuronové sítě. Skriptum VŠB - TU Ostrava, (1994)
2. Mohylová, J., Krajča, V.: Aplikace shlukové analýzy pro zpracování EEG záznamů, Ostrava:, Katedra teoretické elektrotechniky, FEI, VŠB - TU Ostrava, 80-7078-922-6, (2001)
3. Arbib, Michael A.: The Handbook of Brain Theory and Neural Networks, (1995).
4. Wilkes, A.L. & Wade, N.J.: "Bain on Neural Networks". Brain and Cognition 33: 295–305, (1997).
5. Kvasnička V., Beňušková L.: Úvod do teórie neurónových sietí
6. MATLAB, http://www.mathworks.com/

Verification of Temperature Fields in the Bimetallic Thermometer

David Grobelný, Pavel Nevřiva

Department of Measurement and Control, FEECS,
VŠB – Technical University of Ostrava, 17. listopadu 15, 708 33 Ostrava – Poruba
{david.grobelny,pavel.nevriva}@vsb.cz

Abstract. Mechanical parts in many field tested sensors are now replaced by electronic equipment. Such electronic equipment is sensitive to ambient temperature and ambient temperature changes. One example is the bimetallic thermometer used for oil temperature measurement in an automobile oil pan. To replace the bimetallic strip with electronics, the mathematical model of the dynamic behavior of the bimetallic thermometer was constructed. The sensor measures the temperature of oil in automobile oil bath. The task serves as a pilot example for the larger project focused on the study of thermal load of sensors. This paper deals with verification of temperature fields in the bimetallic thermometer obtained by mathematical simulation of the sensor by the measurement. The measurement was made by infrared camera FLIR THERMACAM SC2000. The image processing methods was used to calculate the correlation of the measured data with the data calculated from analytical model numerically by the finite element method.

1 Introduction

The temperature of oil in automobile oil bath is often measured by a bimetallic thermometer. The bimetallic thermometer was selected as a prime case of a sensor that is affected by the thermal energy. The mathematical model of the dynamic behaviour of the sensor was constructed. It serves as a pilot example for the larger project focused on the study of thermal load of sensors. This paper deals with verification of dynamics of temperature fields in the bimetallic thermometer obtained by mathematical simulation by the measurement. The measurement was made by infrared camera FLIR THERMACAM SC2000. The image processing methods will be used to recognize the temperature field of the bimetallic thermometer in the image with the noisy background. The similarity between the mathematical model and the measurement of the temperature field of the bimetallic thermometer is computed by the two-dimensional correlation coefficient. MATLAB is used for digital image processing.

© Václav Snášel (Ed.): WOFEX 2007, pp. 190–195, ISBN 978-80-248-1571-8.
VŠB – Technical University of Ostrava, FEECS, 2007.

2 Physical model of the system

The mathematical simulation describes the simple physical model. The measurement by the infrared camera has to verify the results generated by the mathematical model described above. Therefore, the physical model of the system was constructed in laboratory of VSB TU Ostrava. In Figure 1 is shown the diagram of the physical model of the system and the configuration of the measurement. The dimensions in the physical model correspond to those in mathematical model. The thermostat is filled with oil Marloth SH and keeps a constant temperature 365,2K. An insulating wooden board is placed on the top of the thermostat. The width of the board is 4 mm. The board should prevent from heating dissipation to surrounding air. A hole is drilled into the board for the thermometer placing. The stem of thermometer is put into the oil and the hexagonal head of the thermometer is influenced by the surrounding air. The temperature of the air is 294,2K. The hexagonal head of the thermometer is blackened by the Thermo spray to increase a coefficient of emissivity to 0.96. Note, that the coefficient of emissivity was set directly at the infrared FLIR THERMACAM SC2000 camera.

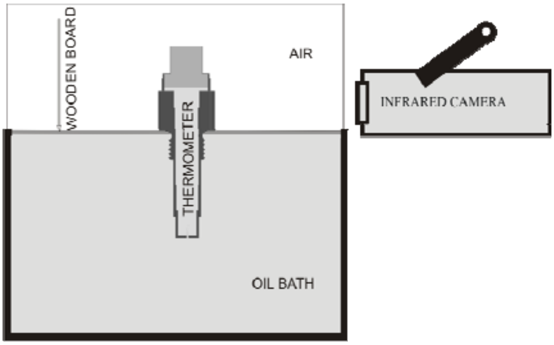

Figure 1. Physical model of the system and the configuration of measurement.

3 Mathematical model of the system

From the physical point of view, the mathematical description of the process is very simple. It is given by the Fourier partial differential equation of the second order

$$\frac{\partial T}{\partial t}=\frac{\lambda}{c_p\cdot\rho}\left(\frac{\partial^2 T}{\partial x^2}+\frac{\partial^2 T}{\partial y^2}+\frac{\partial^2 T}{\partial z^2}\right), \qquad \textbf{(1)}$$

Initial value of the solution is given by the initial temperature T of the thermometer. Boundary conditions of the solution come out from the formula

$$q=\alpha\left(T_O-T_P\right), \qquad \textbf{(2)}$$

q ... density of heat flow rate [W.m--2]
α ... heat transfer coefficient [W.m-2.K-2]
λ ... heat conductivity [W.m-2.K-1]
c_p ... specific heat capacity [J.kg-1.K-1]
ρ ... specific density [kg.m-3]
T_P … surface temperature of the solid [K]
T_O … ambient temperature [K]

The calculation of the equation (1) was made numerically in the software product ANSYS.

4 Measurement

For the measurement, two bimetallic thermometers were selected. The bimetallic thermometers were of the same type, they differ only by the serial number. The results obtained by the measurement differ also only by a value that can be explained by a measurement error. The infrared camera was set approximately 20cm from the thermometer. The temperature of the surrounding air was kept on 294,2K. Therefore the bimetallic thermometer was in its initial state given by the initial condition 294,2K. It was emerged by its stem in to oil of temperature 365,2K. The transient responses on the model were measured. Images were logged either in 1s time interval. Data logging time was 800s. The experiments were repeated 12 times. Total duration of the measurement was about 4 hours. The composition of the thermostat, bimetallic thermometer and infrared camera FLIR THERMACAM SC2000 shows Figure 2a. The local view at bimetallic thermometer is shown in Figure 2b.

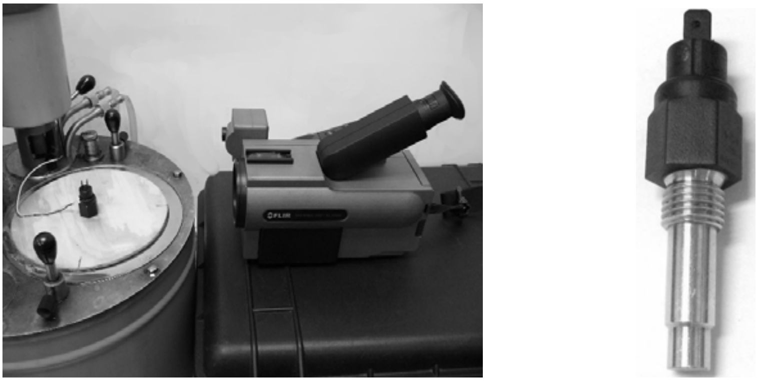

Figure 2. a) The measuring by the infrared camera. **b)** Picture of bimetallic thermometer.

5 Digital image processing

The infrared camera FLIR THERMACAM CS2000 has logged the images to the associated camera PC laptop computer in the image 14 bit IMG format. The format IMG had the corresponding resolution 240x320 pixels. To use the MATLAB software, the data were transferred into the PC computer. The transfer was done at the end of the measurement period. It was made off-line by the RS 232 channel using the ThermaCAM researcher 2001 software. One raw image of the infrared camera is shown in Figure 3a. The every raw image of the transient response of the bimetallic sensor was processed by method of digital image processing. Several problems were resulted. The temperature field of bimetallic sensor was separated from the noisy background. The temperature field was rotated to the regular location. It was selected only the perpendicular part of the temperature field on the object lens of infrared camera. The perpendicular part of the temperature field is marked in Figure 3b. The gray scale of these images corresponds with degrees Kelvin. The temperature emission of the bimetallic sensor depended on the rotation degree in Z direction from the object lens of infrared camera. Whole part of the temperature field was not correctly measured because of the geometric shape of bimetallic sensor.

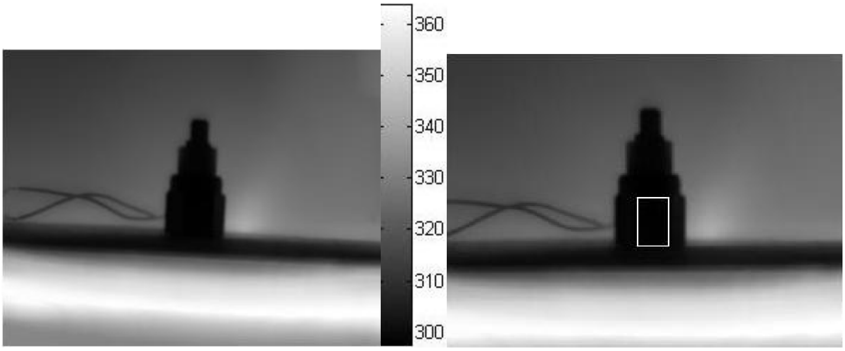

Figure 3. a) The raw image. **b)** The correct image.

For image segmentation functions the standard edge detector was used. It was used edge detector, which approximates digitally the first-order derivate. The first-order derivative of choice in image processing is the gradient. The gradient of a 2D function f(x,y), is defined as the vector

$$\nabla f(x,y) = \begin{bmatrix} \dfrac{\partial f}{\partial x} \\ \dfrac{\partial f}{\partial y} \end{bmatrix}, \tag{3}$$

The magnitude of this vector is

$$|\nabla f(x,y)| = \sqrt{\left(\frac{\partial f}{\partial x}\right)^2 + \left(\frac{\partial f}{\partial y}\right)^2}\,, \tag{4}$$

It was selected Prewitt edge detector. The Prewitt edge detector uses the mask

$$h = \begin{bmatrix} -1 & 0 & 1 \\ -1 & 0 & 1 \\ -1 & 0 & 1 \end{bmatrix}, \tag{5}$$

Then the convolution is made between the image and The Prewitt edge detector. It was applied to develop the vertical edges of the thermometer from the noisy background. Then, the noisy background of the image was partially smoothed out. The refined image was transformed into a binary one. It was used correct the thresholding. The position of thermometer bounds in the image was calculated. By this way, the position of the thermometer and the value of temperature of all points of thermometer measured by the infrared camera were fixed. The Radon transform was chosen for estimation of rotation in direction Y of the temperature field of the bimetallic sensor in the image. The Radon transform is described by the term

$$R_\Theta(x') = \int_{-\infty}^{\infty} f(x'\cos\Theta - y'\sin\Theta, x'\sin\Theta + y'\cos\Theta)dy',$$

where (6)

$\begin{bmatrix} x' \\ y' \end{bmatrix} = \begin{bmatrix} \cos\Theta & \sin\Theta \\ -\sin\Theta & \cos\Theta \end{bmatrix} \begin{bmatrix} x \\ y \end{bmatrix}$ is given by the rotation transform.

The central line of the temperature field of the bimetallic sensor in the horizontal direction was counted. Then the Radon transform was used. Maximum of Radon transform is rotation degree in Y direction of the temperature field. If rotation degree is known then is made correction of the temperature field by Rotation transform. Finally is found the perpendicular part of the temperature field on the object lens of infrared camera by global thresholding. The perpendicular part is selected and used for correlation.

6 Verification between perpendicular parts

Verification is done by the two-dimensional correlation coefficient. The correlation coefficient is the best estimate of the correlation of the mathematical model and the measurement. For correlation was chosen only perpendicular parts of temperature fields of mathematical model and measurement. If those parts have high correlation coefficient then whole part of mathematical model and whole part of measurement have high correlation coefficient. Both of parts are matrices of the same size. The two-dimensional correlation coefficient is described by

$$r = \frac{\sum_m \sum_n \left(A_{mn} - \bar{A}\right)\left(B_{mn} - \bar{B}\right)}{\sqrt{\left(\sum_m \sum_n \left(A_{mn} - \bar{A}\right)^2\right)\left(\sum_m \sum_n \left(B_{mn} - \bar{B}\right)^2\right)}}, \tag{7}$$

where $\bar{A}$ and $\bar{B}$ are means of matrices
The correlation coefficient between these perpendicular parts is in the range
0,9 – 0,98.

7 Conclusion

We have about 10 000 images of measurement. The verification of mathematical model and measurement is time-consuming. Algorithms were developed and process images of measurement by digital image processing methods. These algorithms can automatically find interesting parts in the image of the measurement and can compare these parts with mathematical model by statistical methods. The results indicate good correspondence between the calculated and measured data.

8 References

1. Nevřiva P., Grobelný D., Plešivčák P., *Simulation and Experimental Verification of Heat Transfer Dynamics of Sensors*, WSEAS 2006, Vol. 1, Athens 2006.

2. Kerlin T., Grobelný D., Nevřiva P., *Measurement of the temperature transient response of the bimetallic thermometer*, Proceedings of PDeS 2006, Brno 2006.

3. Grobelný D., Nevřiva P., Plešivčák P: Měření teplotního pole bimetalového senzoru s využitím analýzy obrazu. Technical Computing Prague 2006, Praha, Czech Republic, 2006, ISBN 80-7080-616-8

4. Nevřiva P., Plešivčák P., Grobelný D.: Experimental validation of mathematical models of heat transfer dynamics of sensors. WSEAS TRANSACTIONS on SYSTEMS, Athens , Greece, 2006, ISSN 1109-2777

5. GONZALEZ, Rafael C., WOODS, Richard E., EDDINS, Steven L. *Digital Image Processing using MATLAB*. Upper Saddle River, New Jersey: Pearson Prentice Hall, 2004. 609s.

Measuring of Vibrations in Medicine

Lukáš Martinák

Department of Measurement and Control, FEECS,
VŠB – Technical University of Ostrava, 17. listopadu 15, 708 33 Ostrava – Poruba
`lukas.martinak@vsb.cz`

Abstract. The goal of this project is the patient's bed vibrations measurement in hospital. This project is localized to detection of epileptic fit of patients. The sensor – accelerometer is mounted to patient's bed. This sensor is continuously monitoring vibrations in three dimensions. The accelerometer is connected to the PC via Bluetooth. The measurement process included the procedure of processing values using the created software.

1 Introduction

The main goal of this project was design and realization of measurement of vibrations of patient bed during epileptic fit. It is good to use for this measurement acceleration and some wireless technology. It was decided to use Bluetooth technology, because of good characteristics of range and transmission. The next was necessary to realize any software for visualization and data saving.

2 Materials and methods

In recent years, silicon micromachined sensors have made tremendous advances in terms of cost and level of onchip integration for measurements such as acceleration and/or vibration. These products provide the sensor and the signal conditioning circuitry on chip, and require only a few external components. Some manufacturers have taken this approach one step further by converting the analog output of the analog signal conditioning to a digital format such as duty cycle. This method not only lifts the burden of designing fairly complex analog circuitry for the sensor, but also reduces cost and board area. Micromachined accelerometers are now being incorporated into products such as joysticks and airbags, applications that were previously impossible due to sensor price and/or size.

Accelerometers are devices for measuring dynamic acceleration (power created by changing of velocity of this accelerometer) or static acceleration (power created by cavity of Earth). Detection of vibration is one of the measuring types of dynamic acceleration. When we want to measure only vibrations we must use a filtration. The output signals are analog voltages proportional to acceleration

© Václav Snášel (Ed.): WOFEX 2007, pp. 196–199, ISBN 978-80-248-1571-8.
VŠB – Technical University of Ostrava, FEECS, 2007.

The most often are used capacitance accelerometers. Capacitance accelerometers using special technology where all mechanical structure is on the one monolithic integration circuit with electronics. Principle of measuring is on changing of capacity of inside regulated integrated capacitors. This structure (Fig. 1) is capable of measuring both positive and negative accelerations. The sensor is a surface-micro machined polysilicon structure built on top of the silicon wafer. Polysilicon springs suspend the structure over the surface of the wafer and provide a resistance against acceleration forces. Deflection of the structure is measured using a differential capacitor that consists of independent fixed plates and plates attached to the moving mass. Acceleration will deflect the beam and unbalance the differential capacitor, resulting in an output square wave whose amplitude is proportional to acceleration.

For measuring is used tree dimensions accelerometer (Fig. 1) Freescale MMA7260.

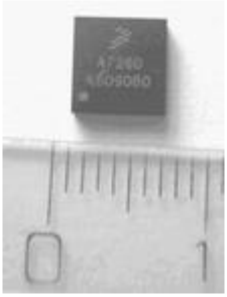

Fig. 1. Accelerometer Freescale MMA7260

BluesenseAD (Fig.2) is an OEM module for wireless sensor data transfer by using Bluetooth technology. BluesenseAD is equipped with two different ports, a common UART and eight 12 bit A/D converters for connecting to a measurement device or an analogue circuit.

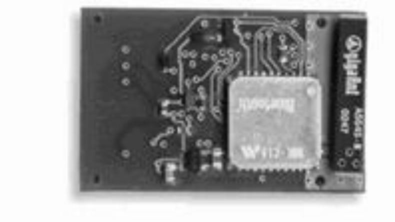

Fig. 2. Bluetooth moduleBluesenseAD

BluesenseAD can be used in every sensor system with data rates lower than 115.2 kbit/s. The range of this Class 2 Bluetooth module is about 25 m. BluesenseAD is designed for low power applications.

3 Results

For realization was created device, which is contained from Bluetooth module BluesenseAD, accelerometers MMA7260 and circuit for power stabilization (Fig.3). The device is powered by two AAA accumulators. This device is used for monitoring of vibrations of patient's bed. This measuring device is possible to easy connect with patient bed, because it contains two screws.

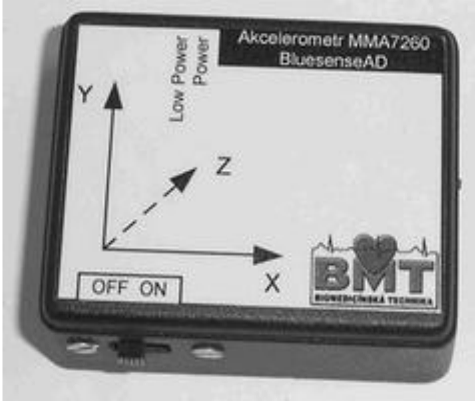

Fig. 3. Measuring device

Part of realization is software for visualization and data saving. Main part of user interface are three strip charts where are displayed measured values of acceleration. There are two control LED diodes, which easily inform about state of measuring process. The first LED is active in case of the serial communication was successfully set. The second is active when the measurement was successfully started. There are next two command buttons in user interface. Close button ends application, Start and Stop button serve to start or stop of measuring process.

Data are saved to standard text file and measured values are separated by tabs, to be easily processed in other programs.

4 Conclusions

It was created device which is in the first case designed or measurement of patient bed in hospital. The visualization and data saving program was realized too. But this created device and software is used for demonstration of function of accelerometers in lessons of biotelemetry engineering course too. The created software is more universal, because it will be used for visualization and data saving of various measured parameters by BluesenseAD modules. The monitoring will be realized in child neurology clinic in Faculty hospital of Ostrava.

References

1. ČERNÝ, M. - MARTINÁK, L. - PENHAKER, M. - SPIŠAK, J. Embeeded portable biotelemetry system of humans, In Proceedings of 3rd International Medical and Biological Engineering Conference EMBEC 2005, 20.-25. listopadu 2005, Praha. Praha: IFBME, 2005, ISSN 1727-1983
2. ČERNÝ, M. - MARTINÁK, L. - PENHAKER, M. - SPIŠAK, J. Biotelemetry system of human, In sborník Programmable devices and systems – IFAC PDS Brno. Brno: PDS, 2006, ISBN 80-214-3130-X
3. ČERNÝ, M. - MARTINÁK, L. - PENHAKER, M. - SPIŠAK, J. – VÁLKOVÁ, A. Systém HomeCare pro sledování životních funkcí člověka, In sborník semináře Medsoft 2006 Praha. Praha: Agentura Action, 2006, ISBN 80-86742-12-1.
4. ČERNÝ, M. - MARTINÁK, L. - PENHAKER, M. - SPIŠAK, J. Vzdálené monitorování pacientů v domácí péči. In sborník souhrnů XXXI. Pachnerovy dny pracovního lékařství Rožnov pod Radhoštěm. Ostrava: Ostravská univerzita, Zdravotně sociální fakulta, ISBN 80-7368-181-1

Strain Gages and Position on Circular Diaphragm

Aleš Oujezdský

Department of Measurement and Control, FEECS,
VŠB – Technical University of Ostrava, 17. listopadu 15, 708 33 Ostrava – Poruba
`ales.oujezdsky@vsb.cz`

Abstract: Strain gages are often used while measuring the pressures, forces and mechanical tensions in industrial systems. The basic element of such measurements is suitable selection of deformation component (beam, diaphragm etc.), suitable placement of gages on deformation component and gages connection (Wheatston´s bridge). Placement and connection of strain gages on deformation component is chosen with respect to thermal compensation and maximal responsiveness of gages. This article deals with the use of deformation component in the form of circular diaphragm, placement of strain gages on this diaphragm and their connection. It systematically continues the paper "Analytical Solution and Modelling of Circular Diaphragm" presented on the Wofes 2006 conference.

1 Introduction

Strain gages are used in many industrial branches. They find their place everywhere, where the solid is deformed. The first strain gage was used already in 1938. Since then architects, builders, project engineers and others use it. The first strain gage was in the form of metal wire, however, in 1952 foil strain gage was created and it is used till now. At present foil strain gages compete with semiconducting strain gages, which have nearly sixty times higher responsiveness. However, foil gages are more accurate and are characterized by linearity.

Foil gages are for example used in folowing areas:

- Measuring of forces, pressure and mechanical tensions,
- Measuring of torsional deformation,
- Measuring of bending on built-in beam,
- Measuring of axial and radial deformation of rods,
- Measuring of stress of constructions (bridges, buildings, etc.).

Foil gages are placed straight on deformation component. They are glued there by special pastes and glues, which do not increase the measurement error by their thermal expansivity. Individual gages differ by their shape and size. During measurement it is necessary to place the gage in correct direction. If we measure force in more directions, more gages are connected, possibly we can use gage, which contains more meanders for measuring in more directions.

© Václav Snášel (Ed.): WOFEX 2007, pp. 200–205, ISBN 978-80-248-1571-8.
VŠB – Technical University of Ostrava, FEECS, 2007.

2 Principle of measuring by strain gages

Ohmic resistance of conductor R depending on its length 1, cross section area S and measured resistance of wire material ρ is given by relation:

$$R = \rho . \frac{l}{S} \qquad \textbf{(1)}$$

If we consider all these values during deformation as variable, then for total function differencial (1) stands:

$$dR = \frac{l}{S} d\rho + \frac{\rho}{S} dl - \frac{\rho . l}{S^2} dS \qquad \textbf{(2)}$$

From the equations then results relation:

$$\frac{dR}{R} = \frac{d\rho}{\rho} + \frac{dl}{l} - \frac{dS}{S} \qquad \textbf{(3)}$$

If we indicate relative elongation:

$$\frac{dl}{l} = \varepsilon \qquad \textbf{(4)}$$

If we expect relative change of measured resistance linearly dependent on relative elongation ε:

$$\frac{d\rho}{\rho} = p . \varepsilon \qquad \textbf{(5)}$$

The change of cross section of the conductor of circular cross section we calculate as difference of the cross section before and after deformation:

$$dS = \pi (r - \Delta r)^2 - S = \pi . r^2 \left(1 - \frac{\Delta r}{r} \right)^2 - S = S(1 - \mu . \varepsilon)^2 - S \cong -2 . \mu . \varepsilon . S \qquad \textbf{(6)}$$

Then we can arrange the equation to:

$$\frac{dR}{R} = \rho . \varepsilon + \varepsilon + 2 . \mu . \varepsilon = (p + 1 + 2 . \mu) . \varepsilon = k . \varepsilon \qquad \textbf{(7)}$$

For certain final change of resistance R we can rewrite the equation (6) to:

$$\frac{\Delta R}{R} = k.\varepsilon \tag{8}$$

Value k in equation (8) is called deformation factor (k-factor). For most commonly available gages the k-factor is k=2 and for their production materials are used, for which this k-factor is invariable in huge extent of deformations.

2.1 Wheatston Bridge

Connection of Wheatston Bridge and marking of its parts is in Figure 1. Four resistances marked R1, R2, R3 and R4 (bridge arms – individual gages or their replacements) are placed into bridge. Feeding diagonal between nodes 2 and 3 is connected to the constant voltage supply $U_{N,}$ output voltage of the bridge U_V between nodes 1 and 4 (output diagonal) is connected to machine booster with theoretically infinite inner resistance.

Output resistance Uv (difference of the resistance between nods 1 and 4) is given by this relation:

$$U_V = U_N \frac{R_1R_3 - R_2R_4}{(R_1 + R_2).(R_3 + R_4)} \tag{9}$$

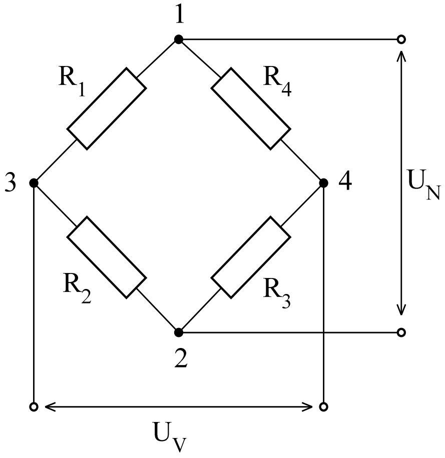

Fig.1. Connection of gages into full bridge

If all the bridge arms are set by active gages with similar resistance, it is full bridge. Output resistance will be maximal achievable, thermal dependence of the gages resistance is fully compenstated. It is used for the most exact experimental measuring with high demands on long-time stability. The most common area of use is construction of tensometric sensors.

Output resistance of the full bridge is given by the relation:

$$U_V = U_N . \frac{\Delta R_1}{R_{10}} = U_N .k.\varepsilon_1 \tag{10}$$

3 Special application for gages placement on diaphragm

While using circular diaphragm as deformation component it is necessary to know the basic parameters of the diaphragm.

- Maximal pressure, which will operate on the diaphragm,
- Diaphragm radius,
- Module of diaphragm flexibility (in dependence on used material),
- Diaphragm thickness.

We come out the assumption that diaphragm is fixed around the whole circumference.

Special application, which was created for diaphragm modelling and placing the strain gages on diaphragm is able to model and graphically display individual basic parametres of deformation component for given parameters (Fig. 2):

- Relative radial elongation,
- Relative tangential elongation,
- Radial tension,
- Tangential tenstion,
- Maximal diaphragm flexure.

We can store all values into the file.

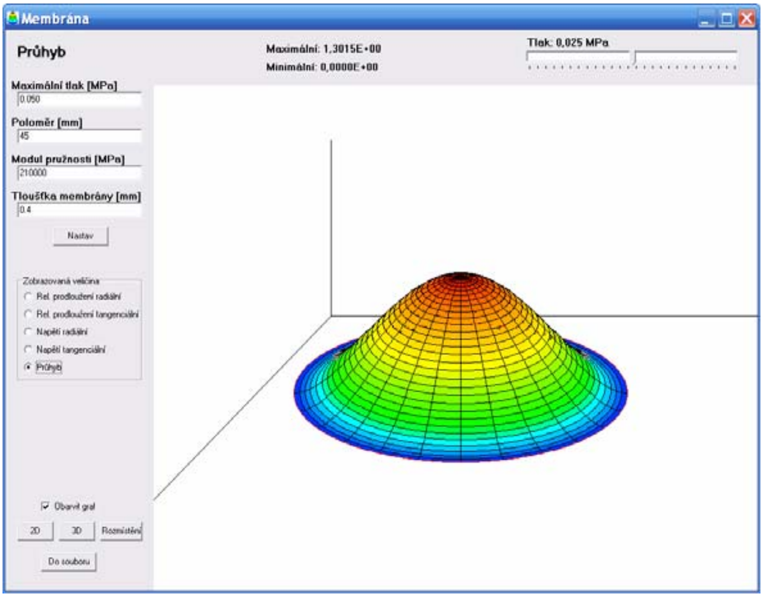

Maximální: 1,3015E+00
Minimální: 0,0000E+00
Tlak: 0,025 MPa

Maximální tlak [MPa]: 0.050
Poloměr [mm]: 45
Modul pružnosti [MPa]: 210000
Tloušťka membrány [mm]: 0.4

○ Rel. prodloužení radiální
○ Rel. prodloužení tangenciální
○ Napětí radiální
○ Napětí tangenciální
● Průhyb

☑ Obarvit graf

Fig.2. Picture of maximal diaphragm flexure

While modeling the placing of gages we come out from the assumption that we use ideal point gage.

Because strain gages will be placed on the diaphragm, it is necessary to set their precise position. When using the full gage bridge we have to place the gages in such way so we gain maximal responsiveness of the bridge and that the individual relative enlongations (in radial and tangential directions) gain the same values.

For output resistance we can afterwards use the relation 10.

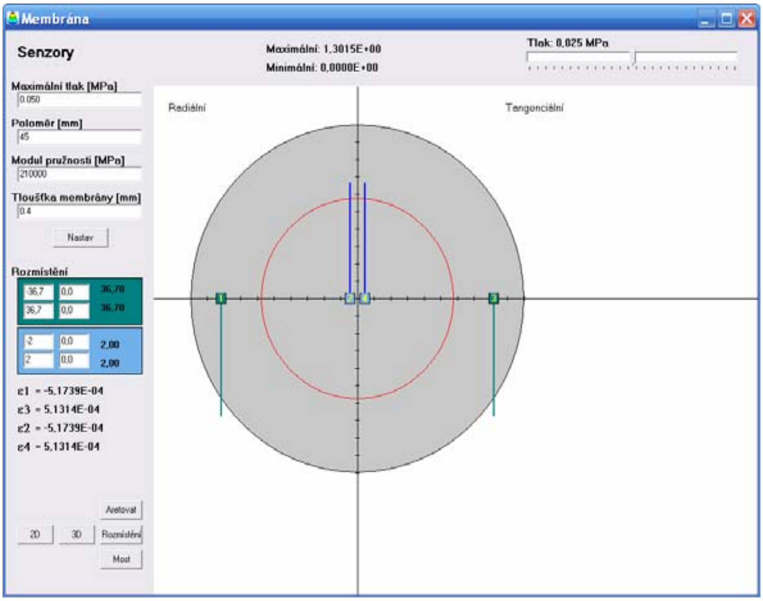

Membrána

Senzory

Maximální: 1,3015E+00

Minimální: 0,0000E+00

Tlak: 0,025 MPa

Maximální tlak [MPa] 0.050

Poloměr [mm] 45

Modul pružnosti [MPa] 210000

Tloušťka membrány [mm] 0.4

Rozmístění

36,7 0,0 36,70

36,7 0,0 36,70

-2 0,0 2,00

2 0,0 2,00

ε1 = -5,1739E-04

ε3 = 5,1314E-04

ε2 = -5,1739E-04

ε4 = 5,1314E-04

Fig.3. Placement of gages on diaphragm

While placing gages we come out from simulated values of relative elongation in radial and tangential direction. Position of individual gages in both axises, and also value of relative elongation in given point is pictured on the board on the left (Fig.3).

For possibility to move all gages into random position there was created function “adjust”, which locks gages as the unit. By using random positioning of gage all the gages move at the same time.

After positioning of individual gages (two scan radial and two tangential relative elongations) it is necessary to connect gages to bridge. Connection to bridge is pictured in Fig.4. In this type of connection the gage bridge will have the highest responsiveness.

When selecting voltage supply of bridge U_N (in our case 5V) we can find output voltage U_V during maximal pressure. For better image it is possible to picture graph of dependence of output voltage U_V and pressure p. Resulting values can be stored into file.

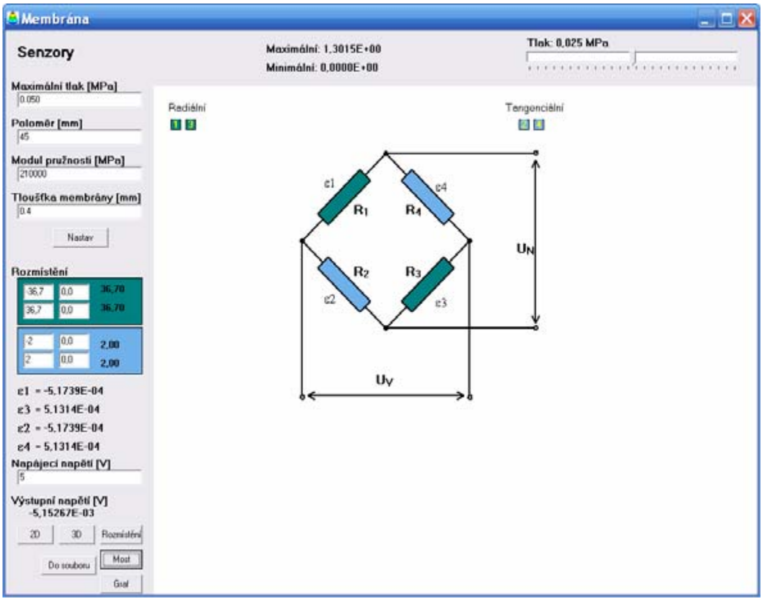

Membrána

Senzory

Maximální: 1,3015E+00
Minimální: 0,0000E+00

Tlak: 0,025 MPa

Maximální tlak [MPa]: 0.050
Poloměr [mm]: 45
Modul pružnosti [MPa]: 210000
Tloušťka membrány [mm]: 0.4

Rozmístění

36,7	0,0	36,70
36,7	0,0	36,70
-2	0,0	2,00
2	0,0	2,00

ε1 = -5,1739E-04
ε3 = 5,1314E-04
ε2 = -5,1739E-04
ε4 = 5,1314E-04

Napájecí napětí [V]: 5
Výstupní napětí [V]: -5,15267E-03

Fig.4. Conection of individual gages into full bridge

4 Conclusion

Use of circular diaphragm as deformation component for measuring pressure is common in practice. With the help of created model and known values of radial and tangential relative elongation we can precisely set the possition of individual gages before the fixation itself. The important factor is fixation of gages in such way so they react in correct direction. Two gages measure radial elongation; two of them measure tangential elongation. When suitably chosen placement of gages we gain fully thermally compensated Tensometric Bridge with maximal responsiveness.

References

1. Slíva, A., Oujezdský, A., Martinák, L., *Tříosý snímač tlaků v sypkých hmotách*, časopis Automa 06/2005.
2. Oujezdský, A., *Measurement of pressures in silos using strain-gauge bridges*, Wofex 2005, Ostrava.
3. Slíva, A., Oujezdský, A., Martinák, L., *Měření napětí sypkých hmot pomocí vyvinutého 3Dimenzionálního snímače*, AT&P žurnál, 10/2005, Bratislava.
4. Oujezdský, A., *Analytical Solution and Modelling of Circular Diaphragm*, Wofex 2006, Ostrava.

Using Knowledge System Module in Genetic Algorithm

Pavel Petránek, Miroslav Pokorný

Department of Measurement and Control, FEECS,
VŠB – Technical University of Ostrava, 17. listopadu 15, 708 33 Ostrava – Poruba
{pavel.petranek, miroslav.pokorny}@vsb.cz

Abstract. The Genetic Algorithms deal with two basic problems. The first of them is probability to get stuck in local extreme. This question is solved by many different accesses but scope of our work is dealing with the second problem – used computer time. Genetic algorithm is very demanding on computing resources. The way how to solve this problem is in increasing computer power, using parallel computation or try to introduce some advanced technique into computational process. Our paper deals with the last proposed method. Our aim is including artificial intelligence approach to restrict need of fitness's function computation. All aspects of our access are in the following article.

1 Introduction

A principle of genetic algorithm (GA) is based on biological background. [1] Although this approach for solving problem is not so old, these basics make this principle as one with the oldest practical results. Terminology is naturally overcome from biology because of similarity.

Conditions for using GA are simple. We have to be able to code our problem into string called chromosome. This is typically vector with one possible solution of the problem. This chromosome is made from genes. Each gene represents one parameter of the solution. This is often a number, but it is not necessary we can works with letters symbols etc. The second condition of using GA is ability to evaluate each solution (chromosome) by cost (fitness) function, which assignees a value for chromosome which expresses how close this solution to the ideal chromosome is.

Fitness function could be hard to complete in case of difficult problems. Time consumption is also depending on type of problem which is solved. In case of simple equation is needed time irrelevant, but if (for example) the costs function is constructed as simulation of some process the time which is spent for its calculation very dramatically excessive cost for all other operation.

All operations are made above group of chromosomes which is called population. GA is iteration algorithm. Population in one iteration is called generation. Transition from one generation to next follows this scenario. Selected chromosomes in actual generation are cross over. There are many selection methods for example one of the most common is called tournament selection. Among group of randomly taken chromosomes is chosen the best one. The best one chromosome from actual population is

© Václav Snášel (Ed.): WOFEX 2007, pp. 206–211, ISBN 978-80-248-1571-8.
VŠB – Technical University of Ostrava, FEECS, 2007.

not automatically taken because of degeneration which causes this approach to the solution. Children (results of cross over) are inserted into new generations. With small possibility could be mutation performed over products of cross over. This random factor helps GA also to overcome problem with stuck in local extreme. Transit from one generation to another expresses iteration base of algorithm. The average fitness during these generations is also improving.

There are few ways how to terminate the algorithm. We can it limit by number of generation, stall time or time of run.

As was mentioned the biggest disadvantage of an approach is possibility to get stuck in local extreme. Some advanced techniques are usually implemented into GA. [2] The second disadvantage is computation time, which is needed for finding solution. In this article we will try to introduce new method for its reducing

2 Knowledge system

We have introduced purpose of cost function. It is essential part of algorithm, but on the other side is also reason why are GA computationally so demanding.

The new access for the architecture of GA is settled in this article. Our way how to increase efficiency of GA is implementation of knowledge (expert) module. The goal for this module is simple. We try to reduce needs for calling fitness function. Solutions which are coded into chromosomes could be similar. We can find similar solution in one or during more generations. The main idea is find a solution (module) which is able to discover such situations and use stored information instead of wasting computation time on just know results.

The module is implemented into new layer (totally transparent for the GA), which is inserted on the position of interface of GA's program code and calling of fitness function.

The module analysis GA's calling for computation of fitness function. It analyses input parameters (chromosome) and is trying to find match with its knowledge base. If there are no results, then execution of fitness function will be done. Result is return back to the main part of GA and also is saved (with input parameters - chromosome) into knowledge base of expert module.

Different situation, in positive way, is when input parameters are for the expert module known. In this case are similar parameters saved in the knowledge base – question of similarity depends on decision of expert module. The probability of the exactly same know parameters is very small so in the most cases is decision of expert module needed. It of course must take into account more factor than only numeric similarity with input parameters.

If the result of comparison is positive, then there will not be execution of cost function but just only saved result will be return to GA. Inner structure of expert module will be discussed in next chapter.

3 Structure of knowledge system

The start point (Fig. 2) represents call of cost function. Symbol CH_T (1) is actual chromosome (with N genes), which should be evaluated by fitness function.

$$[a_{11,T}, a_{12,T}, a_{13,T}, .. a_{1N,T}] = CH_T \qquad (1)$$

Database stores known solutions. Extraction of the similar chromosomes is done according to equation (2), where $P_1 - P_N$ is precision for each gene of chromosome. Output from the database search is group of parameters (we describe here situation with positive results, if no result is obtain then progress in expert module will be terminated and classical cost function will be computed) - $CH_{k,T}$ is group of similar chromosomes, with their appropriate values of fitness function FIT_k.

$$\forall CH_{k,T}; \left|a_{k1} - a_{11,T}\right| \le P_1 \wedge \left|a_{kN} - a_{1N,T}\right| \le P_N \qquad (2)$$

Character K is symbol for number of founded similar chromosomes and R represents ratio of average of selected to the best know solution. Input to the fuzzy system [3] is pair of parameter R and K. In fuzzy system is inferred value S, which sets precision for computation of estimated fitness value for input chromosome CH_T.

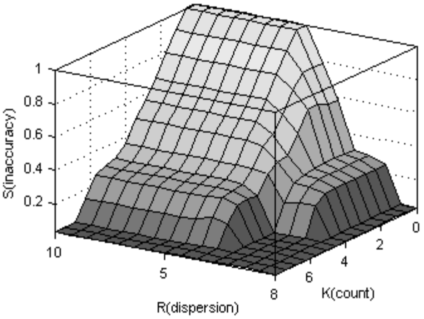

Fig. 1 Model of fuzzy system's knowledge base

If the result with such precision is not calculated, then fitness value will be calculated by classical way.

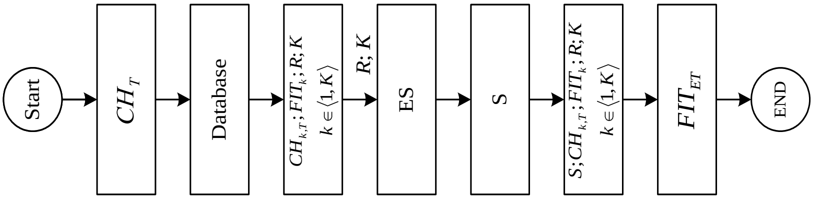
Start
CH_T
Database
$CH_{k,T};FIT_k;R;K$ $k \in \langle 1,K \rangle$
$R;K$
ES
S
$S;CH_{k,T};FIT_k;R;K$ $k \in \langle 1,K \rangle$
FIT_{ET}
END

Fig. 2 Scheme with structure of expert module

Coefficient S is used as multiplier of precision coefficients $P_1 - P_N$. The increased precision (S coefficient) is used for selection chromosomes in modified equation (2). Finally the estimated fitness value is computed from chromosomes, which fits these stronger conditions.

$$\forall CH_{k,T}; \left|a_{k1} - a_{11,T}\right| < S \cdot P_1 \wedge \left|a_{kN} - a_{1N,T}\right| < S \cdot P_N \tag{3}$$

The output value is estimated as a weighted sum of cost values of selected chromosomes by equation (4). Where *K* presents number of similar chromosomes, *N* symbols length of chromosome, FIT_k is fitness value of the *k* chromosome.

$$FIT_{ET} = \frac{\sum_{K} \left(\sum_{N} \left(S \cdot P_n \cdot a_{1n,T} - abs(a_{kn} - a_{1n,T}) \right) \right) \cdot FIT_k}{\sum_{K} \sum_{N} S \cdot P_n \cdot a_{1n,T}} \tag{4}$$

The computed value is considered as fitness value of input chromosome but in fact it is only mathematical approximation. The value is returned to the main part of GA finally.

Important mechanism that is not shown in scheme (Fig. 2) takes care about dangerous of stuck in small area near real solution. This is done by ageing of records in database. If record with similar solution is in database, than it will use. Next action is simple. Age of used record will be increased by one. Record will be erased from the database if its age is over settled limit.

As we will see on the practical results the computation costs for running of expert module are insignificant.

4 Case Study

Simulated experiments were performed to verify our study. MATLAB environment was used to model situation how great impact has early expert module on computation a results of GA's run. This software is suitable because of integrated environment of GA and easy connectivity with other toolboxes.

The base of experiment is overtaken from our paper. [4] The work deals with optimization of fuzzy regulator by GA. The idea is simple.

Design stage of fuzzy controller is easy. There are recommended rule bases for fuzzy regulators type PID, PD, PI - so there is no need to develop new one. Unfortunately it is not enough. Setting of universes will follow to ensure that the regulator will work fine. An expert access is normally used for tuning over universes, but it is possible to use GA instead of human intervention.

It takes a lot of time to set right coefficients for people without experiences. Using GA for replacing expert role is good way. In our system was used following transfer function (5):

$$G_{S,1} = \frac{1}{s^2 + 0.5s} \tag{5}$$

Parameters of GA's settings and fitness function are shown in the article. We have modified fitness function for only two thinks. There was set allowed overrunning of unit response for absolute size 0.01 and early expert module implementation was done also. Results of the experiments are shown in next chapter.

5 Results

Algorithm was run with expert module and without it to verify how big impact the module has on computation parameters and quality of the results. The numbers of the runs of algorithm are same for both cases.

Table 1. Results without and with expert module

fval=	10,35369	time=	5294,39	fval=	10,44291	time=	4089,16
fval=	11,10054	time=	4903,34	fval=	10,70208	time=	3373,73
fval=	10,57117	time=	4915,76	fval=	10,82383	time=	3784,09
fval=	10,49794	time=	4905,74	fval=	10,55071	time=	4329,37
fval=	11,81779	time=	4960,31	fval=	10,48918	time=	4258,33

As we can see the approximate time, necessary for the computation of 25 generations is about 4 950 s. Fitness values are very similar.

Results from system with expert module show that time which is needed for computation of 25 generations is significantly lower. Next remarkable thing is that the lowest value of fitness function is also nearly the same as the best result of the run without expert module.

Table 2. Average results

Expert Module	Average Fitness Value	Average Time [s]
NO	10,8682	4995,908
YES	10,6017	3966,936

Exact number of expert module impact is shown at Tab. 3. Time consumption is less than approximately 20 %. Average fitness value is also lower, but the difference is not so significant.

The average time of fitness function's computation is about 4.8 s (expert module activation cost in average 0.02 s only). This system is useful in case that at least one successful expert module result is obtained during 240 fitness counts.

6 Conclusion

The new access for the GA's computation is shown in this paper. Our goal is finding the way how to save computation time with using some advanced technique. The solution consists of knowledge module implementation, which seems to be original idea for saving time consumption of GA. The module represents for the algorithm transparent layer with only one target. It tries to find solution by using local database of previous runs of fitness function. If no previous solution is present, than fitness value is computed by classical way.

We made experiments with focus on verifying or disproving our thoughts. The program was run for several times to obtain average results. We can notice remarkable time saving. It is about twenty percent fall of computed time, which satisfies our expectation. On the other side average fitness value is even better than we supposed. It means that the result is not worse than in case of normal run. This fact seems to be hard to explain but we think that it is due to small absolute error in the last phase of computation (the differences are so small, that it almost play no role on result of computation).

Next work will deal with implementation of the module into proprietary GA at our department. Next possible way of progress could be improvement of expert module.

7 Acknowledgement

This work was solving on the VSB Technical University of Ostrava, Czech Republic. This work was supported in part by the Grant Agency of Czech Republic under Grant, 102/05/H525, Racionalizace studia doktorského studijního programu na FEI VŠB-TU Ostrava and under Grant, 102/06/1332, Computational Intelligence in Metallurgical Process Control.

8 References

1. Mařík, V.; a kol., *Umělá inteligence (3)*, Academia Praha, 1997
2. Želasko, P., *Využití znalostních přístupů v genetických algoritmech*, Ph.D. thesis, Ostrava 2006
3. Pokorný, M., ***Řídící systémy se znalostní bází*,** Ostrava, 1999
4. Petránek, P., Šišpera, P., Pokorný, M., *„Fuzzy Controller Optimization Using Genetic Algorithms"*, IWCIT 2005, str.67 – 70, Ostrava 2005

The V4DB Real-time Database System: Admission Control and Priority Assignment

Jan Pokorný

Department of Measurement and Control, FEECS,
VŠB – Technical University of Ostrava, 17. listopadu 15, 708 33 Ostrava – Poruba
`jan.pokorny@vsb.cz`

Abstract. I am a member of a research group and our main objective is to design and implement an experimental real-time database system suitable for study of real time transaction processing. The experimental system is implemented as an integrated set of the most important functional parts of a veritable real-time database system. It serves as a support platform for performance evaluation of known and new algorithms of the particular processing components, including CPU scheduling, concurrency control and conflict resolution strategies. Because of the strong interactions among the processed components, proposed system can help us to understand their effect on system performance and to identify the most influencing factors. You can find continuous results on the V4DB project as well as my contribution on this project in the following paper.

1 The V4DB Project

The research group was established in 2005 and supported by Czech Science Foundation. Detail research is focused on developing experimental real-time database system. We have implemented an experimental real-time database system suitable for study of real-time transaction processing.

Our research group consists of two cooperative teams. The first is situated in the VSB Technical University in Ostrava. Next part of the research group has been set up in Silesian University in Opava, Faculty of Business Administration in Karviná.

1.1 Project history

The main objective was focused on analyzing of existing real-time database systems during the first year of the project. The next fields of study were classical database system mechanisms and possibilities of adapting these methods into real-time systems.

We had created analysis model and basic concept of the V4DB system. We call it as a V4DB version 1. We selected VxWorks as a real-time operating system and there were implemented fundamental functional blocks. We were presented significant

© Václav Snášel (Ed.): WOFEX 2007, pp. 212–214, ISBN 978-80-248-1571-8.
VŠB – Technical University of Ostrava, FEECS, 2007.

results inside the papers [1][2][3][4][5][6]. In the dissertation thesis [7] were presented the most important ideas and the whole V4DB system.

1.2 Current Status of the Research

We are deeply working on the (V4DB) version 2. We decided that the VxWorks platform is not suitable for progressive research and the next development. New version of the RTDB system is associated with the change of a real-time platform. It is used RTX extension as a base real-time operating system. We added two new blocks into the existing system schema - Indexing Manager, Buffer Management and changed block - Concurrency Control. This improved system as a whole has not been tested yet.

Next research is divided into separate directions. One of the directions is admission control and priority assignment policy.

1.3 Admission Control Mechanism and Priority Assignment

Admission control and priority assignment is one of the important areas in real-time database systems. In general, it avoids system overloading and dispatches for execution as to the priority assignment policy and the way of transaction processing. The priority assigned to a transaction execution process is mapped to a real operating system process priority and the context (transaction) switching is relied on an underlying operating system.

Especially, I am analyzing and designing adaptive admission control concepts based on system feedback. I try to find proper design of a mechanism for optimal cooperation between concurrency control and priority assignment policy. My following focus within the project is transaction processing strategies as well.

These spheres of study will be described in my dissertation thesis. There will be evaluated their pros and cons of admission control mechanisms in comparison with others, as a further priority assignment policies, transaction processing strategies and relating important ideas and results.

Publications

I cooperated on the following papers (from September 2006 to July 2007):

1. Krol, V., Pokorny, J.: Design of the experimental platform for testing real-time database transaction processing, 3rd IFAC Workshop on Discrete-Event System Design (DesDes06), Leszno, Poland, September 2006.
2. Krol, V., Pokorny, J.: Design of V4DB - Experimental Real-Time Database System, The 32nd Annual Conference of the IEEE Industrial Electronics Society, Paris, France, November 2006.
3. Krol, V., Pokorny. J.: The V4DB Testbed - Evaluating of Real-Time Database Transaction Processing Strategies, The 11th WSEAS International Conference on COMPUTERS, July 2007

References

1. Krol, V., Cernohorsky, J., Pokorny, J.: Towards the Evaluation of Algorithms used in Real-Time Databases, in Proceedings of the 7th WSEAS International Conference: Automatic Control, Modelling and Simulation, ISBN 960-8457-12-2, pp. 67-71, Prague, 2005.
2. Pokorný, J., Król, V., Černohorský, J.: Návrh databázového systému v prostředí operačního systému založeného na specifikaci real-time, Sborník přednášek Tvorba Software 2005, ISBN 80-86840-14-X, str. 207-210, Ostrava, 2005.
3. Krol, V., Pokorny, J., Cernohorsky, J.: Architecture of experimental real-time databases for embedded systems, in Proceedings of IFAC Workshop on Programmable Devices and Embedded Systems PDeS 2006, ISBN 80-214-3130-X, pp. 384-388, Brno, 2006.
4. Pokorný, J., Król, V.: Testování rt algoritmů při zpracování transakcí v experimentálním real-time databázovém systému, in Proceedings of the 7th International Scientific - Technical Conference - PROCESS CONTROL 2006, ISBN 80-7194-860-8, pp. 187-192, Kouty nad Desnou, 2006.
5. Krol, V., Pokorny, J.: The V4DB project - support platform for testing the algorithms used in real-time databases, in Proceedings of the 10th WSEAS Int. Conf. on Computers, ISBN 960-8457-47-5, Athens, Greece, 2006.
6. Krol, V., Pokorny, J.: Design of experimental platform for testing real-time database transaction processing, 3rd IFAC Workshop on Discrete-Event System Design (DesDes06), Leszno, Poland, September 2006.
7. Król, V.: Metody ověřování vlastností real-time databázového systému s použitím jeho experimentálního modelu, disertační práce, 2007

Flow Sensor for Biomedical Applications

Jan Spišak

Department of Measurement and Control, FEECS,
VŠB – Technical University of Ostrava, 17. listopadu 15, 708 33 Ostrava – Poruba
jan.spisak@vsb.cz

Abstract. This contribution deal with description and properties of differential pneumotachograph for volumetric flow measuring. The construction of this pneumotachograph is modified for using in education for subjects orientated on applications with biomedical sensors. This equipment demonstrated volumetric flow of air along patient respiration.

1 Introduction

The sense of laboratory exercises in subjects with a view to biomedical sensors is make a presentation of a new technologies of biomedical sensors with students. For maximum plasticity is this pneumotachograph modified into special preparation which is supplemented other components as filter and amplifier. This preparation also includes input and output protection.

2 Analysis

Breathing is one of more essential fhysiological declarations of human. It is the process when it´s realized gas exchange between blood and organs of body. Differential pneumotachograph provides measuring of volumetric flow when it is possible to survey quality of patient breathing with good accuracy. Measuring, record and processing of these parameters is called spirometry or also spirography. [1]

© Václav Snášel (Ed.): WOFEX 2007, pp. 215–218, ISBN 978-80-248-1571-8.
VŠB – Technical University of Ostrava, FEECS, 2007.

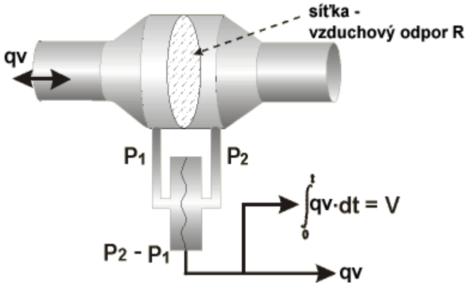
síťka -
vzduchový odpor R
qv
P1
P2
P2 - P1
$\int_0^t qv \cdot dt = V$
qv

Fig. 1. Principle of differential manometer

Pneumotachograph with differential manometer is measured flow on the basis scanning differential pressure between two areas of sensor. It is available many types of construction sensor when the difference pressure is created by air resistance (small metal reticulum or system of slim tubes). The pressure is measured before and behind of this air resistance. For this application was used differential manometer with type Lilly when his principle of function is described on figure 1. This type of differential manometer is used as a elementary module of anestetic equipment in surgery and incubators in maternal hospital for example.

Air resistance *R* is defined as a difference pressure *Dp* when this parameter presents unit flow:

$$\mathrm{D}p = p_2 - p_1 = R.q_v \tag{1}$$

Eventually it´s possible to calculated dimension of inspire or respire air by the help of volumetric flow integration. Generally considered that air resistance must have enough full diameter because it may created turbulent air flowing. In this case the functional dependance is nonlinear.

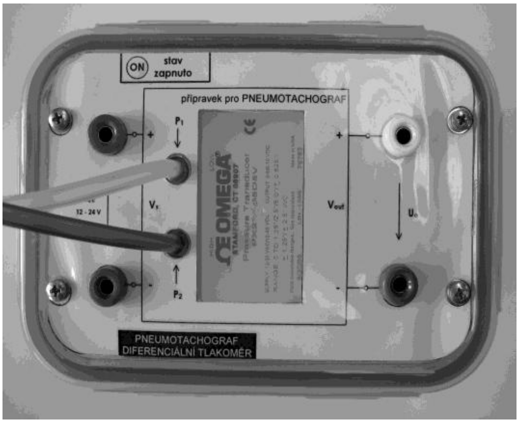
ON
stav
zapnuto
přípravek pro PNEUMOTACHOGRAF
P1
P2
+
-
12 - 24 V
Vs
OMEGA
Vout
U0
+
-
PNEUMOTACHOGRAF
DIFERENCIÁLNÍ TLAKOMĚR

Fig. 2. Detail of preparation with pneumotachograph

3 Results and conclusion

The main component of this equipment is differential manometer - type Lilly which is proposed for measuring pressure within the range 1,25 psi (8618,45 Pa). Input voltage of this senzor is max. 10V and output voltage is 5V in case zero pressure difference. This fact allows pressure difference measuring in both roads of air flow. For conversion of measured voltage into pressure is used constant value 861,845 Pa/V. Also this value determine sensitivity of sensor.

The following pictures describes result of this work. On the figure is differential pneumotachograph connected with other components for using as laboratory exercise whereas the goal this exercise is measuring of funcionality U = f(qv) where qv is air flow.

References

1. Penhaker, M., Imramovský, M., Tiefenbach, P., Kobza, F.: Lékařské diagnostické přístroje, ISBN 80-248-0751-3.
2. www.spirxpert.com

Acknowledgment

I would like to thank M. Penhaker and M. Imnramovský for cooperation on this project.

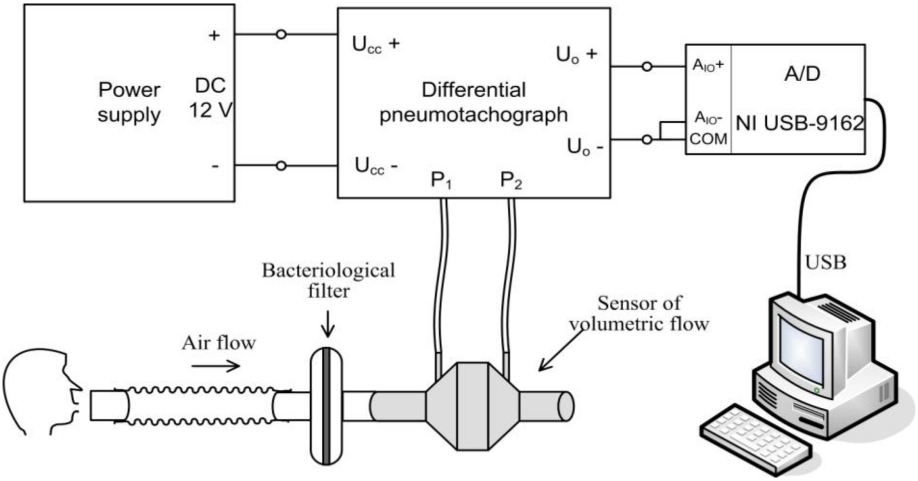
Power supply
DC 12 V
+
-
Ucc +
Ucc -
Differential pneumotachograph
Uo +
Uo -
P1
P2
AIO+
AIO-
COM
A/D
NI USB-9162
USB
Bacteriological filter
Air flow
Sensor of volumetric flow

Fig. 3. Measuring chain of laboratory exercise

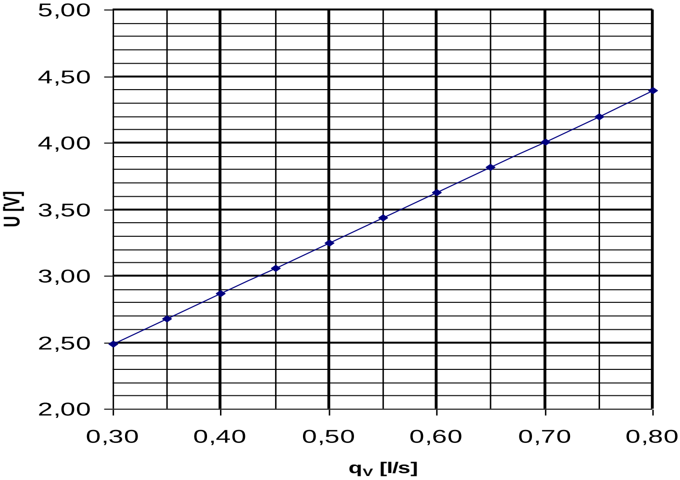

Fig. 4. Measuring chain of laboratory exercise

A Benchmark on Dynamic Reliability: Analysis of the Modeled System*

Petra Škňouřilová

Department of Applied Mathematics, FEECS,
VŠB – Technical University of Ostrava, 17. listopadu 15, 708 33 Ostrava – Poruba
`petra.sknourilova@vsb.cz`

Abstract. In this paper, the results of a dynamical-behavior analysis of an examined system are presented. As the analysed system I used a benchmark taken from the literature. This benchmark was previously implemented using Stochastic Colored Petri Nets (SCPNs). The modeled net serves for the acquisition of the system-reliability evaluation. As another system modification I considered the maintenance action. I implemented two types of maintenance : a preemptive (periodic) maintenance and a repair process. These modifications were also modeled by SCPNs and the obtained analysis results are presented. My final objective is to compare these results with the analytical approach.

Keywords: dynamic reliability, cumulative distribution function, maintenance action

1 Introduction

The discipline of dynamic reliability has arisen as a mean to study the interactions of systems, taking into account not only the stochastic failures but also the deterministic evolution of the process variables.

The dynamical aspects concern the ordering and timing of events in the accident propagation, the dependence of transition rates and failure criteria on the process variables values, the human operator and control actions.

The formal description for the dynamic reliability analysis: Let $x(t) \in R^n$ be the set of the process variables describing the state of the system at time t. The system behavior can be described as follows: starting from an initiating event occurred at $t_{k_0} = 0$ with the system in a given initial state k_0 and process variables vector x_0, the system will evolve deterministically in phase space according to the corresponding dynamic model m_{k_0} as given by the vector equation

$$\frac{dx(t)}{dt} = m_{k_0}(x(t), t). \tag{1}$$

---

* Presented results had been obtained during solving the grant project Dynamic Reliability Quantification and Modeling under grant code T401940412 supported by the Academy of Sciences of the Czech Republic.

© Václav Snášel (Ed.): WOFEX 2007, pp. 219–224, ISBN 978-80-248-1571-8.
VŠB – Technical University of Ostrava, FEECS, 2007.

This equation describes the time evolution of the system up to the occurrence at time t_{k_1} of another event which moves the system to state k_1. Then, the system will evolve according to the new dynamics, m_{k_1}, and so on.

2 The case study

2.1 Presentation of the system

The system (taken from [1]) is composed of a tank where the fluid level (h) must be kept between two values ($h_0 - 1$) and ($h_0 + 1$). The tank is supplied by a main pump P1, an emergency pump P2, and is drained by a valve V. A control system regulates the fluid level by switching on/off the pumps and the valve according to the fluid level measured by sensors.

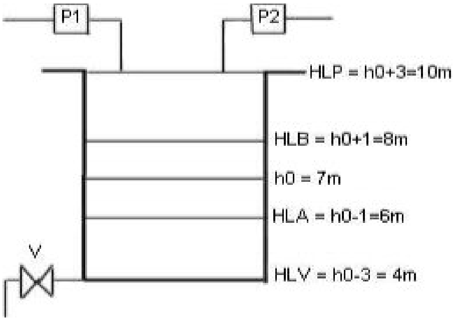

Fig. 1. System scheme.

2.2 Presentation of the hypothesis

I made the following functional and dysfunctional hypothesis:

1. Functional hypothesis
   - the flow from the valve and the pumps are supposed to be identical and equal to 0.6 m^3/h. The tank section is 1 m^3, so we can represent the flow as an hourly rate of level variation equal to 0.6 m/h.
   - initially (at time t=0), the fluid level is supposed to be equal to $h_0 = 7$ m, the pump P1 is on, the valve V is on and the pump P2 is off
   - sensors are located at different levels of the tank and the detection of a specific fluid level threshold will send orders to the actuators according to the Table 1.
2. Dysfunctional hypothesis
   - I only consider failures of the valve and the pumps

- these actuators are independent from each other and in the first case there are not repairable
- I consider the following failure modes: the components (P1,P2,V) can lock in the state on, or in the state off
- failure occurrence of these components obey the exponential law with a rate α_1=$4,566 \cdot 10^{-3}$ h^{-1} for P1, α_2=$5,714 \cdot 10^{-3}$ h^{-1} for P2 and α_3=$3,125 \cdot 10^{-3}$ h^{-1} for the valve V.

The fluid level	P1	P2	V
$h < h_0 - 1$	ON	ON	OFF
$h_0 - 1 \leq h \leq h_0 + 1$	ON	OFF	ON
$h > h_0 + 1$	OFF	OFF	ON

Table 1. The control laws.

2.3 System modeling in Stochastic Colored Petri Nets

The forementioned system, as well as its maintenance action extention, is modeled by SCPNs in [2].

2.4 Simulation of the modeled nets

The tank dryout ($h <$ HLV) and the fluid overflow ($h >$ HLP) are two possible unwanted situations. The failure of the whole system happens, when the dryout or the overflow occurs. The simulation was realized for all three modifications of the systems:

1. the system with non-repairable components
2. the system with repair service - the components are repairable
3. the system with preemptive (periodic) maintenance.

In order to evaluate the reliability of these system modifications, I determined the dryout and the overflow cumulative distribution function (cdf) as the probability of the presence of a token in the places Dry_out and Overflow, at the mission time. The obtained results are numerically reported in Table 2 and 3, and graphically in Fig. 2 and Fig. 3.

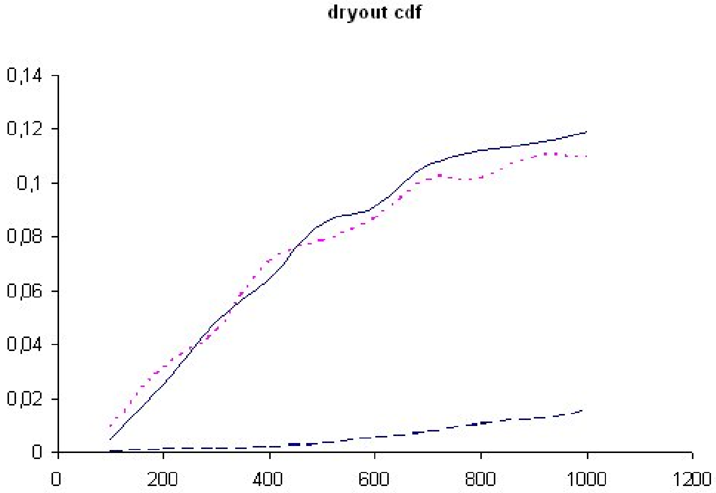

Fig. 2. Dryout cdf. The solid line shows cdf for the system with non-repairable components; the dashed line shows cdf for the modified system with the repair service and the dotted line shows cdf for the modified system with the preemptive maintenance.

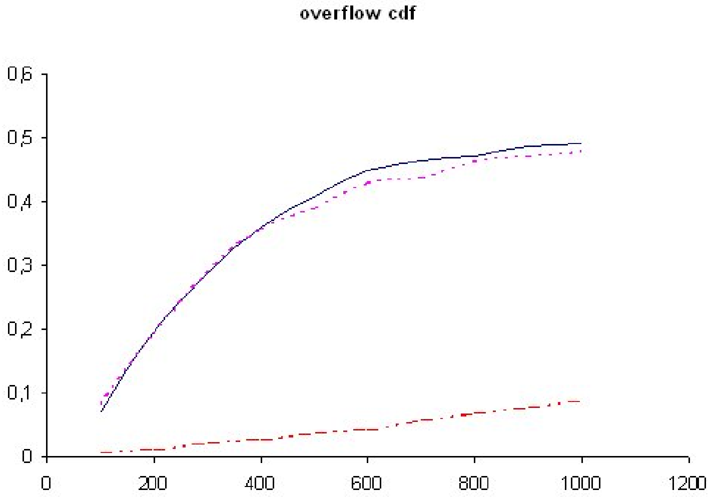

Fig. 3. Overflow cdf. The solid line shows cdf for the system with non-repairable components; the dashed line shows cdf for the modified system with the repair service and the dotted line shows cdf for the modified system with the preemptive maintenance.

hours	non-repairable components	repair service	preemptive maintenance
100	0.00524	0.0092	0.00006
200	0.0251	0.0312	0.00095
300	0.0486	0.045	0.00124
400	0.0645	0.0712	0.0019
500	0.085	0.0781	0.00323
600	0.0911	0.087	0.00554
700	0.1068	0.101	0.0075
800	0.112	0.102	0.0105
900	0.115	0.1095	0.0124
1000	0.1191	0.11	0.0153

Table 2. Dryout cdf.

hours	non-repairable components	repair service	preemptive maintenance
100	0.0712	0.0821	0.0042
200	0.1981	0.192	0.00945
300	0.289	0.291	0.021
400	0.361	0.356	0.0265
500	0.409	0.389	0.0361
600	0.4492	0.4286	0.0413
700	0.4651	0.4371	0.056
800	0.471	0.461	0.067
900	0.486	0.468	0.076
1000	0.493	0.4765	0.086

Table 3. Overflow cdf.

3 Conclusion

The objective of my work was to analyse the dynamical behavior of the benchmark by the simulation method. As a second analysed problem, I considered the benchmark modification while I added the possibility to repair the components. I used SCPNs to model the dynamical behavior of the systems. These nets were used as the simulation input while the values of cdf for two unwanted states of the systems are the simulation results. These results may be sumarized in two major points : the overflow state takes place a with higher probability and the preemptive maintenance is more suitable. After the evaluation and comparsion of my results with the analyticaly acquired outcomes I can say that the usage of SCPNs for this type of systems is suitable and usefull.

This research serves as a groundwork for a modeling and analysis of a dynamical behavior of more complicated systems and real problems.

References

1. Marseguerra,M., Zio,E. Monte Carlo approach to PSA for dynamic process systems. *Reliability Engineering and System Safety,52: 227-241.*
2. Škňouřilová,P. Solving a dynamic reliability problem by Colored Petri Nets. *Proceedings of WOFEX 2006*, 282-287.
3. Devooght,J., Smidts,C. Probabilistic dynamics as a tool for dynamic PSA. *Reliability Engineering and System Safety,52*,185-196.
4. Walter, M., Schneeweiss, W. *The Modeling World of Reliability / Safety Engineering.*. Hagen: LiLoLe-Verlag GmbH.
5. Labeau, P.E., Smidts, C., Swaminathan, S. Dynamic reliability: towards an integrated platform for probabilistic risk assessment. *Reliability Engineering and Safety System,68*, 219-254.
6. Cabarbaye A., Faure, J., Laulheret, R. Optimization and recursive simulation modelling *Proceedings of ESREL 2006.*
7. Schneeweiss. W.G. *Reliability modeling*, Hagen: LiLoLe-Verlag GmbH.
8. Dutuit, Y., Chatelet, E., Signoret, J.-P., Thomas, P. Dependability Modelling and Evaluation by Using Stochastic Petri Nets: Application to Two Test Cases. *Reliability Engineering and System Safety, 55*, 117-124.
9. Chen, C. H., Lin, J., Yucesan, E., Chick, S. E. Simulation budget allocation for further enhancing the efficiency of ordinal optimization. *Journal of Discrete Event Dynamic Systems : Theory and Application, 10(3)*, 251-270.

Adaptive Filter for Speech Signal Processing

Jan Vaňuš

Department of General Electrical Engineering, FEECS,
VŠB – Technical University of Ostrava, 17. listopadu 15, 708 33 Ostrava – Poruba
jan.vanus@vsb.cz

Abstract. This paper describes the method of design Adaptive filter parameters for speech signal processing. I used the LMS algorithm for adaptive filtering. One part of design Adaptive filter parameters is correct adjustment of initialization filter vector $\boldsymbol{w}(0)$. In this paper is solving influence setting up optimum tap weight vector of LMS algorithm on speech signal processing.

Key words: Adaptive filter, LMS algorithm, speech signal processing, tap weight vector

1 Introduction

The LMS algorithm is the most widely used adaptive filtering algorithm, in practice. I chose the LMS algorithm of Adaptive filter for speech signal processing. This algorithm is a member of stochastic gradient algorithms and its iterative procedure involves: a) computing the output of an FIR adaptive filter produced by set of tap inputs (filter coefficients), b) generation of an estimated error by comparing the output of the filter to a desired response, and c) adjusting the tap weights (filter coefficients) based on the estimation error. I obtained the optimum tap-weight vector, $\boldsymbol{w}_0$, according to the Wiener – Hopf equation.

2 The LMS Algorithm

2.1 Derivation of the LMS Algorithm

Figure 1 depicts an M-tap transversal adaptive filter. The filter input $\boldsymbol{x}(n)$, desired output $d(n)$ and the filter output $y(n)$ are assumed

$$y(n) = \sum_{i=0}^{N-1} \boldsymbol{w}_i(n)\boldsymbol{x}(n-i) \tag{1}$$

© Václav Snášel (Ed.): WOFEX 2007, pp. 225–230, ISBN 978-80-248-1571-8.
VŠB – Technical University of Ostrava, FEECS, 2007.

The tap weights $w_0(n)$ $w_1(n)$ … $w_{M-1}(n)$ are selected so that difference (error) $e(n)$ is minimized in some sense.

$$e(n) = d(n) - y(n) \tag{2}$$

Tap weights are time varying, since they are continuously being adapted so that any variations in the signal's statistics could be tracked.

The LMS (least mean square) algorithm changes (adapts) the filter tap weights so that $e(n)$ is minimized in the mean-square sense. When the processes $\boldsymbol{x}(n)$ a $d(n)$ are jointly stationary, this algorithm converges to a set of tap weights which are equal to the Wiener Hopf solution. LMS algorithm is a practical scheme for realizing Wiener filters, without explicitly solving the Wiener-Hopf equation. It is a sequential algorithm which can be used to adapt the tap weights of a filter by continuous observation of its input, $\boldsymbol{x}(n)$, and desired output $d(n)$. The conventional LMS algorithm is a stochastic implementation of steepest descent algorithm.

$$\boldsymbol{w}(n+1) = \boldsymbol{w}(n) - \mu\nabla e^2(n) \tag{3}$$

Meaning of symbols in the equation (3):

$\boldsymbol{w}(n)$ = $[w_0(n)\ w_1(n)\ \ldots\ w_{M-1}(n)]^T$, filter taps at time n,
μ is algorithm step size parameter,
∇ is the gradient operator.

Adjustment of equation (3) we obtain

$$\boldsymbol{w}(n+1) = \boldsymbol{w}(n) + 2\mu e(n)\boldsymbol{x}(n) \tag{4}$$

Meaning of symbols in the equation (4):

$\boldsymbol{x}(n)$ = $[x(n)\ x(n-1)\ \ldots\ x(n-M+1)]^T$, input data.

Equation (4) is referred to as the LMS recursion. It suggests a simple procedure for recursive adaptation of the filter coefficients after the arrival of every new input sample, $\boldsymbol{x}(n)$, and its corresponding desired output sample, $d(n)$. Equations (1), (2) a (4) specify the three steps required to complete each iteration of the LMS algorithm. Equation (1) is referred to as filtering. It is performed to obtain the filter output. Equation (2) is used to calculate the estimation error $e(n)$. Equation (4) is the tap weight adaptation recursion.[1]

2.1 Describe of calculate the optimum tap weight vector w_o

In the event of the input, $\boldsymbol{x}(n)$, and its desired output, $d(n)$, are assumed to be real-valued stationary processes. In that case the optimum tap-weight vector, $\boldsymbol{w}_0$, of the transversal Wiener filter is fixed and can be obtained according to the Wiener-Hopf equation (5). The filter tap weights, w_0, w_1, … w_{M-1}, are also assumed to be real-valued. After calculate the optimum tap weight vector $\boldsymbol{w}_o$ is Wiener filter set and we can use $\boldsymbol{w}_o$ for calculate minimum mean square error.

$$\boldsymbol{R}\boldsymbol{w}_0 = \boldsymbol{p} \tag{5}$$

Meaning of symbols in the equation (5):

p denotes Mx1 cross correlation vector of input signal $\boldsymbol{x}(n)$ and desired signal $d(n)$.

$$\boldsymbol{p} = \mathrm{E}[\boldsymbol{x}(n)d(n)] = [p_0 p_1 \cdots p_{M-1}] \tag{6}$$

E [ ] denotes statistical expectation,
R denotes M x M autocorrelation matrix of input signal $\boldsymbol{x}(n)$.

$$\boldsymbol{R} = \mathrm{E}[\boldsymbol{x}(n)\boldsymbol{x}^T(n)] \tag{7}$$

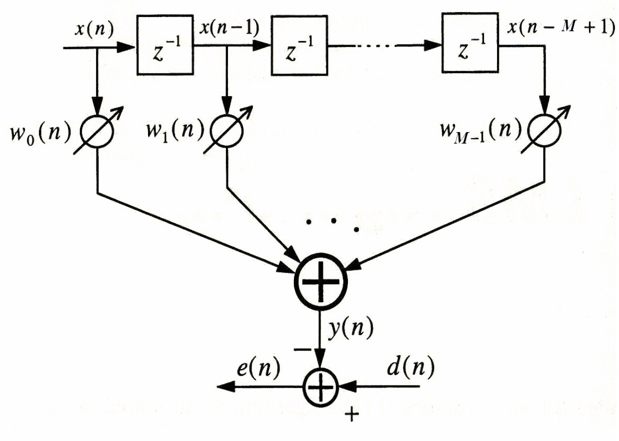

Fig. 1. An M – tap transversal adaptive filter

3 Implementation the LMS algorithm in MATLAB

The algorithm defined by (1), (2), (4) constitute the adaptive LMS algorithm. The LMS algorithm at each iteration requires that $\boldsymbol{x}(n)$, $d(n)$ a $\boldsymbol{w}(n)$ are known. The algorithm is a stochastic gradient algorithm, because input signal $\boldsymbol{x}(n)$ is a stochastic process. An FIR adaptive filter realization is shown in Figure 3. Figure 4. shows the block-diagram representation of the LMS filter. Table 1. presents the LMS algorithm.[2]

For setting up M and μ I used recommendation values at [6]. Figure 5a. shows input signal to adaptive filter $\boldsymbol{x}(n) = d(n)$ + white noise. Figure 5b. depicts desired signal $d(n)$ of speech signal separate word “jeden”. Figure 2a. depicts the optimum tap weight vector $\boldsymbol{w}_0$ of Wiener filter accordance with Wiener – Hopf equation for M= 32 and Figure 2b. is vector $\boldsymbol{w}_0$ for M=128.

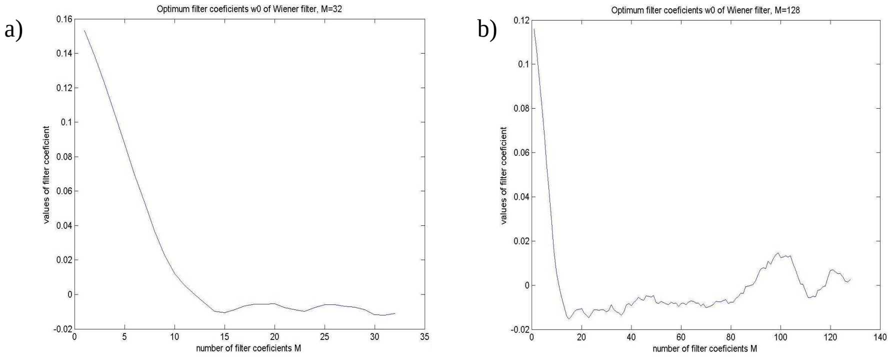

Fig.2. The optimum tap weight vector $\boldsymbol{w}_0$ of Wiener – Hopf equation for a) M=32, b) M=128

Table 1. The LMS Algorithm for an M = 32, M = 128 – Order FIR Adaptive Filter

Inputs:	M = filter length (32,128), values were chosen accordance with [6], μ = step size factor (0,75; 0,125), values were chosen accordance with [6], $\boldsymbol{x}(n)$ = input signal to the adaptive filter (speech signal of czech word “jeden” + additive white noise), $\boldsymbol{w}(0)$ initialization filter vector a) $\boldsymbol{w}(0) = 0$, b) $\boldsymbol{w}(0) = \boldsymbol{w}_0$ (the optimum tap weight vector).
Outputs:	$y(n) = \boldsymbol{w}^T(n)\boldsymbol{x}(n)$, adaptive filter output, $e(n) = d(n) - y(n)$, error estimation, $\boldsymbol{w}(n+1) = \boldsymbol{w}(n) + 2\mu e(n)\,\boldsymbol{x}(n)$, Tap weight vector adaptation.

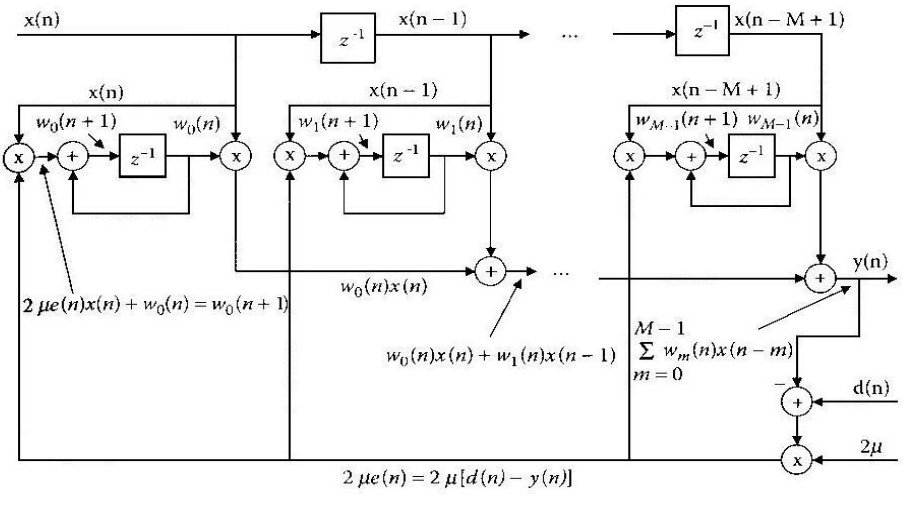
x(n)
z^{-1}
x(n − 1)
...
z^{-1}
x(n − M + 1)
x(n)
$w_0(n+1)$
$w_0(n)$
x(n − 1)
$w_1(n+1)$
$w_1(n)$
x(n − M + 1)
$w_{M-1}(n+1)$
$w_{M-1}(n)$
x
+
z^{-1}
y(n)
$w_0(n)x(n)$
...
$2\mu e(n)x(n) + w_0(n) = w_0(n+1)$
$w_0(n)x(n) + w_1(n)x(n-1)$
$\sum_{m=0}^{M-1} w_m(n)x(n-m)$
−
d(n)
2μ
$2\mu e(n) = 2\mu[d(n) - y(n)]$

Fig.3. FIR LMS filter realization

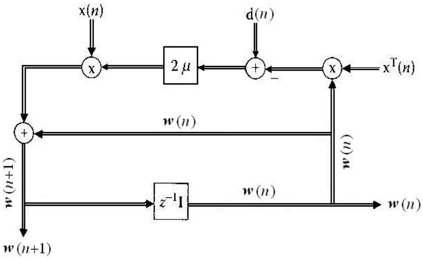

Fig. 4. Block diagram of the LMS algorithm

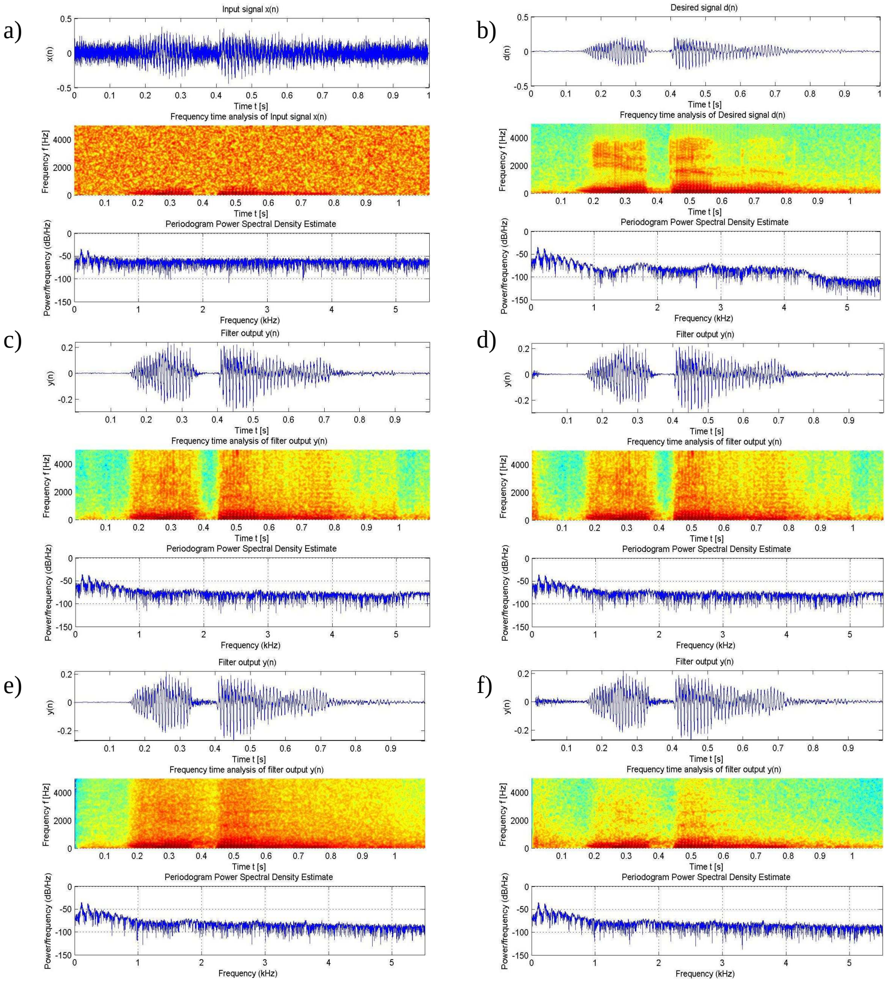

Fig.5. Waveform, spectrogram (frequency time analysis) and periodogram power spectral density estimate of a) input signal $\boldsymbol{x}(n)$, b) desired signal $d(n)$ and output signal y(n) for adjustment conditions: c) $M = 32$, $\mu = 0{,}75$ and $\boldsymbol{w}_0(n) = 0$, d) $M = 32$, $\mu = 0{,}75$ and $\boldsymbol{w}_0(n) = \boldsymbol{w}_0$, e) $M = 128$, $\mu = 0{,}125$ and $\boldsymbol{w}_0(n) = 0$, f) $M = 128$, $\mu = 0{,}125$ and $\boldsymbol{w}_0(n) = \boldsymbol{w}_0$

4 Conclusion

Optimal speech signal processing of adaptive filter with LMS algorithm is biased in this test by setting up order of adaptive filter M, step size factor μ and setting up initial conditions of tap weight vector adaptation.

For $M = 128$, $\mu = 0{,}125$ and $\mathbf{w}_0(n) = 0$ is output signal $y(n)$ distortion (it is shown in Figure 5e.) and is not possible exactly recognize single speech sound of word „jeden“ [8].

For $M = 128$, $\mu = 0{,}125$ and $\mathbf{w}_0(n) = \mathbf{w}_0$ is muting energy of speech output signal $y(n)$ of high frequency (it is shown in Figure 5f.). In time $t = 0$ - 0,1s is additive interfering signal.

Figure 5c. and 5d. shows, that processing speech signal $y(n)$ is better for recognize single speech sound of word „jeden“ (for conditions 5c) $M = 32$, $\mu = 0{,}75$ and $\mathbf{w}_0(n) = 0$ and 5d) $M = 32$, $\mu = 0{,}75$ and $\mathbf{w}_0(n) = \mathbf{w}_0$).

At the end I would resume, that initial conditions of tap weight vector adaptation with $\mathbf{w}_0$ has better characteristics output speech signal $y(n)$ for higher adaptive filter length $M = 128$.

References

1. Farhang – Borounjeny B.: Adaptive Filters, Theory and applications, John Wiley & Sons, Chichester, 2005, str. 139 - 200
2. Poularikas D. A., Ramadan M. Z.: Adaptive filtering primer with MATLAB, Taylor & Francis Group, 2006
3. Davídek V, Sovka P.: Číslicové zpracování signálů a implementace, ediční středisko ČVUT, Praha, 1999
4. Jan J.: Číslicová filtrace, analýza a restaurace signálů, nakladatelství VUTIUM, Brno, 2002, ISBN 80-214-1558-4 (2. uprav. vydání)
5. Uhlíř J. Sovka P.: Čislicové zpracování signálů, Vydavatelství ČVUT, Praha 1995
6. Smékal Z., Sysel P. Signálové procesory, nakladatelství Sdělovací technika, Praha 2006, ISBN 80-86645-08-8
7. Vaňuš J., Kolář V.: Použití signálového procesoru TMS320C50 pro adaptivní potlačení šumu řečového signálu, Sborník konference SEKEL 2006, ISBN 80-8070-584-4
8. Vaňuš J., Kolář V.: Zpracování řečového signálu v časové oblasti, Sborník konference SEKEL 2006, ISBN 80-8070-584-4

Using FPGA Technology in Medical Diagnostic Ultrasonography

Petr Žůrek

Department of Measurement and Control, FEECS,
VŠB – Technical University of Ostrava, 17. listopadu 15, 708 33 Ostrava – Poruba
`petr.zurek.fei@vsb.cz`

Abstract. The ultrasound is the most practical and the most considerate method of the examining in this time. It is using in the examining of tender tissues in the organism. The output of these examines can be various types of visual representations. The individual parts of tissues and blood vessels are represented by the B-mode ultrasound representation. D-mode ultrasound representation is using for the representation of the bloody values. This mode is operating on the dependence of the Doppler Effect principal. There is the possibility of using FPGA technology to make the results of acquired signal from the ultrasound. This technology is allowing realizing constituted proposal with the VHDL programmer language. This work continues the information about the Doppler sound processing in the ultrasonography, basic information about using the FPGA technology, the proposal and results of realization of the sound processing with developmental Xtreme DSP kit with FPGA Virtex II-Pro

1 Introduction

Diagnostic ultrasound devices have not any bad effects for the patient, if you observe the maximally power levels of radiated signal (stay in power case). The advantage of this method is that the doctor is in the first hand contact with the patient.

Only the ultrasound diagnostic devices with the special function called D-mode can put information about the blood flowing inside the body. It is made by using the Doppler's effect principal.

We can process the signal from the ultrasonic probe not only in the ultrasonic device, but also by using FPGA technology-technology of field programmable gate array. The advantage of using this technology is to use very good property of hardware for implementation developed software, and the possibility of using very good and easy hardware control, when we use JTAG cosimulation.

There is not moving only blood in the researched tissue just in the moment. There are much more moving elements, etc. soft tissues, which transmit the heart frequency. This process affects the dopllers measured signal. To eliminate these disturbing signals should be used the wall filter. The maximum limit for the transmission is from 25 Hz to 1500 Hz for this filter.

The information about the frequency drifts are modulates into the received signal with using the QAM modulation.

© Václav Snášel (Ed.): WOFEX 2007, pp. 231–236, ISBN 978-80-248-1571-8.
VŠB – Technical University of Ostrava, FEECS, 2007.

To process the information signal from the ultrasound we need the signals, which give us information about:

- the Begin of frame (BOF)
- the Begin of sampling links (BDRPT)
- the type of mode, which is used (switching between D-mode and B-mode) (DENABLE)

For this application is possible to use signal from the F/E (front/end) block of ultrasound device (Fig. 1).

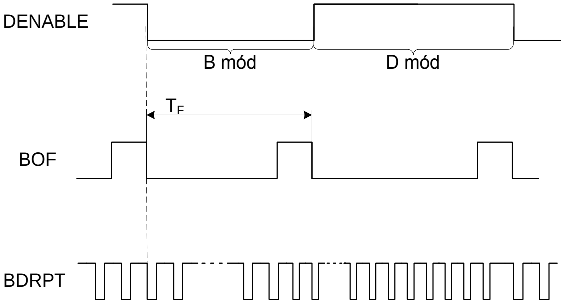

Fig. 1: Synchronization signals

Hardware, which we use, is Xtreme DSP development kit. This kit has two A/D and two D/A convectors. This dual channel high performance ADCs and DACs, as well as the user programmable Virtex-II device are ideal to implement high performance signal. The core of this module is Virtex-II Pro User FPGA: XC2VP30-4FF1152

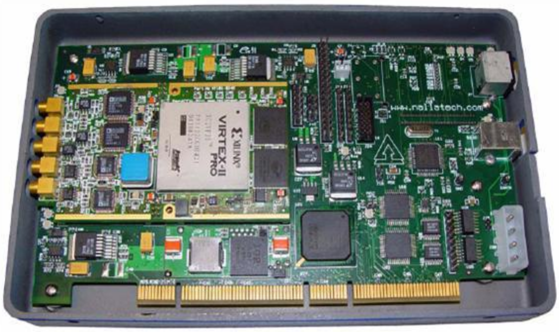

Fig. 2: Xtreme DSP development kit

For the development of the software and configuration of the hardware we can use various type of software. The System Generator software is created for using with Matlab Simulink software is implemented in it as library files, which provides the possibility to make and simulate the designed concept in the same time. System Generator can compile the concept to the various formats. [1], [2], [5]

2 Project signal processing

The signal from the F/E block of the ultrasound device is used for the processing. This signal contains the information about the Doppler frequency drift. We must adjust this signal before processing in the kit, because these signals have too high amplitude for the A/D convectors in the kit. The amplitude is changing in the dependence of the attenuation of the tissues whichever the signal is coming through. The resistance of the tissue has exponential course. So we developed special amplifier. Amplification of this amplifier is changing in the time and it is synchronising with the ultrasound transmitter is through the D/A convector. For the picking the synchronization impulses from the ultrasound device, the digital I/O bus on the kit, used is. This signal must be also modificated for the kit, because the I/O buses interface support 3, 3 V logic. The ultrasound device use 5V logic.

For connecting the kit with the computer we used the JTAG cosimulation. This connection between the kit and PC is made with the USB and also with the JTAG interface. Than these two devices can work in the loop. We can control the process and in the same time we can have background control of this process. This connection is used only for development and testing the application, not for transmission of the dates to the PC.

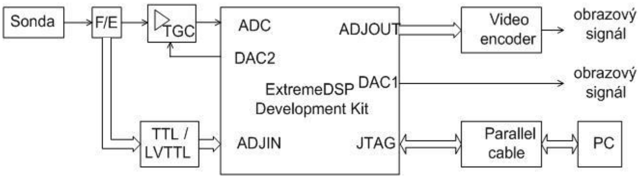

Fig. 3: Conecting FGA and ultrasound device

3 Developed software

The whole transmission chain was developed with the help of Matlab 7.0.1 with the System Generator toolbox upgrade. The block of The Xilinx Blockset, Xilinx Reference and the library of Xilinx XtremeDSP kit toolbox were used as the elementary blocks.

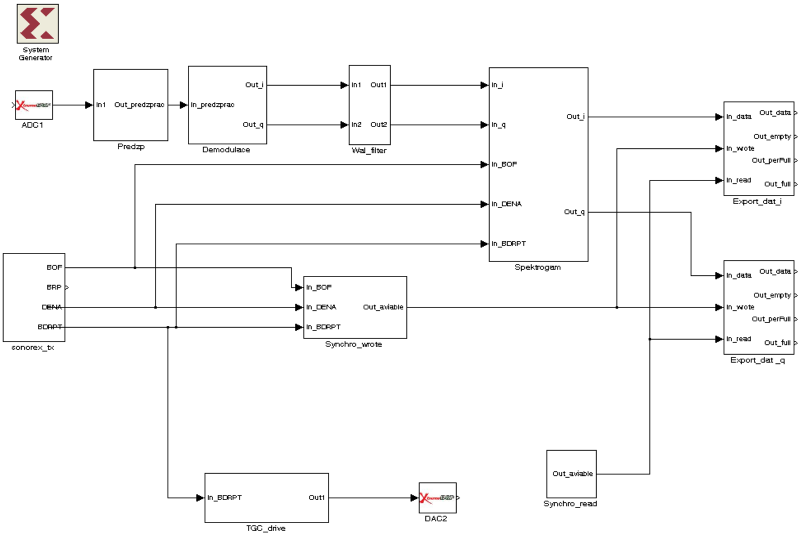
System Generator
ADC1
In1
Out_predzprac
Predzp
In_predzprac
Out_i
Out_q
Demodulace
In1
Out1
In2
Out2
Wal_filter
In_i
In_q
In_BOF
In_DENA
In_BDRPT
Out_i
Out_q
Spektogam
In_data
Out_data
Out_empty
In_wote
Out_perFull
In_read
Out_full
Export_dat_i
In_data
Out_data
Out_empty
In_wote
Out_perFull
In_read
Out_full
Export_dat _q
BOF
BRP
DENA
BDRPT
sonorex_tx
In_BOF
In_DENA
In_BDRPT
Out_aviable
Synchro_wrote
Out_aviable
Synchro_read
In_BDRPT
Out1
TGC_drive
DAC2

Fig. 4: Scheme of designed system for process ultrasound signal

The input signal contains the DC component, which must be removed from the signal before the next processing. In the input to Pre-processing signal block is the sample signal, which is in fix 14_13 form from the A/D convector. This signal is going to the FIR filter. This filter is set as a band-pass filter with the pass from 7-8 MHz adjust for 7, 5 MHz, which is the carrier frequency of the ultrasound device. This frequency is changed with the using probe. The sampling rate in this case is the same as a sampling rate of the A/D convector 40MHz in a fact. The filtration with the window type Kaiser with the 16 coefficients was used for. The coefficients are set with the help of the FDA Tool.

The input nonmodulated signal is getting into subsystem Signal demodulation, where is separated into the two directions. Both signals are sending to the same blocks Multi ii_ (qq). In these blocks there are the signals multiple with the signal, which has the same frequency as a carrier signal.

There are some low-pass filters. The cutting frequency of these filters are calculated in accordance with the maximally phase drifts of Doppler signals define with the Nyqusit limit. These frequencies are in rank about kHz and the sampling rate is 40 MHZ.

The block entrance called Out_i matches nonmodulated inphase component part of the input signal and the signal on the Out_q output matches quadratur component part of the signal.

The Block Wall_filter removes aliasing signals from the inform signal. These signals are from the moving parts of the body. This block is developed as a low-pass filter. The cutting frequency of this filter could be changed by the wishes of user.

Subsystem Spektrum contains blocks for the processing of encoding signal and getting out information about spectrum of signal. We make FFT of signal. On the output of this block we have two parts of signal-separately spectrum of inphase part of signal and quadrature part. Inphase part of spectrum gives information about forward direction of the blood flowing and the quadrature part of spectrum gives information about the backward direction.

At the end of the processing chain is block which contains the stored dates for the next step-for visualization.

The FIFO memory blocks are two for each part of signal. The synchronization of this procedure is one of the most important parts. This block has to be synchronization whit the signal, whose index begins of the active link for each frame in each mode. The same one must be prepared for reading from this block

The subsystem for the control of the module of TGC amplifier

The module of external TGC amplifier is directs to eliminate the decrement of the tissue in every moment. The amplitude of the signal must not ever be higher than maximum value for the A/D converter.

This amplification is changing in dependence of the depth of tissue, from which came the measure signal. The controlled signal of this module is signal, which gives information about the begin of vertical links.

Physically is the controlled signal transmits to the module via D/A convector. The convector converts the signal from the bit word to the analogy signal. On the module we use AD602 amplifier, which is controlled with analogy signal.

The testing results are on figure 5. [3], [4], [6], [7], [8]

4 The Conclusion

The whole system was tested continuously during the project. Each of subsystem was tested with simulated signals from Matlab Simulink and than with the signals from the ultrasound device.

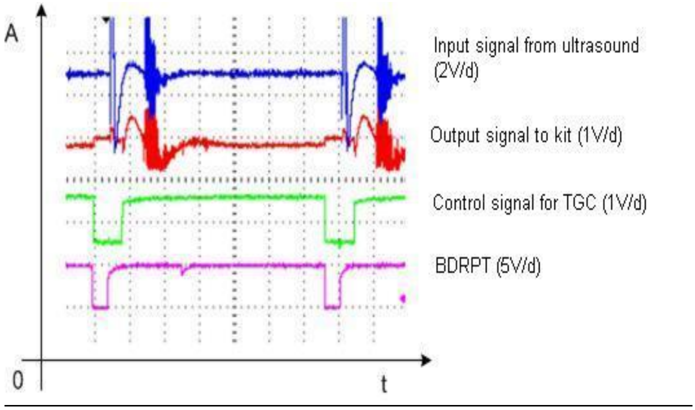

Fig. 5: Signals processed on TGC amplifier

TGC amplifier module was tested with the simulations signals from the generator at first and after that was tested with the original signals. The output information dates are saving to the FIFO memory and they are prepared to the visualization, which is the next step of this work.

The possibility of transition the dates to PC via JTAG connections was tested too. But this connection is prepared for testing and control the system only. The connection was not as fast as was required. And the speed of connections is changing according to the loading of the system.

5 Acknowledgement

This work was solving on the VSB Technical University of Ostrava, Czech Republic. This work was supported in part by the Grant Agency of Czech Republic under Grant 102/05/0467, Architectures of embedded system networks.

References

1. Zuna, I., Poušek, L., *Úvod do zobrazovacích metod v lékařské diagnostice.* Dotisk prvního vydání. Praha: ČVUT, 2002.
2. Eliáš, P., Žižka, J., *Dopplerovská ultrasonografie* Nucleus, Hradec Králové, 1998
3. Xilinx online <http://www.xilinx.com>.
4. Texas Instruments online <http://www.ti.com>.
5. Analog Devices online <http>//www.an.com>
6. *Přednášky k předmětu Lékařská přístrojová technika I.*, VŠB-TU Ostrava
7. *SonoAce 4800HD Operation manual,* Medison 1994 – technická dokumentace
8. Nallatech online < http>//www.nallatech.com>

An Indexing Approaches to Efficient Processing XPath Queries

Radim Bača, Michal Krátký, Václav Snášel

Department of Computer Science, FEECS,
VŠB – Technical University of Ostrava, 17. listopadu 15, 708 33 Ostrava – Poruba
{`radim.baca,michal.kratky,vaclav.snasel`}`@vsb.cz`

Abstract. XML (Extensible Mark-up Language) has been embraced as a new approach to data modeling. Nowadays, more information are formated as semi-structured data, e.g. articles in a digital library, documents on the web and so on. Implementation of an efficient system enabling storage and querying of XML documents requires development of new techniques. The indexing of an XML document is enabled by providing an efficient evaluation of a user query. XML query languages, like XPath or XQuery, apply a form of path expressions for composing more general queries. The evaluation process of regular path expressions is not efficient enough using the current approaches to indexing XML data. Comparison with MS SQL Server 2005 shows that our path-based method can overcome commercial product in more than order of magnitude.

Keywords: compression scheme, compression method, multi-dimensional data structures, R-tree

1 Introduction

In recent years, many approaches to indexing XML data have appeared. There are holistic approaches giving good results for XPath queries without content-based predicates [1, 11, 8]. Basic principles of wider support of XPath queries was outlined in works [10, 16, 15] based on *structural joins*. These works evaluate every node of XML query pattern and then results are joined together by structural join. Query execution time grows with number of nodes in a query pattern.

However, there are also different approaches to XML query processing which are not based on nodes in XML query pattern, but on paths [2]. Handling the paths during the query processing can have some advantages. If the `a/b/c//e/f/g` simple-path query is considered, then the query is evaluated by five structural joins. The evaluation can be very inefficient compared to path-based [12, 9] approaches which can perform these queries by finding matched labeled paths, which is a very small problem, and then find relevant nodes with a single index search [12]. Since there is significantly lower number of labeled paths

© Václav Snášel (Ed.): WOFEX 2007, pp. 237–242, ISBN 978-80-248-1571-8.
VŠB – Technical University of Ostrava, FEECS, 2007.

than nodes in an XML document, the search can be performed very quickly. When we have the set of matched labeled paths we can finish the simple-path query process only by finding the nodes corresponding to those labeled paths in an inverted list.

We explored the features of path-based approaches and we developed and implemented two path-based approaches [7, 9] and compared them with MS SQL 2005 on the 1 GB XMARK XML document. Our first approach (MDX) is based on multi-dimensional data structures and we also tested the dynamic compression of this structure [6, 4], which lead to significant index reduction with slight execution query time improvement. The second solution (PBX) is based on the work [9]. It employs the dewey labeling scheme for better support of updates and it is based only on inverted list.

2 A Model

2.1 A Model of an XML document

Let $\mathbb{X}.Tree$ be the XML tree of an $\mathbb{X}$ XML document. A path, p, is a sequence $(n_0, n_1, \ldots, n_l)$ of nodes from the root node to a leaf. The length of the path is l. For each p path, there is a labelled path as a sequence of $(t_0, t_1, \ldots, t_l)$, where $t_i, 0 \leq i \leq l$, is the tag of n_i. Let us consider the *lp* attribute of the p path including the labelled path and the unique *lpnumber* number of this labeled path. There are differences between path-based approaches. For a content-based query, some path-based approaches [7, 9] include a string value, an element content or an attribute value of the last element to each path. Let $\mathbb{X}.P$ be a set of all root-to-leaf paths in an $\mathbb{X}.Tree$. Let $\mathbb{X}.LP$ be a set of all labelled root-to-leaf paths in an $\mathbb{X}.Tree$.

There is many ways how to label nodes in the XML tree. The Figure 2 shows three different labeling schemes. We tested dewey and global labeling, where the label (vector) is path p from root to node. Dewey labeling is more suitable for updates, but global labeling should be faster during query processing. The interval labeling scheme is widely used by methods based on structural joins and can not be applied on path-based query execution scheme described in Section 3.

2.2 Path-based Indexes

Even though our two path-based approaches are different they share *term index* and *labeled paths index*. The term index only map the string values into numbers for easier handling of labeled paths. The labeled path index store the $\mathbb{X}.LP$ and map every labeled path to its *lpnumber*. Due to the fact, that the number of labeled paths is usually much smaller than the number of paths, this index can be implemented only by sequential search.

The major difference between our path-based approaches is in path index which store the $\mathbb{X}.P$. The MDX concatenate *p.lpnumber*, p and content value of the node. The result is a vector for every leaf node of $\mathbb{X}.Tree$, which is stored in

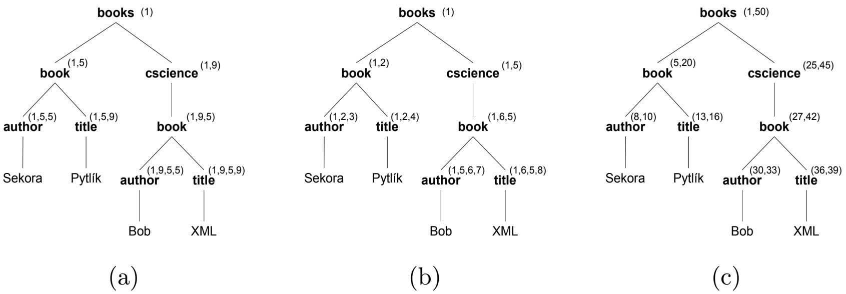
books (1)
book (1,5)
cscience (1,9)
author (1,5,5)
title (1,5,9)
book (1,9,5)
Sekora
Pytlík
author (1,9,5,5)
title (1,9,5,9)
Bob
XML
(a)
books (1)
book (1,2)
cscience (1,5)
author (1,2,3)
title (1,2,4)
book (1,6,5)
Sekora
Pytlík
author (1,5,6,7)
title (1,6,5,8)
Bob
XML
(b)
books (1,50)
book (5,20)
cscience (25,45)
author (8,10)
title (13,16)
book (27,42)
Sekora
Pytlík
author (30,33)
title (36,39)
Bob
XML
(c)

Fig. 1. Labeling schemes (a) Dewey (b) Global (c) Interval

a R-tree. Since the vectors have variable length they are stored in a forest of R-trees. The PBX store the same information in two indexes called the path index and the element index. The path index is inverted list where key is concatenated numbers *p.lpnumber* and content value of the node and *p* is unindexed value in leaf records of inverted list. The element index is very similar to DATAPATH index described in a work [9], only headId is not number but the whole dewey.

The PBX has to has two indexes to have the same functionality as a MDX with one R-tree forest, therefore, the MDX has lower space complexity. However, the PBX has often lower query time evaluation as we can see in Section 5.

3 XPath Query Execution

Firstly, we decompose the query pattern into query paths. For example XPath query $Q1$ $/books//book[author =' Bob']/title$ can be decomposed into two query paths $/books//book/author$ and $/books//book/title$. These query paths are searched in a labeled path index. We find two labeled paths for the first query path $(books, book, author)$ and $(books, cscience, book, author)$ and two labeled paths for the second query path $(books, book, title)$ and $(books, cscience, book, title)$. We get the *lpnumbers* of this labeled paths and these numbers are used for searching relevant nodes in the path index.

This query processing gives very good results for query pattern with one query path, because we only find the *lpnumbers* and then we resolve the result by few queries over path index. As we show in Section 5 even query paterns with more than one query path are resolved very quickly. We only have to join the intermediate results together.

4 Future work

The indexes described above provides two possible ways of the processing of the query pattern over the path index. One solution is to resolve the nodes of every labeled path only with knowledge *lpnumbers* and than to join the results together. However, this approach can lead to unnecessary handling of

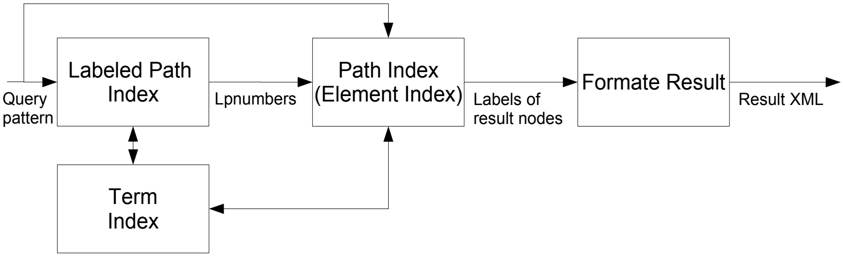

Fig. 2. Query plan

large intermediate results. The second approach firstly resolve nodes of one query path and then resolve other query path with usage of previous results and with corresponding *lpnumber*. This is possible in the case of MDX, because the whole nodes vectors are indexed. In the case of PBX the element index provides such functionality.

Suitability of each way of processing is dependent on a query. There are cases when the first approach is more efficient than the second one and vice versa. Also order of query path processing can have significant influence on a query time evaluation. These aspects lead us to develop the query plan which can help us to optimize the query processing [5]. The query plan is based on a estimation of a query path result size. This help us to choose a query path which is processed first and then decide which way of processing should be applied.

We also made some experiments with R-tree compression utilizing the fibonacci compression to reduce the path index size in the case of MDX. We achieved average compression ratio about 25% of the original index, but the speed of query was much worse then in the case of uncompressed R-tree [6]. We identified the speed of the fibonacci decompression as a botleneck and we developed the fast fibonacci decompression algorithm [3, 14]. This algorithm is so fast that queries are even faster in a case of compressed index then in a case of uncompressed index, because we save some time with lower number of I/O opperations.

5 Experimental Results

In our experiments[2], we test the XMARK collection [13] with the factor 10. The collection contains one file, 1.1 GB in size. It includes 20,828,540 elements. Characteristics of both MDX and PBX indices are put forward in Table 1.

We compared the query time of PBX and MDX with MS SQL Server 2005 on the queries in the table 2. Every query was processed twice and we have chosen the better result. We can see that the results of our approaches are significantly better. This is due to the fact that MS SQL Server 2005 use structural joins for the query execution and the intermediate results are quite high even though the result can be very small.

---

[2] The experiments were executed on an Intel Pentium ®4 2.4Ghz, 1GB DDR400, under Windows XP.

Table 1. Characteristics of indices

Approach	**Path Index**	**Element Index**	**Labeled-Path Index**	**Term Index**
PBX	797 MB	3.5 GB	66 KB	268 MB
MDX	1.7 GB		66 KB	268 MB

Table 2. XPath queries evaluated in our experiments

Query	**XPath query**	**Query size**
$\mathbb{Q}_1$	`site/regions/namerica/item[mailbox/mail/to= 'Cort Penn mailto:Penn@uic.edu']/location`	1
$\mathbb{Q}_2$	`site/regions/namerica/item[location='United States' and mailbox/mail/to='Cort Penn mailto:Penn@uic.edu']/name`	1
$\mathbb{Q}_3$	`site/regions/namerica/item[quantity='1' and location='United States' and payment='Money order']/name`	4,637
$\mathbb{Q}_4$	`site/open_auctions/open_auction[quantity='1' and bidder/increase='3.00' and type='Regular']/@id`	16,972
$\mathbb{Q}_5$	`site/regions/namerica/item[location='Thailand']/ name`	108
$\mathbb{Q}_6$	`site/regions/namerica/item[location='United States']/name`	74,917

Query	**Time [s]**		
	PBX	**MDX**	**MS SQL Server 2005**
$\mathbb{Q}_1$	0.07	0.032	103
$\mathbb{Q}_2$	0.07	0.032	131
$\mathbb{Q}_3$	2.01	2.8	162
$\mathbb{Q}_4$	7.9	8.5	321
$\mathbb{Q}_5$	0.07	0.04	102
$\mathbb{Q}_6$	4.4	6.8	107
Avg.	**2.44**	**3.14**	**154.3**

6 Conclusion

In this article, we briefly outline bath-based approaches, which we implemented. We also show the comparison, where our solution outperform MS SQL Server

2005 in more than order of magnitude. We also developed a query plan, which tries to find good query plan to achieve optimal query performance. Another issue was index compression, which lead to 25% size of original index with preserving query performance.

References

1. S. Al-Khalifa, H. V. Jagadish, and N. Koudas. Structural Joins: A Primitive for Efficient XML Query Pattern Matching. In *Proceedings of ICDE'02*, 2002.
2. R. Bača and M. Krátký. Indexing XML Data The State of the Art. In *Proceedings of ITAT conference, Slovakia*, 2007.
3. R. Bača, M. Krátký, J. Platoš, E. El-Qawasmeh, and V. Snášel. The fast fibonacci decompression algorithm. In *Submitted in Software Practise and Experience Journal.* Wiley, 2007.
4. R. Bača, M. Krátký, and V. Snášel. A Compression Scheme for the R-tree Data Structure. In *Proceedings of ITAT conference, Slovakia*, 2006.
5. R. Bača, M. Krátký, and V. Snášel. An Efficient Path-join for Twig Content-based Queries of XML Data. In *Submitted at 9th ACM International Workshop on Web Information and Data Management (WIDM)*, 2007.
6. R. Bača, M. Krátký, and V. Snášel. Evaluation of Multidimensional Approach to Indexing XML data with Compressed R-trees. In *Proceedings of the ZNALOSTI conference.* Technical University of Ostrava, Czech Republic, January 2007.
7. R. Bača, M. Krátký, and V. Snášel. On the efficient processing regular path expressions of an enormous volume xml data. In *Proceedings of DEXA 2007*, LNCS. Springer–Verlag, September 2007.
8. S. Chen, H.-G. Li, J. Tatemura, W.-P. Hsiung, D. Agrawal, and K. S. Candan. Twig2stack: bottom-up processing of generalized-tree-pattern queries over xml documents. In *Proceedings of VLDB'2006*, pages 283–294. VLDB Endowment, 2006.
9. Z. Chen, G. Korn, F. Koudas, N. Shanmugasundaram, and J. Srivastava. Index Structures for Matching XML Twigs Using Relational Query Processors. In *Proceedings of ICDE'05*, pages 1273–1273. IEEE Computer Society, 2005.
10. T. Grust. Accelerating XPath Location Steps. In *Proceedings of the 2002 ACM SIGMOD, Madison, USA.* ACM Press, June 4-6, 2002.
11. H. Jiang, H. Lu, W. Wang, and B. Ooi. XR-Tree: Indexing XML Data for Efficient Structural Join. In *Proceedings of ICDE, 2003, India.* IEEE, 2003.
12. T. S. M. Yoshikawa, T.Amagasa and S. Uemura. Xrel: a path-based approach to storage and retrieval of xml documents using relational databases. *ACM Trans. Inter. Tech.*, 1(1):110–141, 2001.
13. A. R. Schmidt and at al. The XML Benchmark. Technical Report INS-R0103, CWI, The Netherlands, April, 2001, `http://monetdb.cwi.nl/xml/`.
14. V. Snášel, R. Bača, M. Krátký, and J. Platoš. An Implementation of Fast Fibonacci Coding. Technical Report ARG-TR-01-2007, Amphora Research Group (ARG), Department of Computer Science, VŠB–Technical University of Ostrava, 2007, `http://www.cs.vsb.cz/arg/techreports/ffibonacci.pdf`.
15. I. Tatarinov and at al. Storing and querying ordered XML using a relational database system. In *Proceedings of the ACM SIGMOD 2002*, pages 204–215, New York, NY, USA, 2002. ACM Press.
16. C. Zhang, J. Naughton, D. DeWitt, Q. Luo, and G. Lohman. On supporting containment queries in relational database management systems. In *Proceedings of the ACM SIGMOD 2001*, pages 425–436, New York, USA, 2001. ACM Press.

Parallelization of Process Functional Language

Marek Běhálek

Department of Computer Science, FEECS,
VŠB – Technical University of Ostrava, 17. listopadu 15, 708 33 Ostrava – Poruba
`marek.behalek@vsb.cz`

Abstract. Process Functional Language (PFL) was developed to integrate good properties of functional and imperative languages. PFL came out from pure functional languages and preserve their good properties. In the other hand we may define processes or use environment variables in PFL. So we can easily express structures like loops in PFL. This article focuses on a parallelization of PFL. It presents an extension of PFL for parallel programming. Article also describes different implementations of runtime environments.

Keywords: Process Functional Language, algorithmic skeletons, parallelization, Java Threads

1 Introduction

Purely functional languages are concise, composable, and extensible. They allow developing and reasoning about reliable programs using mathematical methods. The role of the state is often crucial in real systems. Expressing a state in pure functional languages (for example using monads) could be difficult and hard to understand. All advantages of pure functional approach are gone when the imperative approach is used. Process functional language was developed to integrate good properties of imperative languages and to still preserve properties of functional languages.

Programs written in some functional language are often much shorter than their imperative equivalents. In the other hand they are usually much slower when they are executed. Parallelization could improve a running performance and it also brings a new insight into properties of a programming language. This article aims to parallelization of *PFL*.

2 Process Functional Language

PFL was described in [6–9]. *PFL* is a functional language. It implements all constructions common in pure functional languages and it also preserves their semantics. Syntax comes out from functional language Haskell.

This set of constructions was extended by environment variables and processes.

© Václav Snášel (Ed.): WOFEX 2007, pp. 243–248, ISBN 978-80-248-1571-8.
VŠB – Technical University of Ostrava, FEECS, 2007.

2.1 Environment Variables in *PFL*

New unit type () was included to the *PFL*(() have another meaning in Haskell). This type represents only a control value [6].

One of the main differences between pure functional languages and *PFL* is that *PFL* uses environment variables. A usage of environment variables is bound to processes. A process application is the only place where we can access or update environment variables. The scope of environment variables is defined by the scope of processes that use them. In other words the environment variables are in the same scope as well as processes that manipulates with them.

2.2 Processes

The *PFL* processes are similar to functions from pure functional languages. The only difference is in their type definition. This definition extends syntax and semantics from pure functional type definition. Type definition of a process contains:

1. the unit type () - for an argument or a value type;
2. an argument in form `x T` - where `x` is an environment variable and `T` a data type.

Following example shows process definition.

Listing 1.1. A process in PFL

```
f :: a Int -> b Int -> Int
f x y = x + y
```

The process uses two environment variables (namely `a` and `b`). These variables are defined within the same scope as the process `f`. There is no partial process application. This approach has been chosen to simplify identification of program parts which manipulate with a state.

The process may be applied either to: control values and computed using values accessed from the environment variables; data values and computed using them (updating the environment variables by this value before).

Suppose an application (`f 3 4`) exist somewhere in an expression of a *PFL* program, such that `f` is accessible. Then the result of the application will be 7. Side effects to pure function evaluation will be update of the environment variable `a` by value 3 and update of the environment variable `b` by value 4.

Another possibility is that the argument will be a control value `()`. Assume that right after the previous process application (`f 3 4`) will be this process applied to the control value () and value 5 (`f () 5`). Then the result of the application will be 8. The value of `x` will be accessed from the environment variable `a`. Another side effect will be update of the environment variable `b` by value 5.

3 Parallel Functional Languages

Functional languages have three key properties that make them attractive for parallel programming [10].

- **Abstraction** - Functional languages have excellent mechanisms that can be applied to both computation and coordination [4]. Two important abstraction mechanisms are *function composition* and *high-order function.*
- **Elimination of unnecessary dependencies** - The absence of side-effects makes relatively straightforward to identify potential parallelism.
- **Architecture independence** - Good parallel abstractions encourage high-level portability by abstracting over lower level issues.

There are several approaches how we can parallelize functional languages. First we may extend language with constructions like threads, forks or semaphores. However the language is usually made into a strict, call by value, sequentional language to bring to these imperative futures a meaningful semantics. This makes also language dependent on low level architecture. So presented advantages and declarative nature are gone.

Parallelism is implicit in pure functional languages. Annotations for parallelism may by used but they may be viewed as hints and do not add to intellectual burden of a programmer. For example in traditional parallel programming the communication is explicit: programmer uses explicit message-passing primitives or communicates trough explicit shared variables. In parallel functional languages communication occurs as a consequence of shared data dependencies between tasks. The system automatically uses low-level mechanism to share data and automatically protects them against concurrent modification as required. When using this approach the parallelization is made by a compiler or by a run-time system or combination of both. We can use mechanisms like algorithmic skeletons or evaluation strategies for these languages.

4 Parallel Extension of PFL

Parallel extension of PFL was presented in [1, 2]. To preserve presented advantages of parallel programming from pure functional languages then some high-level mechanism must be implemented in *PFL*. For parallelization of PFL we use algorithmic skeletons [4]. This approach was extended by implementation skeletons [5].

First we extend the Process Functional Language by syntactic constructs for explicit definition of parallel tasks. Parallel task identifies a part of program that can be usefully evaluated in parallel. It is on a lower level than algorithmic skeletons but it still does not represent a low-level process. It can be realized like a process or a thread or must not even be executed in parallel at all. This decision depends on appropriate compiler (that maps tasks to a low-level architecture) and on used low-level architecture.

Functional languages distinguish between function definitions and functions applications. Similarly *PFL* offers task abstractions and task instantiations.

First we represent new polymorphic type:

```
Task a b
```

Using this new type we can define a task abstraction:

```
some_task :: Task a b
some_task = task x -> e where eqv_1 ... eqv_n
```

where type of `x` is `a` and type of `e` is `b`. Tasks could be compared to functions of type `a -> b`. Main difference is that tasks has to be evaluated in parallel. Tasks can use *PFL* processes.

Tasks are dynamically created using task instantiations. A task instantiation provides a task abstraction with actual input parameter. The process instantiation is achieved by using the predefined infix operator:

```
# :: Task a b -> a -> b
```

Each time an expression `e1 # e2` is evaluated a new task is created to evaluate the application of `e1` to `e2`. Because we use an eager evaluation in *PFL* the expression `e2` will be fully evaluated in the time of instantiation.

Presented approach is based on two basic principles: explicit process/tasks management (parallel tasks can be defined and used) and implicit communication.

Communication and synchronization mechanisms are still implicit and must be solved by a compiler or by a runtime environment.

Main difference between pure functional languages and *PFL* is that an evaluation of functions has no side effects in pure functional languages. This is not true in *PFL*. But side effects are bound to *PFL* processes. We are able to compute them using static analysis at a compile time [9, 11]. Using high order functions (algorithmic skeletons) for composition of processes does not affect this possibility. Obtained information is sufficient for an implicit synchronization mechanism.

Environment variables are normally shared between tasks. Implicit synchronization mechanism takes care of their concurrent modification and correct usage with respect to evaluation order. Within the `where` part of task's definition we may include processes definitions. Scope of these processes is bound to task and environment variables defined by them are visible only within appropriate instance. Using this approach we may define a sort of *private* variables and avoid unnecessary communication and other synchronization issues.

Now we present an implementation skeleton for a simple version of parallel map. In this example one task is created for each element of the input list `xs`. This example also describes how function `f :: a ->b` can be embedded into a task abstraction (function `mkTask`).

Listing 1.2. Simple parallel map

```
mkTask :: (a -> b) -> Task a b
mkTask f = task x -> f x

map_par1 :: (a -> b) -> [a] -> [b]
map_par1 f xs = [(mkTask f) # x |x<- xs]
```

4.1 Programming Using Parallel PFL

First we may directly use a parallel task definition in our program. Another option is that we may use an algorithmic skeleton. Typical algorithmic skeletons are functions `map` and `fold`.

In *PFL* we named them `parallel_map` and `parallel_fold`. Programmer can easily build parallel applications simply by replacing all occurrence of `map` with `parallel_map` respectively `fold` by `parallel_fold`. Parallelizing compiler can then exploit rules provided for this skeletons and produce parallelized result and thus gets programmer parallel solution with very little overhead. Another advantage of this solution is that when composing two parallel applications we should easily obtain their parallel composition. This is not true for all languages especially one with low level architecture dependencies.

Another possibility is usage of different algorithmic skeletons. Different variants for functions `map` and `fold` are defined using implementation skeletons and they are a part of basic libraries. Finally programmer may define his own algorithmic skeleton (using implementation skeleton).

5 Parallelizing compiler and runtime environment

There exists compiler to Java for *PFL*. For the experimental reasons we use this compiler and extend it to produce parallel (respectively concurrent) programs using native Java Threads and shared memory. This solution is strongly dependent on used Java Virtual Machine. In one hand Java Threads and shared memory represents a sort of bottleneck for parallelization of PFL programs, on the other hand this technology is commonly used and easy to obtain.

6 Future work

Now we are trying to use some sophisticated low-level architectures. We are especially interested in usage of MPI combined with Java. This brings us much closer to distributed computing. We must solve other problems like process placement or data distribution. The work is still in progress.

Another area of our interest is high-order processes. For parallelization of PFL we use high-order functions (algorithmic skeletons). To be able to use this method we allow a composition of processes using a high order functions. If fact now are able now to pass some process to a function or even to a parallel task. This process can access some environment variables and we can use theses variables for example for synchronization of parallel tasks.

7 Conclusions

We present our extension of *PFL* that solve parallelization on a high level of abstraction. We believe that this solution preserve advantages of parallel programming in pure functional languages and also preserve its declarative nature. Article also presents how we can use this extended language for parallel applications implementation.

References

1. M. Běhálek, P. Šaloun Paralelization of Process Functional Language. In *ECI2006*, Košice, Slovak Republic, September 2006, ISBN 80-8073-598-0.
2. M. Běhálek, P. Šaloun Parallel Process Functional Language. In *SOFSEM 2007 SRF*, Harrachov, Czech Republic, January 2007, ISBN 80-903298-9-6.
3. M. I. Cole. Algorithmic skeletons: Structured management of parallel computations. In *Research Monographs in Parallel and Distributed Computing.* Cambrige, MA: The MIT Press, 1989.
4. R. Hughes. Why functional programming matter. *The Computer Journal*, 32(2):98–107, 1989.
5. U. Klusik, R. Loogen, S. Priebe, and F. Rubio. Implementation skeletons in eden: Low-effort parallel programming. *Lecture Notes in Computer Science*, 2011:71–??, 2001.
6. J. Kollár. Process functional programming. In *33rd Spring International Conference MOSIS'99 - ISM'99*, pages 41–48, Ronov pod Radhotm, Czech Republic, April 1999.
7. J. Kollár. Comprehending loops in a process functional programming language. *Computers and AI*, 19:373–388, 2000.
8. J. Kollár and V. Novitzká. Semantical equivalence of process functional and imperative programs. *Acta Polytechnica Hungarica*, 1(2):113–124, 2004.
9. J. Kollár, J. Poruban, and P. Václavík. From Eager PFL to Lazy Haskell. *Computing and Informatics*, 1, 2006.
10. H. Loidl, F. Diez, N. Scaife, K. Hammond, U. Klusik, R. Loogen, G. Michaelson, S. Horiguchi, R. Mari, S. Priebe, A. Portillo, and P. Trinder. Comparing parallel functional languages: Programming and performance. In *Higher-order and Symbolic Computation.* Kluwer Academic Publisher, 2003.
11. J. Poruban. *Profilácia procesných funkcionálnych programov.* PhD thesis, KPI TU FEI Košice, 2004. in Slovak.
12. P. W. Trinder, K. Hammond, H.-W. Loidl, and S. L. P. Jones. Algorithms + strategy = parallelism. *Journal of Functional Programming*, 8(1):23–60, 1998.

Adaptive Mechanisms and Adaptation of Navigation in Virtual Education Environment

Marek Bober, Jana Šarmanová

Department of Computer Science, FEECS,
VŠB – Technical University of Ostrava, 17. listopadu 15, 708 33 Ostrava – Poruba
`marek.bober, jana.sarmanova@vsb.cz`

Abstract. Knowledge mining process based on logs in virtual education systems is one from many techniques, which can help to receive information for automated adaptation – selection of study materials. Target of this Article is to describe possible ways of Automated Adaptation for walk-through study materials in virtual education environment. Article describes goals and weaknesses for several adaptive algorithms in opposite to manual modification of study materials. Algorithms respect Student Activity Protocol, Study Groups and Authors for finding best available adaptation. Benefit of this solution is to simplify user orientation in study materials and growing efficiency of their education.

1 Introduction

Use of typical information systems or if you like e-learning system which offers study materials and obtaining knowledge about users from these systems in order to feedback has some constraints. Adaptive hypermedia in learning process can be used for personalization of content, navigation or presentation of information presented to users. Personalization can increase effectiveness of users learning process.

Adaptation of presentation or navigation in system depends on previous or actual knowledge of the student in system and actual student's behavior. For the preparation purpose of better learning materials personalized for user it is necessary to obtain knowledge about user behavior in the system. There are some different methods how to analyze obtained data. We can target to specific area such as course productivity, course quality, suitability of usage course, etc. [9]. Our target is to improve course by the adaptive techniques and personalization, which is backed by data analysis from protocol activities.

1.1 Adaptive hypermedia

Adaptive hypermedia allows adaptation of content, style of presentation and navigation to particular user or group of users. Advantage of use of adaptive hypermedia (not only for learning) is that they allow increasing effectiveness of the learning by the adaptation of learning material to individual user [1].

© Václav Snášel (Ed.): WOFEX 2007, pp. 249–254, ISBN 978-80-248-1571-8.
VŠB – Technical University of Ostrava, FEECS, 2007.

Adaptation in adaptive hypermedia systems is based on knowledge about content of individual pages, relationships between them and hypothesis about knowledge, preferences and other characteristics of the user [1]. Adaptive systems not only offer learning material to the user, but also collect information about user's behavior in system and based on this adapt content and style of offered materials.

Every adaptive hypermedia system is using adaptation techniques for adaptation of learning material. There are two groups of adaptation techniques – adaptation of content and adaptation of navigation. Nowadays, adaptation is often called personalization [4, 8]. Most systems working with adaptive hypermedia are based on specific model, e.g. AHA! system is based on AHAM model [4, 6].

2 Adaptive mechanisms

Adaptive mechanisms can be divided on two types: manual and automatic adaptive mechanisms.

In the first case are not adaptive mechanisms exactly. That means, all modification making authors by self depending on some analysis. One of the ordinary mechanisms is usage of statistic evaluation on the end of course. Author makes statistic evaluation and then modifies content of study materials. For example, authors want to analyze if there are differences between students behavior of full and part time students and on this base decide, if is necessary modify course separately for full time and separately for part time students. After course finishing author makes a statistic evaluation and on this based modifies content to next students. For evaluation of course can be used: statistical analysis, data analysis such as clustering or decision trees, etc.

In the second case exists some algorithms, which makes decides and modification (adaptation) based on protocol activities of user. Premise is algorithm designed for work in real time. For example, author wants to advise to user which toward a given topic is relevant other topic in study materials. Mostly, there have been related pages with specific 'relevancy' weight to understanding study material to study topic [3]. Some examples for automatic adaptation: Full Scan algorithm, mining sequential patterns, hash based algorithm, etc.

2.1 Manual and automatic adaptive mechanisms differences

Manual adaptive mechanisms (MAM) are effective after some part of time proceeding of course or on the end of course. Automatic adaptive mechanisms (AAM) can be used in real time. This is big advantage of AAM.

Modification of offered study materials in MAM makes author by self. This is time consuming. Author has to know structure of study materials mostly. AAM can modify offered study materials self. System has properties and rules for these modifications. There is no need author's knowledge of structure offered study materials.

Author or person, who wants to make manual adaptation, has to know some kinds of analysis, their usage and understanding their results. AAM have logic for data evaluation and usage of results. These results can be modified by author, if it is necessary.

AAM automatically can provide adaptation to actual user or group of users. But MAM are not possible to target to actual user in the system. It is possible target to group of users for next session, in MAM.

It is possible combine both mechanisms MAM and AAM. In a future we want to try to find new mechanisms which will be full automatic for adaptation of study materials. These mechanisms will be return results for every user exact and will be without modification of study materials by author. There are three basic algorithms for data mining and usage in adaptive environment. Because user activities in system looks like transactions in electronic shops, it is possible to use tree basic techniques for data mining: association rules mining, sequential patterns mining and traversal patterns mining.

For all algorithms is premise that system holds sessions of user and data for concrete sessions, e.g. who accessed the page, what pages were requested, how long each page was viewed, etc. On this data can be used algorithms such as clustering, classification, association rules or sequential patterns. The results of these algorithms can be used for several aspects, e.g. searching path profiles of users for predict future, predict future user behavior or offering recommended links (see next chapter).

Clustering techniques can be used for searching similar sessions based on occurrence patterns of URI references. User session can be mapped into a multidimensional space as vectors of URI references. By this can search relevant or significant features.

2.3 Algorithms for adaptation of navigation

One of the most usage techniques is base on student model [10]. Binary vector denote v represents student's knowledge where vi = 1 means that the student has successfully mastered concept (page) i, and ki = 0 means the opposite. This technique is based on session and current state of his knowledge in system. The state of variable is change by the click to link of some concept (page) and reviews the concept (page) to value 1. As the student reviews concepts, newer concepts become available. For annotation about new concepts are used colored icons [10].

Other technique appears from previous. For annotation of relevant links to concept are used colored icons with more states. This relevancy is calculated based on the threshold parameter for each concept individually.

The most technique for adaptation of navigation is based on Social Navigation Support (SNS). This technique is based on social navigation theory (Dourish & Chalmers 1994). These man define SNS as "moving towards cluster of people" or "selecting subjects others have been examining them". For example (Brusilovksy) used two type algorithms (traffic based and annotation-based) in system AnnotatEd system [7].

3 Modified results of full scan algorithm

This part describes usage of full scan (FS) algorithm for finding recommended links and our new possibilities of modification of FS algorithm results for creating recommended links. The main of target is notified to user, which has the highest weight (relevancy) of link context to specific page and made easier decision for user about relevant page reference to visit it or not. Modified results can improve orientation in hyperspace than non-modified results of FS algorithm. For modification of results we introduce pages and links relevancy weight, as you can see in next chapter. These values are necessary for modification of FS algorithm results.

3.1 Problem Description

To notify user about specific link relevancy for him and his study process, is necessary to determinate not only weight of link but weight of content offered by other page. Weight determination is not simple and all weight values should have been given to every user individually. Every user has a different style of learning and personalization is basically difficult. The next problem is occasion of author to advise which content of text are more and which less important. One of the possibilities is non automatic weights setting of pages by author. Non automatic weights setting are necessary for creation new pages. The better occasion is for example automatic (semi-automatic) setting by the ontology and modifying by the neural networks. It is subject of next research.

We can determinate several relevancy weights (WR) for all pages. For example we can use percentage valuation by displaying weights in every page. Now is possible say to user, which is the important study content for him in light of relevancy in concrete subject. The traditional case of referencing to several pages is self WR page poor. From the other one point of view can be one page more relevant (it has greater valuation) than other page for some case based on study material. There are necessary to determinate WR between the links of several pages. If page has references at each other then weights can have same or different valuation in both ways of relevancy view within actual topic. Relevancy from the one side can be different than from the other side. It is necessary set WR into links every way. Usage of weights in pages and links show figure 1.

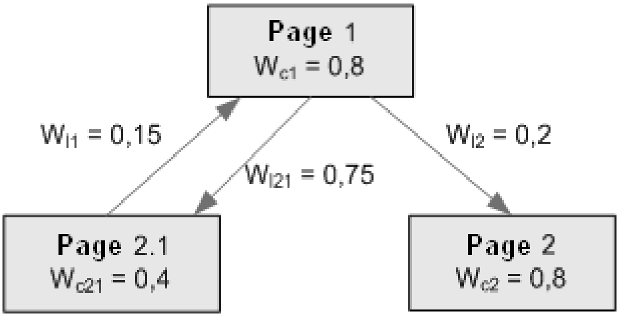

Fig. 1. Different WR for links in opposite direction

WR of hypertext links and pages can have relevancy restriction. WR can be determinate in case of summary study material, one chapter, paragraph etc. In adaptive environment system it can offer related links in ordered list by the value of weights (link recommendation), for example by the traversal pattern algorithm [5]. Recommended (related) links and the most frequently links from all users can be string together by interconnection with properties of concrete user or user group and the result is offered to concrete user or group[7].

Usage modified results of FS algorithm

Specification of FS algorithm outgoes from DHP (direct hashing and pruning) algorithm [5]. Our main idea is integrate results of FS algorithm with WR within the scope of all subject matter, and with WR of links within the scope of actual topic of concept. As a result are recommended links to pages in two categories: recommended links within the scope of all study material and recommended links within the scope of actual topic of page. Usage of FS algorithm and modified results is shown on Figure 2.

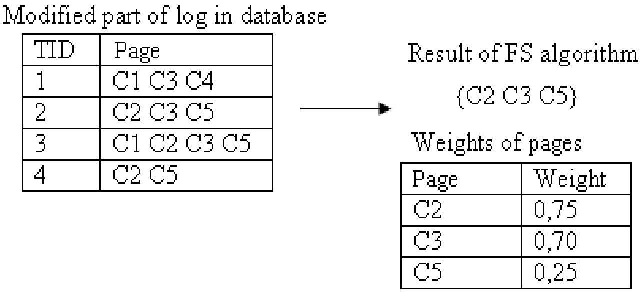

Modified part of log in database

TID	Page
1	C1 C3 C4
2	C2 C3 C5
3	C1 C2 C3 C5
4	C2 C5

Result of FS algorithm

{C2 C3 C5}

Weights of pages

Page	Weight
C2	0,75
C3	0,70
C5	0,25

Fig. 1. Results of FS algorithm

Left table in Figure 2 contains session identifier TID, and set of visited pages. Results of FS algorithm are tree qualifications for page recommendation C2, C3 and C5. System can display user links to pages. But in case of pages have WR within the scope of all study material; see right table in Figure 2, the result of algorithm can be modified. From the table we can see, that pages C2 and C3 have relevancy within the scope of all study material 'relatively big'. Page C5 has relevancy 'relatively small'. We determinate a minimum limit of relevancy within the scope of all study material, denote L and determinate value to 0,35. By applying limit LA to results of recommended pages is possible to eliminate pages, which are not relevant for link in study material.

In case of results, as shown Figure 2, are relevant recommended pages only C2 and C3. Page denoted C5 have not to be displayed. It is possible to use another technique than displaying and hiding recommended links, for example highlighting of background color. In the case of page C5 can be highlighted of other color. More information about usage modified results of FS algorithm, see [3].

We propose relevancy weights determination to every user individually. There are two possibilities. If we have on the beginning of course the entrance test, we can set the weight by the results of this test for every user individual. In case that we have not entrance test, there are next two possibilities. Set the weights for every user the same to default value (for example to 80 %) and during user sessions in systems modify these values individually. Another access is let the choose user how is fill. That means: user is thinking that know study subject very well or good or he does not know. By this decision we can determinate relevancy values for current user and in next time modified by the results of tests.

4 Conclusion

Next our works is design new adaptive mechanisms or modify the most usage mechanisms for virtual education system called Barborka. Mechanisms integration to e-learning system will offer more flexible responds to student's knowledge. The main target is offer a proposal of explanation of basic term or hyperlink to basic term explanation for student which do not understand term consists of basic term. Next target is offer more different explanations of terms based on knowledge of student. Different explanations of terms means describe terms by other definitions or use different visualization, e.g. text, picture or graph etc. All piece of knowledge about student behavior automatically store, modify and use for next student proceedings in virtual education system by the adaptive mechanisms.

References

1. Bielikova M. Tvorba obsahu v adaptivnych hypermediach pre e-vzdelavanie. Technologie pro e-vzdelavani 2004. Praha 2004. ISBN 81-01-03167-5. (in Slovak)
2. Bober M, Velart, Z. Adaptive hypermedia and PDF forms in AHA! For e-learning. Wofex 2005. Ostrava 2005. ISBN 80-248-0866-8.
3. Bober, M. and Saloun. P.: Adaptation of navigation by the modified results of full scan algorithm in adaptive hypermedia systems, ISIM 2007. ISBN 978-80-7248-006-7, pp. 111-120.
4. Brusilovsky P. Methods and Techniques of Adaptive Hypermedia, Adaptive Hypertext and Hypermedia, Kluwer Academic Publisher 1998. ISBN 0-7923-4843-5
5. M. S. Chen, J. S. Park, and P. S. Yu. Data mining forpath traversal patterns in a web environment. In Proc.of 16th Int. Conf. on Distributed Computing Systems, pp. 385-392, 1996.
6. De Bra P., Aerts A., Berden B., De Lange B., Rousseau B., Santic T., Sints D., Stash N. AHA! The Adaptive Hypermedia Architecture. ACM Hypertext Conference. Nottingham 2006.
7. Farzan R. & Brusilovsky P. (2006) AnnotatEd: A Social Navigation and Annotation Service for Web-based Educational Resources. In Proceedings of E-Learn 2006--World Conference on E-Learning in Corporate, Government, Healthcare, and Higher Education.
8. Matuskova, K., Bielikova, M.: Personalized Navigation in Open Information Space Represented by Ontology. Adaptive Hypermedia and Adaptive Web-Based System AH 2006, Springer LNCS 4018, 2006, ISBN 3-540-34696-1.
9. Mendes E., Mosley N.: Web Engineering. Springer, 2006. ISBN 3-540-28196-7.
10. Sosnovsky, S., Brusilovsky, P., and Yudelson, M. (2004) Supporting Adaptive Hypermedia Authors with Automated Content Indexing. In: Proceedings of Second International Workshop on Authoring of Adaptive and Adaptable Educational Hypermedia at the Third International Conference on Adaptive Hypermedia and Adaptive Web-Based Systems (AH'2004), Eindhoven, the Netherlands.

DSP in Image Processing - Face Detection

Petr Delong, Michal Krumnikl, Boris Polikarpov

Department of Computer Science, FEECS,
VŠB – Technical University of Ostrava, 17. listopadu 15, 708 33 Ostrava – Poruba
`petr.delong@centrum.cz, michal.krumnikl@vsb.cz, mironov@volny.cz`

Abstract. This work deals with the face detection, using directly connected camera to the signal processor Blackfin. The paper consists of description of interconnection between monochromatic camera KAC-9618 and DSP processor Blackfin BF-537 (product of Analog Devices). An algorithm of face detection and algorithm for communication between the camera and DSP are also included. The first of them is based on using the back–propagation neural network. The camera is controlled over I2C serial bus. In addition, there is an overview of used neural network.

Keywords: Blackfin, DSP, Face detection, I2C, Neural network, training set

1 Introduction

The main goal of this work is to design interconnection between DSP Blackfin BF–537 and the camera, which was mentioned above. The connection was realized without any auxiliary components. The next part consists of the software solution of this interconnection, neural network design, and the verification of implemented algorithms. We aimed at using DSP processors in the field of image processing. In contrast to general purpose processors, the main advantage of digital signal processors are fast vector computation blocks and arithmetic units designed for processing digital signals. Moreover these processors are less demanding on power source.

2 Camera Interface

The camera is connected to Blackfin BF–537 development kit through PPI interface. All pins of camera are directly connected to the DSP (by using PF and PG ports), except for the MCLK pin, which is connected to the external oscillator with required frequency. The oscillator is the only additional part needed for the interconnection, because the DSP board does not provide suitable clock source for the camera. It is necessary to connect SCLK and SDA pins of the camera with appropriate pins on the PPI interface in order to exploit the hardware implementation of I2C bus on the chip. It is not necessary to use an external power source because we can use the power source provided by PPI, which is sufficient for driving the camera. Camera data (D0-D11) and control (HSYNC, VSYNC,

© Václav Snášel (Ed.): WOFEX 2007, pp. 255–260, ISBN 978-80-248-1571-8.
VŠB – Technical University of Ostrava, FEECS, 2007.

PCLK) lines are accessible through PF and PG ports. It is important to connect matching pins of camera and DSP by software routines.

The camera provides several modes of operations. In our application we have used camera controlled data transfer. Using this way of communication, camera handles HSYNC, VSYNC, and PCLK signals. The horizontal synchronization output pin (*hsync*) is used as an indicator for row data. The *hsync* output pin reaches the specified level at the start of each row and remains at that level until the last pixel of that row is read out on D0-D11 as shown in Figure 1.

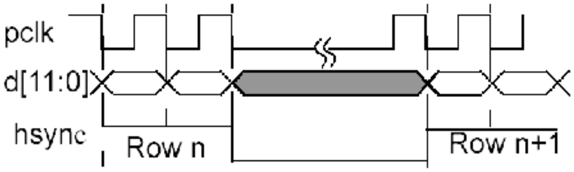

Fig. 1. Horizontal Synchronization Timing

The *hsync* level is always synchronized to the active edge of *pclk*. The vertical synchronization output pin, *vsync*, is used as an indicator for pixel data within a frame. The *vsync* output pin will go to the specified level at the start of each frame and remain at that level until the last pixel of that row in the frame is placed on D0-D11 as shown in Figure 2. The *hsync* level is always synchronized on the active edge of *pclk*.

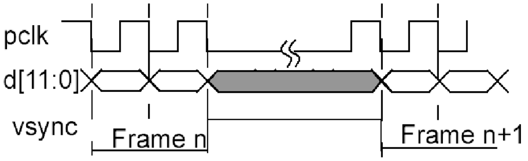

Fig. 2. Vertical Synchronization Timing

3 Face Detection

We will describe briefly how our implementation of the method for face detection works. This method is based on special structured neural network which is prepared for face detection. The decision about absence or presence of face in proper part of input image is made by neural network. The neural network could be considered classificatory which means we have a "black box" with squared input image of fixed size and the output provides information whether there is face present or not.

The classificatory is used for all possible parts of input image where a face could be found. According to a decision made during the processing by the classificatory, the specific part is considered a face or not. This method will be described more precisely further. It is convenient to unify the image before the image processing in order to make the conditions of face detection similar in various types of images. The histogram equalization and correct lighting are applied. The detection of various sized faces is processed by this method. The neural network tests areas of various sizes in different positions. We used the classificatory with the input size 20 × 20 pixels. The detection of faces can be started when input image is successfully retrieved from the camera. Sub-sampling is required for various sized faces. The term sub–sampling represents a gradual size reducing. The classificatory is applied at all positions for every reducing step.

3.1 Light Correction

The correction of lighting and histogram equalization (which is described in [1]) is carried out for every image which is processed by the classificatory. We assume that input image can be represented by function $f(x, y)$. This function describes input image which is distorted by irregular lighting.

Function $g(x, y)$ represents correctly lightened image. Relationship between these functions is:

$$f(x, y) = g(x, y) + u(x, y) \tag{1}$$

where $g(x, y)$ is fault caused by irregular lighting. The evaluation of function $u(x, y)$ is needed to evaluate $g(x, y)$ by subtraction $u(x, y)$ from $f(x, y)$.

Several premises are considered to compute the value of function $u(x, y)$. At first we assume that this function is linear. Further, the linear approximation of correctly lightened input image is straight. This premise is not fulfilled in the case of irregular lighting. From these premises we can assume that $u(x, y)$ is a linear approximation of input image. In this way we will compute all necessary details to process lightning correction. Our implementation of computation uses mask that ignores boundary and corner pixels. It is because pixels in these positions do not provide useful information about faces.

3.2 Neural Network Structure

The structure of neural network can be seen in the Figure 3. Used network structure is taken from the article [2]. The first layer serves as an input layer. This layer consists of 26 neurons. Neuron inputs are raw image data transformed into interval $\langle 0, 1\rangle$. These neurons could be divided into three different parts. Number of neuron inputs and shape of observed area differ through these groups.

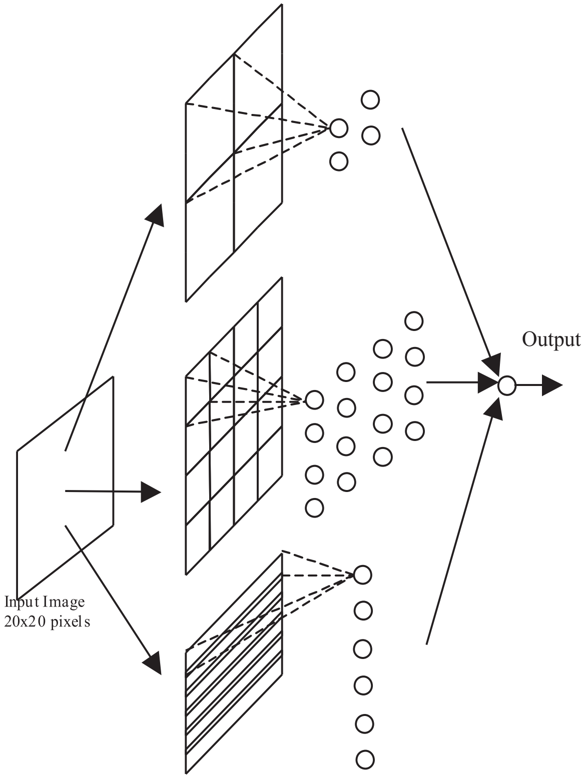

Fig. 3. Structure of Neural Network

The first part consists of four neurons observing square areas of 10×10 pixels. Another group contains 16 neurons. These neurons work as same as neurons from the first group. However, they handle areas of 5×5 pixels. The last group contains six neurons with input size of 20×5 .

This means that areas observing neurons from this group are overlapped by two pixel rows. There is also the second layer consisted of output neuron, which is connected with outputs of the first layer through its inputs. It is necessary to teach neural network to perform face detection. Therefore it is needed to create training set, which contains two kinds of patterns - the first group contains images of face, while another one consists of images without the presence of faces. We have chosen back–propagation method for teaching.

In the future we would like to create a new training set with images of faces with better localization of face. We assume that the neural network will learn better and the results of the detection will be better as well.

The expected output of the network in case of face presence is value close to 1 (0 in the other case). The value of the network output means the probability of face presence in tested image.

Results of face detection method can be used in several ways. For instance, DSP can create images marking regions with selected faces or separate the parts of images where faces can appear. The example of marked face in the image can be seen in figure 4.

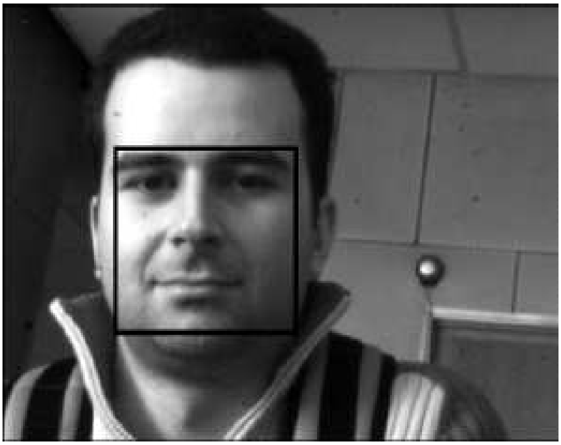

Fig. 4. Example of Detected Face

4 Conclusions

As mentioned above we worked with BlackFin BF-537 development board. This board provides port for Ethernet connection. We used it to get images from camera and to manage the process of testing as well. In addition, we had implemented a communication via serial link. Our implementation of this system is based on using threads. Communication with camera, via Ethernet (or serial link), face detection and control all these parts of our system are implemented as separate threads. We used VDK library to handle these threads and network connection.

Our goal is to create a smart camera system. This system might work without any human control – producing information for users who are connected to this system. For instance, system that tries to search for people in places where cameras are placed. The system can provide information about the presence of human being in the area of interest or it can store faces of people who have visited some place. The main advantage of using DSP is that camera with DSP can be placed anywhere (more precisely where connection to the network is available). Thus we do not have to transfer all data via network and process it on place. The data sent by the system are composed of either results or at least pre-processed data.

The results were presented on POSTER 2007, held annually in Prague.

References

1. SOJKA, E., *Digitalni zpracovani a analyza obrazu*, VSB-TU Ostrava, 2000.
2. ROWLEY, H., BALUJA, S., *Neural Network-Based Face Detection* , IEEE Transactions on Pattern Analysis and Machine Intelligence, vol 20, number 1, pages 23-38, January 1998.
3. SMITH, S., *The Scientist and Engineer's Guide to Digital Signal Processing*, Hard Cover, 1997.

Projector Preconditioning for the Solution of Quadratic Programming Problems*

Marta Domorádová

Department of Applied Mathematics, FEECS,
VŠB – Technical University of Ostrava, 17. listopadu 15, 708 33 Ostrava – Poruba
`marta.domoradova@vsb.cz`

Abstract. Our focus is concentrated on the solution of the large sparse bound constrained quadratic programming problems, such as those arising from the discretization of elliptic boundary variational inequalities. Applying preconditioning is a general way how to improve the performance of the conjugate gradient based algorithms. Conjugate projector preconditioning is connected with MPRGP algorithm. The unique feature of this preconditioning strategy is that it affects all steps of the MPRGP algorithm, so that guarantees better bound on the rate of convergence than the original MPRGP. Numerical experiments (using FEM and FETI-DP) show this improvement.

Keywords: Quadratic programming, bound constraints, boundary variational inequalities, preconditioning.

1 Introduction

The results that we show here come from joint research with my supervisor. For more detail see Domorádová and Dostál [3]. It is a continuation of my thesis [1]. My contribution consisted mainly in numerical experiments.

We are concerned with the partially bound constrained quadratic programming problem to find

$$\min_{\mathbf{x}\in\Omega} f(\mathbf{x}), \quad \Omega = \{\mathbf{x}\in\mathbb{R}^n :\ \mathbf{x}_{\mathcal{I}} \geq \ell_{\mathcal{I}}\}, \quad \mathcal{I} = \{1,\dots,m\}, \tag{1}$$

where $f(\mathbf{x}) = \frac{1}{2}\mathbf{x}^T\mathbf{A}\mathbf{x} - \mathbf{x}^T\mathbf{b}$, ℓ and $\mathbf{b}$ are given column n-vectors, $1 \leq m \ll n$, and $\mathbf{A}$ is an $n\times n$ symmetric positive definite matrix. We are interested in large, sparse problems, such as those arising from the discretization of elliptic boundary variational inequalities.

We combined conjugate projector preconditioning, for example [4], with the algorithm MPRGP proposed by Dostál and Schöberl [7]. MPRGP algorithm combines the proportioning algorithm with the gradient projections. It uses a given constant $\Gamma > 0$, a test to decide about leaving the face, and three types of steps to generate a sequence of iterates $\{\mathbf{x}^k\}$ that approximate the solution of (1).

---

* This paper was supported by GA CR 201/07/0294, AS CR 1ET400300415, and the Ministry of Education MSM6198910027.

© Václav Snášel (Ed.): WOFEX 2007, pp. 261–266, ISBN 978-80-248-1571-8.
VŠB – Technical University of Ostrava, FEECS, 2007.

2 Preconditioning by Conjugate Projectors

First, let us describe some basic properties of conjugates projectors.

Let $\mathbf{A} \in \mathbb{R}^{n\times n}$ be a symmetric positive definite matrix. A projector $\mathbf{P}$ is an $\mathbf{A}$-*conjugate projector* if $\mathrm{Im}\mathbf{P}$ is $\mathbf{A}$-conjugate to $\mathrm{Ker}\mathbf{P}$, or equivalently

$$\mathbf{P}^T\mathbf{A}(\mathbf{I}-\mathbf{P}) = \mathbf{P}^T\mathbf{A} - \mathbf{P}^T\mathbf{A}\mathbf{P} = \mathbf{O}.$$

It follows that $\mathbf{Q} = \mathbf{I} - \mathbf{P}$ is also a conjugate projector. Let us denote $\mathcal{V} = \mathrm{Im}\mathbf{Q}$. If $\mathbf{x} \in \mathbf{A}\mathcal{V}$, then $\mathbf{Q}^T\mathbf{A}\mathbf{Q}\mathbf{x} = \mathbf{A}\mathbf{Q}\mathbf{x}$, so that $\mathbf{Q}^{\mathrm{T}}\mathbf{A}\mathbf{Q}(\mathbf{A}\mathcal{V}) \subseteq \mathbf{A}\mathcal{V}$. Thus $\mathbf{A}\mathcal{V}$ is an invariant subspace of $\mathbf{Q}^T\mathbf{A}\mathbf{Q}$.

Let us assume that $\mathcal{U}$ is the subspace spanned by the full column rank matrix $\mathbf{U} \in \mathbb{R}^{n\times p}$,

$$\mathbf{U} = \begin{bmatrix} \mathbf{O} \\ \mathbf{U}_2 \end{bmatrix}, \quad \mathbf{U}_2 \in \mathbb{R}^{n-m\times p}.$$

We shall decompose our partially constrained problem (1) by means of the conjugate projectors

$$\mathbf{P} = \mathbf{U}(\mathbf{U}^T\mathbf{A}\mathbf{U})^{-1}\mathbf{U}^T\mathbf{A}$$

and $\mathbf{Q} = \mathbf{I} - \mathbf{P}$ onto $\mathcal{U}$ and $\mathcal{V} = \mathrm{Im}\mathbf{Q}$, respectively. Some manipulation yields

$$\min_{\mathbf{x}\in\Omega} f(\mathbf{x}) = f(\mathbf{x}^0) + \min_{\substack{\mathbf{z}\in\mathbf{A}\mathcal{V} \\ \mathbf{z}_{\mathcal{I}}\geq \ell_{\mathcal{I}}}} \frac{1}{2}\mathbf{z}^T\mathbf{Q}^T\mathbf{A}\mathbf{Q}\mathbf{z} + \left(\mathbf{g}^0\right)^T\mathbf{z},$$

where $\mathbf{x}^0 = \mathbf{P}\mathbf{A}^{-1}\mathbf{b}$ and $\mathbf{g}^0 = -\mathbf{Q}^T\mathbf{b}$. We have thus reduced our bound constrained problem (1) to the problem

$$\min_{\substack{\mathbf{z}\in\mathbf{A}\mathcal{V} \\ \mathbf{z}_{\mathcal{I}}\geq \ell_{\mathcal{I}}}} \frac{1}{2}\mathbf{z}^T\mathbf{Q}^T\mathbf{A}\mathbf{Q}\mathbf{z} + \left(\mathbf{g}^0\right)^T\mathbf{z}. \tag{2}$$

It follows that we can obtain the correction $\widehat{\mathbf{z}}$ which solves the auxiliary problem by the standard MPRGP algorithm [3]. Since the iterations are reduced to the subspace $\mathbf{A}\mathcal{V}$, the *projector preconditions all three types of steps* and we can give an improved bound on the rate of convergence [3, Th. 5.2]. The solution $\widehat{\mathbf{x}}$ of the bound constrained problem (1) can then be expressed by $\widehat{\mathbf{x}} = \mathbf{x}^0 + \mathbf{Q}\widehat{\mathbf{z}}$. We conclude that with a suitable choice of $\mathbf{U}$, we can improve the bound on the rate of convergence of the MPRGP algorithm by the preconditioning by the conjugate projector.

3 Numerical experiments

We have implemented algorithms MPRGP and MPRGP with conjugate projector preconditioning (MPRGP-CP) in Matlab language and compared their performance to show preconditioning effect. We have used experiments similar to Dostál [6, Sec. 5.11].

3.1 Model problem

Let $\Omega = (0,1)\times(0,1)$ denote an open domain with the boundary Γ and its three parts $\Gamma_u = \{0\}\times[0,1]$, $\Gamma_l = \{1\}\times[0,1]$, and $\Gamma_f = [0,1]\times\{0,1\}$. See also Fig. 1a. The obstacle l on the contact boundary Γ_l is defined by the upper part of the circle with the radius $R=1$ and the center $S=(1;1;-1.3)$.

Let $H^1(\Omega)$ denote the Sobolev space of the first order in the space $L^2(\Omega)$ of functions on Ω whose squares are integrable in the Lebesgue sense. We shall consider the problem to find

$$\min f(u) = \frac{1}{2}\int_\Omega \|\nabla u(x)\|^2 \mathrm{d}\Omega + \int_\Omega u \mathrm{d}\Omega \quad \text{subject to} \quad u \in \mathcal{K}, \tag{3}$$

where

$$\mathcal{K} = \{u \in H^1(\Omega) : \ u = 0 \ \text{ on } \ \Gamma_u \quad \text{and} \quad c \le u \ \text{ on } \ \Gamma_c\}.$$

Since the Dirichlet conditions are prescribed on the part Γ_u of the boundary with the positive measure, the cost function f is coercive, which guarantees the existence and uniqueness of the solution. The solution of this problem is shown in Fig. 1b. It can be interpreted as the displacement of the membrane under the traction defined by the unit density. The membrane is fixed on Γ_u and is not allowed to penetrate the obstacle on Γ_l.

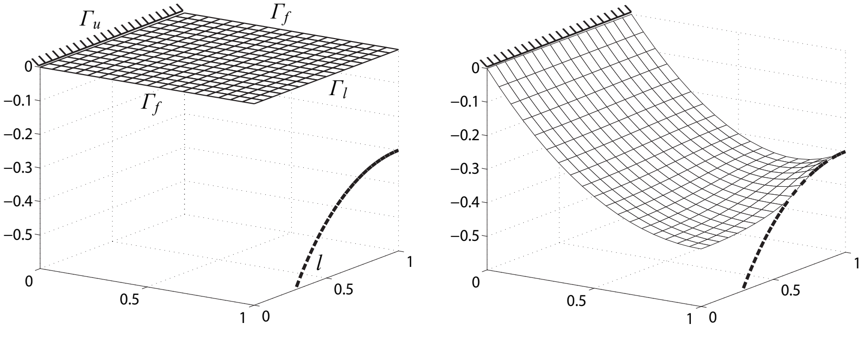

Fig. 1. [**a**] Model problem with regular grid; [**b**] Solution to the model problem.

We have discretized the problem (3) by the piece-wise finite elements using regular grids defined by the discretization parameter h. After the discretization, we got the problem of the form (1). The computations were performed with the parameters $\overline{\alpha} = \|\mathbf{A}\|^{-1}$ and $\Gamma = 1$. The stopping criterion was $\|\mathbf{g}^P(x)\| \le 10^{-4}\|\mathbf{b}\|$.

3.2 Projector defined by aggregations

Firstly, we have used the projectors defined by the elements of the aggregation basis such as those depicted in Fig. 2a. Each element of such basis can be represented by the column $\mathbf{u}_{j\ell} \in \mathbb{R}^n,\ \ell = 1, \ldots, p$, with all the entries equal to zero except the entries which correspond to the aggregated variables and are equal to one. For example, if $\mathbf{u}_\ell = [u_{i\ell}]$ corresponds to the element of the aggregation basis depicted in Fig. 2a, then $u_{i\ell} = 1$ and $u_{j\ell} = 0$.

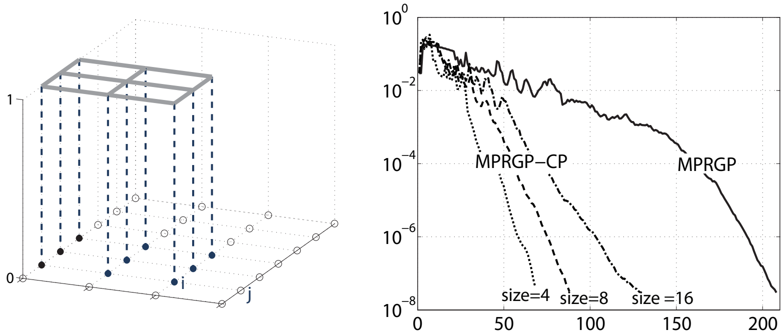

Fig. 2. [**a**] Aggregation basis function; [**b**] The norm of projected gradient against the number of iterations.

Let *size* denotes number of variables that are aggregated in one direction. For example, this number is equal to three for basis function of Fig. 2a. Fig. 2b shows the norm of projected gradient against the number of iterations for $size \in \{4, 8, 16\}$. This results were obtained with $h = 1/34$, which corresponds to 1156 variables. We can see that projector preconditioning using aggregation basis can considerably reduce the number of iterations.

3.3 Projector defined by the traces of linear functions on coarse grid

Secondly, we used the projectors defined by the traces of linear functions on the coarse grids such as that depicted in Figure 3a. Each element of such basis can be represented by the column $\mathbf{u}_j \in \mathbb{R}^n,\ j = 1, \ldots, p$, with all the entries equal to zero except the entries which correspond to the support. For example, if $\mathbf{u}_\ell = [u_{i\ell}]$ corresponds to the coarse space basis function depicted in Fig. 3a, then $u_{i\ell} = 0$, $u_{j\ell} = 0.5$, and $u_{k\ell} = 1$.

Let *size* now denotes the maximal number of variables in the element in one direction. The results depicted in Fig. 3b were obtained with $h = 1/34$ and $size \in \{5, 9, 17, 33\}$. We can see that preconditioning reduce the number of iterations.

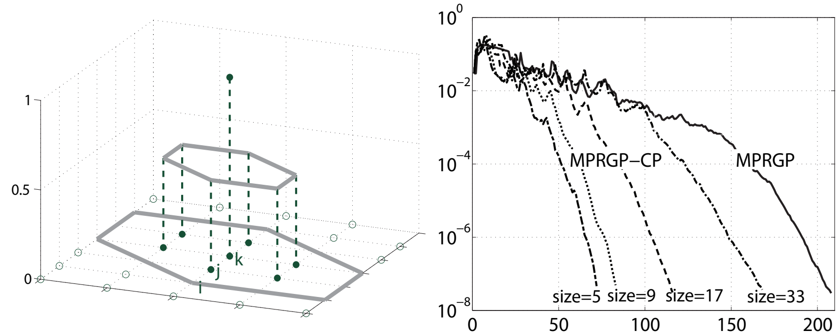

Fig. 3. [**a**] Coarse linear basis functions; [**b**] The norm of projected gradient against the number of iterations.

3.4 Dual-Primal Finite Element Tearing and Interconnecting

The FETI-DP method [5] is based on decomposition of the original domain into several smaller non-overlapping subdomains (Fig. 4a) where the continuity conditions are enforced by Lagrange multipliers. This method defines so-colled corner nodes, which belong to more then one subdomain.

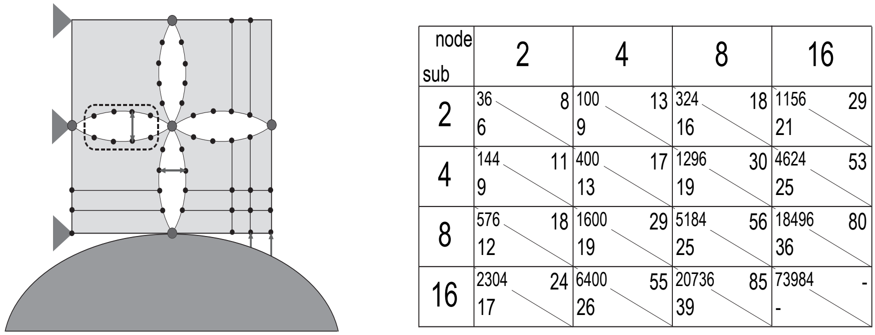

node / sub	2	4	8	16
2	36 8 6	100 13 9	324 18 16	1156 29 21
4	144 11 9	400 17 13	1296 30 19	4624 53 25
8	576 18 12	1600 29 19	5184 56 25	18496 80 36
16	2304 24 17	6400 55 26	20736 85 39	73984 - -

Fig. 4. FETI-DP: [**a**] Decomposition of the original domain into four subdomains; [**b**] Results of numerical experiments: Small number in the left-upper corner is dimension. The number in left-lower corner is number of MPRGP-CP iterations and the number in the right-upper corner is number of MPRGP iterations..

Thirdly, we solved the problem (3) by FETI-DP method, implemeted by D. Horák. This implementation also includes solving the “dual” quadratic programming problem by MPRGP algorithm. We applied MPRGP with projector preconditioning (MPRGP-CP) to solve this “dual” problem. We used the projectors defined by aggregations consist of dual variables (Lagrange multipliers) depicted in Fig. 4a in dashed rectangle.

Fig. 4b shows the results with the stopping criterion $\|\mathbf{g}^P(x)\| \leq 10^{-6}\|\mathbf{b}\|$, where *sub* denotes number of subdomains in one direction, *node* denotes number of nodes in one direction in one subdomain. Small number in the left-upper corner is dimension. The number in left-lower corner is number of MPRGP-CP iterations and the number in the right-upper corner is number of MPRGP iterations. We can see that preconditioning reduce the number of iterations.

4 Comments and Conclusions

We have presented experimental results which indicate that the performance of MPRGP algorithm for the solution of the partially bound constrained quadratic programming problem (1) can be considerably improved by preconditioning by a conjugate projector on the coarse grid.

As mentioned before this is joint research with my supervisor Prof. Dostál. It is a continuation of my thesis *Projector Preconditioning for the Solution of the Large Scale Bound Constrained Quadratic Programming Problems* [1], which was awarded 2nd place in SVOČ 2006 in Bratislava and 3rd place in Professor Babuška’s Prize 2006.

References

1. Domorádová, M.: Projector Preconditioning for the Solution of the Large Scale Bound Constrained Quadratic Programming Problems, Master Thesis, 2006, VSB-TU Ostrava, Supervisor: Prof. Dostl
2. Domorádová, M., Dostál, Z.: Projector Preconditioning for the Solution of the Large Scale Bound Constrained Quadratic Programming Problems, Seminar on Numerical Analysis and Winter School: proceedings of the conference SNA ’07, Ostrava, January 22-26, 2007, editor: Blaheta, R., Starý, J.
3. Domorádová, M., Dostál, Z.: Projector preconditioning for partially bound constrained quadratic optimatizion, Numerical Linear Algebra with Applications, submitted
4. Dostál, Z.: Conjugate gradient method with preconditioning by projector. Intern. J. Computer Math. **23**, 315–323 (1988)
5. Dostál, Z., Horák, D., Stefanica, D.: A scalable FETI-DP algorithm for coercive variational inequalities. IMACS Journal Applied Numerical Mathematics **54,3–4**, 378–390 (2005)
6. Dostál, Z.: Optimal Quadratic Programming Algorithms, with Applications to Variational Inequalities,1st Edition, Springer, submitted
7. Dostál, Z., Schöberl, J.: Minimizing quadratic functions subject to bound constraints with the rate of convergence and finite termination, Comput. Optimiz. and Applications 30,1 (2005) 23-44.

Task Generators, and Environment Simulator, Evaluation of Special Tasks

Radoslav Fasuga

Department of Computer Science, FEECS,
VŠB – Technical University of Ostrava, 17. listopadu 15, 708 33 Ostrava – Poruba
`radoslav.fasuga@vsb.cz`

Abstract. Goal of this article is to describe automatic evaluation of special tasks by using computers. This Article inspects evaluation possibility from different point of view. Especially is this topic oriented to technical realization aspects. Here is suggested also pedagogical point of view, discuss the possibility of typical task (variant question, quizzes) generator, in opposite to environment simulators with numerical evaluation methods. Content describes different evaluation methods, their goals, and weaknesses demonstrated on elementary tasks. Target of this document is to inspire actual and future study matter, and test authors with this problematic. It can help them to choice good class of tasks, and purpose the solution possibilities, by using variant question generator or assembling environment simulator based on numerical result evaluation for student result with author template. This article is published without orientation to concrete LMS system, and purpose common theory that can be implemented into your LMS or interactive study material.

1 Introduction

When authors transform study matter, and explanation methods into electronic form they must to answer the question, How to solve testing process, and automated evaluation of question answers. Most of LMS systems allow completing quizzes based on question with variant answers. Authors define questions, and variants that are purposed to student. Student select one or more correct variant from given set. This testing method is extremely fast, their abilities are very limited. For many tasks this way of knowledge testing is not acceptable, and limited. Next set is represented by created answers, where student must to build or create the answer. For this set is basic problem with flexibility. Author must set into system all possible templates of correct answers. This solution is very complicated, and for example for mathematical tasks is possible to type correct formula in many acceptable formats. Not only in this situation have we started to speak special task types which we want to solve. Commonly our LMS does not support given class of tasks, and it is necessary to choice alternative solution (transform to created question) that can sole this problematic. [1.][2.]

© Václav Snášel (Ed.): WOFEX 2007, pp. 267–272, ISBN 978-80-248-1571-8.
VŠB – Technical University of Ostrava, FEECS, 2007.

2 Productive ways for special tasks assembling

2.1 Define theme of special task

Special task is commonly solved for really narrow problematic. By theme specification process is good to from elementary tasks, which can be enlarged in future. In math discipline we can start to solve simply algebraic formulas, and then add most complicated mathematical operations. For our purposes we will be focused on mathematic problematic, bud common ways we can in difference scientific disciplines. For natural sciences we can commonly find some rights, and rules that can be simulated. In human disciplines is this solution exact less.

2.2 Describes behavior rules for solved problem

Before we start to solve the task, we must to understand the background problematic. Captured reality is good to describe by mathematical rules or by list of typical tasks. As an environment simulator designer we must to know the limit values for given problem. For example for which mathematical formulas has no solution, assumption problematic, tolerance, and other supporting rules.

2.3 Choice simulation method or task generator approach

Based on received request we must to decide if we will develop task generator. It will generate set of tasks in given type based on predefined parameters. Result is classic created or variant question that is possible to evaluate with traditional LMS.

Most difficult is solution based on environment simulator. Environment simulator can be based on several rules oriented to problematic solve. For our example we will think about math algebraic formulas. We can produce semantic analysis for given formula or use numerical substitution method. For tasks with own logic like electrical circuits or physics phenomenon we can implement virtual environment that will simulate this phenomenon. We can design system for circuits, magnetic power, dimensions, pressures, weights etc. Commonly we design system for constructive task when student must to complete some electrical circuit which simulates physics phenomenon.

2.4 Complete the requirements for special task

When we have simulator for solving some class of tasks, we will start to complete task requirements. First step is exact textual task formulation. Second step represent template task results. For some task is necessary third step. This step requires some controlling data that data will be used for evaluation of final solution. In next three main chapters we will discuss about three basic sets of special tasks which we are able to automatically evaluate.

2.5 Evaluation algorithm for given task

Based on type of simulation environment is necessary to choice correct evaluation algorithm. Algorithms can be divided into two groups. First group is represented by common algorithms that can be used for different task classes. When we create non-specialized environment simulator based on graph theory. Here we can define properties for nodes, and relations. Based on this simply schema we can simulate many problems like – electrical circuits connection, UML (Unified Modeling Language), database schemes etc. Evaluation algorithms are not based on absolute position of used objects. Objects are situated in relative space, for us are necessary values of objects properties, and their interconnections. Algorithm returns level of similarity based on (author) template model, oriented to whole schema, special properties or defined errors that can be corrected.

Special algorithms solves (evaluates) just limited class of task. They are strictly oriented to concrete problematic without larger area of usage. For example algorithms for chemistry formulas, and tests, physics simulators etc. To improve quality of these algorithms we can accept larger set of tasks. Sam simulation algorithms are so difficult that are impossible to use them in on-line application. Evaluation results are received with long (hours, days) delays.

3 Task generator

Task generators can be divided by theme or type of generated examples. For geometry and mathematical tasks are often used generators of created answers. For example we can generate task requirements for quadratic formulas with results. We generate typical task formula with correct results. Student inserts only solution (key values) for given formula.

Most effective is generator based on templates (here are often generated variant question). In this case we use as example query in SQL (Structured Query Language). We create the template with common task. For example select from table A that are also included in table B. Then we will formulating SQL queries which will solve current problem + generate set of wrong queries. When we will generate some task based on this template, we can say that Table A = Teacher, Table B = Student, then we formulating the task requirements Select all Teachers that are also students. System substitutes Tables A, and B ant their attributes by concrete attribute instances from our task, and generate the whole task. This is method of basic generator (Tab. 1 – Basic generator). Weakness of this solution is fact that all templates must include set of correct and also wrong answers.

Advanced generator uses different strategy. Task template contains only task description, and correct answers (without wrong answers). Then author define similar solutions (with different results) (Tab. 1 – Advanced generator). In final stage author creates Final task template. Here is selected correct solution template, modify task requirements, and solution constants, and select similar solution (similar count of tables, attributes, constant, problematic) which will be source for wrong answers.

In final stage we will add generation parameters. In which format we want to show the task, count of variants, and how many variants will be correct. When we use advanced generator with large set of similar solutions, we can create opposite questions. Task requirements will be concrete SQL query, and sentences from task preamble will be variants for answering. For template description is best to use XML (eXtensible Markup Language) documents.

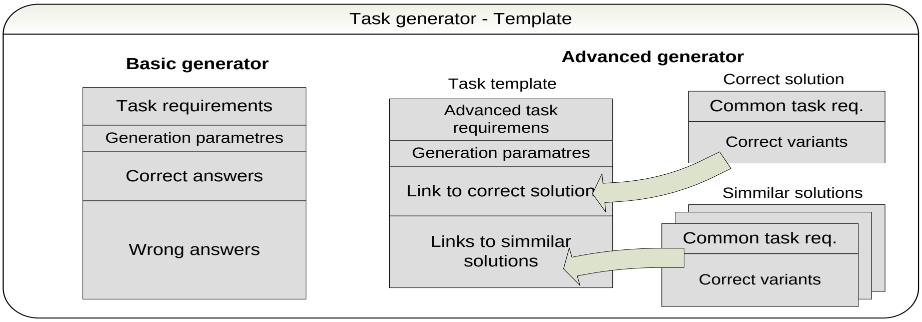
Task generator - Template
Basic generator
Task requirements
Generation parametres
Correct answers
Wrong answers
Advanced generator
Task template
Advanced task requiremens
Generation paramatres
Link to correct solution
Links to simmilar solutions
Correct solution
Common task req.
Correct variants
Simmilar solutions
Common task req.
Correct variants

Tab 1: Task generator template

4 Environment simulator

Other way to solve difficult task evaluation problem is environment simulator. As we say before often goes about physics phenomenon simulator. We can use this phenomenon to solve current problem. To evaluate this type of tasks we use two basic approaches. Semantic approach explodes given construction into comparable tree structure. Numerical approach that substitute constants with real values, and compare the results.

Semantic approach is more complicated for evaluation in opposite case is here possible to represent solution steps, for example for difficult mathematic formulas, and deductions. Simulators based on semantic approach are not so often especially based on difficult of evaluation algorithms.

Numeric methods are very effective, and simply solution. Author defines template formula with several checkpoint values. These values are inserted into formula, and receive results. Then are same values inserted into student solution. Now we can compare author, and student values. Student can write formula in different format or order but finally receives total score. By using this approach is impossible to watch deductive or inductive steps. Numeric methods require from author special skills – select ideal data for entry evaluation, to determine student correct solution. Author especially select values where formula has no result or exception, to verify student solution. Control values cannot be ideal but it must be limit values that exactly determine author template, and student solution equivalence. [5.]

5 Statistical method used for selected data

Here we will describe evaluation possibilities for question with created answer. Evaluation system can be divided into two basic parts. Firs part compares elementary items (number, word). Second part solves difficulty structure (sets, vectors of items) on this items comparing.

4.1 Elementary item comparing

For elementary item comparing like – text or number we can convert them into standard form. It is necessary for author template, and student result (solution). Both of them (student and author) can break the rules about solution format. For numbers we can find absolute equal, or accept tolerance to make a round of solutions. For textual answers we can accept grammar, capital letters etc. Elementary items (with accepter rules) can by compared only like absolute evaluation equal/non-equal.

4.2 Complicated item structures comparing

For elementary task student build the answer like single value. For difficulty tasks student can answer by using set of elementary values like – numbers, words, sentences, special solutions. System must process correct separation (based on defined separator), and divide answer into elementary comparable components. Whole set of elementary items we can evaluate by using percentage similarity. Absolute equal is represented by 100% non-equal by 0%. Elementary items are compared absolutely like – item is identical (in template and result) or not.

Evaluation by using sets is traditional evaluation method. Author commonly gives the set on correct items. Student builds as an answer own set of items. In set is not respect item order (Tab. 2 Set 100%). Evaluation process works in this way. Authors defined set represents 100% of correct answer, and then we go through student set, and control items. When we find the item if author template, student receive given percentage representation (for for item in template receives 25% for one correct item). When student result does not contain author item (he didn't receive the percentage) (Tab. 2 Set 66.6%). When student put into result item that s not in author defined set template, it is mean like mistake, and student lost one of correct answers, (Tab. 2 Set 33.3%). By this way is defined total percentage of similarity.

Evaluation by using vector is identical principle like for sets evaluation, only with strictly given item order. Unfortunately vector evaluation is more complicated. Here exists several strategies how to compare vectors, and how to represents mistakes in answers. Ideal situation is, when student set correct whole vector (same values in same position) (Tab. 2 Vector 100%). Other frequently used evaluation is method from left to right until firs mistake. In this method when student produce mistake in first step receives 0% similarity (Tab. 2 Vector 33.3%). We can use same strategy in opposite way (from right to left) to find the mistake from the end of a vector (Tab. 2 Vector 55.5%). Other strategy is to compare strictly position in vector, so given value must be in correct place like in author template. Some movement in vector (lost or add some item) devalues result (Tab. 2 Vector 44.4%). Other more tolerant method is finding largest similar subsequence in vector that is similar in both vectors (student and author) (Tab. 2 Vector 77.7%). Last here published method is evaluation based on interrupted sequence (Tab. 2 Vector 88.8%). Here we jump over missing items or wrong items in respecter vector order. [3.][4.]

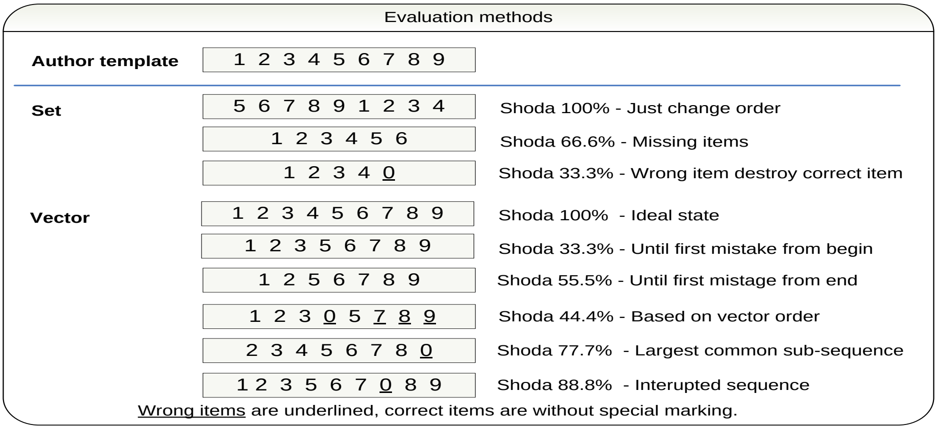

Evaluation methods

Author template	1 2 3 4 5 6 7 8 9	
Set	5 6 7 8 9 1 2 3 4	Shoda 100% - Just change order
	1 2 3 4 5 6	Shoda 66.6% - Missing items
	1 2 3 4 0	Shoda 33.3% - Wrong item destroy correct item
Vector	1 2 3 4 5 6 7 8 9	Shoda 100% - Ideal state
	1 2 3 5 6 7 8 9	Shoda 33.3% - Until first mistake from begin
	1 2 5 6 7 8 9	Shoda 55.5% - Until first mistage from end
	1 2 3 0 5 7 8 9	Shoda 44.4% - Based on vector order
	2 3 4 5 6 7 8 0	Shoda 77.7% - Largest common sub-sequence
	1 2 3 5 6 7 0 8 9	Shoda 88.8% - Interupted sequence

Wrong items are underlined, correct items are without special marking.

Tab 2: Ways of evaluation for sets, and vector of values

6 Conclusions

Proposed material is some preview of possible automated testing solutions. Here exists a lot of variants, and many authors produce own tools for special task environment simulation. Results and solution of many authors come to same solutions that can by generalized into one system.

Resources

1. Bober, M., Fasuga, R., Holub, L.: Traditional tasks in Computer Science and their Automatic Evaluation. In EAEEIE 2007, 2007, ISBN 978-80-01-03745-4
2. Holub, L., Fasuga, R., Šarmanová, J.: Metody automatického vyhodnocení se zaměřením na tradiční způsoby hodnocení kvizů a variantních otázek. In sborník. Ed. Petr Sojka, Martin Kvizda, Brno:Masarykova univerzita, 2007, S. 49-54, ISBN 978-80-210-4296-4
3. Fasuga, R.: On-line teaching and statistic evaluation inside study materials and tests. VSB-TU Ostrava 2004. Course project – Statistical methods in Engineer practice
4. Fasuga, R.: On-line education process: Statistical Method, Ostrava University Editorial Centre:, University of Ostrava, 2004. ICTE 2004.
5. Fasuga, R.: Using artificial intelligence in education process, CVUT Praha 2004, technology for e-education 2004

An Image Analysis Based Method for Measuring the Surface Tension of Liquids*

Jan Gaura[1], Michal Krumnikl[1], Eduard Sojka[1], Rostislav Dudek[2]

[1]Department of Computer Science, FEECS,
VŠB – Technical University of Ostrava, 17. listopadu 15, 708 33 Ostrava – Poruba
{jan.gaura.fei,michal.krumnikl,eduard.sojka}@vsb.cz
[2]Department of Physical Chemistry and Theory of Technological Processes, FMME,
VŠB – Technical University of Ostrava, 17. listopadu 15, 708 33 Ostrava – Poruba
rostislav.dudek@vsb.cz

Abstract. In this paper, we present a method for measuring the surface tension of liquids. The method is based on automatically recognizing and extracting the shape of drop, which is followed by fitting the theoretical Laplacian profile by the least-squares method. In the experimental part, achieved results are presented.

Keywords: image analysis, surface tension, sessile drop, liquids, differential geometry of surfaces, least-squares method

1 Introduction

In fluid dynamics, the equilibrium pressure balance at the interface between the liquid and gas is described by the Laplace-Young equation

$$p = \gamma \left(\frac{1}{R_1} + \frac{1}{R_2} \right) = 2\gamma H. \tag{1}$$

In the above equation, p is the pressure difference over the interface, γ is the surface tension, H is the mean curvature, and R_1 and R_2 are the principal radii of curvature at the interface. (Note that the expression $H \equiv (1/R_1 + 1/R_2)/2$ as well as the meaning of R_1, R_2 are introduced in differential geometry of surfaces.) In the case of sessile drop, $p = p_0$ at the apex of drop and it increases due to the hydrostatic pressure in the drop as we proceed down along the y coordinate (left image in Fig. 1). The pressure may be expressed by $p = p_0 + \rho g y$, where ρ is the density difference across the liquid-gas interface, g is the acceleration due to gravity, and y is the depth measured from the apex of the drop.

Let us consider the axisymmetric surfaces that are created by rotating the curve $y = h(x)$. If we introduce the values $ds = \pm\sqrt{(dx)^2 + (dy)^2}$, $\varphi = \arctan(dy/dx)$, the following expression may be derived for $2H$

---

* This work was partially funded from the grant 106/06/1225 of the Czech Science Foundation.

© Václav Snášel (Ed.): WOFEX 2007, pp. 273–278, ISBN 978-80-248-1571-8.
VŠB – Technical University of Ostrava, FEECS, 2007.

$$2H = \frac{1}{R_1} + \frac{1}{R_2} = \frac{d\varphi}{ds} + \frac{\sin\varphi}{x}. \tag{2}$$

A capillarity constant is usually introduced in this context. It is defined by $c = \rho g/\gamma$. Moreover, for the apex of the drop, we have $1/R_1 = 1/R_2 \equiv b$. It follows that $p_0 = 2\gamma b$, where b is the curvature of the drop at its apex.

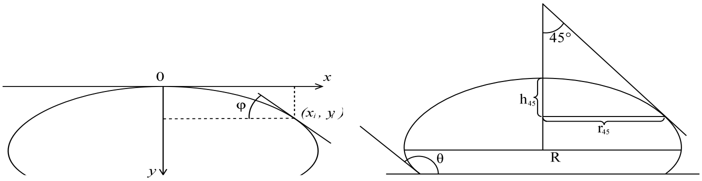

Fig. 1. Geometry of axisymmetric sessile drop (left image), the contour of drop and the geometrical parameters of interest (right image)

Surface tension is an important physical characteristic of liquids and melts. For its measuring, some authors still use the traditional graphical methods [1]. The axisymmetric drop shape analysis (ADSA) is a technique that has already been used by several authors [2]. Recently, the methods based on finite element modelling have appeared too [3]. The method we propose follows the ADSA technique. The new feature is that efficient image processing and recognising steps have been exploited that make it possible to use the method also in the cases that the drop is not seen well (e.g., images from a furnace) and in the case of noisy images.

In this paper, we propose a method for measuring the surface tension of liquids that is based on analysing the images of sessile drops that are considered to be axisymmetric (Fig. 2). The method may be divided into the following steps: (1) finding and recognising the drop and its boundary in image; (2) preliminarily estimating the value of surface tension and other parameters that are needed for the subsequent more precise computation; (3) determining surface tension, mass density, and wetting (contact) angles. The mentioned steps are described in Sections 2, 3, and 4, respectively. In Section 5, experimental results are presented.

2 Recognition of the drop and determining its boundary

Recognition of the drop in an image is accomplished in a few steps. The first step is to estimate the approximate height of drop in the image. This estimation is based on finding the base plane and apex part of the drop. In this step, we assume that the base plane is seen as a line segment, and the apex part of the drop may be approximated as an arc of a circle. Both the base plane and the arc of the circle are searched for by the Hough transform. In the first case, it is

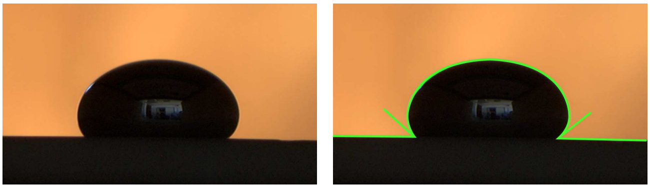

Fig. 2. An example of images used for measuring: A sessile mercury drop (left image), the result of fitting the Laplacian profile (right image)

the line transformation. In the second case, it is the transformation of the circle arc.

In the second step, the contour segments of the drop are found. In this analysis, we are processing gray scale images of drop. Let $f(\mathbf{x})$ denote the brightness at $\mathbf{x}$. To find the pixels that form the contour of drop, we compute the derivatives $\partial f/\partial x$, $\partial f/\partial y$. These derivatives are then tested in the four variants of thresholding: $\partial f/\partial x < t$, $\partial f/\partial x > t$, $\partial f/\partial y < t$, $\partial f/\partial y > t$, where t is a chosen threshold. The result of each mentioned thresholding contains continuous sets of pixels that form particular contour segments of the drop. Moreover, it may also contain noise pixels. Recognising the contour segments is based on measuring the size of the areas produced by thresholding. Because the estimated dimensions of drop are available from the previous step, we can exclude the areas that are not big enough to be considered a contour segment. This procedure is illustrated in Fig. 3, in which the result of the thresholding $\partial f/\partial x < t$ for the drop from Fig. 2 is shown. It can be seen that in this case, the upper part of the drop was found. The remaining three thresholding variants followed by filtration similarly detect contour segments laying attached to the heel of drop.

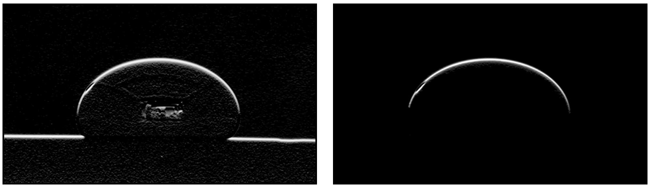

Fig. 3. The result of the thresholding $\partial f/\partial x < t$ (left image) and the result of filtering according to the size of objects (right image)

The contour of the whole drop is acquired as a sum of all particular segments that were recognised. This sum is also filtered by checking its size. In this way, possible false segments are excluded that are not connected to others, which is why they cannot form a part of the drop boundary. Fig. 4 shows an example of recognised drop contour.

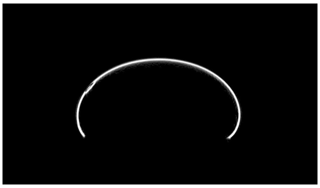

Fig. 4. The result of finding the contour pixels of drop

3 Preliminarily determining the surface tension

To precisely determine surface tension, we are using an iterative technique that requires an estimation of initial values (Section 4). If the value of surface tension is not known at least approximately, we carry out its preliminary estimation by the Dorsey method. Dorsey found, coming from the Laplace-Young equations, the following approximate expression for the surface tension

$$\gamma = \left(\frac{0.052}{q} - 0.1227 + 0.0481q \right) R^2 g\rho, \tag{3}$$

where q is $q = \frac{r_{45} - h_{45}}{R} - 0.4142$.

The meaning of the values r_{45}, h_{45}, and R is shown in Fig. 1 on the right. We introduce a polynomial representation of the drop contour to determine the volume of drop, values r_{45}, h_{45}, R, and the intersection between the drop contour and the base line. The polynomial representation of the drop contour consists of cubic parabolas that are fitted to the pixels of contour by the least-squares method. In a similar way, the polynomial representation of the base is also obtained. The left and right part of the base line are also represented by cubic parabolas constructed by the least-squares method.

4 Precisely determining the surface tension

For the axisymmetric drops, the Laplace-Young equation may be rewritten into the following system of ordinary differential equations as a function of the arc length s (Section 1)

$$\frac{dx}{ds} = \cos\varphi, \tag{4}$$

$$\frac{dy}{ds} = \sin\varphi, \tag{5}$$

$$\frac{d\varphi}{ds} = 2b + cy - \tfrac{\sin\varphi}{x}. \tag{6}$$

In the above equation, b is the curvature at the origin of coordinates (at the apex of drop), and $c = \rho g/\gamma$ is the capillary constant. It should also be noted that at the apex of drop, we have $\frac{\sin\varphi}{x} = b$ at $s = 0$, which yields $\frac{d\varphi}{ds} = b$ at $s = 0$.

For given values of b and c, a unique shape of a Laplacian axisymmetric liquid-gas interface can be obtained by simultaneous integration of the above initial value problem. However, there is no known analytical solution to this problem, except for very limited cases, and a numerical integration scheme must be used. In our implementation, we use the fourth-order Runge-Kutta method with satisfactory results.

Unfortunately, neither b nor c are known beforehand when carrying out the measurement of surface tension. They should be determined as a result of measurement. The problem can be formulated as an optimisation task: Find the values of b and c so that the curve defined by Eqs. 4, 5, and 6 fits best the contour of drop that was determined from image (Fig. 4). In addition to b and c, also further parameters must be taken into account and found during optimisation. Namely, the coordinates of the drop apex in the image, denoted by $\mathbf{x}_0 = (x_0, y_0)$, and θ, the possible rotation of the drop in the image, are needed for transforming the coordinates from the coordinate system in which Eqs. 4, 5, 6 are written to the coordinate system of image and vice versa.

The value that is minimised during fitting the theoretical shape of drop is the sum of the weighted normal distances between the points that were found in the image as a drop contour and the theoretical Laplacian profile. The objective function may be expressed as follows

$$E(\mathbf{x}_0, \theta, b, c) = \sum_{\mathbf{x} \in \Omega} w(\mathbf{x}) d^2 \left(\mathbf{x}, \mathcal{L}(\mathbf{x}_0, \theta, b, c)\right). \tag{7}$$

In the above equation, Ω stands for the area in image in which the pixels creating the contour of drop have been found (Fig. 4). $\mathcal{L}(\mathbf{x}_0, \theta, b, c)$ stands for the Laplacian profile generated for the parameters b, c, placed to $\mathbf{x}_0$ in image, and rotated by θ; $d(\mathbf{x}, \mathcal{L})$ is the distance between $\mathbf{x}$ and $\mathcal{L}$. As $w(\mathbf{x})$, which is the weight of pixel at $\mathbf{x}$, we use the size of the gradient of brightness at $\mathbf{x}$. The value of $E(\mathbf{x}_0, \theta, b, c)$ is minimised with respect to all its indicated parameters, i.e., $\mathbf{x}_0$, θ, b, c. We use the Levemberg-Marquardt algorithm to carry out the minimisation.

In this step, we also seek for a more exact representation of the base the drop is lying on. The base is approximated by two parabolas, denoted by $\mathcal{B}_L$, $\mathcal{B}_R$, of the third order representing the left and the right part of the base, respectively. Fitting the parabolas may again be formulated as an optimisation problem. This problem is not discussed here in details since it may be regarded as well known.

The intersections of $\mathcal{L}(\mathbf{x}_0, \theta, b, c)$ with $\mathcal{B}_L$ and $\mathcal{B}_R$ are found by numerically solving the corresponding set of equations. At intersection points, the contact angles between the Laplacian profile and the parabolas are computed. Fig. 2 (right image) shows the result of fitting the Laplacian profile. The parabolas approximating the base and the wetting angles are shown too.

5 Experimental evaluation of the method

To verify the functionality and accuracy of the method, we carried out an experiment in which the surface tension of mercury was measured. The drop weight was 1.3456g. The images were taken by a CCD camera with the resolution of 1520 × 1144 pixels. For the given drop, we performed four measurements in total. The values of surface tension, density, and contact angles obtained from particular images are shown in Tab. 1.

Table 1. The values obtained from particular images

Measurement	Volume [mm^3]	Density [g/cm^3]	Surface Tension [mN/m]	Left Contact Angle [°]	Right Contact Angle [°]
1	99.15	13.571	469.72	166.54	162.74
2	99.12	13.575	470.08	165.32	162.29
3	99.29	13.552	469.35	162.68	159.28
4	99.18	13.567	465.37	160.60	159.25

The values of density that are stated in various sources are usually about 13.54 g/cm^3 with a relatively small variance. At present, the value of surface tension is reported from the interval 465 to 485 mN/m. It follows that, from the point of view of today's knowledge, the method may be considered correct.

6 Conclusion

A method for automatically measuring the surface tension of liquids has been presented. Fully automated recognition and extraction of the drop shape with subsequently fitting the theoretical Laplacian profile to the shape belong to the features of the method. Achieved results showing that the method is successful have been presented. Since the computation has proved to be time-consuming, we are considering the parallelisation of the computationally intensive parts.

References

1. H. Chiriac, M. Marinescu. Surface tension of intergranular regions of NdFeB nanocomposite magnets. *Materials Science & Engineering, Elsevier* (2004) A 375-377: 1032-1035
2. O.I. del Río and A.W. Neumann. Axisymmetric drop shape analysis: Computational methods for the measurement of interfacial properties from the shape and dimensions of pendant and sessile drops. *Journal of Colloid and Interface Science, Elsevier* (1997) 196: 136-147
3. P.H. Saksono, D. Peri. On finite element modelling of surface tension, variational formulation and applications part I: quasistatic problems. *Computational Mechanics, Springer* (2006) 38: 265-281

The Analogy between Polymorfic Gates and Linear Threshold Units

Vladimír Havel

Department of Computer Science, FEECS,
VŠB – Technical University of Ostrava, 17. listopadu 15, 708 33 Ostrava – Poruba
`vladimir.havel@vsb.cz`

Abstract. The paper deals with behavioural (or functional) similarities between polymorfic gates and linear threshold units. It is shown that linear threshold unit can be viewed as polymorfic gate.

1 Introduction

Polymorphic electronics provides a new way for obtaining circuits that are able to perform two or more functions depending on the environment in which they operate. [6]. These functions can be activated under certain conditions by changing control parameters of the circuit (such as temperature, power supply voltage, light etc.).

We can find many areas in which polymorphic electronics could be utilized. The following list provides some examples [6, 7]:

- The automatic control of power consumption when battery voltage decreases (a circuit realizes another function for lower battery voltage; however, its structure remains unchanged).
- Implementation of a hidden function, invisible to the user, which can be activated in a specific environment (e.g. watermarking at the hardware level).
- Intelligent sensors for biometrics, robotics, industrial measurement, etc.
- Reverse engineering protection.
- Implementation of low-cost adaptive systems that are able to adjust the behavior inherently.

The Linear Threshold (*LT*) unit is a Boolean version of an artificial neuron [2]. It computes a neural-like Boolean function of n binary inputs, which means that it outputs the sign of a weighted sum of its Boolean inputs. The function computed by a *LT* unit is given by setting its weight and threshold values. In this paper we show that all weights can be set to 1, and then the function computed by given *LT* unit depends only on the threshold value. This is obviously the same behaviour as every polymorfic gate has. Thus, an *LT* unit can be viewed as polymorfic gate.

The aim of this paper is to point the behavioural analogy out.

© Václav Snášel (Ed.): WOFEX 2007, pp. 279–284, ISBN 978-80-248-1571-8.
VŠB – Technical University of Ostrava, FEECS, 2007.

2 Polymorfic electronics and polymorfic gates

In the recent years, several polymorphic gates have been discovered [6, 7]. For example, NAND/NOR gate controlled by the power supply voltage (Vdd) is available: This circuit operates as NAND when Vdd is 3.3V and as NOR when Vdd is 1.8V. Some of them have been fabricated and evaluated in a real environment [8].

In other research [4, 3, 1], multifunctional combinational modules composed of polymorphic gates were designed by means of evolutionary techniques. The resulting circuits are composed of standard as well as polymorphic gates and exhibit various unusual functions, for example, one of these circuits could operate as a two-bit adder when Vdd is 3.3V and as a two-bit multiplier when Vdd is 1.2V. However, it was assumed in these papers that polymorphic gates can be utilized as standard building blocks and that these gates are reliable and electrically fully functional.

Multifunctional digital circuits are circuits composed of *polymorphic* (multifunctional) gates. In addition to its standard logic function (such as NAND), a polymorphic gate exhibits another logic function (such as NOR) which is activated under a specific condition, for example, when Vdd, temperature or illumination reaches a certain level. It was shown that it is possible to consider polymorphic gates as standard building blocks and to use them, together with ordinary gates, to design multifunctional digital circuits [4]. These multifunctional circuits exhibit interesting behaviors not visible in standard digital circuits. Importat is, that the topology of the circuit is invariable; the only feature which is changed with Vdd is the functionality of some gates. The main problem is their design: All the existing polymorphic gates were discovered by means of evolutionary design techniques. It seems that a human designer is not able to accomplish this task at all.

Thus, having polymorphic and ordinary gates, the task is to find a graph representing the digital circuit which performs the first desired function under first condition and the second desired function under second condition (see Fig. 1). Unfortunately, standard methods for logic synthesis are not able to solve this problem. In order to find simple multifunctional circuits at the gate level, an evolutionary approach has been utilized in the recent papers [4], [1], [5]. The evolved circuits have up to 5 inputs and outputs and consist of a few tens of gates.

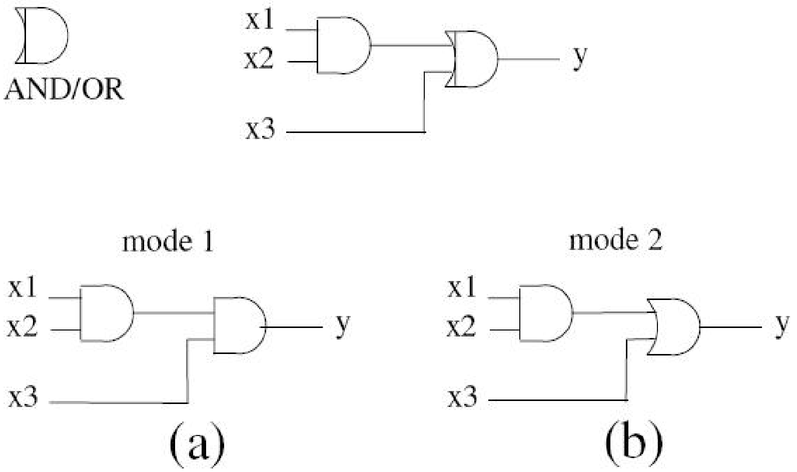

Fig. 1. Example of a polymorphic module with AND/OR gate: (a) $y = x1.x2.x3$ (b) $y = x1.x2 + x3$ [9].

3 Linear Threshold Unit

In this section a formal definition of the function computed by a linear threshold gate is given. Then, we show examples of Boolean functions that can be implemented by a single *LT* element, in particular, we show how to compute *AND*, *OR*, and *MAJ*, defined below. Circuits composed of linear threshold gates are called *linear threshold circuits*, or *LT* circuits. Those have binary inputs and output. They are mathematically described by a *linear threshold function*.

Definition 1. (Linear Threshold Function)

A linear threshold function of *n* variables is a Boolean function $f : \{0,1\}^n \rightarrow \{0,1\}$ that can be written, for any $x \in \{0,1\}^n$ and a fixed $w \in \Re^{n+1}$, as:

$$f(x) = \operatorname{sgn}(F(x)) = \begin{cases} 1 & \text{for } F(x) \geq 0 \\ 0 & \text{otherwise} \end{cases} \tag{1}$$

$$\textit{where } F(x) = w \cdot (1, x) = w_0 + \sum_{i=1}^{n} w_i x_i$$

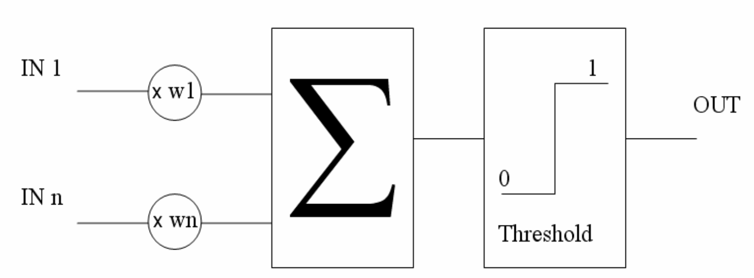

Fig. 2. Linear threshold element $y = \operatorname{sgn}\left(-t + \sum_{i=1}^{n} w_i x_i\right)$

3.1 *LT* representation of *OR*

The logical disjunction, *OR*, is a simple Boolean function of *n* variables:

$$OR(x_1,\ldots,x_n) = \begin{cases} 0 & \text{if} \quad (x_1,\ldots,x_n) = (0,\ldots,0) \\ 1 & \text{otherwise} \end{cases} \tag{2}$$

It can be implemented by a threshold gate, i.e., for all *n*, there exists a weight vector, $(w_1,\ldots,w_n)$, such that:

$$\forall x \in \{0,1\}^n, \qquad OR\,(x_1,\ldots,x_n) = \operatorname{sgn}\left(w_0 + \sum_{i=1}^{n} w_i x_i\right) \tag{3}$$

To implement *OR* one needs unit weights and a threshold, w_0, of -1.

$$w = (-1,1,\ldots,1)$$

$$OR(x_1,x_2) = \operatorname{sgn}\left(-1 + \sum_{i=1}^{n} x_i\right) \tag{4}$$

Table 1 shows the case of $n = 2$.

Table 1. 2-variable disjunction, $OR(x_1,x_2) = \operatorname{sgn}(-1 + x_1 + x_2)$

x_1	x_2	$-1 + x_1 + x_2$	$\operatorname{sgn}(-1 + x_1 + x_2)$	$OR(x_1,x_2)$
0	0	-1	0	0
0	1	0	1	1
1	0	0	1	1
1	1	1	1	1

3.2 *LT* representation of *AND*

The logical conjunction, *AND*, is also a linear threshold function ($AND \in LT$):

$$AND(x_1, x_2) = \operatorname{sgn}\left(-n + \sum\nolimits_{i=1}^{n} x_i\right) \tag{5}$$

Table 2 shows the case of $n = 2$.

Table 2. 2-variable conjunction, $AND(x_1, x_2) = \operatorname{sgn}(-2 + x_1 + x_2)$

x_1	x_2	$-2 + x_1 + x_2$	$\operatorname{sgn}(-2 + x_1 + x_2)$	$OR(x_1, x_2)$
0	0	-2	0	0
0	1	-1	0	0
1	0	-1	0	0
1	1	0	1	1

3.3 *LT* representation of *MAJ*

The majority function, *MAJ*, is a Boolean function that outputs 1 if half or more than half of its input variables are 1s. Definition of the majority function:

$$MAJ(x_1, \ldots, x_n) = \begin{cases} 1 & \text{if } \sum_{i=1}^{n} \mathrm{x_i} \geq \left\lceil \frac{n}{2} \right\rceil \\ 0 & \text{otherwise} \end{cases} \tag{6}$$

One choice of weights is:

$$w = \left(-\left\lceil \frac{n}{2} \right\rceil, 1, \ldots, 1 \right) \tag{7}$$

$$MAJ(x_1, \ldots, x_n) = \operatorname{sgn}\left(-\left\lceil \frac{n}{2} \right\rceil + \sum_{i=1}^{n} x_i \right) \tag{8}$$

All these three Boolean functions are symmetric, which means that the output depends on the number of 1s in the input vector irrespective of their position. For all symetric function that are also linear threshold functions, $w_1 = w_n = \ldots = w_n$. That is quite convinient, because the weights can then be set all to 1. Note that parity function, *XOR*, is also symmetric, but it is not linear threshold function ($XOR \notin LT$).

4 Conclusion

It was shown, that it is possible for one *LT* gate to compute different simple *LT* functions like *OR, AND,* and *MAJ* in dependence on choosing the threshold value. Thus, the *LT* unit can behave like polymorfic gate. The question is: How can this fact be useful? As above, the main problem area concerning polymorfic circuits is design of those circuits. Can we use the well-known theory of *LT* units on solving problems of polymorfic circuits mentioned above? This remains the subject of our further work.

References

1. M. Bidlo and L. Sekanina: Providing information from the environment for growing electronic circuits through polymorphic gates. In *Genetic and Evolutionary Computation-Conference (GECCO2005) workshop program*, pages 242–248, Washington, D.C., USA, 2005. ACM Press.
2. M. Muroga: Threshold logic and its applications. Wiley-Interscience, 1971
3. L. Sekanina. Design Methods for Polymorphic Digital Circuits. In *Proc. of the 8th IEEE Design and Diagnostics of Electronic Circuits and Systems Workshop DDECS 2005*, pages 145–150, Sopron, Hungary, 2005. University of West Hungary.
4. L. Sekanina. Evolutionary design of gate-level polymorphic digital circuits. In *Applications of Evolutionary Computing*, volume 3449 of *LNCS*, pages 185–194, Lausanne, Switzerland, 2005. Springer Verlag.
5. L. Sekanina: Design and Analysis of a New Self-Testing Adder Which Utilizes Polymorphic Gates, In: 2007 IEEE Workshop on Design and Diagnostics of Electronic Circuits and Systems, Gliwice, PL, IEEE CS, 2007, s. 243-246, ISBN 1-4244-1161-0
6. A. Stoica, R. S. Zebulum, and D. Keymeulen: Polymorphic electronics. In *Proc. of Evolvable Systems: From Biology to Hardware Conference*, volume 2210 of *LNCS*, pages 291–302. Springer, 2001.
7. A. Stoica, R. S. Zebulum, D. Keymeulen, and J. Lohn: On polymorphic circuits and their design using evolutionary algorithms. In *Proc. of IASTED International Conference on Applied Informatics (AI2002),* Insbruck, Austria, 2002.
8. A. Stoica, R. Zebulum, X. Guo, D. Keymeulen, I. Ferguson, and V. Duong: Taking Evolutionary Circuit Design From Experimentation to Implementation: Some Useful Techniques and a Silicon Demonstration. *IEE Proc.-Comp. Digit. Tech.*, 151(4):295–300, 2004.
9. L. Sekanina, T. Martínek, Z. Gajda: Extrinsic and Intrinsic Evolution of Multifunctional Combinational Modules, In: 2006 IEEE World Congress on Computational Intelligence, CA, US, IEEE CIS, 2006, s. 9676-9683, ISBN 0-7803-9489-5

Spectral Graph Partitioning

Pavla Kabelíková

Department of Applied Mathematics, FEECS,
VŠB – Technical University of Ostrava, 17. listopadu 15, 708 33 Ostrava – Poruba
`pavla.kabelikova@vsb.cz`

Abstract. For parallel computing, large computational graphs are partitioned into subdomains and distributed over individual processors. Finding partitioning with minimum edge cut is, in general, an NP-complete problem. We will present suitable heuristics for graph partitioning based on spectral methods. Spectral methods for graph partitioning have been known to be robust but computationally expensive, however, recent development of hardware and software makes these methods interesting for practical applications. The separator produced by spectral methods is related to second smallest eigenvalue of discrete Laplacian matrix - the Fiedler value and to corresponding eigenvector - the Fiedler vector.

Keywords: graph partitioning, spectral methods, Lanczos algorithm, sparse matrix, Fiedler value, Fiedler vector

1 Introduction

For parallel computing, large computational graphs are partitioned into subdomains and distributed over individual processors. The cost of communication between processors depends on the number of edges between different subdomains. Load balance constraints require (approximately) equal-sized subdomains.

Finding a partition with minimum number of edges cut is, in general, an NP-complete problem. Suitable heuristics are based on spectral methods. Spectral methods for graph partitioning have been known to be robust but computationally expensive, however, recent development of hardware and software makes these methods interesting for practical applications. The separator produced by spectral methods is related to second smallest eigenvalue of discrete Laplacian matrix - the Fiedler value and to corresponding eigenvector - the Fiedler vector.

For computational needs, the graph partitioning algorithms have been implemented under C++. Results of numerical experiments are also presented. They show spectral methods can effectively generate the partitions of computational graphs in reasonable time.

2 Basic technique

The basic technique for partitioning of graphs is spectral bisection. In its simplest form, one step of spectral bisection comprises the generation of the discrete

© Václav Snášel (Ed.): WOFEX 2007, pp. 285–290, ISBN 978-80-248-1571-8.
VŠB – Technical University of Ostrava, FEECS, 2007.

Laplacian matrix of the graph, the evaluation of an eigenvector corresponding to the second-smallest eigenvalue, and the partitioning of the graph into two components A and B, according to the sign pattern of the eigenvector components. The set of edges joining A and B is an edge separator in the graph G.

Spectral bisection algorithm

Input: a graph $G = (V, E)$
Output: graphs $G_1 = (V_1, E_1)$, $G_2 = (V_2, E_2)$

```
1. set up the discrete Laplacian matrix L of G
2. compute the second eigenvector $v$
3. search median of $v$
4. for each node i of G
   4.1. if ( $v(i) \leq median$) put node i in partition $V_1$
   4.2. else put node i in partition $V_2$
5. $E_1$ ... set of edges with both end vertices in $V_1$
   $E_2$ ... set of edges with both end vertices in $V_2$
6. set up the graphs $G_1 = (V_1, E_1)$, $G_2 = (V_2, E_2)$
7. end
```

Since L (Laplacian matrix of given graph) is a sparse symmetric positive semidefinite matrix in all practical applications, suitable algorithm for computing the second eigenvector (Fiedler eigenvector) is the Lanczos algorithm.

3 Improvements of basic algorithms

In the simplest form, the spectral bisection decomposes graphs recursively into a power of two partitions. To alow decomposition of the graphs into arbitrary number of partition there is considered also k-way partitioning. The main idea is to apply the spectral bisection as much as necessary, exactly until we have desired count of parts (say k). There are two posibilities. When k is power of two, we use recursive bisection in its simple form and median as the splitting value. When k is not power of two, we have to use another quantil to get appropriate partitions.

Furthermore, some modifications to the Lanczos algorithm for computation of the second smallest eigenvector are necessary. The original Lanczos algorithm delivers very good approximations to the large eigenvalues instead of converging to the desired second smallest eigenvalue. At first, we explicitly orthogonalize the current Lanczos vector v to the first eigenvector $e = (1, 1, .., 1)^T$. In this way, we always stay in the subspace orthogonal to e while the eigenvalue zero is removed from the problem. Second, shift of spectrum follows.

For working purposes, we have also included partitioning of disconnected graphs. We have found that a Breadth First Search algorithm is an efficient tool for finding all connected components. After obtaining a list of all components, the problem is reduced to partitioning of one connected component.

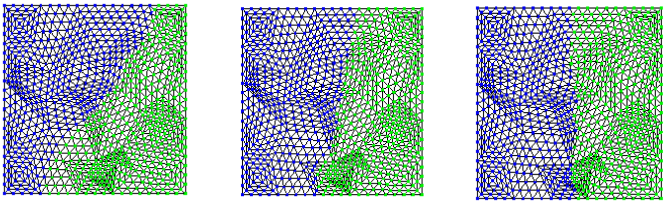

(a) tolerance=10^{-4}, $|E'| = 63$

(b) tolerance=10^{-3}, $|E'| = 64$

(c) tolerance=10^{-2}, $|E'| = 67$

Fig. 1. `square2` in two parts

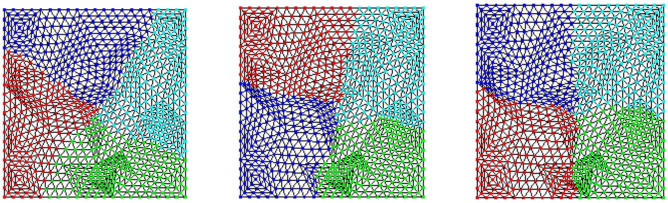

(a) tolerance=10^{-4}, $|E'| = 134$

(b) tolerance=10^{-3}, $|E'| = 129$

(c) tolerance=10^{-2}, $|E'| = 126$

Fig. 2. `square2` in four parts

4 Results

We have tested the algorithms on a given testing set of graphs. The partitioning corresponding to the discretization of one of them[1] is shown in Figures 1,2. In Figure 1, there is shown two parts partitioning in dependence on tolerance in the Lanzcos algorithm, In Figure 2, there is four parts partitioning correspondingly. The tolerance 10^{-4} turned out to be sufficient to get the optimal edge cut $|E'| = 63$. In case of two parts, it turned out that increasing of the precision of tolerance has only small influence on count of divided edges as we assumed. Different situation arises in case of partitioning into four parts. There is a turn in points $[10^{-3}, 129]$ and $[10^{-2}, 126]$. Explanation of this situation is as following. In k-way partitioning, there should hold the conditions of optimality in each level separately, but in global view there could exists some better partitioning which is not optimal in lower levels but which is optimal in global view. Specifically, the optimal four-cut $|E'| = 126$ corresponds to suboptimal two-cut $|E'| = 67$.

For testing maximal performance, we have worked with large graphs. The biggest graph that we have tested has 3 375 000 vertices and 1 005 750 edges. The

---

[1] `square2`, 857 vertices, 2 488 edges

Table 1. Software performance in dependence on count of nodes - large graphs

NAME	$\|V\|$	$\|V\|$	time[s]	L. steps	$\|E'\|$	VM size .. max size
`large_cube1`	125000	367500	4	120	4669	18 MB .. 146 MB
`large_cube2`	421875	1248750	54	160	9565	59 MB .. 670 MB
`large_cube3`	857375	2545050	106	199	18317	88 MB .. 260 MB
`large_cube4`	1000000	2970000	137	197	19133	101 MB .. 315 MB
`large_cube5`	1520875	4522950	233	201	23483	149 MB .. 463 MB
`large_cube6`	2197000	6540300	372	217	31399	214 MB .. 670 MB
`large_cube7`	3375000	10057500	599	242	41405	325 MB .. 1048 MB

results are presented in Table 1, where $|V|$ denotes the size of vertex set (count of vertices), $|E|$ denotes the size of edge set (count of edges), L.steps means count of steps in Lanczos algorithm, $|E'|$ denotes the size of edge separator (count of cutted edges), the VM size means the count of bytes allocated at the beginning in virtual memory, and the max size means the maximum of bytes used during computation. The fourth column shows total computing time.

We have used the *number of partition = 2* and *Lanczos tolerance = 0.001*. All this graphs represent cubic grid with maximal degree of vertex equal six. As we can see from the table, the main limitation is the space memory. Starting from `large_cube3` we had to swap (on hard disk memory). This explains that the maximal size required for the partitioning of `large_cube3` is smaller than that for the two previous graphs. We can also see that the main limitation is the size of operating memory (or the size of addressable space).

We can see the quality of graph partitioning in Figure 3. This graph contains 26 487 vertices and 152 938 edges. In part (a), there the two-parts partitioning is shown, in part (b), there we can see the four-parts partitioning. We have used the *Lanczos tolerance = 0.0001*.

5 Conclusion

We have investigated various strategies how to achieve an optimal mesh partitioning in a reasonable time. The set of test matrices was used to test the influence of parameters to resultant quality of partitioning. There were also used some large graphs to find the limitation of written software.

As we have found out, the main limitation is the size of operating memory. This bottleneck can be partially relieved by an external memory. There is also the possibility to use another store structure in the program to decrease the storage space requirements. Moreover, using of another algorithm for computing of the second smallest eigenvector instead od the Lanczsos algorithm is a good way how to decreace time and space requirements.

On the other hand, we have also brought a new tool for visualization of mesh partitioning.

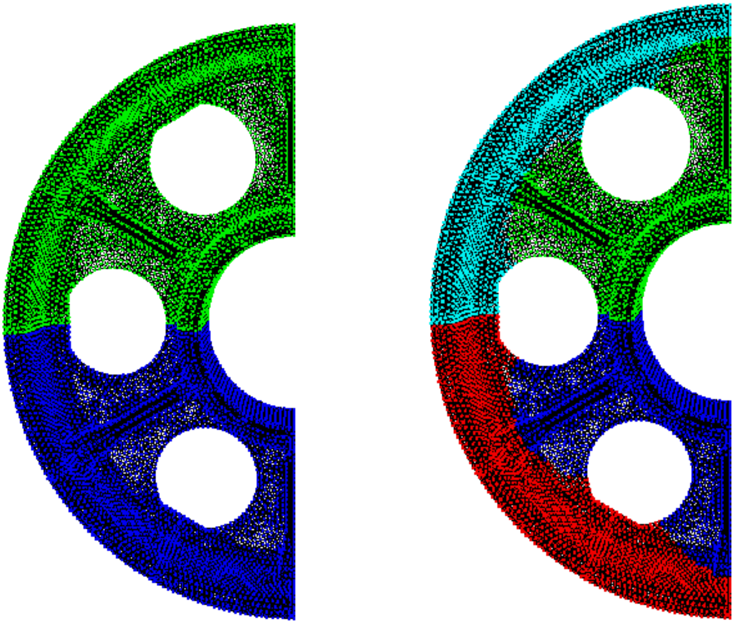

(a) Graph in two parts (b) Graph in four parts

Fig. 3. Example of partitioning

The results of this work were published in collection of SNA 2007 conference and they were also presented in CSGT 2007 conference. An article to Digital Technology Journal is in preparation.

References

1. W. N. Anderson and T. D. Morley, *Eigenvalues of the Laplacian of a graph*, Linear and Multilinear Algebra, 18:141-145, 1985
2. S. T. Barnard and H. D. Simon, *A Fast Multilevel Implementation of Recursive Spectral Bisection for Partitioning Unstructured Problems*, Concurrency: Practice and Experience, 6(2):101-117, 1992
3. J. Demmel, *http://www.cs.berkeley.edu/∼demmel/cs267/*, University of California at Berkeley, 1996
4. F. R. K. Chung, *Spectral Graph Theory*, Regional Conference Series in Mathematics, 92:0160-7642, 1994
5. M. Fiedler, *Algebraic connectivity of graphs*, Czech. Math. J., 23(98):298-305, 1973
6. M. Fiedler, *A property of eigenvectors of nonnegative symmetric matrices and its application to graph theory*, Czech. Math. J., 25(100):619-633, 1975
7. G. H. Golub and C. F. Loan, *Matrix Computation*, John Hopkins University Press, Baltimore, MD, Second edition, 1989
8. P. Kabelikova, *Graph partitioning using spectral methods*, Institute of Geonics, Ostrava, 978-80-86407-12-8, 2007

9. B. Mohar, *The Laplacian spectrum of graphs*, Preprint Series Dept. Math. University E. K. Ljubljana 26, 261, 1988
10. B. N. Parlett, H. Simon and L. M. Stringer, *On Estimating the Largest Eigenvalue With the Lanczos Algorithm*, Math. Comp., 38(157):153-165, 1982
11. A. Pothen, H. D. Simon and K. Liou, *Partitioning Sparse Matrices with Eigenvectors of graphs*, SIAM J. Matrix Anal. Appl., 11(3):430-452, 1990
12. R. Pozo, K. Remington and A. Lumsdaine, *SparseLib++ Sparse Matrix Class Library, http://math.nist.gov/sparselib++/*, 1996
13. W. H. Press, S. A. Teukolsky, W. T. Vetterling, B. P. Flannery, *Numerical Recipiens in C*, Cambridge University Press, Second edition, 1992
14. H. D. Simon and S.-H. Teng, *How good is Recursive Bisection*, SIAM J. Sci. Comput., 18(5):1436-1445, 1997
15. D. A. Spielman and S.-H. Teng, *Spectral Partitioning Works: Planar graphs and finite element meshes*, Technical Report UCB//CSD-96-898, University of Berkeley, 1996

Brain for Agents in Multi-agent Systems

Ondřej Kohut

Department of Computer Science, FEECS,
VŠB – Technical University of Ostrava, 17. listopadu 15, 708 33 Ostrava – Poruba
ondrej.kohut.fei@vsb.cz

Abstract. This paper concerns with suggestion of a software brain for agents in multi-agent systems. The base schema of the whole brain is presented and one of its units – Prolog-brain – is described in detail. It is shown how the data translation is performed in order to prepare suitable conditions for correct decision making. Also manners of usage of the agent's brain is written here.

1 Introduction

Currently the Laboratory of intelligent systems (LabIS) is working on the project "Logic and Artificial Intelligence for multi-agent systems". This research group consists of several teams. I am a member of the team of logicians. The object of our research is to develop software brain for agents in multi-agent systems (MAS). The agents in MAS have to be able to do independent determination, so it is for each agent necessary to have his own efficient brain. In following sections it will be described a suggestion of agent's brain and current state of research.

2 Concept of the agent's brain

Any final vision of the whole agent's brain is not set yet. But I describe my idea which is gradually realizing. At this time the brain is divided into four parts: *Prolog-brain*, *TIL-brain*, *Computational-brain* and *Brain-interface*. In the future it could be added other brain units written in various programming languages. Now the *Prolog-brain* makes simple decisions by use of *Prolog*[1]. The *TIL-brain* based on Transparent intensional logic (TIL) will provide communication among agents and supports artificial intelligence rules solving more complex problems whereas for simple tasks could be called the *Prolog-brain*. It is also planned to use this unit for execution logical analysis of the natural language in the future. TIL is described for example in [1]. These both inference units will keep at disposition the services of the *Computational-brain* for auxiliary computations (e.g. finding the shortest path in a graph). Thus this unit can be seen as a library of computational procedures. The

---

[1] In the project is used tuProlog, software engine programmed in JAVA language. http://www.alice.unibo.it:8080/tuProlog/

© Václav Snášel (Ed.): WOFEX 2007, pp. 291–296, ISBN 978-80-248-1571-8.
VŠB – Technical University of Ostrava, FEECS, 2007.

choice of proper inference unit for decision-making will be made by the *Brain-interface*. The schema of the brain is illustrated in fig. 1.

Today the operational and still evolving unit is the Prolog-brain. The *TIL-brain* is under development. The *Computational-brain* is still empty because it's no need of complex calculations at present. Also the *Brain-interface* is not implemented yet; all queries are implicitly sent to *Prolog-brain*. The selection of the correspondent inference unit could be executed by the *Brain-interface* as follows.

If the incoming message came from agent's sense organs[2] (it usually contains a description of the agent's environment and as an answer is required some action) then it is called the *Prolog-brain*. For example an agent-driver is going on a road and his perception is sending to his brain the information about the infrastructure he's moving over. That is what lane is he moving on, how far is a following crossroad, how the crossroad looks like, which other agents occur in the environment and lot of others. Afterwards the *Prolog-brain*, according to these information and his own knowledge (rules written in *Prolog*), chooses the most proper reaction to given situation, i.e. speed up, speed down, change lane and others.

If the message is coming from another agent then they are used services of the *TIL-brain*. Agents will communicate mutually by means of *TIL-Script* language what is computer version of the language of TIL-constructions. It results from TL OWL language which has been published in [2]. The *TIL-Script* language is still in development. The *TIL-brain* unit will be working for example during the communication between agent-driver and agent-dispatcher.

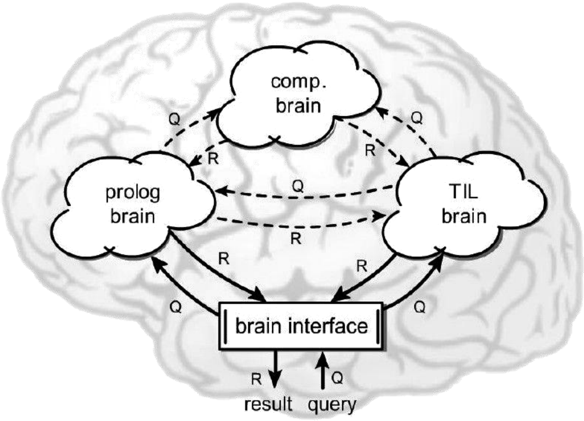

Fig. 1. Schema of the agent's brain.

---

[2] Of course the agent under consideration has no real sense organs. Information about agent's environment is sent by infrastructure which is an agent too. Nevertheless for clearness and some analogy with the real world I keep this term.

3 Prolog-brain

Function of this unit is to transform data sent by agent perception in XML format to prolog query, give to the Prolog and obtained answer-action convert to XML document again and send to agent's "body". The data contain agent's visibility, i.e. a part of the static infrastructure, obstacles and other agents seen by the agent. It's necessary to translate this data into relative point of view of the observing agent, i.e. enumerate road elements and lanes and convert orientation of agents and all elements in the face of observer. This is performed by *Prolog-brain interface*. Each agent keeps at disposition his own *memory* in the brain. In the *memory* an agent can remember what the maximum allowed speed is in the actual segment in accordance to traffic signs passed by the agent during his journey. From the *Prolog-brain interface* goes a prolog query to the *Prolog-engine*. Prolog answer is then packed by the *Prolog-brain interface* to XML. Schema of the *Prolog-brain* unit is shown in fig. 2.

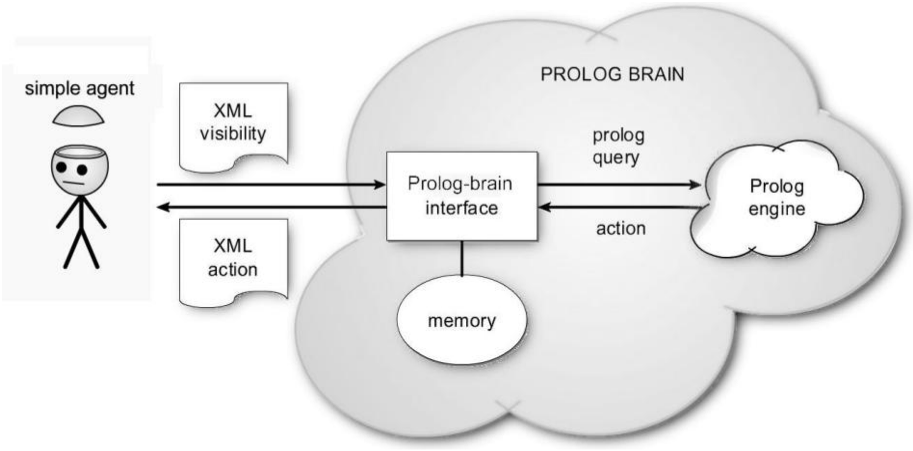

Fig. 2. Schema of the *Prolog-brain*

3.1 Transformation to the relative point of view

Before the Prolog engine makes decision it's necessary to transform data in absolute form to the relative form. The infrastructure contains roads and crossroads. Every road is divided into road-elements and each road-element includes traffic lanes. All these elements are defined absolutely and they form a static infrastructure. The infrastructure is occupied by agents. To resolution by Prolog it's useful to renumber road-elements and lanes, and convert orientation of lanes and other agents. For illustration I describe how is the direction-translation performed.

All roads has some direction in the static infrastructure. This direction is inherited by included road-elements. The orientation of lanes is set with respect to the road-element. For the agent it is significant to know about each lane if its direction is consistent with his orientation. As regards other agents it's essential if an agent is going in the same direction as the agent-observer or against him.

At first we must determine as the roads are consistent with the agent's direction. If the processed road is the agent's current road than the consistency is computed as follows:

Let's define logical variable A_O and L_O.

$$A_O = \begin{cases} true, & \text{if the } \textit{absolute direction} \text{ of the } \textit{observer}- \text{agent is } \textit{forward} \\ false, & \text{otherwise} \end{cases}$$

$$L_O = \begin{cases} true, & \text{if the } \textit{absolute direction} \text{ of the } \textit{observer}\text{'s lane is } \textit{forward} \\ false, & \text{otherwise} \end{cases}$$

Then C is defined as follows:

$$C = A_O \wedge L_O \vee \overline{A_O} \wedge \overline{L_O} \tag{1}$$

The current road is consistent if C is true, inconsistent otherwise. For determination the consistency of other road we result from the fact that orientation of the road is defined by its start and end intersection. The roads over the crossroad are consistent if the current following intersection corresponds to their start-intersection. And further roads (which are not connected to the current road) are irrelevant.

Obtaining the relative lane's direction is very simple:

$$lane's\ relative\ direction = \begin{cases} lane's\ absolute\ direction, \text{if the road is } \textit{consistent to observer} \\ reverse\ lane's\ absolute\ direction, \text{otherwise} \end{cases}$$

Now we can determine orientation of the other agents. Let's define logical variable A and L:

$$A = \begin{cases} true, & \text{if the } \textit{absolute direction} \text{ of the agent is } \textit{forward} \\ false, & \text{otherwise} \end{cases}$$

$$L = \begin{cases} true, & \text{if the } \textit{relative direction} \text{ of the agent's lane is } \textit{forward} \\ false, & \text{otherwise} \end{cases}$$

Then RA is defined as follows:

$$RA = A \wedge L \vee \overline{A} \wedge \overline{L} \tag{2}$$

Now we can obtain agent's relative direction:

$$Agent's\ relative\ direction = \begin{cases} forward, & if\ RA\ is\ true \\ backward, & otherwise \end{cases}$$

The modification of the orientation is illustrated in fig. 3. There are also shown renumbered road-elements. Renumbering of lanes isn't presented with regard to greater clarity.

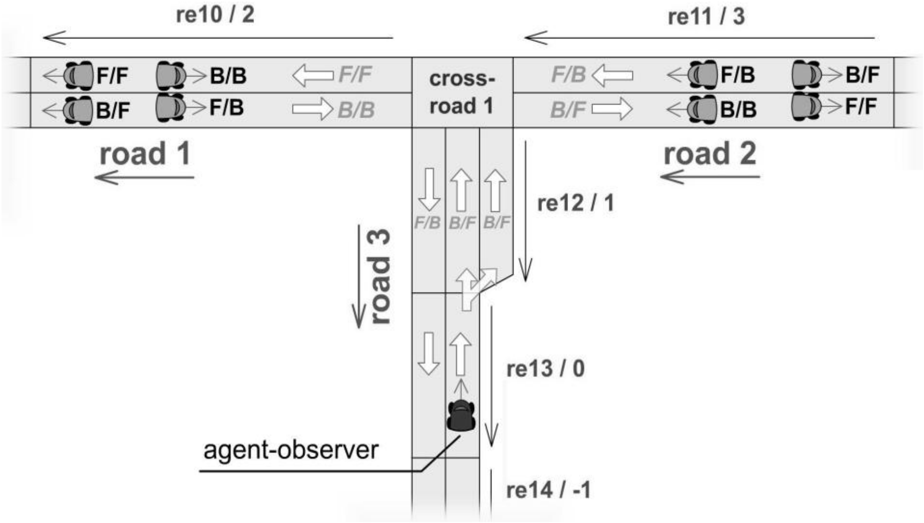

Fig. 3. The illustration of the modification the data into the form relative to the agent-observer. Before the slash is the absolute orientation, behind it is the relative orientation. F-*forward*, B-*backward*

After the data conversion to the observer's point of view and forming the prolog query, this query is given to the prolog engine. I won't describe the prolog rules because it's business of the other members of the team. I take care of the data preparation and the brain as a whole.

4 Usage of the brain

Prolog-brain is programmed in JAVA language. Thus the agent made by use of JAVA technology can keep his own brain as a JAVA object and use its services very simply and very fast. The both query and result are sent in XML format. If an agent cannot have his own brain (e.g. an agent created in a different programming language) then it's possible to use the Brain Server which manages particular brains and provides their inference services. The server keeps a collection of brains and it asks appropriate brain according to agent's ID. Internal and external brain are diagrammed in fig. 4.a and 4.b respectively. Both these alternatives were tested in multi-agent system created by JADE framework [3].

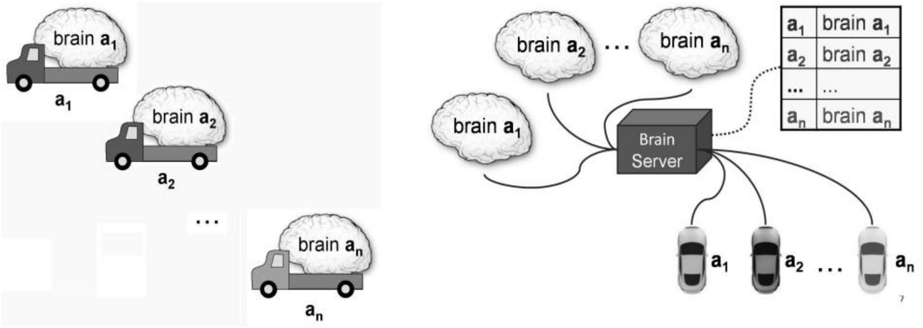

(a) (b)

Fig. 4. Variations of using the brain: (a) internal brain, (b) external brain

5 Conclusion

In this paper I present my design of the agent's brain. It's shown what important units should be contained in the brain and how the present state looks like. Also it's briefly described how the data are transformed from absolute form to the description relative to agent-observer. The prolog brain is working and has been tested in a simulation environment and is still in development.

6 Future work

In the future I propose to further evolve the brain and to attempt to make it universal as much as possible. The Prolog-brain will be advanced henceforth. Particularly I intend to deal with the TIL-brain, in the concrete with its fuzzy module for vague concepts processing. Fuzzy approach is not still defined in TIL while it is very important.

This research has been supported by the program "Information Society" of the Czech Academy of Sciences, project No. 1ET101940420 "Logic and Artificial Intelligence for multi-agent systems"

References

1. Duží, M.: Intensional Logic and the Irreducible Contrast between de dicto and de re, ProFil Vol. 5, No. 1, 1-34, (ISSN 1212-9097), 2004
2. Müller, J.: TL - Content Language Based on Transparent Intensional Logic. In WOFEX 2005, 2005
3. http://jade.tilab.com/

Control System for Robot Soccer Game Category MiroSot and SimutoSot

Jan Kožaný[1], Petr Tučník[2]

[1]Department of Computer Science, FEECS,
VŠB – Technical University of Ostrava, 17. listopadu 15, 708 33 Ostrava – Poruba
`jan.kozany@vsb.cz`
[2]Department of Information Technologies, Faculty of Computer Science and Management, University of Hradec Kralove, Rokitanskeho 62, 500 03 Hradec Kralove, Czech Republic
`petr.tucnik@uhk.cz`

Abstract. Control system is an important component of the robot soccer game. Control system runs at the computer and has to do all necessary work at every game's iteration: image recognition, strategy computation, data logging etc. We have developed our control system with strategy module and we used them in two robot soccer category: at the real case with real robot and camera (MiroSot) and at the simulated case with robot soccer simulator (SimuroSot).

Keywords: Robot soccer control system, MiroSot, SimuroSot

1 Introduction

The control mechanism of the robot soccer team is generally difficult to design. Because every individual player has to make decisions accordingly to his actual situation and the team as a whole has to coordinate its actions, there is a need to make proper decisions and to make them quickly. For every decision-making cycle, there is a time limit given above all by the speed of image processing mechanism.

The multicriterial decision-making principle was chosen to be control mechanism of the strategic module because of its adaptability potential. In the robot soccer environment, the situation is evolving quickly and adaptability to the given situation is utmost necessity. The robots are moving in the speed about 1,5 [m/s] (they may be faster, but we are limited by the playground dimensions and image processing speed) and when the image transfer speed and its processing speed are taken into account, there is a limit of approximately 33 [ms] in which every individual agent (and a team as a whole) has to make a decision.

© Václav Snášel (Ed.): WOFEX 2007, pp. 297–302, ISBN 978-80-248-1571-8.
VŠB – Technical University of Ostrava, FEECS, 2007.

This is quite a strict condition, as there is a huge number of possible solutions, options and developments.

For better understanding (or basic overview) of agent-oriented terms see [6] or [1]. We will not present definitions of these terms here for it is not necessary.

2 Robot soccer control system

Naturally, good strategies are needed to decide the roles and actions of the team robots during the game. But to be effective, they need to be organized into an architecture for proper management and control. The general performance of the host system depends on the selected control architecture [5].

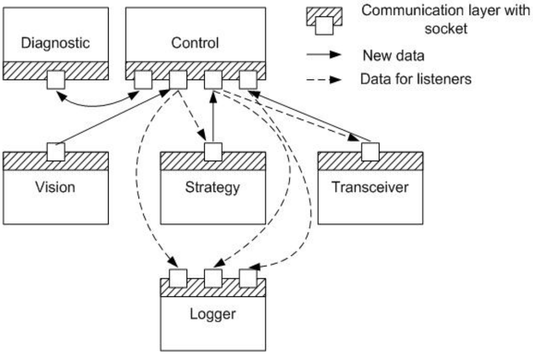

Fig. 1. The control system for robot soccer MiroSot category

Our system is divided into 6 modules, as depicted at Fig. 1. Communication among them is realized via sockets. We use the client/server architecture. The clients can communicate only via the server, which is the control module.

The data flow begins in the vision module, which analyzes the camera data in order to recognize all the robots (agents) and the ball. The vision system then sends the coordinates of the recognized agents and the ball to the control server module, which forwards the vision data to the strategy module. The data processing here is quite involved so that it will be described later on in more details. The output strategy data contains instructions for the robots on how to move next. They are forwarded to the transceiver module via the server again. At the end, the transceiver sends the instructions to the agents, which ends the data flow. This process runs more than 10 times per second while using multiple threads for the particular module processes. Moreover, there are two additional modules in the system. The diagnostic module serves as a real time diagnostic utility. The logger module is important for the subsequent game analysis, as it monitors the work of the whole system.

The strategy module is divided into three levels, according to the nature of the decisions to be made. There is a gradual degradation of the centralized nature of the decisions towards an autonomous control during the process. The high level strategy is responsible for situation assessment and reaction selection. The medium level deals with roles assignment and task specification and instructions are generated at the low level. Detailed description of our strategy module has been introduced in our publications.

3 Differences between real and simulated robot soccer

We have tried to use our strategies developed for "real world" robot soccer in the simulated robot soccer. We are dealing with FIRA robot soccer platform, middle MiroSot league (5-a-side) [2]. Two wheel robots are playing soccer on the pitch [3]. A vision camera overlooking the pitch is used for centralized video processing. The pictures from camera are transformed to host computer. There are recognized robots' positions and their angles and ball's position. This information is forwarded to our strategy module. There are some decision-making processes performed and instructions of our robots' wheel velocities are the result. This result is transferred to robot by wireless transceiver and robots immediately adjust these velocities accordingly to these instructions. This is the iteration cycle of robot soccer game in the middle MiroSot league.

The simulated-robot soccer tournament (SimuroSot) is basically similar as MiroSot but it is played in a computer simulated environment. Without the robot and vision processing hardware, the problems with physical environment of the robot soccer are reduced and it becomes possible to focus on strategy development for the middle league (5-a-side) in SimuroSot [4]. The computer simulated environment consists of simulator and two teams strategies. Simulator simulates physical motion of two wheel robots, checks and solves collisions among robots and among robots and ball. Robots are controlled by settings their wheel velocities. The control is very similar to the real robot hardware. Because of similar nature of strategies and robot control in MiroSot and SimuroSot we have decided to try our strategies developed for MiroSot into SimuroSot.

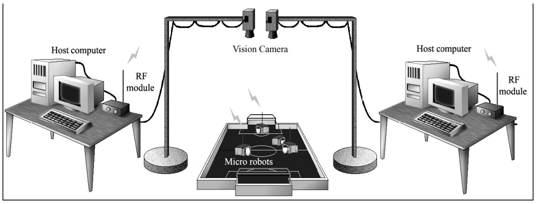

Fig. 2. The overall system for robot soccer MiroSot category

As it is depicted at Fig. 2, the strategy module is one part of robot soccer control system. We have modified the strategy module interface, so now we can use it with the simulator. The interface between simulator and strategy module is well-defined. From the strategy developer point of view, the start of the game iteration is in the moment when the simulator provides positions and angles of all robots and position of the ball at the pitch to the strategy module. Then it expects wheel velocities for our team robot. The strategy module has to make strategy decisions, transfer them into wheel velocities and return them to the simulator. This is the end of the game iteration. Simulator asks both teams for wheel velocities simultaneously. In the next step, it internally sets the wheel velocities to robots' wheels, compute physical motion, checks and solve the collisions. The next iteration begins after a certain time period.

After modifying the strategy module interface we have to revise low-level component of our strategy module due to the different physical motion of real robot hardware and of the simulated robot. Other modifications were not necessary; we were able to play a game. It was due to the proper design of strategy module.

As we expected, the main differences between real and simulated case are physical motion of the robot and the image recognition. There are usually non optimal conditions in the real case, because there are always some noises present. We will describe the main issues that we have to deal with when we are trying to develop a strategy for MiroSot and SimuroSot.

In the real case, the robot can slip on the surface of the pitch when the robot's wheel velocity is changing. In addition, the strategy module recognises slipping after a certain time period due to the image processing delay. In order to minimize robot's wheels' slipping it is necessary to recognize three states of robot movement: acceleration (robot accelerates, its velocity rapidly increases), main movement (robot's velocity is approximately constant) and breaking (robot's velocity rapidly decreases). We must not allow changing robot's velocity too rapidly, especially at the acceleration and breaking phases, in order to minimize the probability of slipping. The simulator does not simulate any slipping and it is easier to develop the robot soccer motion for simulator than for real case.

Another big difference is in the image recognition. In the real case the camera situated over the playground takes the picture and transfers them into host computer. Then there are recognized colour segments at the picture, the colour segments are matched with robot labelling, robots' positions and angle and ball position are recognized and transferred to the strategy module. During image recognition process it is possible that some inaccuracies occurs in robot's or ball positions due to some reflections of beholders' shadows on the surface of the pitch or different noise at the picture. Strategy has to make its decisions-making with (reasonably) inaccurate and incomplete information. The simulator does not simulate any noise from image recognition module. All information provided by the simulator is accurate and complete.

Generally, it is easier to develop a strategy for the simulator. But simulator has one big disadvantage: it should simulate real life environment and no simulator can do this faultlessly. Moreover, SimuroSot simulator contains some big mistakes, for example it allows two robots to be at the same place at the same time etc. It is easier to transfer strategy developed for real robot soccer hardware to simulator than transfer strategy developed for simulator to real robot soccer due to the unresolved real-life conditions issues.

There is no generally working mechanism how to objectively evaluate successfulness of the robot soccer strategy at the FIRA robot soccer platform. MiroSot teams with faster and more accurate image recognition and robots, win over the slower opponents. They have more accurate information from image recognition and they are able to use them for more effective robots' control. Robots process their order with minimum delay. It is easier to acquire the ball and shoot the goal. They do not need a sophisticated strategy; often, the good camera, image recognition and robots' hardware is enough to gain advantage and shoot at least one goal more than the opponent team. SimuroSot team that have better control of simulated robot and are able to exploit improper physical simulation of robot soccer simulator to win. They do not need a sophisticated strategy; it is enough shoot at least one goal more then opponent team due to certain errors in physical simulation of the robot motion. Therefore, the final score of the robot soccer game does not reflect the quality of strategy control only. The quality of all parts of the robot soccer system is assessed as a whole, not separately, in the game. The handicap of FIRA robot soccer platform is that we are unable to compare the qualities of strategic control mechanisms only.

4 Conclusion

The robot soccer environment brings up a challenging task in designing the control mechanism. The presented decision-making mechanism provides a great deal of adaptability potential, but it is still difficult for analysis and design. Nevertheless, the analysis and debugging issue is a problem common to all similar attempts in solving the robot soccer strategic control task. Generally, the tremendous amount of tests must be run in order to get the system work properly.

We have attended to the robot soccer European championship and World Championship. We have obtained the bronze medal from European championship. At the World Championship we did not advance in the playoff so we have been placed at the fifth to eight place. We would like to improve our robots and algorithms in order to be better in the future robot soccer tournaments.

Acknowledgement

The work and the contribution were supported by the project from Grant Agency of Czech Academy of Science - Strategic control of the systems with multiagents, No. 1ET101940418 (2004-2008) and by the project from the Czech Republic Foundation – AMIMADES, No. 402/06/1325.

References

1. J. Ferber. *Multi-Agent Systems: An Introduction to Distributed Artificial Intelligence.* Addison-Wesley, New York, 1999.
2. FIRA, federation of international robot-soccer association, *http://www.fira.net.*
3. FIRA, mirosot rules, *http://www.fira.net/soccer/mirosot/MiroSot.pdf.*
4. FIRA, simurosot rules, *http://www.fira.net/soccer/mirosot/MiroSot.pdf.*
5. J. Kim, D. Kim, Y. Kim, and K. Seow. *Soccer Robotics (Springer Tracts in Advanced Robotics).* Springer-Verlag, 2004.
6. Aleš Kubík. *Inteligentní agenty – tvorba aplikačního software na bázi multiagentových systémů.* Computer press, 2004.

Authors' publications

1. J. Kožaný: Hybrid control architecture for robot soccer. *Ed. V. Snášel, Proceedings of WOFEX 2005*, VŠB - Technical University of Ostrava, 2005, ISBN 80-248-0866-8, p. 399-404
2. J. Kožaný and P. Tučník: Multicriterial decision-making in a robot soccer game. *Ed. V. Snášel, Proceedings of WOFEX 2006*, VŠB - Technical University of Ostrava, 2006, ISBN 80-248-1152-9, p. 364-369
3. J. Kožaný, P. Tučník, J. Pokorný, D. Lukáš and V. Srovnal: Software structure of a control system for the mirosot soccer game. *Ed. N. Weiss, N. Jesse, B. Reusch, Proceedings of FIRA RoboWorld Congress 2006*, Dortmund: University of Dortmund, 2006, ISBN: 3-00-019061-9, p. 183-188
4. P. Tučník and J. Kožaný: Multicriterial decision-making in a robot soccer strategies. In *Proceedings of ICINCO 2007*, Angers, France, 2007, ISBN 978-972-8856-82-5, p. 428-431
5. P. Tučník and J. Kožaný: Application of the multicriterial decision-making in the robot soccer game. In *Sborník konference Řízení procesů ŘÍP 2006*, Fakulta chemicko-technologická, Univerzita Pardubice, 2006, ISBN 80-7194-860-8, p. R114-1 - R114-8
6. P. Tučník, J. Kožaný and V. Srovnal: Multicriterial Decision-Making in Multiagent System. In *Lecture Notes in Computer Science. Ed. Vassil N. Alexandrov, Geert Dick van Albada, Peter M.A. Sloot, Jack Dongarra*, Berlin: Springer, 2006, ISBN: 3-540-34383-0, ISSN: 0302-9743, p. 711-718
7. P. Tučník, J. Kožaný and V. Srovnal: Kognitivní aspekty vícekriteriálního rozhodování při rozpoznávání prostředí ve fotbale robotů v kategorii MiroSot. In *Kognice a umělý život VII*, 2007, ISBN: 978-80-7248-412-6, p. 357-364.

Embedded Vehicle Systems and Networks

Michal Krumnikl, Jan Martinovič

Department of Computer Science, FEECS,
VŠB – Technical University of Ostrava, 17. listopadu 15, 708 33 Ostrava – Poruba
{michal.krumnikl,jan.martinovic}@vsb.cz

Abstract. This paper is dealing with online communication among embedded systems in vehicles and data acquisition from on-board controlling systems and auxiliary sensors. The goal of the conducted research is to develop embedded system capable of interconnecting with standard vehicle systems and communicating via wireless networks. Several wireless technologies were presented and evaluated, considering the usability in traffic environment. These types of network architecture were considered - adhoc, infrastructure and piconet networks. The concept of the system is set to allow the basic functionality without the central node/server, by spreading information across the scattered network of mobile clients.

The proposed system is composed of embedded computers inside the vehicles and remote central storage – the informational system consisting of data storage, geographic systems, statistical and analytical modules. Such models can be used in the future for preventing and forecasting traffic jams, accidents, etc.

Keywords: embedded system, OBD–2, vehicle diagnostics, wireless networks, traffic analysis

1 Introduction

Embedded vehicle systems are subject of the research currently carried out in many laboratories of car manufacturers. The goal of conducted research is to provide safety for driver and expand potential of on-board electronics.

Despite the development of safety features, car accidents kill an estimate 1.2 million people worldwide each year, and injure about forty times this number. This means that every one and half second one man is killed or injured. Projections indicate that these figures will increase by about 65% over the next 20 years unless there is new commitment to prevention[1]. Although many accidents are caused by human factor or unpredictable situations that are difficult to alter (mechanical failures, or bad road conditions), there are already available technical solutions preventing some circumstances. Despite the fact that today's cars are equipped with anti lock braking system (ABS), electronic stability control (ESP) and many other systems enhancing the stability of vehicle, there is still a lack of more sophisticated systems actively avoiding dangerous situations.

© Václav Snášel (Ed.): WOFEX 2007, pp. 303–308, ISBN 978-80-248-1571-8.
VŠB – Technical University of Ostrava, FEECS, 2007.

Knowing these facts, we are trying to develop an embedded vehicle computer, interconnected with already existing electronic networks in the vehicle. It would be responsible for gathering data from on-board systems, analysing them and communicating with other vehicles in the range of wireless network. The analyses done by the system are aimed at providing more details concerning the traffic situation and possible threats.

2 Embedded System Overview

Several types of embedded systems were developed during the last year. The first version, using mobile phones was part of M–Net project lead by Roman Szturc. The second version was still based on M–Net protocol, but used it's own hardware consisting of Siemens TC65 modules and embedded processor controlling the communication with vehicle control units. The third version is based on PXA processors and was supported by Microsoft Academy.

The system can be divided into two parts – a computer and wireless interfaces. Each vehicle should be equipped with an embedded computer – a mobile client responsible for data processing and analysis. The solution used during the experiments consisted of these parts : embedded computer based on PXA270, vehicle diagnostics interface, GPS unit, auxiliary sensors (digital accelerometer, camera etc.) and wireless communication devices.

Data transmitted by the mobile clients are either sent to the central server or spread across the network made by vehicles – dynamical scattered networks.

2.1 Embedded Computer

The platform used in the last revision of the embedded system is Toradex Colibri - development board for Intel PXA processors. It provides serial and CAN interfaces as well as connection for LCD display used for communication with the driver.

PXAs are wide spread processors used in the majority of mobile devices, such as mobile phones, PDA etc. ARM core is fully supported by vendors, several development toolsets are available. The controlling software is running on Windows CE, providing support for real-time applications. The application itself uses .NET Framework for compatibility with other platforms supported by the framework.

Control application has modular design, each module is used for a specific purpose: program logic is stored in the core module, data acquired from local sources or remote clients are processed in input modules. The system is designed to use universal message passing between the modules, allowing to separate module specific behaviour from the rest of the application. Communication with the central server and remote clients is held by the communication modules which will be described in the detail in the following section.

2.2 Diagnostics Interface

Embedded computer is connected with the car via OBD-2 interface. This is a standard interface providing access to electronic control units (ECU) of cars and small trucks. Modern cars usually have several control units linked together, providing a variety of functions ranging from engine control to anti-theft protection.

The specification of OBD-2 was introduced in the United States in 1990s to simplify and standardize the ECU connection with the emission testing hardware. The EOBD (European OBD) is mandatory in Europe by European Directive for all petrol vehicles manufactured since 2001 [2][3].

The OBD2 interface provides access to diagnostic trouble codes (DTC) stored in the control units, which have been stored during the failure, as well as real–time data gathered by on-board sensors. Additionally the interface provides functions to erase the DTC codes after the car was fixed.

The interface used in this project is using auxiliary Atmel microcontroller maintaining real time access to vehicle bus. This device was developed according to SAE [3][4] and ISO[2] standards and should be able to communicate with all EOBD cars equipped with the K-line. Additionally, experimental implementation of Volkswagen proprietary protocol was added, based on experiments with VAG 1552. Unfortunately this protocol is no longer used by Volkswagen.

2.3 Wireless Interfaces

The crucial parts of the system are wireless parts that provide connection to other vehicles on the road. Several types of wireless technologies were used to determine its suitability for transmitting information among vehicles.

Despite the fact that packet radio is obsolete technology used by radio amateurs in the past, it is interesting to compare it with today's wireless networks. The tests were done with radio modem using Bell 202 modulation – 1200 bps. The system was sufficient only for transmitting the GPS position of the car. Similar system is used for Automatic Packet Reporting System (APRS), real time tactical digital communication protocol for exchanging information between stations covering large area. It is used for transmitting reports of the exact location of an object via amateur radio frequencies.

More effective wireless technology, designed for low power consumption, high resistance to interference and low price is Bluetooth. It supports several types of configurations – point-to-point connection and point-to-multipoint. The latter is also referred as a piconet. It supports sharing the channel among all devices in the piconet, which can be composed of seven slaves and one master. The Bluetooth specification [6] provides also scenario of two piconets that have overlapping coverage areas. Each of the piconets are operating in its own frequency hopping channel while any of the device can participate in multiple piconets. In this way information can be transmitted from one piconet to the other. Such networks are called scatternet.

The Bluetooth communication among the vehicles was realized by using Bluetooth Network Encapsulation Protocol (BNEP), encapsulating Ethernet frames to Bluetooth and vice versa. This ensures transparent operation for TCP/IP protocol used in applications. The ability of creating scatternets seemed to be perfect for vehicle networks but appeared to be ineffective for quickly changing environment. The technology does not have effective mechanisms for fast reconfigurations – nodes entering and leaving the network. Further research will be done in terms of altering Bluetooth for such environment.

The most promising technology appeared to be well known ad-hoc mode of WiFi, which allows to form a wireless network spontaneously. It is able to cope with rapid changes in network topology and provides fast channel for data transmissions. The IEEE 802.11 standard[7] defines this peer-to-peer mode for small networks, but for larger networks its effectiveness rapidly falls due to common clock synchronization problem. Several solutions[8] were introduced to solve this task. The IEEE 802.11 networks are easy for implementation in applications and are supported in the majority of embedded systems.

The last used communication device was GPRS module. Key features, pros and cons of this technology are generally known and are well described in many sources. As an alternative to embedded PXA270 computer, we have developed smaller device based on Siemens TC65 module which acts as a thin client in our network. It is sufficient to send data to the central server, but it does not provide any user interface because of its simplicity.

The solution used at the end of this phase of development is the combination of IEEE 802.11 networking and GPRS connection. The part of application responsible for the connection is selecting the communication channel based on the message priority. Data that are not essential and are not changing very often are send via the slower channel if both connections are available. The main emphasis was put on applicability of the idea of inter-vehicle networks and sharing the information of vehicles among them.

2.4 Data Types

Dealing with multiple sources of various information raises the question of the demands for their processing. The system deals with data that need to be processed in the term of time variance more than actual value, e.g. accelerometer readings reflect the actual acceleration vector, but for motion analysis we need its development in time. On the other hand some information are valid for longer period due to physical laws, e.g. engine coolant temperature cannot change rapidly in a few seconds.

The first type of information we need to process are data from on-board electronic control units. Nowadays we use diagnostics interface running OBD–2 or CAN bus. The former was developed mainly for diagnostics purposes, the latter is used as the main bus for communication among the control units. The communication can be generally described as testing device interrogation. After the initialisation phase, testing device sends requests for services (vehicle identification, diagnostic trouble codes, actual measured values etc.) and the vehicle unit responds with appropriate messages. The other approach that can be used to obtained vehicle data is to connect directly to CAN bus lines in the vehicle.

There are usually two independent CAN buses, usually called the "fast" and "slow". The fast CAN bus is used between engine, brakes, steering assistant etc. The slow, also called the comfort, among other systems, such as air conditioning, car security system, navigation. The embedded computer acts in this situation as the CAN bus message analyser. Intercepted known messages are decoded and sent to the core module.

The second type of data are geographic information obtained from GPS units. Almost all commercial low cost units support NMEA data exchange format. This is a standard that permits marine electronics (including GPS) to send information to computers and other marine equipment. This standard was developed in 1983 and has undergone several revisions[5].

At last we should mention the sensor data and camera images that must be processed as well.

Vehicle data from two independent sources were used for analysis and model calculations. The first source of information were embedded devices as described in this paper, but because of insufficient records from multiple vehicles only a part of analysis can have been done. The other source of data was obtained from the NAM a.s. [9], company cooperating with the university. The first dataset contains the position obtained by GPS, engine telemetry from OBD2 interface, acceleration vector measured by digital accelerometer and images taken by mounted camera. The second dataset contains only the data from GPS.

3 Usability of Acquired Data

All incoming data are stored in the spatial database on the central server for further analysis. Geographic information system is used to connect the positions of cars with proper road segments and points of interests. All statistical values are connected with road segments.

Data produced by our system can be used in various informational systems such as FLOREON[10] (FLOods Recognition on the Net) [1]. In the Figure 1 we can see the FLOREON interface. The map is showing the traffic jam near Havlickuv Brod. The red dots are representing cars moving with avarage speed below 30 kmph.

4 Conclusion and Future Work

The system presented in this chapter is the combination of the Internet technologies, embedded systems and visualisation tools. The purpose is to provide all

---

[1] The main concern of project is to proof that the combination of newest information technologies and results from the disciplines that are somehow connected to the solving of floods simulations and predictions can be very helpful. The list of the disciplines whose results must be combined comprises hydrology, meteorology, integration of prediction models, development of new models, etc. The information system itself is focused on the development of the reliable architecture and is also concerned of the graphical user interface (2D, 3D) that should be able to satisfy all types of users that can interact with the system.

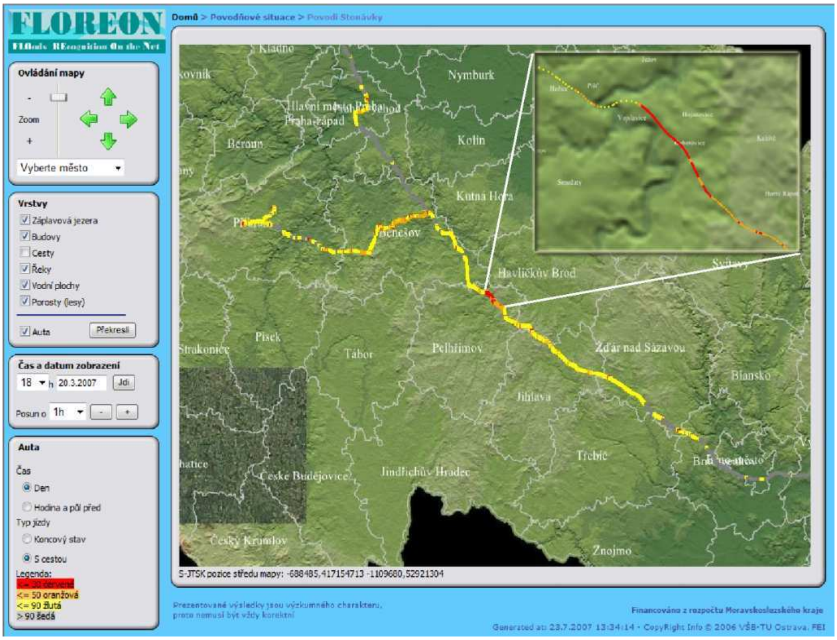
FLOREON
FLOods REcognition On the Net
Domů > Povodňové situace > Povodí Stonávky
Ovládání mapy
Zoom
Vyberte město
Vrstvy
Překresli
Čas a datum zobrazení
Jdi
Auta
Kladno
Kovník
Nymburk
Hlavní město Praha
Praha-západ
Beroun
Kolín
Kutná Hora
Příbram
Benešov
Havlíčkův Brod
Svitavy
Písek
Tábor
Pelhřimov
Žďár nad Sázavou
Strakonice
Blansko
Jihlava
Třebíč
Brno-město
České Budějovice
Jindřichův Hradec
Český Krumlov
Znojmo

☑ Záplavová jezera
☑ Budovy
☐ Cesty
☑ Řeky
☑ Vodní plochy
☑ Porosty (lesy)
☑ Auta

18 h 20.3.2007

Posun o 1h

Čas
● Den
○ Hodina a půl před

Typ jízdy
○ Koncový stav
● S cestou

Legenda:
<= 30 červená
<= 50 oranžová
<= 90 žlutá
> 90 šedá

S-JTSK pozice středu mapy: -688485,417154713 -1109680,52921304

Prezentované výsledky jsou výzkumného charakteru, proto nemusí být vždy korektní

Financováno z rozpočtu Moravskoslezského kraje

Generated at: 23.7.2007 13:34:14 - CopyRight Info © 2006 VŠB-TU Ostrava, FEI

Fig. 1. FLOREON Visualisation of Traffic Jam

available traffic information in one place and one common interface. Moreover the system can be used as a part of larger informational system such as FLOREON. In contrast to the current available systems, we can exploit the potential of embedded computers mounted in the vehicles involved in this project. Extra data provided by this system may be found useful for the future research involving the intelligent traffic systems. Research teams of major vehicle manufacturers have already announced several solutions involving embedded computers and mobile networks that will be released in oncoming car models.

References

1. World Health Organization, *World report on road traffic injury prevention*, 2004
2. International Organization for Standardization, *ISO 9141–2*, 1994
3. SAE International, *Surface Vehicle Standard J1979*, 2002
4. SAE International, *Diagnostic Connector J1962*, 2002
5. National Marine Electronics Association, *NMEA 0183 Standard*, 2002
6. Bluetooth SIG *Bluetooth Protocol Specifications, Profile Specifications*, 2003–07
7. IEEE Standards Association, *IEEE 802.11 Standard for Information technology*, 1999
8. Huang H., Lai T., *On the Scalability of IEEE 802.11 Ad Hoc Network*, MOBIHOC, 2002
9. NAM system a.s., Orlova, www.nam.cz
10. FLOREON, floreon.vsb.cz

The Usage of Polarization During Logic Synthesis Using Ashenhurst Disjunctive Decomposition

Pavel Moravčík

Department of Computer Science, FEECS,
VŠB – Technical University of Ostrava, 17. listopadu 15, 708 33 Ostrava – Poruba
`mor196@vsb.cz`

Abstract. In this paper we present some results of experiments with logic synthesis of polarization logic functions using Ashenhurst disjunctive decomposition. It is chance that the results of synthesis for polarizated function will be better (for a lot of functions) than results for non-polarizated function. We must make a lot of experiments to decision if it is fact. First results we present in this paper (mainly for ACTELS's FPGA).

1 Introduction

The synthesis techniques, that is fragmentation of the model written in the hardware description language to simple logical functions and its implementation (most often in programmable logic array of FPGA type) are know-how of separate compa-nies that creat synthesis tools to logical arrays produced by them.Of course there is aspiration so that resulting chip was as small as possible and the computing process as fast as possible. So synthesis tools minimalize and design ways and connections inside the logical array so there won´t happen time delays.

One of known methods of fragmentation of logical function if so called Ashenhurst disjunctive decomposition, published at [1] and in short form described in this document. Disadvantage of this method is that couldn´t be applied to all logical functions, but only on that ones that fulfills one specific condition. However, it couldn´t be a problem for the synthesis tool to uncover if the method can be applied on given function. If it is not possible, we have to choose a different method, for example Curtis disjunctive decomposition.

2 Reed-Muller spectrum, reverse transformation

Before we explain principles of Ashenhurst disjunctive decomposition, it is necessary to remind some terms known from algebra. Terms are closely explained in [1], [2], possibility of their use during the logical synthesis was outlined in [3], [4].

Reed-Muller functions are orthogonal functions defined over unity interval $\langle 0;1 \rangle$ which is continuous and closed. The Walsh functions form an orthogonal and com-

© Václav Snášel (Ed.): WOFEX 2007, pp. 309–314, ISBN 978-80-248-1571-8.
VŠB – Technical University of Ostrava, FEECS, 2007.

plete set of functions representing a discretized function. An interval over each Walsh functions are specified is divided into 2^n subintervals, $n = 1,2,3,...$ Let us assign number 0 to the most left interval and number $2^n - 1$ to the most right subinterval. Under such conditions Reed-Muller functions are defined as (see [3]):

$$R_\omega(x) = \prod_{i=0}^{n-1} \omega_i^{x_i} \tag{1}$$

The values of Reed-Muller function are usually presented in matrix form. Matrix R(n) is calculated using formula:

$$R(n) = R(1) \otimes R(n-1) \tag{2}$$

where operation $\otimes$ means Kronecker product of matrices and matrix $R(1)$ is:

$$R(1) = \begin{bmatrix} 1 & 0 \\ 1 & 1 \end{bmatrix} \tag{3}$$

Examples can the reader find in [3] or [4].

Reed-Muller transformation of logic functions in matrix form is defined as:

$$\tilde{f} = R(n) \cdot f \quad \text{over } GF(2) \tag{4}$$

where: $R(n)$ is Reed-Muller matrix;

f is truth vector of boolean function $f(x_{n-1}, x_{n-2}, ..., x_0)$;

$\tilde{f}$ is Reed-Muller spectrum (usually called as vector of spectra factor);

$GF(2)$ is Galois field with two elements (0 and 1).

Reverse Reed-Muller transformation is calculated as:

$$f(x_{n-1}, x_{n-2}, ..., x_0) = X_R \cdot \tilde{f} \quad \text{over } GF(2) \tag{5}$$

where: $X_R = \bigotimes_{i=0}^{n-1} \begin{bmatrix} 1 & x_{n-i-1} \end{bmatrix}$

$\begin{bmatrix} 1 & x_{n-i-1} \end{bmatrix}$ is basis of reverse Reed-Muller transformation

2.1 Polarization

Let $x_{n-1}, x_{n-2}, ..., x_0$ be a vector of variables of logic function. Let us define polarization by the following way [4]:

$x_i \to a_i = 0$

$\overline{x_i} \to a_i = 1$

where: $a_n, a_{n-1}, ..., a_0$ be a polarization vector

Then polarization p is calculated as:

$$p = \sum_{i=0}^{n-1} a_i 2^i \tag{6}$$

Matrix of spectrum conversion is calculated as :

$$M_p = \bigotimes_{i=0}^{n-1} M(a_{n-i-1}) \tag{7}$$

where:

$$M(0) = \begin{bmatrix} 1 & 0 \\ 0 & 1 \end{bmatrix} \qquad M(1) = \begin{bmatrix} 1 & 1 \\ 0 & 1 \end{bmatrix} \tag{8}$$

Reed-Muller spectrum of polarity p is calculated as:

$$\tilde{f}_p = M_p \cdot \tilde{f} \tag{9}$$

where $\tilde{f}$ is Reed-Muller spectrum of polarity 0 of logic function *f*

3 Ashenhurst disjunctive decomposition

Ashenhurst disjunctive decomposition was presented in [1]. Boolean function is splitted in two subfunctions *g* and *h*.

$$f(x_{n-1}, ..., x_{r+1}, x_r, x_{r-1}, ..., x_0) = h[A, g(B)] \qquad A \cap B = \{\ \} \tag{10}$$

where $A = \{x_{n-1}, ..., x_{r+1}, x_r\}$ and $B = \{x_{r-1}, ..., x_1, x_0\}$

The methods of Ashenhurst decomposition in Reed-Muller spectral domain is presented in work [5]. The details of this metod are contained in the following algorithm (which was in same way presented in [3]).

4 Usage of polarisation in Ashenhurst disjunctive decomposition

The aim of our future work is to uncover if polarisation of the variables of logical function can have an influence to results of the synthesis, in the concrete if is possible to find some polarisation, that can be for particular function prefereable than if the variables of this function weren´t polarised. The advantage of the polarisation lie in that after the synthesis of polarised function into the programmable logical array less logic tables or logic cells will be used than after the synthesis without using a polarisation (if look-up tables or logic cells, that depends on type of programmable gate array, because FPGA from different producers have various internal structure). If such a polarisation exists, that is a question. In following part of this document we will present results of experiments with the synthesis of several differently polarised and non-polarised logical functions (we present one example in this paper).

5 Synthesis of polarised and non-polarised logical functions

As an experiment we made synthesis of polarised logical functions fragmented by using Ashenhurst disjunctive decomposition. At first there was necessary to determine, if it is even possible to fragment given function by using the Ashenhurst disjunctive decomposition. For this purpose was written the program in C language, which for given logical function with selected number of variables and given vector of functional values determines, if the method can be used on given function and if so the method is applied. The output of the program consists of two vectors: spectra of subfunction g and spectrum of function h, from which is easy to determine the expressions for computing the functional values. Program also allows the user to submit the polarisation of logical function and compute the spectra of subfunction g and spectra of function h for these polarised variables.

We tried to perform a synthesis of always non-polarised and differently polarised function. Particulary we synthetised functions with low number of variables (particulary four and five variables) because for functions with bigger number of variables it is not easy to get known, if the Ashenhurst disjunctive decomposition is exercisable for them. Because of this reason it is not possible to say if for example one polarisation is better than other one, it will require more tests with big amount of differetly polarised functions with different number of variables. But it is centrain that we can consider the polarisation.

The synthesis was performed into FPGA series ProAsic from Actel company with usage of software IDE Libero. Subsequently the synthesis was performed also into the FPGA arrays from Spartan series from Xilinx company, with usage of software kit called ISE Webpack. Results showed that upon the different polarisations various number of basic elements in programmable arrays are used and so it is reasonable to consider the polarisation when performing the synthesis. As example, we show in this work results of synthesis for function

$$f(x_4, x_3, x_2, x_1, x_0) = \sum m(2,3,6,8,9,10,11,12,13,14,15,16,17,18,19,20,21,22,23,26,27,30)$$

where $\sum m$ means sum of minterms over $GF(2)$ for different polarisations into circuit of ProAsic series (see tables 1-3).

As far as synthesis into arrays of ProAsic fields from Actel company, it turnet out that the polarisation has relevant reason to the number of basic build items used. Basic build item of this arrays is so called logic tile [7], which has three inputs, from which two only are used for combination logic during the synthesis. So it is possible to compare results of synthesis for different polarisations also at the functions with low number of variables (see pictures 1-3). It can be seen that it is reasonable to consider polarisation when using this FPGA type. The number of used logic tiles may be markedly lower in opposite to non-polarised synhetised function.

```
cell        count       area        count*area
XOR2        6           1.0         6.0
NAND2       3           1.0         3.0
AND2        3           1.0         3.0
XOR2FT      1           1.0         1.0
TOTAL       15                      13.0
```

Table 1. Synthesis results for polarization $p = 0$.

```
cell        count       area        count*area
XOR2        9           1.0         9.0
OR2FT       3           1.0         3.0
AND2        3           1.0         3.0
NAND2       2           1.0         2.0
XOR2FT      1           1.0         1.0
TOTAL       20                      18.0
```

Table 2. Synthesis results for polarization $p = 1$.

```
cell        count       area        count*area
XOR2        6           1.0         6.0
NAND2       4           1.0         4.0
XOR2FT      2           1.0         2.0
OR2FT       2           1.0         2.0
NOR2FT      1           1.0         1.0
AND2        1           1.0         1.0
TOTAL       18                      16.0
```

Table 3. Synthesis results for polarization $p = 2$.

Synthesis into arrays of Spartan series from Xilix company was also performed. But the FPGA arrays from Xilinx have different inner structure than Actel arrays. Basic build FPGA item from Xilinx is so called logic cell [8]. It contains two four-input

LUTs (Look-Up Table) in which basic logical operation is realized. Because LUTs are of four inputs, two will be used for example when performing logical function with five variables, independent from polarisation. It will be necessary to explore the results of synthesis of dirrefently polarised functions with higher number of variables, if we want to analyze the advantage of polarisation.

6 Conclusion

From performed tests can be seen that performing of good polarisation has sense for sure.The question is if some particular polarisation for significant amount of logical functions is always better than other polarisation. The question also is if for example polarisation is significant, but only for procentually insignificant number of functions. Some, but not much sophisticated and hardware and time demanding solution would if every logical function would simulately synthetised for all possible values of polarisation and physically realized would be that one which performs best results.

Acknowledgment

This work was written during my study intership in Departmet of Electronics, Silesian University of Technology, Gliwice, Poland (from March to June 2007). The special thanks goes to author‘s temporary supervisor – (prof.) dr hab. inż. Edward Hrynkiewicz

References

1. Ashenhurst, R.L.: The decompositions of switching functions. In Proceedings of International symposium on the Theory of switching functions, 1959
2. Curtis, H.A.: A new approach to the design of switching circuits., Van Nostrand, Princeton, New Jersey, 1962
3. Hrynkiewicz, E., Kołodziński, S.: Decomposition of logic functions in Reed-Muller spectral domain. In Proceedings of 10.DDECS, Kraków, Poland, 2007
4. Hrynkiewicz, E.: Funkcje prostokątne Reeda-Mullera w syntezie układów logicznych. Author's lecture on Silesian University of Technology, Gliwice, Poland, 06.03.2007
5. Varma, D., Trachtenberg, E.A.: Design automation tools for efficient implementation of logic function by decomposition. In IEEE trans. on computer aided design, vol. 8, nr. 8, 1989
6. Kołodziński, S.: Dekompozycja funkcji logicznych metodami spektralnymi zorientowana na realizację tych funkcji w układach FPGA typu tablicowego. PhD thesis, Silesian University of Technology, Gliwice, Poland, 2003
7. Actel logic tile, URL http://www.actel.com
8. Xilinx logic cell, URL http://www.xilinx.com

Compression of Small Text Files

Jan Platoš[1], Václav Snášel[1], and Eyas El-Qawasmeh[2]

[1]Department of Computer Science, FEECS,
VŠB – Technical University of Ostrava, 17. listopadu 15, 708 33 Ostrava – Poruba
{jan.platos, vaclav.snasel}@vsb.cz
[2]Computer Science Dept., Jordan University of Science and Technology, Jordan
eyas@just.edu.jo

Abstract. This paper suggests a novel compression scheme for small text files. The proposed scheme depends on Boolean minimization of binary data accompanied with the adoption of Burrows-Wheeler transformation (BWT) algorithm. Compression of small text files must fulfill special requirements since they have small context. The use of Boolean minimization and Burrows-Wheeler transformation generate better context information for compression with standard algorithms. We tested the suggested scheme on collections of small and middle-sized files. The testing results showed that proposed scheme improve the compression ratio over other existing methods.

Keywords: Compression, Small files, Quine-McClusky, Decompression

1 Introduction

Data compression aims to remove redundant data in order to reduce the size of a data file [7, 11]. The compression of a file into half of its original size increases the free memory that is available for use [6]. The same idea applies to transmission of messages through the network with limited bandwidth channels.

Currently, the volume of all data types is increasing continuously. This holds for all data types including textual data. Many lossless compression techniques and algorithms for normal and large texts exist and most of them need sufficient context information.

Very small files, like SMS, chat messages and emails, have different characters. These files has very small context and therefore is not possible to use any compression method designed on large or medium sized files. But we may transform this data into another form or we may use Boolean minimization for data compression, which was presented by El-Qawasmeh and Kattan in 2005 [3]. In this technique, the compressed stream is splitted into 16 bit blocks. These blocks represents truth-table of Boolean function of 4 variable. This function is minimized using Quine-McClusky algorithm. After minimization, Huffman code is used and obtained code is stored into file.

© Václav Snášel (Ed.): WOFEX 2007, pp. 315–320, ISBN 978-80-248-1571-8.
VŠB – Technical University of Ostrava, FEECS, 2007.

This paper suggests a novel compression scheme for small text files. The proposed scheme is designed for small text files and it uses Burrows-Wheeler transformation besides Boolean minimization at the same time.

The organization of this paper will be as follows: Section 2 presents a review of the Quine-McClusky algorithm. Section 3 explains the improvements and enhancements suggested. Section 4 shows the performance results and Section 5 contains the conclusion of this paper.

2 Quine-McClusky algorithm

The Quine-McClusky algorithm is a technique for presenting Boolean functions [10]. It seeks to collect "product terms" by looking for entries that differ only in one bit. The Quine-McClusky algorithm is capable of minimizing logical relationships for any number of inputs. It starts with the truth table and extracts all the "product terms" (all input combinations that produce a true output). After that, it groups all the "product terms" by the number of ones they contain. Then it combines the "product terms" from adjacent groups [4].

3 Suggested improvements and enhancements

In this section, we will describe the basic ideas behind our suggested scheme. the best compression ratio in experiments in [3] was achieved on data with very small or very high probability of ones. Therefore, if we transform vectors from compressed file into more suitable vectors and their "product-terms", then we can achieve a better compression ratio.

The first improvement is based on idea that vectors with less count of ones have shorter length of Boolean minimization.

The second improvement is based on the idea that the shortest Boolean minimization is used the more frequent occurrence "product terms" is and then better context for context-based compression algorithm is created.

In the compression algorithm that were suggested by El-Qawasmeh and others, they use Quine-McClusky algorithm combined with the static Huffman encoding.

By using Quine-McClusky, we reduce the alphabet of the file from 256 symbols into 82 product terms and one extra symbol for separating between vectors after Boolean minimization. In this case, we can get better context information in transformed data than we have in original, non-minimized data. Currently, there are many compression methods that need good context for achieving a good compression ratio. One of them is the BWT (Burrows-Wheeler) compression algorithm [2].

BWT needs for a good compression ratio sufficient context which is formed by frequent occurrences of symbols with same or similar prefixes. This can be achieved with sorting product terms in some order. Our proposal consists in enumeration of any possible terms and their sorting by these numbers. The term "0" is assigned 0, the term "1" is assigned 1, and so on until the term " A'B'C'D' " which assigned 82 and a comma which assigned 83.

Another improvement can be achieved with separator elimination. Since product terms are sorted by their number, i.e. lowest to highest, the passing between product terms of adjacent vectors can by detected by decreasing the term number. This principle works in most cases but not in all.

The most recent tested improvement was not compression by product terms, but compression by smaller parts. One possibility is logical variables A, A', B, , D'. In this case, of course, the separator between product terms, '+', must be compressed too. A second possibility is compression by separate characters A, B, C, D, +, ' and comma. The volume of original data significantly increases in both cases, but the alphabet size decreases, also significantly.

4 Performance Results

The suggested method was compared with four different methods. The first compression method is Semi-static Huffman encoding [5] which was used in [3]. The second compression method is Adaptive Huffman encoding [8], which is also well known. The third method that we used is LZW, which is described in [9]. The fourth algorithm which we compared with is based on a BWT compression algorithm. In this algorithm, Burrows-Wheeler transformation is applied to the data block. Then MTF transformation is used. Data from MTF is compressed using the RLE algorithm which uses Fibonacci for counting and encoding symbols Adaptive Huffman encoding. This compressor was used for normal compression and also for compression of product terms.

Experimental results showed that the maximal compression efficiency was achieved by applying another transformation which was used as the first step in any used algorithm. The vectors were mapped by their frequency. This transformation is realized by a priority queue. The range of used vectors is decreased by this transformation, which simplifies mapping for each file.

The Compression efficiency was tested in many tests over several files. In the first step, the algorithm described in [3] was compared to the suggested algorithms. In the second step, the described algorithm was compared to another compression algorithm. Several files were used for testing. The first one is *sms.txt*[96 704 B], which is a collection of SMS [1]. This collection was collected from a public SMS stored server and was prepared for processing by Monojit Choudhury and his team. The second file is *bible.txt*[4 138 536 B] from Canterbury compression corpus [1]. This file was processed by lines, which contains one verse from the English bible.

The second group of files that we used for testing was parts of Enron corpus; *enron_nh.txt*[36 971 613 B] contains the 20,000 emails without headers, *enron_sh.txt*[14 484 583 B] contains the 20,000 emails smaller than 1kB without headers and *enron.ssh.txt*[8 175 564 B] contains 20,000 emails smaller than 512B.

---

[1] http://www.mla.iitkgp.ernet.in/ monojit/sms.html

4.1 Comparison of described compression algorithm

The following part of this section describes the variants of the algorithm. It describes comparison results for the algorithm described in [3] and our proposed algorithm based on BWT and Boolean minimization at the same time. The base algorithm is designed *MinHuff*, algorithms with Boolean minimization and BWT over product terms is designed as *MinBwt*, same algorithm with separator elimination as *MinBwtS*, algorithms with minimization and BWT over logical variables as *MinBwtL* and algorithms with minimization and BWT over character representation as *MibBwtC*. All variants of *MinBwt* algorithms had block sizes set at 1MB.

Results for non-Enron files are shown in Table 1[2]. Both of them contain very short messages. The compression ratio of the *MinHuff* method is greater than 100%, which is caused by storing of Huffman trees into file. All variants of *MinBwt* algorithms are better than *MinHuff* algorithms. Base *MinBwt* versions achieved the best compression ratio, results achieved by *MinBwtS* variant are a little worse. Variants with compression on logical variables or characters are still better than *MinHuff*, but quite worse than *MinBwt*.

Table 1. Comparison between base algorithm and algorithms with BWT

	sms.txt		bible.txt	
	CS [bytes]	CR [%]	CS [bytes]	CR [%]
MinHuff	108 696	112.40	4 447 367	107.46
MinBwt	73 941	76.46	2 946 782	71.20
MinBwtL	96 786	100.08	3 891 008	94.02
MinBwtC	88 934	91.97	3 590 441	86.76
MinBwtS	81 881	84.67	3 260 340	78.78

Results for Enron files are depicted in Table 2. Achieved ratios are similar to the previous table.

Table 2. Comparison between base algorithm and algorithm based on BWT - Enron files

	enron_nh.txt		enron_sh.txt		enron_ssh.txt	
	CS [bytes]	CR [%]	CS [bytes]	CR [%]	CS [bytes]	CR [%]
MinHuff	29 548 821	79.92	7 909 173	96.74	5 018 207	108.76
MinBwt	21 055 382	56.95	6 345 648	77.62	3 706 019	80.32
MinBwtL	26 657 872	72.10	7 851 240	96.03	4 667 562	101.16
MinBwtC	25 353 586	68.58	7 470 631	91.38	4 416 945	95.73
MinBwtS	21 391 560	57.86	6 511 943	79.65	3 912 122	84.79

---

[2] CS means the size of the compressed file and CR is the compression ratio.

4.2 Comparison with standart compression algorithm

Comparison with standard compression algorithm is described in this section. *MinBwt* variant was chosen as the best compression method based on Boolean minimization and BWT. This algorithm was compared with standard, character based, algorithms. Three algorithms were tested. *BWT* is an algorithm based on BWT. Block size was set on 1MB for testing. *LZW* is a traditional compression algorithm described previously. The size of the dictionary was set at 1MB again. The most recently used algorithm was Adaptive Huffman encoding, which is designed as *AHuff*. *MinHuff* algorithm was only included in the results for the purpose of comparing.

Results for non-Enron files are depicted in Table 3.The MinBwt algorithm was the best for both files. Other algorithms are significantly worse. This is probably caused by very short messages which do not have sufficient context.

Table 3. Comparison with standard algorithms

	sms.txt		bible.txt	
	CS [bytes]	CR [%]	CS [bytes]	CR [%]
BWT	92 502	95.65	3 701 212	89.43
LZW	83 624	86.47	3 405 503	82.29
AHuff	78 110	80.77	3 291 873	79.54
MinHuff	108 696	112.40	4 447 367	107.46
MinBwt	73 941	76.46	2 946 782	71.20

Results for Enron files are depicted in Table 4.These files contain messages with variable lengths. The average length of messages in enron_nh.txt is 1845 B, in enron_sh.txt is 405 B and in enron_ssh.txt is 227 B. The previous two files have message lengths mostly shorter than 400 B. Messages in Enron files are so long that context based algorithms are effective on these files.

The best result for enron_nh.txt file was achieved with a BWT algorithm. MinBwt is in second place, just before LZW algorithm. AHuff and MinHuff algorithms have the worst results. BWT algorithm was the best also for enron_sh.txt file. AHuff algorithm was a little worse. MinBwt and LZW algorithms were worse by 3% of compression ratio. MinHuff was the worst again. Enron_ssh.txt file contains shorter messages than other Enron files. Compression algorithms that need large context are worse than MinBwt, because context in messages from these files is insufficient. The best result, however, has been achieved by AHuff algorithm. MinBwt was worse by 1%. LZW algorithm came in third place with BWT coming in fourth.

5 Conclusion

This paper describes a novel compression scheme for very small text files. This scheme may be useful for many applications which need to store or transfer

Table 4. Comparison with standard algorithms - Enron files

	enron_nh.txt		enron_sh.txt		enron_ssh.txt	
	CS [bytes]	CR [%]	CS [bytes]	CR [%]	CS [bytes]	CR [%]
BWT	17 469 403	47.25	6 050 234	74.00	3 876 253	84.01
LZW	21 321 651	57.67	6 298 213	77.04	3 840 240	83.23
AHuff	24 570 316	66.46	6 099 495	74.61	3 647 439	79.05
MinHuff	29 548 821	79.92	7 909 173	96.74	5 018 207	108.76
MinBwt	21 055 382	56.95	6 345 648	77.62	3 706 019	80.32

many small files, e.g. instant messaging, SMS, chat communication. The described scheme is more effective for small text files than standard compression algorithms. The advantage of this algorithm is usability in any other system, because it works independently to other systems. Therefore it can be used at the lowest level of any application, which needs to store or transfer data of this type.

Future work may focus on modification of minimizing algorithms for 32-bit length vectors accompanied with applying other mapping transformation and using other compression algorithms in the second phase of compression.

References

1. R. Arnold and T. Bell. A corpus for the evaluation of lossless compression algorithms. In J. A. Storer and M. Cohn, editors, *Proc. 1997 IEEE Data Compression Conference*, pages 201–210. IEEE Computer Society Press, Los Alamitos, California, Mar. 1997.
2. M. Burrows and D. J. Wheeler. A block-sorting lossless data compression algorithm. Technical report, Digital Systems Research Center Research Report 124, 1994.
3. E. El-Qawasmeh and A. Kattan. New technique for data compression. In N. Guimarães and P. T. Isaías, editors, *IADIS AC*, pages 365–373. IADIS, 2005.
4. M. D. Ercegovac, T. Lang, and J. Moreno. *Introduction to Digital Systems.* John Wiley and Sons Inc, 1999.
5. D. A. Huffman. A method for the construction of minimum-redundancy codes. *Proceedings of IRE*, 40(9):1098–1101, 1952.
6. J. Mandal. *An Approach Towards Development of Efficient Data Compression Algorithms and Correction Techniques.* PhD thesis, Jadavpur University, 2000.
7. G. J. Mathews. Selecting a general-purpose data compression algorithm. In *Proceedings of the Science Information Management and Data Compression Workshop*, NASA Publication 3315, pages 55–64, 1995.
8. M. Nelson and J.-L. Gailly. *The Data Compression Book.* M&T Books, 1995.
9. T. A. Welch. A technique for high-performance data compression. *IEEE Computer*, 17(6):8–19, 1984.
10. D. Zissos. *Logic Design Algorithms.* Harwell/Oxford University Press, 1972.
11. N. Ziviani, E. Moura, G. Navarro, and R. Baeza-Yates. Compression: A key for next-generation text retrieval systems. *IEEE Computer*, 33(11):37– 44, 2000.

A Detection of Structural Damage of Brain Tissue in Parkinson's Disease Patients

Josef Schreiber

Department of Computer Science, FEECS,
VŠB – Technical University of Ostrava, 17. listopadu 15, 708 33 Ostrava – Poruba
`josef.schreiber@vsb.cz`

Abstract. Parkinson's disease (PD) is very complex neurodegenerative brain disease with very complicated diagnostics. Recently, several studies dealing with the usage of transcranial sonography for a diagnostics of PD, were published. These studies showed that ultrasound has very good results in revealing the structural damage of nerve cells in substantia nigra area. Since this method has to deal with a scull during the process of images acquisition, the provided images suffer from a very poor quality. This implicates the equivocation of the diagnosis made by different physicians. Therefore, the final objective of my research is to develop a method that could be used by medical doctors for the objective evaluation of brain-stem ultrasound images.

Keywords: transcranial sonography, ultrasound imaging, substantia nigra, Parkinson's disease, brain stem

1 Parkinson's disease diagnostics

Neuroimaging methods are increasingly used as diagnostic tools in patients presenting with Parkinson's disease (PD). Since the dysfunction of dopamine transfer is a primary (but unfortunately not the only) cause of PD, we can use different diagnostics methods like PET, DaT scan - SPECT to see the metabolism and the transfer of dopamine in the patient's brain. However, the usage of these methods is significantly limited because more frequent examinations can be dangerous to the patient.

Another way how to determine the existence or seriousness of the disease is to analyse the structural damage of brain tissue in the neural center called substantia nigra. Unfortunately, traditional methods like brain computed tomography or magnetic resonance imaging are only able to detect other aetiology than Parkinson's disease[1] and they are not considered to be conclusive. [2].

In 1995 Becker et al. published a study dealing with a diagnostics of PD using transcranial sonography [3]. They showed that increased echogenicity of substantia nigra is closely associated with PD. Their research was later followed by other publications [4] [5]. They proved that hyperechogenic substantia nigra can be found at more than 91% patients with PD. Nowadays the transcranial

© Václav Snášel (Ed.): WOFEX 2007, pp. 321–326, ISBN 978-80-248-1571-8.
VŠB – Technical University of Ostrava, FEECS, 2007.

sonography is considered to be the best possible diagnostic tool for a detection of structural damage of brain tissue in Parkinson's disease patients.

The ultrasonic imaging is based on detecting reflected and scattered waves arising as a response to the emitted wave with various frequencies. Generally, the higher the frequency is the better and more detailed output images can be obtained. Unfortunately, in case of transcranial sonography, we need to deal with the scull that behaves as a barrier stopping all high-frequency waves. This means that only the low frequency probes (1-4 MHz) may be used. As a consequence of this, transcranial sonography provides images of significantly lower quality.

The interpretation of ultrasound images is generally a difficult task and the opinion of different medical doctors is generally not equivocal. The problem is even more serious in transcranial sonography. Even if the image is carefully evaluated by a physician, there is a significant influence of subjectivity. By two different medical doctors, a different diagnosis may be determined from one image. Another problem is a long time treatment when a progress of disease must be determined from old images and a repeating of examination is no longer possible. [6] That is why there appeared a demand to create a tool that would help physicians to objectivize the diagnosis process.

The processing of ultrasound images is widely discussed in literature. Still, according to my knowledge, there are no studies dealing with the processing of brain-stem transcranial images or with the computerized recognition of objects in the substantia nigra area.

2 Localization of brain stem

The method, I developed for the processing of brain-stem transcranial sono images, is divided into two phases. In a first one, I try to locate the position of a minimal window in the processed image containing the brain stem. For this, I use the modified pattern matching algorithm.

Since every human being is unique, the brain stems may slightly differ in shape and size in images. Moreover, the objects being sought inside the stem may have different position, size, and echogenicity, depending on the disease progress. Therefore, for creating the template of the stem, I choose several images that best represent various possible shapes and sizes of the stem. I also considered the seriousness of the disease by choosing images depicting the situation in various stages of the disease progress (from healthy persons to persons with an advanced stage of the disease). The selection of images, used for the template construction, was widely discussed with medical doctor to best fulfil previously mentioned parameters. Overall there were 15 selected images used for the template construction.

I construct the template that is used for matching by averaging the particular selected images of the brain stem. Firstly, the images are normalised to the same size. In my experimental implementation, I use the size of 120×120 pixels. After normalising the size, I normalise the images of stem also with respect to the mean value and the variance of brightness. In the pattern matching algorithm, I will also use the variance of brightness in particular pixels. An example of the template that was obtained by averaging the brain-stem images is depicted in Figure 1.

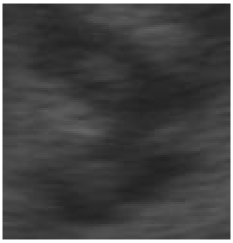

Fig. 1. The constructed template

As a next step of my method I try to locate the position of the brain stem (it is $p \times r$ pixels large) in the processed image. This image is $s \times t$ pixels large. The i-th pixel is defined by vector $\mathbf{x} = (x_1, x_2)$, where x_1 denotes x-coordinate and x_2 the y-coordinate of a i-th pixel in the template. The k-th pixel in processed image is defined by vector $\mathbf{u}_k = (u_1, u_2)$, where $u_1 = 0, \ldots, (s - p)$ denotes x-coordinate and $u_2 = 0, \ldots, (t - r)$ the y-coordinate of a k-th pixel.

I introduce now a possibility, denoted by $\pi(\mathbf{u}_k, \mathbf{x})$, of the event that the template point with the coordinates $\mathbf{x}$ corresponds to the image point with the coordinates $\mathbf{x} + \mathbf{u}_k$. This possibility may be determined from the difference

$$\varDelta b = b(\mathbf{x} + \mathbf{u}_k) - t(\mathbf{x}), \tag{1}$$

where $b(\mathbf{x}+\mathbf{u}_k)$ is the brightness of pixel in processed image with coordinates $(x_1 + u_1, x_2 + u_2)$ and $t(\mathbf{x})$ is brightness in corresponding template pixel.

I suppose that the possibility distribution may be described by a certain chosen function φ. Fig. 2 shows an example of such a function. For the construction of φ function I use the deviation $\sigma_b(\mathbf{x})$ that was determined during the template construction.

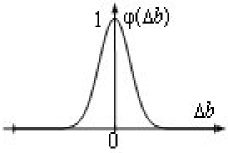

Fig. 2. The distribution of possibility φ (the Gaussian function)

To obtain the possibility of the event that the image pixel just being processed corresponds to the pixel from the template, I use the following equation

$$\pi(\mathbf{u}_k, \mathbf{x}) = \varphi(b(\mathbf{x} + \mathbf{u}_k) - t(\mathbf{x})). \tag{2}$$

To characterize the quality of matching at the position $\mathbf{u}_k$, I introduce the quantity $S(\mathbf{u}_k)$ characterizing the number of pixels, i.e., the "net area" that can successfully be matched to the template. I have

$$S(\mathbf{u}_k) = \sum_{x_1, x_2} \pi(\mathbf{u}_k, \mathbf{x}). \tag{3}$$

The final goal is to find the value of $\mathbf{u}$ that maximizes the value of $S(\mathbf{u}_k)$. The value of $\mathbf{u}$ then determines the position of the window that should contain the brain stem object (Fig. 3).

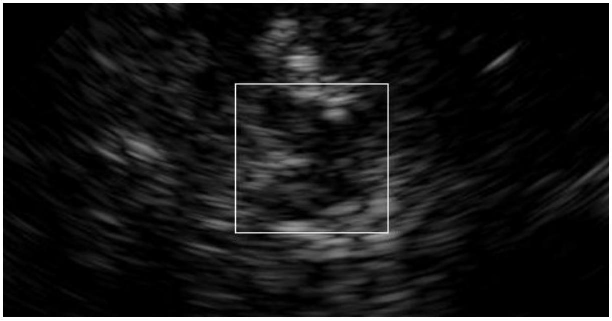

Fig. 3. Image with recognized brain stem

It is obvious that during the brain-stem detection each processed window from analysed image must be normalized in the same way like the images used for the template construction.

3 Region of interest analysis

To obtain the information about the disease progress I need now to locate and measure objects inside the brain stem. In the image, these objects appear as the areas with higher level of echogenicity inside the substantia nigra area. To correctly identify these objects is a very difficult task because areas may have insufficient contrast.

I locate the objects in the brain stem as the areas with a higher level of brightness that are found using the region growing method. Homogeneity of brightness is a criterion that is used for growing. After growing, the regions of interest are usually partitioned into several smaller areas (Figure 4). Therefore, morphological closing is carried out after growing to connect the sub-areas together.

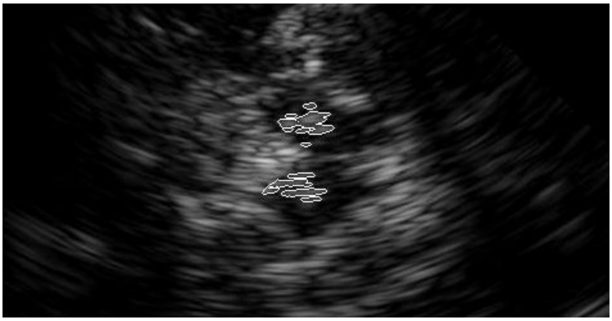

Fig. 4. Image with recognized brain stem and highlighted objects

It often happens, that ultrasound speckle or noise fragment one larger object into several smaller parts. Therefore, I utilize a clustering method based on distances. If the distances between gravity centers of the objects that have been found do not exceed a pre-defined limit, I consider all of them to be parts of one bigger object.

4 Achieved results

To test the successfulness of my method in brain stem localization, I used a sample of 170 images where I tried to locate the correct position of brain stem in processed image. The result (the quality of recognition) was classified with the marks between 1 and 3. The mark 1 means that the position was recognized correctly and accurately. The mark 2 means that the position was determined inaccurately but not completely incorrectly. In this case, the position was usually determined with an error up to 10-15 pixels. The mark 3 means that the method determined an incorrect position. For our set of test images, I obtained the results that are summarized in Table 1.

Table 1. The results of brain-stem localization by presented method. The first column determines the quality of recognition. The second one show the number of images recognized with corresponding quality and last column displays the overall percentage.

Recognition	Number of images	Results in %
1	129	75.9
2	4	2.3
3	37	21.8

5 Conclusion

The computer processing of transcranial ultrasound images is very complicated task. Images often suffer from a very poor quality and they have got a high level of noise and speckle. Displayed objects are often discontinuous, in worse cases even incomplete. Searched objects, inside the brain stem, have often insufficient contrast and they are usually fragmented by some ultrasound speckle. Still, the objective evaluation of these images can be very helpful in Parkinson's disease diagnostics and treatment. It can help the medical doctors to determine the correct diagnosis as well as the level of the disease progress.

Achieved results, obtained during testing, make me believe that the method I have developed for the analysis and processing of the brain-stem images is successful. Considering the quality of processed images, I obtained good results. In 75% cases, the position of the brain stem in the image was determined correctly.

From the medical domain, there is a big demand for a computer aided analysis of transcranial ultrasound images. The novelty of this research in medical area implicates its novelty in computer vision. Also as it was already stated, there are no other authors referring about the brain-stem sono images processing or about the computerized recognition of objects in the substantia nigra area.

The results of the presented method were already published [7], [8]. Also, based on this research, a new project was send to Czech Science Foundation (GAČR). This project is currently being evaluated and approved.

References

1. P. Ressner, D. Školoudík, P. Hlustik, P. Kanovsky. Hyperechogenicity of the substantia nigra in Parkinson's disease. *Journal of Neuroimaging, Vol. 17, Issue 2*, 164-167,2007.
2. U. Bogdahn, G. Becker, F. Schlachetzki. *Echoenhancers and transcranial color duplex sonography.* Blackwell Science, 1998, Berlin.
3. G. Becker, U. Bogdahn, C. Gehlberg, et al.. Transcranial color-coded real-time sonography of intracranial veins. Normal values of blood flow velocities and findings in superior sagittal sinus thrombosis. *Journal of Neuroimaging, Vol. 5*, 87-94, 1995.
4. D. Berg, G. Becker, B. Zeiler, O. Tucha, E. Hofmann, et. al.. Vulnerability of the nigrostriatal system as detected by transcranial ultrasound. *Neurology, Vol. 53*, 1026-1031 1999.
5. D. Berg, C. Seifker, G. Becker. Echogenicity of the substantia nigra in Parkinson's disease and its relation to clinical findings. *Journal of Neurology, Vol. 248*, 684-689, 2001.
6. D. Školoudík, T. Fadrná, P. Bártová, K. Langová, P. Ressner, O. Zapletalová, P. Hlustik, R. Herzig, P. Kanovsky. Reproducibility of sonographic measurement of the substantia nigra *Ultrasound in Medicine & Biology, Jun 1*,[Epub ahead of print],2007.
7. J. Schreiber, E. Sojka, L. Ličev. Analysis and diagnostics of the brain-stem ultrasound images. *14th International Conference on Systems, Signals and Image Processing.* Maribor, Slovenia, 489-492. 2007.
8. J. Schreiber, L. Ličev, E. Sojka. Recognition and diagnostics of special objects in ultrasound images. *8th ICCC 2007.* Štrbské pleso, Slovak Republic, 643-646, 2007.

Using of BIBD Designs with Parallel Class for B-trees

Jan Šútora[1]

Department of Computer Science, FEECS,
VŠB – Technical University of Ostrava, 17. listopadu 15, 708 33 Ostrava – Poruba
jan.sutora.st@vsb.cz
Department of Computer Science, Science Faculty, University of J. Palacky Olomouc,
Tomkova 40, 779000 Olomouc
jan.sutora@upol.cz

Abstract. There is an algorithm for making a B –tree which takes as input parameter so called minimum degree of the B- tree. After finishing this algorithm we get B – tree which has a height, every its node contains a number of elements of initially set of keys so that nodes without the root of the B – tree are half full. These properties are not known before using the algorithm. If we knew that parameters, we would choose minimum degree of the B – tree in such a way that we can get B – tree with nodes which are full more and the B – tree has lower height. We are going to investigate the possibility of using of block design with parallel class for making B – trees. We are also going to show properties of these B – trees.

Key words: parallel class, block design, group divisible designs, B - tree

1 Introduction

The B –tree was introduced in 1970 by R. Bayer and E. M. McCreight. The B – tree serves as efficient data structure for searching key in set of keys. The B- tree can be use in database systems. Properties, algorithms can be found [2].

As example of a B – tree for set *{1, 2, 3, 4, 10, 16, 6, 7, 9, 11, 12, 15, 16, 17, 22, 36}*, minimum degree *t = 4* we can see in following picture:

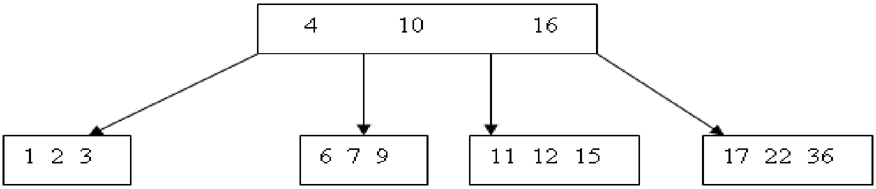

Fig. 1. B - tree

---

[1] Advisor: prof. RNDr. Snášel Václav, CSc.

© Václav Snášel (Ed.): WOFEX 2007, pp. 327–332, ISBN 978-80-248-1571-8.
VŠB – Technical University of Ostrava, FEECS, 2007.

Theory of combinatorial designs concerns questions about whether it is possible to arrange elements of finite set into subset so that certain balanced properties are satisfied. Theory of combinatorial designs was roughly investigated from 1950 by Bose. Combinatorial designs can be used for example in cryptography, tournament scheduling, mathematical biology. Properties, algorithms creating some combinatorial designs we can find [1], [3], [5].

We can see B – tree as division of initially finite set of keys into finite subsets. Number of these subsets has to satisfy the properties of B-tree.

We are going to look for ways of using a block design for creating B – trees we are going to show properties of these B – trees, too.

This paper has following structure:

- Section 2 contains combinatorial model of a B- tree
- Section 3 shows B – trees from block designs
- Section 4 contains properties B – tree from block designs
- Section 5 contains conclusions

2 Combinatorial model of a B – tree

We can see that B – tree contains subsets from initially finite set of keys see fig.1. The number of these subsets has to satisfy property of B – tree. With respect to the fact that nodes of a B – tree contain subsets keys we can use block design (v, k, λ) – *BIBD*. This block design has to have so called parallel class i.e. $k|v$ hence $v = kq$ $q \in Z$. We have to find values of these parameters:

- covalency function $\lambda = 1$ (every pair different element is contained in one subset)
- number element of set of keys v (depend on k parallel class)

We are going to choose blocks from all blocks of $(v, k, 1)$ – *BIBD*. The number of the blocks equals to number of blocks in parallel class in this design (the set – covering problem). We can find that the number of blocks in parallel class is minimum ($q < r; r \leq k$).

This block design with parallel class is also thought to be group divisible design with index *1*:

- groups of the group divisible design are blocks of the parallel class,
- blocks of the group divisible design are other blocks of the block design.

We have set parameters for block design with parallel class i.e.

$$(k^n, k, 1) - BIBD,\ n \in N \tag{1}$$

We have to show that the design exists

- $k^n - 1 \equiv 0 \bmod (k-1)$ (number *1* is root of polynomial $k^n - 1$ above ring of Z)
- $k^n(k^n - 1) \equiv 0 \bmod (k(k-1))$ (number *0, 1* are roots of polynomial $k^n(k^n-1)$ above ring of Z) **(2)**
- $\frac{k^n}{k}\frac{k^n-1}{k-1} = k^{n-1}(k^{n-1} + k^{n-2} + \ldots + k + 1) > k^n$ (Fisher's inequality)

3 Creating of a B – tree from *(k^n, k, 1) – BIBD* with parallel class

We are going to present how we can create B- tree from the design (1) for different heights. We are going to use blocks (their size is *k*) from the parallel class as free space where elements of set of keys will be put.
We are not going to create blocks of the design (1). This B – trees have to satisfy properties of B – trees.

3.1 The B – tree with height 1

We use $(k^2, k, 1) - BIBD$ with parallel class. Hence the parallel class contains *k* blocks of the design. If number of keys was ideal square, we would create following B – tree:

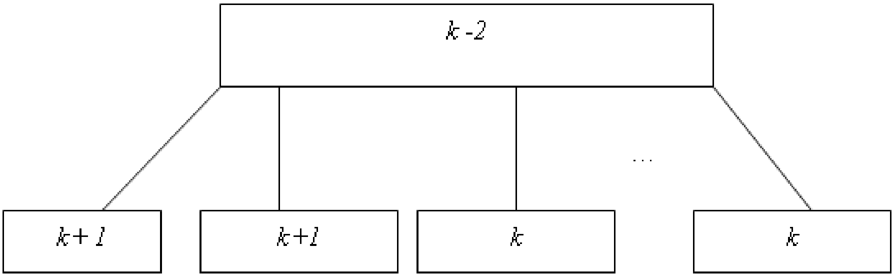

Fig. 2. B – tree from $(k^2, k, 1) - BIBD$

In case that the number of keys is not ideal square we have to put remaining elements into nodes of the B – tree (= blocks of the parallel class). Maximum number of remaining elements is *2k.*

3.2 The B – tree with height 2

We use $(k^3, k, 1) - BIBD$ with parallel class. Hence the parallel class contains k^2 blocks of the design. We have to create B – tree with height *2* from the k^2 blocks. First we find how many times blocks in fig. 3 contain in k^2 i.e.

$$k^2 = (k-2)(k+2) + 4 \tag{3}$$

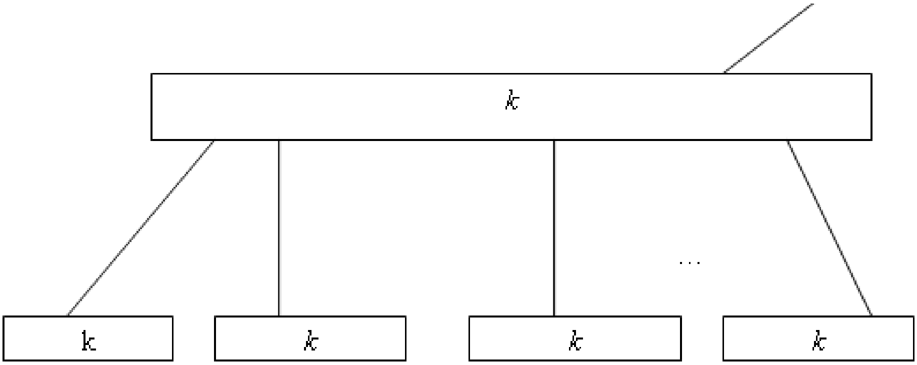

Fig. 3. Sub tree of B – tree with height 2

From (3) we can create B – tree with height 2

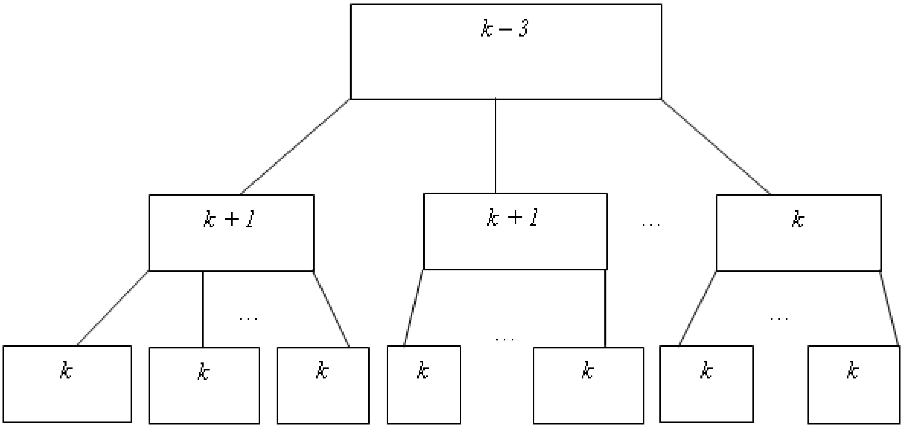

Fig. 4. B – tree with height 2

4 Properties B – tree from block design with parallel class

We are going to use following properties from B – trees:

Theorem 1: If $v \geq 1$, then for any v-key B-tree of height h and minimum degree $t \geq 2$

$$h \leq \log_t \frac{v+1}{2} \tag{4}$$

Proof: [2]

□

If we sort out this logarithmic inequality (4) for unknown parameter t we will get distribution of minimum degree t of a B – tree because of height of the B-tree for initially input set of keys as following picture shows:.

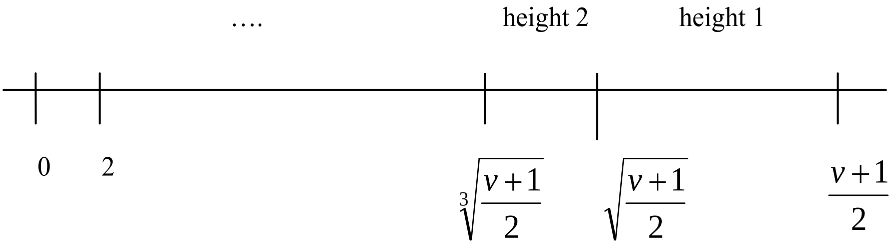

Fig. 5. Distribution minimum order of a B - tree

If we use results from section 3 and theorem 1 (fig. 5) we will create following table which shows properties of the B-tree for initially set of keys for example $v = 125$:

Cardinality set of keys: $v = 125$			
Height of a B-tree h	Minimum order of a B-tree t	Properties of a B – tree from design	
		Parameters of design	Minimum order
1	$t \in \{8, 63\}$	*(121,11,1) - BIBD*	$t \in \{8, 12\}$
		• root: *9* • leafs: *4x12*; *6x11*	for $t = 8$ min. full: *73.3%* for $t = 9$ min. full: *64.7%* for $t = 10$ min. full: *57.9%* for $t = 11$ min. full: *52.4%* for $t = 12$ min. full: *47.8%*
2	$t \in \{4, 7\}$	*(125, 5, 1) - BIBD*	$t \in \{4, 6\}$

		- root: *2* - first level: *3x6* - leafs: *21x5*	for $t = 4$ min. full: *71.4%* for $t = 5$ min. full: *55.5%* for $t = 6$ min. full: *45.5%*

Tab.1. Different B – tree for initially set of keys cardinality *125* from block designs

5 Conclusions

We presented the way of creating of a B – tree from the block designs $(k^n, k, 1) - BIBD$ with parallel class. From these block designs we use:

- size of blocks (= minimum degree of a B-tree)
- number blocks in parallel class (= height of a B – tree)

By using these block designs we can see properties of a B – tree – height, minimum degree, capacity of all nodes – it depends on cardinality of the initially set of keys. We can find these properties before we create B – tree. We know these properties of B – tree for a number of different B – trees.
If we know these properties of a B – tree we will choose more suitable parameters for a B – tree.
If we want to create B – tree with parameters – minimum degree- we will perform the following:

1. external sorting of set of keys (we find cardinality of the set keys)
2. we find some parameters of B – trees for the set of keys
3. creating of B - tree

Reference

1. Colbroun, Ch.J. – Dinitz,J.H.: CRC Hanbook of Combinatorial designs, CRC Press 1996
2. Colrmen, T.H. – Leiserson,Ch.E.-Rivest,R.E.-Stein,C.: Introduction to Algorithms, MIT 2003
3. Stinson,D.R.: Combinatorial Designs, Construction and Analysis, Springer, 2004
4. Šútora, J.: Group divisible desings and B – tree, Information Science (running review)
5. Wallis, W.D.: Combinatorial Designs, Marcel Dekker, 1988

Ontology Based Course Structure for Adaptive Web-based Systems

Zdeněk Velart

Department of Computer Science, FEECS,
VŠB – Technical University of Ostrava, 17. listopadu 15, 708 33 Ostrava – Poruba
`zdenek.velart.fei@vsb.cz`

Abstract. Personalization – this word is nowadays used in many contexts. Amount of existing information is increasing and there is a need for delivering personalized information to the user. One of these areas, where personalization is needed is adaptive web-based learning systems. This article present an idea of ontology based course structure, where the interconnection between particular concepts is defined by prerequisite and outcome sets with elements of ontology. The structure is created by the use of keyword of domain and mapping between keywords and particular elements of ontology. For purpose of evaluation of these approach a prototype is developed.

Keywords: personalization, adaptive hypermedia, web-based systems, ontology

1 Introduction

Personalization of information is nowadays primary goal of many existing search engines, recommending, shopping and learning systems and other usefull systems, which we can meet in our everyday lives. The ideas behind these systems are based on research and technologies and standards, which are in development for several years now. The ideas of adaptive web-based systems, which are focusing on adaptation of the presented information or adaptation of navigation as well as ideas of semantic web offers us many possibilities in personalization.

One big group of systems, which utilize these ideas are learning systems, which offer courses or learning material of some subject to the students. Many of these systems works with courses not as collection of individual pages, interconnected through link, but with defined ontologies, connections between them and associated learning material.

In this text adaptive web-based (sometimes referenced as hypermedia) systems are described together with the idea of adaptation and techniques – adaptive navigation and adaptive presentation, which are used in these systems to deliver personalized information to the user. My work is concerning with ontology based course structure. The structure of a course is based on relations between element of ontology, rather than on interconnection between pages, which are

© Václav Snášel (Ed.): WOFEX 2007, pp. 333–338, ISBN 978-80-248-1571-8.
VŠB – Technical University of Ostrava, FEECS, 2007.

connected with links. For every concept two distinct sets are defined – prerequisite and outcome set – which contain elements of ontology. According these sets and occurrences of mapped keywords interconnection between pages based on knowledge can be defined.

2 Adaptive web-based systems

The branch of adaptive web-based systems, which is in development since beginning of the 90's, is focused on personalization of offered hypermedia materials to the users. To this purpose adaptive web-based (hypermedia) systems are used. They are collecting information about users and according their requirements, preferences and goals adapts the presented information.

Adaptive web-based systems can be used in areas, where exists a presumption, that system will be used by different people with different requirements. Therefore these systems are used in the following areas:

- **Information retrieval systems** – purpose of these systems is to help the user in the search in the hyperspace in situations where the user is unable to create a formal query and the user is searching information sequentially following hyperlinks in the documents.
- **On-line information systems** – the main goal of these systems, which represents on-line documentation or on-line encyclopedia, is to help users with different levels of knowledge and with different requirements to offer a reference access to the information.
- **On-line help systems** – these systems are almost like previous systems, but they are focusing only on one particular application (for example spreadsheed application) and to the users are only information usefull to work with the application are presented.
- **Learning hypermedia** – these systems represents to the user only a part of the hyperspace, mostly these systems offers to users learning course or other learning material. The main goal of these systems is to help users/students to learn the presented learning material.

Adaptive web-based systems, which lie within these categories, are using techniques for adaptation of presented information. Adaptation techniques can be divided into two main categories which are *adaptive presentation* and *adaptive navigation*. Each of these categories is further divided into subcategories and particular techniques.

There exists different adaptive web-based systems. Many of these systems were only a testing prototypes, which did not evolve into mature systems. Some of these systems are: AHA! [4, 5], ALEA, NavEx [7], QuizGuide and SQLTutor.

Adaptive presentation These techniques are working with whole pages or with fragments of pages, such as paragraph: *Inserting/removing fragments* –

particular fragments can be removed or inserted in the final presentation of information according the application settings, user preferences or learned knowledge. *Altering fragments* – this technique represents a possibility to choose a fragment from several options for presentation. *Strechtext* – for every fragment there is defined a representative, which can be presented to the user. The system decides if the content of the fragment is visible or only the representative of the fragment. The user can by the mouse click on the representative of the fragment view or hide the content of the fragment. *Sorting fragments* – the fragments in the result are dynamically sorted, that they present the most wanted information on the top of the list. *Dimming fragments* – these technique represent a possibility to shade fragments with non-relevant information.

With the technologies, which are nowadays available in modern browsers (dynamic HTML, CSS, etc.) these techniques can be easily implemented. Together with new and emerging technologies, like AJAX, there is a possibility to offer rich and powerfull user interfaces.

Adaptive navigation These techniques are working with link or with groups of links. *Direct guidance* – the user is guided by the system to the required information by the use of hyperlinks and buttons **next** and **previous**. *Adaptive link sorting* – the presented links are sorted in a way, that the user prefers, or by the preferences of the system or that the links at the top are leading to the most relevant information. These technique is the most used technique for presenting links in the result of the search engines. *Adaptive link hiding* – the links are presented to the user or presented in a different way or completely hidden. *Adaptive link annotation* – these technique represent links textually or graphically differently according their relevance, for example interesting links are represented by the green color, irelevant with red color. *Adaptive link generation* – the system can find new or interesting interconnection within existing pages and generate new links a present them to the users. *Map adaptation* – this technique represent a link map adaptation, which is graphically represented to the users.

3 Ontology based course

The structure of a course is dependent on several factors, which can be following – learning style usual in the school, preferences of the author of the course and requirements of the used system. In the most common structure the course is divided into several chapters. Every chapter is than divided into one or many concepts (concept usually describes in the language of the used system page or fragment of a page or set of pages). Every concept contains learning material, which is presented to the user and one or more learning examples. Usually every chapter ends with a test, where the author of the course can test the students skills and knowledge.

The proposed structure of the course is based on knowledge mined by semantic web technologies and connections between the knowledge rather than on connection between pages. Particular concept is described by two distinct sets – *prerequisite set* and *outcome set.*

The prerequisite and outcome sets consists of elements which represent elements of ontology. Elements placed in particular outcome set can be members of another prerequisite set, creating thus prerequisite – outcomes relation. The basic mapping between learning material and particular elements of ontology, which are in these sets is provided by the use of keywords of the domain.

So defined course structure together with a system, that will offer these courses allows students to take different paths through the course according the knowledge they gained and their goal or information they are seeking. The path through the course is, as was mentioned before, defined by the connection between elements of ontology, more precisely by the outcome and prerequisite sets. The system for every student keeps a set of elements of ontology, which the student already learned.

The basic idea of movement through the course is, that student is allowed to access ontology and learning material associated with it, when he meets all the elements in prerequisite set. When student learns some new learning material, the elements of the outcome set are added to his “achieved knowledge” set. So the students is allowed to learn only such learning material for which he already has all the necessary knowledge. This basic approach can be modified by different extensions, such as allowing student to view learning material afther he meets at least some defined percentage of prerequisite set – therefore there is a need to keep the record of keywords in students “achieved knowledge” set.

The entry point of the course can be defined by prerequisite – outcome relations, where the starting concept is that with empty prerequisite set. This can lead to multiple entry points of the course. The entry point can be also explicitly set by the author of the course. For example that is possible to start C++ learning classically with mathematical and logical expressions as well as with string processing. Student’s needs imply both such a paths.

This approach allows teacher to let student “skip” learning material, which he already knows. For example when student is learning second programming language from the same family of languages (for example students is starting with Java as first language and then C++ as second), he can skip the knowledge and associated learning material, that is same. Ontology and gained knowledge is mapped from the first course to the second. So the students does not have to learn the same knowledge for twice – for example *for, while, do–while* loops are same in Java and C++, so the students by learning loops in Java already can skip learning loops in C++. With this approach student is learning only the new, by applying previously learned. This also needs, that for both courses exists defined ontology and a mapping from one course ontology to the other.

4 Related works

Though the application of ontologies in e-learning environments is still in an early stage, recent researches imply that it will be a promising direction in the future. New published research Ontology based content management and access framework for supporting e-learning systems [6] employ ontology in three ways: – help classifying the learning materials according to the schema of the ontology; – organize and visualize major topics of a course; – provide effective methods to support students access to relevant materials in a semantic way. In contray with their approach of explicitly markup the connection "relate to topic" relationship in the ontology our approach allows to teacher to collect vocabulary semi-automatically from teaching materials and such vocabulary describes the content of its origin.

There is a NavEx system [7] which uses an efficient adaptive prerequisite-based annotation approach. However, unlike other systems that use this approach, NavEx does not require any manual indexing of educational objects. But NavEx is focussed on examples for programming languages learning where our approach would like to mine vocabulary for ontologies in general texts.

The authors in [1] propose a method for adaptive application content modeling using ontology that allows the content reuse between applications. It is based on designed core ontology that is open and can be used for integrating other aspects of adaptive behavior and other layers of reference models. Adaptive applications benefit also from generated domain-dependent part of user model.

5 Conclusions and future work

The previous text was describing, the branch of adaptive web-based systems, together with techniques (adaptive navigation and adaptive presentation), which were and are used in adaptive web-based systems.

The next part of this work, the basic idea of ontology based course structure was presented. The choice of the course structure is essential part of the course creation process.

The future goals of my work is to provide a sequence of steps need to successfully interconnect existing learning material with existing ontology, by defining prerequisty and outcome set based on ontology - keyword mapping. There is also need to create metrics for extraction of keyword or their synonyms from existing text.

To test these ideas a prototype of a tool is developed. This tool will enable the author of the course to define or load definition of keyword, load existing ontology, create mapping between element of ontology and keyword, go through the learning material and to create a description in XML or other intermediate format usable for import into learning or adaptive systems or extend existing material with found metainformation.

References

1. BIELIKOVÁ M., MORAVČÍK M. Modeling the Content of Adaptive Web-Based System Using an Ontology. *In proceedings of* 1^{st} *International Workshop on Semantic Media Adaptation and Personalization SMAP06.* IEEE Computer Society. ISBN: 0-7695-2692-6

2. BIELIKOVÁ M., KURUC J., ANDREJKO A. Learning Programming with Adaptive Web-Based Hypermedia System AHA!, *In Proc. of ICETA 2005*, Košice, Slovakia, September 2005, p. 251-256, ISBN 80-8086-016-6
3. BRUSILOVSKY P. Methods and Techniques of Adaptive Hypermedia, *Adaptive Hypertext and Hypermedia*, Kluwer Academic Publisher, 1998, p. 1-44, ISBN: 0-7923-4843-5
4. DE BRA P., AERTS A., BERDEN B., DE LANGE B., ROUSSEAU B., SANTIC T., SMITS D., STASH N. AHA! The Adaptive Hypermedia Architecture. *In Proceedings of the ACM Hypertext Conference*, Nottingham, UK, August 2003, pp. 81-84
5. DE BRA P., AERTS A., BERDEN B., DE LANGE B., ROUSSEAU B., SANTIC T., SMITS D., STASH N. AHA! The Adaptive Hypermedia Architecture. *In Proceedings of the ACM Hypertext Conference*, Nottingham, UK, August 2003, pp. 81-84
6. MAO M., PENG Y., HE D. Ontology-based Content Management and Access Framework for Supporting E-Learning Systems. *Proceedings of the 2006 IEEE/WIC/ACM International Conference on Web Intelligence and Intelligent Agent Technology (WI-IAT 2006 Workshops)(WI-IATW'06)*
7. YUDELSON M., BRUSILOVSKY P., SOSNOVSKY S. Acessing Interactive Example with Adaptive Navigation Support. *Proceedings of the IEEE International Conference on Advanced Learning Technologies (ICALT'04)* ISBN 0-7695-2181-9/04
8. VELART Z. Adaptivní informační systém pro podporu e-vzdělávání. *In Technologie pro e-vzdělávání 2005*, Praha: ČVUT FEL, 2005, pp. 32-36, ISBN 80-01-03274-4
9. VELART Z., ŠALOUN P.: Využití adaptivního hypermediálního systmu AHA! při výuce programovacího jazyka C++. *In Objekty 2005*, 2005, pp. 280-288, ISBN 80-248-0595-2
10. VELART Z., ŠALOUN P. Výuka programování C++ v adaptivním systému AHA!. *In Technologie pro e-vzdělávání 2006*, ČVUT FEL, 2006, ISBN 80-01-03512-3
11. ŠALOUN P., VELART Z. Adaptive Hypermedia as a mean for learning programming. *In Workshop proceedings of the* 6th *ICWE 2006*. ACM Digital Library, 2006, ISBN 1-59593-435-9
12. VELART Z., ŠALOUN P. User Behavior Patterns in the Course of Programming in C++. *In Proceedings of the joint international workshop on Adaptivity, personalization & the semantic web*. ACM Digital Library, 2006, ISBN 1-59593-453-7
13. VELART Z. Utilization of adaptive hypermedia for learning programming. *In Proceedings of WOFEX 2006*, 2006, pp. 440-445, ISBN 80-248-1152-9
14. VELART Z., ŠALOUN P. Evaluation testing with strong motivation. *In Proceedings of the Seventh International Scientific Conference Electronic Computers and Informatics ECI 2006*, 2006, pp. 64-69, 80-8073-598-0
15. VELART Z., ŠALOUN P., KALINSKÁ M. Znalostmi řízený průchod kurzem. *1st Workshop on Intelligent and Knowledge oriented Technologies - WIKT 2006 Proceedings*. 2006. Bratislava, Slovakia. ISBN 978-80-969202-5-9
16. VELART Z., KOŘENEK P., ŠALOUN P.: Získávání ontologií z připraveného kurzu a z nich vycházející návrh pruchodu kurzem v prostředí hypermediálního personalizovaného systému, *to be published on Technologie pro e-vzdělávání 2007*, Praha 2007.

DRM Reception - the Practical Experience

Marek Dvorský

Department of Electronics and Telecommunications, FEECS,
VŠB – Technical University of Ostrava, 17. listopadu 15, 708 33 Ostrava – Poruba
`marek.dvorsky.fei@vsb.cz`

Abstract. **DRM** (Digital Radio Mondiale) is the most perspective system of the new digital radio broadcasting systems that works below 30MHz. It means that **DRM** sooner or later overtakes a position of present **AM** (amplitude modulated) systems working at Long Wave (**LW**), Medium Wave (**MW**) and Short Wave (**SW**) frequency bands. In contrast to an abroad experience, our ordinary listener does know not so much about this technically and economically advantaged system. This paper deals with practical experience of long distance reception abroad transmitters **DRM** on our territory.

1. Introduction

It seems that the time of the radio broadcasting at **LW**, **MW** and **SW** bands have already gone. The opposite is true – **LW**, **MW** and **SW** bands are before their renaissance. It is obvious that it cannot remain in a classical analogue broadcasting method of an amplitude modulation but there have to be used new digital modulation principles.

In September 2001 ETSI (*European Telecommunications Standards Institute*) published a technical specification of system for digital broadcasting "*ETSI-TS 101980: Digital Radio Mondiale, System Specification*", in which this system recommend for radio broadcasting bellow 30MHz. DRM was approved by ITU-R in October 2002 as "*Recommendation ITU-R BS 1514-1: Digital Sound Broadcasting Bellow 30 MHz*". Nowadays Consortium **DRM** have 90 members from 30 countries and more than 40 associated members. The group called High Frequency Co-ordination Conference (**HCCF**) presents the Czech Republic. **DRM** is broadcast in more than 30 countries all around the word. While **DRM** currently covers the broadcasting bands below 30 MHz, the **DRM** consortium voted in March 2005 to begin the process of extending the system to the broadcasting bands up to **120 MHz**. The design, the development and the testing phases are expected to be completed by 2007-2009. [1], [4]

Since there has not been working a DRM transmitter in the Czech Republic yet, the reception of DRM signals relays just on signals from abroad transmitters. Under this consequence is a long distance reception meant to be more like a hobby for the **DRM** enthusiasts.

© Václav Snášel (Ed.): WOFEX 2007, pp. 339–344, ISBN 978-80-248-1571-8.
VŠB – Technical University of Ostrava, FEECS, 2007.

2. Type of receivers

At the beginning it has to be said that the long distance reception does not pick up some of the great advantages such as a mobile reception that offers **DRM** broadcasting, the principles of a single frequency network (**SFN**) are meaningless and at least the information broadcasting through a data channel (traffic information, weather forecast e.g.) is uninteresting for a foreign listener. Currently, there are three basic types of the **DRM** receivers.

2.1. Commercial receivers

This type of the receivers is the most spread in the areas perfectly covered by **DRM**. However, the receivers which dispose of DRM standard are just rarely seen on the market. Contemporary the problems linked with the technology **DRM** are caused by an increasing demand for receivers which are now missing on the market or are just presented by narrow choice which is often expensive.

Some of them indicate that many other technologies such as **T-DAB** (Digital Audio Broadcasting - Terrestrial) may be used in different countries around the world. Accordingly, many chip manufacturers who are addressing this market are catering for them and developing systems that will be able to switch between the varieties of bands that will be used around the globe.

Fig. 1. Example of **DRM** commercial receivers

Since we talk about the long distance reception and a few fanciers who will not spend a huge money for expensive receivers, is this kind of receivers not suitable. We have to start looking for the alternatives.

2.2. Software receivers

One of the most reasonable alternatives is a software receiver. It can be guess from the name that this receiver is assembled from "*an ordinary* ***AM***" receiver and a software demodulator. No special requirements might be needed for the receiver. It should be enough sensitive and able to bring out an intermediate frequency (**IF**) signal after conversion.

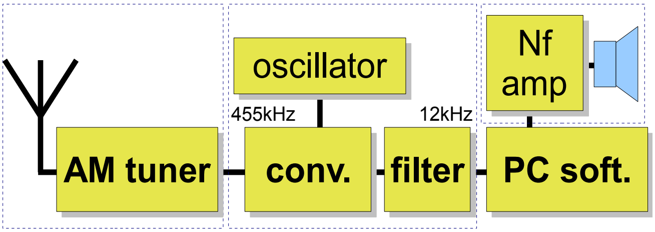
oscillator
Nf amp
455kHz
12kHz
AM tuner
conv.
filter
PC soft.

Fig. 2. Software Radio block diagram

A receiver's adjusting consists in finding and bringing out the intermediate frequency (455kHz or 10,7MHz) and inserts an extra converter (**conversion 455kHz into 12kHz**). By that we get a baseband signal which can be brought to a PC sound card. The decoding and the demodulation are done by a special software (e.g. freeware **DREAM** or licensed **DRM Software Radio**).[1]

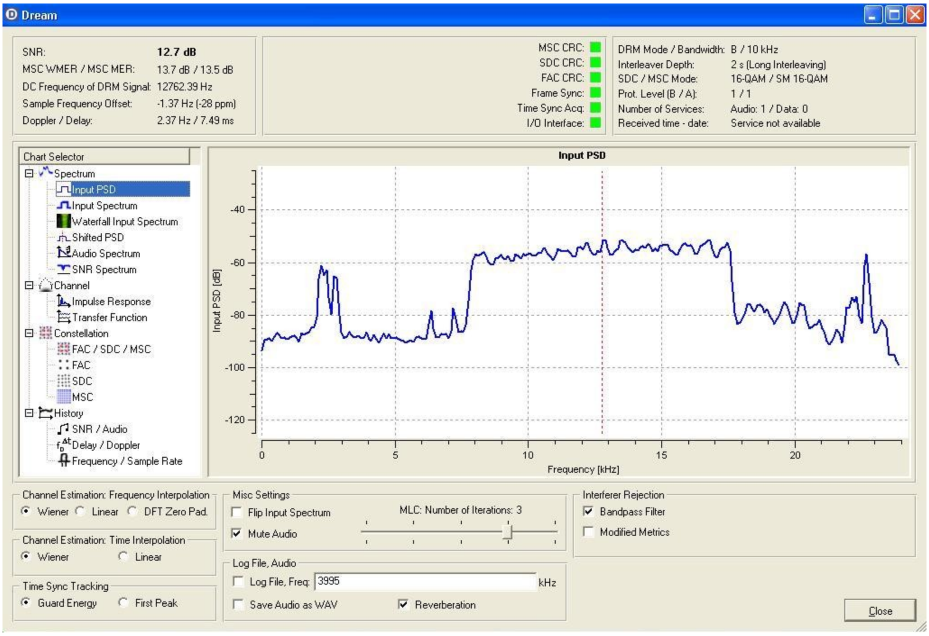
Dream
Chart Selector
Spectrum
Input PSD
Input Spectrum
Waterfall Input Spectrum
Shifted PSD
Audio Spectrum
SNR Spectrum
Channel
Impulse Response
Transfer Function
Constellation
FAC / SDC / MSC
FAC
SDC
MSC
History
SNR / Audio
Delay / Doppler
Frequency / Sample Rate
Input PSD
Input PSD [dB]
-40
-60
-80
-100
-120
0
5
10
15
20
Frequency [kHz]
Close

SNR: **12.7 dB**
MSC WMER / MSC MER: 13.7 dB / 13.5 dB
DC Frequency of DRM Signal: 12762.39 Hz
Sample Frequency Offset: -1.37 Hz (-28 ppm)
Doppler / Delay: 2.37 Hz / 7.49 ms

MSC CRC: 🟩
SDC CRC: 🟩
FAC CRC: 🟩
Frame Sync: 🟩
Time Sync Acq: 🟩
I/O Interface: 🟩

DRM Mode / Bandwidth: B / 10 kHz
Interleaver Depth: 2 s (Long Interleaving)
SDC / MSC Mode: 16-QAM / SM 16-QAM
Prot. Level (B / A): 1 / 1
Number of Services: Audio: 1 / Data: 0
Received time - date: Service not available

Channel Estimation: Frequency Interpolation
● Wiener ○ Linear ○ DFT Zero Pad.

Channel Estimation: Time Interpolation
● Wiener ○ Linear

Time Sync Tracking
● Guard Energy ○ First Peak

Misc Settings
☐ Flip Input Spectrum
☑ Mute Audio
MLC: Number of Iterations: 3

Log File, Audio
☐ Log File, Freq: 3995 kHz
☐ Save Audio as WAV ☑ Reverberation

Interferer Rejection
☑ Bandpass Filter
☐ Modified Metrics

Fig. 3. Software Radio DREAM

2.3. Professional Receivers

The last type of the receivers is the professional communication receivers. This type is more suitable for a research and a development than for an ordinary listener. The resulting factor here is their high price.

Within the framework of the research project **FRVŠ** *(Fond Rozvoje Vysokých Škol)* ***459/2007*** *„Demonstrační pracoviště využívající nové digitální vysílací technologie“* was a laboratory of Radio-communication at The Telecommunications Department equipped by a front-end receiver **WINRADIO WR G313. WR G313** has had an extended bandwidth from **9kHz to 180MHz.** The sensitivity goes up to -116dBm (0.35µV with AM service). By these features G313 enables monitoring not only DRM transmitters in wild frequency range. [2]

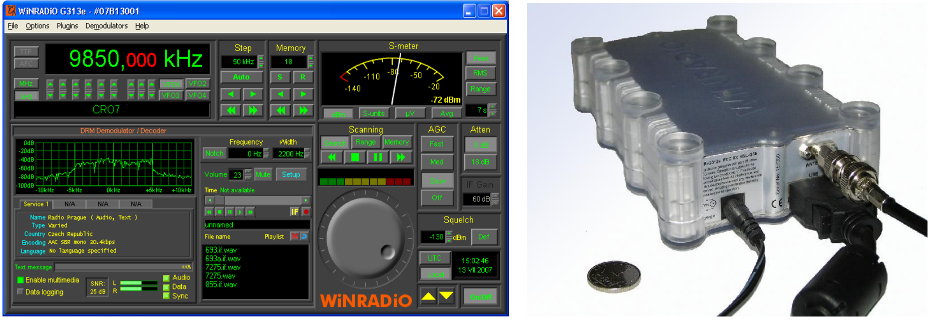
WiNRADiO G313e - #07B13001
File Options Plugins Demodulators Help
9850,000 kHz
CRO7
Step
Memory
S-meter
-72 dBm
DRM Demodulator / Decoder
Scanning
AGC
Atten
Squelch
WiNRADiO

Fig. 4. Winradio WR G313 – the remote software and the hardware parts

3. Long distance reception

More than 130 International, National and Local DRM Broadcasters are on Markets Worldwide (updated 7.7.2007) on http://drm.org/livebroadcast. [1] In our case when we talk about the foreign broadcasters, the reception conditions are fully depended on a daytime, a ionosphere condition and a used frequency. That is logical, due to way of a wave propagation which is mostly done by a ionosphere wave. A frequency scanning has to be analyzed and suit to a daytime and the actual wave propagation conditions.

One of the FRVŠ 459/2007 project solutions is focused on searching foreign DRM transmitters in the frequency bandwidth c. 500kHz-15MHz while is used **WR G313** and a broadband matched antenna **LW** (Long Wire).

The captured stations are recorded and compared to the radiation pattern published at [1]. The present results are good beyond expectation. The receiver is able to decode a signal with **SNR≥7dB.** It has to be mentioned that once is DRM signal tuned, it is available in a full quality. If the broadcast is also a data channel (headlines, traffic info., weather forecast etc.), it takes some time than the data are available (usually 3 to 5 min).

In contrast to professional receivers, there was made an experiment with a software radio (overview receiver **SONY ICF-7600DS** with an external decoder and the software **DREAM**). It had been achieved the similar results. However, from time to time

DREAM could not decode a signal due to a decoder overloading by a high level of noise. It can be caused by a high sensitivity level of DREAM and an electrical disturbance.

The choice and placing the receiver's antenna has a considerable sense. Under taken experiences, an indoor antenna has shown as useless. Electrical noise goes from the fluorescent tubes with a poor quality inductor, a laptop with a plastic case, LAN (local area network) networks etc. negatively influence clear reception by DREAM. In this condition "**the magnetic loop antenna**" (MLA) takes a right place. The essence of the loop antenna is that it responds mainly to the magnetic field component of an electromagnetic wave (the H-field component) rather than the electric (E-component). This feature gives the magnetic loop a non-sensitivity of the electrics interferences. It is usually used for receiving in the small places, where cannot be used a proper length antenna as well as in the places with a high electric noise level.[3]

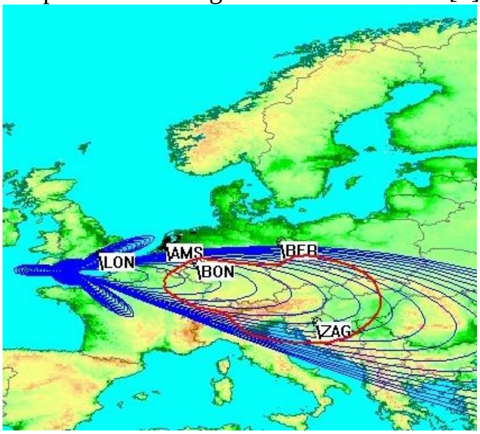

Fig. 6. Radiation pattern of transmitter Rampisham, Great Britain, f=9850 kHz, Power 35kW, program: **Radio Prague** [1]

4. Conclusion

The actual results prove the theoretical advantages of DRM in quality of the signal and the interruption robustness. The type of the receivers does not influence the quality of the output signal. There might be a difference in a remote control comfort. Software Radio is more likely to be overload by electrical noise. The most important component of a radio-communication chain is an antenna, its type and the placement. Although a universal solution does not exist.

We can still hope that a future of DRM in our country will not fall behind the west part of the world for long time and we soon come from a long distance reception to a local.

References

1. *Digital Radio Mondiale* [online]. c1999-2007 [cit. 2007-07-07]. Available from WWW: <http://www.drm.org>.
2. *WINRADIO* [online]. c2006 [cit. 2007-07-07]. Available from WWW: <http://www.winradio.com/>.
3. DVORSKÝ, Marek. THE MAGNETIC LOOP ANTENNA. In *7. Seminar of Telecommunications Department* [s.l.] : [s.n.], 2007. s. 104-108. ISBN 978-80-248-13.
4. DVORSKÝ, Marek. DIGITAL RADIO IN THE BROADCASTING BANDS BELLOWS 30MHz. In *7. Seminar of Telecommunications Department*. [s.l.] : [s.n.], 2007. s. 95. ISBN 978-80-248-13.

Appendix: An example of DRM broadcasters

Table 1. Extract from a list of relevant DRM broadcasters

f		**Sound**		**Data**
[kHz]	**Program**	**Quality**	**Bitrate [kbps]**	**Bitrate [kbps]**
693	RAI WAY DRM TEST	AAC SBR stereo	19,60	
855	Berlin	AAC SBR stereo	17,60	0,4+1
1 296	BBC World	AAC SBR stereo	25,90	-
3 995	Deutsche Welle	AAC SBR mono	14,50	-
5 990	RTL	AAC SBR mono	17,40	-
6 085	BR-B5akt	AAC SBR mono	17,50	-
6 095	RTL	AAC SBR stereo	20,90	-
6 175	RMC (Audio)	AAC SBR mono	17,50	-
7 240	Bouquet Flevo NL	AAC SBR mono	17,40	-
7 275	Deutsche Welle	AAC SBR stereo	18,00	0,40
9 460	Deutsche Welle	AAC SBR stereo	18,00	0,40
9 760	VT Digital	AAC SBR stereo	20,70	-
9 770	VT Digital	AAC SBR stereo	21,70	-
9 850	**Radio Prague**	**AAC SBR stereo**	**20,40**	**-**
9 880	Kuvajt	AAC SBR mono	11,60	-
12 060	Voice of Russia	AAC SBR mono	17,40	-
13 620	MOI Kuwait	AAC SBR mono	11,60	-
13 810	Deutsche Welle	AAC SBR stereo	17,40	-
15 715	Deutsche Welle	AAC SBR stereo	20,70	0,40

Fiber Optical Sensors in Biomedical

František Hanáček

Department of Electronics and Telecommunications, FEECS,
VŠB – Technical University of Ostrava, 17. listopadu 15, 708 33 Ostrava – Poruba
`frantisek.hanacek.fei@vsb.cz`

Abstract. : Fiber optics sensors in biomedicals are very perspective for the future using. FOS in medicals use all of advantage of fiber optics. Construction of FOS allow use in wide range in all biomedical application.

1 Introduction

Optical techniques developed for sensing purposes proved to be essential in many applications fields, ranging from aerospace, industry, process control, to security, and also medicine. The capability of these sensors are generally enhanced when a bulk-optical configuration is replaced by optical fibre sensors. Fiber optical sensors based on telecommunication fibers or adapting special fibers are main component for the future, for precious measurement system.

2 Fiber optic sensor

The simplest sub-division of optical sensors is into so-called *intrinsic* devices, where the interaction occurs actually within an element of the optical fiber itself and *extrinsic* devices were the optical fiber is used to coule light, usually to and from the region where the light beam is influenced by the measurand. This is external to the fiber, but may be attached to it in some suitable way, by fusion-splicing, glueing or mechanical connection which may often be decoupled. The familiar requirement of a sensor system is the measurement of a particular measurand at a particular location, this usually being achieved with a *point* sensor. This is the way in which most sensors operate, such as those used, for example, in the monitoring of temperature, acceleration, pressure or many chemical parameters. A schematic of the three major sensor schemes point, distributed and quasi-distributed is illustrated in Fig. 1.a. Fig. 1.a shows, for example, a *point* sensor. Many different types of such sensors exist - as examples, they range from liquid level monitors with a prism tip, through chemically-sensitive ‘‘dip-in’’ probes for species monitoring and to resonant structures mounted at the end of the fiber for pressure or acceleration measurement. Alternatively, sensor devices may be designed so that they can discriminate in the spatial mode, and in this

© Václav Snášel (Ed.): WOFEX 2007, pp. 345–349, ISBN 978-80-248-1571-8.
VŠB – Technical University of Ostrava, FEECS, 2007.

way, the measurand can be determined along the *length* of the fiber itself, in a process normally termed *distributed* sensing, illustrated in Fig.1b. This principle has been employed widely in the measurement of temperature using non-linear effects in fibers, such as Brillouin or Raman scattering or in some types of strain sensing. A style of sensor that is somewhat ‘‘in between’’ these two types of sensors is termed *quasi-distributed*, as shown schematically in Fig.1c , where the measurand information is obtained at particular and pre-determined points along the length of a fiber network. Here, the fiber has been sensitized or special materials have been introduced into the fiber loop to allow the measurement to be taken and this technique has been applied to temperature and chemical sensing, e.g., using different fiber types.

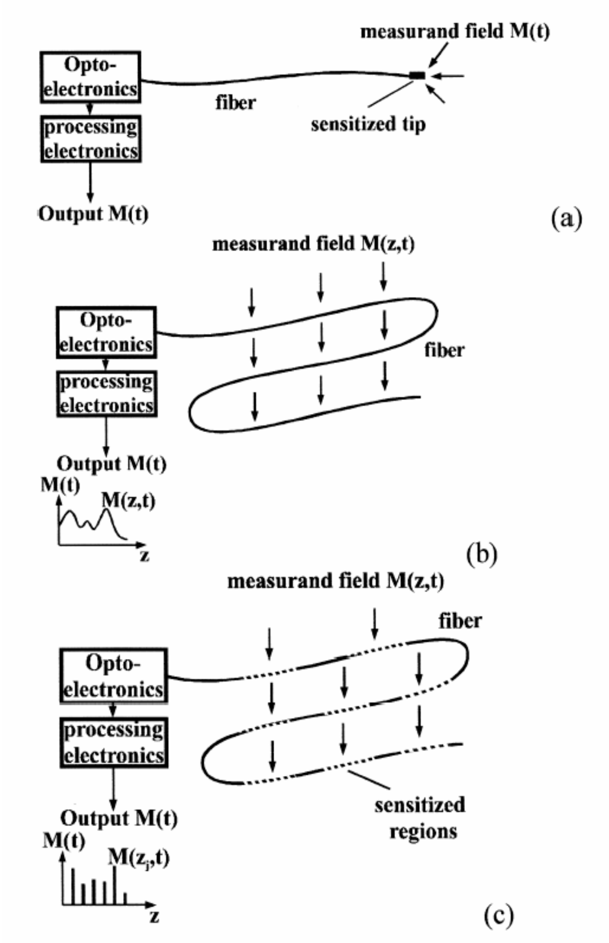
measurand field M(t)
Opto-electronics
fiber
sensitized tip
processing electronics
Output M(t)
(a)
measurand field M(z,t)
Opto-electronics
fiber
processing electronics
Output M(t)
M(t)
M(z,t)
z
(b)
measurand field M(z,t)
fiber
Opto-electronics
processing electronics
sensitized regions
Output M(t)
M(t)
M(z_i,t)
z
(c)

Fig. 1. (a) Point, (b) intrinsic distributed, and (c) quasi-distributed sensing.

3 Fiber optic sensor in medical

Fibre optic sensors overcome some of these drawbacks, owing to the well known inherent characteristics of optical fibre:

- *geometrical versatility*, such as miniaturization, flexibility, and lightness, which allow easy insertion in catheters and needles, and hence highly localized measurements inside blood and tissues;
- *suitable material*, glass or plastic, non-toxic and biocompatible, and can be used for continuous measuremens;
- *intrinsic safety for the patient*, ensure by optical fibre dielectricity and by the low light power used for sensing purposes.

Furthermore, optical fibres present low attenuation, so that long fibre links can be used, if the electronics must be located far from the bedside. Fibres must be cabled, so as to avoid handling problem. Another property is the absence of crosstalk between close fibres, which suggest housing different sensors in the same catheter. In some cases a single elektro-optic unit can be utilized for all the sensor, naturally with an appropriate illumination, detection and signal-processing scheme.

Basic division of FOSs to classification in three main classes: sensors for physical parameter, sensors for chemical parameters and "spectral" sensors, for which spectral analysis is performed in order to know the state of health of particular organ or tissue.

The working principle of FOSs is based on the modulation of the fibre-guided light produced in one of the optical properties (phase, intensity, wavelength, polarization state) by the parameter under investigation. The complexity of the electro-optical system, the type of component selected, and thus cost of the sensor are related to the operating principle.

The ideal FOS for biomedical applications should posses the following characteristics:

- reliability,
- automatic or semiautomatic operation for use by operators who have little or no technical background,
- low-cost installation and maintence

These requirements limit the selection of the sensor's operating principle and impose limitations to the complexity of the electro-optical system. FOSs for biomedical applications are mostly of the intensity modulation type, owing to the low cost of their components and the intensity of their architectures. They can be either *intrinsic* or *extrinsic,* according to whether the intensity modulation is produced by the fibre, which is sometimes modified, or by an external transducer connected to the fibre (Fig.2)

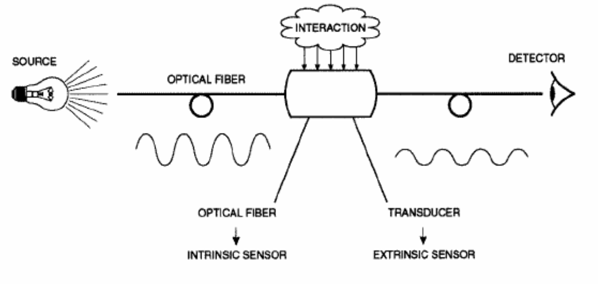
INTERACTION
SOURCE
OPTICAL FIBER
DETECTOR
OPTICAL FIBER
↓
INTRINSIC SENSOR
TRANSDUCER
↓
EXTRINSIC SENSOR

Figure 2. Working principle of intensity-modulated fibre-optic sensor.

A FOS of the intensity modulation type can be viewed as a compact electro-optical module connected to the measuring probe by a multimode optical fibre (Fig. 3.) The module houses source(s) detector(s), and all the electronics for signal processing.

The sources can be either lamps, lasers, LEDs, or laser diodes. Lamps and lasers require beam focus optics and holders for the fibre alignment. If a halogen lamp is used, interferential or dichroic filters may also be necessary when the sensor has a specific operating wavelength. LEDs and laser diodes, the most compact, may be housed in special receptacles that are easily connected to the fibre by commercial connectors. The most recent LEDs and laser diodes offer a wide variety of wavelengths. Laser diodes have a high emission power and can, in many cases, replaces costlier and bulkier lasers.

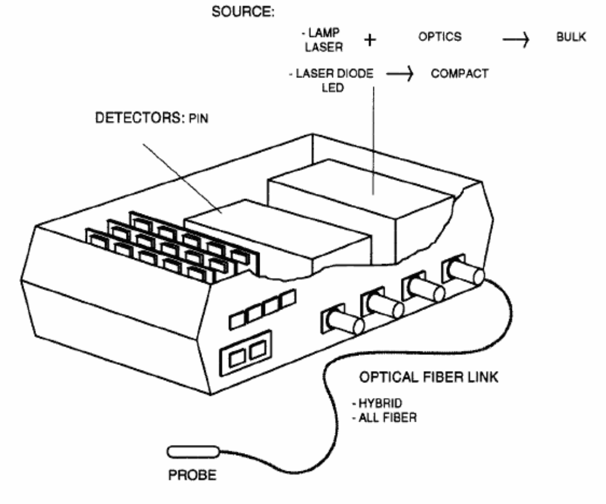
SOURCE:
- LAMP
LASER
+
OPTICS
⟶
BULK
- LASER DIODE
LED
⟶
COMPACT
DETECTORS: PIN
OPTICAL FIBER LINK
- HYBRID
- ALL FIBER
PROBE

Figure 3. Sketch of the instrumentation of a fibre-optic sensor.

References

1. A.Ghatak, K. Thyagarajan, “Introduction to Fiber Optics”, *Cambridge university press.* ISBN 0-521-57120-0
2. J. M. Lopez-Higuera, “Handbook of Fibre Optics sensing technology”, *JOHN WILEY and SONS 2002.* ISBN 0-471-82053-9
3. Mignani A.G., Baldiny F., Biomedical senzors using optical fibres, Report on Progress in physics, 1996 p. 1-28
4. K.T.V. Grattan, Sun T., Fiber optic sensor technology: an overview, Sensors and Actuators A: Physical; 2000 p. 40-61
5. Udd E., Fiber Optic Sensors an Introduction for Engineers and Scientists John Wiley & Sons, New York, 1991 ISBN 0-471-83007-0
6. Hanáček F., Vláknově optické sensory v medicíně. Ostrava 2006. 74 s. Diplomová práce na Fakultě elektrotechniky a informatiky, katedra Telekomunikační techniky

The Influence of the Network Load on a Quality of IP Telephony

František Hromek

Department of Electronics and Telecommunications, FEECS,
VŠB – Technical University of Ostrava, 17. listopadu 15, 708 33 Ostrava – Poruba
`frantisek.hromek.fei@vsb.cz`

Abstract. Raising the counts of users and programs counts that need the network connection have the direct influence on the increasing amount data flows in networks. Individual data flows do not have identical demands of carrier characteristics, which make a possible the usage of QoS; QoS provide a different kind of service that is the most suitable for a concrete information type. However, what will happen in the situation that increased data flows belongs to the one information type and that information type need, in its nature, limited network resources? The IP telephony is one of the most susceptible data flows with very limited network resources. In this article is presented the influence of increased data flow to IP telephony.

1 Introduction

During last few years the telecommunication sector focuses its interest to IP telephony - VoIP (Voice over Internet Protocol). The IP telephony is totally new method of communication that is based on using IP networks. IP networks were originally created for transmission of classic type of data (such as a file transfer). Any information is chopped into small data units called packets in these networks. Packets are transmitted to recipient address independently. They can arrive to recipient in a different time and a different sequence. Voice or Video streams are divided into small transport units too. But for these data flows is necessary to lower packet delay below 200ms, because with greater delay the quality of communication declines dramatically. In this communication is also important to ensure that packets are in correct sequence for additional processing. For this task is necessary to assign exclusive system resources to in every network device. If this is not assured for only one, the quality will be probably dramatically reduced.

IP telephony service models mostly use PQ (Priority Queuing) for a service. That is because PQ in preference services concrete requirements. However it is appropriate manner in cases, when the amount of traffic, which has come to be preferred, is relatively smaller that amount of other traffic. What, however, will happen in the situation that the percentage of VoIP traffic increases? From basic knowledge mode of operation of service queue we can assert, that there will be the increased traffic in an

© Václav Snášel (Ed.): WOFEX 2007, pp. 350–355, ISBN 978-80-248-1571-8.
VŠB – Technical University of Ostrava, FEECS, 2007.

applicable service front. This increased traffic will be obvious, since it increases waiting time and also a jitter. A packet loss can easily happen in the above mentioned network saturation. Question is, how the increased traffic load, that is directed into a concrete queue, influence the quality of communication. Let us to propose an experiment, in which I am more closely intent on monitoring communication parameters, at a step by step raising the load in network components.

2 E-model

An E-model was developed for consideration qualities of communication. The first standardized version has been published below mark ITU- T G.107 already in the year 1998. In the following years a model was improved many times. In the year 2000 came to addition adjustments of comprehensive noise impact in rooms and influence of deformation signal causing quantization. In the year 2002 has been included an influence of accidental packet loss during transmission. Presently holds valid a recommendation from the year 2003, in which a voice model is specified.

A Result of E-model is an R-factor that describes a quality of the talk value in interval from 0 to 100. Include influence noise, echo, delay, quantization distortion, packet loss and many of other partial influences, manifestative in resulting quality talk.

A common expression a quality of talk on the basis interval value R-factor is relatively simple, see Table 1. The quality of talk is generally defined for interval R-factor from 50 to 100. The value of R-factor less than 50 is insufficient for communication. For a consideration talk quality is possible use an older formulation MOS.

Table 1. R-factor of Voice Quality

R-factor	MOS	Voice Quality
$90 \leq R < 100$	>4,3	Best
$80 \leq R < 90$	4,0-4,3	High
$70 \leq R < 80$	3,6-4,0	Medium
$60 \leq R < 70$	3,1-3,6	Low
$50 \leq R < 60$	2,6-3,1	Poor

3 Experiment

An primary task of the experiment is to determine an influence of network load on the quality of IP communication. Remarkable are especially changes of parameters depending on the increase of the network load. An Experimental workplace structure is represented Fig. 1.

A base of experimental workplace was formed by two PCs running application IxChariot Performance Endpoint and one PC running IxChariot Performance Console.

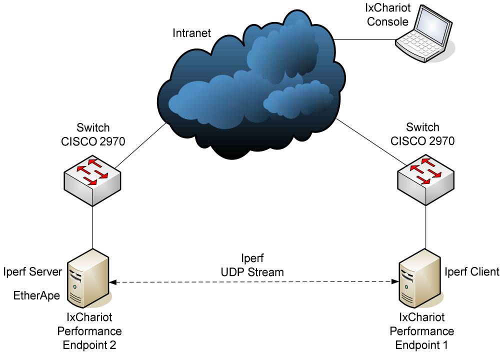
IxChariot Console
Intranet
Switch CISCO 2970
Switch CISCO 2970
Iperf UDP Stream
Iperf Server
EtherApe
Iperf Client
IxChariot Performance Endpoint 2
IxChariot Performance Endpoint 1

Fig. 1. Experimental workplace

Exact flows were predefined in IxChariot Performance Console. These predefined flows were then generated between communication endpoints. Results were sent back to the Console for evaluation.

Table 2. Network load influence to IP telephony quality

Network Load	R-faktor	End-to-End Delay	Jitter	Packet Loss
[%]	[-]	[ms]	[ms]	[%]
0	92,21	31	0	0
10	91,93	32	0	0
20	91,61	33	0,007	0
30	91,32	35	0,059	0
35	90,86	36	0,082	0
40	88,03	38	0,125	0
45	86,83	40	0,202	0
46	86,77	49	0,164	0
47	85,88	162	0,236	0
48	72,78	295	0,161	0
49	47,09	447	0,112	1,246
50	31,08	506	0,195	2,963
51	25,23	529	0,582	4,297
52	19,85	549	1,553	10,83
53	18,35	567	1,268	16,133

The traffic was generated by a support software application for measuring network efficiency Iperf 1.7.0. This application needs to use one workplace as a server and the other as a client. The verification was checked by the support application EtherApe. In every measure IxChariot generated fifty parallel VoIP communications with encoding algorithm G.711. A Network load in the table is introduced without inclusion VoIP traffic. This is because for us is not important when changes happened but its consequences.

4 Queuing models

For the calculation of the delay in router (jitter), with one service queue, we can, under certain condition, use figure (1) [4]:

$$T = \frac{1}{\mu} + \frac{\rho}{2\mu(1-\rho)} \tag{1}$$

Where: μ –Attendance speed of requests [s^{-1}]
α – Intensity speed of requests [s^{-1}]
ρ– System load [-]
After substitution, we get (2) [4]:

$$T = \frac{1}{2} \cdot \frac{P_S + H_L + L_S \cdot T_S}{L_S} \cdot \frac{2P_S \cdot L_S - C_{BW} \cdot M\left(P_S + H_L + L_S \cdot T_S\right)}{P_S \cdot L_S - C_{BW} \cdot M\left(P_S + H_L + L_S \cdot T_S\right)} \tag{2}$$

Where: C_{BW} – Codec Bandwidth [kbit/s]
P_S – Payload size [B]
T_S – Sample time [ms]
H_L – Header length [b]
L_S – Line speed [kbit/s]
When we use model with two priority queues, we could lower jitter in packets in the first queue, but we increase jitter in packets in the second queue.

$$T_1 = \frac{1}{\mu} + \frac{\rho}{2\mu(1-\rho_1)} \tag{3}$$

$$T_2 = \frac{1}{\mu} + \frac{\rho}{2\mu(1-\rho_1)(1-\rho)} \tag{4}$$

When we substitute, we get (5) (6):

$$T_1 = \frac{1}{2} \cdot \frac{P_S + H_L + L_S \cdot T_S}{L_S} \cdot \frac{2P_S \cdot L_S - C_{BW}\left(M_1 - M_0\right)\left(P_S + H_L + L_S \cdot T_S\right)}{P_S \cdot L_S - C_{BW} \cdot M_1\left(P_S + H_L + L_S \cdot T_S\right)} \tag{5}$$

$$T_1 = \frac{1}{2} \cdot \frac{P_S + H_L + L_S \cdot T_S}{L_S} \cdot \frac{2P_S \cdot L_S - C_{BW}(M + 2M_1)(P_S + H_L + L_S \cdot T_S) + 2C_{BW}{}^2 \cdot M \cdot M_1(P_S + H_L + L_S \cdot T_S)^2}{P_S \cdot L_S - C_{BW}(M + M_1)(P_S + H_L + L_S \cdot T_S) + C_{BW}{}^2 \cdot M \cdot M_1(P_S + H_L + L_S \cdot T_S)^2} \tag{6}$$

This could be useful to stop dramatic delay increase in packet with higher jitter. On the other side, there will be a greater jitter increase in packet with lower jitter. The increase of the lower jitter will not be problem in VoIP telephony, because there is used de-jitter buffer.

5 Conclusion

From above started results is perceptible, that the delay increase slowly first. The end-to-end delay begins increase significantly in interval from 46 to 47%. But this is not an overall load, it is only a load generated by an external source. To compute the overall load we have to increment a load done by VoIP too. In this case we have to add roughly 44%. My first expectation was that there will be the jitter increase. Because there was the stable load during measuring all packets (all were delayed) and that express in an end-to-end delay increase. In interval from 48 to 49% (92 – 93%) is evident a degradation of the talk quality. This degradation is given partially by an end-to-end delay and partially by a packet loss.

In our case delay has, however, only minimum influence to the R-factor degradation until 46%, because we communicate in a local area. But when we communicate for a long distance these small delays sums, which means that overall quality will be affected by the delay factor too. On long communication paths we should not have greater substitution of VoIP traffic. A network load between 50-70% has increasing a delay by 2ms in our case. Between 70-90% there was already 5ms increase. With greater counts of network devices, this will be a major affect to the voice quality of degradation.

References

1. Hromek F.: Vliv zatížení sitě na kvalitu IP komunikace. Telecommunication Workshop, Ostrava (2007)
2. RFC 3261: SIP Session Initiation Protocol. IETF, June (2002)
3. ITU-T G.107: The E-model, a computational model for use in transmission planning, 2005
4. Halás,M.: Optimalizácia hlasovej prevádzky s ohľadom na kvalitu hovoru v sieťach s technolóhiou VoIP, dizertačná práca, Katedra telekomunikácií STU Bratislava (2006)
5. Vozňák, M. - Zukal, D.: E-model pro stanovení kvality hlasu. Sborník příspěvků 6. ročníku semináře KETT, Ostrava (2005)

Appendix: Graphs

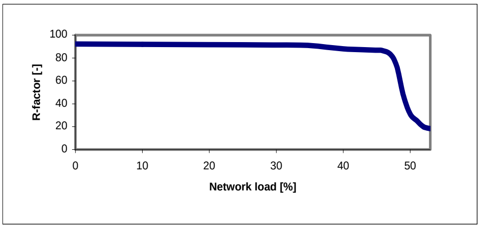

Fig. 2. The R-factor dependence on the network load

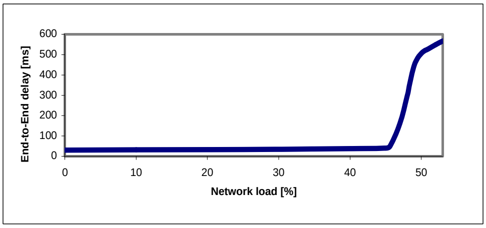

Fig. 3. The End-to-End delay dependence on the network load

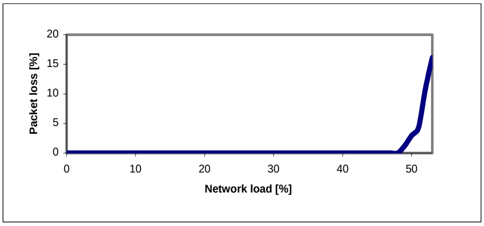

Fig. 4. The packet loss dependence on the network load

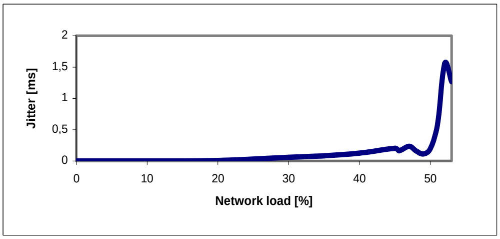

Fig. 5. The jitter dependence on the network load

Mathematical Modeling of EDCF Media Access Mechanism

Petr Machník

Department of Electronics and Telecommunications, FEECS,
VŠB – Technical University of Ostrava, 17. listopadu 15, 708 33 Ostrava – Poruba
`petr.machnik.fei@vsb.cz`

Abstract. The main topic of this paper is to describe the EDCF access mechanism used in the IEEE 802.11 technology and its mathematical modeling by Markov chains.

1 Introduction

The IEEE 802.11 working group chartered the 802.11e task group with the responsibility of enhancing the 802.11 MAC to include bidirectional quality of service (QoS) to support latency sensitive applications such as voice and video. Also, new types of consumer electronics are looking to 802.11 as a wire replacement. Products such as cable and satellite receivers might one day send high definition TV (HDTV) signals via 802.11 to TVs. DVDs and digital video recorders might do the same. The new applications for 802.11 require an effective QoS mechanism to ensure that their latency sensitive data has priority over data such as e-mail and web browsing.

To support QoS, many priority schemes are currently being discussed. IEEE 802.11 Task Group E defined enhancements to the 802.11 MAC, which are called 802.11e. These enhancements introduce two new MAC modes: EDCF and HCF. Both of these QoS-enhanced MAC protocols support up to eight priority levels of traffic, which map directly to the RSVP protocol and other protocol priority levels.

2 Enhanced Distributed Coordination Function (EDCF)

The major enhancement provided by EDCF versus older DCF is the introduction of eight distinct traffic classes. Aside from this, EDCF, as the name suggests, works in a fashion similar to the DCF MAC, except that some of the elements of the MAC are parameterized on a per-class basis. Figure 1 illustrates the functioning of EDCF. Here, each traffic class (TC) starts a back-off after detecting the channel being idle for an AIFS. The AIFS is at least as large as the DIFS, and can be chosen individually for each TC. This is the first per-class MAC parameter added in EDCF.

© Václav Snášel (Ed.): WOFEX 2007, pp. 356–361, ISBN 978-80-248-1571-8.
VŠB – Technical University of Ostrava, FEECS, 2007.

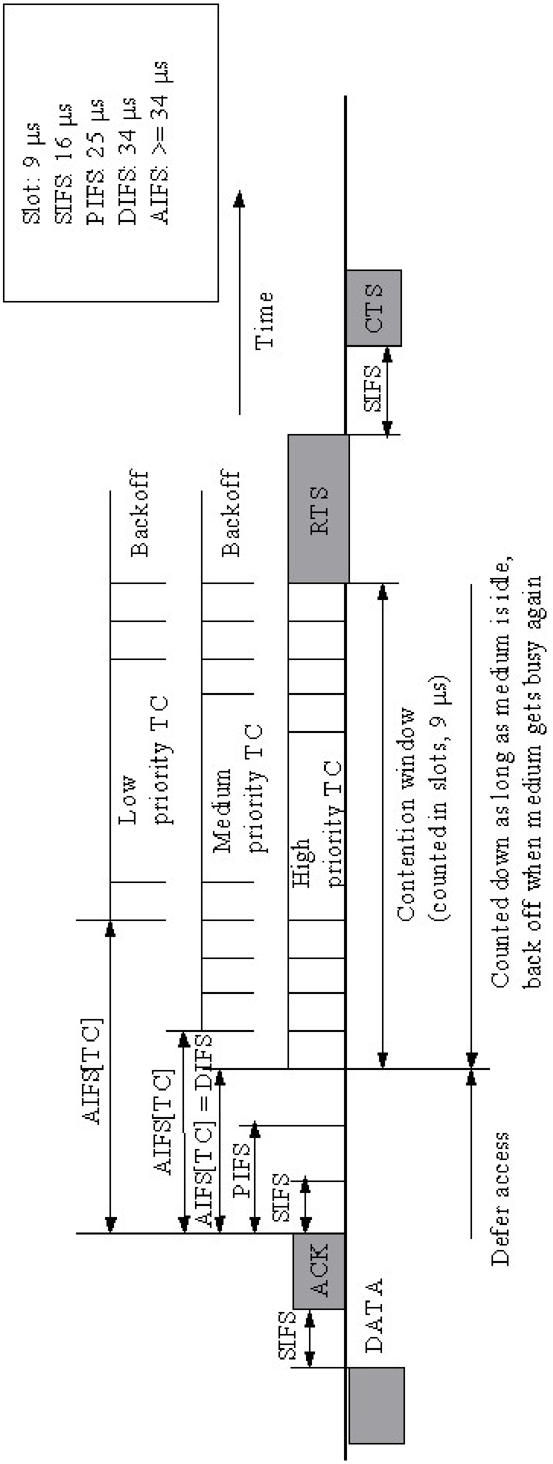
Slot: 9 µs
SIFS: 16 µs
PIFS: 25 µs
DIFS: 34 µs
AIFS: >= 34 µs
Time
DATA
SIFS
ACK
SIFS
PIFS
AIFS[TC] = DIFS
AIFS[TC]
AIFS[TC]
Defer access
High priority TC
Medium priority TC
Low priority TC
Contention window (counted in slots, 9 µs)
Counted down as long as medium is idle, back off when medium gets busy again
Backoff
Backoff
RTS
SIFS
CTS

Fig. 1 EDCF access mechanism

Second, the minimum value of the CW for each traffic class, denoted by CW_{min}, can be selected on a per-TC basis. In DCF a global constant CW_{min} is used to initialize all CW values.

Third, when a collision is detected and the CW has to be increased, the value of CW is increased by a persistence factor (PF), which is also determined on a per-TC basis. A value of 1 the PF gives a CW that stays constant even in the case of collisions, whereas a value of 2 (which is the default) gives binary exponential back-off identical to DCF. The equation to calculate the CW in case of a collision is given by

$$newCW[TC] \geq ((oldCW[TC]+1)\,PF[TC]) - 1$$

The CW_{max} value sets the maximum possible value for the CW on a per-TC basis. However, CW_{max} is typically intended to remain the same for all traffic classes (at the default value used in DCF).

Within a station, the eight TCs have independent transmission queues. These behave as virtual stations with the above-mentioned parameters determining their ability to transmit. If the back-off counters of two or more parallel treats the event as a virtual collision. The transmit opportunity (TXOP) is given to the TC with the highest priority of the "colliding" TCs, and the others back-off as if a collision on the medium occurred. [1, 2]

3 EDCF Modeling by Markov Chains

The most suitable tool to model the EDCF access mechanism is a two-dimensional discrete-time Markov chain (figure 2).

Let us assume that the channel conditions are ideal (e. g., no hidden nodes) and that the system operates in saturation: a fixed number of stations always have a packet available for transmission.

L different types of traffic flows are considered with n_i traffic flows for traffic type i ($i = 1, 2, ..., L$) . Let $b_i(t)$ be the stochastic process representing the back-off time counter for a given traffic flow with type i. Moreover, let us define for convenience $W_i = CW_{\min,\, i}$ as the minimum contention window for traffic type i. Let m_i, "maximum back-off stage" be the value such that $CW_{\max,i} = 2^{m_i} \cdot W_i$, and let $s_i(t)$ be the stochastic process representing the back-off stage ($0, 1, ..., m_i$) for a given traffic flow with type i.

The key approximation in the model is that, at each transmission attempt for a traffic flow of type i, regardless of the number of retransmissions suffered, each packet collides with constant and independent probability p_i. This assumption is very accurate as long as W_i and n_i get larger.

The states in Markov chain are defined as two integers $\{s_i(t); b_i(t)\}$. [3]

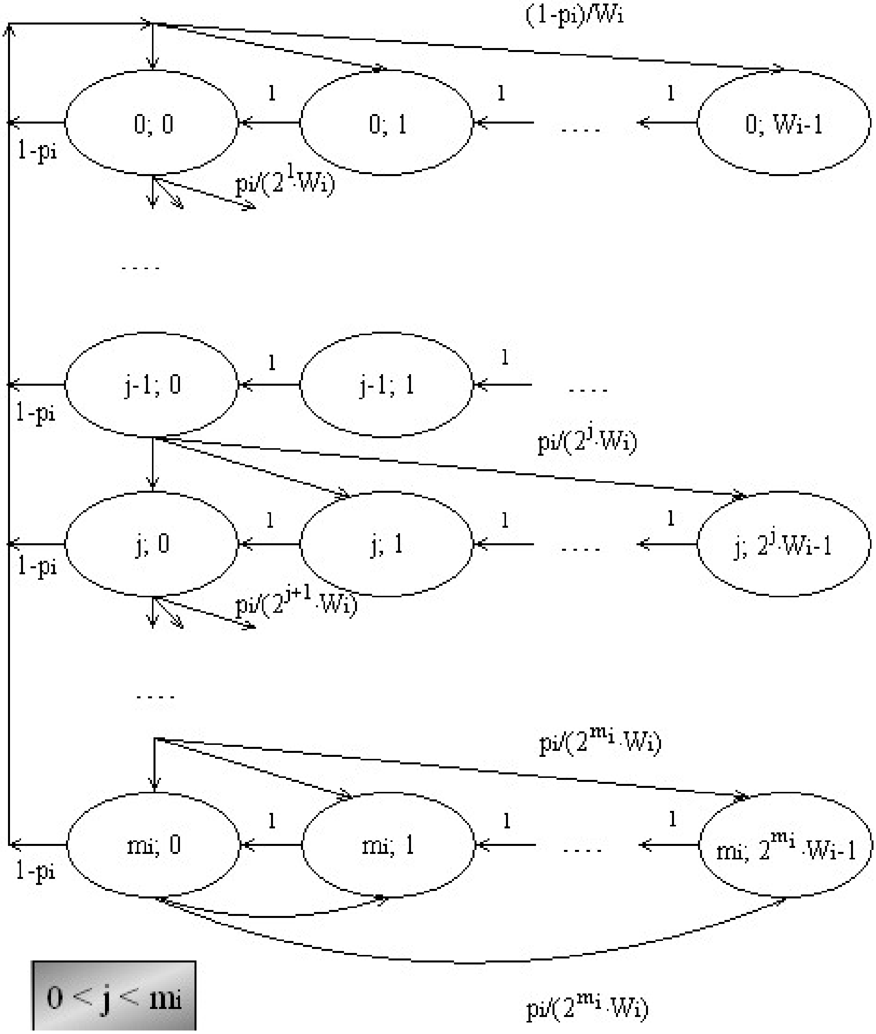
(1-pi)/Wi
0; 0
0; 1
0; Wi-1
1
1
1
1-pi
pi/(2^1·Wi)
j-1; 0
j-1; 1
1
1
1-pi
pi/(2^j·Wi)
j; 0
j; 1
j; 2^j·Wi-1
1
1
1
1-pi
pi/(2^(j+1)·Wi)
pi/(2^mi·Wi)
mi; 0
mi; 1
mi; 2^mi·Wi-1
1
1
1
1-pi
pi/(2^mi·Wi)
0 < j < mi

Fig. 2 Scheme of an EDCF model by a two-dimensional discrete-time Markov chain

Transition probabilities of this process are as follows:

$$P\{j,k|j,k+1\}=1 \quad , \quad j\in\{0,\dots,m_i\}, \quad k\in\{0,\dots,2^j\cdot W_i-2\},$$

$$P\{0,k|j,0\}=\frac{1-p_i}{W_i} \quad , \quad j\in\{0,\dots,m_i\}, \quad k\in\{0,\dots,W_i-1\},$$

$$P\{j,k|j-1,0\}=\frac{p_i}{2^j\cdot W_i} \quad , \quad j\in\{1,\dots,m_i\}, \quad k\in\{0,\dots,2^j\cdot W_i-1\},$$

$$P\{m_i,k|m_i,0\}=\frac{p_i}{2^{m_i}\cdot W_i} \quad , \quad j\in\{1,\dots,m_i\}, \quad k\in\{0,\dots,2^{m_i}\cdot W_i-1\},$$

4 Conclusion

In this paper, it was described the basic function of EDCF that offers eight traffic priority classes to improve QoS in the IEEE 802.11 technology. I was also shown how to model EDCF process by the two-dimensional discrete-time Markov chain.

References

1. ROHAN, P., LEARY, J. *Wireless Local Area Network Fundamentals.* [s.l.] : Cisco Press, 2003. 300 s. ISBN 1587050773.
2. OHRTMAN, F. *Voice over 802.11.* Boston • London: Artech House, 2004. ISBN 1580536778.
3. LI, Bo, BATTITI, Roberto. Performance Analysis of An Enhanced IEEE 802.11 Distributed Coordination Function Supporting Service Differentiation. In *Quality for All: 4th COST 263 International Workshop on Quality of Future Internet Services, QoFIS 2003.* Berlin : Springer, 2003. s. 152-161. ISBN 9783540201922.

My publications

1. MACHNÍK, P., MICHALEK, L. Multimedia transmission over WiFi. In *Proceedings EC-SIP-M 2005, 5th EURASIP Conference focused on Speech and Image Processing, Multimedia Communications and Services.* Bratislava: Slovak University of Technology in Bratislava, Slovak Republic, 2005. s. 251-256, ISBN 80-227-2257-X.
2. MACHNÍK, P. Quality of Service in 802.11 Networks. In *Proceedings Research in Telecommunication Technology 2005, 6th International Conference*. Ostrava: VŠB-TU Ostrava, 2005. s. 325-329. ISBN 80-248-0897-8.
3. MACHNÍK, P. Wireless Networks According to IEEE 802.11 Standard. In *Proceedings Wofex 2005*. Ostrava: VŠB-TU Ostrava, 2005. s. 508-512. ISBN 80-248-0596-0.
4. MACHNÍK, P., MICHALEK, L. Vliv elektromagnetického pole na lidský organizmus. In *sborník VI. Seminář Katedry elektroniky a telekomunikační techniky*. Ostrava: VŠB-TU Ostrava, 2005, s. 23-26. ISBN 80-248-0833-1.

5. MACHNÍK, P. Voice over IP and its objection. In *Proceedings 3rd Scientific Conference with International Participation Communication and Information Technologies* Liptovský Mikuláš: Academy of the Armed Forces of Gen. M. R. Štefánik Liptovský Mikuláš, 2005. s. 142-145. ISBN 80-8040-269-8.
6. MACHNÍK, Petr. Access Methods in IEEE 802.11 Technology. In *Sborník Vršov 2006*. Brno : VUT v Brně, Fakulta elektrotechniky a komunikačních technologií, 2006. s. 95-98. ISBN 80-214-3247-0.
7. MACHNÍK, Petr. Security of Wi-Fi Technology. In *Proceedings Research in Telecommunication Technology 2006*. Brno : Brno University of Technology. 2006. p. 345-348. ISBN 80-214-3243-8.
8. MACHNÍK, Petr. Optimizing of EDCF Access Mechanism in IEEE 802.11 Technology. In *Proceedings of the 4th annual workshop WOFEX 2006*. Ostrava : Faculty of Electrical Engineering and Computer Science, VŠB-Technical University of Ostrava. 2006. p. 457-461. 80-248-1152-9.
9. Machník, Petr. EDCA Simulation by Markov Chains. In *Proceedings VII. Workshop of Telecommunications Department*. Ostrava:VŠB-TU Ostrava, FEI, Department of Telecommunications, 2007. ISBN 978-80-248-1370-7.

Mode Field Visualization Near of Normalized Frequency

Leoš Maršálek, Václav Hamerský, and Vladimír Vašinek

Department of Electronics and Telecommunications, FEECS,
VŠB – Technical University of Ostrava, 17. listopadu 15, 708 33 Ostrava – Poruba
{`leos.marsalek,vaclav.hamersky,vladimir.vasinek`}`@vsb.cz`

Abstract. Nowadays optical fibbers are not only used for transition of information but as a detector of various physical quantities as well. The main aims in optic fibers production are to build a fiber which is as less influence as possible by outer condition. On the other hand detectors based on fiber optic have to be very sensitive. Therefore an idea comes to mind why not use optical fiber as a detector and transition media together in one. The idea seems to be such an interesting that we have decided to build a technology which will be able to merge measurement and telecommunication area together.

Keywords: DSP, LabVIEW, normalized frequency, optical fiber, optics measurement, sensor, telecommunication, virtual instrument

1 Introduction

Optical fibers are mainly used for telecommunication purposes. The idea behind it started to be proven and it is possible to detect quantities via optical fiber such as temperature, pressure, radiation etc. During optical fiber evolution process the main target was to build such a fiber which is not influenced by outer condition at all. Opposite of that optical fiber detector was always designed to be to such a condition sensitive. This is why question remain why not merge the advantage of both concept into one.

2 New optical fiber design approach

Classical telecommunication fiber are by design limited in usage as a detector fibers this is why we try to create a brand new optical fiber type which will connect the telecommunication area with the detector fiber area. It leads into a optical fiber with behavior of telecommunication fiber and will be able to measure physical quantities which occurs over the distance as well. Our aim was to design quasi-single mode optical fiber, which will be able to transmit data over one wavelength and simultaneously measure physical quantities at second wavelength and They have same diameter like standard telecomunication fibers.

© Václav Snášel (Ed.): WOFEX 2007, pp. 362–366, ISBN 978-80-248-1571-8.
VŠB – Technical University of Ostrava, FEECS, 2007.

Fiber with large (greater than $\approx 10\mu m$) core diameter may be analyzed by geometric optics. Such fiber is called multi-mode fiber, from the electromagnetic analysis. In a step-index fiber, rays of light are guided along the fiber core by total internal reflection. Rays that are falling to the core-cladding boundary at a high angle (measured relative to a line normal to the boundary) are completely reflected. The minimum angle for total internal reflection internal reflection depends on the difference in index of refraction between the core and cladding materials. Rays that are falling to the boundary at a low angle are refracted from the core into the cladding, where they are not useful for conveying light along the fiber. In this way, the minimum angle for total internal reflection determines the acceptance angle of the fiber, often reported as a numerical aperture. A high numerical aperture makes it easier to efficiently couple a transmitter or receiver to the fiber.

2.1 Normalized frequency

Normalized frequency is a dimensionless quantity, obtained by taking the ratio between an actual frequency and a reference value or a nominal value.

$$V = \frac{2\pi}{\lambda} a \cdot n_1 \cdot \sqrt{2\mathit{\Delta}} \qquad (1)$$

Where λ is light wavelength, n_1 is refraction index of the core and $\mathit{\Delta}$ is the relative index difference.

Optical fiber is a single mode when normalized frequency is $V \leq 2.405$. If the optical fiber for wavelength of $\lambda = 1550nm$ is single mode and optical fiber for wavelength of $\lambda = 850nm$ is multi mode then you can speak about quasi-single mode optic fiber.

2.2 Quasi-single mode optical fibre

Quasi-single mode fiber is such a fiber which works over one wavelength as single mode telecommunication fiber and over second wavelength as multimode fiber. This condition can be achieved via distribution of refractive index intervention during optical fiber production. Currently we cooperate with UVE, which is able to produce any optical fibred based on our theoretical models.

Quasi-single mode optical fiber theoretical model

During an optical fiber design process we use a software environment Fiber CAD. Fiber CAD is powerful simulation tool where we are able to simulate processes in optical fiber with different refractive index distribution configuration. A light distribute over optical fiber as stable el.mag. Configurations which are called modes. This mode differentiates in a distribution at the optical fiber. The distribution of the particular modes can be controlled via an internal fiber structure. The structure can be control via outer condition as well, for example via temperature when geometrical dimensions of the fibre are changed or via pressure where refractive indexes are cached due to photoelectric phenomenon. Following illustration shows mode array change in dependency of temperature.

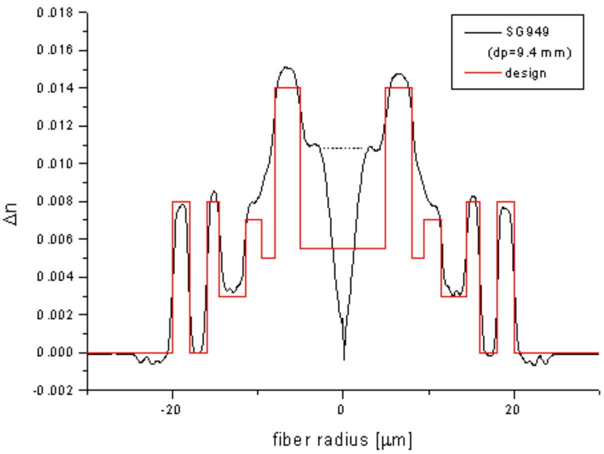

Fig. 1. Picture showed theoretical model of fiber with real fiber profile

Optical fiber in reality

Manufactured optical fibers cannot have parameters like ideal theoretical model, this is caused by imperfect manufacturing process which can try to create as best as possible fiber but it can never reach the ideal properties. This is why we must extend our theoretical model by means of reaching more real states. The real problem is how to find compromise between theoretical requirement and production technology.

Huge changes of refractive index in glass result in negative impact on material properties like fragility or inner tension.

Benefit of new type of optics fiber

Main benefit from designed fiber is usage of optical fiber for acquisition data from all links. An analysis can be resolved into information of a condition on a link.

3 Measurement system

We have an idea about behavior of measure part of optical fiber, but we need to confirm our theoretical opinion.

Measurement part of our project will be used for distribution of energy on face of optical fiber. There are not any measure technologies for energy changes measurement on face of fiber nowadays. This is the reason why we must create new measurement technologies.

Fig. 2 shows change of energy in dependence on temperature. The upper figure shows MFD[1] for 20 Celsius degree and the lower one shows MDF for 85

---

[1] Mode field diameter

Celsius degree. We need to create new measurement system because we want to visualize near field of optical fiber. From this information we will be able to analyze the behavior of the fiber route.

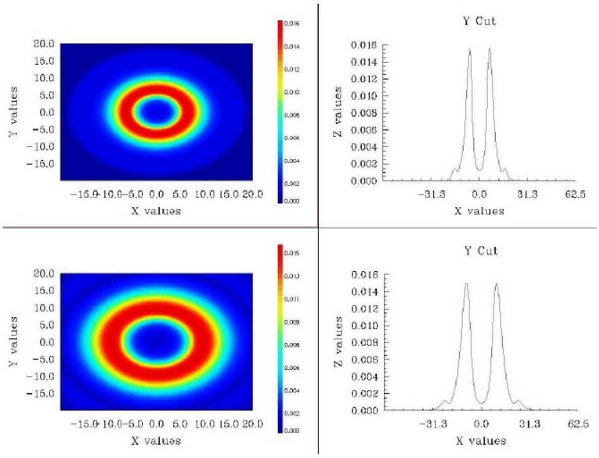

Fig. 2. Change of energy distribution for various temperatures

3.1 System description

All measurement system will be modular. We want to use microscope, camera, computer and optical fiber. Parts of measurement system:

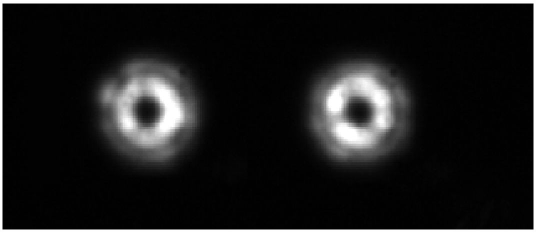

Fig. 3. Picture showing visualization results of our visualization system

- There is a microscope used for zoom of the fiber optic cross section. We need zoom for about $1600x$.

- There is a camera used as a detector for light measurement $\lambda = 850nm$. We will use NIR cameras with interface IEEE 1394 FireWire. We would like to plug this camera directly at computer.
- Optical fiber measure the environment..
- Computer will be used for data analysis from the camera.

3.2 Measurement system practical realization

The measurement system was realized as a microscopic camera system. An optical part of the camera system consists of inverse microscope which is able to reach magnification 1000x. The MS was supplemented by camera Basler A631f which is a digital industrial camera with very high resolution and 12bit depth per pixel. The camera is connected via FW to standard PC which has NI LW installed including Vision Acquisition Module[2] for image processing. The software part of the MS is realized in NI VI concept.

3.3 Virtual instrument - LabVIEW

Concept of virtual instrument[3] is very progressive area of measurement. VI substitutes classical measurement devices by computer with measurement program.

The interest of VI is because programmer can create measurement function in development environment. We have chosen the software environment LabVIEW from National Instrument. The main advantage is simple environment for program creation.

We will use DSP function because we except that the data from camera will corrupt of coherent granularity, because of LASERs source usage.

4 Conclusion

This contribution outlines how to extend optical telecommunication technologies which are commonly used these days. The design is not the issue but problem is to build up and prove the idea in reality. If there will be an optical fiber of such qualities proven than this will able us not only use optics for data transfer but it will give us a new territory for a future research in area of data acquisition.

References

1. Ajoy Ghatak Thyagarajan *Introduction to Fibre optics*, ISBN : 0-521-57120-0
2. Vladimir Vasinek, *Opticka vlakna v blizkosti mezni normalizovane frekvence jednomodovch vlaken a jejich aplikace* 1.vyd, Vysoka skola banska Technicka univerzita Ostrava, ISBN 80-24-0575-8.
3. National Instrument *LabVIEW User Manual* 2005 `www.ni.com`
4. Stergios Stergiopoulos *Advanced Signal Processing Handbook*, ISBN 0-8493-3691-0
5. Leos Marsalek *Opticka vlakna* `goro.czweb.org/publikace.php`

---

[2] Software module to LabVIEW for capturing images.

[3] Next only VI

Bitrate Determination for GPRS/EDGE Service Using Markov Chains

Libor Michalek

Department of Electronics and Telecommunications, FEECS,
VŠB – Technical University of Ostrava, 17. listopadu 15, 708 33 Ostrava – Poruba
`libor.michalek.fei@vsb.cz`

Abstract. Although, the UMTS network enables fast bit rates, the GPRS/EDGE remains the most used service for the Internet connection. In this paper, I analyzed the performance of GPRS/EDGE service. The bit rate determination for the end user using birth-death structure of Markov chains is presented. For this purpose, the special kind of Kendall classification for the characterization of queuing system is used. The fixed sharing policy with varying border is used to optimize the capacity in the GSM radio cell.

1 Introduction

Mobile devices such as cell phones, PDA, notebooks are increasingly being used to transfer data over GSM (Global System for Mobile Communication). More and more people are using them for a many of multimedia applications such as multimedia-messaging (MMS), web browsing for cell phones wireless application protocol (WAP) or downloading specific content like ring-tones or games.

The GPRS/EDGE and GSM circuit switched services share the same radio resources. Whenever a channel is not used by circuit switched services, it may be utilized by GPRS/EDGE. The allocation of physical channels for GPRS/EDGE can be based on the needs for actual packet transfers. The GPRS/EDGE doesn't require permanently allocated Packet Data Channel (PDCH). The operator can decide to dedicate permanently or temporarily some physical channels for GPRS/EDGE traffic. The number of allocated PDCH in a cell can be increased or decreased according to demand. More things about the static principle of sharing between the packet and conventional GSM service within the one radio cell can be found in [1].

This paper is focused on GPRS/EDGE service optimizing, especially to derive a steady-state probability of the birth-death structure Markov chain and then the offered bit rate for the end user. A mathematical model for dimensioning this type of traffic was developed with use the ON-OFF model.

The special kind M/M/m/K/M of Kendall classification was also used to describe the characteristics of GPRS/EDGE queuing system.

© Václav Snášel (Ed.): WOFEX 2007, pp. 367–372, ISBN 978-80-248-1571-8.
VŠB – Technical University of Ostrava, FEECS, 2007.

2 Model Developments

It's necessary to make basic description of mathematical model. I used the probability functions based on birth-death structure of Markov chains.

2.1. Basic Assumptions

I considered a single GSM radio cell divided into the two types of traffic, the fixed sharing policy especially. The first traffic is conventional GSM voice and the second is GPRS/EDGE data flow. My study is focused only on the downlink.
I made the following basic assumptions:
- The Radio Resource Manager (RRM) reallocates every 20ms RLC/MAC block according to the actual demands. 20ms is a basic radio block and must be transmitted always without any dependency.
- All data users at the on-going transfer share the total bandwidth, i.e. capacity in the frame with the fair sharing scheme, e.g. Round Robin scheduling.
- All GPRS/EDGE mobiles have the same multislot class, i.e. the number of timeslots simultaneously used for downlink d and uplink u.
- Finite amount of users belong to the one radio cell.

2.2. Modelling Assumptions

The GPRS/EDGE traffic corresponding to each service is bursty and can be characterized by a typical ON-OFF model (process).

Every terminal (mobile station) generates an ON-OFF traffic. ON periods corresponds to the download of the element (www page, downloading). OFF periods correspond to the reading time. It requires a characterization of the duration of the OFF-period t_{off} and of the size of the ON-period x_{on}.

So, the ON-OFF model is used for the exact description of the GPRS/EDGE traffic behaviour. It consists of the active and passive periods. If the mobile station transmits any data the period is active. During the passive period no data is transmitted. In the model, I made following model assumptions [1], [2]:
- The total number of timeslots available for PDTCH (Packet Data Traffic Channel) and TCH (Traffic Channel) in GSM TDMA frame is 8.
- I neglected the BCCH (Broadcast Control Channel) and other signalling channels in the frame.
- Complete Partitioning sharing scheme is fitted, i.e. a part of time-slots TSL_V is dedicated for voice, the remained part TSL_D is dedicated for data.
- Radio block duration is t_B=20 ms, it's duration of the RLC/MAC (Radio Link Control / Medium Access Control) layer data block.
- A number of bits x_b is transferred during the t_b. x_b/t_b is the throughput of the RLC/MAC layer. The value of x_b depends on the radio coding scheme [3].

2.3 Birth-death Markov process in the GPRS/EDGE traffic

A birth-death process is a special type of continuous time Markov Chain with the restriction that each step, the state transitions, if any, can occur only between neighboring states.

Assume that voice user's arrival is a Poisson process with a rate of λ_V and the call service time is exponentially distributed with a mean of $1/\mu_V$. All GPRS/EDGE users share the physical channels reserved for data and so unused by the voice services. I assume, we have a finite population of *M* customers (in service and in queue), each with an arriving parameter λ. In addition, the system has a number of time-slots TSL_D dedicated in frame only for a data, each with parameter $d\mu$, where *d* is number of time-slots simultaneously used by mobile device. The system also has finite storage room such that the total number of customers in the system is no more than 32 (TBF parameter) [3].

Kendall classification (notation) describes the nature of the arrival process to the queue, the nature of the service process, the number of servers, the maximum number of jobs that may be in the system and some basic queuing disciplines. The notation has been considerably extended to allow it to represent a wide variety of queues.

I assume $M \geq 32 \geq TSL_D$, this leads to the *M/M/m/K/M* Kendall classification and to the following set of birth-death coefficients [4, 5]:

$$\lambda_k \begin{cases} \lambda\left(M-k\right) & 0 \leq k \leq 31 \\ 0 & otherwise \end{cases}$$

$$\mu_k \begin{cases} d\,k\mu & 0 \leq k \leq TSL_D \\ TSL_D\,\mu & k \geq TSL_D \end{cases}$$

In Figure 1 we see the finite state-transition-rate diagram for GPRS/EDGE system with M=32. TSL_D is variable here and depends on the actual capacity demands in the cell.

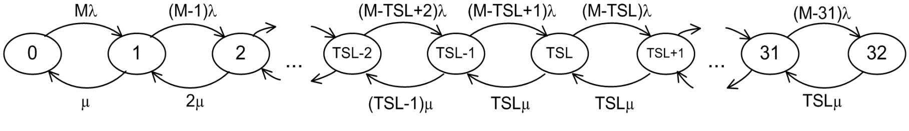

Fig. 1. State-transition-rate diagram for GPRS/EDGE service

2.4 Steady state probabilities determination

In order to apply the Equation 1 (equilibrium probability p_k) we must consider two regions.

$$p(k) = p_0 \prod_{i=0}^{k-1} \frac{\lambda_i}{\mu_{i+1}} \qquad k = 1,\ 2,\ \ldots\ \infty \tag{1}$$

The stationary probability of having *k* mobile devices in ON period in the radio cell is derived from the initiated state-transitions-rate diagram birth-death Markov chain. We have thus [4], [5]:

First, for the range $0 \le k \le k_{\max} - 1$ we have

$$p(k) = p_0 \prod_{i=0}^{k-1} \frac{\lambda(M-i)}{(i+1)d\mu} = p_0 \rho^k \cdot \begin{pmatrix} M \\ k \end{pmatrix} \frac{1}{d^k} = \ldots = p_0 \rho^k \frac{M!}{(M-k)!k!d^k} \tag{2}$$

For the range $k_{\max} \le k \le 32$ we have

$$p(k) = p_0 \prod_{i=0}^{k_{\max}-1} \frac{\lambda(M-i)}{(i+1)\cdot d \cdot \mu} \cdot \prod_{i=k_{\max}}^{k-1} \frac{\lambda(M-i)}{TSL_D \cdot \mu} = \ldots = \frac{p_0 \cdot \rho^k \cdot M!}{(M-k)! \cdot d^{k_{\max}} \cdot k_{\max}! \cdot TSL^{k-k_{\max}}} \tag{3}$$

Since probabilities must sum to 1, it follows that:

$$p(0) = \frac{1}{\displaystyle\sum_{k=1}^{k_{\max}} \frac{\rho^k \cdot M!}{(M-k)!k!d^k} + \sum_{k_{\max}+1}^{32} \frac{\rho^k \cdot M!}{(M-k)! \cdot d^{k_{\max}} \cdot k_{\max}! \cdot TSL^{k-k_{\max}}}} \tag{4}$$

I defined the rate λ and the data service time-rate μ from the ON-OFF model structure as:

$$\lambda = \frac{1}{t_{off}} \tag{5}$$

$$\mu = \frac{x_B}{x_{on} \cdot t_B} \tag{6}$$

$k_{\max}$ is the maximum value of *k* such that *k* mobiles with *d* class occupy less than TSL_D timeslots:

$$k_{\max} = \frac{TSL_D}{d} \tag{7}$$

Parameter $\rho = \dfrac{\lambda}{\mu}$ is the traffic utilization and must be less than value one to have a stable system.

2.5 Bit rate Determination

To obtain the bit rate that can mobile device achieve is necessary do derive some parameters.

The average number S of mobile station in the cell is:

$$S = \sum_{k=1}^{32} p(k) \cdot k \qquad \textbf{(8)}$$

The average number of busy timeslots depends on average number S and either on d or TSL_D. So, we must again consider two regions.

First, for the range $TSL_D \leq d$ we have:

$$T = \sum_{k=1}^{32} p(k) \cdot TSL_D \qquad \textbf{(9)}$$

For the range $TSL > d$ we have:

$$T = \sum_{k=1}^{32} p(k) \cdot d \qquad \textbf{(10)}$$

The average number of timeslots for one mobile device is obtained as:

$$Y = \frac{T}{S} \qquad \textbf{(11)}$$

Then, the offered bit rate by one cell for the one mobile device is:

$$v_p = \frac{x_B \cdot Y}{t_B \cdot 125} \quad [kbit/s] \qquad \textbf{(12)}$$

3 Performance Results

In this section, I use the analytical model developed in Section 2. For a GPRS/EDGE multislot service, the result from the approximation is presented. All mobiles are assumed to use the same performance parameters, i.e. x_B (based on used coding scheme), t_{off}, x_{on}, t_B [1].

The offered bitrate changing by amount of transferred file size (x_{on}) for one mobile device is presented on Figure 2. These values were used: x_B=112 bytes (EDGE MCS-7), t_B=20ms, t_{off}=7s, M=40. We can see that as the number of bytes increases, the offered bitrate degrades early but after xon=5000B degrades slowly. The changes between bigger sizes of file aren't significant. We must also consider the assumed amount of population M, used coding scheme (depends on actual radio conditions) and the reading time (depends on the type of application).

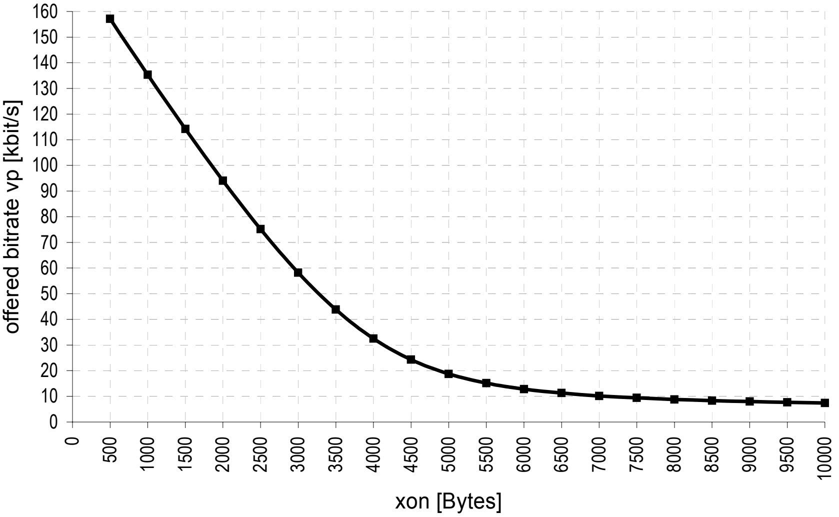

Fig. 2. Offered bitrate for one mobile device with variable x_{on}.

4 Conclusion

In this paper, an approximation method is used for evaluating the GPRS/EDGE performance of multislot service in the variable radio resource. It assumes Poisson distributed voice traffic and ON-OFF sessions performed by a finite number of users for the data traffic part. I developed a model based on a birth-death structure of Markov chain and on the Kendall classification. It's possible to obtain the mean number of mobiles in ON period and the mean number of timeslots for the one mobile device. According to equation 12, I performed the offered bitrate for the one mobile station. It's the possibility how to determine the offered bitrate for the one subscriber without any trace network data.

References

1. MICHALEK, Libor. Providing Quality of Service in the GPRS/EDGE Networks. In SNÁŠEL, Václav. *Wofex 2006*. Ostrava, 2006. p. 467-472. ISBN 80-248-1152-9.
2. NOGUEIRA, Georges. An Erlang-like law for GPRS/EDGE engineering and its first validation on live traffic. In *Valuetools 2006*. Italy : [s.n.], 2006. ISBN 1-59593-504-5.
3. HEINE, Gunnar, SAGKOB, Holger. *GPRS: gateway to third generation mobile networks*. [USA] : Artech House, 2003. 295 p. ISBN 1-58053-159-8.
4. KLEINROCK, Leonard. *Queueing Systems : Volume 1: Theory*. 1st edition. USA : Wiley, 1975. 417 p. ISBN 0-471-49-110.
5. BOSE, Sanjay K. *An Introduction to Queueing Systems*. 1st edition. USA : Kluwer Academic/Plenum Publishers, 2002. 287 p. ISBN 0-306-46734-8.

Reflectivity of the Wall Surfaces and Its Influence on Fibreless Optical Diffused Networks within Interiors

Jaromír Nečesaný

Department of Electronics and Telecommunications, FEECS,
VŠB – Technical University of Ostrava, 17. listopadu 15, 708 33 Ostrava – Poruba
`jaromir.necesany@centrum.cz`

Abstract. Fiberless optical diffused networks use the scattering of light radiation, when the rays are sent to the various directions and by the reflection from the walls they will get to the place of destination (detector). The most important problem in these networks is high signal loss during transmission path, especially at reflection. These losses depend on the surface roughness of sample, pigment as well as on the wavelength of incident light. Graphs of surface roughness and values transfer from the time domain to the frequency domain, we get answer that low frequency correspond surface waving by the both surface. Directive characteristics after the reflection are asymmetric, mainly thanks to surface waving.

1 Introduction

Optical diffused networks work mainly in reserved rooms and make possible voice, data and video transmission. Their advantage is independence of wavelengths, they are highly safety because they cannot leave the room and signal remains inside of the intended area. This is the same reason why infrared systems are not regulated by license. The frequency spectrum can be reused in different rooms and doesn't have to be shared like in radio systems. Diffused infrared networks are afflicted by several different problems. The most important problem is small sensitivity of receiver and mainly high signal loss during transmission path.

Fig. 1 shows, how the light from the source incidents on the surface of the sample. In the case, when the light is reflected only from the surface, the reflexes are very directional. Of course, at special samples, the light can also penetrate to the certain depth. The depth penetration depends on many factors, for example the light wavelength or the angle of incidence. This effect, reflection under surface, is called diffusion. The metals reflect only from the surface and dielectrics (plastics, color coats) have both reflected mechanisms, reflection from the surface and under the surface. It leads to distortion of received signals and to the growth of noise and bit error rates (BER) of communication systems. Conclusions of these research works are significant for simulation of light distribution coverage in space and solving of bit error rate distribution in space.

© Václav Snášel (Ed.): WOFEX 2007, pp. 373–378, ISBN 978-80-248-1571-8.
VŠB – Technical University of Ostrava, FEECS, 2007.

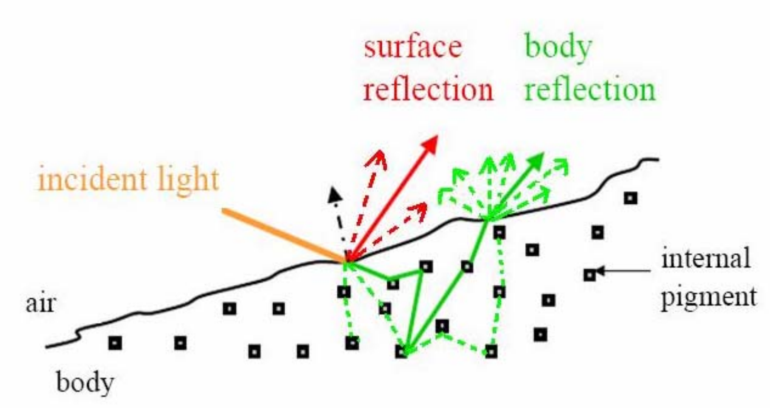

Fig. 1. Reflections from the surface and under the surface

2 Surface characteristics

2.1 Measurement of surface roughness

I measured by roughness meter Mitutoyo on distance 12,5 mm with 8330 samples. From results it stands to reason, that surface waving has a big influence on directive characteristics after the reflection. It measured with plaster boar and indoor walling. Each surface was paint of indoor white colors. In my case are colours from corporation primalex especially polar, plus, standard. This color differs in level of whiteness and therefore capabilities of reflect incident light in wide of range of wavelengths.

2.2 Graphs of surface roughness

On Fig. 2a we can see measurement two surfaces roughness. Paint is primalex polar with whiteness 92%. It stands to reson that plaster board is smoother than indoor walling. In both cases is direct current component zero, which means that surface is not ideal smooth. By the indoor walling is bigger surface waving, it stands to reson by granulity of indoor walling, which is 0,6mm.

On Fig. 2b we can see two surfaces again, with color prilamex plus, with whiteness 82% and on Fig. 2c is color primalex standard with whiteness 77%.

Results of all measurements show it, that same sample of surface with various type of color appearing differently. By influence of surface waving is directive characteristic after the reflection asymmetric, which shows later in this paper.

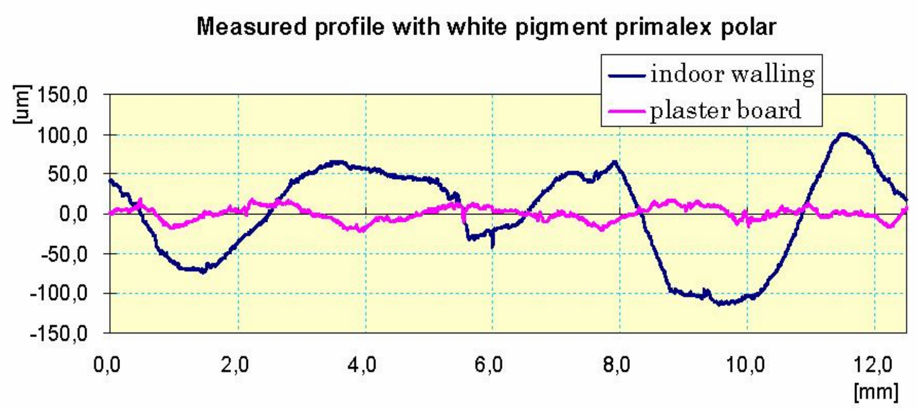

(a)

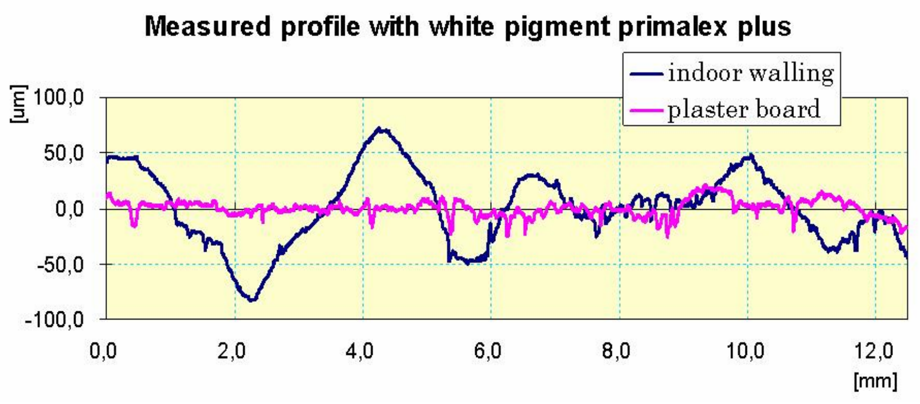

(b)

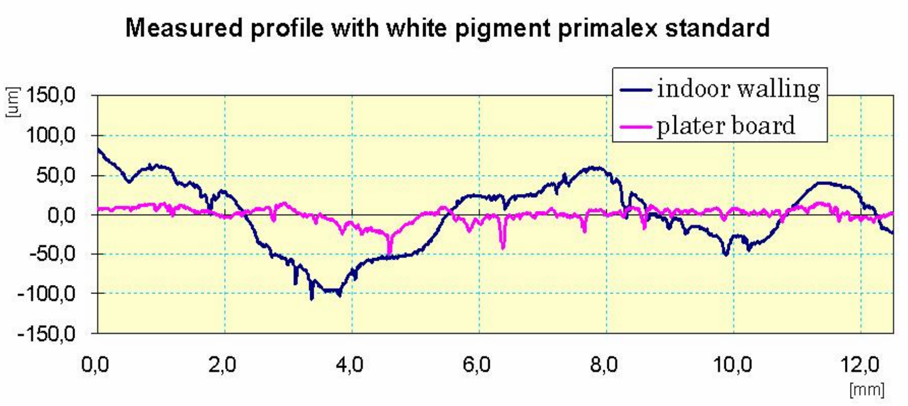

(c)

Fig. 2. Graphs of surface roughness

3 Formulation in frequency spectrum

I transferring measured process by help Fourier transformation to the frequency domain. On Fig. 3 is power spectrum of color primalex polar. On axis x is space frequency and on axis y is power. From spectrum it stands to reson, that low frequency correspond surface waving by the both surface. On Fig.4 is power spectrum of color primalex plus and on Fig. 5 is primalex standard.

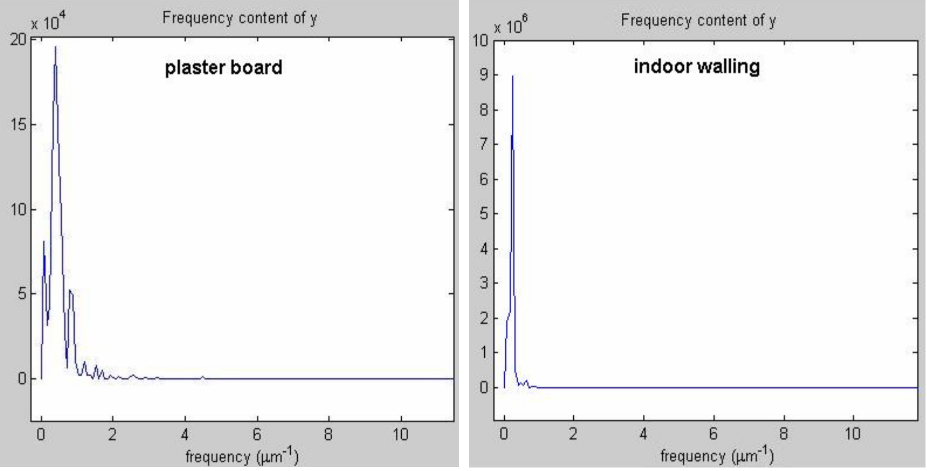

Fig. 3 Power spectrum of color primalex polar

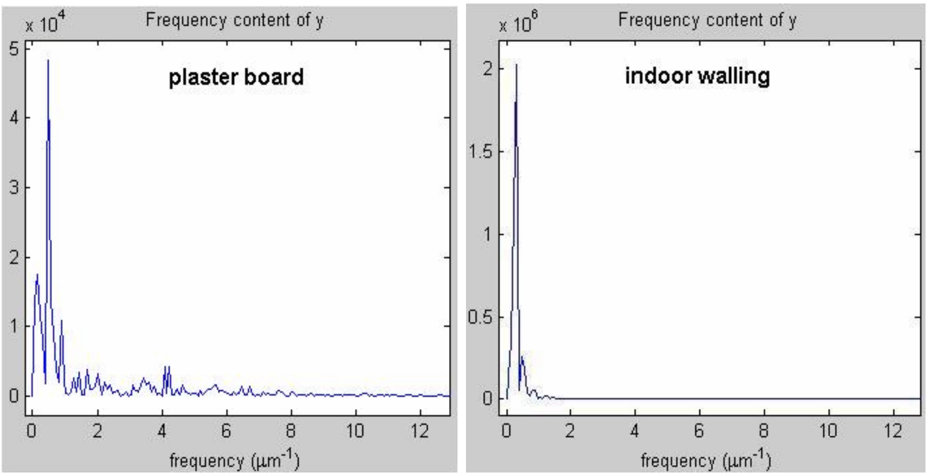

Fig. 4. Power spectrum of color primalex plus

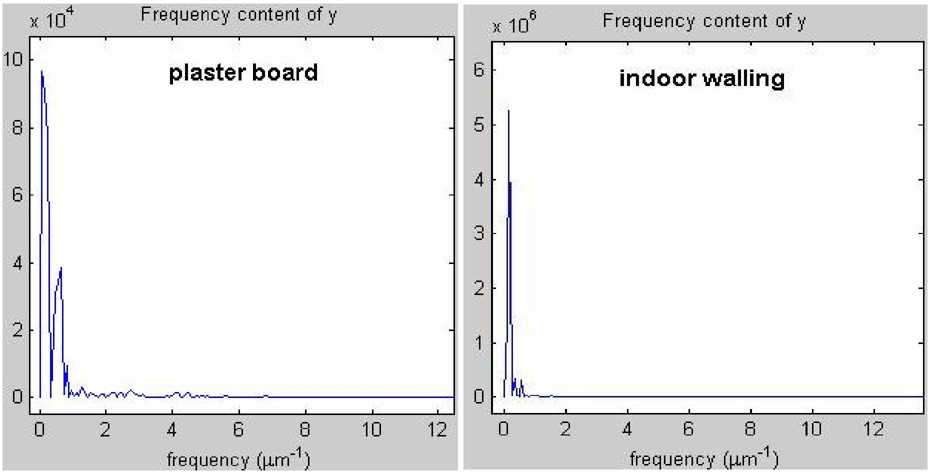

Fig. 5. Power spectrum of color primalex standard

It is interesting, that this color has smallest whiteness and it leads to assume, that maximum will be have less value than color with higher whiteness. Values of maximums are different; it confirms that the same material with various type of color has different characteristics.

4 Directive characteristics after the reflection

On Fig. 6a we can see graph of directive characteristics after the reflection in case of plaster board. Incident power is 10,6mW and wavelength is 650nm. Incident angle is 45°. Directive characteristic represent distribution of constant power in space. In this case it is power 4,5uW in distance from sample of 20 centimeters. Characteristic is asymmetric thanks to surface waving.

On Fig. 6b we can see graph of directive characteristics after the reflection in case of indoor walling. In this case it is power 4,7uW and other parameters are uniform. Here is asymmetric less than last paper.

Next research work is find out relationship between space frequencies of surface waving and degree of asymmetric characteristics for better simulation of light distribution in space.

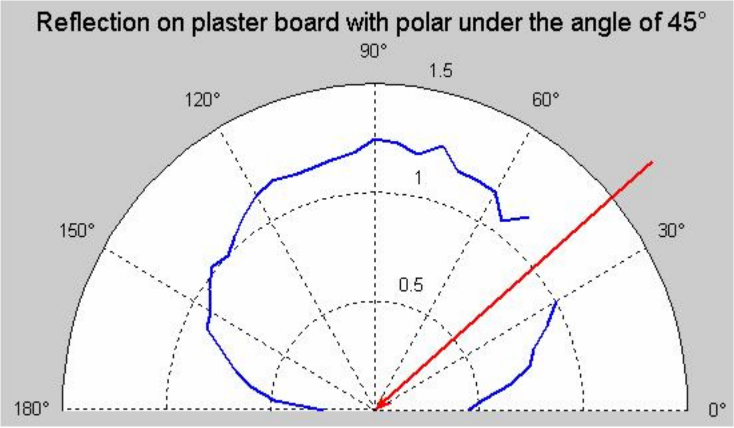

(a)

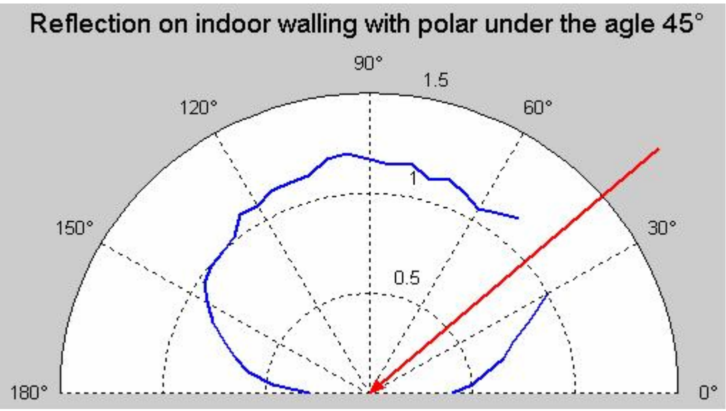

(b)

Fig. 6. Directive characteristics after the reflection

5 Conclusion

Optical diffused networks represent an attractive choice for many indoor applications. Its advantages include the availability of a wide bandwidth that is unregulated worldwide and that can be reused in a very dense fashion, immunity to eavesdropping the ability to achieve very high bit rates. The most difficult challenge in wireless optical network is achieving a high noise-to-ratio (SNR).

I analyzed of materials characteristics, static measurement and directive characteristics after the reflection in this paper. Next research work is dynamic measurement which we obtain information needed for suitable choice of construction materials.

Interleaver Improvement for the New Scheme of Combined Turbo Code with Public Key Cryptosystem

Nabil Ouddane

Department of Electronics and Telecommunications, FEECS,
VŠB – Technical University of Ostrava, 17. listopadu 15, 708 33 Ostrava – Poruba
`nabil.ouddane.st1@vsb.cz`

Abstract: A new combination for a public key cryptographic system with Turbo Codes was proposed in [1], in this paper we will present the contribution of the interleaver and it important development to perform the cryptosystem, this model will yields important gain and security improvement. Incoming data is embedded at the interleaver process of the Turbo encoder and its security is derived from the one-way functions provided by elliptical curves.

1 Introduction:

The appearance of the elliptic curve cryptosystems offer new horizons for public-key cryptography, they provide a methodology for obtaining high -speed, efficient, and scalable implementations of network security protocols [3][4][5][6]. The security of these protocols depends on the difficulty of computing elliptic curve discrete logarithms in the elliptic curve group [1]. The group operations utilise the arithmetic of points that are elements of the set of solutions of an elliptic curve equation defined over a finite field. Turbo codes were first introduced to the coding community in 1993 [2].Turbo Codes give a new direction for the channel encoding field, especially since they were adopted for multiple norms of telecommunications, such as deeper communication them invention involved reviving some dormant concepts and algorithms. Turbo codes are linear block codes, the encoding operation can be viewed as the modulo 2 matrix multiplication of an information vector with a generator matrix. This arithmetic is exactly the same as the proposed elliptic curve.

© Václav Snášel (Ed.): WOFEX 2007, pp. 379–385, ISBN 978-80-248-1571-8.
VŠB – Technical University of Ostrava, FEECS, 2007.

2 System description:

The public key cryptosystem and a turbo encoder/decoder will be used as a unique entity, with shared secret keys between the transmitter and receiver.
The same size at the initialisation stage of the interleaver and the deinterleaver of the Turbo/ECC encoder and Turbo decoder.

The incoming block data is using the ECC module, the encrypted data is encrypted using the upper and lower encoder of the turbo those output are multiplexed before enter to the channel as it shown in the figure1. Since the encryption module compress the information a recalculation of the amount of systematic transmitted data must be performed and send back to the ECC encryption module to check the synchronization of the data. The input data from the channel is used to decode the encrypted data using the systematic, the upper and lower decoder in an iterative way as shown in the figure 2 the amount of systematic received data is send forward to the ECC decryption module to check the synchronization and to decompress the data from where can be possible to compute the errors. as that proposed for the standard elliptic curve [1].

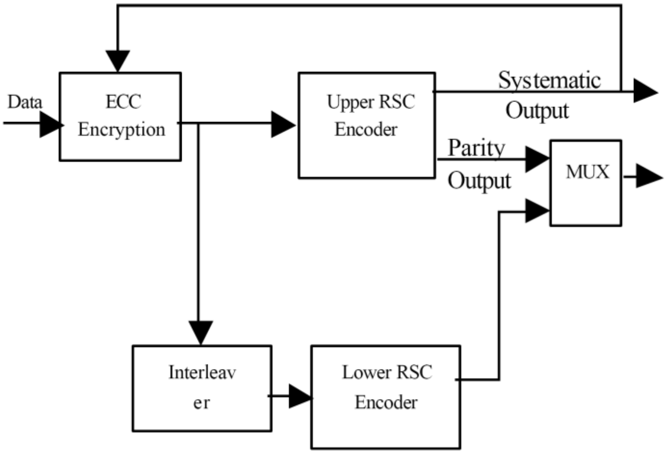

Fig.1. Turbo/ECC encoder

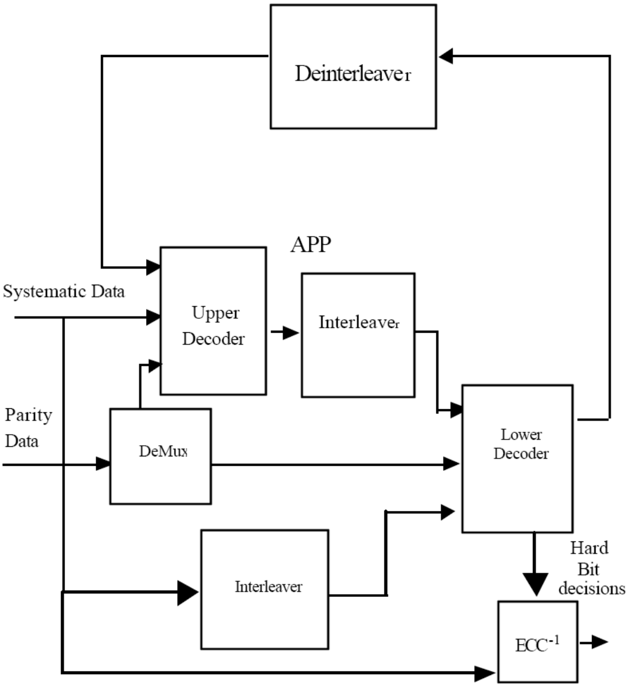

Fig.2. Turbo/ECC decoder

To realise this combination ECC/Turbo, an optimal choices such the type of the underlying finite field, algorithms for implementing the elliptic arithmetic, the type of elliptic curve, algorithms for implementing the elliptic group operation. In order to determinate the size of the system interleaver the number of points in the ECC is used, also is interesting to define the Turbo encoding/decoding group operations and finally elliptic curve protocols.

The recent evaluation of the binary error rate was in function of security level with the iteration process of the Turbo Codes systems, as it is shown in the figure 3 and 4, The main task of this presentation of the subject, is to try to give to the Turbo codes better parameters set, and to use the interleaver performed with the Genetic algorithms with the HLC and semielitary selection recently developed by [N]. It is known that if we use the semi random interleaver, we will obtain in the output random channel, and it is very useful for the BER measurement, but what about if we try to study the possibility to secure the network access with the Turbo/ECC that process with the new interleaver pattern distinated for deep communication applications [N], and what about the compromise between BER and the reliability of the security.

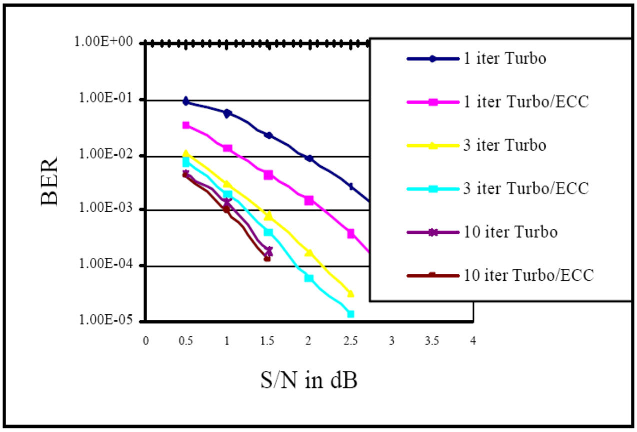

Fig.3 Comparison between Turbo codes and the combination Turbo/ECC

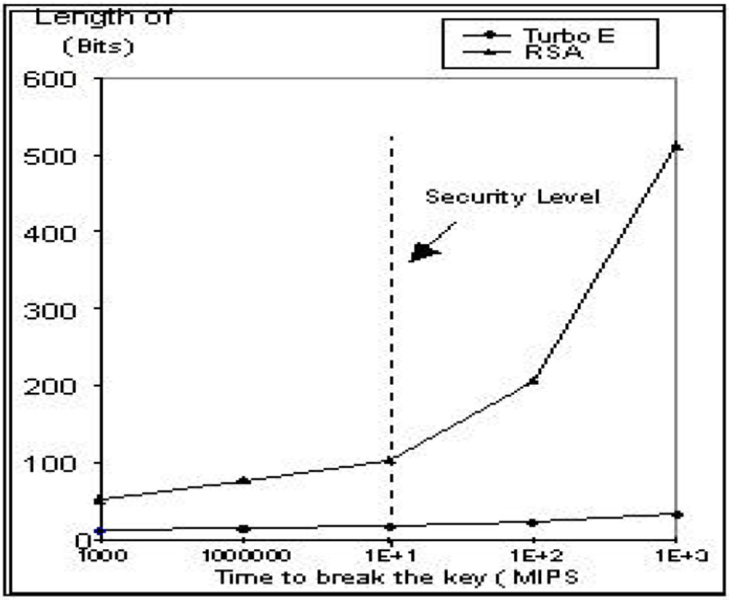

Fig;4 Comparison security levels of Turbo/ECC and the other standard RSA and DSA algorithms. Assuming that a reasonable security level of years of MIPS (Million Instructions per second) to break the key.

There are several important details that have to be considered when setting up a cryptosystem to implement the combination. The first consideration is how much time is taken to compute an elliptic curve secret key in the underlying field. The second consideration is how the elliptic curves are chosen in the underlying field, where the number of points on an elliptic curve determines the interleaver size and the security level. Figure 3 shows a comparison between a Turbo/ECC combination and ordinary Turbo codes, the bit error rate is plotted for different iterations. Also shown is the tendency of the error rate to decrease more rapidly, while the number of iterations increases. This increases the computational effort in the transmission of the symbol set, since in spite of errors taking place in the channel, an iterative decoding with a greater depth, has a greater probability of correcting these errors. To quantify in precise form, for 1 iteration there is an approximately 0.8 dB improvement, and for 3 iterations 0.4 dB approximately in relation to the ordinary Turbo Codes, which are enough for some real time applications. Nevertheless, as the iterations increase it is observed that the gain diminishes between the simulations. Indeed, for 10 iterations the simulation emphasised a gain of around 0.2 dB, which is very good for the security level introduced by the Turbo/ECC combination proposed and experimentally proposed by [1].

3 The new interleaver pattern:

We used the genetic algorithms as evolutionary algorithm to optimize the matrix interleaver, especially for satellite real time transmissions applications. The objective was to attend an optimal matrix to permit reduction in the delay and the codec complexity, in this experience we encoded the random as reference interleaver as permutation $\sigma_{N,}$,and we used two types of selection: roulette wheel selection for speeding up the convergence of the algorithm a semi-elitary selection scheme choosing one parent by elitary manners and the second by proportional manners of roulette wheel selection.

Mutation is simply realized by swapping positions of two coordinates in σ_N. On the contrary, traditional crossover operators (except of uniform crossover) will break the structure of permutation σ_N and hence cannot be used without post processing. Authors of [7] have fully omitted crossover and the crossover application in [8] lead to the need to repair every new chromosome created via crossover. This is a remarkable fact since crossover is referred as the primary operator for GA [9].

To enable the application of crossover for interleaver optimization, expecting performance increase, we have investigated the effect of uniform crossover on convergence ability of the classical interleaver optimizing GA. In the second phase, we have designed modified GA allowing the use of virtually any crossover operator for permutation evolution without breaking the chromosome. New crossover friendly GA is based on separation of chromosomes into groups of the same size called higher level chromosomes, (HLC's). Genetic operators are then applied on HLC's while original chromosomes act as genes. We have tested all above introduced techniques on benchmarking problem consisting of search for identity matrix. The evaluation was for the objective function it means binary error rate in function of the signal to noise rate as shown in the figure 5.

The results was very promising, with clear binary error rate improvement realized and obtained for the first time, with the new combination of the GA.

For interleaver length of 512 bits the new interleaver gives 0.75 db of gain ahead of the initial reference random interleaver.

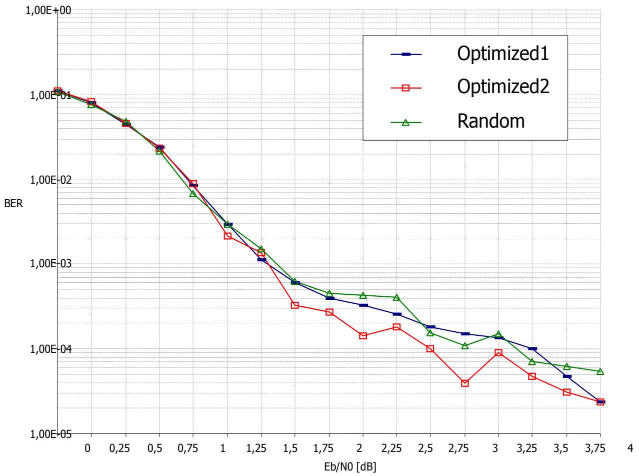

Fig.5 GA for interleaver length 512 bits

The improvement of the Turbo codes performances for correction capacity with the new biological pattern interleaver can lead also to develop the turbo codes applications and reliable the capacity of security with the Turbo/ECC combination with public key for the cryptosystem, this idea can be one of the ways to apply the evolutionary algorithms for the cryptosystems using the turbo codes.

References:

1. Ontiveros, Beatriz – Soto, Ismael- Carrasco, Rolando.
2. C. Berrou, A. Glavieux, and P. Thitimajshima, "Near Shannon limit error-correcting coding and decoding: turbo codes," in Proc. Int. Conf. on Commun., pp. 1064–1070, 1993.
3. N. Koblitz. "A Course in Number Theory and Cryptography". New York, NY: Springer- Verlag, Second edition, 1994
4. N. Koblitz. "Elliptic Curve Cryptosystems". Mathematics of Computation, January 1987.
5. A. Menezes. "Elliptic Curve Public Key Cryptosystems". Kluwer Academic Publishers, 1993.
6. V.Miller. "Uses of elliptic curves in cryptography". In H.C. Williams, editor, Advances in Cryptology —CRYPTO85,Proceedings ,Lecture Notes in Computer Science, No. 218,pages 417 –426.New York,NY:Springer-Verlag,1985.
7. N. Durand, J. Alliot, and B. Bartolomé, "Turbo codes optimization using genetic algorithms," in Proceedings of the Congress on Evolutionary Computation (P. J. Angeline, Z. Michalewicz, M. Schoenauer, X. Yao, and A. Zalzala, eds.), vol. 2, (Mayflower Hotel, Washington D.C., USA), pp. 816–822, IEEE Press, 6-9 1999.

8. S. Rekh, S. Rani, W. Hordijk, P. Gift, and Shanmugam, “Design of an interleaver for turbo codes using genetic algorithms,” The International Journal of Artificial Intelligence and Machine Learning, vol. 6, pp. 1–5, 2006.
9. M. Mitchell, An Introduction to Genetic Algorithms. Cambridge, MA: MIT Press, 1996.
10. N.Ouddane, P.Kromer, V.Snasel, ,“Optimizing Interleaver for Turbo Codes for Satellite Communications by Genetic Algorithms”.GEM 07, Las Vegas, 25-28 june 2007.

Analysis of Optical-Power Redistribution for Hybrid Optical Fiber Sensors

Jan Skapa, Jan Vanda

Department of Electronics and Telecommunications, FEECS,
VŠB – Technical University of Ostrava, 17. listopadu 15, 708 33 Ostrava – Poruba
`jan.skapa.fei@vsb.cz`

Abstract. This paper brings a short view into the hybrid communication-sensing fiber analysis. In our research we are trying to include properties of communication and sensor optical fibers into one fiber. A special type of fiber (a hybrid fiber), which preserves character of the standard communication fiber, was design and maintained for this purpose. We use a microscope with a high-resolution camera to watch the power redistribution between individual modes at the output end of the fiber. The coupled power equations are being used to predict changes in the optical power redistribution after the coupling coefficients are determined. The key problem is how to excite individual modes to determine the coupling coefficients because of very small diameter of the fiber.

The Fourier and wavelet analysis is used to find out the significant points in the progression of the optical power. From the Fourier analysis we can predict the progression, wavelet analysis enables us to find out singularities. It is expected, that every change on the fiber has its own "fingerprint" in the redistribution of the optical power. So we believe that we will be able to say, what affects to the fiber, if it is heat, pressure, tension etc.

Keywords: Coupled optical power, hybrid fibers

1 Introduction

Telecommunication companies use lots of thousands kilometers of optical fibers for telecommunication purposes like Internet, voice services, video on demand service etc. In most of this cases the single-mode fibers are being used for their properties like the smallest total-dispersion parameters. The only thing these fibers are used for is to carry the light-power from one end of the fiber to the another end with the smallest attenuation, amount of time for one bit period and dispersion. One can ask: "Can we use the same fiber for telecommunication signals and as a sensor at the same time?".

The standard telecommunication fibers are designed to be independent on external conditions as much as it is possible. The only thing we can find out using this fibers is whether there is a light-power on the output end or not. That is not enough information to identify the external quantities. We have had to

© Václav Snášel (Ed.): WOFEX 2007, pp. 386–391, ISBN 978-80-248-1571-8.
VŠB – Technical University of Ostrava, FEECS, 2007.

design a new fiber with a special refractive-index profile. These fiber carries only one mode at wavelength $\lambda = 1550$ nm, so in that case the parameters important for telecommunication purposes are preserved. But there can be four next modes carried at wavelength $\lambda = 850$ nm, which do not affect the one mode used to carry telecommunication signals. These additional modes are used for measuring the optical-power redistribution in the circumference of the fiber. Using a high-resolution digital camera the changes of the optical-power redistribution are observed at the end of fiber. Now we are going to find out some method to convey changes of the light-power distribution into quantities like force, heat, moisture or pressure.

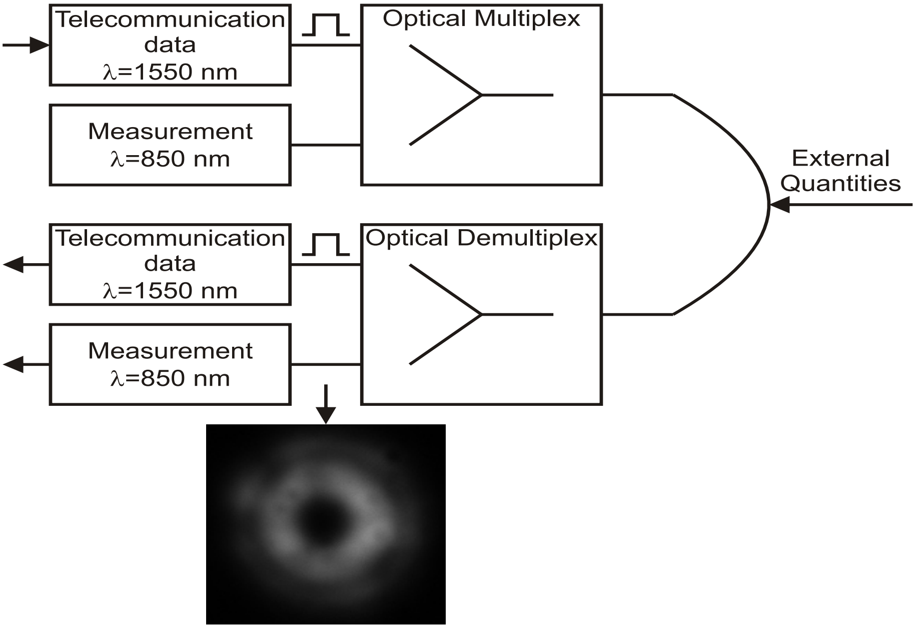
Telecommunication data λ=1550 nm
Measurement λ=850 nm
Optical Multiplex
External Quantities
Telecommunication data λ=1550 nm
Measurement λ=850 nm
Optical Demultiplex

Fig. 1. Measuring configuration.

2 Coupled-power equations

The *coupled mode* equations, which follows directly from the wave equations for individual modes, contain a detailed description of the phase and amplitude of all the modes at any point z along the waveguide. But we are usually not interested in the phases and amplitudes of the individual modes. For most practical intentions, it is sufficient to know the average of the amount of power carried by each mode. *Coupled power* equations for the average mode power are derived for weak coupling between modes. It means that coupling requires a distance of

1000 wavelengths for a complete exchange of power between two modes. It is a set of finite number of first-order differential equations with symmetric constant coefficients. Coupling to forward traveling guided modes occurs for distortion function $f(z)$ whose Fourier spectra are limited to spatial frequencies. Most of the optical fibers have spatial Fourier spectra, always with a background of a nearly flat Fourier spectrum caused by the Rayleigh scattering.

Very important idea is that the average is taken over statistically similar waveguides. We assume, that waveguides manufactured using the same technology will have the same probability distribution of imperfections. We thus assume that $f(z)$ is a stationary random process that can be described by an autocorrelation function $R(u)$ with a finite correlation length D. Using this presumptions we can write

$$\frac{\mathrm{d}P_\mu}{\mathrm{d}z} = -2\alpha_\mu P_\mu + \sum_{\nu=1}^{N} h_{\mu\nu}(P_\nu - P_\mu) \tag{1}$$

where P_μ is power carried by the μth mode, $2\alpha_\mu$ is the power loss coefficient and $h_{\mu\nu}$ is the power coupling coefficient.

We assume that $P(z)$ has its initial power distribution $P(0)$ and $P(z)$ vanishes at $z \to \infty$. The power loss coefficient $2\alpha_\mu$ is a combination of radiation and heat losses.

If we assume that at some point z only mode μ carries power, then

$$\frac{\mathrm{d}P_\mu}{\mathrm{d}z} = -\left(2\alpha_\mu + \sum_{\nu=1}^{N} h_{\mu\nu}\right) P_\mu. \tag{2}$$

It means that the guided mode μ losses power to all the other guided modes. If the mode μ carries no power at a point z, than

$$\frac{\mathrm{d}P_\mu}{\mathrm{d}z} = \sum_{\nu=1}^{N} h_{\mu\nu} P_\mu. \tag{3}$$

The mode μ gains power by coupling with all the other modes.

The coupling coefficients are symmetric,

$$h_{\mu\nu} = h_{\nu\mu}. \tag{4}$$

2.1 Coupling coefficients

If the system operates with the continuous waves, the system of coupled fist-order differential equations, using substitution

$$P_\nu(z) = A_\nu e^{-\sigma z} \tag{5}$$

converts into a homogeneous system of N equations of N unknowns

$$\sum_{\nu=1}^{N} \left[h_{\mu\nu} + \left(\sigma - 2\alpha_\nu - \sum_{\mu=1}^{N} h_{\mu\nu} \right) \delta_{\mu\nu} \right] A_\nu = 0. \tag{6}$$

Its solutions are the N eigenvalues $\sigma^{(n)}$ and eigenvectors $A^{(n)}$. The symbol $\delta_{\mu\nu}$ means that only diagonal terms are nonzero.

The first eigenvalue and eigenvector thus have important physical meanings. The first eigenvalue represents the steady state power loss coefficient, while the first eigenvector determines the shape of the power versus mode number distribution once the steady state is reached. The other eigenvalues and eigenvectors do not have a physical significance.

This equation looks always the same way, but it is not independent, where the external parameters act. The power distribution reaches a steady state after a distance $z = L_s$ which is determined by the difference between $\sigma^{(1)}$ and $\sigma^{(2)}$. The distance between $z = 0$ and $z = L_s$ is called transition region. The speed with which the power redistributes itself in the transient region $0 \leq z < L_s$ is determined by the strength of the eigenvalues $\sigma^{(n)}$. Once the steady state is reached, the average power carried by each mode decreases at the same rate, so the total power distribution decreases without change of its shape according to the loss coefficient $\sigma^{(1)}$. In the lossless case is $A_\nu^{(1)} = 1/\sqrt{N}$, $\sigma^{(1)} = 0$.

The key problem is how to obtain the coupling coefficients $h_{\mu\nu}$. This step can not be done analytically. One can use simulation tools or make an experiment. We have simulated the output distribution of the light-power using the specific modes as the excitation on the input end. It is possible to excite the fiber with just one mode. Then all the power in the other guided modes is gained trough the effect of coupling. The sum of the output power (in the lossless case) must match the initial power $P(0)$. Neglecting the loss coefficient (one can do that for relatively short fibers with known attenuation) we get

$$\frac{\mathrm{d}P_1(z)}{\mathrm{d}z} = h_{11}P_1(0) \ \tfrac{\mathrm{d}P_2(z)}{\mathrm{d}z} = h_{21}P_1(0)$$
$$\frac{\mathrm{d}P_3(z)}{\mathrm{d}z} = h_{31}P_1(0) \ \tfrac{\mathrm{d}P_4(z)}{\mathrm{d}z} = h_{41}P_1(0)$$

Then we can use first two modes to obtain the coupling coefficients that redistributes power from the first and the second mode to the others, first three modes to obtain the coupling coefficients that redistributes power from the first three modes to the others etc.

$$\frac{\mathrm{d}P_1(z)}{\mathrm{d}z} = h_{11}P_1(0) + h_{12}P_2(0) \ \tfrac{\mathrm{d}P_2(z)}{\mathrm{d}z} = h_{21}P_1(0) + h_{22}P_2(0)$$
$$\frac{\mathrm{d}P_3(z)}{\mathrm{d}z} = h_{31}P_1(0) + h_{32}P_2(0) \ \tfrac{\mathrm{d}P_4(z)}{\mathrm{d}z} = h_{41}P_1(0) + h_{42}P_2(0)$$

2.2 Solution of coupled-power equations for 3 modes

We can use equation (6) in matrix form. Solution of the determinant 2.2 with the unknown σ (MATLAB – Symbolic Math Toolbox – elapsed calculation time

48.557463 s, computer Intel Celeron 1.7 GHz, 500 MB RAM):

$$\begin{vmatrix} \sigma - 2\alpha_1 - h_{12} - h_{13}, & h_{12}, & h_{13} \\ h_{12}, & \sigma - 2\alpha_2 - h_{12} - h_{23}, & h_{23} \\ h_{13}, & h_{23}, & \sigma - 2\alpha_3 - h_{13} - h_{23} \end{vmatrix} = 0.$$

The analytical solution takes 20 pages for 3 modes. The MATLAB software could not solve it for 4 modes anlytically.

3 Experiments

The experimental system was created to measure the optical-power redistribution at the end of the fiber. We use a microscope with a high resolution camera to gain images like is shown on figure 1. Images are taken by sampling with periode $T_s = 35$ ms.

Using the wavelet decomposition by the 'db2' wavelet, applied to the signal taken around the circumference we can see strong coefficients at time 17 s and 40 s where pressure was applied to the fiber.

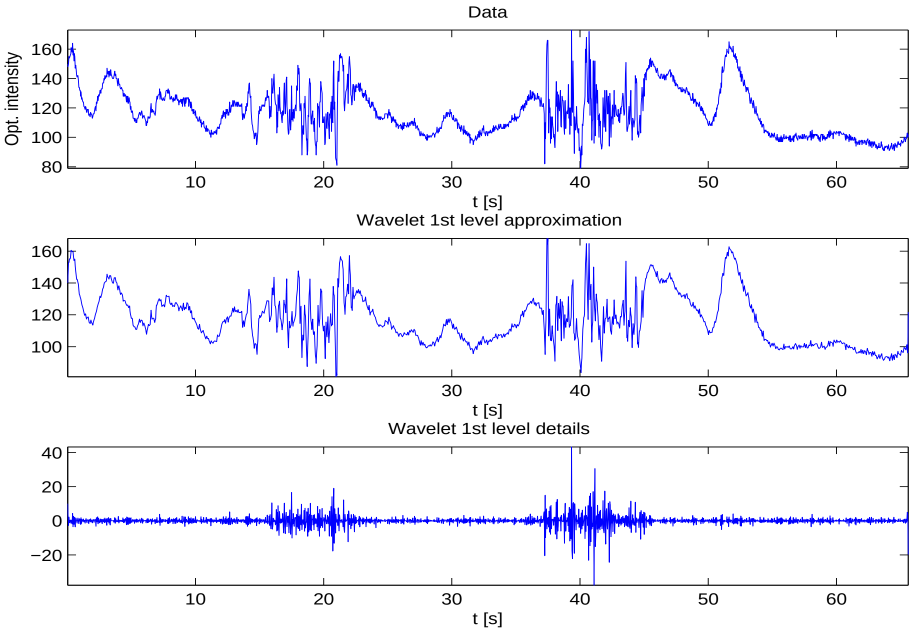

Fig. 2. Wavelet coefficients.

At the present time selective excitation of individual modes is being prepared. Individual modes differs by the angle they reach the input end of the fiber. There are two ways to excite modes selectively – one by masking in space domain and the second by is provided by masking in frequency domain using the optical Fourier transform. The second method seems to be more useful. At the same time we prepare experiments with controlled effect on the fiber with heat and tension.

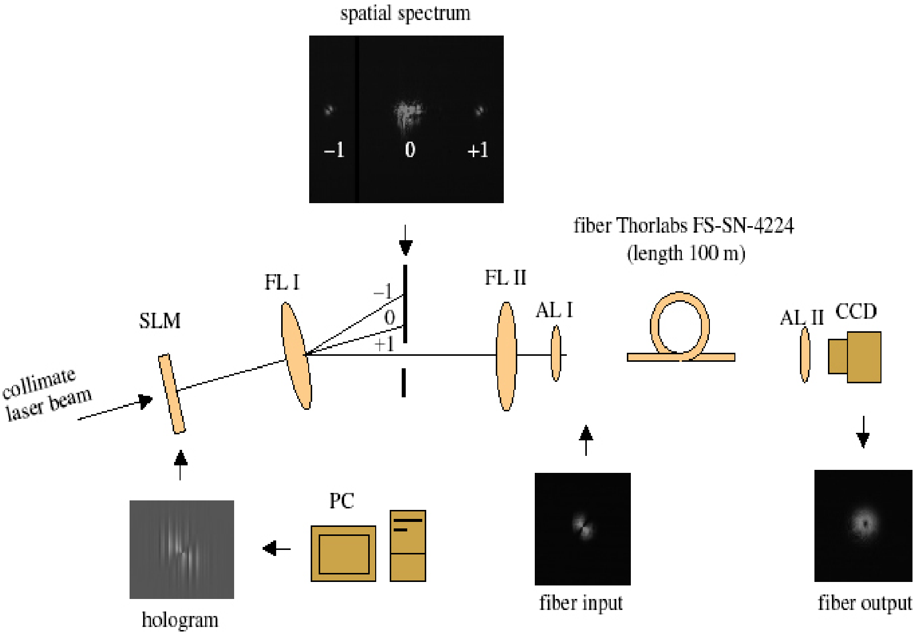
spatial spectrum
–1
0
+1
fiber Thorlabs FS-SN-4224
(length 100 m)
FL I
FL II
AL I
AL II
CCD
SLM
–1
0
+1
collimate laser beam
PC
hologram
fiber input
fiber output

Fig. 3. Selective excitation by masking in frequency domain – see [1].

References

1. Bouchal, Z. – Haderka, O. – Celechovský, R. `http://www.iop.org/EJ/article/1367-2630/7/1/125/njp5_1_125.html`.
2. Chui, CH. K. *Wavelets; A Mathematical Tool for Signal Processing.* Philadelphia (USA): SIAM, c1997. ISBN -0-89871-384-6.
3. Frazier, M. W. *An introduction to wavelets through linear algebra.* New York (USA): Springer, c1999. ISBN 0-387-98639-1.
4. Marcuse, D. *Theory of dielectric optical waveguides.* 2nd edition. Boston (USA): AT&T, 1991. ISBN 0-12-470951-6.
5. Vidakovic, B. *Statistical Modeling by Wavelets.* New York, Chister, Toronto: Wiley, 1999. ISBN 0-471-29365-2.
6. Yu, F. T. S., Yin, S. *Fiber optic sensors.* New York (USA): c2002. ISBN 0-8247-0732-X.

The Hybrid Optical Fibers Based on Redistribution of Power

Petr Šiška

Department of Electronics and Telecommunications, FEECS,
VŠB – Technical University of Ostrava, 17. listopadu 15, 708 33 Ostrava – Poruba
`petr.siska.fei@vsb.cz`

Abstract. The main topic of this paper is to show other steps that were made over the past year and describe how optical fibers might be used in a near future. Paper recapitulate theoretical expectations, designing of new types of optical fiber models and describe results obtained from the real fiber samples.

1. Introduction

Sensors build on optical fibers can measure almost all magnitudes in these days. Article describes a new developing area of optical fiber sensors. These sensors use for their function fundamentals of redistribution of power inside a fiber, which is one of the most sensitive effects that appear inside a fiber. This fact allows to constructing a very sensitive optical fiber sensor.

2. Hybrid optical fiber - a new type of optical fiber

In our research we design new hybrid optical fiber that affords concurrently utilizing of optical fiber for telecommunications and measurement. This fiber is designed to work on two wavelengths. On telecommunications wavelength of 1550 nm this fiber works in single mode regime and on measurement wavelength of 850 nm is working in quasi-single mode regime.

The major part of today's constructed optical communication routes are based on the single mode optical fibers which are the best possibility for data transmission. Single mode optical fibers are constructed to be insensitive on acting external forces which can have influence on a data transmission.

On the other side, optical fiber sensors are constructed to be utmost sensitive on acting external forces and to be able to realize them.

We are trying to eliminate this conflict by using an optical fiber with specially constructed change of a refractive index.

For evaluation of acting external forces on optical fiber we assume that total power value inside fiber is constant.

© Václav Snášel (Ed.): WOFEX 2007, pp. 392–397, ISBN 978-80-248-1571-8.
VŠB – Technical University of Ostrava, FEECS, 2007.

As a possibility how to solve a problem of evaluation of acting external forces on optical fiber can be used a redistribution of power among several modes by phenomena of coupling between modes or differential modal attenuation.

The construction of a new optical fiber was created to satisfy with three conditions. Fiber must be in single mode regime and his transfer characteristics must be close to characteristics of a classic single mode fiber at communication wavelength λ=1550 nm. Fiber must support propagation of four modes which will be strong enough for their measurement at working wavelength λ=850 nm. Finally, total proportions of the fiber must be same as proportions of classic single mode optical fiber and MFD must be close to MFD of classic single mode fiber.

3. Construction of a new hybrid fiber

For design of a new optical fiber we use specialized software Optifiber from Canadian company OptiwaveLtd. Software Optifiber is effective instrument for engineers, scientists or students which are designing optical fibers or optical telecommunication systems.

By the help of this software was created a new fiber construction with closest properties to ours requirements. From figure 1 is evident that new fiber have total proportions 62,5 μm which is the same diameter as standard single mode fiber. Only core diameter is double to standard single mode fiber, but MFD is only slightly bigger.

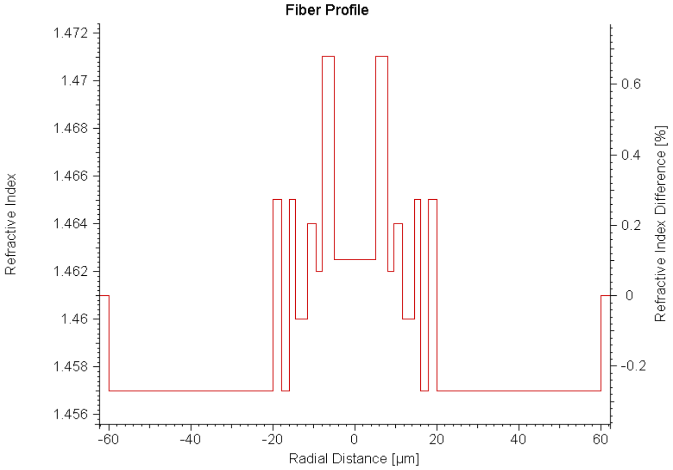

Figure 1 – A new fiber profile

From simulations in OptiFiber we recognize that this fiber satisfy with other two conditions. Fiber is single mode for wavelength λ=1550 nm. In fact this fiber supports propagation of next three modes, but theirs energy contribution are so small that we can vanish those modes.

For wavelength λ=850 nm fiber supports four strong modes. As in single mode regime another higher modes are supported by fiber, but they represents only marginal value of energy so that we can vanish them as well.

We managed a fiber whose simulated characteristics satisfy with set conditions. Next step was real producing of this fiber. To this end was together with ÚFE AV ČR requested and obtained shared grant project. From figure 1 is evident that structure of this fiber is relatively complicated. Specially, sharp changes of refractive indexes are technologically very difficult. For that reason we still continue with designing of a new fiber as will be shown below.

The first produced sample shows technological problems with manufacturing of this complicated profile. As you can see from figure 2 his profile parameters are relatively far away from ideal parameters.

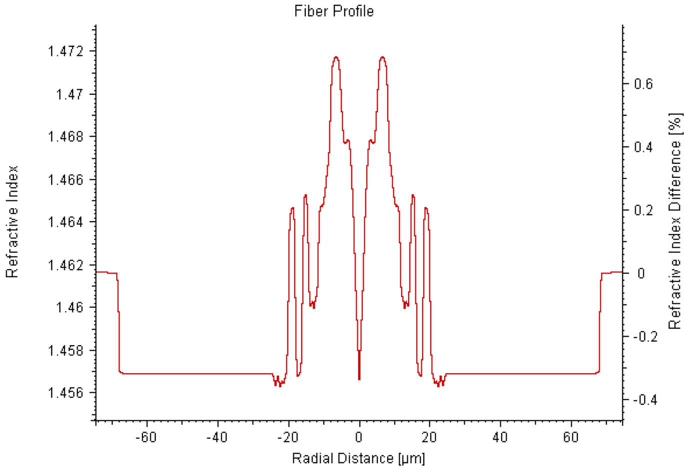

Figure 2 – Real profile of a new fiber

Simulations shows main problem of the real fiber profile. This fiber is not a single mode fiber for communication wavelength, because fiber supports propagation of two significant modes. Thereby transmission parameters were markedly worse, especially modal dispersion. Properties of this fiber would be considerably worse then properties of standard single mode fiber.

When we tests this fiber profile for measurement wavelength in our software, was found out that fiber supports propagation of three significant modes. This fact was not a problem for our purposes, if this fiber would be single mode at communication wavelength.

Researchers from ÚFE AV ČR are still working on improvements of production technology of complicated indexes profiles to keep designed profiles as best as possible. Real fiber profile improvements shows figure 3.

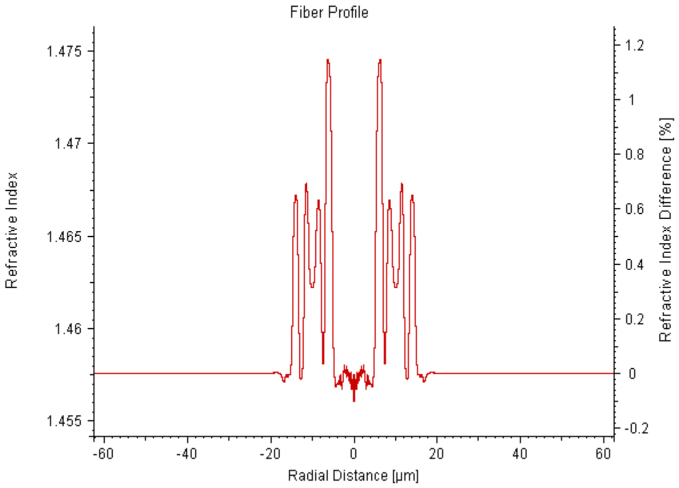

Figure 3 – Fiber profile improvements

4. Other design of hybrid fiber

As mentioned earlier we still continue with designing of new optical fiber profiles follow all set conditions together with new condition of easier fabrication of the fiber. We are trying to design a fiber without sharp changes of refractive indexes and simple as it is possible. For reason of limited article range is describe only one newer design. This design shows figure 4.

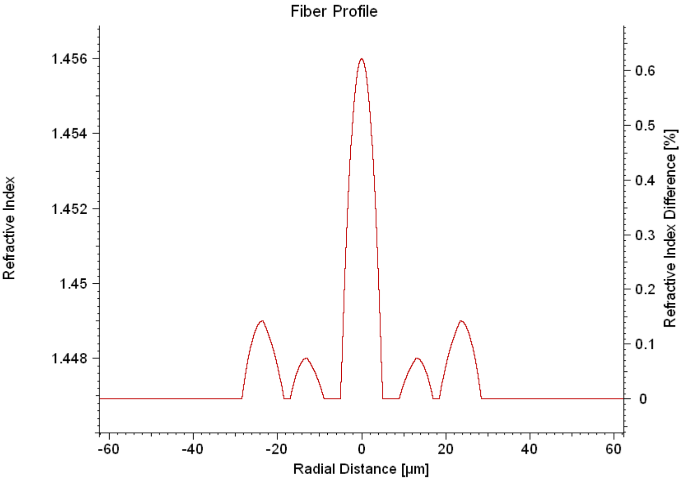

Figure 4 – Newest fiber design

This fiber profile has closest parameters to set conditions from all newest profiles that we design till now, but his parameters are still not so good like parameters of first designed profile with sharp changes of refractive indexes.

All our fiber samples are testing in our laboratory for their sensitivity on external magnitudes. Was build measurement system where we tested fiber for bending and vibrations. Figure 5 shows a redistribution of energy on the head of the fiber. Left side pertains to fiber in resting state and right side pertains to fiber with acting external magnitude.

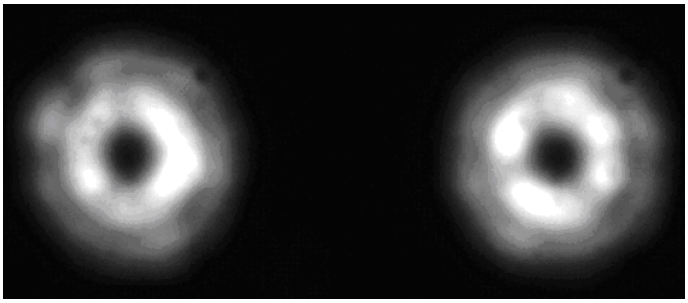

Figure 5 – Redistribution of energy

5. Conclusion

At the present time are designed and fabricated new hybrid optical fibers which satisfy with theoretical expectations for concurrently utilizing of the optical fibers. Were realized first laboratory measurements for bending and vibration sensitivity of hybrid fibers. Results describe that fibers has high sensitivity for those magnitudes. Unfortunately, real samples still show technological problems with manufacturing of complicated profiles to exactly keep set conditions.

References

1. ETTEN, W., PLAATS, J.: *Fundamentals of Optical Fiber Communications*. 1st.edition, Prentice Hall International (UK) Ltd, 1991, ISBN 0-13-717513-2.
2. VAŠINEK, V.: *Optická vlákna v blízkosti mezní normalizované frekvence jednomódových vláken a jejich aplikace.* 1.vyd, Vysoká škola báňská – Technická univerzita Ostrava, ISBN 80-24-0575-8.
3. VAŠINEK, V.: *Podklady k výuce předmětu Optoelektronika*
4. Technical Documentation, *OptiFiber*, Optical Fiber Design Software, Optiwave Corporation. 14.6.2000
5. ŠIŠKA, P.: *Současné využití optických vláken pro telekomunikace a měření*. 2005
6. MARCUSE, D.: *Theory of Dielectric Optical Waveguides*. 2nd. edition, Academic Press, Inc. (1991), ISBN 0-12-470951-6.

Publications

1. VASINEK, V., SISKA, P., MARSALEK, L.: *Quasi single-mode fibers and their applications.* In: The 10th World Multi-Conference on Systemics, Cybernetics and Informatics WMSCI 2006, July 16-19, 2006, Orlando, Florida, USA, p. 317-122, ISBN 980-6560-70-1.
2. VASINEK, V., SISKA, P., MARSALEK, L.: *Quasi Single-Mode Optical Fibers and their Applications.* Journal of SCI, (potvrzené přijetí k publikování v roce 2007), ISSN: 1690-4524.
3. VASINEK, V., SISKA, P., MARSALEK, L.: *Mode visualization for fiber optic temperature sensor.* In: European Symposium on Optics and Optoelectronics, Praha, duben 2007, (přijato k publikování).
4. SKAPA, J., SISKA, P., VASINEK, V.: *Coupled power analysis for hybrid optical fibers.* Radioelektronika 2007, Brno, 24-25 dubna (2007), s. 363-366, ISBN 978-80-214-3390-8.
5. SISKA, P., MARSALEK, L., VASINEK, V.: *Současné využití optických vláken pro telekomunikace a měření.* In: Sborník příspěvků konference IEEE Vršov 2006, Vyd.: VUT v Brně, září 2006, ISBN 80-214-3247-0.
6. MARSALEK, L., SISKA, P., VASINEK, V.: *Vizualizace módových polí v blízkosti normalizované frekvence.* In: Sborník příspěvků konference IEEE Vršov 2006, Vyd.: VUT v Brně, září 2006, ISBN 80-214-3247-0.
7. SISKA, P.: *The concurrently utilizing of the optical fibers for data transmission and measurement.* In: Sborník WOFEX 2006, Vyd.: VŠB-TU Ostrava, září 2006, ISBN 80-248-1152-9.
8. SISKA, P., MARSALEK, L., VASINEK, V.: *Použití telekomunikačních optických vláken pro účely vláknových optických senzorů.* In: Sborník VII. Seminář katedry telekomunikační techniky. 13.4.2007, Ostrava, ISBN 978-80-248-1370-7.
9. MARSALEK, L., SISKA, P., VASINEK, V.: *Vizualizace módových polí v blízkosti normalizované frekvence.* In: Sborník VII. Seminář katedry telekomunikační techniky. 13.4.2007, Ostrava, ISBN 978-80-248-1370-7.

Using Fourier Transform for Solving Problems with Photonic Crystals by PWM

Jan Vanda, Jan Skapa

Department of Electronics and Telecommunications, FEECS,
VŠB – Technical University of Ostrava, 17. listopadu 15, 708 33 Ostrava – Poruba
{jan.vanda.fei,jan.skapa.fei}@vsb.cz

Abstract. Analysis of propagating plane waves is the original and most applied method for analysis of electromagnetic wave characteristics in periodic dielectric media. Due to penetrating of photonics into various areas of human efforts subsequently arise number of various methods for description of behavior electromagnetic waves during propagation in photonic structures. Although these methods, neither of computing time and results accuracy point of view, can reach better results than plane wave method (PWM) in particular cases, generally is plane wave method the most effective in solving of ordinary arbitrary arranged photonic structures in principle. Fundamental in this method is Fourier transform; hence good understanding to its appointment and decision procedure is necessary.

Keywords: Photonics, Photonic crystal, Plane wave method, Fourier transform

1 Introduction

Plane wave method was first theoretical method for accurate photonic crystals analysis and is probably still the most applied of all known methods (others methods are for example localized basis functions, finite difference or finite elements). PWM is simple in general and utilizes periodicity of photonic crystals for description of propagating light almost in same manner like is the periodicity of semiconductors and others solid-state crystals utilized for solving Schrödinger equations in electron band gaps prediction [1].

PWM provides us with the fast suitable tool for frequency domain analysis of full periodic photonic crystals, but it has poorer results in solving large computing problems (2D or 3D photonic crystals with defects). However, utilization advanced implementations may improve PWM efficiency for solving wide problems as are real photonic crystals (PBG optical fibres for example). One of the best implementation is utilization of advances provided by a FT (Fourier Transform). Here we can use both benefits descended from periodicity and translation to reciprocal lattice.

© Václav Snášel (Ed.): WOFEX 2007, pp. 398–404, ISBN 978-80-248-1571-8.
VŠB – Technical University of Ostrava, FEECS, 2007.

2 Analysis

First will be stated some basic conditions, which will be applied for the rest of the paper. Photonic crystals realized in dielectric material without free charges will be considered, for which applies Maxwell's equations in differential form [1]. Presuming, that the photonic crystal is consisted from linear, isotropic and non-magnetic materials, so equations for electric and magnetic flux density is:

$$D = \varepsilon_0 \varepsilon_r E \,; \qquad B = \mu_0 \mu_r H \tag{1}$$

where μ_0 is free space permeability and μ_r is relative permeability and ε_0 is free space permittivity and ε_r is relative permittivity. Only non-absorbing media will be considered, that means ε_r is real.

By utilizing equations expressing position dependence of E and H fields on angular frequency in harmonic time domain into Maxwell equations can be determined wave equation, which fully represents propagation of electromagnetic waves. For E – field or H – field should be expressed as:

$$\text{rot rot}\, E(r) = \frac{\omega^2}{c^2}\varepsilon(r)E(r) \quad \text{or} \quad \text{rot}\left[\frac{1}{\varepsilon(r)}\text{rot}H(r)\right] = \frac{\omega^2}{c^2}\varepsilon(r)H(r) \tag{2}$$

Due to periodicity of photonic crystals is possible to find solution one of equation, according to Bloch's theorem, as plane wave modulated be a function with the same periodicity as photonic crystal:

$$E(r) = V_k(r)e^{-jkr} \quad \text{or} \quad H(r) = U_k(r)e^{-jkr} \tag{3}$$

where $V_k(r)$, $U_k(r)$ are the periodic functions and k is the wave vector of solution. For determination of solution is useful to operate in reciprocal space and utilize fact, that the periodic functions should be expressed as a Fourier series expansion based on reciprocal lattice vectors G for reaching of following expression of E and H – fields:

$$E(r) = \sum_G E_k(G)e^{-j(k+G)r} \quad \text{or} \quad H(r) = \sum_G H_k(G)e^{-j(k+G)r} \tag{4}$$

In reciprocal space is then possible to find corresponding wave equations via FT:

$$-(k+G)\times\left[(k+G)\times E_k(G)\right] = \frac{\omega^2}{c^2}\sum_{G'}\varepsilon_r(G-G')E_k(G') \quad \text{or} \tag{5}$$

$$-(k+G)\times\left[\sum_{G'}\varepsilon_r^{-1}(G-G')(k+G')\times H_k(G')\right] = \frac{\omega^2}{c^2}H_k(G) \tag{6}$$

where $\varepsilon_r(G)$ are the Fourier coefficients of $\varepsilon_r(r)$ and $\varepsilon_r^{-1}(G)$ are the Fourier coefficients of $\varepsilon_r^{-1}(r)$. Equations (**5**) and (**6**) should be expressed in matrix form and solved with using standard numerical routine as eigenvalue problems. Suffix k denotes fact, that the eigenvalue problems are solved for fixed wave vector k to match allowed angular frequencies ω of allowed modes. Truncating sums into N reciprocal lattice vectors a $3N$ x $3N$ matrix will be obtained. However, this matrix should be reduced into the size $2N$ x $2N$ utilizing transversal condition of H-fields $\left(\text{e.g. } (\text{rot rot } H(r) = 0\right)$, as is mentioned in [2], which is very important for computing times reduction.

3 Reciprocal lattice

Reciprocal space is also called Fourier space, k-space or moment space. This space is designed synthesizing two important characteristics of crystal planes: tangent and inter-plane distance. Reciprocal lattice is a set of imaginary points constructed that the vector direction from one point to other is parallel to normal direction in planes in real space and points distance (vector absolute value) equals to reciprocal value of real inter-plane distance.

It is appropriate to determine reciprocal lattice vector as 2π multiples of inter-plane distance. This convention converts period units on length units to radians on length units. This simplifies different periodic processes comparison. Reciprocal lattice should be described in same manner like real periodic lattice, but there must be difference kept on mind: real lattice indices real objects arrangement (rods or holes in photonic crystal) and has size **m**, but reciprocal lattice indices position of imaginary points (amplitude, impulse) and has size $\mathbf{m}^{-1}$.

The green dots on the picture 1 indicates atoms position (holes or rods in photonic crystals) in common real lattice, cyan indicates arrangement of imaginary points in reciprocal lattice (is possible to observe diffraction points under certain conditions). Black point determines beginning. Gray point in real lattice shows orientation in 3D space (during assembling of more planes). Gray point in reciprocal lattice labels direction according to point in real lattice at rotating along crystal symmetry. Even if position of gray point in real and reciprocal lattice consists with position of the atom, in doesn’t shows atom position (hole or rod), but only designates orientation of picture. A red line determines position of planes of periodicity, which are perpendicular to plane of figure. Normal direction N and inter-plane distance d is marked with red bolts. Reciprocal lattice vector G is demonstrated by a blue bolt and yellow points shows points in reciprocal lattice translated by this vector $\mathrm{G} = \dfrac{2\pi}{\mathrm{d}}$ [3].

Consequently, it is possible to say, that the general construction of reciprocal lattice is consist (after choose and determine of beginning) from three points:

1. from choose beginning layout normal to arbitrary group of planes in real direct lattice
2. set length of each normal to 2π multiple of reciprocal value of inter-plane distance for assigned group of planes
3. place point onto end of each normal

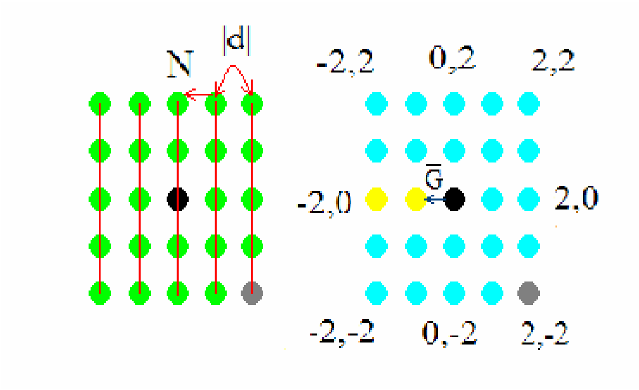

Fig. 1. General real (left) and reciprocal (right) lattice.

For visualization is possible to show relation between real and reciprocal lattice on example of relation between frequency and period. Therefore, for conversion of reciprocal lattice is used Fourier transform in the same way, like in study of any else periodic function respectively. This is the reason, why is reciprocal space also called Fourier space. That's mean the function must fulfill some general condition and than will be possible to reach complex Fourier transform of examined function. Closer overview on mathematical apparatus is in [4].

4 Transformation of photonic crystal's lattice

In most popular case of 2D photonic crystals is necessary to apply general procedure (see points 1-3 above) on special case of translation symmetry abstention in normal direction. In this special case consider symmetry in normal direction equal to infinity. Since reciprocal value of infinity equals to zero, in normal direction appears number of points placed infinity close to each other. Sets of these points are called Bragg rods. Let's assume function $f(\mathrm{r})$, $\mathrm{r} \in \mathbf{R}^2$, which is periodical on lattice; its mean assumption $f(\mathrm{r}) = f(\mathrm{r+R})$ for all vectors R, which translates lattice on it own (i.e. connect lattice points with following). Example of this function is dielectric function ε(r). Set of vectors R is called lattice vectors. Natural consecution in periodic function analysis is to use Fourier transform; that's mean to construct wave periodic function outside of plane of periodicity f(r) with various wave vectors. FT of this function will be:

$$f(\mathrm{r}) = \int_{\Omega} g(\mathrm{q}) e^{i\mathrm{q}\cdot r} d\mathrm{q} \tag{7}$$

where $g(\mathrm{q})$ is function of plane wave with wave vector q, r is variable in real space and Ω is unit cell area. From prescript f(r) = f(r+R) transform should be written as:

$$f(\mathrm{r}+\mathrm{R})=\int_{\Omega} g(\mathrm{q})e^{i\mathrm{q}\cdot r}\cdot e^{i\mathrm{q}\cdot\mathrm{R}}d\mathrm{q} \tag{8}$$

which leads to

$$g(\mathrm{q})=g(\mathrm{q})\exp(i\mathrm{q}\cdot\mathrm{R}) \tag{9}$$

Equation (**9**) should be fulfilled for three conditions:

1. $g(q) = 0$
2. $\exp(iq\cdot R) = 1$
3. $g(q) = 0 \cup \exp(iq\cdot R) = 1$

however for our purposes is important condition 3. In other words the case, where FT is zero everywhere except the peaks on values q such that applies $\exp(iq\cdot R) = 1$ for all R – that means zero everywhere except points in reciprocal lattice. These vectors q, for that applies $\exp(iq\cdot R) = 1$ or equivalently $q\cdot R = n2\pi$ is than labeled as $\overline{\mathrm{G}}$ and called *reciprocal lattice vectors*.

5 Application

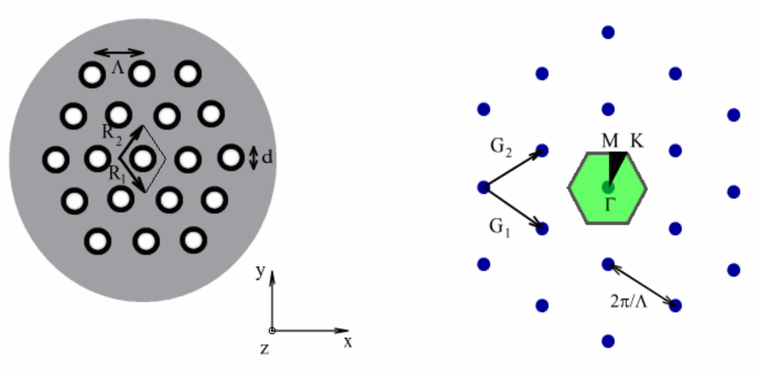

Fig. 2. 2D ideal photonic crystal example with hexagonal symmetry. Left is original photonic crystal with refractive indices n1 (grey) and n2 (white), where primitive lattice vectors in real space $\vec{R}_1$, $\vec{R}_2$ and unit cell are marked. Right is reciprocal lattice with reciprocal lattice vectors $\vec{G}_1, \vec{G}_2$. Green area shows 1st. Brillouin zone and black irreducible 1st. Brillouin zone. Points of symmetry hexagonal structure labels letters Γ, M a K.

For this structures are primitive lattice vectors defined as:

$$\mathrm{R}_1=\frac{\Lambda}{2}\left(x-y\sqrt{3}\right),\quad \mathrm{R}_2=\frac{\Lambda}{2}\left(x+y\sqrt{3}\right) \tag{10}$$

$$\mathrm{G}_1 = \frac{2\pi}{\Lambda}\left(x + y\frac{\sqrt{3}}{3}\right), \quad \mathrm{G}_2 = \frac{2\pi}{\Lambda}\left(x - y\frac{\sqrt{3}}{3}\right) \tag{11}$$

where Λ is distance between two lattice nods. Consequently, unit cell should be defined as $\left|\mathrm{R}_1 \times \mathrm{R}_2\right|$, $\mathrm{R}_1, \mathrm{R}_2 \in \mathbf{R}^2$, $x, y \in \mathbf{R}$ respectively. Using simplifies for triangular structures [5] should be constructed reciprocal vectors (**11**).

Last necessary step is determination of $\varepsilon_r^{-1}(\overline{G})$ coefficients for matrix equation (**3**). Here is used periodicity of photonic crystal and FT for crossing from real to reciprocal space in the same way like above. Dielectric distribution is expanded to Fourier series:

$$\frac{1}{\varepsilon(r_{\|})} = \sum_{\overline{G}_{\|}} \varepsilon_r^{-1}(\mathrm{G}_{\|}) e^{-i\mathrm{G}_{\|}\cdot r_{\|}} \tag{12}$$

where Fourier coefficients are determined as

$$\varepsilon_r^{-1}(\mathrm{G}_{\|}) = \frac{1}{\left|\mathrm{R}_1 \times \mathrm{R}_2\right|} \int_{\Omega} \frac{1}{\varepsilon(r_{\|})} e^{-iG_{\|}\cdot r_{\|}} d^2 r_{\|}, \tag{13}$$

and surface integral is executed on unit cell. In equations (**12**) and (**13**) index || indicate 2D vectors with components only in plane of periodicity. For circular holes/rods with dielectric constant ε_1 and background matrix ε_2 are Fourier coefficients:

$$\varepsilon^{-1}(\mathrm{G}_{\|}) = \begin{cases} \dfrac{1}{\varepsilon_1} f + \dfrac{1}{\varepsilon_2}(1-f), & \mathrm{G}_{\|} = 0 \\ \left[\dfrac{1}{\varepsilon_1} f - \dfrac{1}{\varepsilon_2} f\right] f \dfrac{2J_1\left(\dfrac{\mathrm{G}_{\|}\Lambda}{2}\right)}{\left(\dfrac{\mathrm{G}'_{\|}\Lambda}{2}\right)}, & \mathrm{G}_{\|} \neq 0 \end{cases} \tag{14}$$

where J_1 is first order Bessel function.

6 Conclusion

Although, analytical expression for dielectric distribution in reciprocal space should be found in special case of circular rods/holes in triangular lattice, for arbitrary general photonic crystal (real photonic crystal) is necessary to found Fourier coefficients numerically. This should be done by discretization of real space resolution and transform to reciprocal space using discrete Fourier transform (DFT).

Utilization of mentioned advantages and techniques should reduce computing time dramatically at maintain versatility and accuracy of plane wave method for solving wide computational problems, as real photonic crystals are.

References

1. J. D. Joannopoulos, R. D. Meade, J. N. Winn. Photonic crystals: molding the flow of light. Princeton University Press, 2005, 0-691-03744-2.
2. Bjarklev, J. Broeng, A.S. Bjarklev. Photonic Crystal Fibres. Springer Science Business media, Inc. 2003, 233 Spring Street, New York NY 10013, USA. 1-4020-7610-X.
3. http://www.chembio.uoguelph.ca/educmat/chm729/recip/3vis.htm
4. N. Castova, T. Kozubek. http://www.am.vsb.cz/studium/integralni_transformace/. VŠB-TU Ostrava, 2004.
5. M. Plihal, A. Maradudin. Photonic band structure of two-dimensional systems: The triangular lattice. Physical Rewiev B, vol. 44, Oct. 1991.
6. S. Guo, A. Albin. Simple plane wave implementation for photonic crystal calculations. Optics Express 175, 11/2, 2003

Related publications

1. J. Vanda, J. Necesany, V. Vasinek, J. Skapa. A. Argyros, M. van Eijkelenborg, M. Large. Nonlinear effects in microstructured polymer optical fibres. Published at SPIE Optics and Optoelectronics 2007, Prague. DOI: 10.1117/12.722367.
2. J. Vanda, J. Necesany, L. Marsalek, V. Vasinek. Basic characterization of suspended-core microstructured polymer optical fiber. Published at Radioelektronika 2007, Brno. 1-4244-0821-0.
3. J. Vanda, J. Necesany. Mikrostrukturni polymerova opticka vlakna. Published at VII Seminar telekomunikacni techniky 2007, Ostrava. 978-80-248-1370-7.

Languages of the Environment in PM-Colonies

Adam Kožaný

Silesian University in Opava, Faculty of Philosophy and Science, Bezručovo náměstí
13, 746 01 Opava, Czech Republic
`adam.kozany@fpf.slu.cz`

Abstract. To study structural properties of PM-Colonies the special classes of languages: Alive, Dead, Reachable, Unreachable, Garden-of-Eden, Life, Doomsday and Non-Life were introduced. In this paper we study these languages of the environment for both the original PM-Colonies and PM-Colonies with modified definition. We express these languages in regular notation, compare if and how differs possible combinations of empty and non-empty languages of the environment for different types of PM-Colonies and show other interesting structural properties of PM-Colonies.

1 Introduction

A colony introduced in [3] is a system manipulating with symbols, which consists of components as simple as possible cooperating is such way that its common competence can be strictly larger than competence of individual components.

In [6] we devote to sets of states of environment defined in [10], its relations and properties in PM-Colonies were described in [9] and [10]. After study of these properties in [7] at t-mod colonies [1], we express these languages in regular expression for both sequential and parallel colonies in [5]. In this paper we show regular expressions of languages of the environment for PM-Colonies and PM-Colonies with modified definition. We compare these types of PM-Colonies and its properties.

2 Colonies

Colonies are grammar models of multi-agent systems motivated by subsumptial architecture and they are a special form of cooperating grammars. A Colony consists of a finite number of simple components generating finite languages.

A colony influences the environment represented by string of symbols and through the medium of components makes changes in it. Each state of the environment is denoted by finite string of symbols. Components of the colony change the strings of symbols in a sequential or in a parallel way. The set of all possible states of the environment, which can be generated from a given starting string, forms the language of the colony.

© Václav Snášel (Ed.): WOFEX 2007, pp. 405–410, ISBN 978-80-248-1571-8.
VŠB – Technical University of Ostrava, FEECS, 2007.

2.1 PM-colonies

In a PM-colony environment the location of an agent is fixed. The area, where the PM-colony [9, 10] works, is represented by a string of agents and environment symbols (those can be changed) and boundary markers of the environment. Boundary markers labels the begin and end of a word, it is not allowed to erase, to overstep or to produce them.

The actions take place only in strict vicinity of the symbol representing the agent. These actions can add one environment symbol or one agent symbol (a new agent can be also created), can move agent one step on left or right, can erase neighbouring agent or environment symbol, or can substitute an environment symbol to another one.

All agents work in parallel. The activity of an agent depends maximal on one symbol in front of it and one symbol behind it. To solve a conflict, when agents have a common neighbour, we arrange the set of agents by a priority set relation. Agents can‘t change its own name or name of any other agent. Agents with the same name may be present on more than one position in the string.

Definition 1: PM-colony is a construct $C = (E, \#, N, >, R_1, .. , R_n)$, where

- E an alphabet (of the environment),
- # is the boundary marker,
- N the alphabet of agents names,
- $>$ the partial order relation over N (the priority relation for agents)
- $R_1, .. , R_n$ are finite sets of action rules of the agents. The action rules can be of the following forms:
- Deletion: $(a, Ai, b) \rightarrow (\varepsilon, Ai, b)$, *where* $a \in E \cup N$, $b \in E \cup N \cup \{\#\}$, $(a, Ai, b) \rightarrow (a, Ai, \varepsilon)$, *where* $a \in E \cup N \cup \{\#\}$, $b \in E \cup N$,
- Insertion: $(a, Ai, b) \rightarrow (a, c, Ai, b)$, *where* $a, b \in E \cup N \cup \{\#\}$, $c \in E \cup N$, $(a, Ai, b) \rightarrow (a, Ai, c, b)$, *where* $a, b \in E \cup N \cup \{\#\}$, $c \in E \cup N$,
- Substitution: $(a, Ai, b) \rightarrow (c, Ai, b)$, *where* $b \in E \cup N \cup \{\#\}$, $a, c \in E$, $(a, Ai, b) \rightarrow (a, Ai, c)$, *where* $a \in E \cup N \cup \{\#\}, b, c \in E$,
- Move: $(a, Ai, b) \rightarrow (Ai, a, b)$, *where* $a \in E \cup N$, $b \in E \cup N \cup \{\#\}$, $(a, Ai, b) \rightarrow (a, b, Ai)$, *where* $a \in E \cup N \cup \{\#\}$, $b \in E \cup N$,
- Death: $(a, Ai, b) \rightarrow (a, \varepsilon, b)$, *where* $a, b \in E \cup N \cup \{\#\}$.

Let $(a, A_i, b) \rightarrow \alpha$ be an action rule of an agent, then symbols a, b represent the context of agent A_i.

3 Categories of environment states

In [10] there were introduced important classes of states of the environment. It serves to study structural properties of PM-colonies. In this paper we are interested in in all symbol strings, which a colony is able to generate from any starting symbol.

Definition 2: Let C = $(E, \#, N, >, R_1, .. ,R_n)$ be a PM-colony. A state $y \in \#(E \cup N)^*\#$ is said to be *reachable* in C, if there is a state $z \neq y$ such that $z \Rightarrow y$ with respect to C.

The state, which is not *reachable* is said to be *unreachable*. A state $y \in \#(E \cup N)^*\#$ is said to be *alive*, if there is a state $z \neq y$ such that $y \Rightarrow z$. A state which is not *alive* is said to be *dead*.

By intersecting the classes in the two classifications above, we get four classes of states, hence four languages. We denote by *Reachable(C)*, *Unreachable(C)*, *Alive(C)*, *Dead(C)* the languages of all reachable, unreachable, alive, and dead states of *C*. We denote also:

$Garden\text{-}of\text{-}Eden(C) \quad = \quad Unreachable(C) \cap Alive(C)$
$Life(C) \quad = \quad Reachable(C) \cap Alive(C)$
$Doomsday(C) \quad = \quad Reachable(C) \cap Dead(C)$
$Non\text{-}Life(C) \quad = \quad Unreachable(C) \cap Dead(C)$

Note: In further text we will the environment states *Garden-of-Eden, Life, Non-Life* and *Doomsday* (just like the languages associated with them) mark by codes *GE, LF, NL* and *DD*.

4 Languages of the environment in PM-colonies

4.1 Original PM-colonies

Notation: If the languages of the environment are regular [9], then it must be possible to record them in regular expression. All rules in PM-colonies has the form: $(a, A_i, b) \to \alpha$, we can simplify this notation into $\alpha \to \beta$. *A*s α we mark all alive rule-configurations and as β we mark all reachable configurations consisting of three symbols.

By χ we mark set of configurations unreachable agent-conflict, that cannot be solved via priority rules and δ, $\delta \not\in (E \cup N)^* \cap \beta$, we mark reachable conflicts that are not belonging to the set β.

Lemma 1:

$Alive(C_{PM}) = (E^*\alpha E^*)^* \qquad Dead(C_{PM}) = (E \cup N)^* - (E^*\alpha E^*)^*$

$Reachable(C_{PM}) = (E^*\beta E^*)^* \qquad Unreachable(C_{PM}) = (E \cup N)^* - (E^*\beta E^*)^*$

Theorem 1:

$GE(C_{PM}) = (E \cup N - \chi - \delta)^* \, (\alpha - \beta) \, (E \cup N - \chi - \delta)^*$

$LF(C_{PM}) = (E^*\alpha E^*)^* \cap (E^*\beta E^*)^*$

$DD(C_{PM}) = ((E^*\beta E^*)^* - (E^*\alpha E^*)^*) \cup (E \cup N)^*\delta(E \cup N)^*$

$NL(C_{PM}) = ((E \cup N)^* - (E^*\beta E^*)^* - (E^*\alpha E^*)^*) \cup (E \cup N)^*\chi(E \cup N)^*$

Proof: Flows from Lemma 1.

Definition 3: for *GE, LF, DD, NL* we use a characteristic function $X(L)$:
$X(L) = 0$ for $L = \emptyset$; $X(L) = 1$ else.
And a characteristic vector of the system $X(S)$:
$X(S) = (\ X(GE(S)), X(LF(S)), X(DD(S)), X(NL(S))\ )$.

Proposition 1 [6]: $X(C_{PM}) = (\ (1,1,1,1),\ (1,1,0,1),\ (1,0,1,1),\ (1,1,0,1),\ (1,0,0,1),\ (0,0,0,1))$.

4.2 PM-colonies without agent priority relation

Let us think of PM-colonies, which are not using priorities between agents.

Theorem 2: Colonies without agent priority relation cannot derivate some configurations, that original PM-colonies can do.
Proof: $C_{PM}=(\ (a)\ ,\ \#,\ (A,B,C),\ >\ =\ (B>A,\ B>C,\ C>A),\ R=\{(\#,B,C)\rightarrow(\#,A,B,C),\ (A,B,C)\rightarrow(A,\varepsilon,C),\ (A,C,\#)\rightarrow(C,A,\#),\ (\#,C,A)\rightarrow(\#,C,a,A),\ (\#,C,a)\rightarrow(\#,C,a,a),\ \ldots\ \})$.

Let us derivate from start configuration $\#BC\#$: $\#BC\# \Rightarrow \#ABC\# \Rightarrow \#AC\# \Rightarrow \#CA\# \Rightarrow \#CaA\# \Rightarrow \#CaaA\# \Rightarrow \ldots$

The configuration $\#ABC\#$ cannot be reached without priority relation – to reach it, we have to erase 4 symbols in one derivation step or to create one agent between two other agents. In the first case we need to do more actions then is the numer of our agents, in the second on there is a conflict and we need the priority relation.

Lemma 2:
$Alive(C_{PMBP}) = (E^*\alpha E^*)^*$ $\quad Dead(C_{PMBP}) = (E \cup N)^* - (E^*\alpha E^*)^*$
$Reachable(C_{PMBP}) = (E^*\beta E^*)^*$ $\quad Unreachable(C_{PMBP}) = (E \cup N)^* - (E^*\beta E^*)^*$

Theorem 3:
$GE(C_{PMBP}) = (E \cup N - \chi - \delta)^*\ (\alpha - \beta)(E \cup N - \chi - \delta)^*$
$LF(C_{PMBP}) = (E^*\alpha E^*)^* \cap (E^*\beta E^*)^*$
$DD(C_{PMBP}) = ((E^*\beta E^*)^* - (E^*\alpha E^*)^*) \cup (E \cup N)^*\delta(E \cup N)^*$
$NL(C_{PMBP}) = ((E \cup N)^* - (E^*\beta E^*)^* - (E^*\alpha E^*)^*) \cup (E \cup N)^*\chi(E \cup N)^*$
Proof: Flows from Lemma 2.

Theorem 4: $X(C_{PMBP}) = (\ (1,1,1,1),\ (1,1,0,1),\ (1,0,1,1),\ (0,1,1,1),\ (0,1,0,1),\ (0,0,0,1))$.
Proof:

- $C = (\{a\},\#,\{A\},\ \{(a,A,a)\rightarrow(a,A,a,a),\ (a,A,\#)\rightarrow(a,\#),\ (\#,A,\#)\rightarrow(\#,A,a,\#)\}$.
  $AAA \in NL(C)$, $\#A\# \in GE(C)$, $\#Aa\# \in LF(C)$, $\#a\# \in DD(C)$.
- $C = (\{a\},\#,\{A\},\ \{(a,A,a)\rightarrow(a,\varepsilon,a),\ (a,A,\#)\rightarrow(a,\varepsilon,\#),\ (\#,A,\#)\rightarrow(\#,\varepsilon,\#),\ (\#,A,a)\rightarrow(\#,\varepsilon,a)\}$.

  - $\#AA\# \in NL(C)$, $\#aAa\# \in GE(C)$, $\#aa\# \in DD(C)$, $LF(C) = \emptyset$.
- $C = (\{a\},\#,\{A\}, \{(a,A,a)\to(a,a,A,a), (a,A,\#)\to(a,a,A,\#), (\#,A,\#)\to(\#,a,A,\#), (\#,A,a)\to(\#,a,A,a)\}$.
  - $\#AA\# \in NL(C)$, $\#Aa\# \in GE(C)$, $\#aA\# \in LF(C)$, $DD(C) = \emptyset$.
- $C = (\{a,b\},\#,\{A\}, \{(X,A,b)\to(X,A,\varepsilon), (a,A,Y)\to(A,a,Y), (b,A,Y)\to(A,b,Y); X \in \{a,b,\#\}, Y\in \{a,\#\}\ \}$.
  - $\#AA\# \in NL(C)$, $\#AbA\# \in DD(C)$, $\#aA\# \in LF(C)$, $GE(C) = \emptyset$.
- $C = (\{a,b\},\#,\{A\}, \{(a,A,a)\to(a,A,b), (a,A,b) \to (b,A,b), (b,A,b) \to (b,A,a), (b,A,a) \to (a,A,a), (\#,A,a) \to (\#,A,b), (\#,A,b) \to (\#,A,a), (a,A,\#) \to (b,A,\#), (b,A,\#) \to (a,A,\#)\}$.
  - $\#AA\# \in NL(C)$, $\#aAa\# \in LF(C)$, $DD(C) = \emptyset$, $GE(C) = \emptyset$.
- $C = (\{a\},\#,\{A\}, \{\}$.
  - $\#AA\# \in NL(C)$, $GE(C) = \emptyset$, $LF(C) = \emptyset$, $DD(C) = \emptyset$.

$C_{PMBP} \subset C_{PM}$, then $X(C_{PMBP})$ cannot contain vectors that are not in $X(C_{PM})$.

4.3 Continuing PM-colonies

Let us think about PM-colonies, that don´t stop the derivation in a case of a conflict and continue with derivation on places in the string where it is possible.

Theorem 5: Continuing PM-colonies are able to generate some strings, that original PM-colonies cannot do.

Lemma 3:

$Alive(C_{PPM}) = (E^*\alpha E^*)^*$ $\quad$ $Dead(C_{PPM}) = (E \cup N)^* - (E^*\alpha E^*)^*$

$Reachable(C_{PPM}) = (E^*\beta E^*)^*$ $\quad$ $Unreachable(C_{PPM}) = (E \cup N)^* - (E^*\beta E^*)^*$

Theorem 4:

$GE(C_{PPM}) = (E \cup N)^* (\alpha - \beta)(E \cup N)^*$

$LF(C_{PPM}) = (E^*\alpha E^*)^* \cap (E^*\beta E^*)^*$

$DD(C_{PPM}) = ((E^*\beta E^*)^* - (E^*\alpha E^*)^*)$

$NL(C_{PPM}) = ((E \cup N)^* - (E^*\beta E^*)^* - (E^*\alpha E^*)^*)$

Theorem 5: $X(C_{PPM}) = (\ (1,1,1,1), (1,1,0,1), (1,0,1,1), (0,1,1,1), (0,1,0,1), (0,0,0,1)\ )$.
Proof: In PM-colonies is the set *NL* always non-empty. This eliminates 8 of 16 (2^4) theoretically possible combinations of languages of the environment. Because of dependence among *GE, DD* and *LF* we eliminate vectors *(0,0,1,1)* and *(1,0,0,1)*. For the remaining 6 vectors can be again used examples from the proof of Theorem 3.

5 Conclusions

We formulated the languages of environment of in PM-colonies and some of its variants – PM-colonies without agent priority relation and Continuing PM-colonies by regular expression. It is very interesting that types of the same colony with different derivation power has that regular expression same. And same remains even the characteristic vector of the system.

Acknowledgement: *This work was supported by Internal grant system of Silesian University in Opava no. 45/2007.*

Literature

1. Csuhaj-Varjú, E, Kelemenová A.: *On the power of colonies,* In *2nd Colloquium on Words, Languages and Combinatorics, Kyoto, 1992,* M. Ito, H. Jürgensen (eds.), World Scientific, Singapore, 1994, str. 222-234
2. Harrison, M. A.: *Introduction to Formal Language Theory*, Addison-Wesley Publishing Company, Inc., 1978
3. Kelemen, J., Kelemenová, A.: *A grammar-theoretic treatment of multiagent systems*, Cybernetics and Systems 23, 1992, str. 210-218
4. Kelemenová, A.: *Colonies*, Lecture notes, Tarragona, October 25-26, 2002
5. Kelemenová, A., Kožaný A.: *Structures of the Environment in Colonies,* WFM'07, v tisku
6. Kožaný, A.: *Třídy jazyků v PM-koloniích*, SVOČ 2005 – Sborník příspěvků, sekce Teoretická informatika, 2005, str. 21-42
7. Kožaný, A.: *Strukturální vlastnosti kolonií s t-moc derivací,* Kognice a umělý život VI, 2006, str. 223-227
8. Kožaný, A.: *Jazyky prostředí v PM-koloniích,* Kognice a umělý život VII, 2007, str. 195-200
9. Martín-Vide, C., Paun, G.: *New Topics in Colonies Theory*, Grammars 1, 1998, str. 209-223
10. Martín-Vide, C., Paun, G.: *PM-Colonies*, Computers and Artificial Intelligence 17, 1998, str. 553-582

Using Artifical Intelligence in e-Commerce

Radek Šilhavý, Petr Šilhavý

Thomas Bata University Zlin, Faculty of Applied Informatics, Nad Stranemi 4511,
760 05 Zlin, Czech Republic
{rsilhavy, psilhavy}@fai.utb.cz

Abstract. E-commerce is the most important process, which is used in the electronic business. E-commerce produces a lot of data and information, which has to be analysed. This contribution wants to show the possibilities of using artificial intelligence in e-commerce.

1 Electronic commerce

Main meaning of electronic commerce is given by position in the field of electronic business. Electronic business is based on the electronisation of processes in the form of internet or intranet applications.

Electronic shopping is rapidly increasing the way of business. Fundamental element of e-commerce is applications based on web technologies. This application allows the presenting and selling of goods and services to customers by internet network. The main advantage of e-commerce is unlimited virtual space for the presentation of goods. Only the physical inspection is not possible, but customers have a lot of other information about the item. E-commerce produces a lot of information, which has to be stored and analysed. In field of the data processing can be used artificial intelligence directly neural networks.

2 Application of artificial intelligence in electronic commerce

Following the development of electronic business a lot of information is collected. The goal of the right application of the electronic business is to produce and display information from stored data. This process is called data mining. The data mining

© Václav Snášel (Ed.): WOFEX 2007, pp. 411–415, ISBN 978-80-248-1571-8.
VŠB – Technical University of Ostrava, FEECS, 2007.

process include selection, searching and modeling. These activities are based on particular data. The task of data mining is to prepare information for use in e-commerce.

Using the analyses of stored information, it is possible to make quicker and better decisions of e-commerce strategy. Good examples of using data mining can be found in the field of customer relationship, stock management, marketing analyses, products offers. The following text discusses using in three main parts.

2.1 Customer relationship

Customer relationship management is a very important part of electronic commerce. This part is useful for a lot of e-commerce companies. Use of data is based on stored path of customer in electronic shop. By following this path customers are divided into several groups. This division is important for the recommendation of the right products or links to individual customers.

Second example is the analyst of the shopping basket. To find the right answer to the question, what product the customer wants, is to find the relation between products in the basket. The right answer is important, because it allows the offering of the right product to the right customer. By using artificial intelligence it is possible to find links between products, which are not obvious at the first view.

2.2 Stock management

Forecast of the future development of sales is very important for two reasons. First of these it is important to make decision what customer will ask for in the future. Second reason is to know how the amount of items will develop.

Distribution of parcels is important too. Customers have to know the price of packaging. . It means that it is necessary to know postage or transport fees. Neural network can help with optimalization of cover size - e. g. by neural network it is possible to optimize box size by knowing the size of items.

Forecasting of stock allows the optimization of the number of staff, inventory or preparing of the marketing campaign.

2.3 Marketing campaign

The electronic commerce is one of the most important marketing solutions, which can be used by companies. The study and analyses of customer habits (already mentioned above) belongs to the important goal of electronic commerce. Marketing campaigns can be formed by the application of neural networks to web server logs or other costumer data stored in the database. Objective of analyst is to prepare prototypes of customers.

3 Way of the implementation to Microsoft SQL Server 2005

Important role in the realization and for searching answers to questions of analyst of electronic business take analytical functions that are included in Microsoft SQL Server 2005. This database system is often used for electronic commerce applications. The extension for Microsoft SQL is called Data Mining. Data mining in Microsoft SQL follows the whole cycle of data flow in the electronic commerce. Data mining extension is used for building intelligent applications, which use all advantages of data mining process in all stages. The advantage of this data mining extension is the possibility of work in real-time (e.g. good example is validation of input by data mining algorithm output.)

Advantages of data mining in MS SQL consist in the integration with all parts of MS SQL. It means that data mining is not a standalone application, but is an integral part of all standard applications.

Data mining in MS SQL is useful for database programmers. They don’t have to be experts in data mining. Working with data mining extension is quite easy. MS SQL data mining extension is based on a well - prepared API, which support call of models directly from user application. This is main reason why is very useful for electronic commerce system based on internet or intranet application. The data mining API is based on language, which is called Data Mining Extensions to SQL (DMX). The language DMX is based on basic SQL language syntax. This syntax is the same in the whole MS SQL Server.

Data mining in MS SQL is based on several different algorithms:

Decision Trees – algorithm counts probability, based on values of training set

Association Rules – algorithm based on bindings among elements.

Naive Bayes – is used for showing difference in selected variable and for prediction.

Sequence Clustering – is used for clustering data. Clustering is based on sequence of events.

Time Series – is used for analyses and prediction based on time data.

Neural Nets – most important part of artificial intelligence. Neural Nets are used for prediction or for searching connections in data, where connections are not clearly visible.

Text Mining – is used for analyses non-structural text data.

Microsoft Neural Network Algorithm (MNNA) is most important part of the list for purpose of this contribution. This algorithm will be described next.

3.1 Microsoft Neural Network Algorithm

Microsoft Neural Network Algorithm is using multilayer Perceptron neural network for data mining model construction. Back-Propagated Delta Rule network, composed of up to three layers of neurons, or perceptrons. These layers are an input layer, an optional hidden layer, and an output layer. In a Multilayer Perceptron network, each neuron receives one or more inputs and produces one or more identical outputs. Each output is a simple non-linear function of the sum of the inputs to the neuron. Inputs only pass forward from nodes in the input layer to nodes in the hidden layer, and then finally they pass to the output layer; there are no connections between neurons within a layer

3.2 Perceptron neural network

The neural network is based on biological principles of the neuron. The neuron is called an elementary part of the network . Neurons are connected to each other and inputs from other neurons are by weight. All inputs are added and offset value is subtracted. Offset value dictate, which value makes the neuron active.

The first implementation of neural network was prepared by Frank Rosenblatt in 1957. This first neural network contains only one neuron. The neuron used sigmoid function for the activation function. It means that output of the neuron can be 1 or -1. The neuron is able to divide patterns only in two groups. The perceptron neural network (basic configuration) has a problem with linear separability. This makes it very sensitive for noise in data.

4 Back propagation Algorithm

Neural networks, that use this algorithm for back-propagated of error. Advantages are given by ability of approximation most of function. The algorithm calculates the error, if any, and adjusts the weights that are associated with the inputs for that neuron, working backward from output neurons to input neurons in a process known as back propagation. The algorithm then repeats the process over the entire set of training data.

The important problem is that network has to know optimal output for particular data.

How the Microsoft Neural Network Algorithm

The algorithm uses a three-layer network, which contain input layer, hidden layer and output layer. . Input neurons represent input to data mining model and state of individual attributes. Hidden neurons transport values from input layer to output layer. Output neurons represent output values for data mining models too.

Input neurons receive values from data mining model and output from other neurons. Each input neuron has weight - the size of weight is set by the importance of each input. The weight can be negative; it means that this neuron will be skipped. Each neuron has a simple non-linear function assigned to it, called the activation function, which describes the relevance or importance of a particular neuron to the layer of a neural network. Hidden neurons use a hyper tangent function for their activation function, whereas output neurons use a sigmoid function for their activation function. Both functions are nonlinear, continuous functions that allow the neural network to model nonlinear relationships between input and output neurons. These two functions are non-linear, which allow them to solve problems, which are not linear-separability.

5 Conclusion

The aim of the contribution was to show the possibility of using artificial intelligence - neural networks in field of electronic commerce. Second point was to show implantation of neural networks in MS SQL Server data mining extensions. Basic of the implementation in MS SQL is the Microsoft Neural Network Algorithm. The algorithm is based on the multilayer Percepron neural network which used back propagation algorithm for error adjustment.

Possibilities of using neural networks in electronic commerce are appreciable. The reason for that in electronic commerce is necessary to make prediction of future. Mainly in the relationship between shop and costumers.

6 References

1. Zelinka, Ivan. Umělá inteligence : V problémech globální optimalizace. 1. vyd. Praha : BEN, 2002. 192 s. ISBN 80-7300-069-5.
2. J.Yao, N. Teng, H.-L. Poh, C.L. Tan. Forecasting and Analysis of Marketing Data Using Neural Net-works. Journal Of Information Science And Enginee-ring Vol.14, 1998, 843-862.
3. B. Prasad. Intelligent Techniques For E-commerce. Journal of Electronic Commerce Research, Vol.4, No.2, 2003, 65 – 71.
4. UTLEY, Craig . Introduction to SQL Server 2005 Data Mining. Microsoft SQL Server 9.0 Technical Articles [online]. 2005 [cit. 2007-03-19]. Dostupný z WWW: <http://msdn2.microsoft.com/en-us/library/ms345131.aspx>.
5. Vellido, A., Neural networks for B2C e-commerce analysis: some elements of best practice. 4th International Conference On Enterprise Information Systems (ICEIS), 2002, Ciudad Real, Spain.

Codeviation Project - Analyzing Software Project From Its History*

Petr Zajac

Software tools, Sun Microsystems Czech, s.r.o., Evropská 33E, 148 00 Praha 6, CZ

Abstract. Maintenance and reliability of software products becomes real problem. This paper describes engine for mining software repositories. The data are mined by using modified compiler. Execution of mining process and visualization are performed in continuos integration system. The paper also shows first applications - computation importance of source code fragments and matching correct category in bug tracking system from exception stacktrace of automated error report.

1 Introduction

The Codeviation[1] project was based in order to study evolution of software projects, analyzing software metrics, mining semantics from the history and predicting software reliability. The prototype analyzes only Java projects. We started to create statistics and models of NetBeans[2] project because we are closely in contact with NetBeans development team.

The architecture of Codeviation prototype is described in section 2. Mining semantics is described in section 3. Plug-in for Hudson[12] is described in section 4. We discuss about computing importance of code by using PageRank algorithm and relation between source code fragment importance and bug severity in section 5. First application of Codeviation project the predicting component(category) name in bugtracking system is described in section 6. Project was inspired by work of other researchers (Section 7).

2 Architecture overview

The architecture of Codeviation project is at Fig. 1. Current implementation allows to work only with CVS [14] source code management(SCM). Gathered metrics and computed information are stored to the Codeviation cache. The Codeviation cache contains data needed for computation and construction of models of our research. Hudson [12] is a continuous integration system for building software. It mines history of semantics from source code in a loop. Hudson

---

[*] I would like to thank my tutor Doc. Ing. Radim Briš, CSc.

[1] `http://www.codeviation.org`

[2] `http://www.netbeans.org`

© Václav Snášel (Ed.): WOFEX 2007, pp. 416–421, ISBN 978-80-248-1571-8.
VŠB – Technical University of Ostrava, FEECS, 2007.

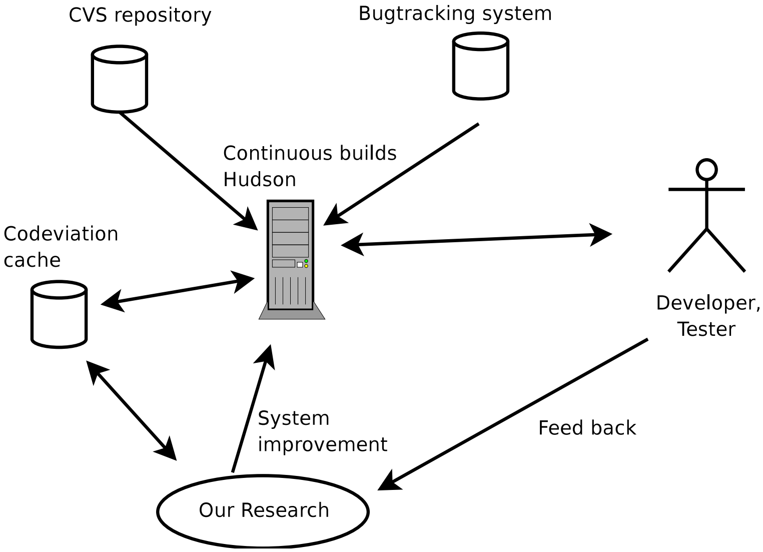

Fig. 1. Set up building of project in web browser

also allows to visualize statistics and create a report. The intention is to show the statistics and the reports from experimental models to NetBeans team. The models will be improved from their feedback. A developer usually fills a bug number to revision information when he fixes the bug, for example:

```
revision 1.7
date: 2006/05/26 08:35:28;
author: john;
#74869 EventDispatchThread hang
```

Bugs are stored in the bug tracking system. We use an algorithm similar to Sliwerski approach[11] to decide whether or not there is a relation[16] between the bug number and the file revision. We describes how to mine metrics in the next section.

3 Mining software metrics

Compiler allows to gather lot of interesting information during compilation time. Javac[1] compiler is standard compiler distributed with Java SDK. We modified Javac to perform static analysis of code during compilation.

Many java applications use Ant [3] building system. To simplify the matters a bit we reduced on this building system. Compilation of java files is done by a javac task in Ant building system. By changing special system property one can easily replace the default compiler. We use this approach to inject the modified compiler into existing build-scripts.

The Patched Ant[3] provides SPI [13] to register custom visitors (design pattern for traversing the tree). A visitor is able to traverse the AST (Abstract Syntax Tree) of a compilation unit (i.e. one Java file). A visitor can be written in separated library. The library is placed to special folder on disk. Patched Ant automatically scans the folder and loads visitors before Ant build script is executed. The Patched Ant also provides an API(application programming interface) to store mined information on disk.

In order to be able to mine historical data about given project. We need to build it as several points in time. This can be easily done with checking out the project at specific date or tag and executing compilation process.

The Patched Ant maps the semantics of code to SCM history. History contains information about developers, comments and time of changes. For example we know all a developer's usages of methods invocations from connection between SCM history and semantics from *cvs annotate* command

```
1.1 (john 06-Jun-04): void main() {}
1.1 (john 06-Jun-04): String v;
1.2 (oleg 30-Jun-06): String getV(){
1.2 (oleg 30-Jun-06):  return v.trim();
1.2 (oleg 30-Jun-06): }.
```

4 Integration with continuous integration system

To be able monitor status of the data mining an extension to continuous building system was needed. We decided to use Hudson continuous building system because it's open source, extensible and well supported by its author. Hudson permits for setting up, running and monitoring the builds through a web interface.

We wrote a Patched Ant plug-in for Hudson[4]. It allows to simplify setting up of a software project for mining metrics for given snapshots at given timestamps. The period is specified by typing date value to first tag's date and last tag's date field. The Hudson will start checking out the source snapshots from the CVS and then building them. We can specify the date interval between two source snapshots.

Hudson provides an interface to show status of projects and for creating online reports. We implemented visualization of gathered data by Patched Ant. Current implementation shows reports for modules [5], java packages and java files.

5 Computation of source code fragment importance

The structure of classes and calls of methods forms a directed graph. The nodes in graph represent classes and the directed links represent calls of methods.

---

[3] for historical we call modified compiler Patched Ant or Pant

[4] `http://codeviation.org/wiki/Wiki.jsp?page=HudsonPlugin`

[5] Source root - folder with files compiled in one time

PageRank[2, 6] algorithm was used to order the classes by their importance. We named the rank of classes the ClassRank [15].

Different bugs are reported with different severity. The severity of bug says how the bug is critical. From mapping between severity of bug and SCM we tested if importance of bug is correlated with the ClassRank. For a type of severity of bug we constructed probability density function (PDF) for positions of classes ordered from the most important class to the least important class. We used rather index of positions than ClassRank value because the ClassRank distribution of nodal degrees is the power law distribution [10]. For our purpose the ClassRank value just only says how to sort the classes. We computed all the probability density functions for all the bug severities types. We estimated whether or not severe bug is in the important source code from probability distribution functions. We fitted the PDF to the polynomial least squares regression [7] to show bugs with higher severity are located in important source code[15].

6 Predicting components from exception stacktrace

NetBeans team is currently developing project which simplify reporting of java exceptions to bugtracking system. The project was named Exception reporter [6]. Program exceptions are collected by using Java logging API and sent to the exceptions web server. The server stores all reported exceptions to database, eliminates duplicates and allows to report a defect to Issuezilla [7] bugtracking system. Unfortunately the defects are reported to different component and subcomponent than name of module in SCM.

The Codeviation project predicts the name of a component from the stacktrace of an exception and connection between history of CVS and Issuezilla. The basic idea will be described in few next sentences. We know from the SCM history the name of classes where was fixed a bug [16]. All the matched bugs in a java package were collected. It was constructed mapping from package name to component name from the collected bugs. A package can contain bugs of different components. The bugs were separated to groups distinguished by components. The component from the largest group was selected. Example of mapping from a package name to a component and a subcomponent is shown in Tab. 1. First column contains java package names, the second contains all matched bugs in the package. The *Component*, *Subcomponent* and *Count* describes component name, subcomponent name with maximum count of issues in the package. The algorithm allows to predict the most appropriate component in the bug tracking system for a java package name. An exception stacktrace consists of frames list (full method names with line positions), for example:

```
Exception in thread "main" java.lang.NullPointerException
       at package_name1.class_name1.method_name1(Main.java:38)
       at package_name2.class_name2.method_name2(Main.java:38)
```

---

[6] `http://statistics.netbeans.org/exceptions/`

[7] Bugtracking system of NetBeans project

Package	*Total*	*Component*	*Subcomponent*	*Count*
org.openide.execution	7	openide	documentation	2
org.openide.explorer.propertysheet	52	openide	property sheet	38
org.openide.explorer.view	48	openide	explorer	24
org.openide.loaders	168	openide	data systems	99

Table 1. Mapping from a package to a component and a subcomponent

Our algorithm starts to predict component from the highest frame (*at package_name1...*). If no component was found it will take next frame (*at package_name2...*) for predicting component, etc. The algorithm sometimes predicts wrong component. It fails for example when a method of other module is invoked with invalid arguments. The method can to throw *IllegalArgumentOperation* exception. The exception says that the method was used incorrectly. After that the algorithm detects wrong component (from the frame with invalid arguments of method). However it also saves time in evaluation in this failure because owner of the detected component know that problem is not on his side and he quickly reassigns the issue to the correct owner (component). Information of manual reassign allows us to detect frames with imprecise prediction and ignore them in prediction of component name.

7 Similar projects and conclusion

Lot of similar research projects to Codeviation are under development. The most interesting will be described in this section. The Software Evolution project [8] analyzes software projects in many areas, for example to detect vulnerable component[9], predicting component failure[5]. The Software Reliability Research group [9] studies how program analysis, program verification and software measurement techniques can be used to improve the quality of software, for example [8]. EvoOnt [10] creates set of software ontologies and data exchange format based on OWL [4]. The results of the research projects are promising and probably will help in software development in many ways.

Project Codeviation allows to extract information from small and large scale software projects. Our technique is effective in storing history of small changes in sources. Integration with Hudson continuous building system allows simple setup mining process history. Goal of the Codeviation project is to analyze opensource software repositories in order to improve reliability and maintenance of software products.

---

[8] Saarland University,`http://www.st.cs.uni-sb.de/softevo/`

[9] http://research.microsoft.com/srr/

[10] `http://www.ifi.uzh.ch/ddis/msr/`

References

1. Jan Bečička, Petr Zajac, and Petr Hřebejk. Using Java 6 Compiler as a Refactoring and an Analysis engine. In *1st Workshop on Refactoring Tools (WRT'07)*, pages 56–57, Berlin, Germany, August 2007.
2. Sergey Brin and Lawrence Page. The anatomy of a large-scale hypertextual Web search engine. *Computer Networks and ISDN Systems*, 30(1–7):107–117, 1998.
3. Erik Hatcher and Steve Loughran. *Java Development with Ant.* Manning Publications Co., 2002.
4. Christoph Kiefer, Abraham Bernstein, and Jonas Tappolet. Mining software repositories with isparql and a software evolution ontology. In *Proceedings of the 2007 International Workshop on Mining Software Repositories (MSR '07).* IEEE Computer Society, 2007.
5. Sunghun Kim, Thomas Zimmermann, Jr. E. James Whitehead, and Andreas Zeller. Predicting faults from cached history. In *ICSE'07, Proceedings of the 29th International Conference on Software Engineering*, Minneapolis, MN, USA, May 23–25, 2007.
6. Amy N. Langville and Carl D. Meyer. *Google's PageRank and Beyond: The science of search engine rankinks.* Princeton University Press, 2006.
7. D.C. Montgomery and G.C. Runger. *Applied Statistics and Probability for Engineers.* Wiley, 3nd edition, 2002.
8. Nachiappan Nagappan and Thomas Ball. Explaining failures using software dependences and churn metrics. Technical report, November 2006.
9. Stephan Neuhaus, Thomas Zimmermann, and Andreas Zeller. Predicting vulnerable software components. Technical report, Universitt des Saarlandes, Saarbrcken, Germany, February 2007.
10. Diego Puppin and Fabrizio Silvestri. The social network of java classes. In *SAC '06: Proceedings of the 2006 ACM symposium on Applied computing*, pages 1409–1413, New York, NY, USA, 2006. ACM Press.
11. Jacek Sliwerski, Thomas Zimmermann, and Andreas Zeller. When do changes induce fixes? In *Proceedings of the Second International Workshop on Mining Software Repositories*, pages 24–28, May 2005.
12. Hudson - Extensible continuous integration engine, `https://hudson.dev.java.net/`.
13. J. Tulach. How to design a (module) api, `http://openide.netbeans.org/tutorial/api-design.html`, 2005.
14. Jennifer Vesperman. *Essential CVS.* O'Reilly, June 2004.
15. Petr Zajac and Radim Briš. Critical software defects are located in important source code. In *Risk, Quality and Reliability - RQR 2007*, Ostrava, Czech Republic, September 2007.
16. Petr Zajac and Radim Briš. Mining software repositories with modified compiler. In *International Workshop Control and Information Technology - IWCIT 2007*, Ostrava, Czech Republic, September 2007.

8 Grants

I have participated in following grants:
Academy of Sciences of the Czech Republic - T401940412.
The Ministry of Education, Youth and Sports of the Czech Republic - CEZ MSM6198910007.

Author Index

Adamovský, Petr, 1
Adamovský, Zbyněk, 7

Babušiak, Branko, 167, 184
Bača, Radim, 237
Běhálek, Marek, 243
Bober, Marek, 249
Božek, Michal, 13

Cigánek, Josef, 77

Černý, Martin, 173

Delong, Petr, 255
Domorádová, Marta, 261
Dostalík, Martin, 155
Dudek, Rostislav, 273
Dvorský, Marek, 339

El-Qawasmeh, Eyas, 315

Fasuga, Radoslav, 267
Floder, Jan, 178

Gála, Michal, 167, 184
Galetka, Martin, 83
Gaura, Jan, 273
Golasowski, Martin, 87
Goňo, Radomír, 87, 116
Grobelný, David, 190

Hamerský, Václav, 362
Hanáček, František, 345
Havel, Vladimír, 279
Hořínek, Pavel, 93
Hrdina, Libor, 19
Hromek, František, 350

Kabašta, Michal, 26
Kabelíková, Pavla, 285
Kohut, Ondřej, 291
Korbel, Petr, 31
Kožaný, Adam, 405
Kožaný, Jan, 297
Krátký, Michal, 237
Krumnikl, Michal, 255, 273, 303
Křeček, Tomáš, 36

Lindovský, Jan, 99

Machník, Petr, 356
Maršálek, Leoš, 362
Martinák, Lukáš, 196
Martinovič, Jan, 303
Michalek, Libor, 367
Minařík, Daniel, 104
Moldřík, Petr, 110
Moravčík, Pavel, 309
Moravčík, Petr, 42

Nečesaný, Jaromír, 373
Nevřiva, Pavel, 190

Osmančík, Lukáš, 48
Ouddane, Nabil, 379
Oujezdský, Aleš, 200

Paszek, Leopold, 110
Petránek, Pavel, 206
Pivoňka, Pavel, 54
Platoš, Jan, 315
Pokorný, Jan, 212
Pokorný, Miroslav, 206
Polák, Martin, 59
Polikarpov, Boris, 255

Rusek, Stanislav, 116

Schreiber, Josef, 321
Skapa, Jan, 386, 398
Skotnica, Petr, 65
Snášel, Václav, 237, 315
Sojka, Eduard, 273
Sokanský, Karel, 104
Spišak, Jan, 215
Stacho, Břetislav, 116

Šarmanová, Jana, 249
Šebesta, Robert, 123
Šilhavý, Petr, 411
Šilhavý, Radek, 411
Šiška, Petr, 392

Škňouřilová, Petra, 219
Škopek, Martin, 161
Škuta, Ondřej, 71
Šútora, Jan, 327

Tinka, Marek, 129
Tran, Khanh Hung, 135
Tučník, Petr, 297

Vanda, Jan, 386, 398
Vaňuš, Jan, 225
Vašinek, Vladimír, 362
Velart, Zdeněk, 333
Vik, Viktor, 142

Zajac, Petr, 416

Žůrek, Petr, 231
Žwak, Zdislav, 148

Editor:	Václav Snášel
Title:	WOFEX 2007
Place, year, edition:	Ostrava, 2007, 1st
Page count:	456
Edit:	VŠB – Technical University of Ostrava, 17. listopadu 15, 708 33 Ostrava-Poruba Czech Republic
Print:	TiskServis Jiří Pustina gen. Sochora 1764, 708 00 Ostrava–Poruba Czech Republic
Impression:	200

Not for sale.

ISBN 978-80-248-1571-8